

INNOVATIVE CLEAN COAL TECHNOLOGY (ICCT)

180 MW DEMONSTRATION OF ADVANCED
TANGENTIALLY-FIRED COMBUSTION TECHNIQUES
FOR THE REDUCTION OF NITROGEN OXIDE (NO_x)
EMISSIONS FROM COAL-FIRED BOILERS

Topical Report
Physical Flow Modeling

DOE Contract Number:
DE-FC22-90PC89653

SCS Contract Number
C-91-000028

Prepared by:

Southern Company Services, Inc.
800 Shades Creek Parkway
Birmingham, Alabama 35209

Patents Cleared by Chicago on June 18, 1991

LEGAL NOTICE

This report was prepared by Southern Company Services, Inc. pursuant to a cooperative agreement partially funded by the U.S. Department of Energy and neither Southern Company Services, Inc. nor any of its subcontractors nor the U.S. Department of Energy, nor any person acting on behalf of either:

- (a) Makes any warranty or representation, express or implied with respect to the accuracy, completeness, or usefulness of the information contained in this report, or process disclosed in this report may not infringe privately-owned rights; or
- (b) Assumes any liabilities with respect to the use of, or for damages resulting from the use of, any information, apparatus, method or process disclosed in this report.

Reference herein to any specific commercial product, process, or service by trade name, trademark, manufacturer, or otherwise, does not necessarily constitute or imply its endorsement, recommendation, or favoring by the U.S. Department of Energy. The views and opinion of authors expressed herein do not necessarily state or reflect those of the U.S. Department of Energy.

EXECUTIVE SUMMARY

This topical report presents the results of the physical flow modeling conducted as part of a U. S. Department of Energy (DOE) Innovative Clean Coal Technology (ICCT) Project demonstrating advanced tangentially-fired combustion techniques for the reduction of nitrogen oxide (NO_x) emissions from a coal-fired boiler. The purpose of this demonstration project is to study the NO_x emissions characteristics of ABB Combustion Engineering's (ABB CE) Low NO_x Concentric Firing System (LNCFS) Levels I, II, and III. These technologies are being installed and tested in stepwise fashion at Gulf Power Company's Plant Lansing Smith Unit 2.

The objective of the physical flow model study was to model the boiler and overfire air ductwork at Plant Smith Unit 2 prior to the installation of the retrofit equipment. These tests were conducted to determine the optimal operating conditions for the unit and to troubleshoot design defects on a small scale prior to the full-scale installation at Plant Smith. To accomplish the modeling in a timely manner, the physical flow modeling study was subdivided into the following tasks:

- TASK I Design and construction of the boiler and ductwork models
- TASK II Test the model of the overfire air ductwork
- TASK III Test the baseline configuration
- TASK IV Test the LNCFS Level II configuration
- TASK V Test the LNCFS Level III configuration.

At the completion of each task (except Task I), an interim report was issued in order to provide the most up to date information about the project. This report is a compilation of the interim reports from each of these tasks. Details concerning Task I are included in the reports from Tasks II and III. The purpose of each task was to investigate the flow characteristics of the Plant Smith boiler and overfire air ductwork using the physical flow model.

Task I involved the design and construction of the 1/12 scale boiler model and the 1/6 scale model of the overfire air ductwork. Following the completion of Task I, the overfire air ductwork (Task II) was tested. Results of these tests showed that the use of turning vanes with trailing edges in the turns of the ductwork could significantly reduce the pressure drop

across the overfire air ductwork. These design recommendations were implemented in the final ductwork design.

Tasks III, IV, and V involved the testing of the baseline, LNCFS Level II, and LNCFS Level III configuration of the boiler. The baseline tests were conducted to determine to original operating conditions of the unit. The results from these tests were compared to the test configurations chosen for LNCFS Levels II and III. Finally, recommended operating conditions for LNCFS Level II and III were presented.

TABLE OF CONTENTS

1. **TASK II** **Overfire Air Duct Work Flow Tests**
2. **TASK III** **Baseline Firing Conditions**
3. **TASK IV** **LNCFS-II Operating Conditions**
4. **TASK V** **LNCFS-III Operating Conditions**

SOUTHERN COMPANY SERVICES
LOW NO_x TANGENTIAL FIRING SYSTEM DEVELOPMENT

C-E CONTRACT #14664

INTERIM REPORT
PHYSICAL FLOW MODELING - TASK II
OFA DUCT WORK FLOW TESTS

Project 901237

Mechanical Systems Engineering
Kreisinger Development Laboratory
KDL-91-5

Robert J. von Hein

February, 1991

DISCLAIMER

This report was prepared as an account of work sponsored by Southern Company Services. Neither Southern Company Services, ABB Combustion Engineering, nor any person acting on behalf of them:

- A. Makes any warranty, expressed or implied, with respect to the use of any information, apparatus, method, or process disclosed in this report or that such use may not infringe privately owned rights: or
- B. Assumes any liability with respect to the use of, or damages resulting from the use of any apparatus, method, or process disclosed in this report.

Table of Contents

<u>Section</u>	<u>Title</u>	<u>Page No.</u>
<i>i</i>	List of Figures	<i>i</i>
<i>ii</i>	List of Tables	<i>ii</i>
1.0	Introduction	1
2.0	Conclusions	2
3.0	Recommendations	2
4.0	Facility Description	3
5.0	Modeling and Testing Techniques	6
5.1	Modeling Theory	6
5.2	Testing Procedures	7
6.0	Results	10
7.0	Future Test Plans	13
8.0	References	14
	Appendix A - Recommended OFA Duct turning Vane	A1

List of Figures

<u>Figure No.</u>	<u>Description</u>
1	Over Fire Air Duct Flow Model
2	Data Acquisition System
3	Model Test Plane Locations
4	Typical Test Plane
A1	Location of Turning vane #1
A2	Details of Turning Vane #1
A3	Location of Turning Vane #2
A4	Details of Turning Vane #2
A5	Location of Turning Vane #3
A6	Details of Turning Vane #3
A7	Location of Turning Vane #4
A8	Details of Turning Vane #4

List of Tables

<u>Table No.</u>	<u>Description</u>
1	RMS Deviation at Multi-cell Venturi Inlet
2	OFA Duct Pressure Drop Coefficient
3	OFA Nozzle Corner to Corner Flow Distribution

1.0 Introduction

Southern Company Services (SCS), the Department of Energy (DOE), and ABB Combustion Engineering (CE) are involved in a program to develop advanced tangentially fired combustion methods for reducing NO_x emissions. The intent of this program is to demonstrate, at "full scale," low NO_x technologies of a commercial prototype design. This demonstration includes the addition of Low NO_x Concentric Firing Systems (LNCFS) to Gulf Power Company's Lansing Smith Unit. To investigate the fluid mechanic performance of the proposed low NO_x configurations, CE is performing a physical isothermal flow model study at its Kreisinger Development Laboratory (KDL) in Windsor, CT.

The LNCFS modifications to the Lansing Smith Unit include the addition of separated over fire air (SOFA.) The duct work for this over fire air is designed to permit reasonable flow measurement through the use of a multi-cell venturi. This type of venturi requires a uniform inlet distribution for successful operation.

In order to insure an acceptable velocity profile at the multi-cell venturi inlet, and to minimize the pressure drop within the duct work, KDL was requested to perform a model study of the system. A secondary objective was to provide a uniform flow at each OFA nozzle. This was accomplished by constructing a one-sixth scale model of the OFA duct and testing a series of flow control. These devices were designed to even out the flow profiles in the duct and to reduce the pressure drop over the entire system.

This report presents the results of the SOFA duct work modeling conducted under Task II of the SCS Low NO_x Development program. This report documents the model study and provides results, conclusions, and recommendations.

2.0 Conclusions

The following conclusions can be drawn from the velocity and pressure testing of the SOFA duct work which was performed at KDL:

- 1.) The velocity profile at the inlet to the multi-cell venturi, with no upstream flow control devices, had an RMS deviation of 8.5%. With the addition of a turning vane with a trailing edge at the upstream elbow, the RMS deviation for this plane was reduced to 4.0%.
- 2.) An even flow distribution in the upstream duct work reduces the pressure drop across the "T" section, that part of the duct where the flow is split to the OFA windboxes.
- 3.) The pressure drop coefficient for the baseline duct configuration (no flow controls) is 5.3. When the recommended turning vanes are added to the duct work, the pressure drop coefficient is reduced to 3.4, a 35% reduction from the baseline configuration.
- 4.) For the baseline duct configuration, approximately one-half of the total flow went to each of the OFA nozzles. The addition of the turning vanes to the duct had little effect on this flow split.

3.0 Recommendations

In order to provide an even flow distribution at the multi-cell venturi inlet plane and to reduce the overall pressure drop in the duct work, the turning vanes, detailed in Appendix A, should be installed for both sets of OFA duct work.

4.0 Facility Description

A one-sixth scale, geometrically similar, isothermal flow model of the OFA duct work was built and tested for this phase of the program. The duct work was modeled from the OFA windboxes back to the secondary air duct. Because the velocity profile at the inlet to the OFA duct work was not known, a uniform inlet profile was used in the flow model. However, due to the long length of the duct, this assumption is not expected to effect the results.

The model was constructed primarily of 1/2" plexi-glas, for ease in construction and modifications. All dimensions were maintained to a tolerance of $\pm 1/16$ " in the flow model, which corresponds to $\pm 3/8$ " full scale. Sheet metal was used for the turning vanes. A lamson blower was used to operate the duct model under forced draft. The model, set up in an inverted position for improved stability, is shown in Figure 1.

Quantitative measurements of pressure and velocity distributions were made with a hand held pitot tube and a data acquisition system developed at KDL. Instrumentation consisted of two (2) 0-10" barocels and two (2) Barocel Electric Manometers. The pitot tube was connected to the barocels such that the total and velocity pressures could be measured. The data obtained by this system was recorded via a personal computer. A schematic of this set up is shown in Figure 2.

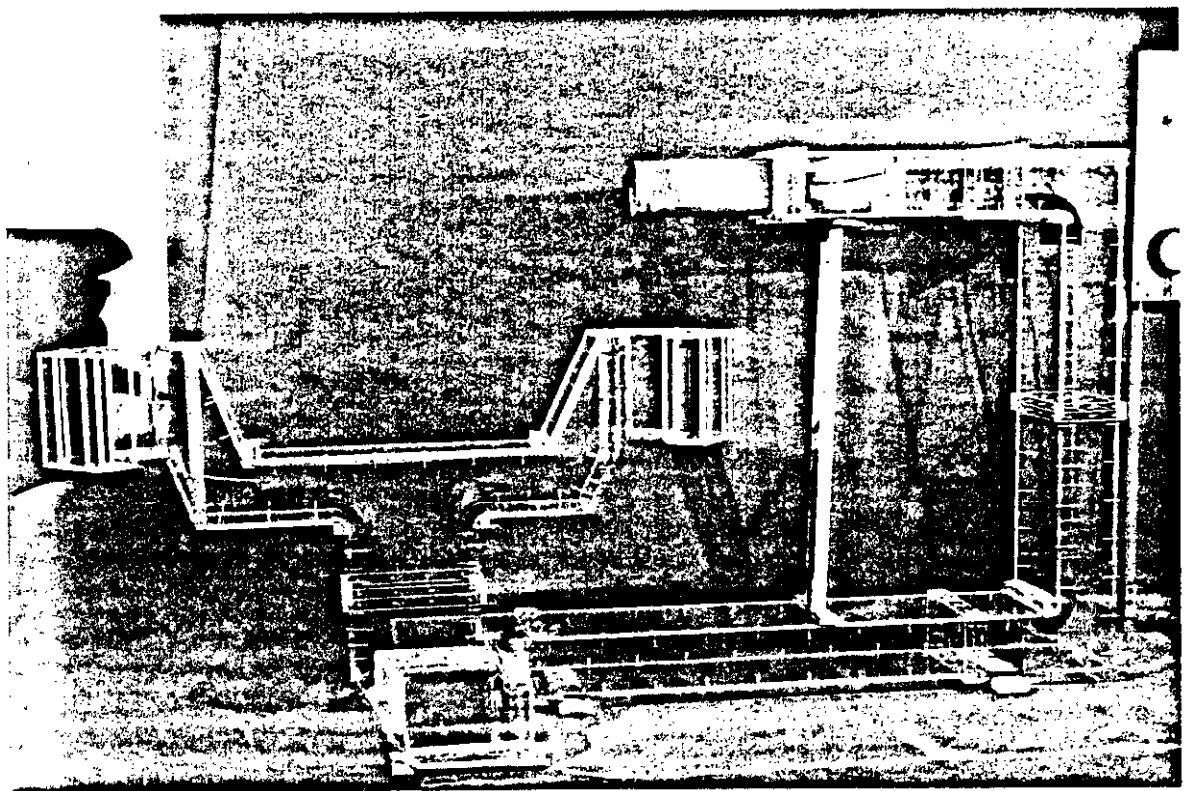


Figure 1
Over Fire Air Duct Model

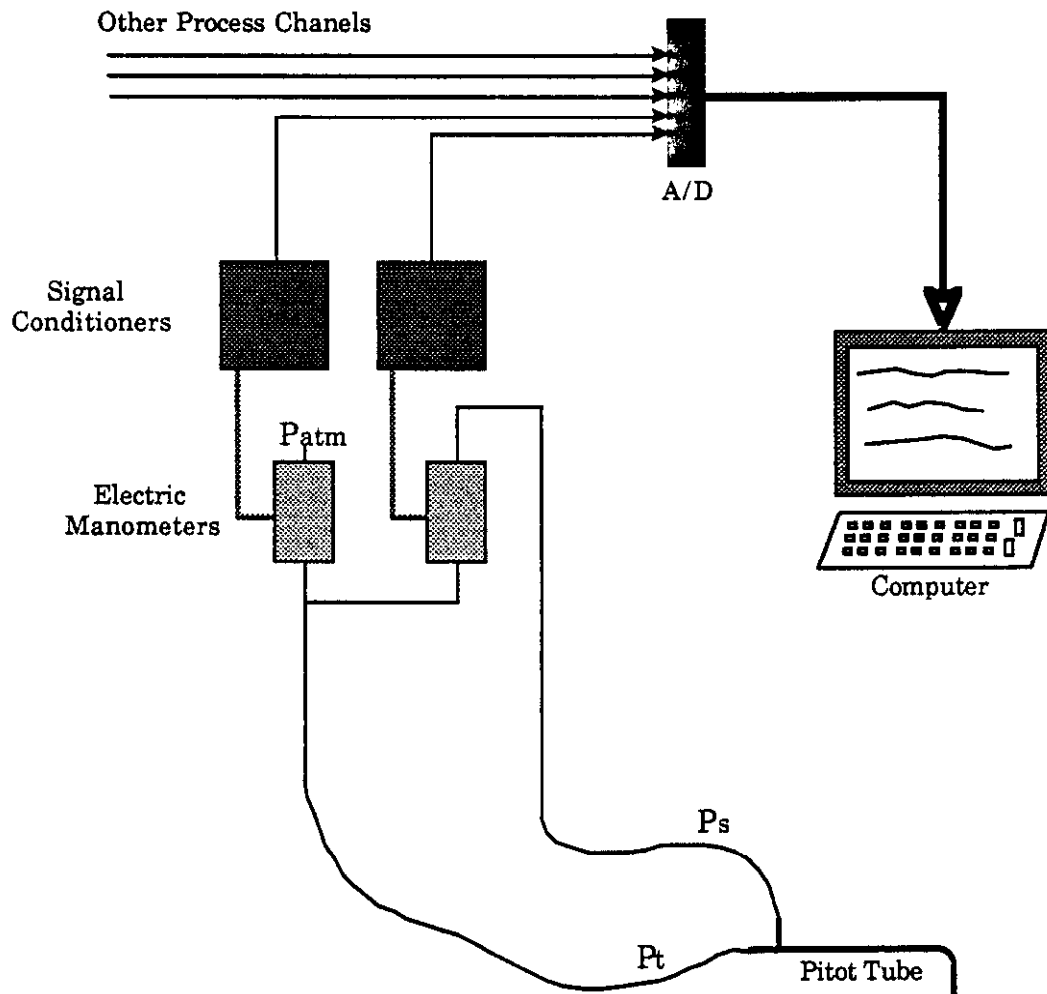


Figure 2
Data Acquisition System

5.0 Modeling and Testing Techniques

5.1 Modeling Theory

Industrial gas flow systems normally operate in the fully turbulent flow regime at MCR conditions. At the same flow velocities, geometrically scaled models of these systems will also operate in the turbulent regime, although at lower Reynolds Numbers. This is due to the characteristic size reduction and the density and viscosity variations of the gas.

Past experience at KDL and other research laboratories has shown that even though the corresponding Reynolds Numbers in the model and prototype are not identical, the model will produce gas flow profiles which are similar to those found in the prototype. Quantitatively, a scaled model will produce similar flow profiles provided a Reynolds Number greater than 10,000 is maintained during its operation. This allows the prediction of actual velocity profiles in a system based on physical model tests.

Velocities for each plane in the model are non-dimensionalized (normalized) by dividing the velocity at each point in the model by the average velocity in that plane. When the flow is turbulent, the normalized velocities in a plane will remain the same, regardless of the actual flow rate in the model or the prototype.

Since flow separation, eddy formation, and stall (flow patterns) are responsible for creating most of the pressure drop in a duct system, it is possible to obtain quantitative pressure drop measurements in the flow model. Quantitatively, the pressure drop, ΔP , can be expressed as a function of the average velocity pressure using Euler's Number (\mathcal{K})

$$\Delta P = \mathcal{K}(\rho * V^2) / 2g_c$$

where:

ΔP = total pressure drop

$(\rho * V^2) / 2g_c$ = average velocity pressure

\mathcal{K} = pressure drop coefficient

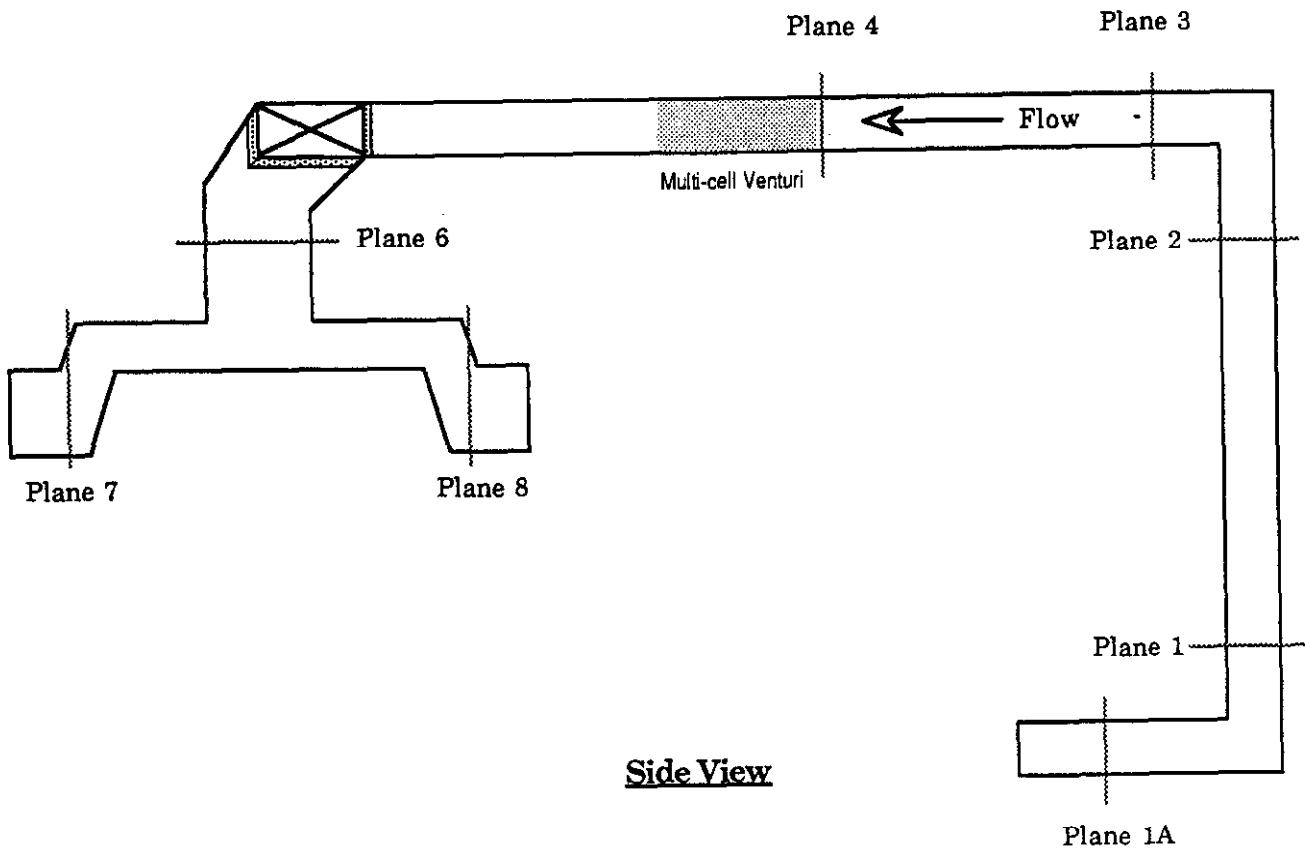
When the model is properly built and operated, the pressure drop coefficient of the model is the same as that of the prototype. However, since the Reynolds Number in the model is less than that of the prototype, the boundary layer of the fluid in the model will be proportionally larger than the prototype. Thus, the pressure drop due to friction in the model will be higher than in the prototype, and the total pressure drop predictions for the prototype should be conservative.

5.2 Testing Procedures

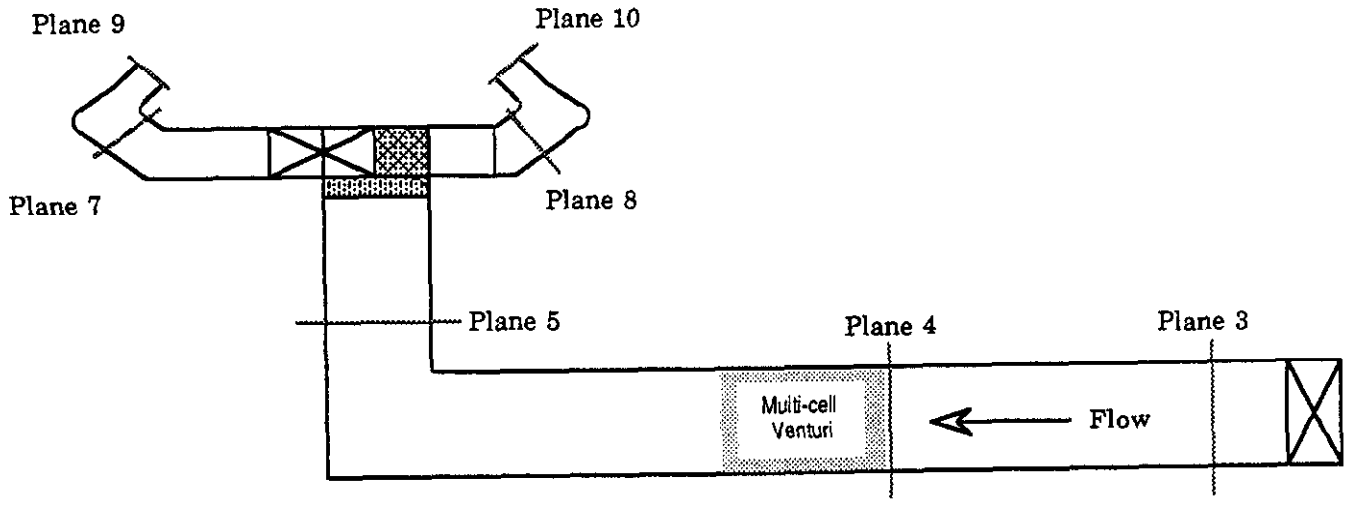
The primary objectives of this study was to obtain a uniform velocity profile at the multi-cell venturi inlet and to reduce the total pressure drop of the duct system. In order to accomplish this, one-dimensional velocity traverses were performed at various planes in the duct work to determine the duct's flow profiles and pressure drop. The results from these tests were then used to design new flow controls and the model retested. The location of these test planes are shown in Figure 3.

At the start of each test, the facility operator input the appropriate test parameters. These included the test number, test plane, number of rows, and number of columns. Once the inputs were entered, testing was done through manual manipulation of the Pitot tube. The model was probed in a plane normal to the nominal flow direction. A typical test plane is shown in Figure 4. Measurements of the total and velocity pressures for each point in the test plane were stored in the PC for later reduction.

Once the testing was completed, the data was reduced through the use of an in house data reduction program and presented in tabular form. This output included the total and velocity pressures, calculated velocity for each point, velocity profiles for the plane in a row/column format and the RMS standard deviation of the distribution.



Side View



Top View

Figure 3 - Model Test Plane Locations

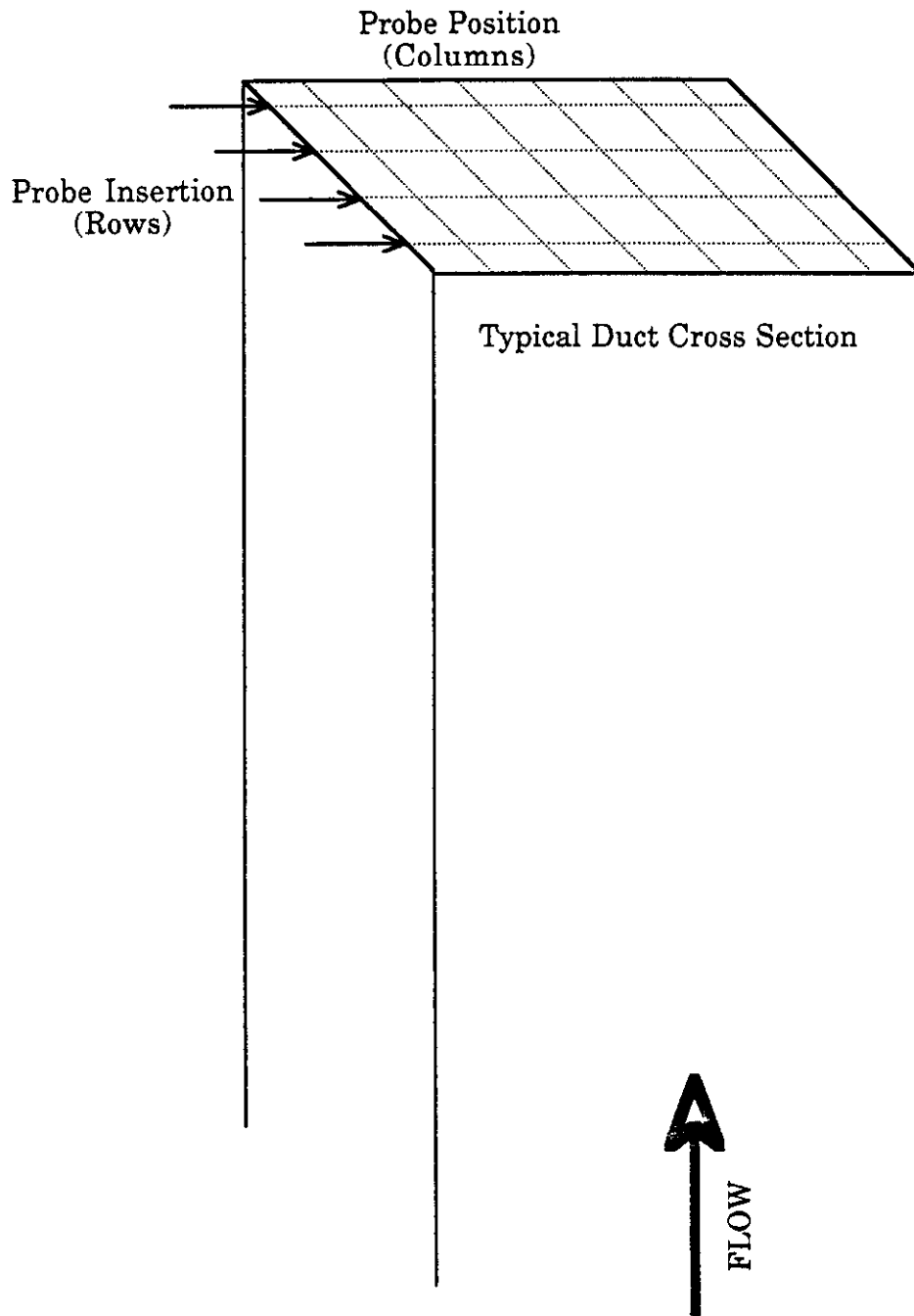


Figure 4 - Typical Flow Model Test Plane

6.0 Results

Testing of the OFA duct work model consisted of obtaining one dimensional velocity and total pressure measurements to determine the flow distribution and pressure drop characteristics. A total of four (4) configurations were tested, with up to eleven (11) planes of data being evaluated for each configuration.

The baseline duct configuration, no flow controls, was the first to be tested. Velocity and total pressure measurements were taken at each of the eleven (11) planes so that the overall pressure drop characteristics of the system could be determined. In addition to this, the velocity profiles at the inlet to the multi-cell venturi and at the outlet of the OFA nozzles were also determined.

Next, in order to reduce the pressure losses in the 90° elbows and to help straighten the flow at the venturi inlet, standard 1/3 turning vanes were installed at each of these elbows. Velocity and pressure measurements were then taken at certain planes in the model.

Next, turning vanes with trailing edges were added to each branch of the "T" section to help reduce the pressure losses further. Again, velocity and pressure measurements were taken at selected planes.

Finally, trailing edges were added to the turning vanes of the second configuration so that the flow could be further straightened and the pressure losses reduced. Again, velocity and pressure measurements were taken.

To simplify this report, details for only the final configuration have been included. These can be found in Appendix A.

One objective of this testing was to evaluate the flow profile at the inlet to the multi-cell venturi, and to establish a uniform flow at this location. Results from the tests performed at the inlet plane to the multi-cell venturi indicate that the addition of standard turning vanes to the upstream elbow has no

effect on the velocity profile, although it does reduce the pressure losses due to the elbow. However, when trailing edges are added to the turning vanes, the RMS deviation of the velocity data is greatly improved. These improvements occur for both the side to side and the top to bottom distribution within the plane and are given in Table 1.

Table 1 - RMS Deviation at the Inlet to the Multi-cell Venturi

<u>Configuration</u>	<u>Plane</u>	<u>Top/Bottom</u>	<u>Side/Side</u>
Baseline	8.5%	8.2%	2.6%
1/3 turning vane	8.9%	8.2%	4.1%
Vanes w/ trailing edge	4.0%	3.6%	2.1%

Another objective was to minimize the pressure drop in the duct work. To do this, pressure drops were analyzed and coefficients determined for each of the four (4) duct configurations. Results from these tests showed that the addition of turning vanes helped to reduce the pressure drop through the duct work. These results also show that the addition of trailing edges to these vanes helped to further reduce the pressure drop. Pressure drop coefficients for each configuration tested are presented in Table 2.

Table 2 - OFA Duct Pressure Drop Coefficient (K)

<u>Configuration</u>	<u>K</u>	<u>% reduction</u>
Baseline	5.3	-----
1/3 turning vane	4.3	18.1%
Vaned "T" section	4.0	24.2%
All vanes w/ trailing edge	3.4	35.0%

Additionally, velocity measurements were taken at the outlets of the OFA nozzles to evaluate the corner to corner flow distributions in the duct work. This was done for the baseline configuration, along with the addition of turning vanes in the upstream elbows and the addition of turning vanes in the "T" section of the duct . For each of these configurations, there was insignificant corner to corner biasing of the flow. The results of these tests are shown in Table 3.

Table 3 - OFA Nozzle Corner to Corner Flow Distribution

<u>Configuration</u>	<u>Corner #1</u>	<u>Corner #2</u>
Baseline	50.7%	49.3%
Vaned "T" section	50.4%	49.6%
All vanes w/ trailing edge	51.0%	49.0%

7.0 Future Test Plans

The next phase of work for the flow model program will be LNCFS-II testing. Changes to the physical flow model for this configuration include modifications to the windboxes and the addition of low set Over Fire Air (OFA.) These will simulate modifications to be made at the Lansing Smith No. 2 Unit.

Evaluation of this configuration will be performed through the use of flow visualization, gas mixing, and three dimensional velocity mapping. The flow visualization tests will be performed in order to screen twenty (20) potential field operating conditions. These conditions will evaluate a combination of furnace load, OFA velocities, and OFA horizontal firing angles. As each of these conditions is run, the effect of OFA tilt will also be evaluated. At the conclusions of these tests, the five (5) "best" configurations will be qualitatively tested via gas mixing and velocity profile tests. The gas mixing tests will be performed by injecting a tracer gas (methane) into the OFA flow. Samples of gas will than be extracted from the furnace model at four (4) elevations above the injection point and a level of mixing at these planes determined. Additionally, velocity data will be taken at the furnace outlet plane so that the exit velocity profile may be evaluated as a function of firing conditions.

8.0 References

1. Anderson, D.K., Bianca, J.D., and McGowan, J.G., "Recent Developments in Physical Flow Modeling of Utility Scale Furnaces," Proc. 1986 Symposium on Industrial Combustion Technologies, Chicago, Illinois, 1986
2. Beer, J.M., "Significance of Modeling," J. Inst. Fuel, November, 1966
3. Johnstone, R.E., and Thirng, M.B., Pilot Plants, Models and Scale up Factors in Chemical Engineering, McGraw Hill, New York, 1947
4. Spaulding, D.B., "The Art of Partial Modeling," 9th International Symp. on Combustion, September, 1973

Appendix A
Recommended OFA Duct Flow Controls

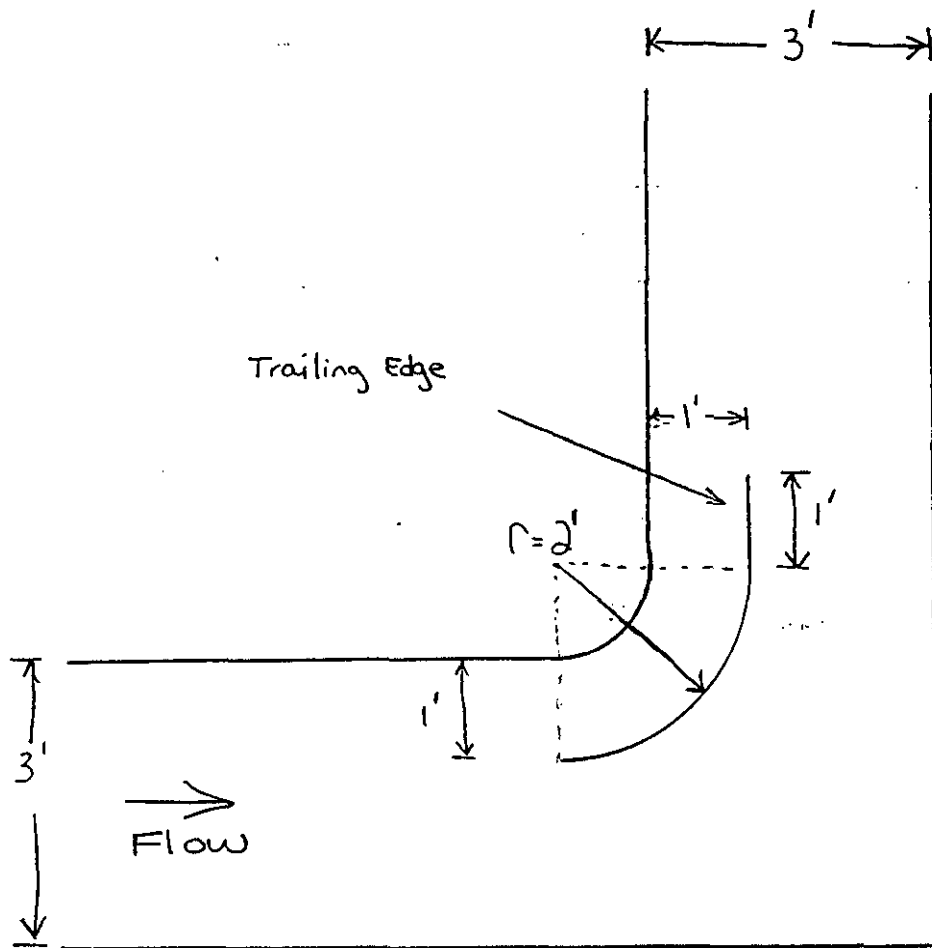


Figure #A2 - Detail of Vane #1

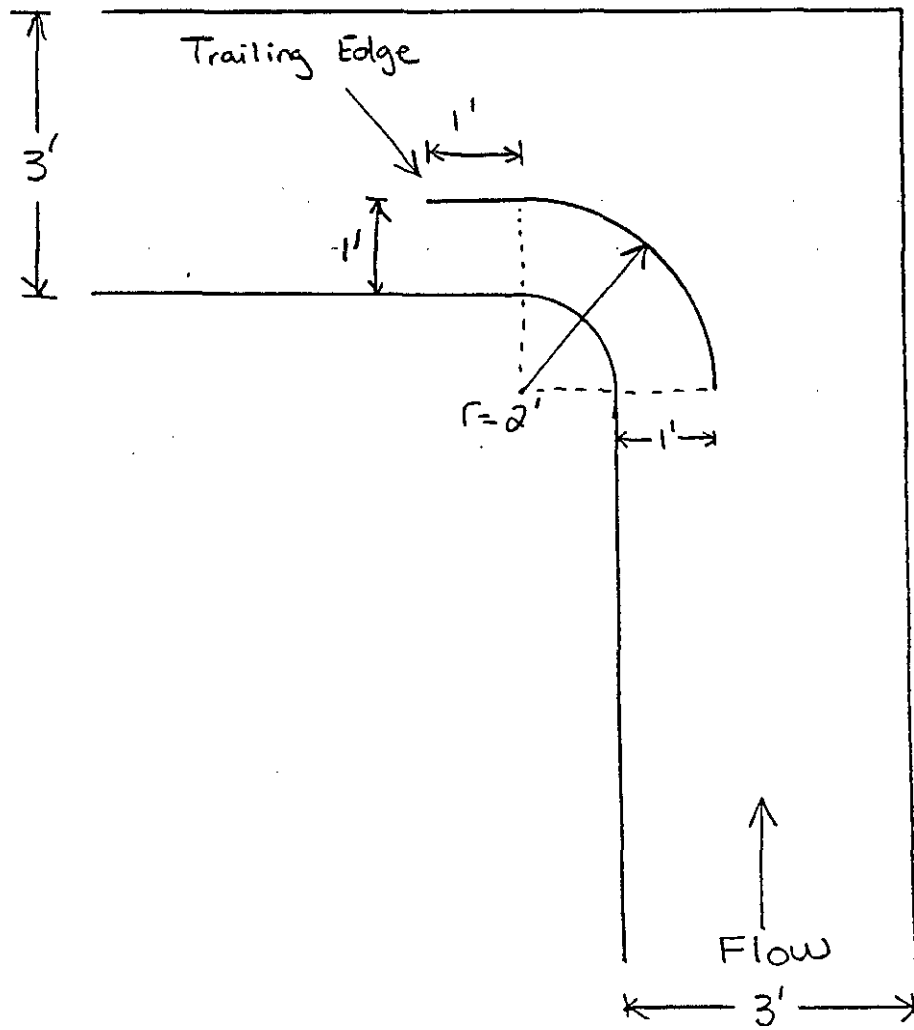


Figure #A4 - Detail of Vane #2

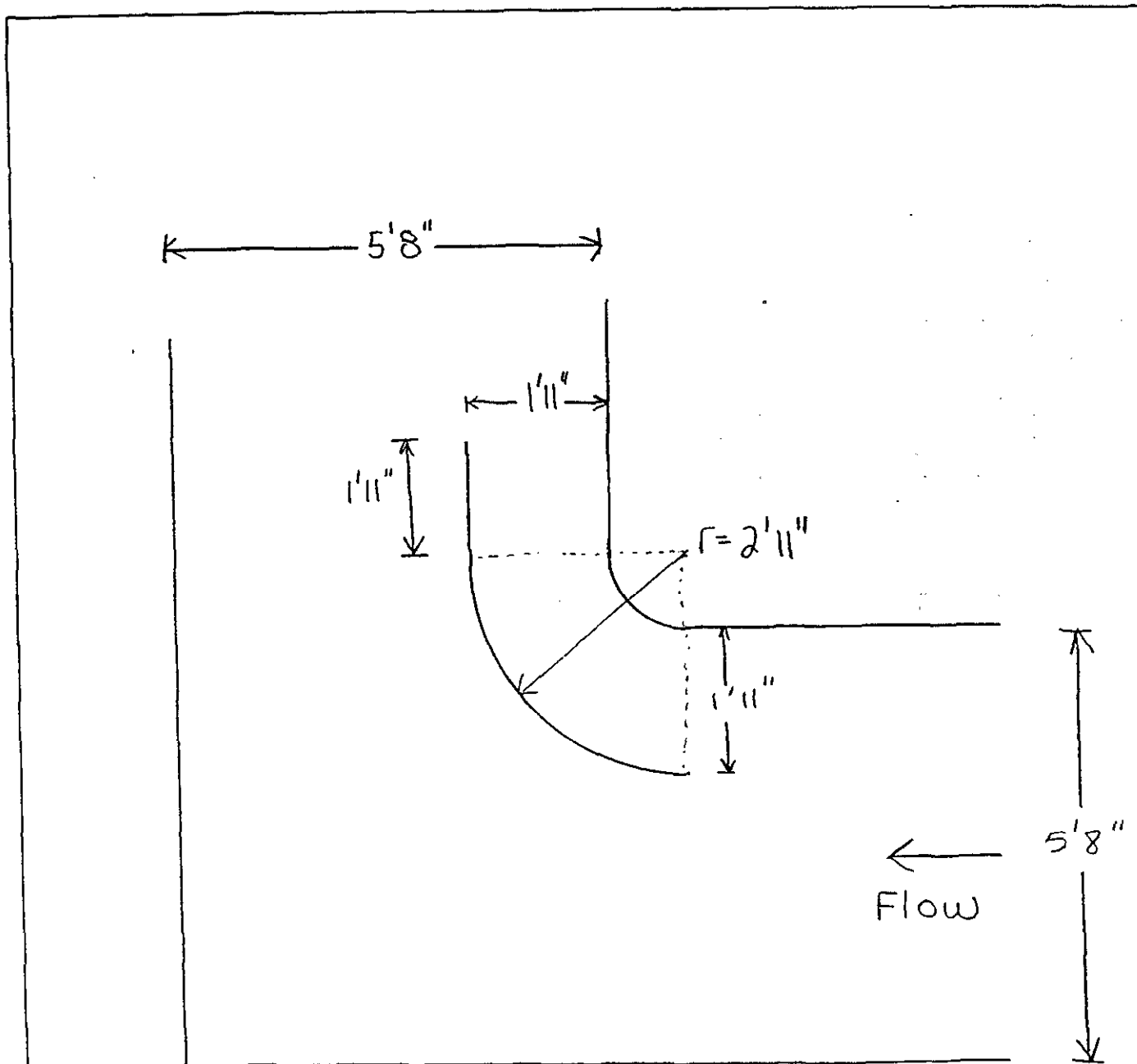
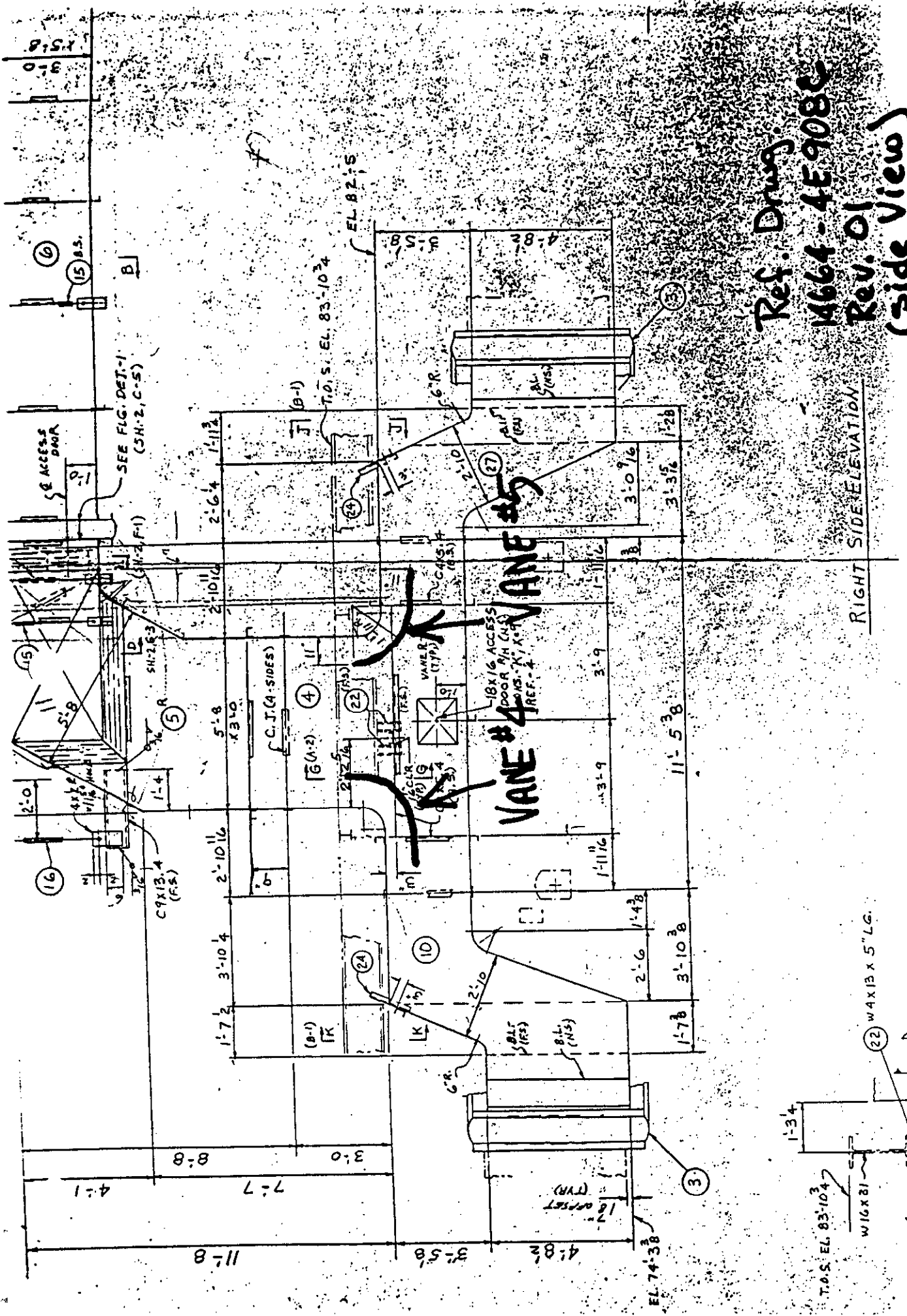


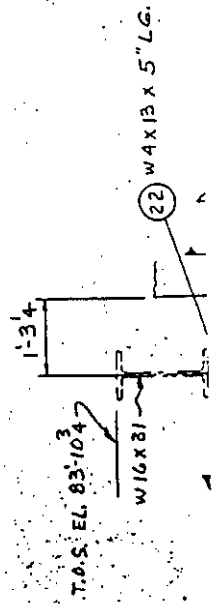
Figure #AG - Detail of Vane #3



Ref. Draw:
 14664-4E908C
 Rev. 01
 (Side View)

RIGHT SIDE ELEVATION

Figure #7



T.O.S. EL. 83'-10 3/4

EL. 74'-3 3/8

EL. 82'-5

T.O.S. EL. 83'-10 3/4

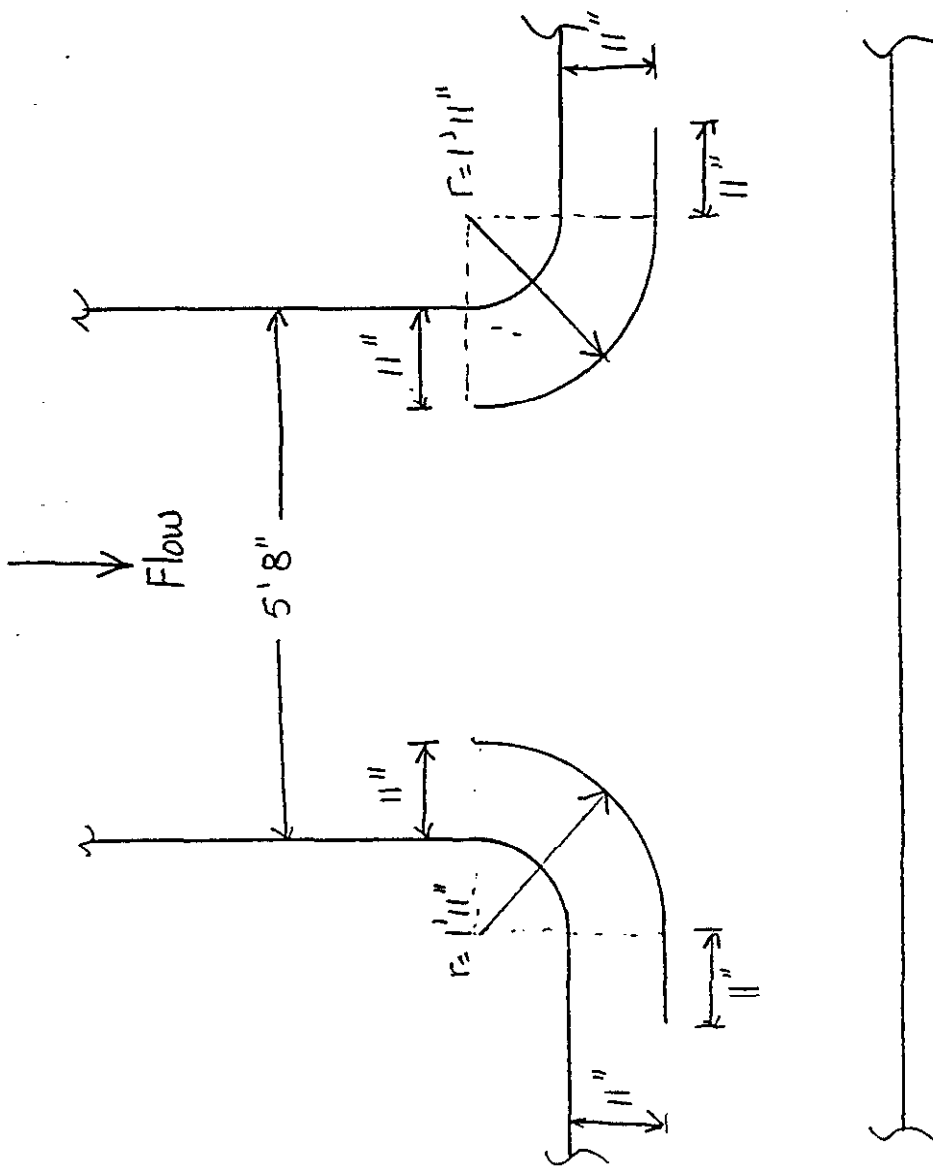


Figure #A8 - Detail of Vanes #4 & #5

SOUTHERN COMPANY SERVICES
LOW NO_x TANGENTIAL FIRING SYSTEM DEVELOPMENT

C-E CONTRACT #14664

INTERIM REPORT
PHYSICAL FLOW MODELING - TASK III
BASELINE FIRING CONDITIONS

Project 901237

Mechanical Systems Engineering
Kreisinger Development Laboratory
KDL-90-41

Robert J. von Hein

December, 1990

DISCLAIMER

This report was prepared as an account of work sponsored by Southern Company Services. Neither Southern Company Services, ABB Combustion Engineering, nor any person acting on behalf of them:

- A. Makes any warranty, expressed or implied, with respect to the use of any information, apparatus, method, or process disclosed in this report or that such use may not infringe privately owned rights: or
- B. Assumes any liability with respect to the use of, or damages resulting from the use of any apparatus, method, or process disclosed in this report.

Table of Contents

<u>Section</u>	<u>Title</u>	<u>Page No.</u>
i	List of Figures	i
1.0	Introduction	1
2.0	Facility Descriptions	3
2.1	Lansing Smith No. 2 Flow Model	3
2.2	Automatic Probe Traversing Device	6
2.3	Three-Dimensional Pitot Tube Probe	9
2.4	Smoke Generator	11
3.0	Results	12
3.1	Flow Visualization	12
3.2	Velocity Testing	15
4.0	Future Test Plans	22
5.0	References	23

List of Figures

<u>Figure No.</u>	<u>Description</u>
1	Lansing Smith #2 Flow Model
2	KDL Flow Model Area
3	Flow Model Firing Circle
4	Automatic Probe Traversing Device
5	Five Hole Pitot Tube
6	Smoke Injection-Lower Windbox
7	Smoke Injection-Upper Windbox
8	Model Test Plane Location
9	Normalized velocity profiles
10	Velocity vectors and normalized velocities

1.0 Introduction

Southern Company Services (SCS), the Department of Energy (DOE), and ABB Combustion Engineering (CE) are involved in a program to develop advanced tangentially fired combustion modifications for reducing NO_x emissions. The intent of this program is to demonstrate, at "full scale," low NO_x technologies of a commercial prototype design. This demonstration includes the addition of Low NO_x Concentric Firing Systems (LNCFS) to Gulf Power Company's Lansing Smith Unit. To investigate the fluid mechanic performance of the proposed low NO_x configurations, CE is performing a physical isothermal flow model study at its Kreisinger Development Laboratory (KDL) in Windsor, CT.

The objective of the isothermal flow model study is to assure optimum performance of the Low NO_x tangential firing system. The proposed effort centers on the understanding of in-furnace flow and mixing phenomena for the various low NO_x firing systems as applied to the demonstration unit. This is to be done through an evaluation of each proposed firing system, along with the evaluation of the burner only configuration, in the isothermal flow model. Following the burner only test, the LNCFS-II configuration will be modeled. This firing system will include the addition of low set OFA to the furnace model. The final configuration to be evaluated will be LNCFS-III. This configuration will consist of close-coupled overfire air (CCOFA) operating in conjunction with low set OFA. Each LNCFS configuration will be evaluated from an Over Fire Air (OFA) penetration, mixing, and dispersion standpoint.

In addition to the furnace flow model, a model of the OFA ductwork from the OFA windboxes to the secondary air duct is being evaluated. The proposed effort is to develop flow control devices which minimize pressure drop and provide uniform flow profiles entering the flow measurement devices.

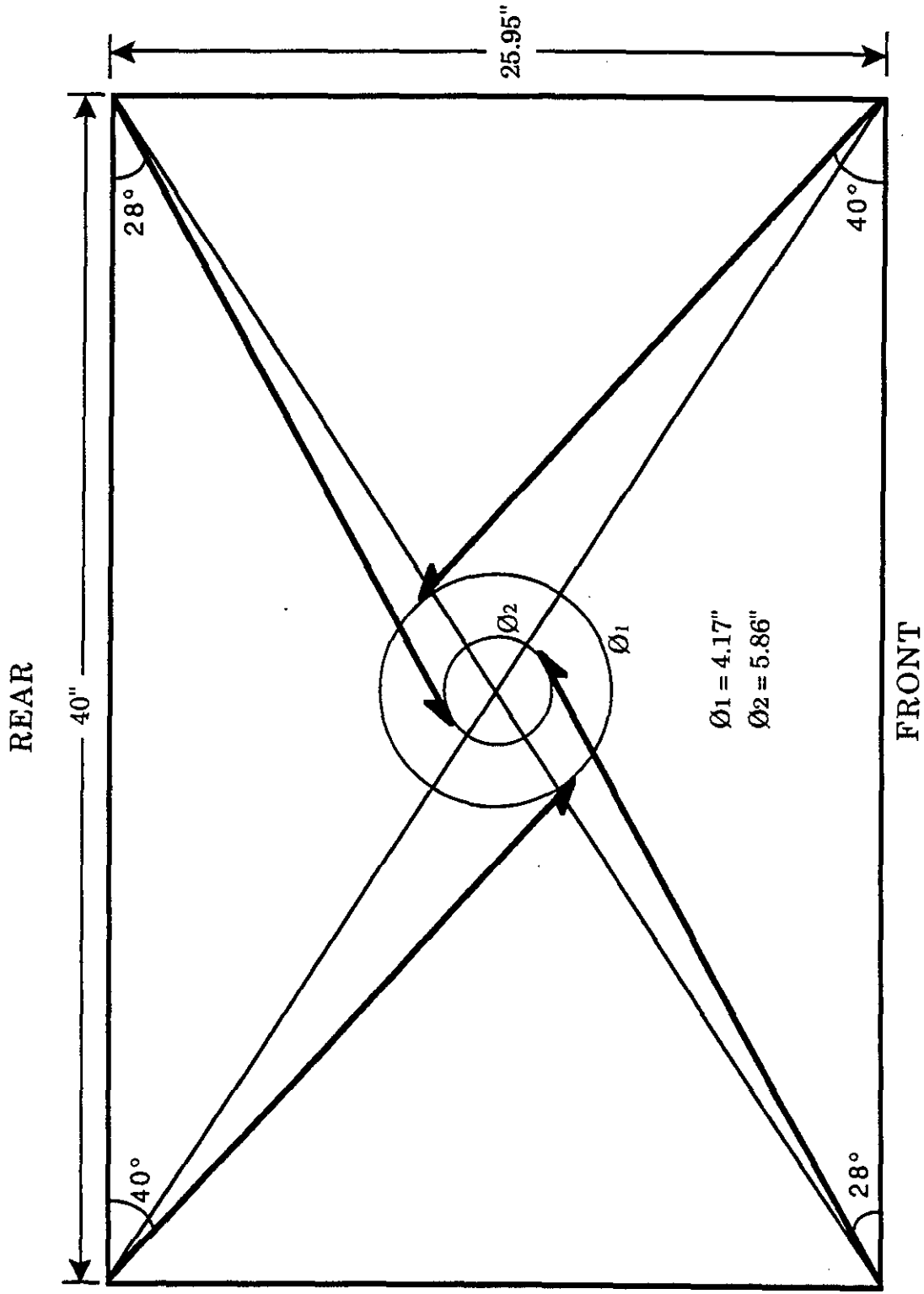


Figure 3 - Firing Circle and Windbox Settings for
Lansing Smith No. 2 Flow Model

probe are then recorded along with probe position, angle, test number, test plane, etc. by the central data acquisition computer.

2.3 Three Dimensional Pitot Tube Probe

A commercially available five-hole, directional sensing, pitot tube, shown in Figure 5, was used. The probe has five pressure sensing holes located at its tip. The centrally located pressure hole, P1, measures the total or impact pressure of the fluid, while two lateral holes, P2 and P3, measure the static pressure. If the probe is rotated around its long axis until P2=P3, the plane of flow can be identified and measured. However, since the condition P2=P3 can be given at two locations 180° apart, the correct vector plane is identified when P2=P3 and P1 has its highest positive value with respect to P2 and P3. An angular encoder is attached to the probe at its base so that the angle of this vector plane, commonly called the yaw angle, can be measured. The yaw angle indicates the plane of flow but does not give the flow angle within this plane. This flow angle, known as the pitch angle, is determined by the differential pressure P4-P5.

In actual practice, four (4) differential pressure readings are required to fully define the flow at a particular point in the flow field of interest. These pressure differentials are:

P1-Patm	= Indicated total pressure with respect to atmosphere
P1-P2	= Indicated velocity pressure
P2-P3	= Yaw angle pressure
P4-P5	= Pitch angle pressure

Calibration curves are used to relate these pressure differentials to the actual pressures and pitch angles. These curves are generated through detailed probe calibrations at the beginning and end of each test series. These curves enable the determination of the actual velocity head and pitch angle at each measuring point. Knowing this data and the yaw angle, the x, y, z, or the normal, radial, and tangential velocity vectors are determined using simple geometric relationships.

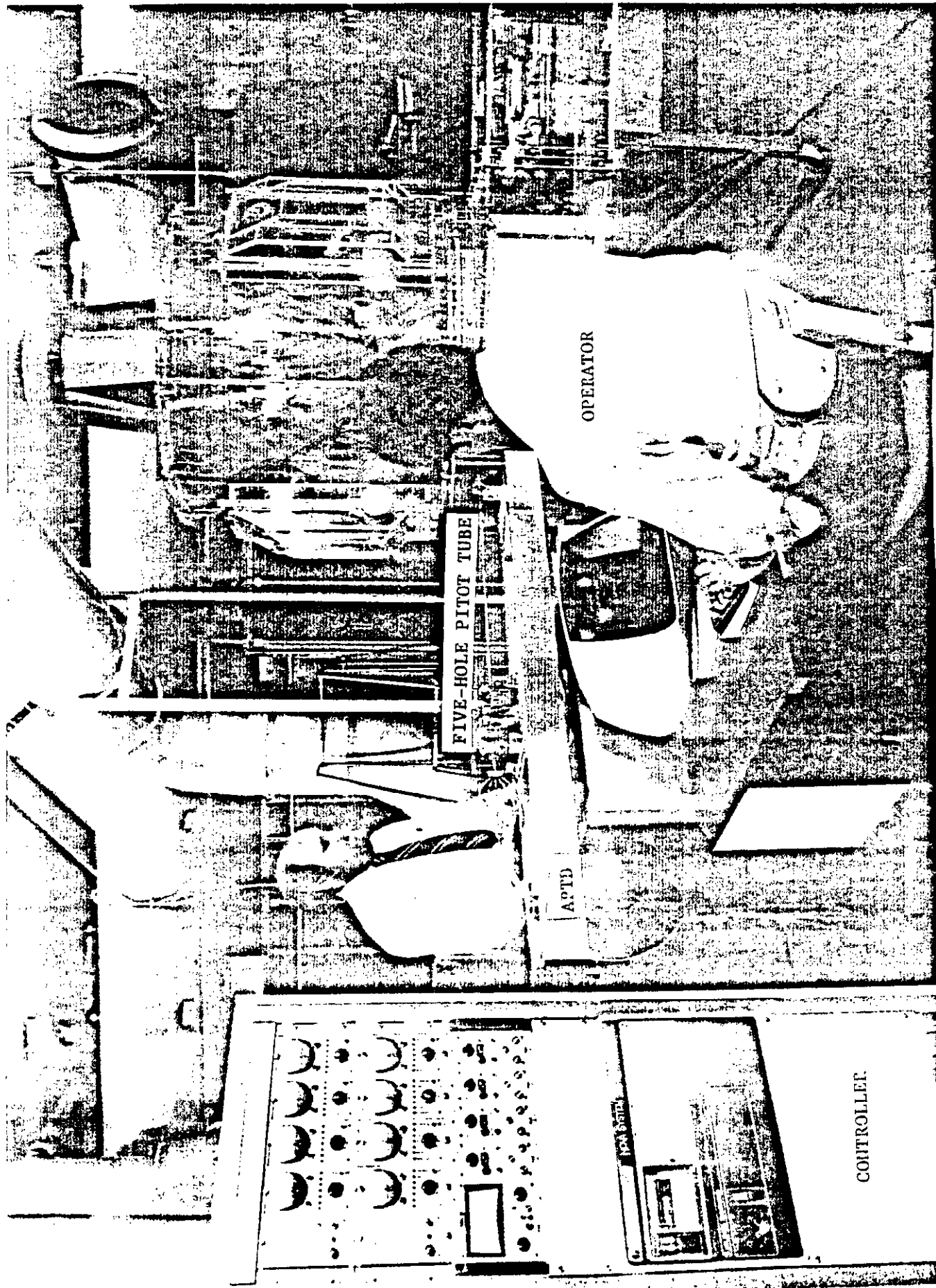


Figure 4 - Automatic Probe Traversing Device

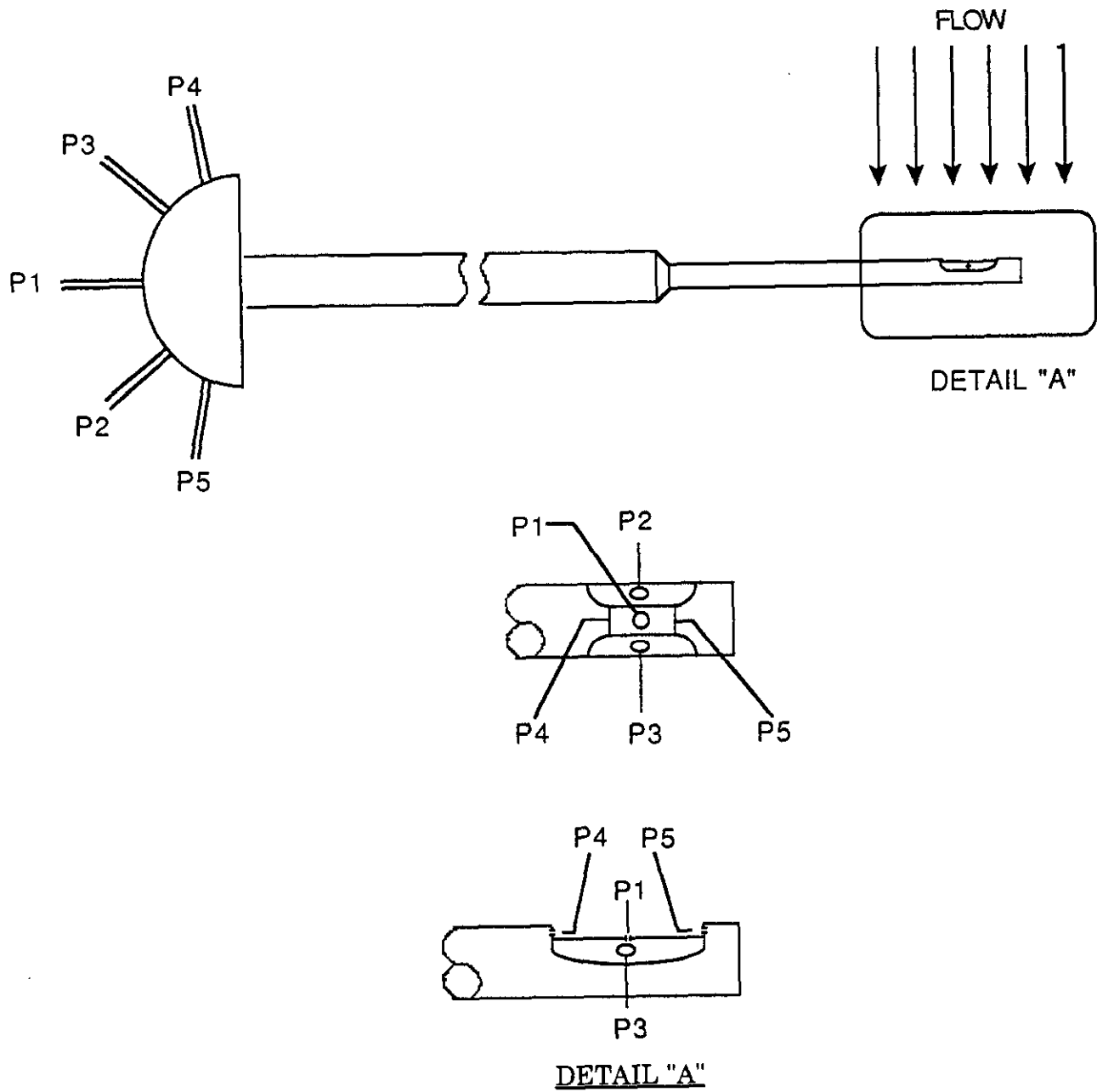


Figure 5 - Five Hole Pitot Tube

2.4 Smoke Generator

A commercially available smoke generator was utilized during the flow visualization tests. The smoke generation system consisted of a gas heater, a light oil smoke fluid reservoir, and tube coil. The fluid was pumped through the tube coil, which was heated, causing it to flash into a dense white stream of smoke. This stream was then injected into the various ports of interest within the model.

3.0 Results

3.1 Flow Visualization

Flow visualization tests were performed on the baseline configuration as a qualitative method of evaluating the flow fields, such as the flow swirl and mixing characteristics. The smoke was injected into the windboxes to qualitatively evaluate the flow swirl and gas mixing characteristics. Testing was performed at reduced model flow rates, while maintaining proper scaling parameters and flow splits. These reduced flow rates improved the visibility of the smoke tracer within the model. A video camera was used to record the flow patterns and a copy of this tape is included as an Appendix. Sketches are included in this report as a visual aid.

Smoke was introduced through each of the four (4) windboxes for this configuration. The furnace swirl was viewed through each windbox, showing the fireball characteristics. The patterns of the smoke as it entered the furnace through different windbox elevations was also observed. The flow entering through the lower part of the windbox experienced recirculation into the hopper, as shown in Figure 6. As the elevation in the windbox increased, the flow was more likely to become entrained in the firing zone, Figure 7. Furthermore, it could be seen that the flow entering the furnace was redirected along all four walls, instead of penetrating towards the furnace center.

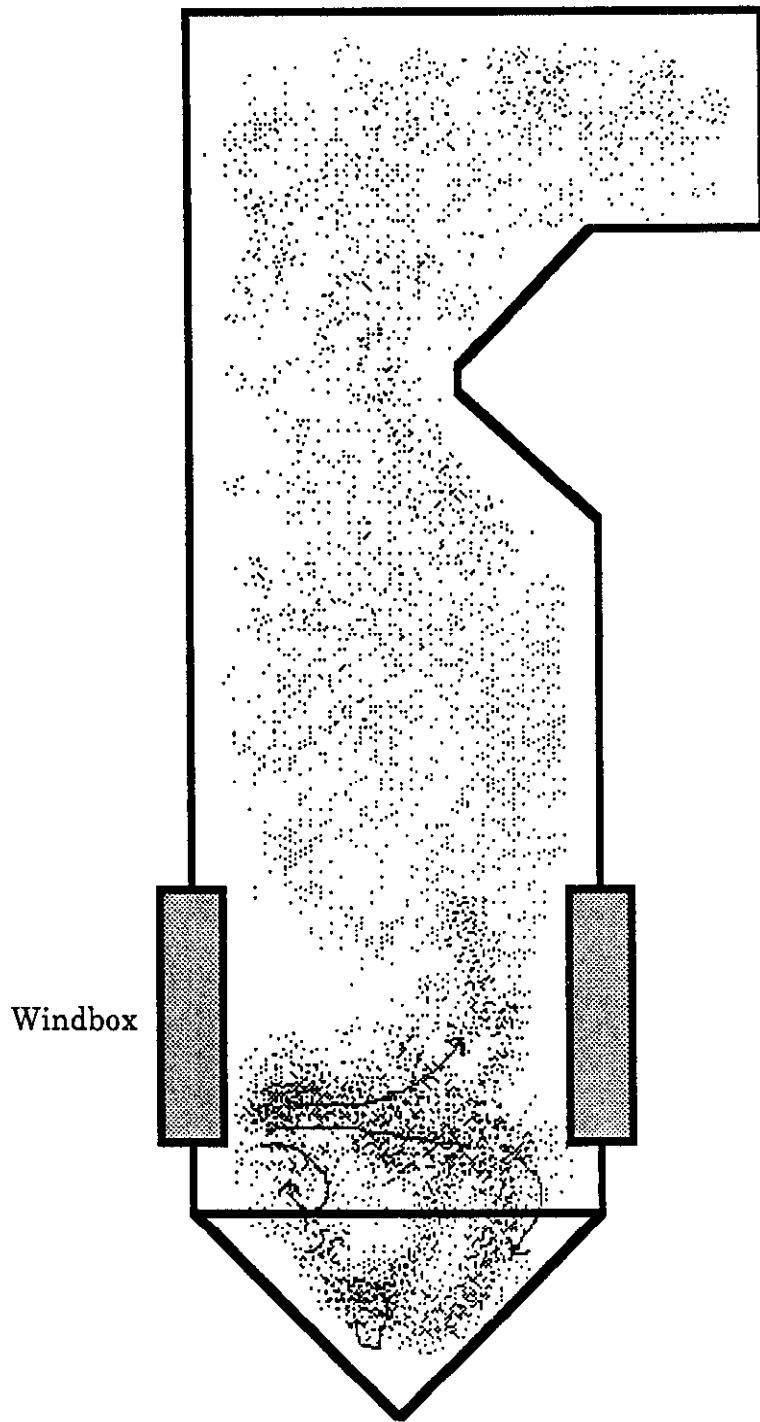


Figure 6 - Smoke Injection Through the Lower Windbox

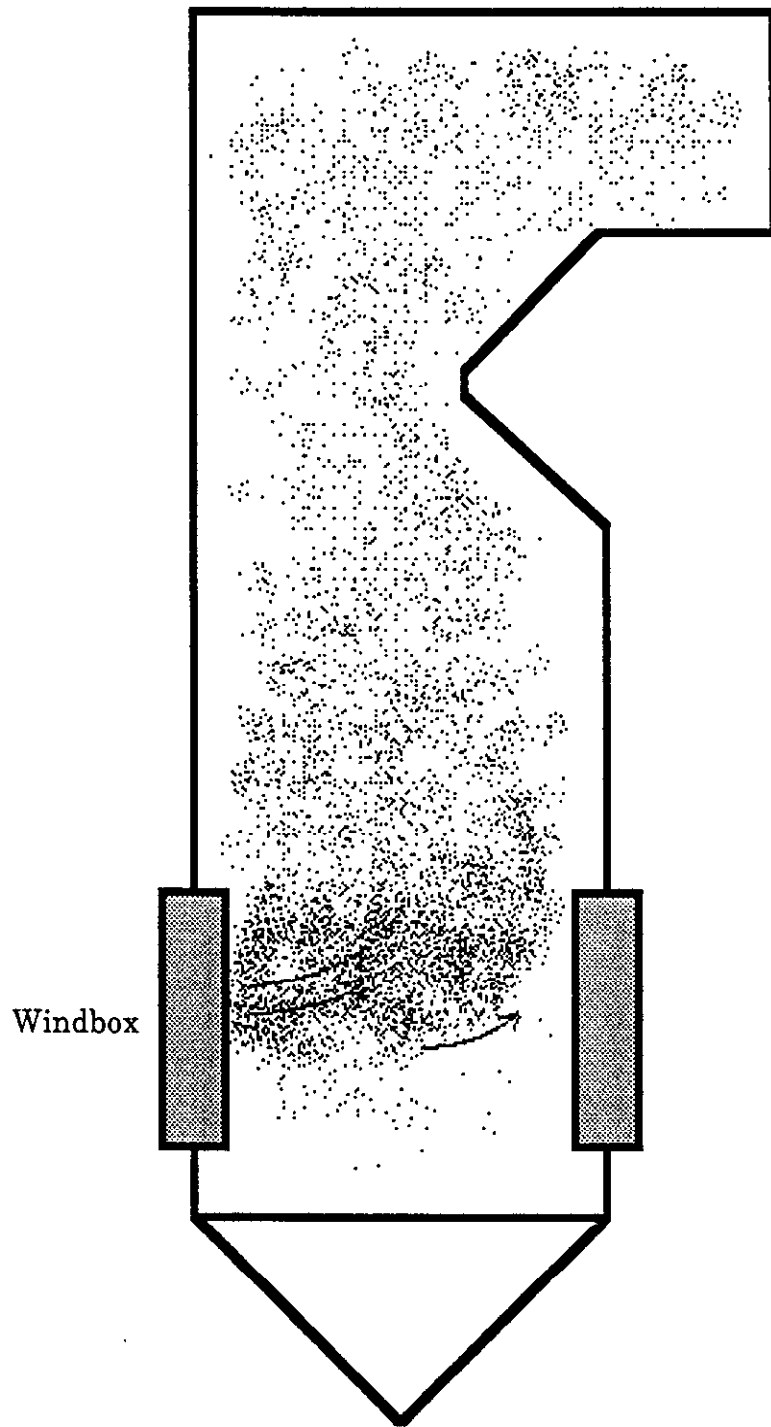


Figure 7 - Smoke Injection Through the Upper Windbox

3.2 Velocity Testing

Three dimensional velocity test data was obtained at the furnace outlet plane to characterize the gas flow distribution leaving the furnace. Velocity data was taken using a five hole pitot probe and the APTD at the furnace outlet plane, shown in Figure 8.

Pressure measurements were collected and stored in the data acquisition system and central computer, coupled to the APTD. This data was reduced to engineering units and is presented in Table 1. The computer calculates the x, y, and z components of the flow, where the x direction is positive as the flow moves along the rear to the front of the furnace, the y direction is positive as the flow moves from left to right in the furnace, and the z direction is positive when the flow is upward in the furnace. From the three dimensional velocity data, the normalized upward velocity data was plotted as surface and contour plots, and is shown in Figure 9. Results show that the upward flow leaving the furnace is concentrated along the left rear corner, typical of tangentially fired units. Furthermore, the higher flows occur along the walls of the model with reduced upward flow through the center.

Additionally, the tangential velocities are presented in the form of a vector plot. This plot, along with the actual normalized normal velocities are presented in Figure 10. The vector plot demonstrates a counter clockwise swirl, illustrated by the flow visualization, which was imposed by the tangential firing system. The center of this swirl is located in the center of the plane, with higher tangential velocities at the rear, left corner.

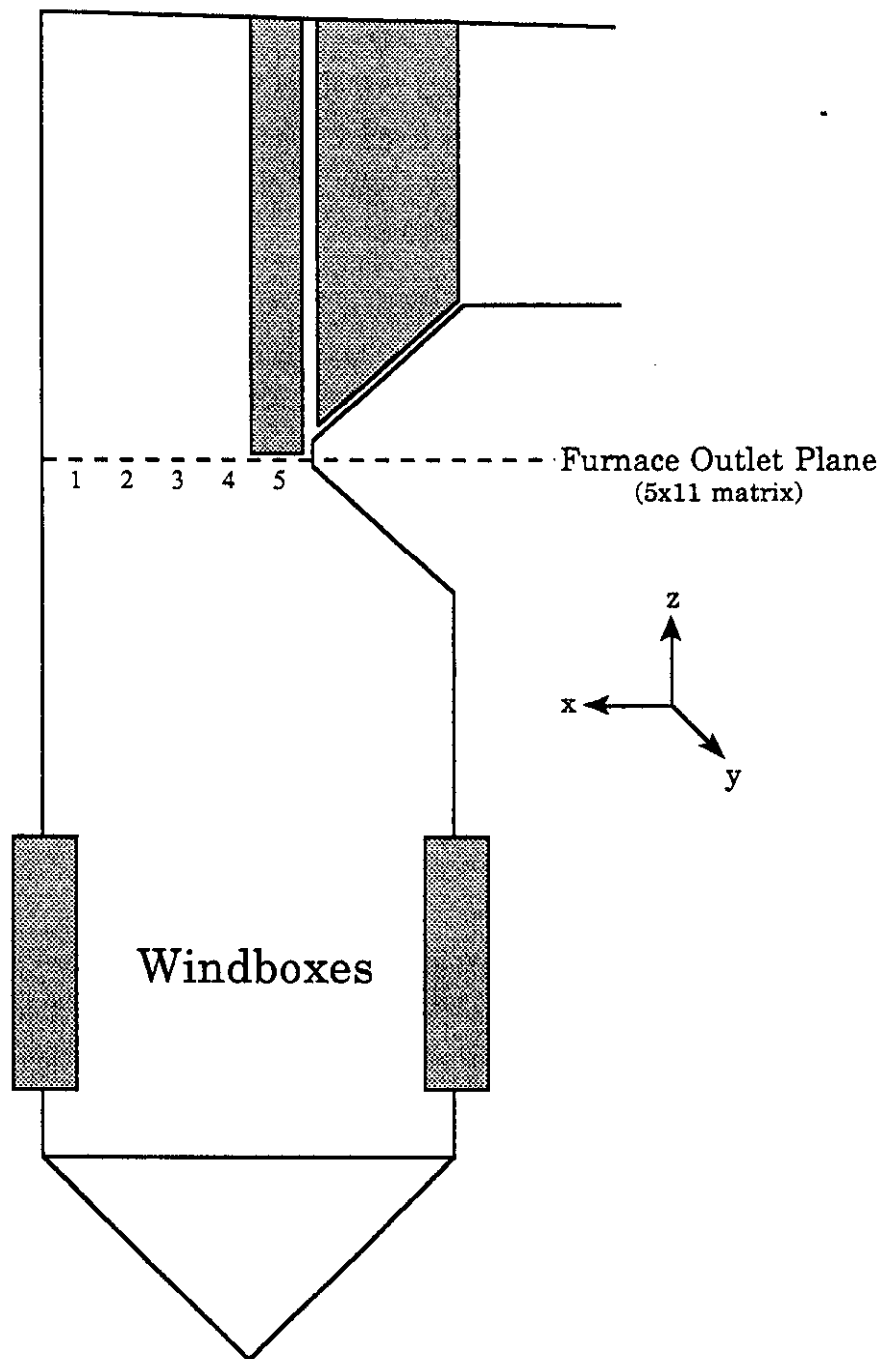


Figure 8 - Test Plane Location

AUTOMATIC PROBE TRAVERSING DEVICE

PROBE NUMBER : B1884-2
 PROBE CAL DATE : 10/23/90

TEST ID : BASE PL4 VEL
 TEST NUMBER : 1004
 TEST DATE : 10/30/90

PLANE NUMBER : 4
 NUMBER OF ROWS : 5
 NUMBER OF COLUMNS : 11

AVERAGE NORMAL VELOCITY = 25.48 FT/SEC

* X-VELOCITY (FT/SEC) *

	1	2	3	4	5	6	7	8	9	10	11
1	-1.40	-6.72	-9.87	-5.69	-3.47	-1.02	2.28	4.02	4.79	8.52	9.57
2	-13.78	-15.34	-12.21	-8.81	-4.92	2.31	11.20	11.38	15.37	19.59	22.87
3	-18.61	-19.39	-13.69	-9.40	-4.44	-0.53	13.72	13.31	18.09	22.21	24.55
4	-12.32	-9.23	-5.47	-5.89	-4.52	1.72	16.71	18.07	17.14	16.26	19.54
5	-14.63	-7.62	-6.10	2.66	-1.44	9.20	13.94	14.71	18.31	18.82	12.54

* Y-VELOCITY (FT/SEC) *

	1	2	3	4	5	6	7	8	9	10	11
1	-0.90	8.92	22.02	28.75	30.25	23.94	20.68	24.12	25.98	12.91	3.93
2	1.89	5.20	4.93	3.80	17.93	12.35	-4.62	8.85	2.63	-0.06	2.73
3	-2.09	3.52	9.85	-10.46	-16.60	1.47	-15.96	-17.10	-12.14	-10.74	-3.60
4	-10.56	-10.18	-20.52	-18.93	-21.13	-17.48	-21.39	-26.58	-22.35	-10.74	-8.64
5	-10.98	-15.87	-18.51	-28.20	-10.06	-39.97	-34.59	-22.42	-28.29	-20.14	-8.01

* NORMAL VELOCITY (FT/SEC) *

	1	2	3	4	5	6	7	8	9	10	11
1	33.35	28.44	23.37	32.57	32.47	24.28	25.04	24.26	25.61	34.16	28.10
2	29.14	25.84	25.36	22.84	19.72	21.65	21.41	20.20	21.79	26.86	32.07
3	28.55	22.70	20.22	24.88	18.63	25.11	19.96	19.44	22.66	23.48	31.77
4	28.21	28.58	25.72	20.54	22.02	20.96	19.23	22.48	20.87	26.44	32.65
5	26.07	24.91	18.67	26.48	20.66	30.34	27.71	22.92	27.15	31.95	40.77

* TOTAL PRESSURE (IN-H2O) *

	1	2	3	4	5	6	7	8	9	10	11
1	-0.91	-1.00	-0.97	-0.91	-0.91	-1.05	-1.09	-1.03	-1.01	-0.93	-0.94
2	-0.95	-0.97	-1.04	-1.13	-1.25	-1.20	-1.11	-1.17	-1.08	-1.05	-0.91
3	-0.93	-1.04	-1.16	-1.05	-1.15	-1.23	-1.13	-1.06	-1.04	-1.01	-0.88
4	-0.88	-0.93	-0.98	-1.02	-1.07	-1.12	-1.08	-1.04	-1.03	-1.01	-0.91
5	-0.90	-0.97	-1.08	-0.95	-1.14	-0.88	-0.95	-1.03	-0.99	-0.96	-0.91

Table 1 - Three Dimensional Velocity Results

AUTOMATIC PROBE TRAVERSING DEVICE

PROBE NUMBER : B1884-2
 PROBE CAL DATE : 10/23/90

TEST ID : BASE PL4 VEL
 TEST NUMBER : 1004
 TEST DATE : 10/30/90

PLANE NUMBER : 4
 NUMBER OF ROWS : 5
 NUMBER OF COLUMNS : 11

AVERAGE NORMAL VELOCITY = 25.48 FT/SEC
 NORMAL VELOCITY RMS = 18.50 %

* NORMALIZED *

* X-VELOCITY *

	1	2	3	4	5	6	7	8	9	10	11
1	-0.05	-0.26	-0.39	-0.22	-0.14	-0.04	0.09	0.16	0.19	0.33	0.38
2	-0.54	-0.60	-0.48	-0.35	-0.19	0.09	0.44	0.45	0.60	0.77	0.90
3	-0.73	-0.76	-0.54	-0.37	-0.17	-0.02	0.54	0.52	0.71	0.87	0.96
4	-0.48	-0.36	-0.21	-0.23	-0.18	0.07	0.66	0.71	0.67	0.64	0.77
5	-0.57	-0.30	-0.24	0.10	-0.06	0.36	0.55	0.58	0.72	0.74	0.49

* NORMALIZED *

* Y-VELOCITY *

	1	2	3	4	5	6	7	8	9	10	11
1	-0.04	0.35	0.86	1.13	1.19	0.94	0.81	0.95	1.02	0.51	0.15
2	0.07	0.20	0.19	0.15	0.70	0.48	-0.18	0.35	0.10	-0.00	0.11
3	-0.08	0.14	0.39	-0.41	-0.65	0.06	-0.63	-0.67	-0.48	-0.42	-0.14
4	-0.41	-0.40	-0.81	-0.74	-0.83	-0.69	-0.84	-1.04	-0.88	-0.42	-0.34
5	-0.43	-0.62	-0.73	-1.11	-0.39	-1.57	-1.36	-0.88	-1.11	-0.79	-0.31

* NORMALIZED *

* NORMAL VELOCITY *

	1	2	3	4	5	6	7	8	9	10	11
1	1.31	1.12	0.92	1.28	1.27	0.95	0.98	0.95	1.01	1.34	1.10
2	1.14	1.01	1.00	0.90	0.77	0.85	0.84	0.79	0.86	1.05	1.26
3	1.12	0.89	0.79	0.98	0.73	0.99	0.78	0.76	0.89	0.92	1.25
4	1.11	1.12	1.01	0.81	0.86	0.82	0.75	0.88	0.82	1.04	1.28
5	1.02	0.98	0.73	1.04	0.81	1.19	1.09	0.90	1.07	1.25	1.60

Table 1 - Three Dimensional Velocity Results (con't)

AUTOMATIC PROBE TRAVERSING DEVICE

PROBE NUMBER : B1884-2
 PROBE CAL DATE : 10/23/90

TEST ID : BASE PL4 VEL
 TEST NUMBER : 1004
 TEST DATE : 10/30/90

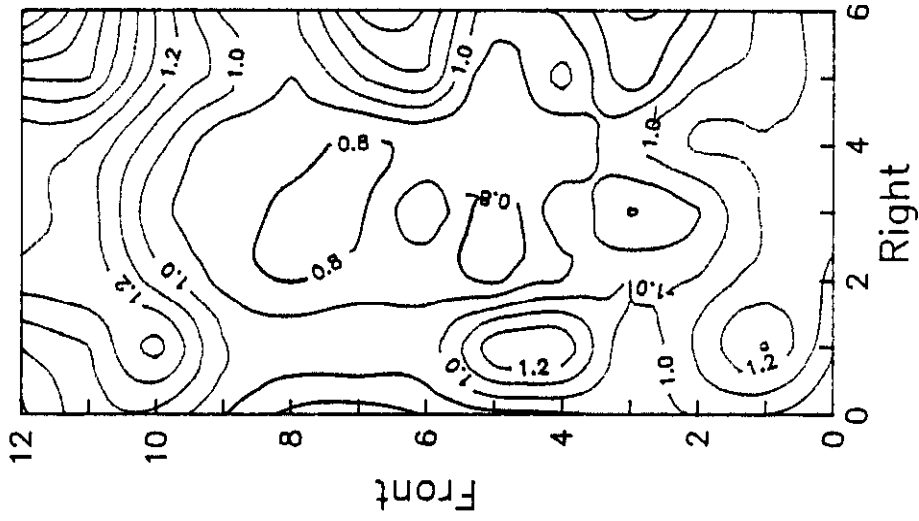
PLANE NUMBER : 4
 NUMBER OF ROWS : 5
 NUMBER OF COLUMNS : 11

AVERAGE NORMAL VELOCITY = 25.48 FT/SEC

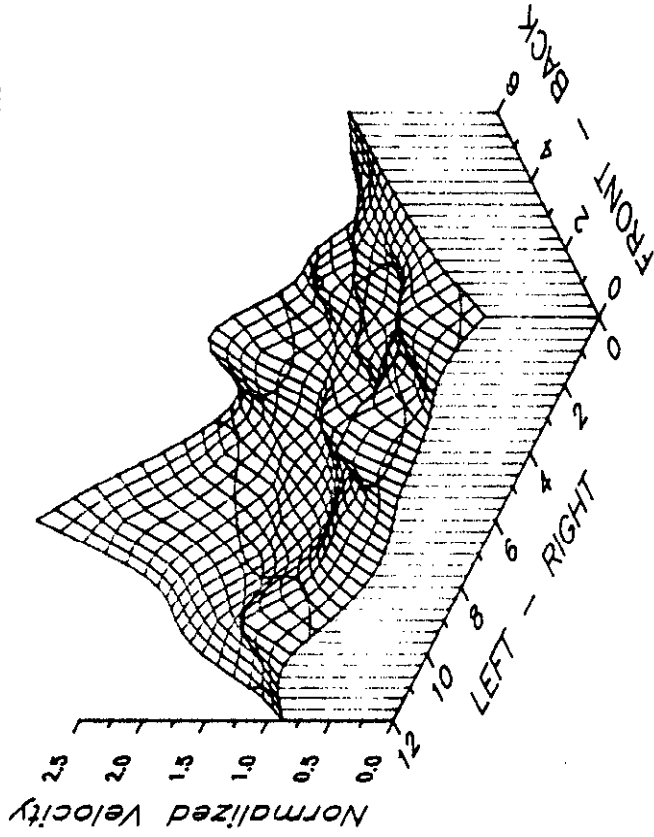
* RESULTANT VELOCITY VECTOR/ANGLE IN THE X-Y PLANE *

	1	2	3	4	5	6	7
1	1.66/237.	11.17/323.	24.14/336.	29.31/349.	30.45/353.	23.96/358.	20.80/ 6.
2	13.90/278.	16.20/289.	13.17/292.	9.60/294.	18.59/345.	12.56/ 11.	12.11/113.
3	18.73/263.	19.70/280.	16.86/306.	14.07/222.	17.18/195.	1.56/340.	21.04/139.
4	16.23/229.	13.75/222.	21.24/195.	19.83/197.	21.61/192.	17.57/174.	27.14/142.
5	18.29/233.	17.60/206.	19.49/198.	28.32/175.	10.17/188.	41.01/167.	37.29/158.
	8	9	10	11			
1	24.46/ 9.	26.41/ 10.	15.47/ 33.	10.34/ 68.			
2	14.42/ 52.	15.59/ 80.	19.59/ 90.	23.04/ 83.			
3	21.67/142.	21.79/124.	24.66/116.	24.82/ 99.			
4	32.14/146.	28.16/143.	19.49/124.	21.37/114.			
5	26.82/147.	33.70/147.	27.57/137.	14.88/123.			

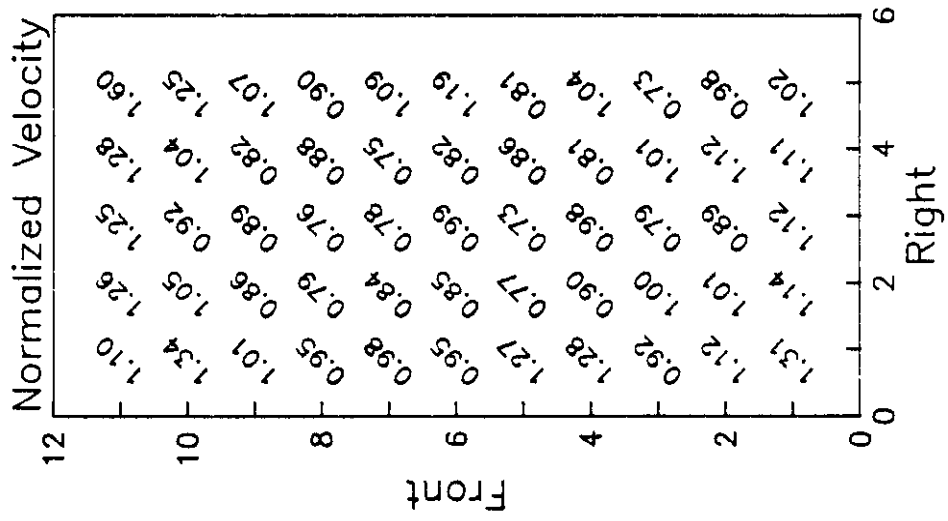
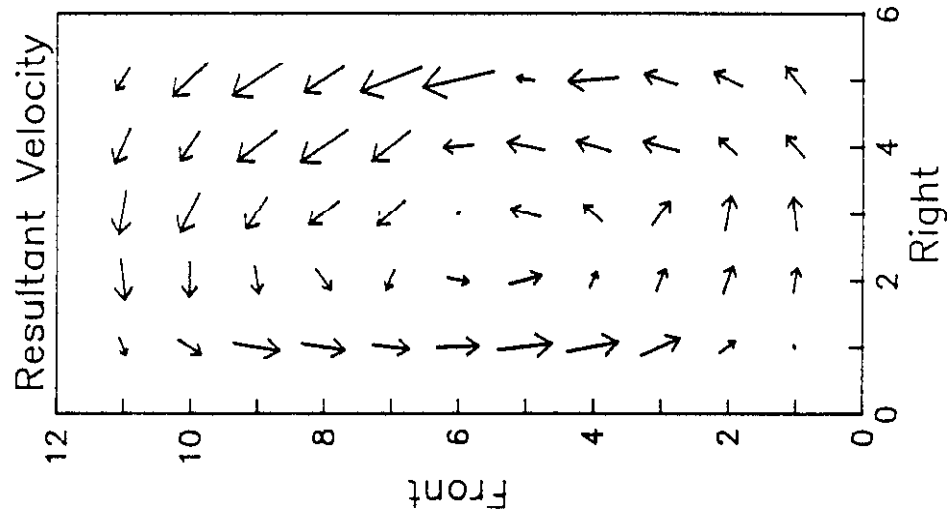
Table 1 - Three Dimensional Velocity Results (con't)



Vel. > 1.0
 Vel. < 1.0



SOUTHERN COMPANY SERVICES
 Baseline Normalized Velocity at Plane 4



SOUTHERN COMPANY SERVICES
Baseline Velocity at Plane 4

Figure 10

4.0 Future Test Plans

The next phase of work for the flow model program will be LNCFS-II testing. Changes to the physical flow model for this configuration include modifications to the windboxes and the addition of low set Over Fire Air (OFA.) These will simulate modifications to be made at the Lansing Smith No. 2 Unit.

Evaluation of this configuration will be performed through the use of flow visualization, gas mixing, and three dimensional velocity mapping. The flow visualization tests will be performed in order to screen twenty (20) potential field operating conditions. These conditions will evaluate a combination of furnace load, OFA velocities, and OFA horizontal firing angles. As each of these conditions is run, the effect of OFA tilt will also be evaluated. At the conclusions of these tests, the five (5) "best" configurations will be qualitatively tested via gas mixing and velocity profile tests. The gas mixing tests will be performed by injecting a tracer gas (methane) into the OFA flow. Samples of gas will then be extracted from the furnace model at four (4) elevations above the injection point and a level of mixing at these planes determined. Additionally, velocity data will be taken at the furnace outlet plane so that an exit velocity profile may be determined.

In addition to this, a one sixth (1/6) scale flow model of the OFA ductwork is being fabricated. Once the ductwork is complete, velocity and pressure measurement tests will be performed. Results from these tests will be incorporated in the design of flow control devices, which will be evaluated in future tests.

5.0 References

1. Anderson, D.K., Bianca, J.D., and McGowan, J.G., "Recent Developments in Physical Flow Modeling of Utility Scale Furnaces," Proc. 1986 Symposium on Industrial Combustion Technologies, Chicago, Illinois, 1986
2. Beer, J.M., "Significance of Modeling," J. Inst. Fuel, November, 1966
3. Beer, J.M., "Recent Advances in the Technology of Furnace Flames," J. Inst. Fuel, July 1972
4. Beer, J.M. and Chigier, N.A., Combustion Aerodynamics, Wiley, New York, 1972
5. Bianca, J.D., Bauver, W.P., and McGowan, J.G., "An Aerodynamic Study of an Operating Tangentially Fired Furnace," Fluid Mechanics of Combustion Systems, ASME, 1981
6. Chigier, N.A., "Application of Model Results to Design Industrial Flames", J. Inst. Fuel, September 1973
7. Johnstone, R.E., and Thiring, M.B., Pilot Plants, Models and Scale up Factors in Chemical Engineering, McGraw Hill, New York, 1947
8. Spaulding, D.B., "The Art of Partial Modeling," 9th International Symp. on Combustion, September, 1973
9. Thiring, M.B., and Newby, M.P., "Combustion Length of Enclosed Turbulent Jet Flames," 9th Symp. on Combustion, September 1953

SOUTHERN COMPANY SERVICES
LOW NO_x TANGENTIAL FIRING SYSTEM DEVELOPMENT

C-E CONTRACT #14664

TEST REPORT
PHYSICAL FLOW MODELING - TASK IV
LNCFS-II OPERATING CONDITIONS

Project 901237

Mechanical Systems Engineering
Kreisinger Development Laboratory
KDL-91-10

Robert J. von Hein

April, 1991

DISCLAIMER

This report was prepared as an account of work sponsored by Southern Company Services. Neither Southern Company Services, ABB Combustion Engineering, nor any person acting on behalf of them:

- A. Makes any warranty, expressed or implied, with respect to the use of any information, apparatus, method, or process disclosed in this report or that such use may not infringe privately owned rights: or
- B. Assumes any liability with respect to the use of, or damages resulting from the use of any apparatus, method, or process disclosed in this report.

Table of Contents

<u>Section</u>	<u>Title</u>	<u>Page No.</u>
<i>i</i>	List of Figures	<i>i</i>
<i>ii</i>	List of Tables	<i>iv</i>
1.0	Introduction	1
2.0	Conclusions	3
3.0	Modeling Theory	4
4.0	Facility Description	8
4.1	Lansing Smith Flow Model	8
4.2	Automatic Probe traversing Device	12
4.3	Three Dimensional Pitot Tube Probe	15
4.4	Laser Absorption Spectrophotometer	18
4.5	Smoke Generator	20
5.0	Modeling and Testing Techniques	21
5.1	Modeling Theory	21
5.2	Testing Procedures	23
6.0	Results	26
6.1	Flow Visualization	26
6.2	Gas Mixing	35
6.3	Velocity	104
7.0	References	135
Appendix A Five Hole Pitot Probe Calibration Curves		
Appendix B Laser Methane Calibration Curves		

List of Figures

<u>Figure No.</u>	<u>Description</u>
3-1	Single Jet in a Crossflow
4-1	Lansing Smith #2 Flow Model
4-2	Side Elevation of Flow Model
4-3	KDL Model Test Facility
4-4	Flow Model Firing Circle
4-5	OFA Nozzles
4-6	Automatic Probe Traversing Device
4-7	5-Hole Pitot Tube
4-8	Laser Absorption Spectrophotometer
5-1	Flow Model Test Matrix
5-2	Model Test Plane Locations
6-1	Typical Flow Visualization Results
6-2	Typical Flow Visualization Results
6-3	Flow Visualization - Close Up of OFA Nozzle
6-4	OFA Firing Circle
6-5	Schematic of Methane Injection System
6-6	Mixing Isoconcentration Plot - Config. #1, Plane 1
6-7	Mixing Contour Plot - Config. #1, Plane 1
6-8	Mixing Isoconcentration Plot - Config. #2, Plane 1
6-9	Mixing Contour Plot - Config. #2, Plane 1
6-10	Mixing Isoconcentration Plot - Config. #3, Plane 1
6-11	Mixing Contour Plot - Config. #3, Plane 1
6-12	Mixing Isoconcentration Plot - Config. #4, Plane 1
6-13	Mixing Contour Plot - Config. #4, Plane 1
6-14	Mixing Isoconcentration Plot - Config. #5, Plane 1
6-15	Mixing Contour Plot - Config. #5, Plane 1
6-16	Normalized Concentration - Config. #1, Plane 1
6-17	Normalized Concentration - Config. #2, Plane 1
6-18	Normalized Concentration - Config. #3, Plane 1
6-19	Normalized Concentration - Config. #4, Plane 1
6-20	Normalized Concentration - Config. #5, Plane 1
6-21	Mixing Isoconcentration Plot - Config. #1, Plane 2
6-22	Mixing Contour Plot - Config. #1, Plane 2
6-23	Normalized Concentration - Config. #1, Plane 2
6-24	Mixing Isoconcentration Plot - Config. #2, Plane 2
6-25	Mixing Contour Plot - Config. #2, Plane 2

6-26	Normalized Concentration - Config. #2, Plane 2
6-27	Mixing Isoconcentration Plot - Config. #3, Plane 2
6-28	Mixing Contour Plot - Config. #3, Plane 2
6-29	Normalized Concentration - Config. #3, Plane 2
6-30	Mixing Isoconcentration Plot - Config. #4, Plane 2
6-31	Mixing Contour Plot - Config. #4, Plane 2
6-32	Normalized Concentration - Config. #4, Plane 2
6-33	Mixing Isoconcentration Plot - Config. #5, Plane 2
6-34	Mixing Contour Plot - Config. #5, Plane 2
6-35	Normalized Concentration - Config. #5, Plane 2
6-36	Mixing RMS Deviation - Plane 2
6-37	Mixing Isoconcentration Plot - Config. #1, Plane 3
6-38	Mixing Contour Plot - Config. #1, Plane 3
6-39	Normalized Concentration - Config. #1, Plane 3
6-40	Mixing Isoconcentration Plot - Config. #2, Plane 3
6-41	Mixing Contour Plot - Config. #2, Plane 3
6-42	Normalized Concentration - Config. #2, Plane 3
6-43	Mixing Isoconcentration Plot - Config. #3, Plane 3
6-44	Mixing Contour Plot - Config. #3, Plane 3
6-45	Normalized Concentration - Config. #3, Plane 3
6-46	Mixing Isoconcentration Plot - Config. #4, Plane 3
6-47	Mixing Contour Plot - Config. #4, Plane 3
6-48	Normalized Concentration - Config. #4, Plane 3
6-49	Mixing Isoconcentration Plot - Config. #5, Plane 3
6-50	Mixing Contour Plot - Config. #5, Plane 3
6-51	Normalized Concentration - Config. #5, Plane 3
6-52	Mixing RMS Deviation - Plane 3
6-53	Mixing Isoconcentration Plot - Config. #1, Plane 4
6-54	Mixing Contour Plot - Config. #1, Plane 4
6-55	Normalized Concentration - Config. #1, Plane 4
6-56	Mixing Isoconcentration Plot - Config. #2, Plane 4
6-57	Mixing Contour Plot - Config. #2, Plane 4
6-58	Normalized Concentration - Config. #2, Plane 4
6-59	Mixing Isoconcentration Plot - Config. #3, Plane 4
6-60	Mixing Contour Plot - Config. #3, Plane 4
6-61	Normalized Concentration - Config. #3, Plane 4
6-62	Mixing Isoconcentration Plot - Config. #4, Plane 4
6-63	Mixing Contour Plot - Config. #4, Plane 4
6-64	Normalized Concentration - Config. #4, Plane 4
6-65	Mixing Isoconcentration Plot - Config. #5, Plane 4
6-66	Mixing Contour Plot - Config. #5, Plane 4
6-67	Normalized Concentration - Config. #5, Plane 4
6-68	Mixing RMS Deviation - Plane 4
6-69	Overall Mixing RMS
6-70	Velocity Isoconcentration Plot - Baseline, Plane 4
6-71	Velocity Contour Plot - Baseline, Plane 4

6-72	Velocity Isoconcentration Plot - Config. #1, Plane 4
6-73	Velocity Contour Plot - Config. #1, Plane 4
6-74	Velocity Isoconcentration Plot - Config. #2, Plane 4
6-75	Velocity Contour Plot - Config. #2, Plane 4
6-76	Velocity Isoconcentration Plot - Config. #3, Plane 4
6-77	Velocity Contour Plot - Config. #3, Plane 4
6-78	Velocity Isoconcentration Plot - Config. #4, Plane 4
6-79	Velocity Contour Plot - Config. #4, Plane 4
6-80	Velocity Isoconcentration Plot - Config. #5, Plane 4
6-81	Velocity Contour Plot - Config. #5, Plane 4
6-82	Normalized Axial Velocity - Baseline, Plane 4
6-83	Normalized Axial Velocity - Config. #1, Plane 4
6-84	Normalized Axial Velocity - Config. #2, Plane 4
6-85	Normalized Axial Velocity - Config. #3, Plane 4
6-86	Normalized Axial Velocity - Config. #4, Plane 4
6-87	Normalized Axial Velocity - Config. #5, Plane 4
6-88	Axial Velocity RMS Deviation - Plane 4
6-89	Side to Side Velocity Profiles
6-90	Velocity Vectors - Baseline, Plane 4
6-91	Velocity Vectors - Config. #1, Plane 4
6-92	Velocity Vectors - Config. #2, Plane 4
6-93	Velocity Vectors - Config. #3, Plane 4
6-94	Velocity Vectors - Config. #4, Plane 4
6-95	Velocity Vectors - Config. #5, Plane 4

List of Tables

<u>Table No.</u>	<u>Description</u>
6-1	Flow Visualization Test Matrix
6-2	Methane and Velocity Mapping Test Matrix
6-3	Methane Mixing Tests - General Output
6-4	Velocity Mapping Tests - General Output

1.0 Introduction

Southern Company Services (SCS), the Department of Energy (DOE), and ABB Combustion Engineering (CE) are involved in a program to develop advanced tangentially fired combustion modifications for reducing NO_x emissions. The intent of this program is to demonstrate, at "full scale," low NO_x technologies of a commercial prototype design. This demonstration includes the addition of Low NO_x Concentric Firing Systems (LNCFS) to Gulf Power Company's Lansing Smith #2 Unit. To investigate the fluid mechanic performance of the proposed low NO_x configurations, CE is performing a physical isothermal flow model study at its Kreisinger Development Laboratory (KDL) in Windsor, CT.

The objective of the isothermal flow model study is to assure optimum performance of the Low NO_x tangential firing systems. The effort centers on understanding in-furnace flow and mixing phenomena for the various low NO_x firing systems as applied to the demonstration unit. This is being done through an evaluation of each proposed firing system, along with the evaluation of the burner only configuration, in the isothermal flow model. Baseline testing was performed on the burner only configuration which exists in the Lansing Smith #2 Unit. Following this testing, the LNCFS-II and LNCFS-III configurations are to be modeled. Each of these configurations include the addition of Separated Over Fire Air (SOFA) to the furnace model. The LNCFS-III configuration also includes the addition of Close Coupled Over Fire Air (CCOFA.) Each LNCFS configuration will be evaluated from an Over Fire Air penetration, mixing, and dispersion standpoint. The results from the flow modeling will provide specific flow field information to help access the merits of each of these configurations in the Lansing Smith #2 Unit.

This report presents the results of the physical cold flow modeling conducted under Task IV of the SCS Low NO_x Development Program. The purpose of this task was to evaluate the flow fields within the LNCFS-II configuration of the flow model. The furnace model, which was constructed under Task I of this project, is a 1/12 scale model of the Lansing

Smith No. 2 Unit, from the hopper through the furnace backpass. In addition to this, modifications were made to the model in order to evaluate the addition of SOFA. The evaluation of this configuration was divided into two (2) screening levels. In the first, flow visualization was used to evaluate a moderate number of operating conditions. These results were then used to select "the best" configurations for additional quantitative tests, three dimensional velocity mapping and gas mixing. The results from this cold flow model will provide a basis to assess the proposed modifications to this unit.

2.0 Conclusions

An evaluation of the proposed LNCFS-II configuration for the Lansing Smith #2 Unit was performed on a 1/12 scale isothermal flow model of this unit. This was done through the use of flow visualization (screening level one), and methane gas mixing, and three dimensional velocity mapping tests (screening level two.) From these tests, the following conclusions have been made:

1. In general, the overall mixing performance for the OFA was found to be pretty good for each of the configurations tested in the second screening level. That is, the RMS deviation of the mixing It was also determined that the mixing could be improved with the adjustment of the OFA firing angles.
2. The recommended configuration for OFA operation, based on the flow model testing, is Configuration #3 (Table 6-2.) For this configuration, the firing angle for each nozzle was determined to maximize the OFA jet penetration, mixing, and dispersion. In addition to this, no horizontal tilt was necessary.
3. For 20% OFA operation, the jets do not penetrate into the center, but are redirected by the cross flow and dispersed along the outer perimeter of the furnace. The overall penetration is increased at higher OFA operating rates, while it is decreased at the lower operating rates.
4. A downward tilt helps to improve the overall mixing level of the OFA jets. However, this occurs at the expense of the separation between the OFA and windbox firing zones. For the recommended configuration, no tilt in the OFA nozzles was necessary to obtain a good level of mixing.
5. An upward tilt to the OFA nozzles will obviously increase the separation between furnace zones. However, the overall mixing is reduced, mainly due to the decrease in the residence time.

6. For the lower OFA operating rates, a down tilt becomes necessary to provide an adequate level of mixing. This is limited to approximately 15° before this flow becomes entrained in the windbox firing zone. This is limited further, to about 10° , in order to establish a clear separation zone.
7. For the higher OFA operating rates, the OFA jets have greater penetration, due to the higher velocities. Because of this, the effect of the OFA nozzle tilt is greater than 20% operation. The jets penetrate into the lower furnace firing zone when a downtilt of approximately 7° is imparted to the OFA nozzles. On the other hand, when the OFA nozzles have an upward tilt, the OFA jets exit the furnace before full mixing can occur.
8. At lower OFA operating rates, the OFA jet penetration, mixing, and dispersion is reduced. In order to improve the overall mixing, it became necessary to adjust the firing angles of the OFA nozzles and to impose a downtilt of 10° .

3.0 Modeling Theory

Isothermal flow models have long been recognized as a cost effective way of evaluating the fluid mechanics within a furnace. Qualitative and quantitative information gathered from these models are especially useful in understanding and explaining unit performance and/or operation. Qualitative information is usually restricted to visual flow observations, whereas, quantitative information includes, but is not limited to, velocity profiles, pressure distributions, and gas mixing data.

For an accurate simulation of the flow within a furnace, a physical model must duplicate the fundamental controlling fluid mechanic phenomena. These include: mixing of fuel and air streams, mixing of crossflow jets with the main swirling flow, and the interaction of these jets in the combustion zone.

As detailed by Beer and Chigier (1972), it is possible to model combustion systems through the use of geometric, mechanical, and thermal similarities. However, Beer (1966) and Spaulding (1963) indicate that it is not possible to simultaneously reproduce all of the prototype's processes in any one model. It becomes an important engineering consideration, then, to critically select the most important parameters. This technique, known as the "art of partial modeling", is based on modeling only the dominant processes and relating the conditions occurring in the furnace to physical observations in the model.

The "art of partial modeling" has been successfully applied and verified in numerous studies at KDL, the most recent by Anderson and Bianca (1989). Here, the results of flow modeling studies were correlated to field observations and measurements in coal fired furnaces. Based on these results, and on those from the previously discussed references, the following criteria was used as guidelines for the isothermal flow modeling of the Gulf Power Company, Lansing Smith Station for Southern Company Services:

1. Geometric Scaling:

To the extent possible, the isothermal flow model must be constructed geometrically similar to the prototype. Scaling is achieved by applying a scale factor between all the dimensions in the model and prototype. As in any physical model, the linear scale factor, **S**, is defined as;

$$S = \frac{\text{dimension in prototype}}{\text{dimension in model}}$$

For the Southern Company Services Program, the value of **S** was 12. This value represents the scale of the physical model, constructed at KDL, to the Lansing Smith No. 2 Station of Gulf Power Company. Geometric scaling of the inlet air/fuel ports was not applicable, as discussed in section 3 below.

2. Reynolds Number

Based on experience in modeling internal flows, if the Reynolds number exceeds 10,000 (based on overall furnace conditions), the transfer process of mass, momentum and heat transfer are controlled by the turbulent flows in the model. In this case, the molecular transport processes can be neglected. Since the Reynolds number for the Lansing Smith No. 2 flow model is approximately 270,000, it is not necessary to equate the Reynolds number between the furnace and the model.

3. Mass and Momentum

As detailed by Beer, et.al. (1984), it is standard practice to oversize the burners in isothermal furnace models to account for the rapid expansion of gasses exiting the burners due to the combustion of the fuel and air. The Thring-Newby criteria (1953) has been utilized to size such burners at KDL for a number of years. In general, the area of the fuel/air admission assemblies is increased such that the total

burner area is equal to the ratio of the prototype's burner inlet to combustion zone gas densities. For the Southern Company Services Program, the windboxes (simulated fuel/air admission assemblies) were scaled according to this criteria.

4. Jet Penetration

In order to simulate jet penetration/dispersion of a "hot" prototype in an isothermal flow environment, it is necessary to scale the jets in the model based on equivalent mass flow ratios. Simplifying assumptions, based on modeling criteria developed by examining single jet trajectories in a crossflow, have been used in designing the jet components of three-dimensional airflow models. This approach insures the modeled jets behave in a similar fashion to furnace jets in the case of a hot uniform flow field. The cold flow model jet velocity and size are optimized to provide a conservative approximation of the jet penetration to the furnace centerline. Figure 3-1 describes the position of the jet centerline in a uniform crossflow. Jet penetration characteristics, as described by Patrick (1965) and Beer and Chigier (1972), have been studied in KDL to determine the appropriate criteria which will provide the desired model to prototype jet similitude.

In general, the mass flow rate ratio of the model is equivalent to the mass flow rate ratio of the prototype, where the mass flow rate ratio is expressed as the ratio of the mass flow rate of the jets to the mass flow rate of the crossflow. For the Southern Company Services flow model, the nozzle sizes were increased to compensate for the gas density differences between the hot furnace gasses and the much cooler over fire air.

Jet Parameters for Replicating Jet in Ideal Uniform Crossflow:

$$\text{Mass: } \frac{\rho_j A_j V_j}{\rho_{cf} A_{cf} V_{cf}}$$

$$\text{Momentum: } \frac{\rho_j A_j V_j^2}{\rho_{cf} A_{cf} V_{cf}^2}$$

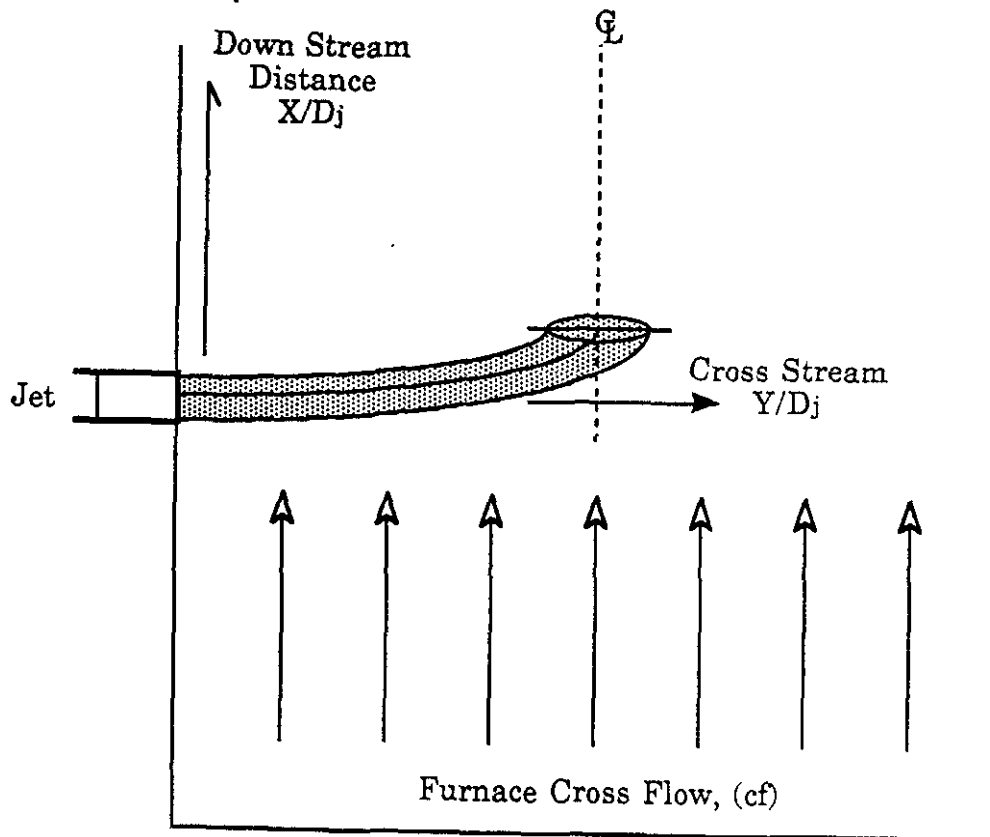


Figure 3-1 Single Jet in a Crossflow

4.0 Facility Descriptions

This section of the report describes the flow model, test facilities, and instrumentation systems used to perform the LNCFS-II evaluations.

4.1 Lansing Smith No. 2 Flow Model Description

Flow modeling was done on a 1/12 scale, geometrically similar model of the Lansing Smith No. 2 Unit, shown in Figure 4-1. The flow model encompasses the entire furnace from the hopper through the economizer outlet. Included in the flow model were the fuel admission assemblies, all radiant and convective heat transfer surfaces within the first sections of the upper furnace, along with the addition of the separated OFA nozzles. Figure 4-2 is a side elevation of the model, showing the nominal model dimensions and the test plane locations.

The furnace model was built primarily of 1/2" acrylic glass, permitting the recording of the flow visualization tests. All dimensions were maintained to a tolerance of $\pm 1/16$ ", which corresponds to $\pm 3/4$ " full scale. The flow model was erected in the KDL Flow Model Test Facility, Figure 4-3. This facility consists of a high volume fan and duct system capable of testing both suction and pressurized models at flow rates up to 20,000 SCFM. Where additional air sources are needed, (i.e. the OFA) supplemental air is supplied via a Lamson high pressure blower (4,000 SCFM @ 4.0 psi) or through the labs compressed air system (1,200 SCFM @ a header pressure of 90 psi.)

The flow model was operated under suction (induced draft) using ambient air as the working fluid. Bell mouths, added to the inlets of the windboxes, reduce the entrance losses and provide uniform velocity profiles at the inlet to the furnace model. Over fire air was supplied via a header which was attached to the high pressure Lamson blower. Each of these flows was independently controlled and monitored, so that the proper air flow splits could be obtained.

The heat transfer surfaces were constructed of perforated metal plate and

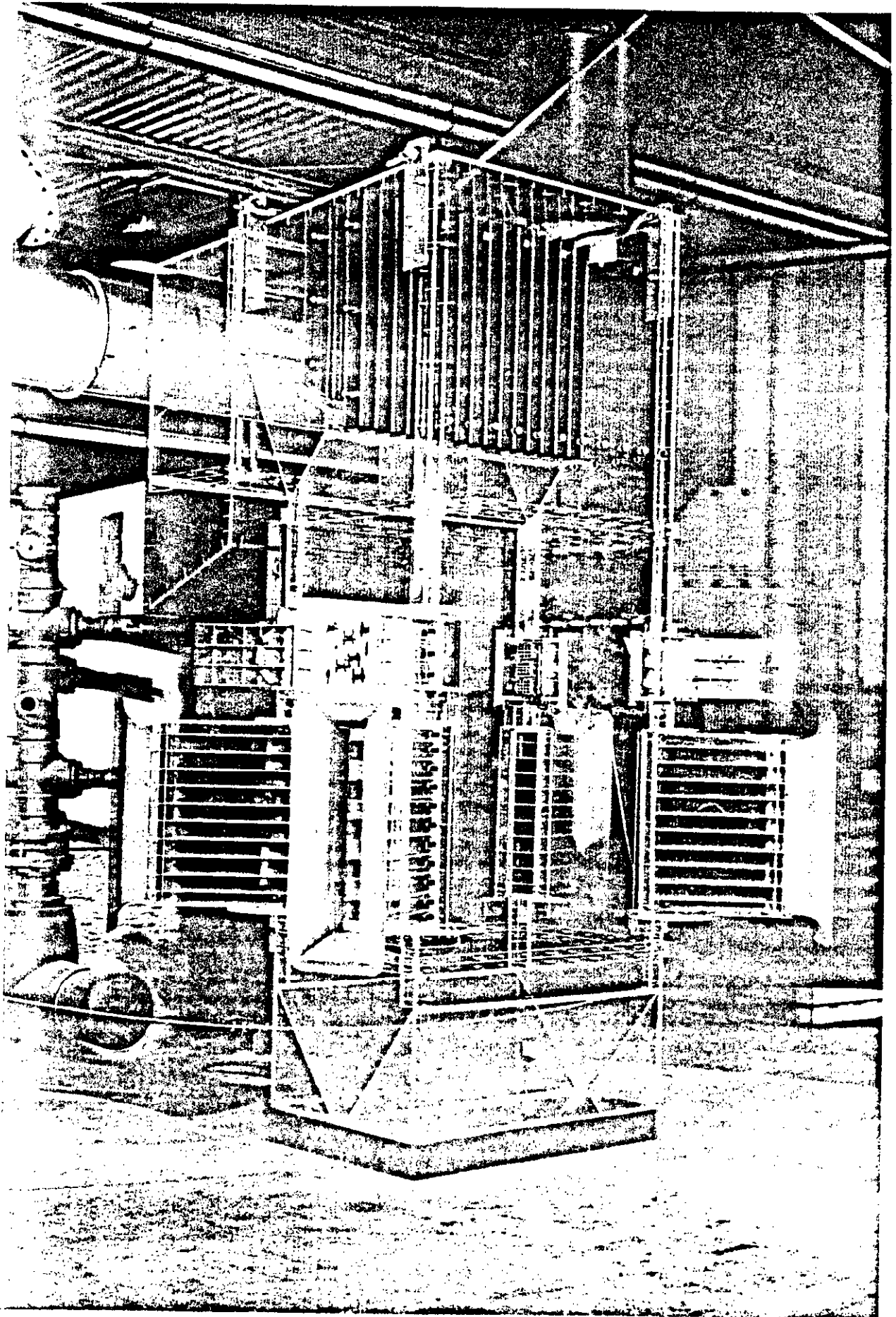


Figure 4-1 Lansing Smith #2 Flow Model (LNCFS-II Configuration)

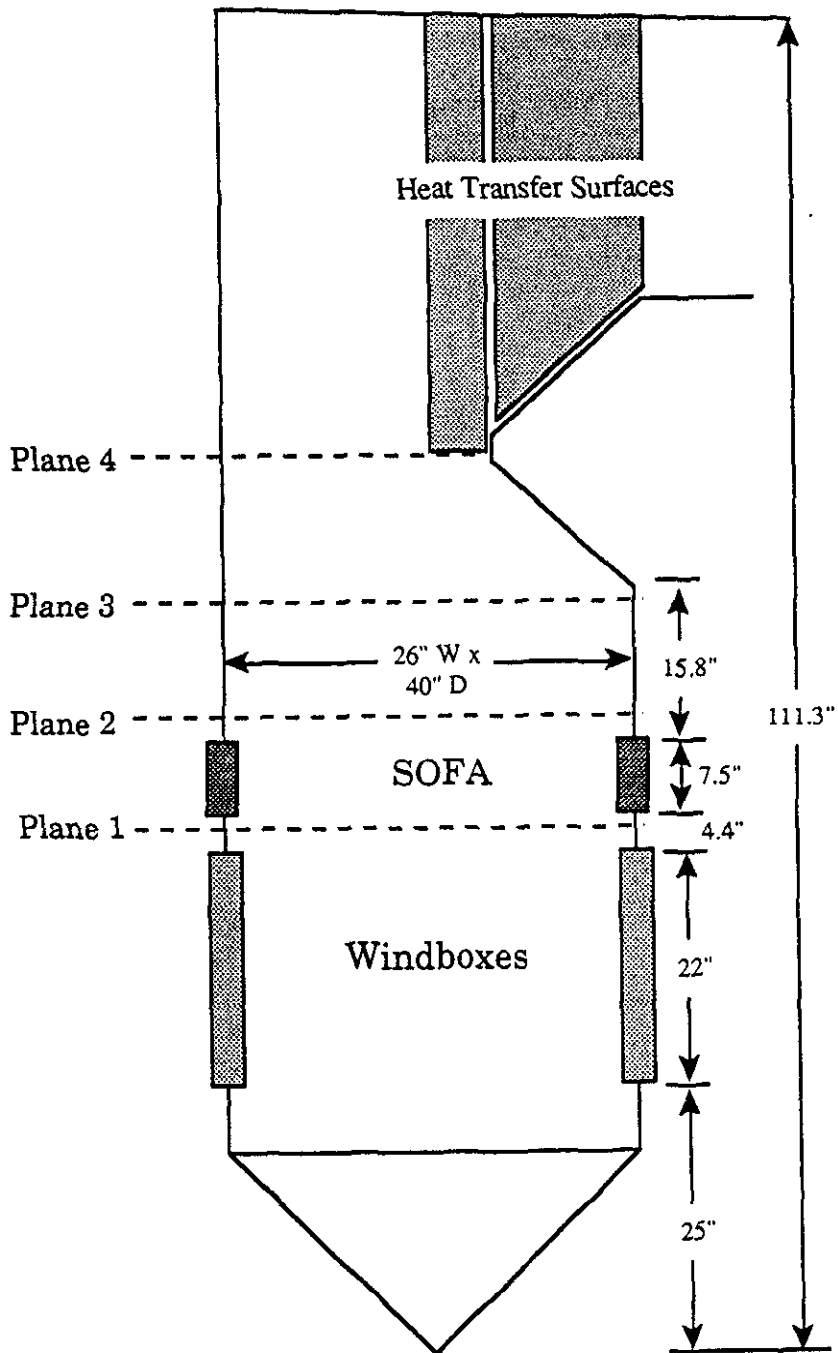


Figure 4-2 Lansing Smith Flow Model (Side View)

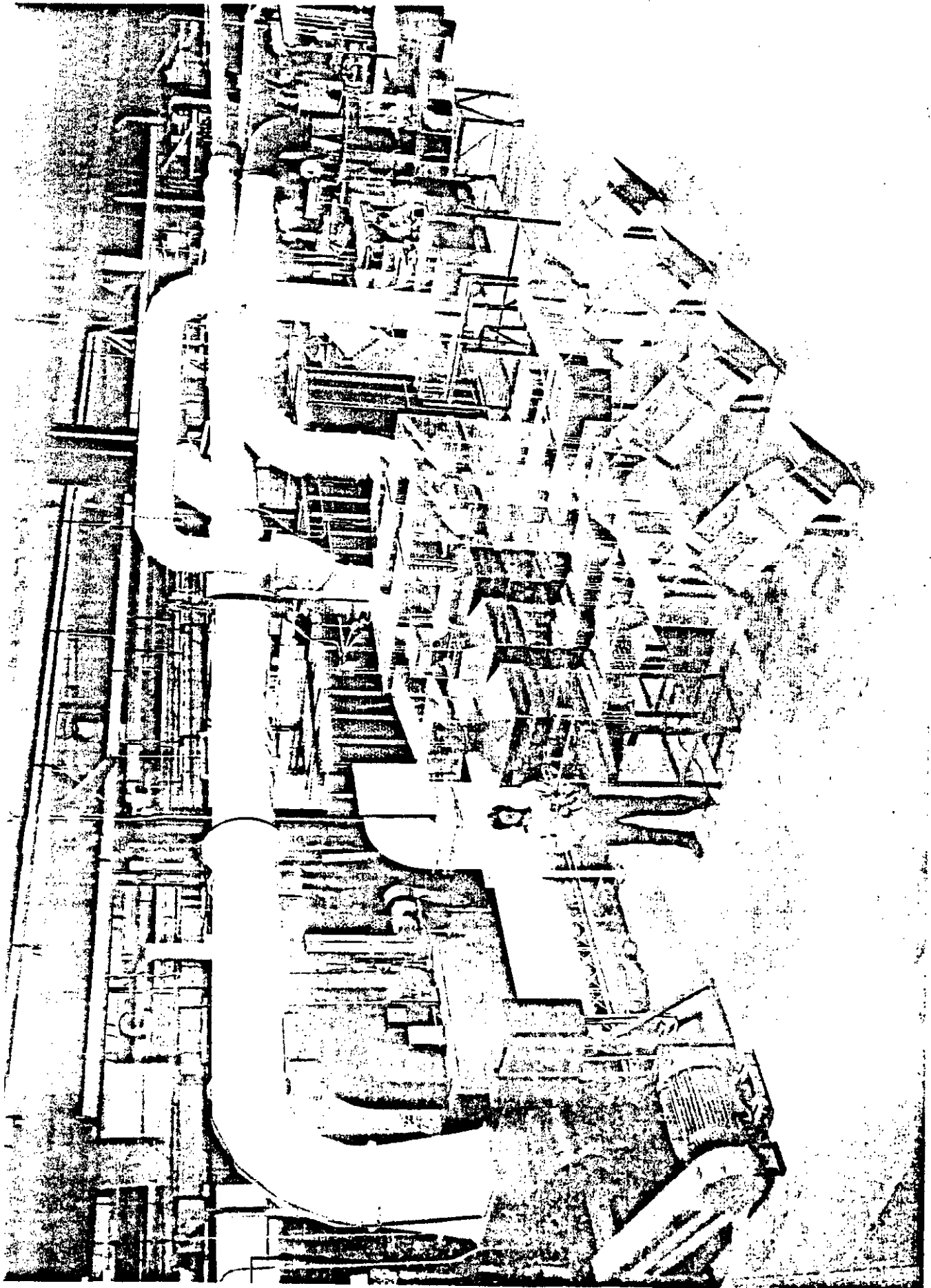


Figure 4-3 KDL Model Test Facility

paper tubing. These sections were shaped to simulate heat transfer surface geometry. The free areas of the plates and their spacing within the model were determined such that the axial and transverse pressure drop coefficients were accurately simulated.

The fuel admission assemblies were modeled as part of the windboxes. The free areas of the compartments were adjusted according to the Thring-Newby criteria, accounting for the change of density which occurs as a result of combustion within the furnace. Perforated plate was added to achieve the proper velocity splits between the primary air /coal nozzles and secondary air nozzles. The firing circle in the model was set to model that of the prototype through geometric scaling. A schematic of the modeled firing circle /angles is shown in Figure 4-4.

The Over Fire Air (OFA) injection nozzles were designed to simulate the corresponding jet trajectories in the prototype. Each nozzle was sized as a single jet, such that the mass and penetration ratios of the prototype jet and the model jet were equivalent. These nozzles were also constructed to allow for variable yaw and tilt settings within the model. Figure 4-5 shows a closer view of these nozzles.

Methane, used as a tracer gas for the mixing studies, was introduced into the over fire air at a point far upstream from the nozzle exits. This insured that the tracer gas was fully mixed with the OFA before entering the furnace.

4.2 Automatic Probe Traversing Device

All quantitative three dimensional velocity and pressure mapping within the flow model was performed with a calibrated five-hole pitot tube coupled to a computer controlled traversing device and data acquisition system. This system, developed and built at KDL, is called the Automatic Probe Traversing Device or APTD.

The APTD is a programmable data acquisition system which automatically positions and nulls the five-hole pitot tube, and records all pressure

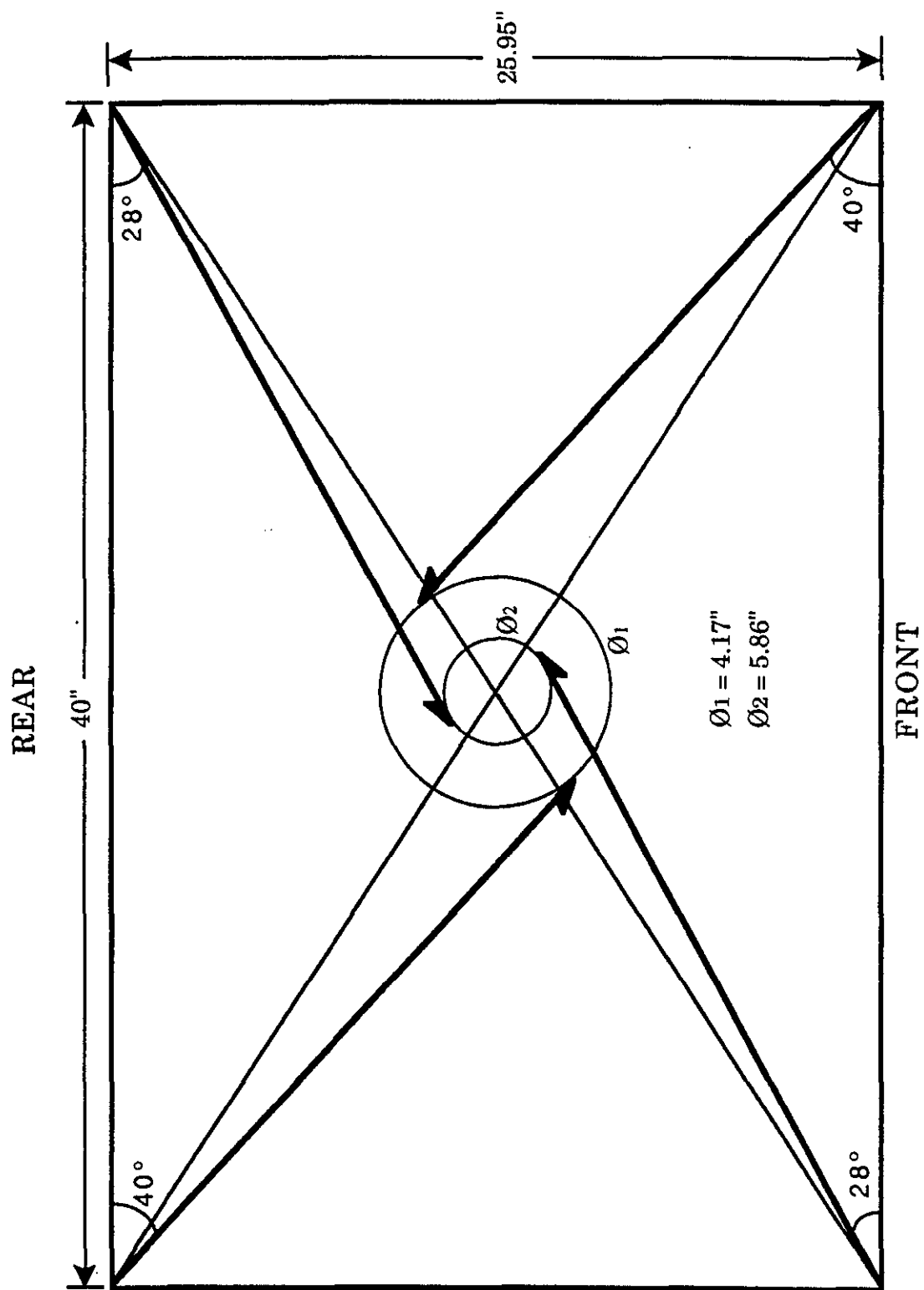
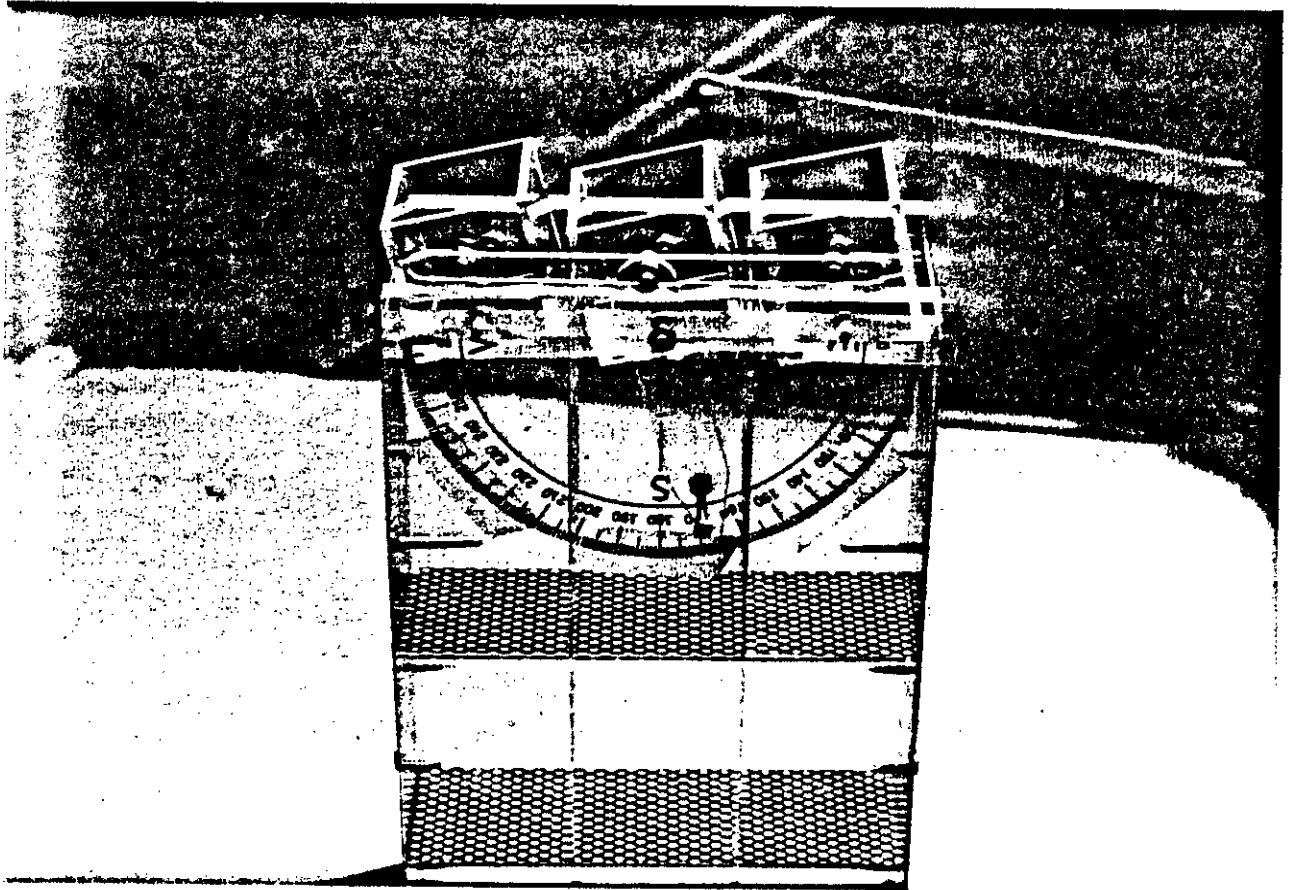


Figure 4-4 Firing Circle and Windbox Settings for Lansing Smith No. 2 Flow Model

Southern Company Services
Lansing Smith Unit #2
LNCFS-II Model Configuration



OFA Nozzle with Variable Tilt

Figure 4-5 OFA Nozzle for Lansing Smith #2 Flow Model

readings on the laboratory's central computer system. Figure 4-6 shows the five-hole pitot tube, the APTD, and the local programmable controller/electronic manometer cabinet. The motion of the probe is controlled by a local processor. This processor is programmed by the facility operator at the start of each traverse by entering the appropriate operational parameters for the particular test. These parameters include: instrument type and serial number (for accessing the most recent calibrations), test number, test plane, the number of data points, the distance between each point, and the maximum distance of probe travel (a safety feature.) Once these operational parameters have been entered, the traverse is started by indicating the desired operational mode.

The processor controls stepping motors which move the probe to the pre-programmed test point location and rotates it until the direction of flow is obtained. The outputs of the four pressure transmitters attached to the probe are then recorded along with probe position, angle, test number, test plane, etc. by the central data acquisition computer.

4.3 Three Dimensional Pitot Tube Probe

A commercially available five-hole, directional sensing, pitot tube, shown in Figure 4-7, was used to obtain the velocity data. The probe has five pressure sensing holes located at its tip. The centrally located pressure hole, P1, measures the total or impact pressure of the fluid, while two lateral holes, P2 and P3, measure the static pressure. If the probe is rotated around its long axis until $P2=P3$, the plane of flow can be identified and measured. However, since the condition $P2=P3$ can be given at two locations 180° apart, the correct vector plane is identified when $P2=P3$ and P1 has its highest positive value with respect to P2 and P3. An angular encoder is attached to the probe at its base so that the angle of this vector plane, commonly called the yaw angle, can be measured. The yaw angle indicates the plane of flow but does not give the flow angle within this plane. This flow angle, known as the pitch angle, is determined by the differential pressure P4-P5.

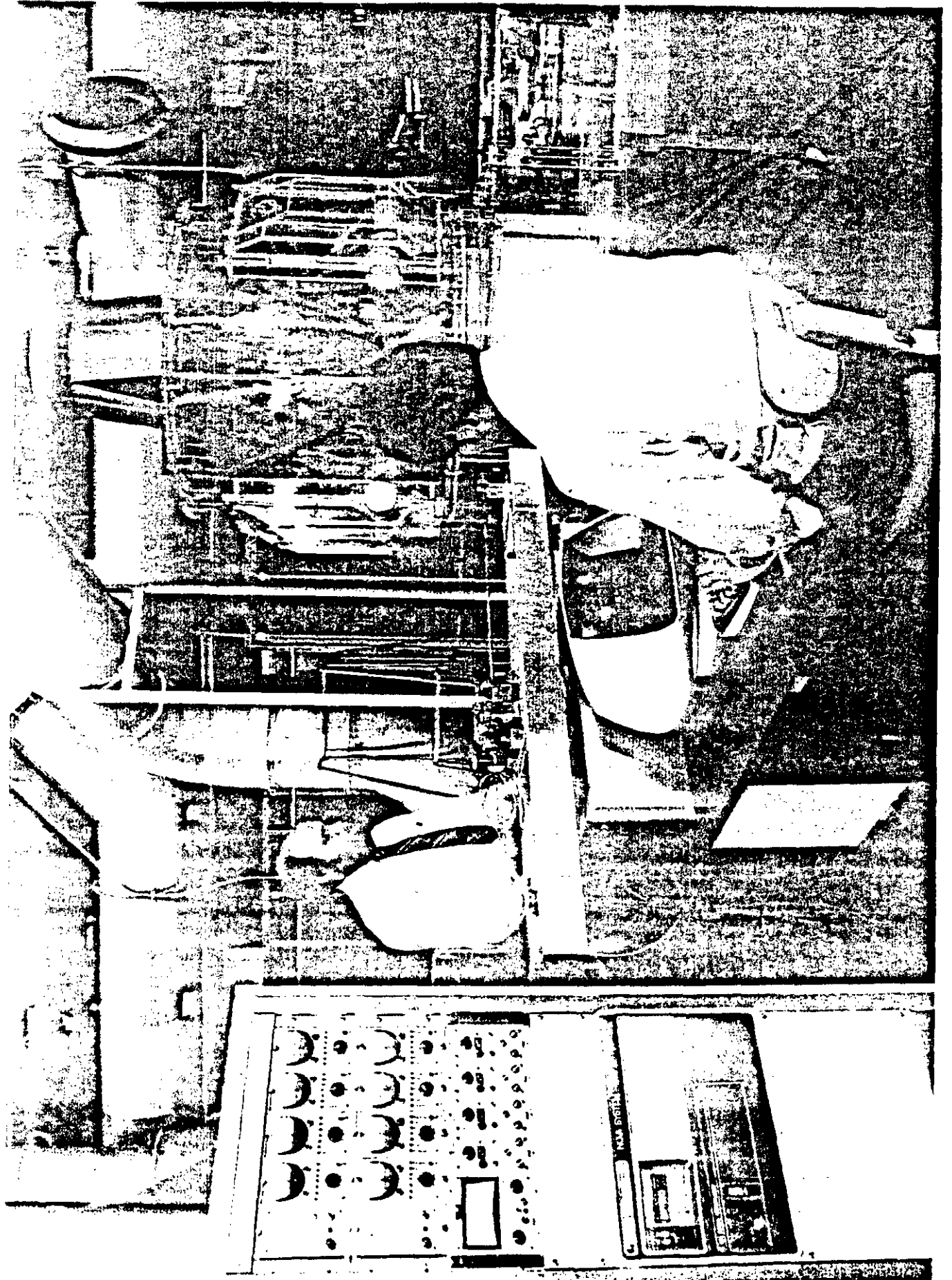


Figure 4-6 Automatic Probe Traversing Device

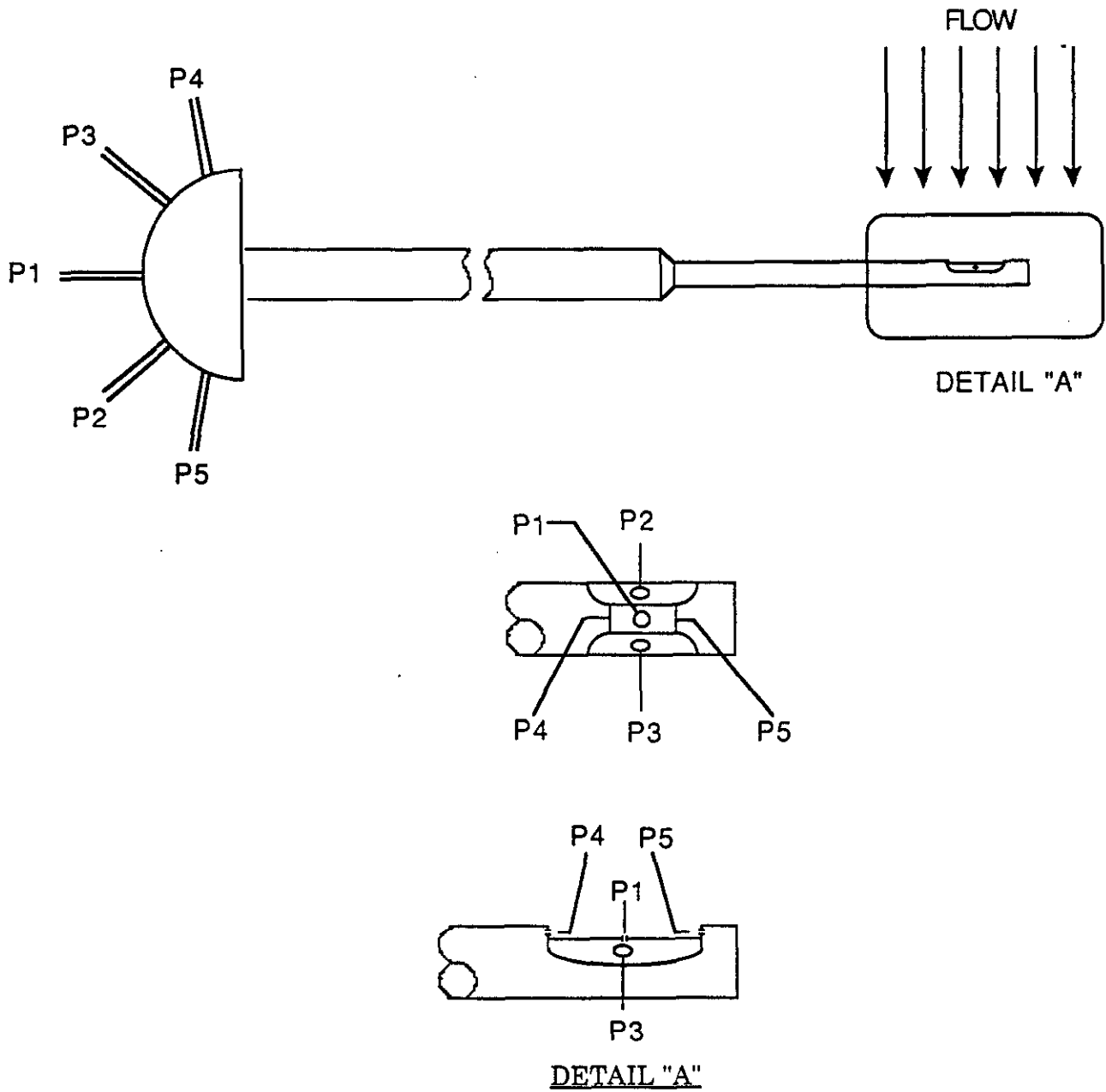


Figure 4-7 Five Hole Pitot Tube

In actual practice, four (4) differential pressure readings are required to fully define the flow at a particular point in the flow field. These pressure differentials are:

P1-Patm = Indicated total pressure with respect to atmosphere
P1-P2 = Indicated velocity pressure
P2-P3 = Yaw angle pressure
P4-P5 = Pitch angle pressure

Calibration curves are used to relate these pressure differentials to the actual pressures and pitch angles. These curves are generated through detailed probe calibrations, which were performed at the beginning of the test series. These curves, given in Appendix A, enable the determination of the actual velocity head and pitch angle at each measuring point. Knowing this data and the yaw angle, the x, y, z, or the normal, radial, and tangential velocity vectors are determined using simple geometric relationships.

4.4 Laser Absorption Spectrophotometer

An automatic laser based system, the Laser Absorption Spectrophotometer, has been developed in KDL to make tracer gas concentration measurements using the available APTD hardware. A schematic of this Laser Absorption Spectrophotometer is shown in Figure 4-8. The APTD positions the five-hole pitot probe at each of a matrix of points in a plane, as specified in the test set-up. A sample of the tracer gas is then extracted from the flow model by a suction pump attached to the probe and analyzed by the spectrophotometer.

The sample, in going from the probe to the pump exhaust, passes through a chamber through which one of two equally intense laser beams is passed. The wavelength of the laser light is tuned to the absorption frequency of the tracer gas, methane. The level of attenuation, when compared to the reference beam, is proportional to the concentration of the tracer gas at the sampling point in the flow model. Before and after each traverse into the model, the system is zeroed. Two samples per test point are drawn and the results sent to the laboratory central data acquisition computer. A full

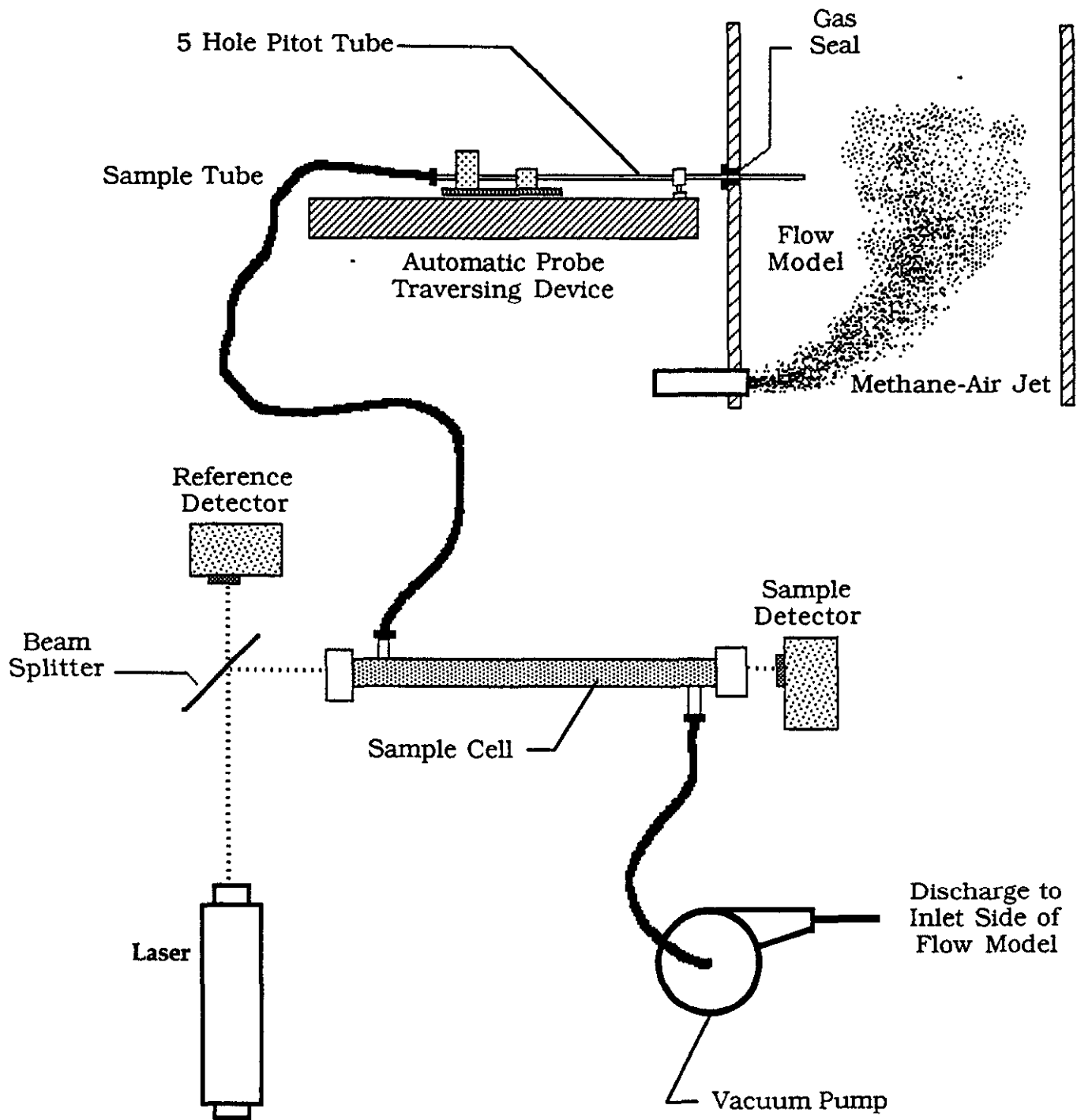


Figure 4-8 Laser Methane System

calibration is performed on this system prior to the model testing. This calibration is given in Appendix B.

4.5 Smoke Generator

A commercially available smoke generator was utilized during the flow visualization tests. The smoke generation system consisted of a gas heater, a light oil smoke fluid reservoir, and tube coil. The fluid was pumped through the tube coil, which was heated, causing it to flash into a dense white stream of smoke. This stream was then injected into the various ports of interest within the model.

5.0 Lansing Smith Flow Model Testing

5.1 Flow Model Set Up

The Lansing Smith flow model and the criteria used to design it have been discussed in the previous sections. In general terms, the flow model is representative of the actual prototype. The final step in achieving model similitude is to configure the model inlet conditions such that they match, as closely as possible, the inlet conditions which exist in the prototype. Since the LNCFS-II modifications are currently underway and actual field data is not available, the model flow splits were modified such that they produced profiles similar to that of the design operating conditions.

The overall distribution of the flow quantities between the sources of air was handled in the following manner. The Lansing Smith flow model was nominally operated under induced draft. The total air flow through the model was measured using a venturi which was installed in the main duct downstream of the Model Area Fan. The OFA flow was supplied through the Lamson blower and was measured independantly via an orifice which was located at the blower inlet. The OFA flow was than subtracted from the total model air flow in order to obtain the flow through the windboxes. Dampers in the air source lines allowed for adjustment of the flow streams until the desired total flow ratios had been achieved.

Correctly modeling the initial flow distributions is necessary where the evaluation of multiple gas streams is considered. For the Lansing Smith model, it was necessary to model the windbox flows as closely as possible in order to obtain meaningful measures of the gas mixing of the OFA at higher levels in the furnace. Velocity ratios between the primary and secondary air nozzles were determined based on MCR operating conditions. Flow splits between the primary and secondary air nozzles were controlled through the use of perforated plate in the windboxes. The velocities through each nozzle were measured with a pitot tube and the flow through each determined.

5.2 Test Matrix

The isothermal flow model test program was divided into two (2) separate screening levels (Figure 5-1) designed to lead, in an interactive manner, to recommended OFA operation. In the first level, flow visualization tests were performed on twenty (20) different OFA configurations to evaluate those conditions which "look the best" from an OFA penetration, mixing, and dispersion standpoint. In the second level, quantitative tests were performed on those configurations which were chosen from the first level. These tests included methane gas mixing tests and 3-D velocity mapping. For each of these configurations, gas mixing data was taken at planes 1, 2, 3, and 4 while 3-D velocity data was taken only at plane 4. Each of these test planes were horizontal planes located above the windboxes, above the OFA nozzles, below the arch, and at the furnace outlet plane, respectively. Figure 5-2 shows the location of these planes in the flow model.

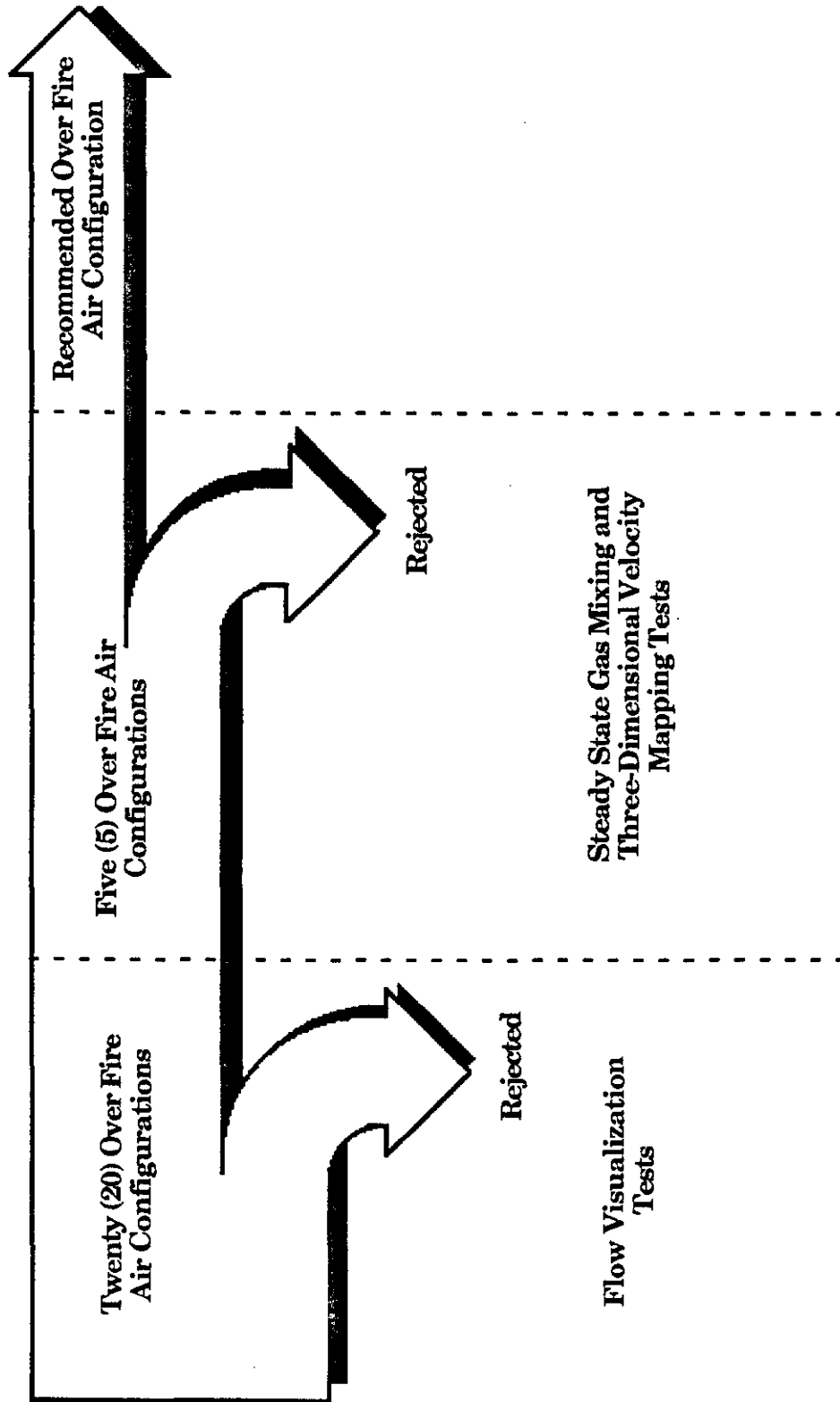


**Figure 5-1 Lansing Smith Unit #2 Flow Model
LNCFS-II Test Matrix**

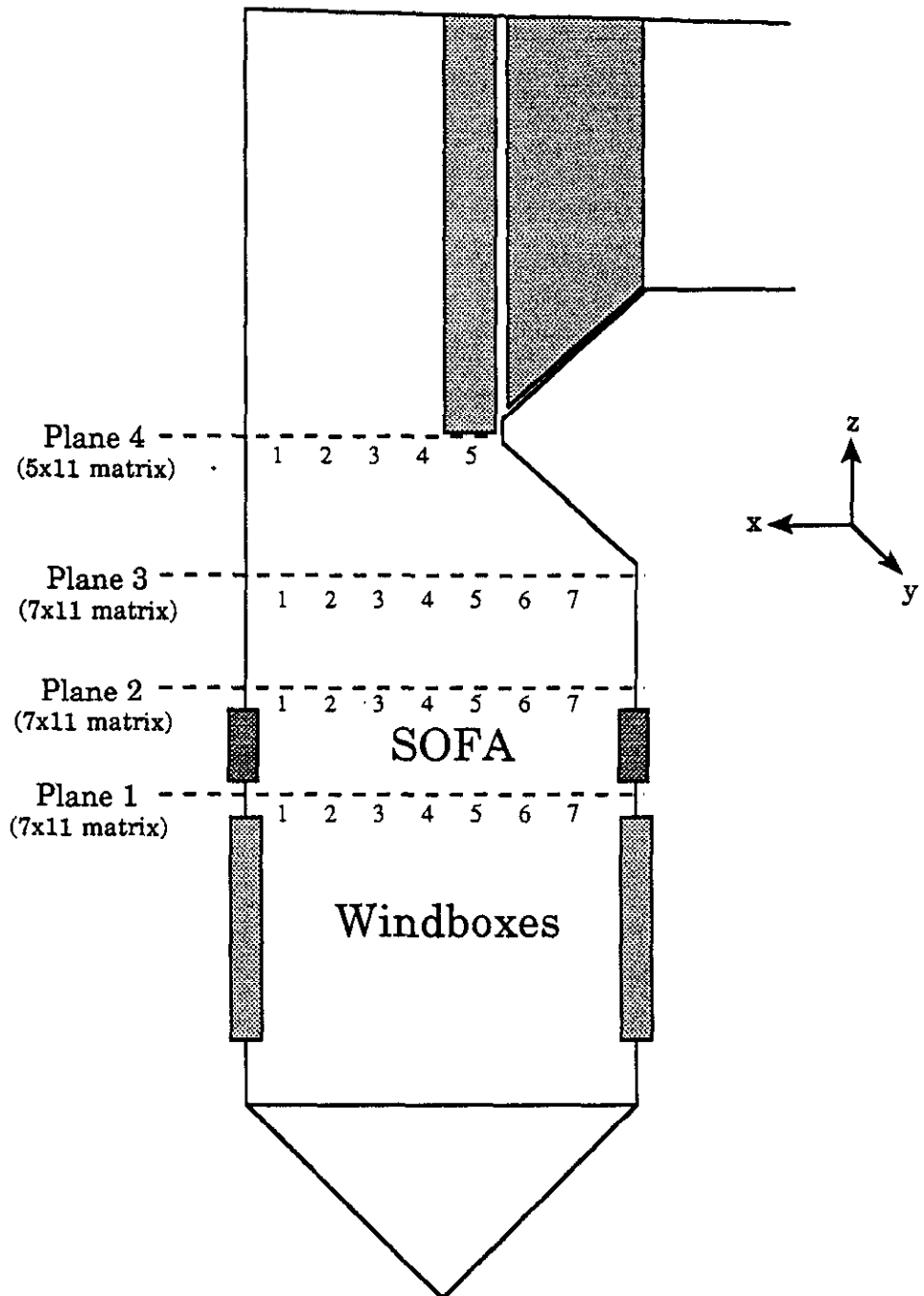


Figure 5-2 Test Plane Location

6.0 Results

The objective of the flow modeling effort was to evaluate the in-furnace flow and mixing phenomena of the LNCFS-II configuration, which is currently being upgraded in the Lansing Smith No. 2 Unit. First, flow visualization tests were used as a preliminary screening tool to evaluate a moderate number of operating conditions. Results from this testing were then used to select those configurations which "looked the best," from an OFA penetration, dispersion, and mixing standpoint, for additional quantitative tests. The quantitative tests, methane gas mixing and three dimensional velocity mapping, were then used to select the OFA configurations providing the desired level of mixing in the furnace.

6.1 Flow Visualization

Flow visualization tests were used as a qualitative method of observing and evaluating the flow fields within the model. These tests were performed on the baseline configuration (no OFA), as well as twenty (22) different operating conditions of the LNCFS-II model configuration with OFA. Each of these tests represented a combination of furnace load and OFA firing angle. In addition to this, the effect of OFA tilt was evaluated for each test configuration.

Model flow patterns were visualized by the injection of smoke through the windboxes and the OFA nozzles. The smoke was used to evaluate the furnace swirl, along with the OFA penetration, mixing, and dispersion. This testing was performed at reduced model flow rates, while maintaining the proper scaling parameters and flow splits. These reduced flow rates were used to improve the visibility of the smoke within the flow model. A video camera was used to record the flow patterns, with a copy of this tape is included as an Appendix. The information gained from these tests was used to develop the matrix for quantitative gas mixing and 3-D velocity tests.

Flow visualization tests were first performed on the baseline configuration to evaluate the flow fields within the furnace. The smoke was injected through each of the four (4) windboxes to qualitatively evaluate the flow

swirl and fireball characteristics. The patterns of the smoke as it entered through the different windbox compartments were also observed. Results from this testing showed that the flow entering the furnace through the lower windboxes experienced recirculation into the hopper. For the higher windbox elevations, the flow penetrated towards the center of the furnace and began to form the "fireball" in the main firing zone. Furthermore, it could be seen that the overall penetration of the windbox jets was not very strong. Typically, the flow would instead be redirected along the wall of the furnace before it reached the center.

After the baseline test was performed, smoke visualization tests were performed on the twenty two (22) OFA configurations. Flow visualization tests for the different configurations were performed for three (3) OFA flow rates. In addition to the design flow of 20%, tests were performed on a reduced flow (12% OFA) and an increased flow (24% OFA.) A summary of these test configurations is given in Table 6-1. Instead of describing the results of each of these tests, the discussion will focus on the OFA performance for each of the three (3) OFA flows tested. For each of these, the performance will be evaluated as a function of the OFA nozzle firing angle and the tilt.

In general, the performance for the 20% OFA condition with a 0° firing angle for each of the four (4) corners was as follows. The jets began to penetrate towards the center of the furnace, but became quickly entrained in the cross flow. As this happened, the jets were redirected towards the walls and were dispersed along the outer perimeter of the furnace flow. Typical results of flow visualization tests are shown in Figures 6-1 and 6-2. When a downward tilt (Figure 6-3) was imparted to these nozzles, the penetration was increased, while the overall dispersion was also improved. However, when this down tilt reaches approximately 10°, the jets begin to mix with the windbox firing zone. In so doing, the separation zone which is required for the staged burning of the separated OFA is eliminated. As an upward tilt was imparted to these nozzles, no improvements were noticed in the jet penetration and mixing. In fact, this type of tilt actually reduced the overall jet dispersion in the furnace.

In general, the penetration and mixing of the OFA jets was improved with the adjustment of the nozzle firing angles, Figure 6-4. In the model, each corner was adjusted to optimize the furnace coverage. That is, a series of tests were performed in which the nozzle firing angles were adjusted to improve the penetration and mixing of individual corners. It was through this technique that those configurations tested in the next screening level were chosen, see Table 6-2.

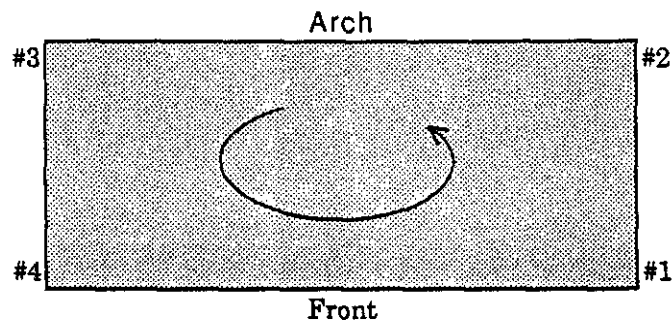
For the reduced operation of 12% OFA, the overall performance was much lower than 20% OFA as far as jet penetration, mixing, and dispersion. At this setting, the jet velocity is reduced, thus reducing the jet penetration. In order to improve the overall mixing for this set up, it was not only necessary to adjust the firing angles of each nozzle, but also to impose a downtilt in the OFA nozzles of 10-15°.

Finally, for the increased operation of 24% OFA, the overall performance tends to improve from a penetration and mixing standpoint. The jets, with higher velocities, are able to penetrate deeper into the furnace cross flow. Increased mixing also occurs at this setting. However, with the higher jet velocities, the nozzle tilts were restricted. Downtilt was limited to about 5° before the jets became entrained in the windbox firing zone. Also, when a positive tilt was imparted on the nozzles, the jets were carried to the back pass much more rapidly.

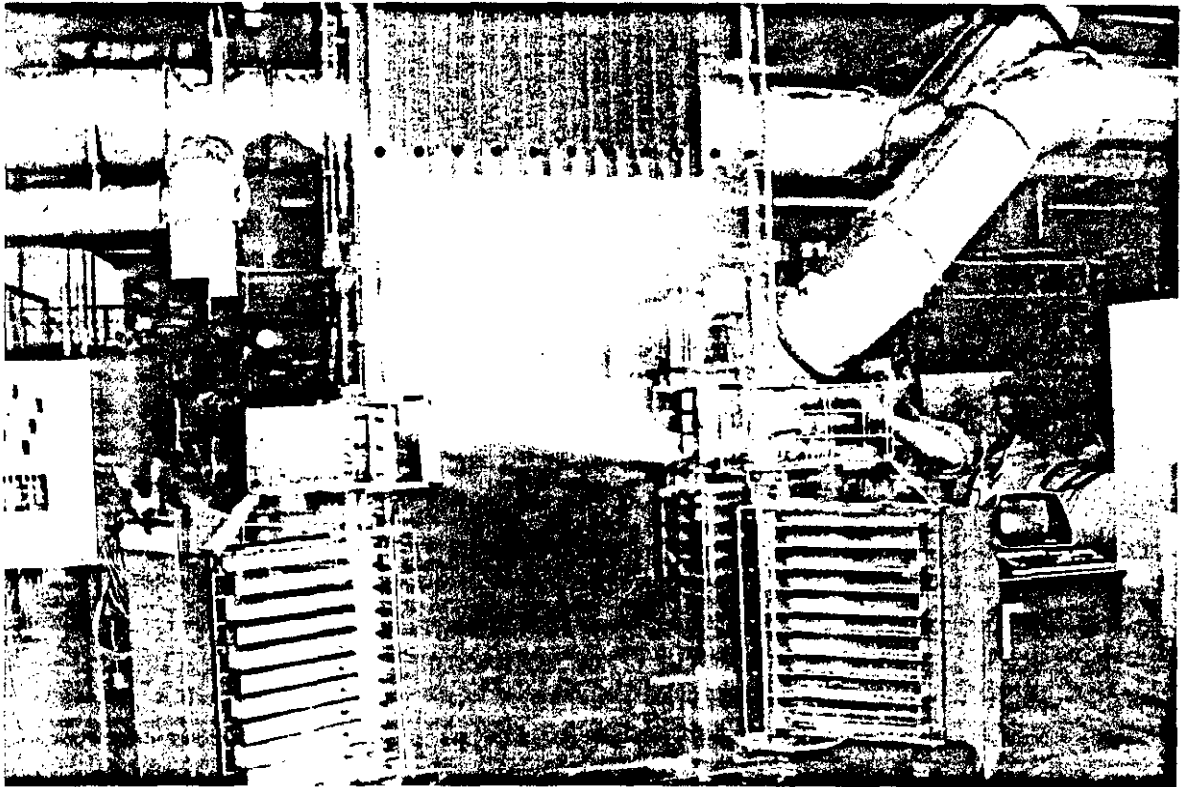
Table 6-1 Flow Visualization Test Matrix

Test No.	Load	% OFA	Corner 1	Corner 2	Corner 3	Corner 4
1	MCR	0%	N/A	N/A	N/A	N/A
2	MCR	20%	0°	0°	0°	0°
3	MCR	20%	-5°	-5°	-5°	-5°
4	MCR	20%	-10°	-10°	-10°	-10°
5	MCR	20%	+5°	+5°	+5°	+5°
6	MCR	12%	0°	0°	0°	0°
7	MCR	12%	-10°	-10°	-10°	-10°
8	MCR	12%	+10°	+10°	-10°	-10°
9	MCR	24%	0°	0°	0°	0°
10	MCR	24%	+7°	+7°	+7°	+7°
11	MCR	24%	+7°	+7°	-7°	-7°
12	MCR	12%	+10°	+10°	+10°	+10°
13	MCR	20%	0°	0°	-7°	-7°
14	MCR	20%	-8°	-8°	-8°	-8°
15	MCR	20%	-8°	-8°	-8°	+5°
16	MCR	20%	-8°	-8°	0°	0°
17	MCR	20%	+5°	-8°	+5°	-8°
18	MCR	20%	+5°	-8°	-10°	-8°
19	MCR	20%	-15°/0°/+15°	-15°/0°/+15°	-15°/0°/+15°	-15°/0°/+15°
20	MCR	12%	-15°/0°/+15°	-15°/0°/+15°	-15°/0°/+15°	-15°/0°/+15°
21	MCR	24%	-15°/0°/+15°	-15°/0°/+15°	-15°/0°/+15°	-15°/0°/+15°
22	MCR	24%	+15°/0°/-15°	+15°/0°/-15°	+15°/0°/-15°	+15°/0°/-15°
23	MCR	20%	+15°/0°/-15°	+15°/0°/-15°	+15°/0°/-15°	+15°/0°/-15°

Lansing Smith Flow Model Corner Reference



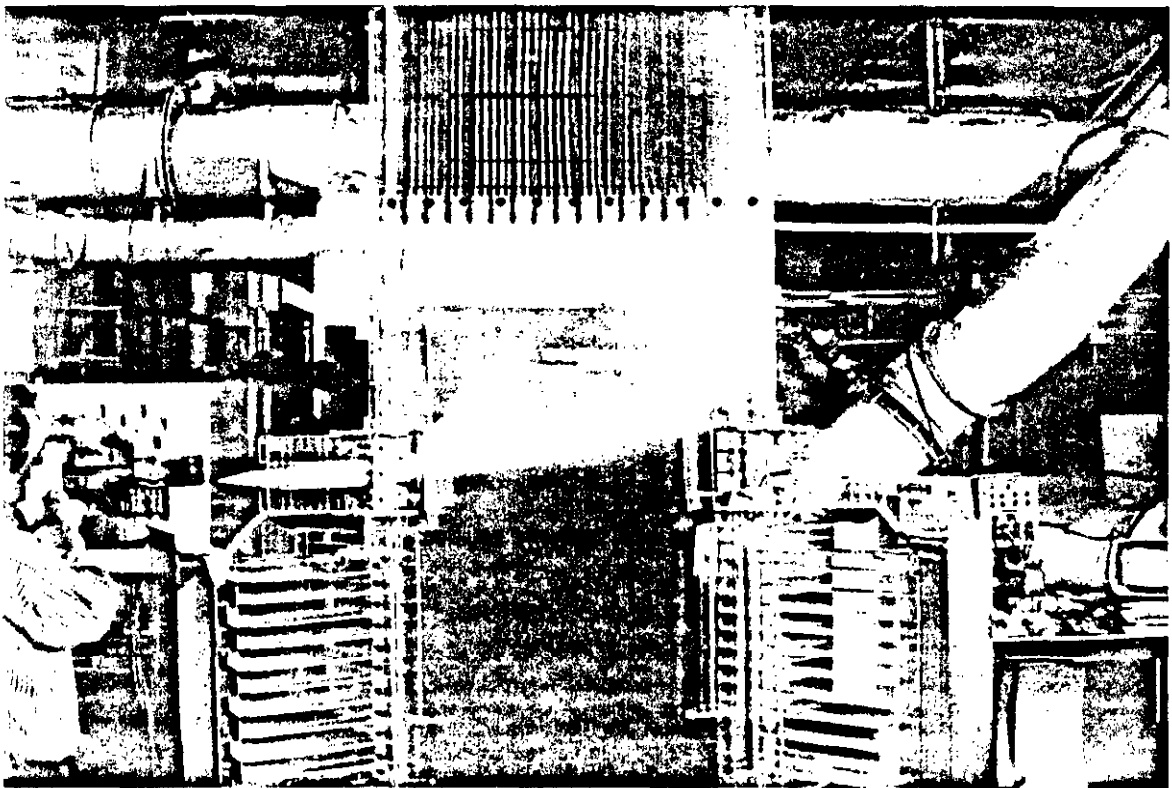
Southern Company Services
Lansing Smith Unit #2
LNCFS-II Model Configuration



Smoke Introduced Through the OFA Nozzles

Figure 6-1 Typical Flow Visualization Results

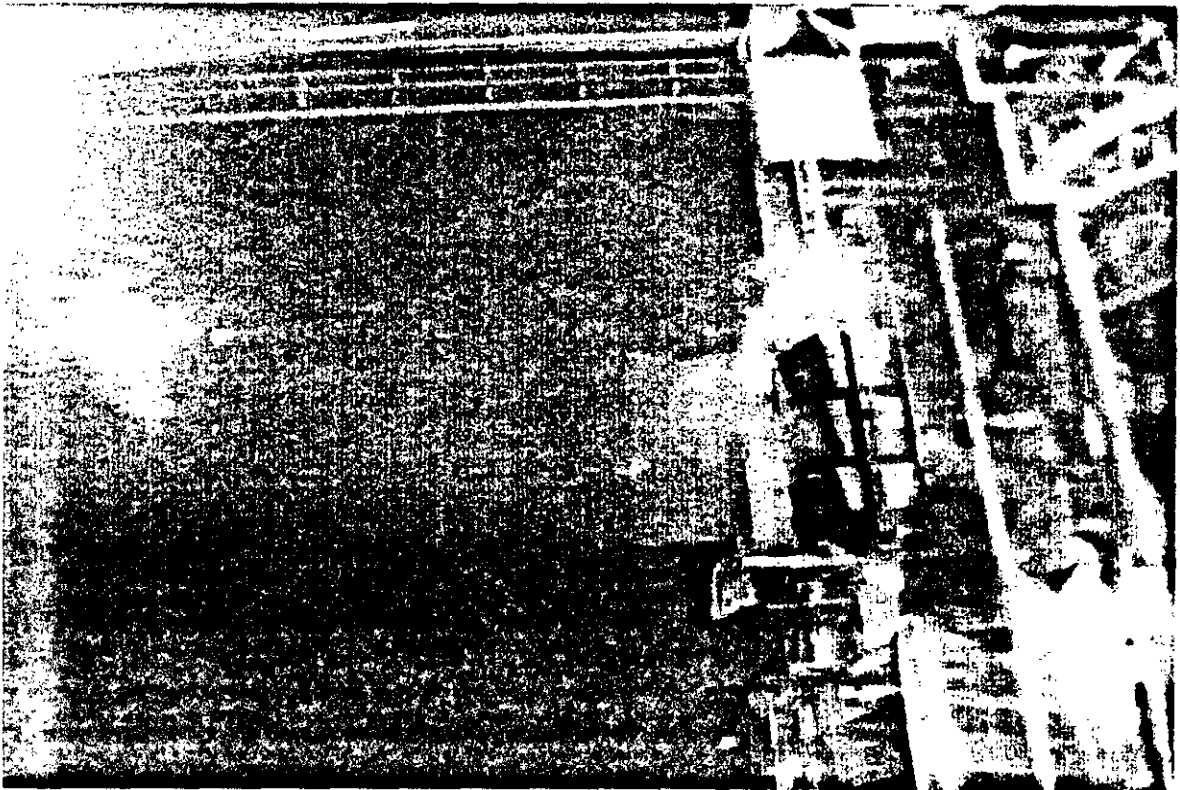
Southern Company Services
Lansing Smith Unit #2
LNCFS-II Model Configuration



Smoke Introduced Through the OFA Nozzles

Figure 6-2 Typical Flow Visualization Results

Southern Company Services
Lansing Smith Unit #2
LNCFS-II Model Configuration



Close Up of Smoke Introduced Through the OFA Nozzles

Figure 6-3 Typical Flow Visualization Results

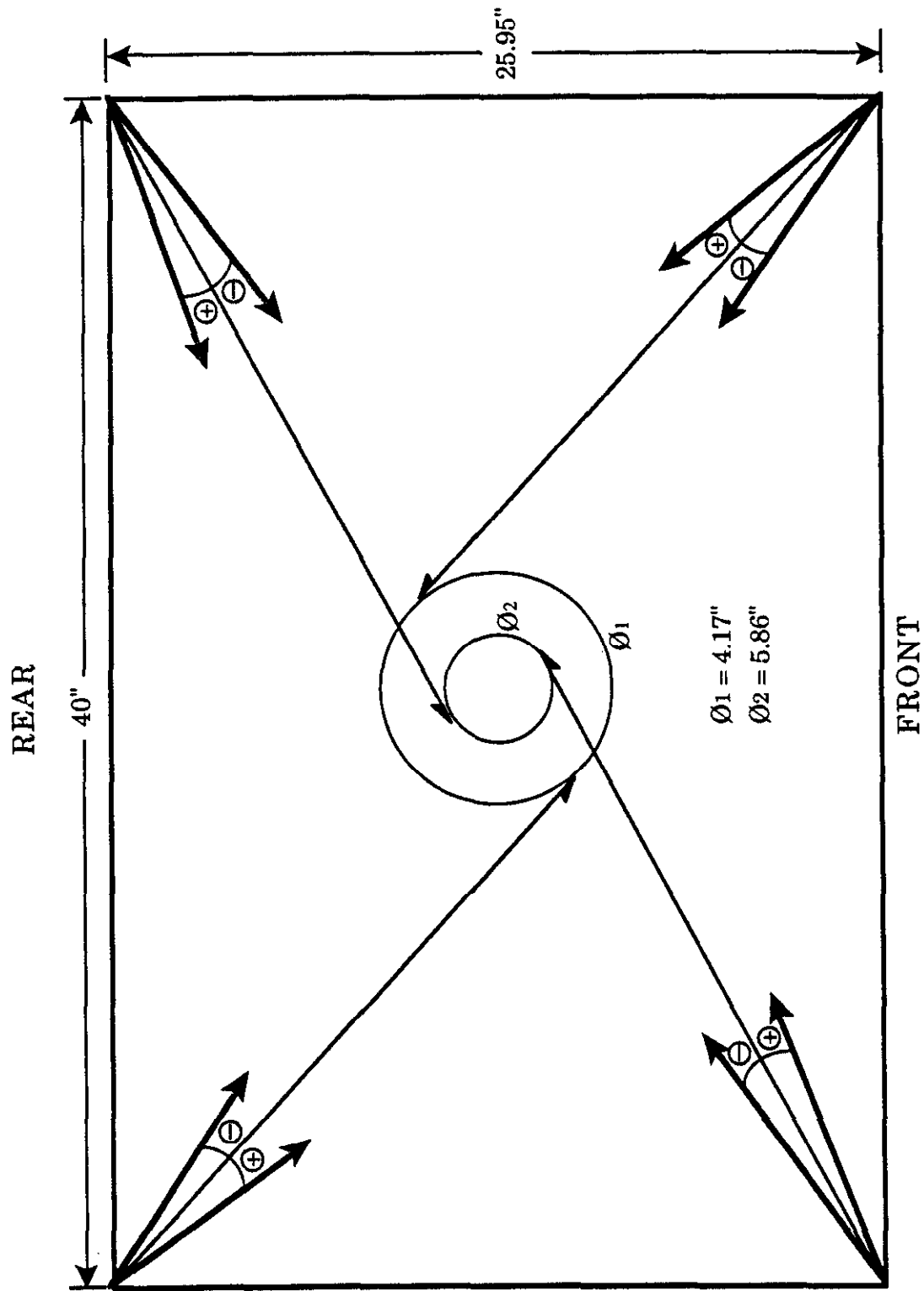


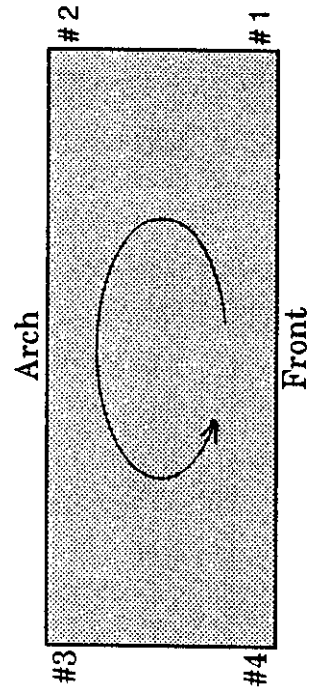
Figure 6-4 OFA Nozzle Firing Circle Lansing Smith No. 2 Flow Model

Table 6-2 Methane Gas Mixing and Velocity Mapping Test Matrix

Configuration #	Load	% OFA	Corner 1	Corner 2	Corner 3	Corner 4	OFA Tilt
Baseline*	MCR	0%	N/A	N/A	N/A	N/A	N/A
1	MCR	20%	0°	0°	0°	0°	0°
2	MCR	20%	-8°	-8°	-8°	-8°	0°
3	MCR	20%	+5°	-8°	-10°	-8°	0°
4	MCR	20%	+15°/0°/-15°	+15°/0°/-15°	+15°/0°/-15°	+15°/0°/-15°	0°
5	MCR	20%	0°	0°	-10°	-8°	-5°

* Velocity mapping only

Lansing Smith #2 Flow Model Corner Reference



6.2 Methane Gas Mixing

Based on the results from the flow visualization testing, a test matrix for the second screening level was developed, as mentioned in Table 6-2. This second screening level involved quantitative mixing tests of five (5) OFA configurations utilizing methane as a tracer gas. The purpose of these tests was to quantitatively measure the penetration, dispersion, and mixing of the OFA with the furnace gases in order to select optimum OFA configurations.

Methane samples were extracted from the flow model through the five hole probe, attached to the APTD. Samples were analyzed by the laser spectrophotometer, previously discussed, and stored in the lab's data acquisition system. This data was later transformed to gas concentrations (ppm) within the model. The measured gas concentrations were normalized to a reference value, taken as the "well mixed" value at the model's outlet. This data was reported in both tabular form, typical of Table 6-3, and graphical form.

For each of these tests, the flow model was operated at a simulated 100% MCR with 20% OFA. The model was operated under induced draft and the OFA under forced draft, the flow being provided by a high pressure Lamson blower. In order to assure a "well-mixed" tracer gas concentration at each of the OFA nozzle outlets, the methane was injected into the discharge of this blower at a point far enough upstream to permit adequate mixing. The flow of methane was set using precision rotometers such that a "well-mixed" value of approximately 1200 ppm at the model outlet was achieved. A schematic of the methane injection system is shown in Figure 6-5. The concentration of the methane gas was then mapped over the four (4) test planes detailed previously in Figure 5-2. The concentration data obtained at each plane was normalized to the "well-mixed" concentration obtained at the model outlet, with each plot generated using the same scaling factors so that they may be compared. For the purpose of clarity, all the plots are presented at the end of this section. The degree of uniformity in concentration across the plane was statistically quantified as the RMS deviation of the mass weighted distribution of methane measured at the test plane. The lower the coefficient, the better the mixing is across the test plane.

Comparing the data at plane 1, contour and isoconcentration plots are presented in Figures 6-6 through 6-15. In addition to these plots, the normalized methane concentrations are shown in Figures 6-16 through 6-20. This plane is located just under the OFA nozzles and is used to show the separation zone between the windbox firing zone and the OFA injection. Generally, it can be seen that there is little OFA recirculation in this zone, with the exception of configuration #5. For this configuration, there is a down tilt of 5° to the OFA nozzles. Thus, it can be seen that a separation zone between the windbox and OFA nozzles exists when the OFA nozzles are firing horizontally. However, the addition of downtilt to these nozzles will decrease this separation. In addition to this, it can be seen that there is recirculation in the rear left corner of configuration #4. However, it should be noted that the peak in this plot is a function of two (2) data points only, and does not encompass as much of the furnace as appears in the plot.

Comparing the data at plane 2, contour and isoconcentration plots, along with the normalized methane concentrations, are presented in Figures 6-21 through 6-35. From this data, the penetration of the OFA jets can be seen as peaks in the isoconcentration plots. Generally, these jets penetrate into the cross flow and, as they mix with the furnace gases, disperse along the furnace walls. This corresponds with the results from the flow visualization tests. It can also be seen that the locally high concentrations, which result from the OFA jets, can be reduced by "fanning" the nozzles. That is, when each of the three (3) nozzles per corner were set at different firing angles, the locally high concentrations of methane at this plane were reduced. Also, it can be seen that those jets which run along the front and rear walls of the furnace tend to have longer penetration lengths than those which run along the sides. Finally, the degree of "mixedness" is limited for this test plane because of the close proximity to the OFA nozzles. Therefore, the RMS deviation, shown in Figure 6-36, for each of these configurations is high.

Again, contour and isoconcentration plots, along with the normalized methane concentration values, for plane 3 are presented in Figures 6-37 through 6-51. This plane, located just under the arch, shows the progression of the methane mixing within the furnace model. Generally, the overall

mixing at this plane is greatly improved, with most of the concentrations falling between $\pm 25\%$ of the well mixed value, as can be seen from the contour plots. As expected, the RMS deviation for this plane, Figure 6-52, is much lower than plane 2, due to the increased mixing time of the OFA jets. It can also be seen that there is also a tendency for higher methane concentrations to be located along the front and rear walls of the furnace model. This is more than likely a result of the aspect ratio and the furnace aerodynamics. With the front and rear walls of the furnace 1.54 times longer than the side walls, the OFA jets which penetrate along the side walls will become entrained along the front and rear walls before those jets which come in along the front and rear walls move along the side walls. That is, there is more OFA mass through the areas along the front and rear walls than there is along the side walls..

Finally, the plane 4 contour and isoconcentration plots, along with the normalized methane concentration values are presented in Figures 6-53 through 6-67. This plane, located at the nose of the arch, shows the progression of the OFA mixing as the flow is exiting the furnace. Typically, an RMS deviation less than 20% at the furnace outlet plane is considered well mixed for OFA injection. For each of the configurations tested, the RMS deviation was less than 18%, with these values shown in Figure 6-68.

The overall best OFA configuration tested from a mixing standpoint was configuration #3. It provided the best overall mixing of any horizontal OFA configuration, with an RMS deviation of 11.8%. Also, the overall mixing was similar to an OFA configuration with a downtilt (configuration #5), without reducing the separation zone between the windbox firing zone and OFA injection. The overall mixing characteristics for each of the configurations tested is shown in Figure 6-69.

STEADY STATE LASER METHANE TRACER

TEST ID : METH 1
 TEST NUMBER : 0044
 TEST DATE : 2/12/91

PLANE NUMBER : 4
 NUMBER OF ROWS : 5
 NUMBER OF COLUMNS : 11

* EXTINCTION COEFFICIENT *

	1	2	3	4	5	6	7	8	9	10	11
1	0.593	0.625	0.643	0.662	0.677	0.692	0.701	0.707	0.690	0.690	0.652
2	0.592	0.635	0.667	0.709	0.724	0.723	0.730	0.724	0.730	0.708	0.652
3	0.579	0.621	0.652	0.704	0.719	0.733	0.733	0.727	0.729	0.690	0.637
4	0.591	0.597	0.614	0.643	0.653	0.672	0.686	0.689	0.680	0.651	0.619
5	0.614	0.608	0.605	0.602	0.598	0.591	0.610	0.613	0.620	0.614	0.583

* CONCENTRATION (PPM) *

	1	2	3	4	5	6	7	8	9	10	11
1	1458.97	1314.97	1234.68	1154.03	1089.34	1029.31	995.25	969.86	1039.47	1038.40	1195.43
2	1467.72	1268.12	1131.35	964.29	905.00	905.64	879.58	902.37	880.69	965.91	1194.11
3	1527.51	1334.42	1196.83	983.48	921.75	868.64	869.32	890.93	885.21	1036.29	1262.63
4	1470.03	1442.36	1362.22	1233.22	1191.60	1114.11	1052.79	1039.68	1078.98	1200.71	1340.58
5	1366.56	1390.71	1404.76	1417.29	1438.74	1472.25	1381.46	1370.71	1338.23	1365.00	1509.40

NORMALIZED BY WELL MIXED CONCENTRATION*
 VALUE : 1186.29 PPM RMS DEV : 17.4 %

	1	2	3	4	5	6	7	8	9	10	11
1	1.2299	1.1085	1.0408	0.9728	0.9183	0.8677	0.8390	0.8176	0.8762	0.8753	1.0077
2	1.2372	1.0690	0.9537	0.8129	0.7629	0.7634	0.7415	0.7607	0.7424	0.8142	1.0066
3	1.2876	1.1249	1.0089	0.8290	0.7770	0.7322	0.7328	0.7510	0.7462	0.8736	1.0644
4	1.2392	1.2159	1.1483	1.0396	1.0045	0.9392	0.8875	0.8764	0.9095	1.0122	1.1301
5	1.1520	1.1723	1.1842	1.1947	1.2128	1.2411	1.1645	1.1555	1.1281	1.1506	1.2724

Table 6-3 Methane Mixing Data - General Output

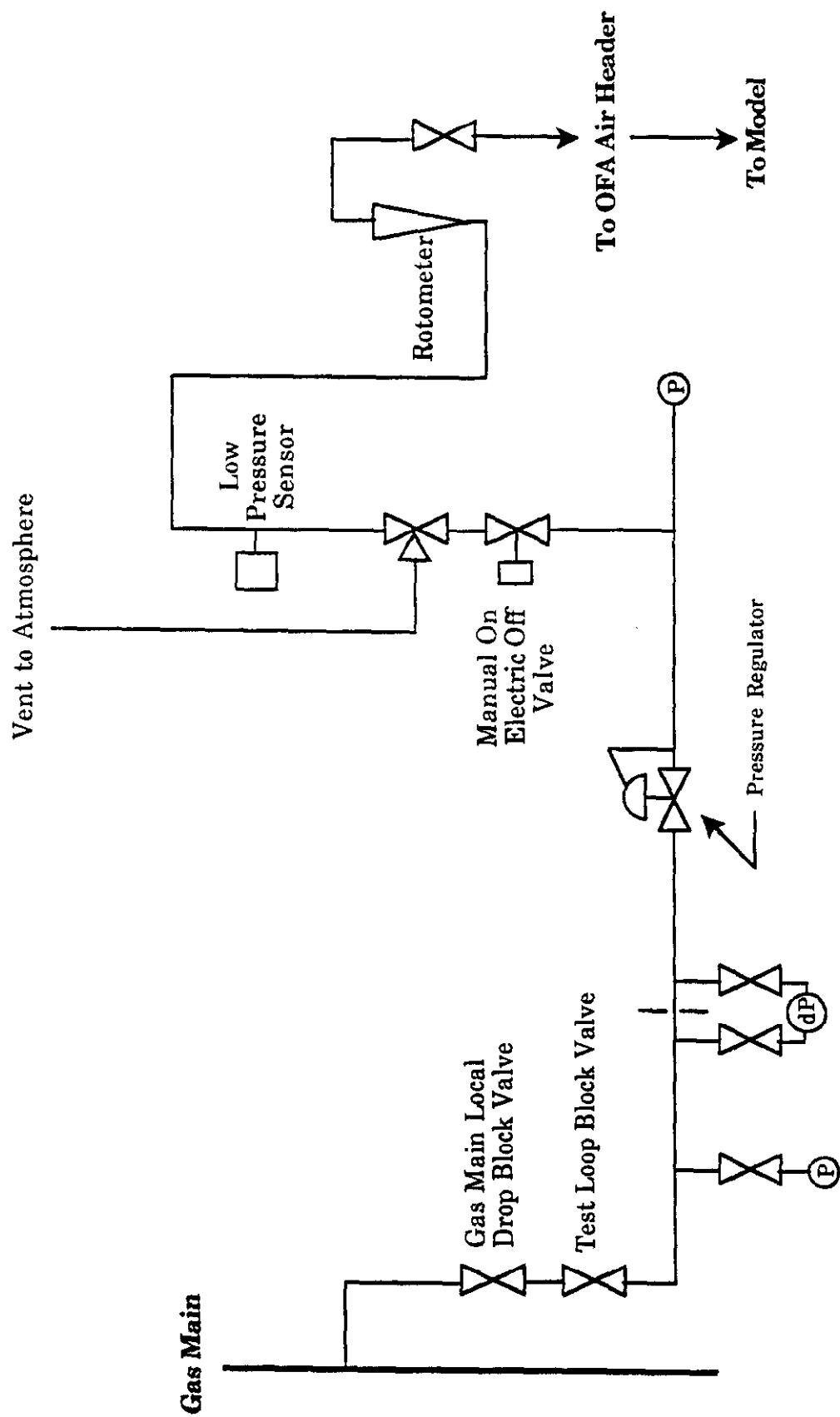


Figure 6-5 Schematic of Methane Injection System

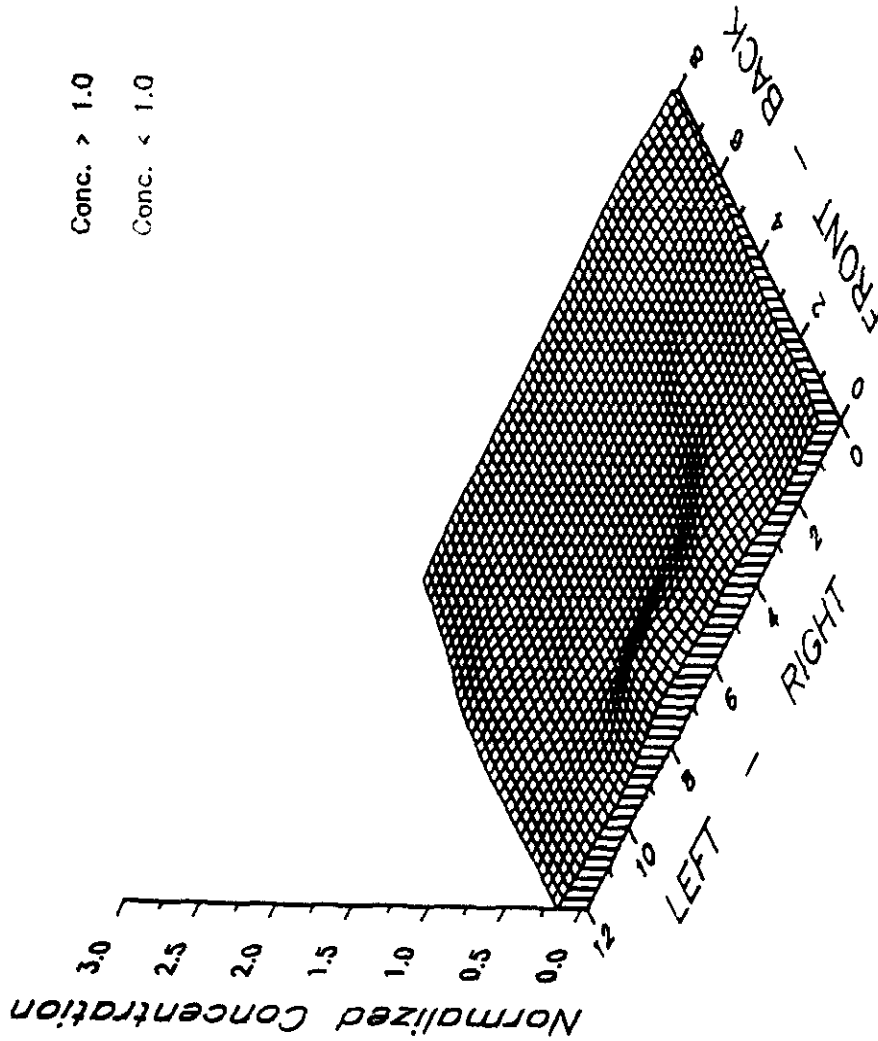
NORMALIZED METHANE CONCENTRATION

Test Plane: 1

Test Date: 2/12/91

Firing System: LNCFS-II

Test ID: Configuration #1



Conc. > 1.0

Conc. < 1.0

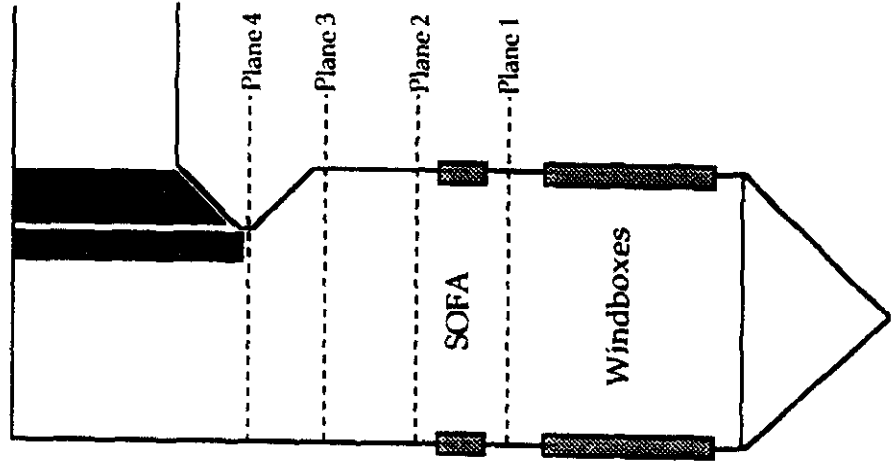


Figure 6-6

**SOUTHERN COMPANY SERVICES
LANSING SMITH #2 FLOW MODEL**

NORMALIZED METHANE CONCENTRATION

Test Plane: 1

Test Date: 2/12/91

Firing System: LNCFS-II

Test ID: Configuration #1

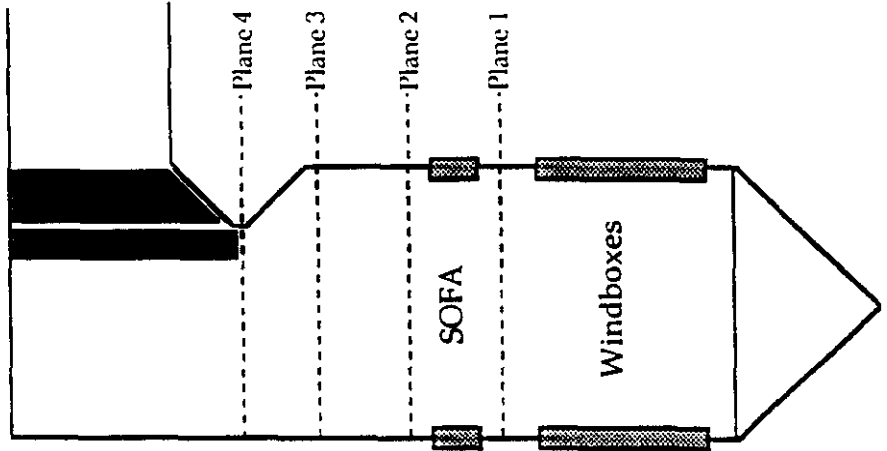
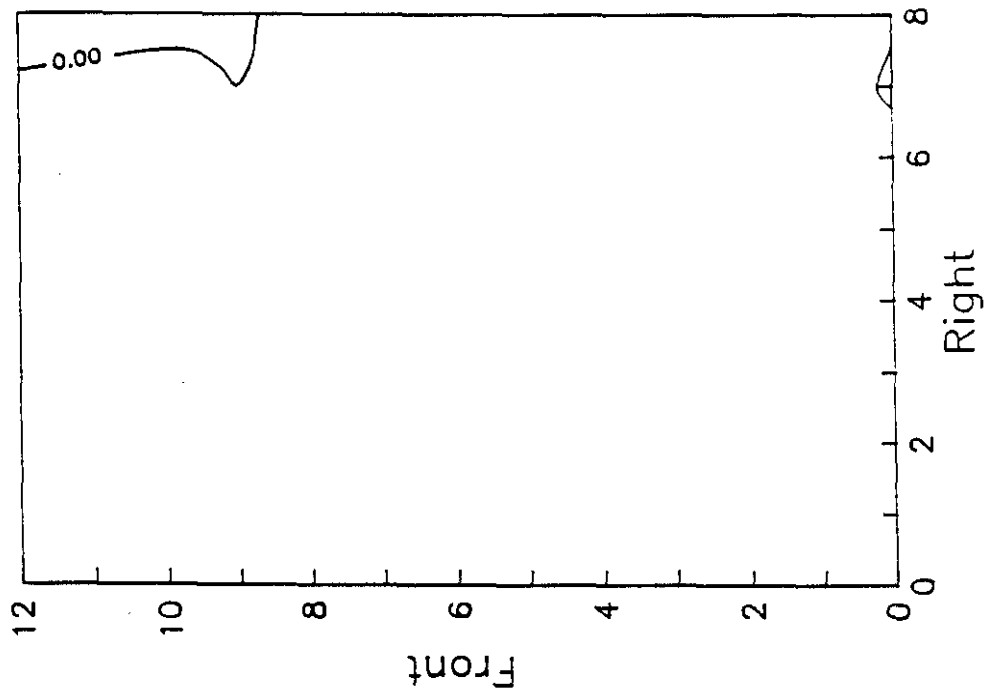


Figure 6-7

**SOUTHERN COMPANY SERVICES
LANSING SMITH #2 FLOW MODEL**

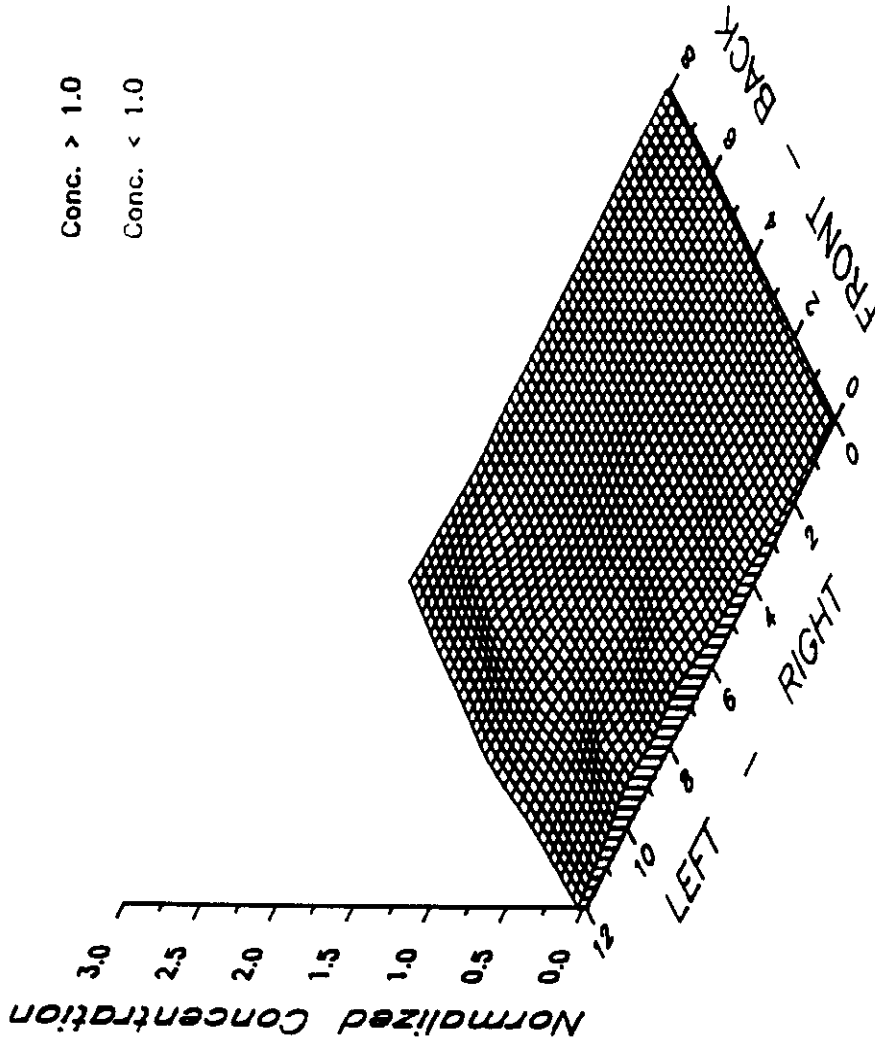
NORMALIZED METHANE CONCENTRATION

Test Plane: 1

Test Date: 2/13/91

Firing System: LNCFS-II

Test ID: Configuration #2



Conc. > 1.0

Conc. < 1.0

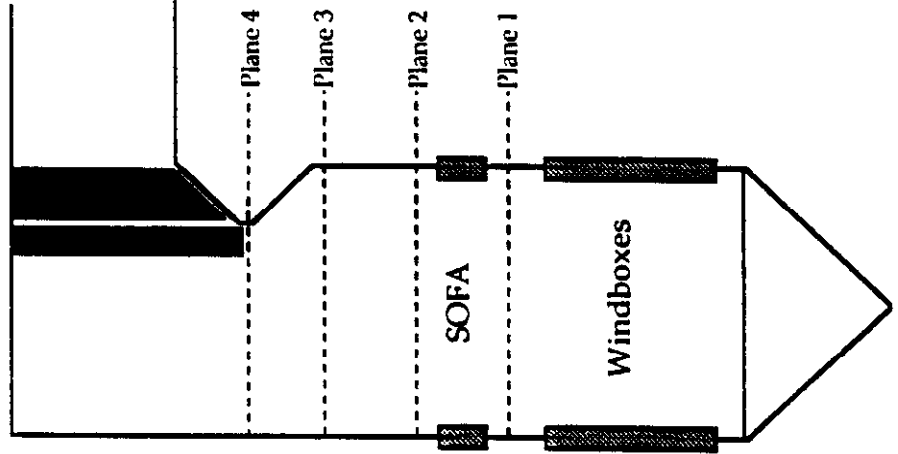


Figure 6-8

**SOUTHERN COMPANY SERVICES
LANSING SMITH #2 FLOW MODEL**

NORMALIZED METHANE CONCENTRATION

Test Plane: 1

Test Date: 2/13/91

Firing System: LNCFS-II

Test ID: Configuration #2

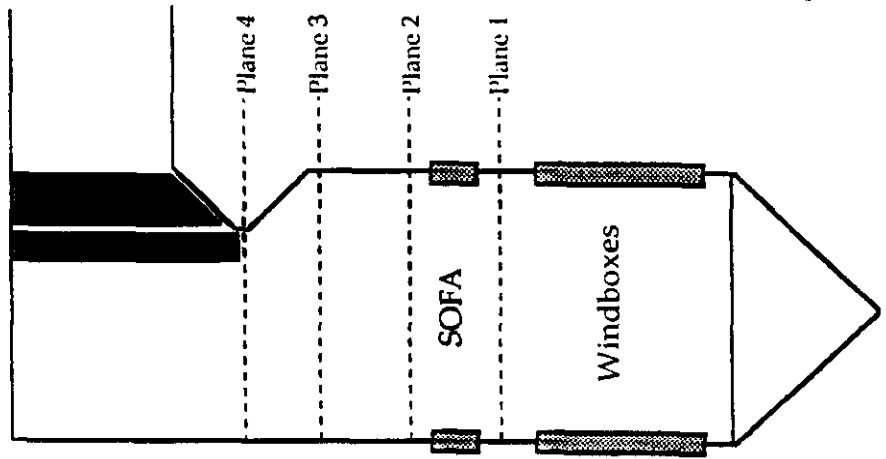
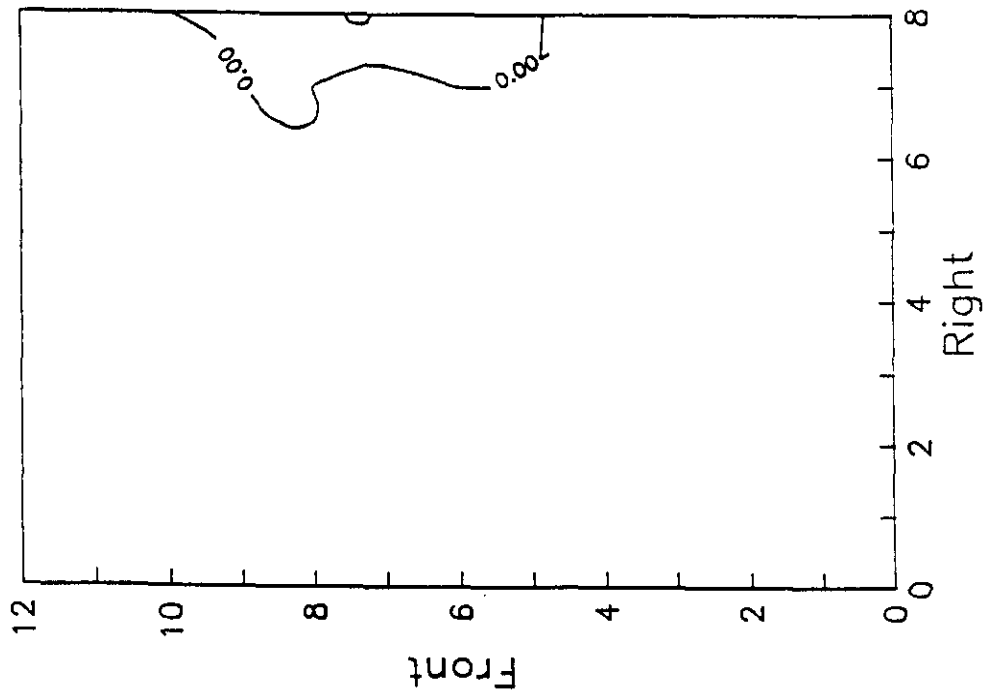


Figure 6-9

**SOUTHERN COMPANY SERVICES
LANSING SMITH #2 FLOW MODEL**

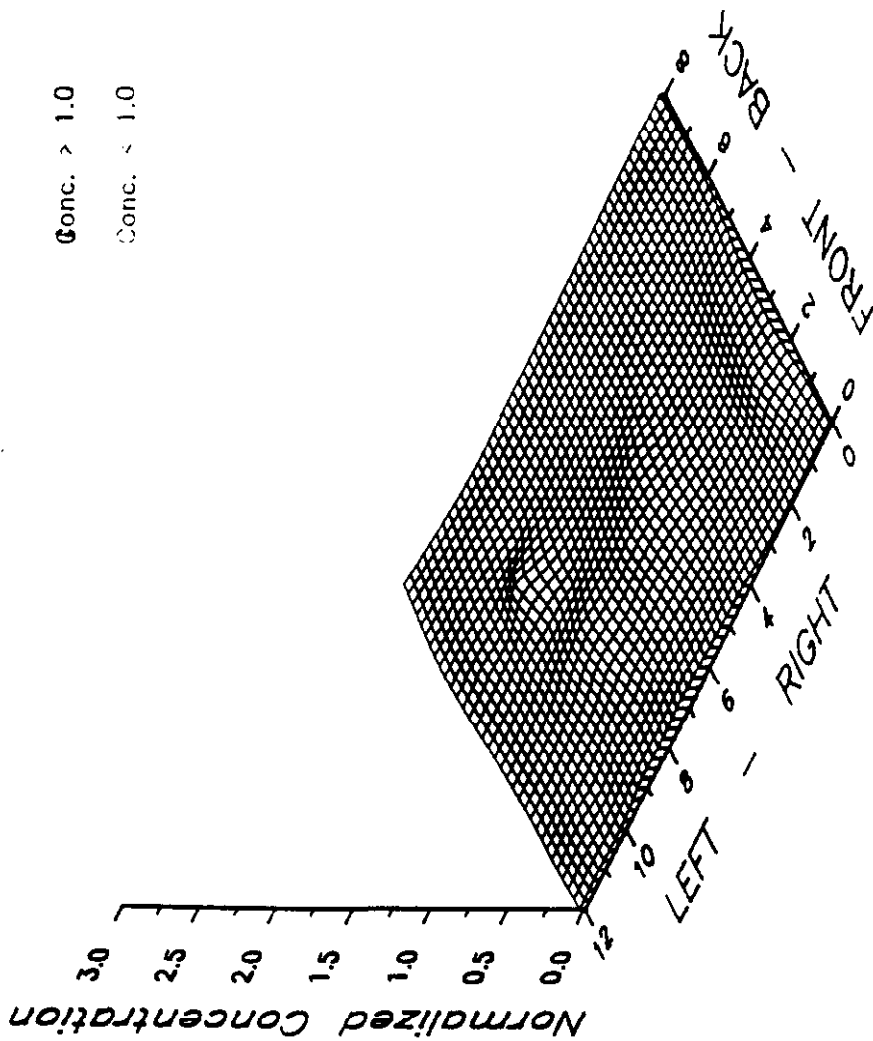
NORMALIZED METHANE CONCENTRATION

Test Plane: 1

Test Date: 2/13/91

Firing System: LNCFS-II

Test ID: Configuration #3



Conc. > 1.0

Conc. < 1.0

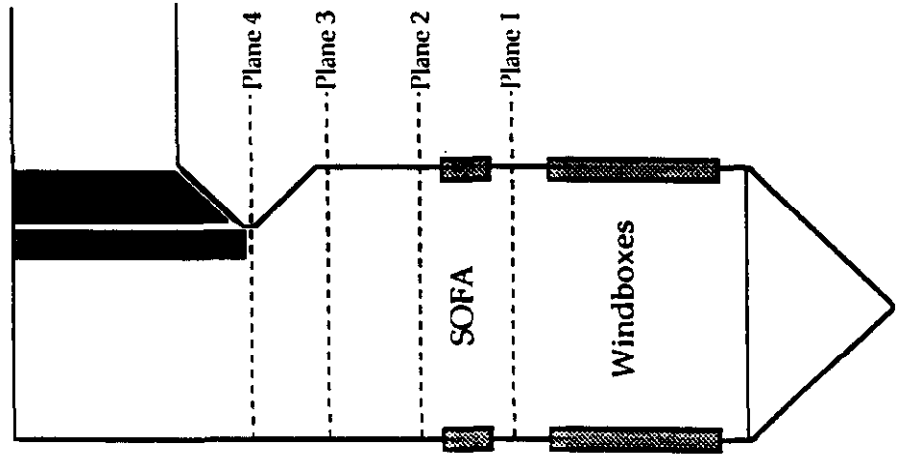


Figure 6-10

**SOUTHERN COMPANY SERVICES
LANSING SMITH #2 FLOW MODEL**

NORMALIZED METHANE CONCENTRATION

Test Plane: 1
Test Date: 2/13/91
Firing System: LNCFS-II
Test ID: Configuration #3

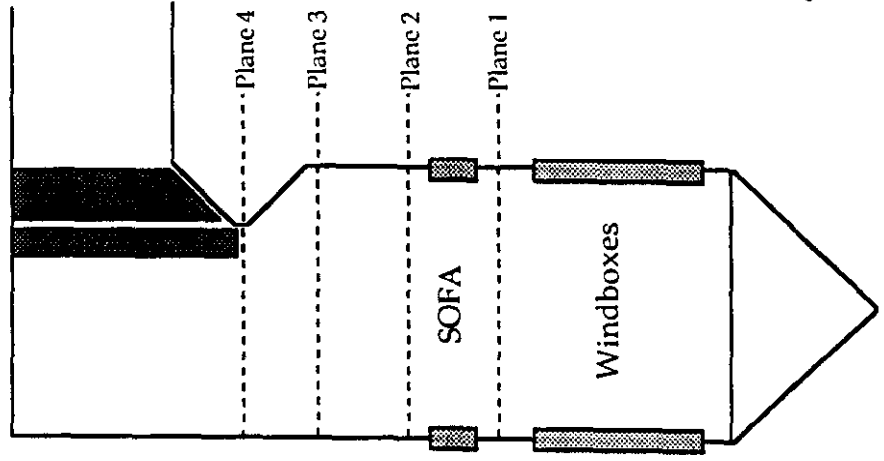
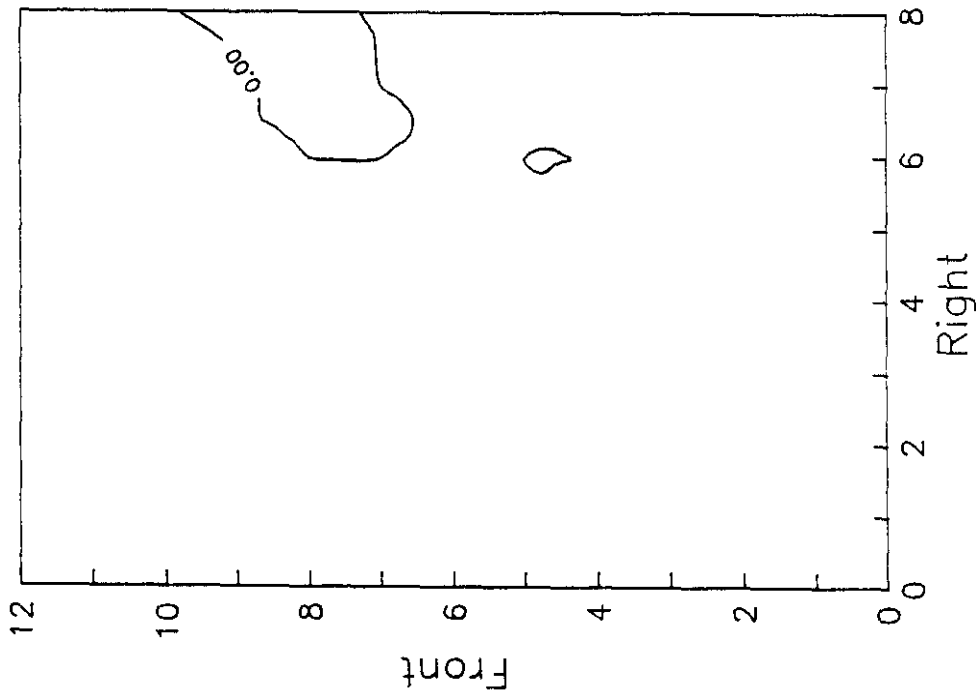


Figure 6-11

**SOUTHERN COMPANY SERVICES
LANSING SMITH #2 FLOW MODEL**

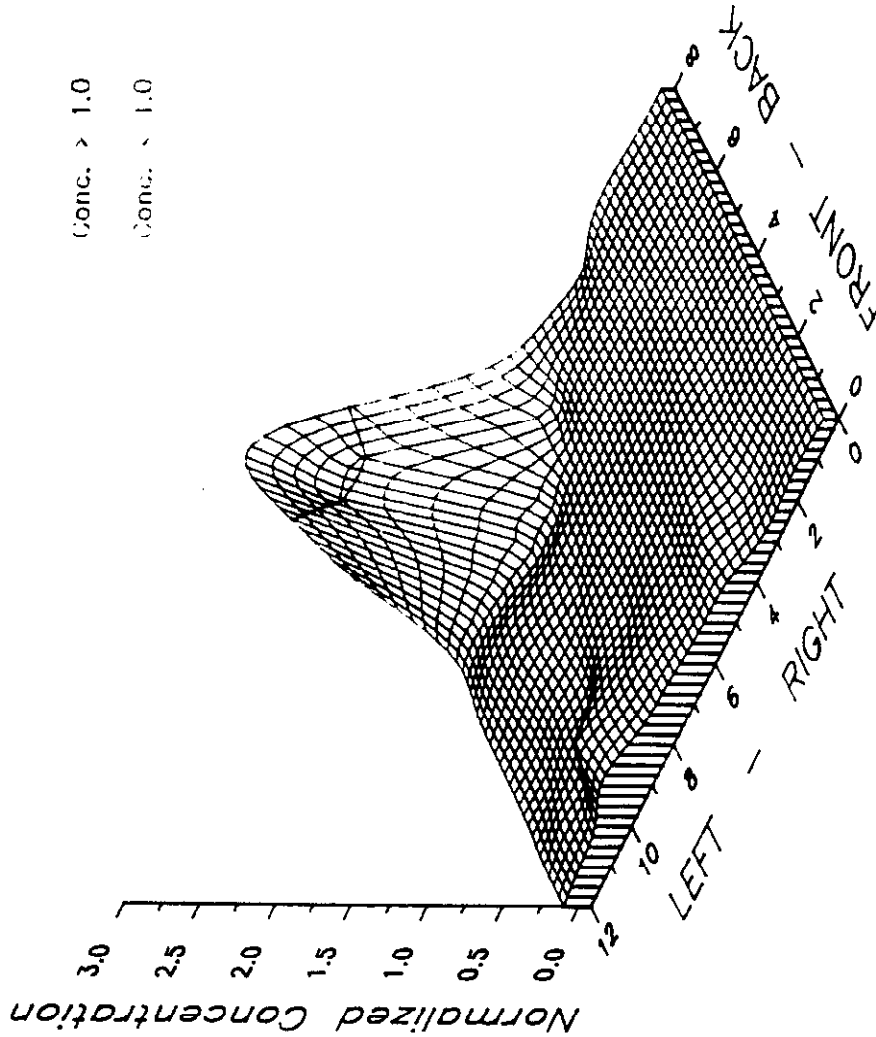
NORMALIZED METHANE CONCENTRATION

Test Plane: 1

Test Date: 2/8/91

Firing System: LNCFS-II

Test ID: Configuration #4



Conc. > 1.0

Conc. < 1.0

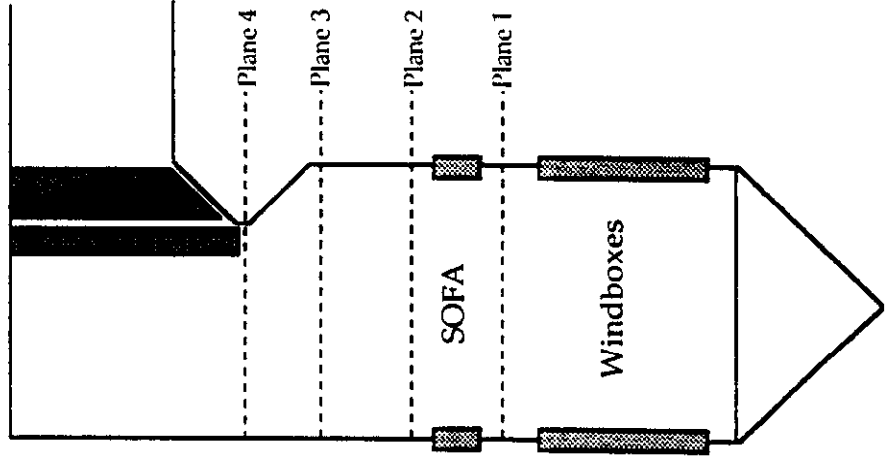


Figure 6-12

**SOUTHERN COMPANY SERVICES
LANSING SMITH #2 FLOW MODEL**

NORMALIZED METHANE CONCENTRATION

Test Plane: 1

Test Date: 2/8/91

Firing System: LNCFS-II

Test ID: Configuration #4

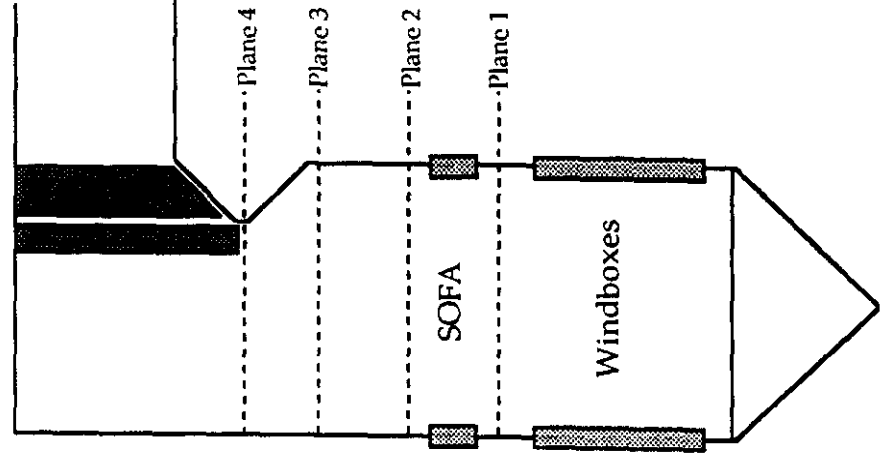
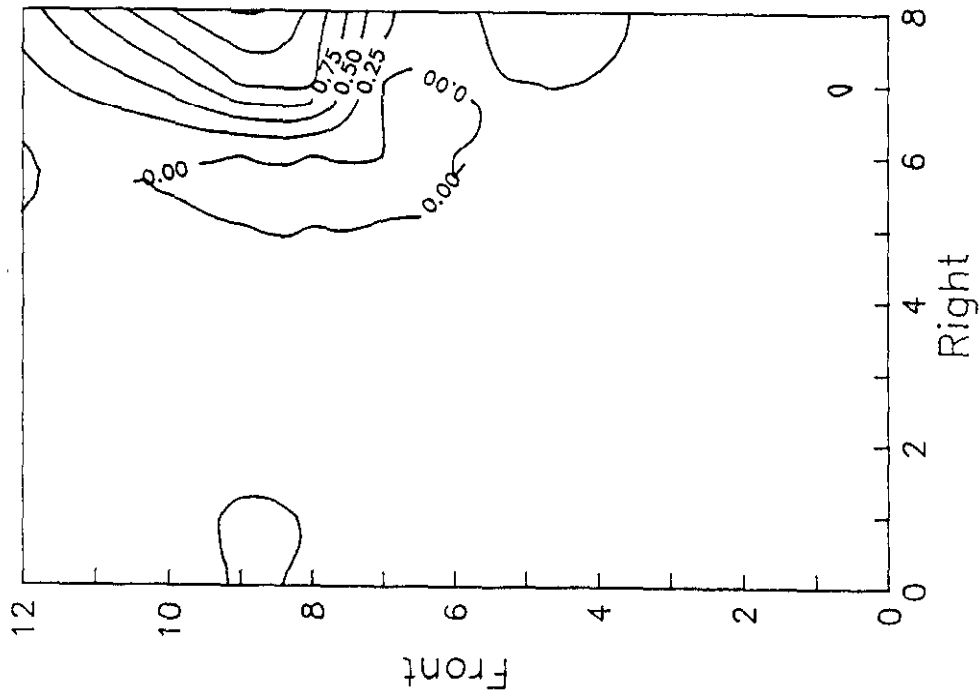


Figure 6-13

**SOUTHERN COMPANY SERVICES
LANSING SMITH #2 FLOW MODEL**

NORMALIZED METHANE CONCENTRATION

Test Plane: 1

Test Date: 2/14/91

Firing System: LNCFS-II

Test ID: Configuration #5

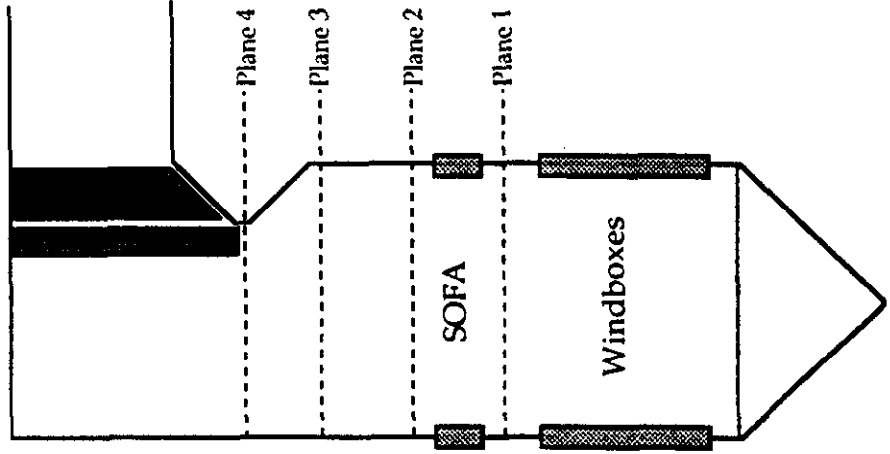
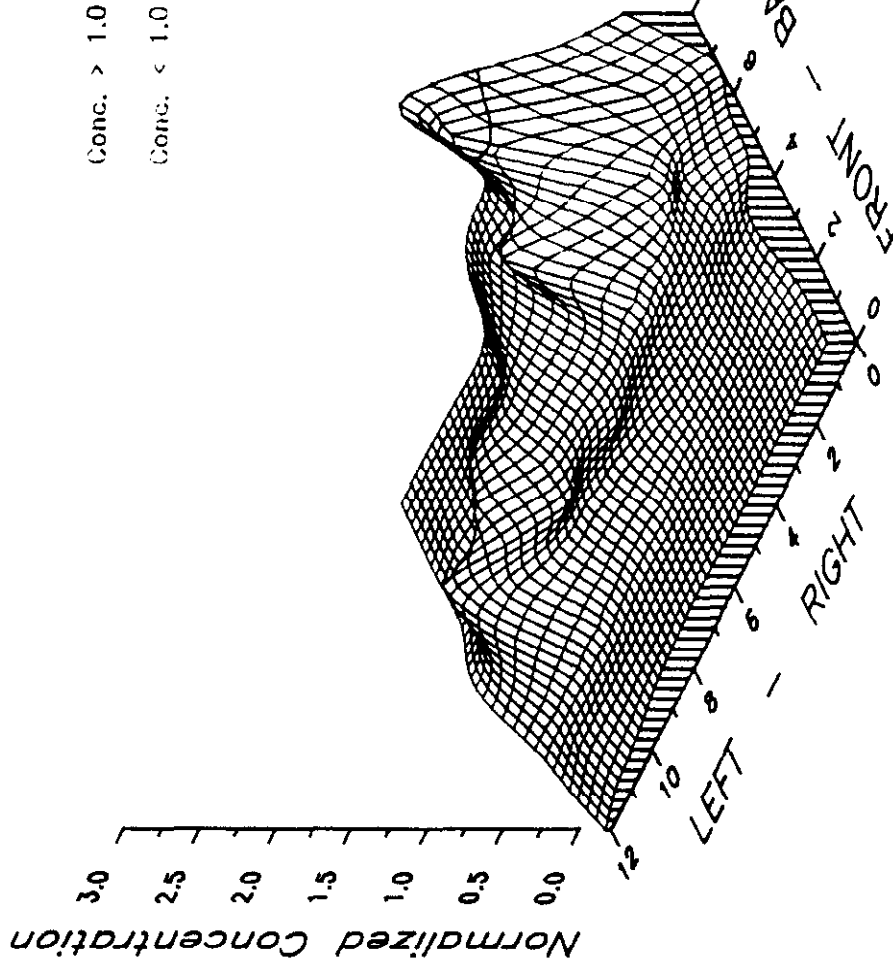


Figure 6-14

**SOUTHERN COMPANY SERVICES
LANSING SMITH #2 FLOW MODEL**

NORMALIZED METHANE CONCENTRATION

Test Plane: 1
 Test Date: 2/14/91
 Firing System: LNCFS-II
 Test ID: Configuration #5

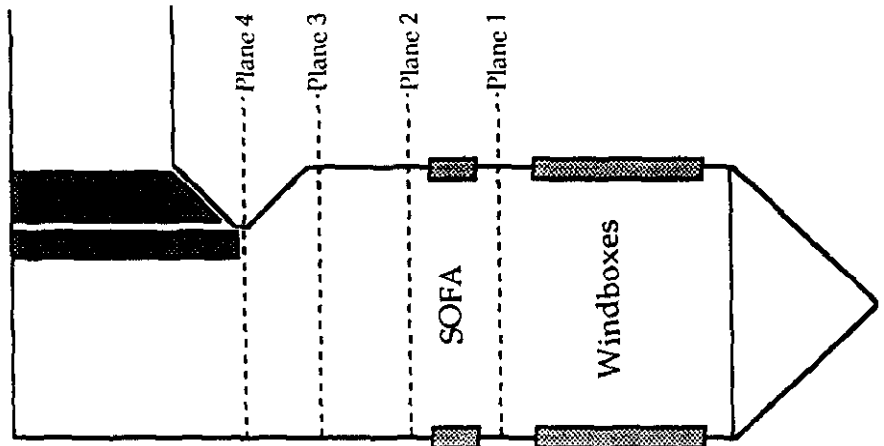
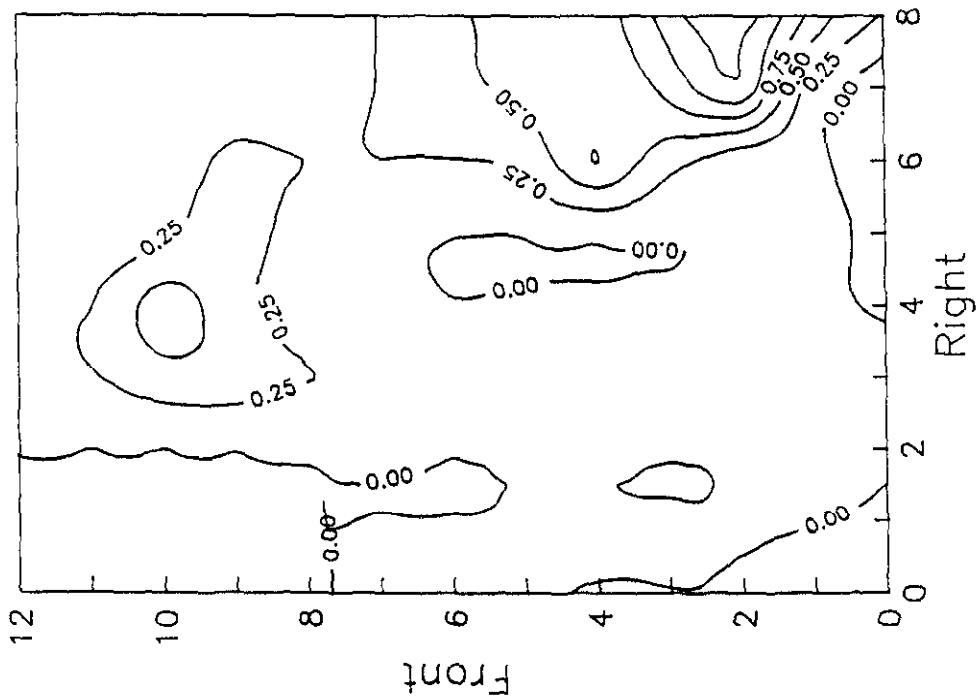


Figure 6-15

**SOUTHERN COMPANY SERVICES
 LANSING SMITH #2 FLOW MODEL**

NORMALIZED METHANE CONCENTRATION

Test Plane: 1
 Test Date: 2/12/91
 Firing System: LNCFS-II
 Test ID: Configuration #1

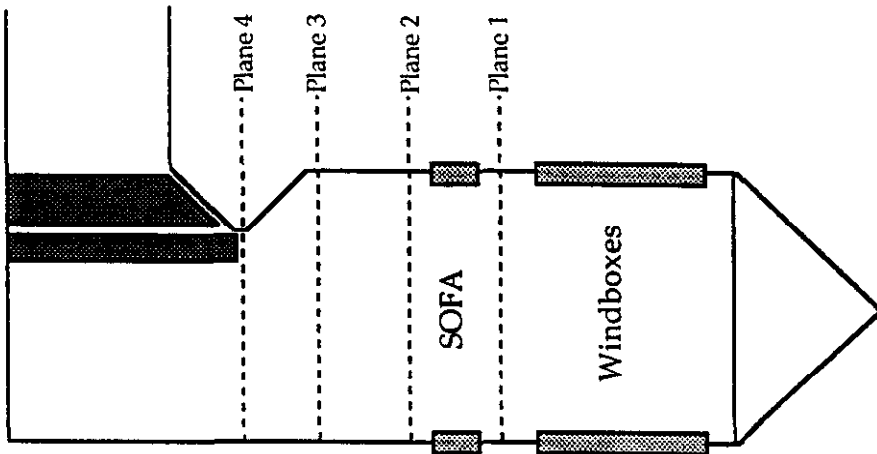
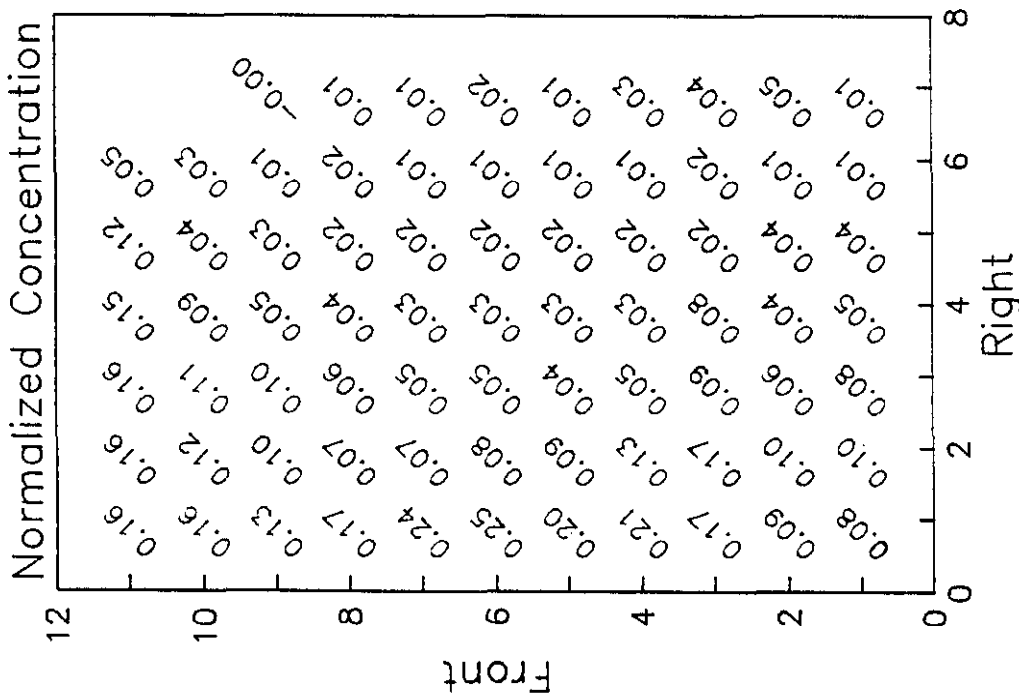


Figure 6-16

**SOUTHERN COMPANY SERVICES
 LANSING SMITH #2 FLOW MODEL**

NORMALIZED METHANE CONCENTRATION

Test Plane: 1
 Test Date: 2/8/91
 Firing System: LNCFS-II
 Test ID: Configuration #4

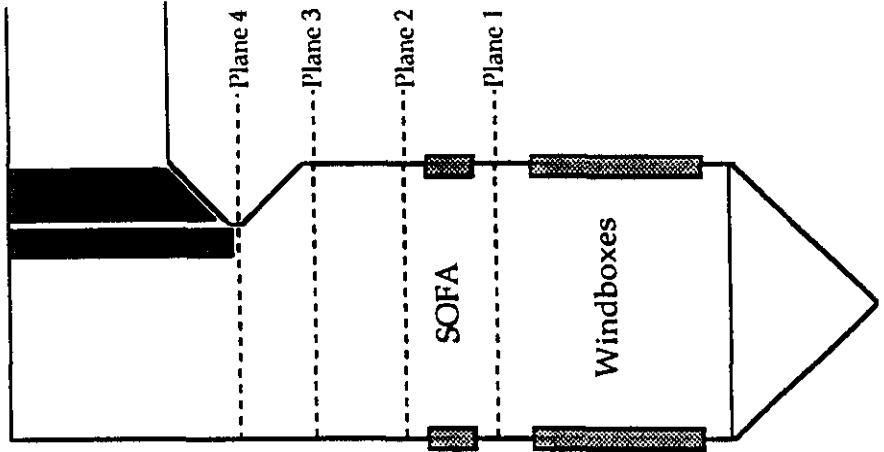
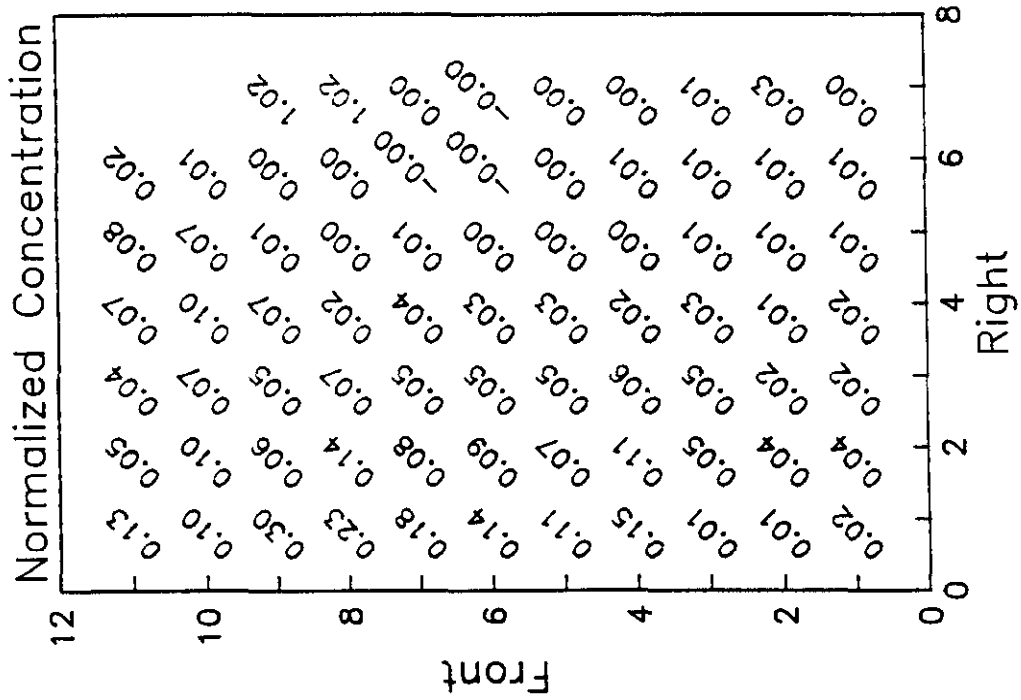


Figure 6-19

**SOUTHERN COMPANY SERVICES
 LANSING SMITH #2 FLOW MODEL**

NORMALIZED METHANE CONCENTRATION

Test Plane: 1
 Test Date: 2/14/91
 Firing System: LNCFS-II
 Test ID: Configuration #5

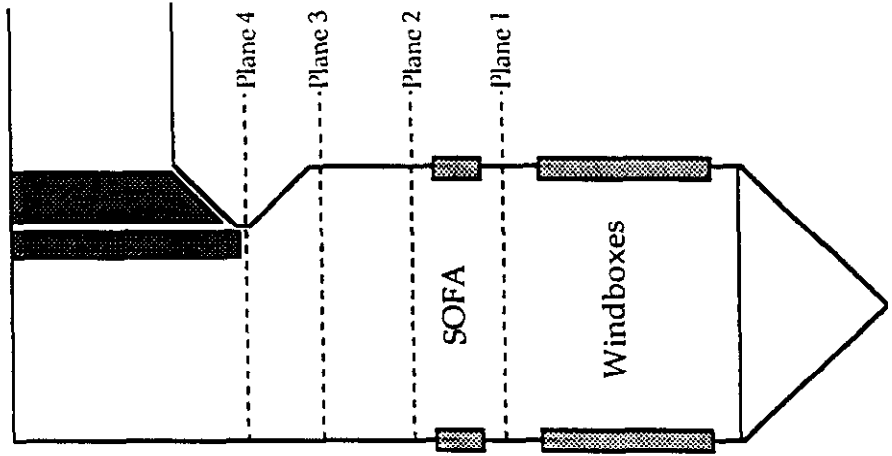
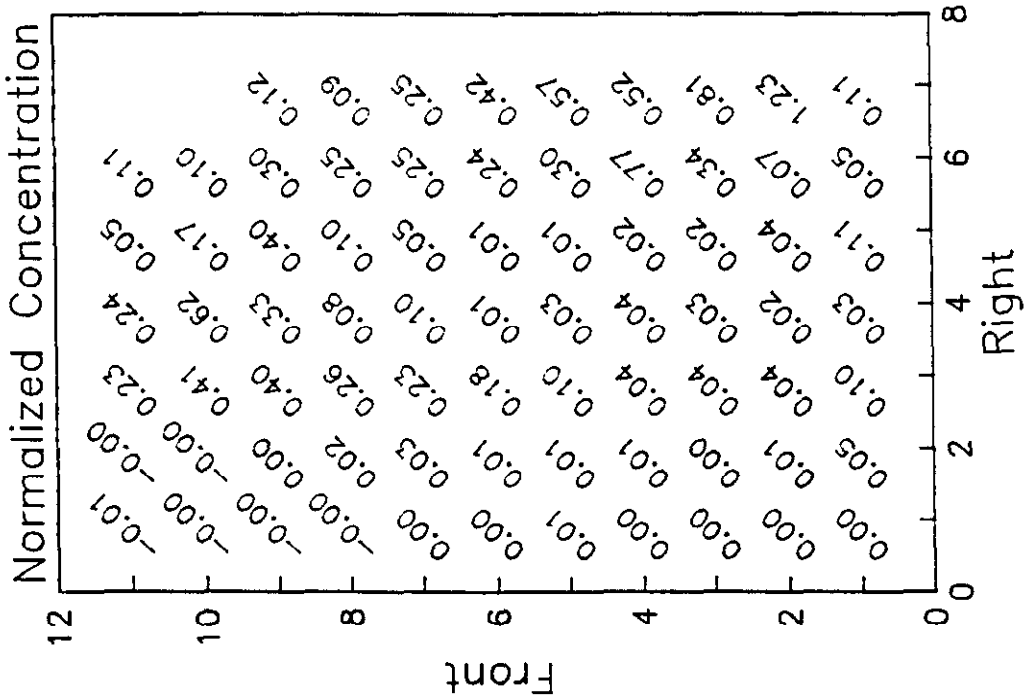


Figure 6-20

**SOUTHERN COMPANY SERVICES
 LANSING SMITH #2 FLOW MODEL**

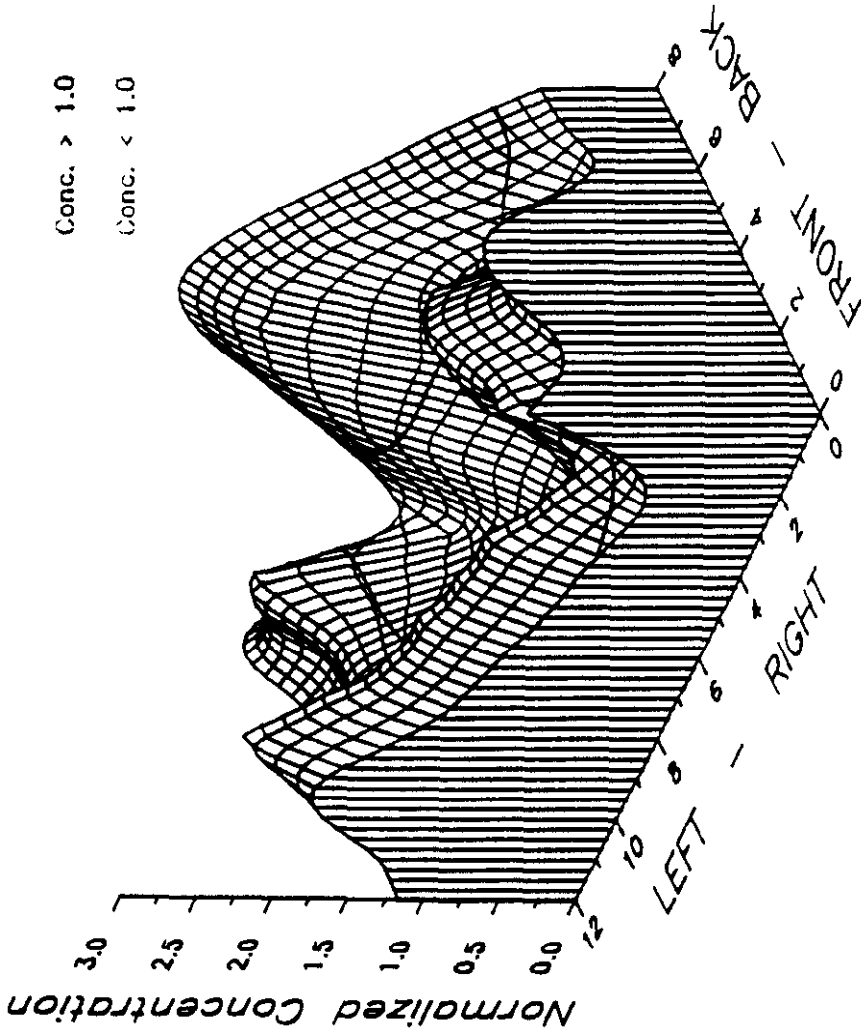
NORMALIZED METHANE CONCENTRATION

Test Plane: 2

Test Date: 2/12/91

Firing System: LNCFS-II

Test ID: Configuration #1



Conc. > 1.0

Conc. < 1.0

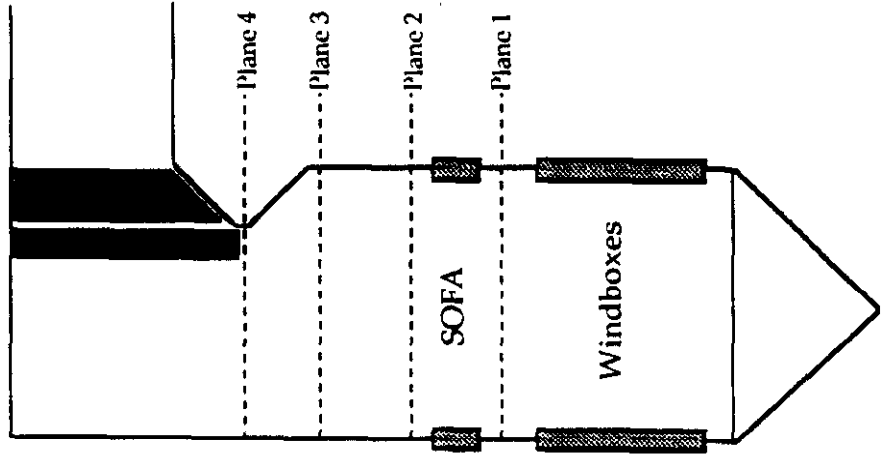
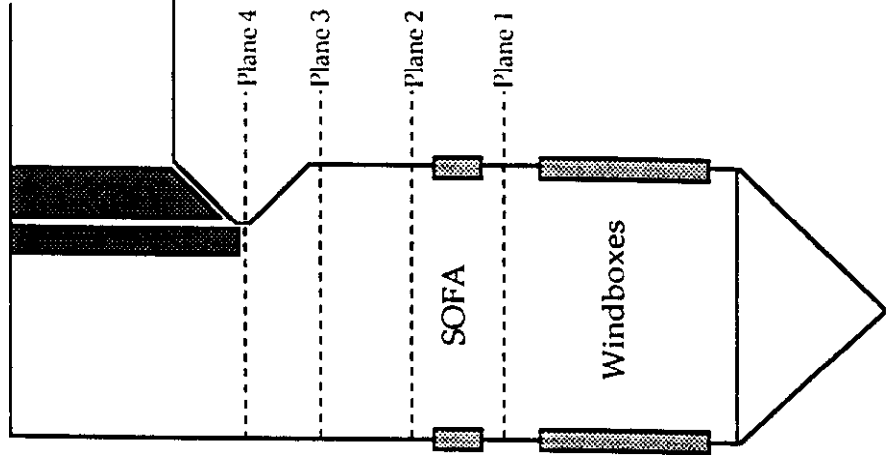
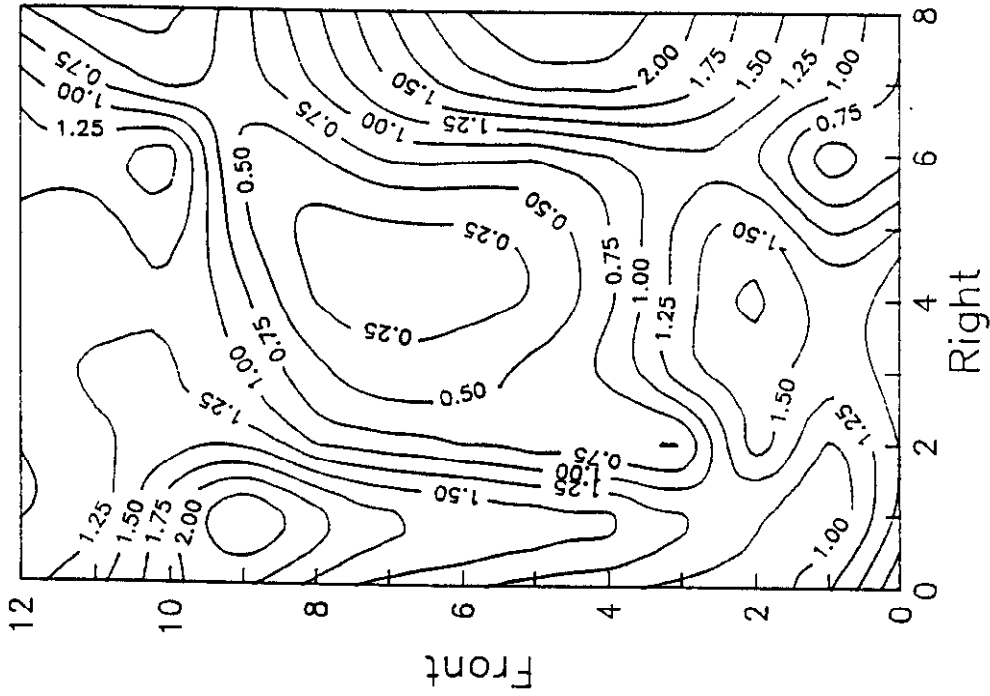


Figure 6-21

**SOUTHERN COMPANY SERVICES
LANSING SMITH #2 FLOW MODEL**

NORMALIZED METHANE CONCENTRATION

Test Plane: 2
 Test Date: 2/12/91
 Firing System: LNCFS-II
 Test ID: Configuration #1

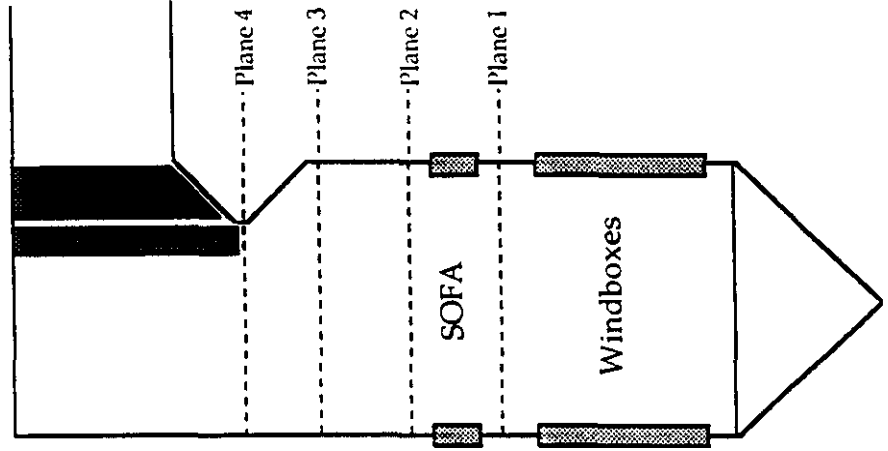
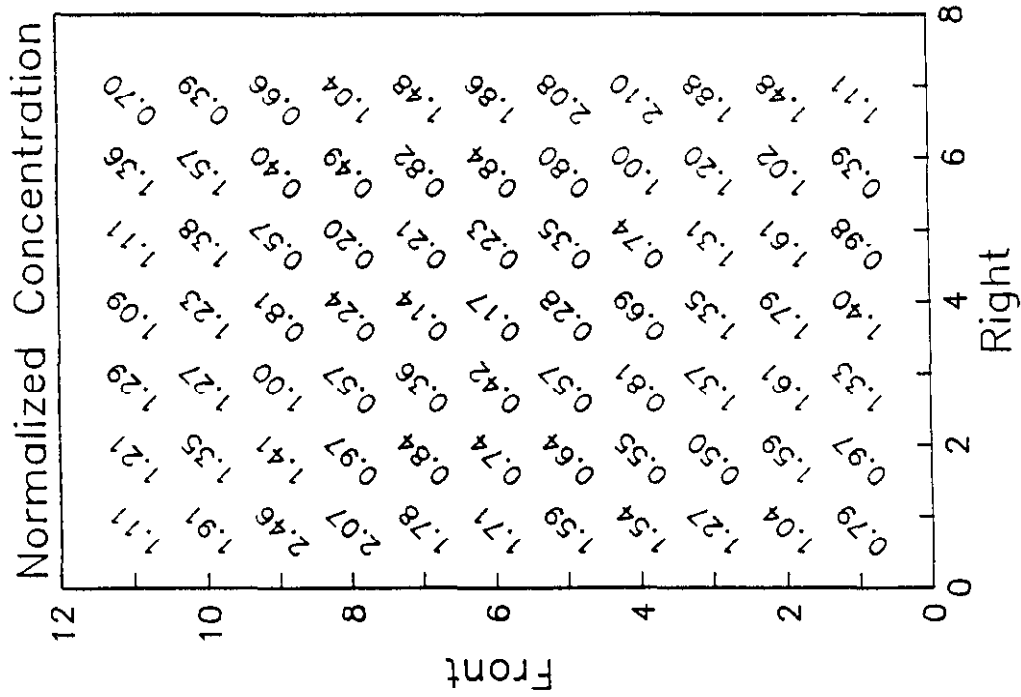


**SOUTHERN COMPANY SERVICES
 LANSING SMITH #2 FLOW MODEL**

Figure 6-22

NORMALIZED METHANE CONCENTRATION

Test Plane: 2
 Test Date: 2/12/91
 Firing System: LNCFS-II
 Test ID: Configuration #1



**SOUTHERN COMPANY SERVICES
 LANSING SMITH #2 FLOW MODEL**

Figure 6-23

NORMALIZED METHANE CONCENTRATION

Test Plane: 2

Test Date: 2/13/91

Firing System: LNCFS-II

Test ID: Configuration #2

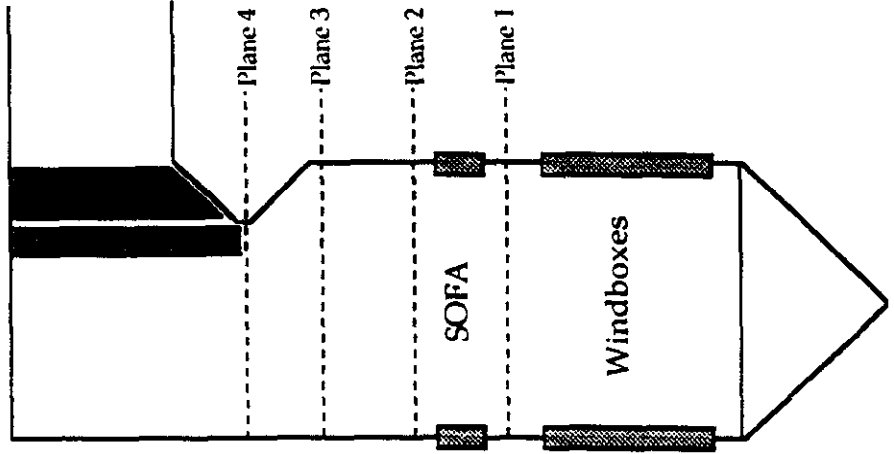
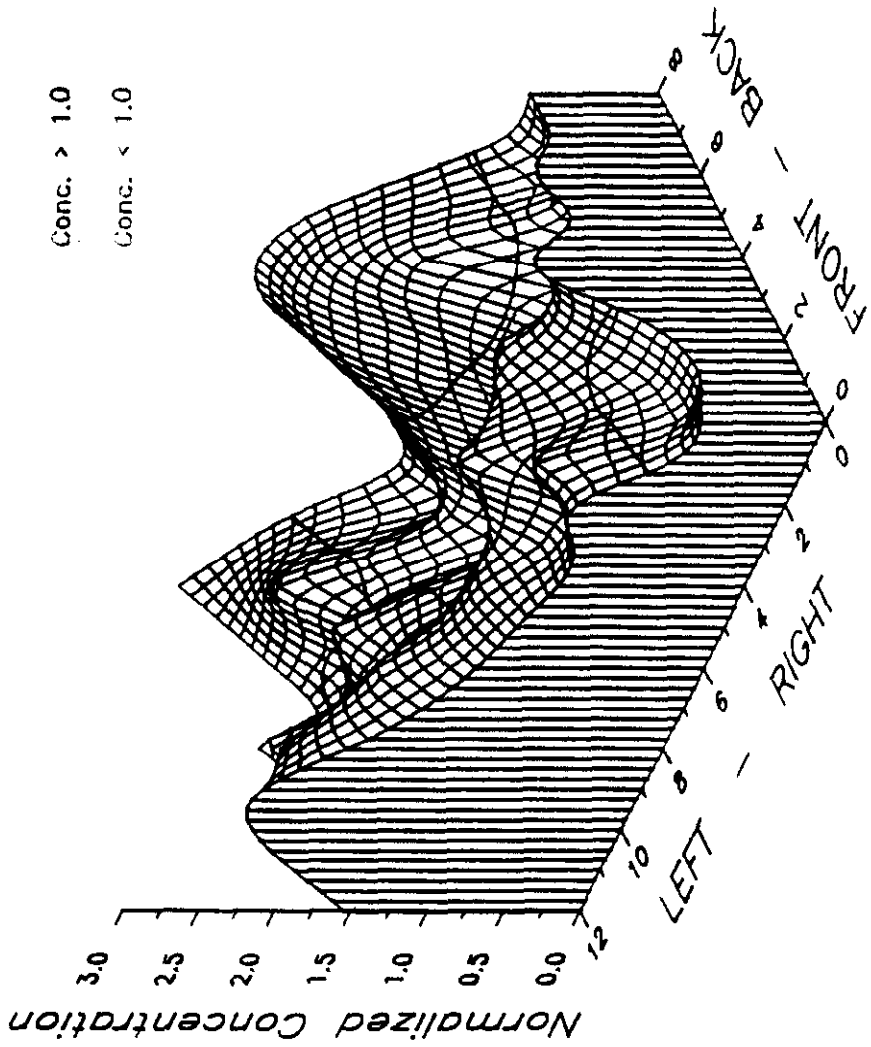


Figure 6-24

**SOUTHERN COMPANY SERVICES
LANSING SMITH #2 FLOW MODEL**

NORMALIZED METHANE CONCENTRATION

Test Plane: 2
Test Date: 2/13/91
Firing System: LNCFS-II
Test ID: Configuration #2

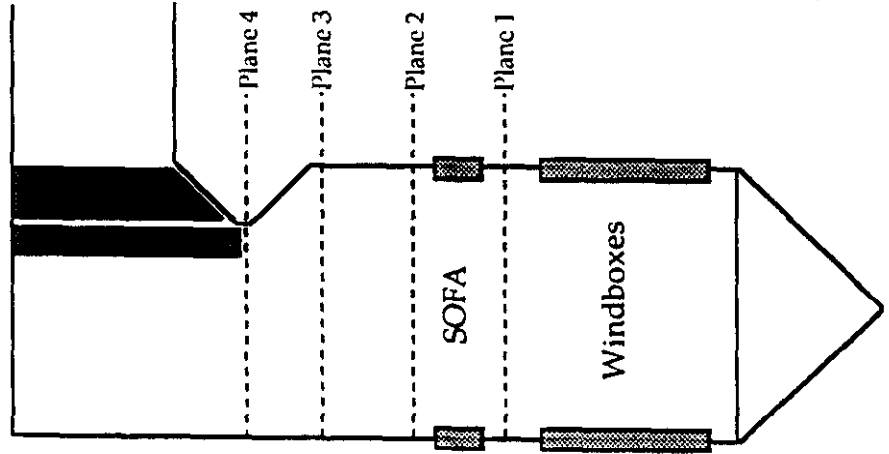
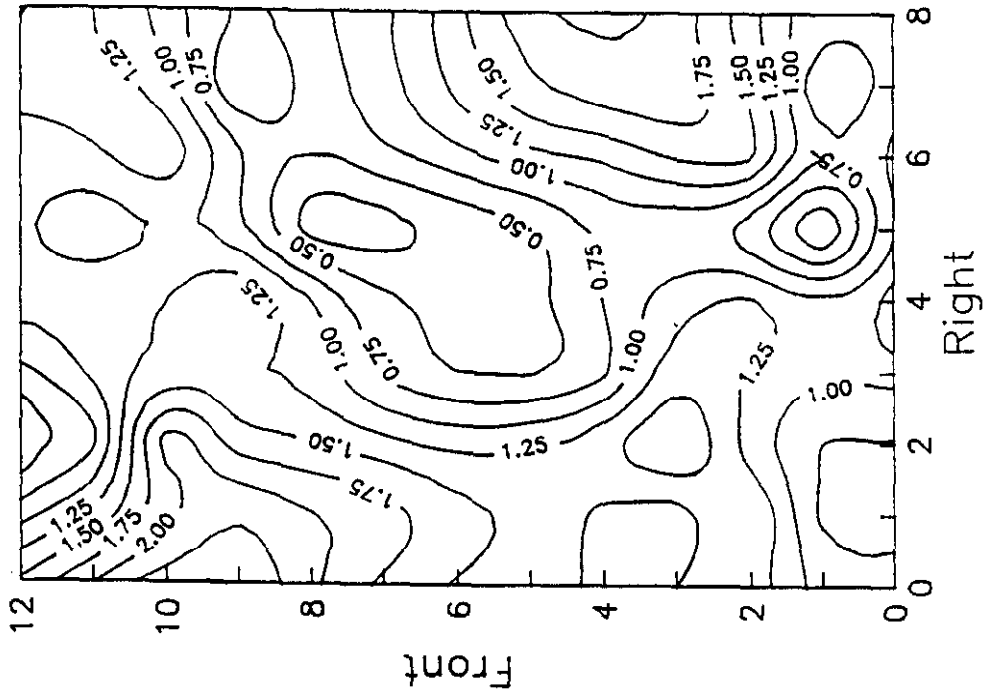


Figure 6-25
**SOUTHERN COMPANY SERVICES
LANSING SMITH #2 FLOW MODEL**

NORMALIZED METHANE CONCENTRATION

Test Plane: 2
 Test Date: 2/13/91
 Firing System: LNCFS-II
 Test ID: Configuration #2

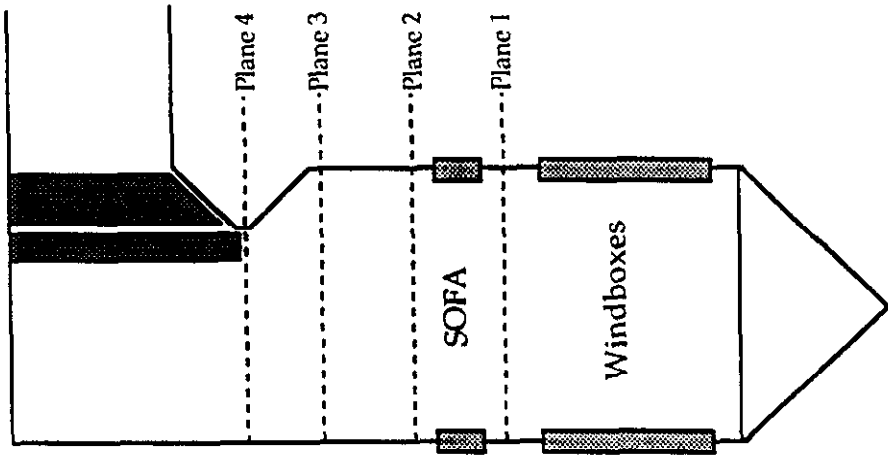
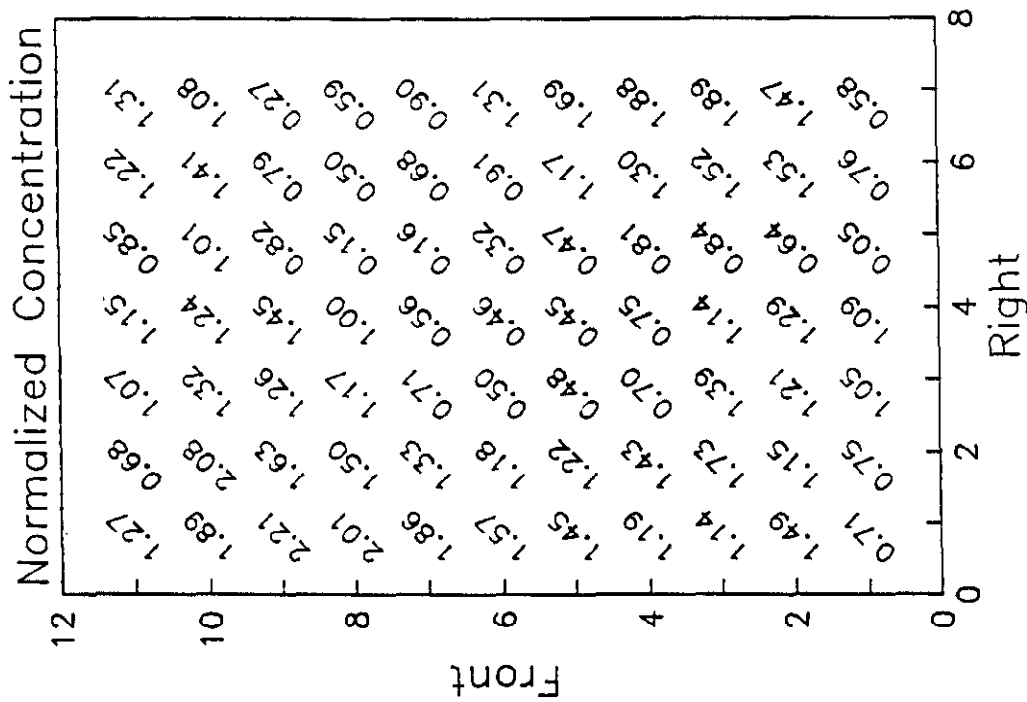


Figure 6-26

**SOUTHERN COMPANY SERVICES
 LANSING SMITH #2 FLOW MODEL**

NORMALIZED METHANE CONCENTRATION

Test Plane: 2

Test Date: 2/13/91

Firing System: LNCFS-II

Test ID: Configuration #3

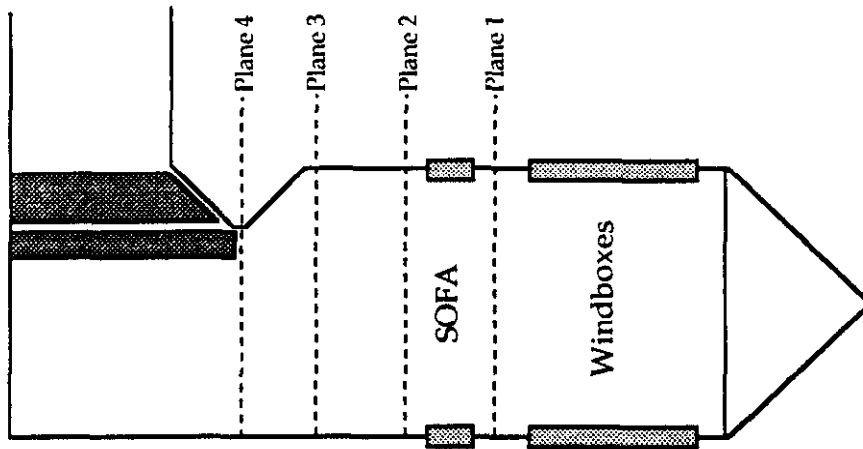
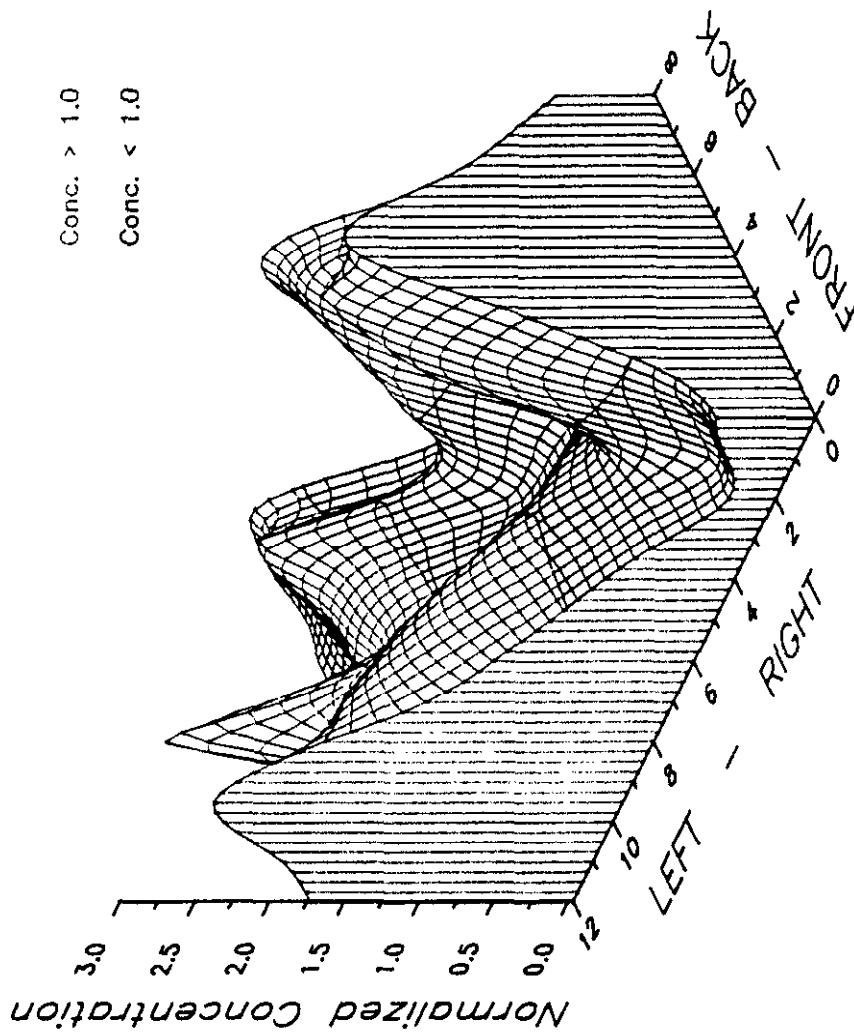


Figure 6-27

SOUTHERN COMPANY SERVICES LANSING SMITH #2 FLOW MODEL

NORMALIZED METHANE CONCENTRATION

Test Plane: 2

Test Date: 2/13/91

Firing System: LNCFS-II

Test ID: Configuration #3

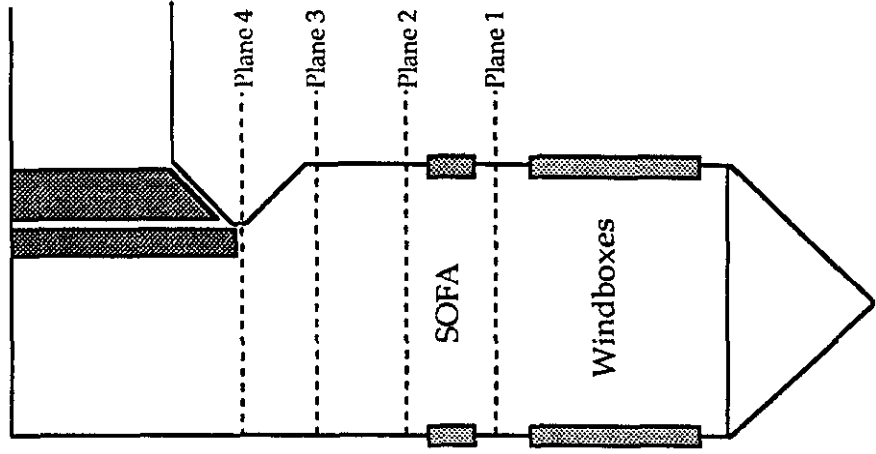
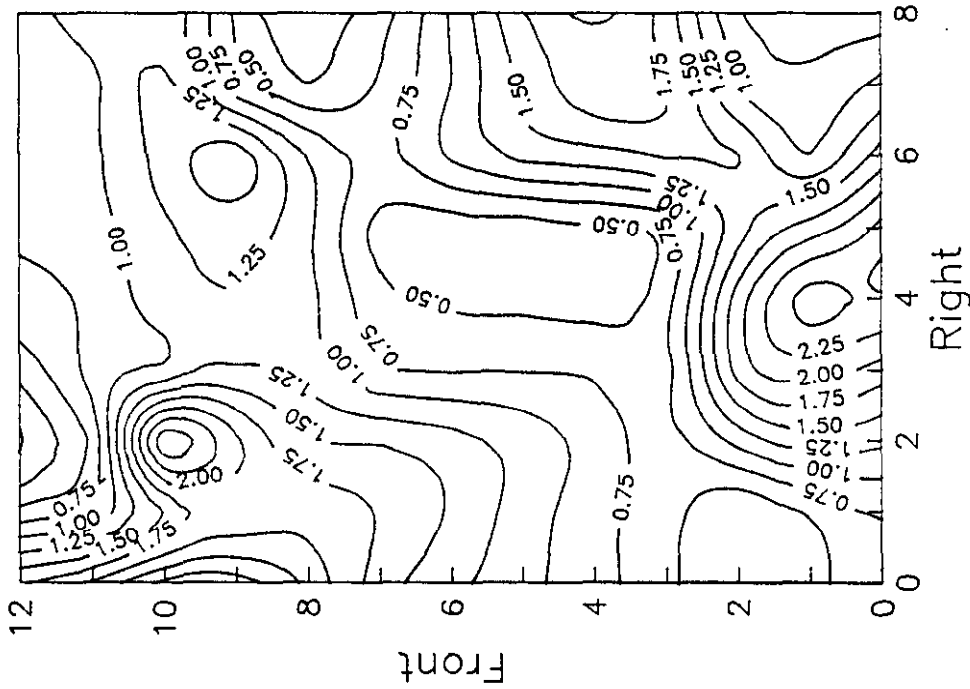


Figure 6-28

**SOUTHERN COMPANY SERVICES
LANSING SMITH #2 FLOW MODEL**

NORMALIZED METHANE CONCENTRATION

Test Plane: 2
 Test Date: 2/13/91
 Firing System: LNCFS-II
 Test ID: Configuration #3

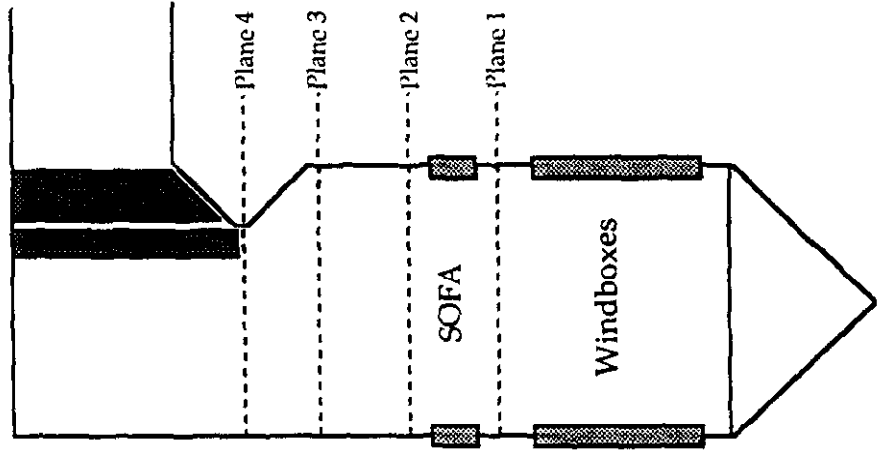
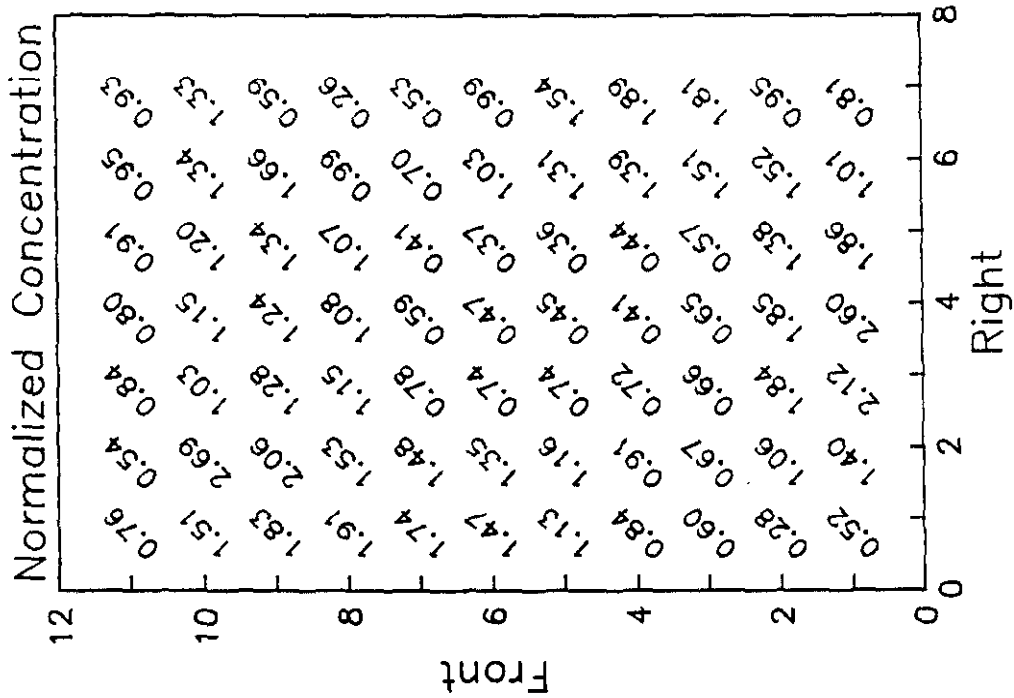


Figure 6-29
**SOUTHERN COMPANY SERVICES
 LANSING SMITH #2 FLOW MODEL**

NORMALIZED METHANE CONCENTRATION

Test Plane: 2

Test Date: 2/8/91

Firing System: LNCFS-II

Test ID: Configuration #4

Conc. > 1.0

Conc. < 1.0

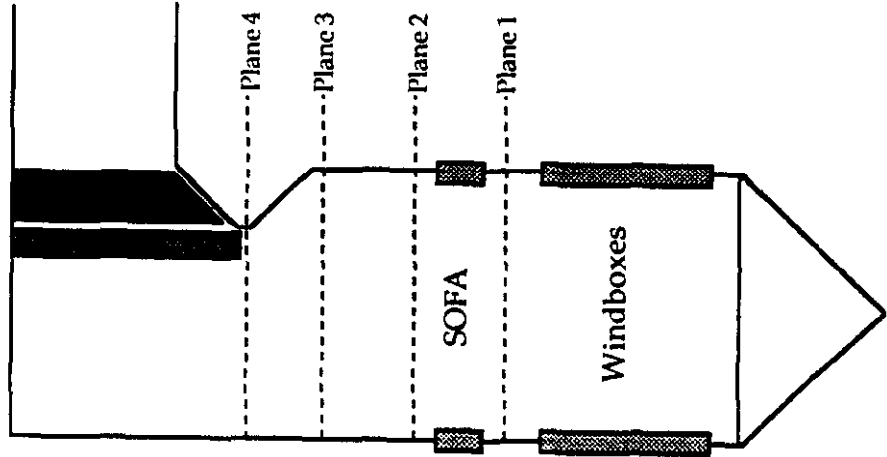
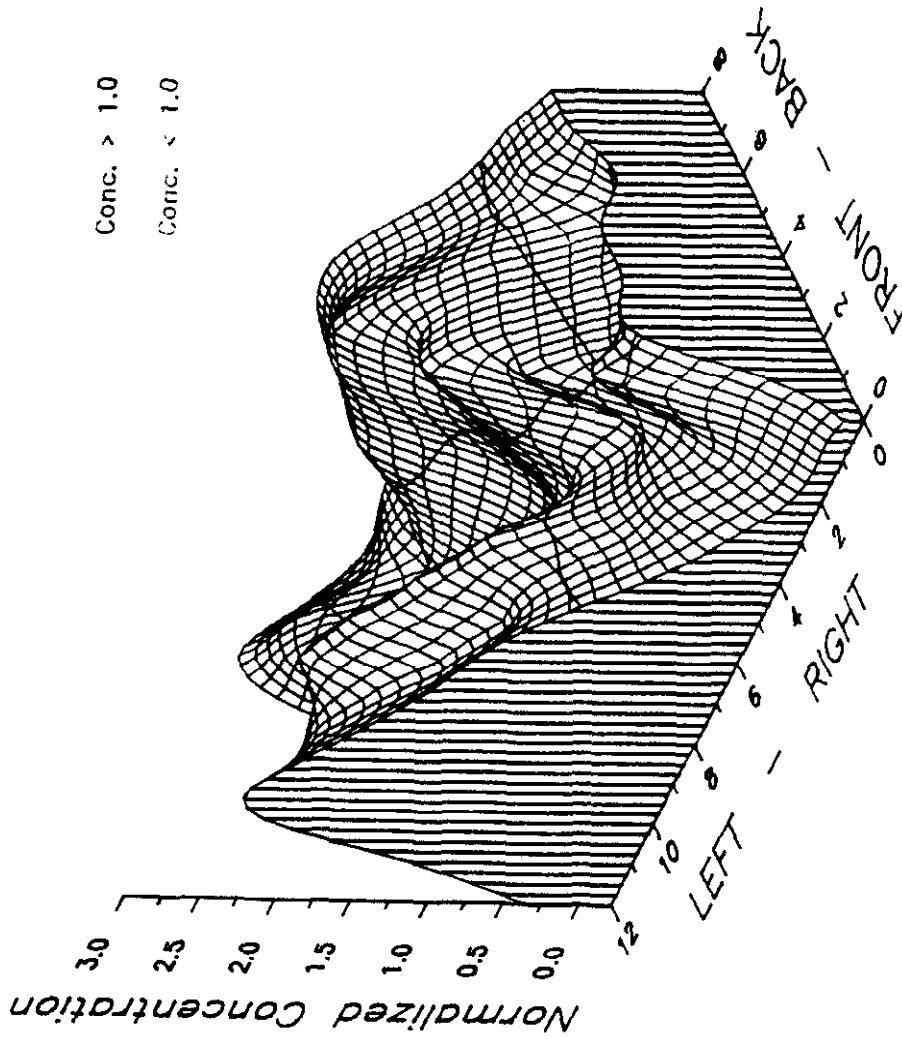


Figure 6-30

SOUTHERN COMPANY SERVICES LANSING SMITH #2 FLOW MODEL

NORMALIZED METHANE CONCENTRATION

Test Plane: 2

Test Date: 2/8/91

Firing System: LNCFS-II

Test ID: Configuration #4

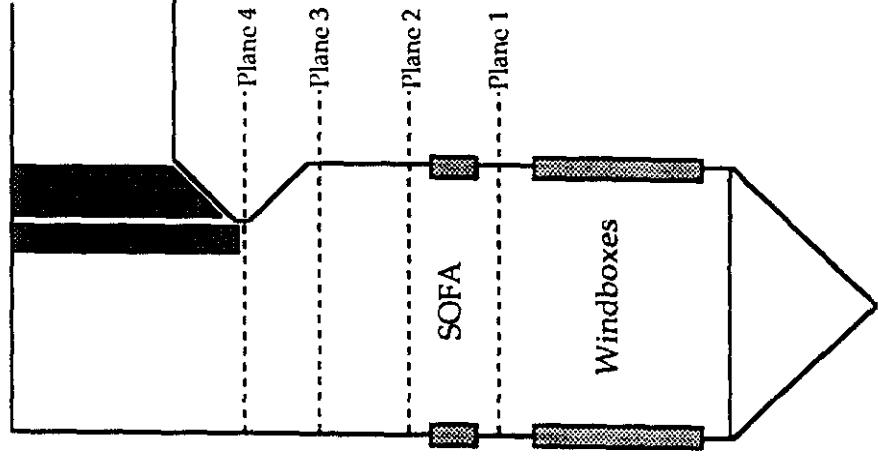
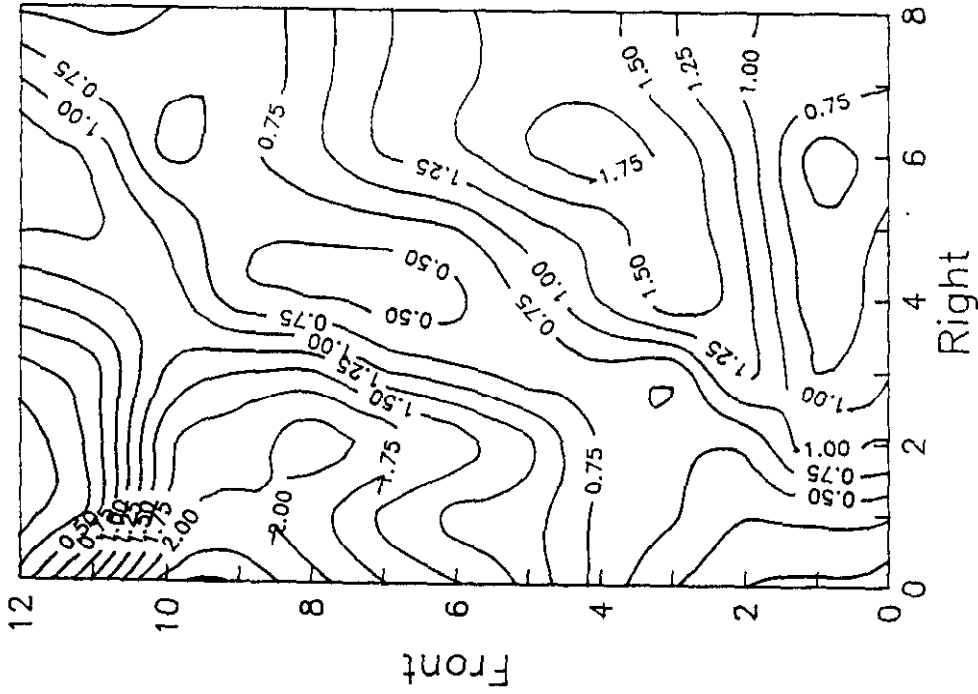


Figure 6-31

**SOUTHERN COMPANY SERVICES
LANSING SMITH #2 FLOW MODEL**

NORMALIZED METHANE CONCENTRATION

Test Plane: 2
 Test Date: 2/8/91
 Firing System: LNCFS-II
 Test ID: Configuration #4

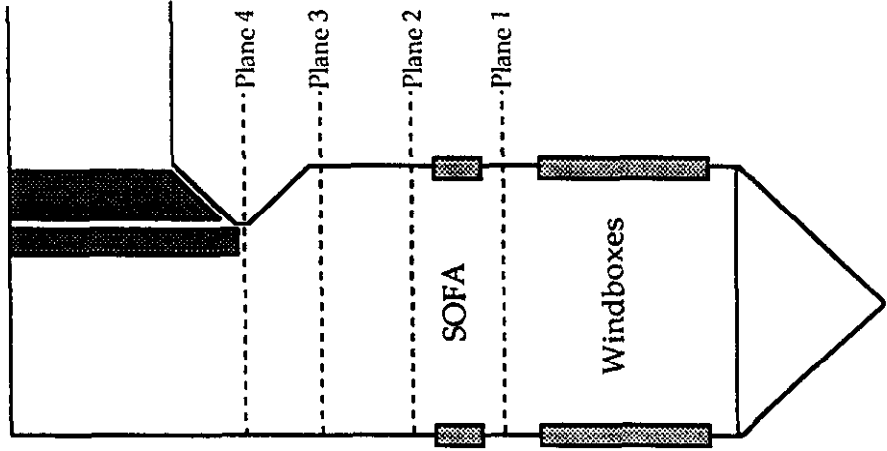
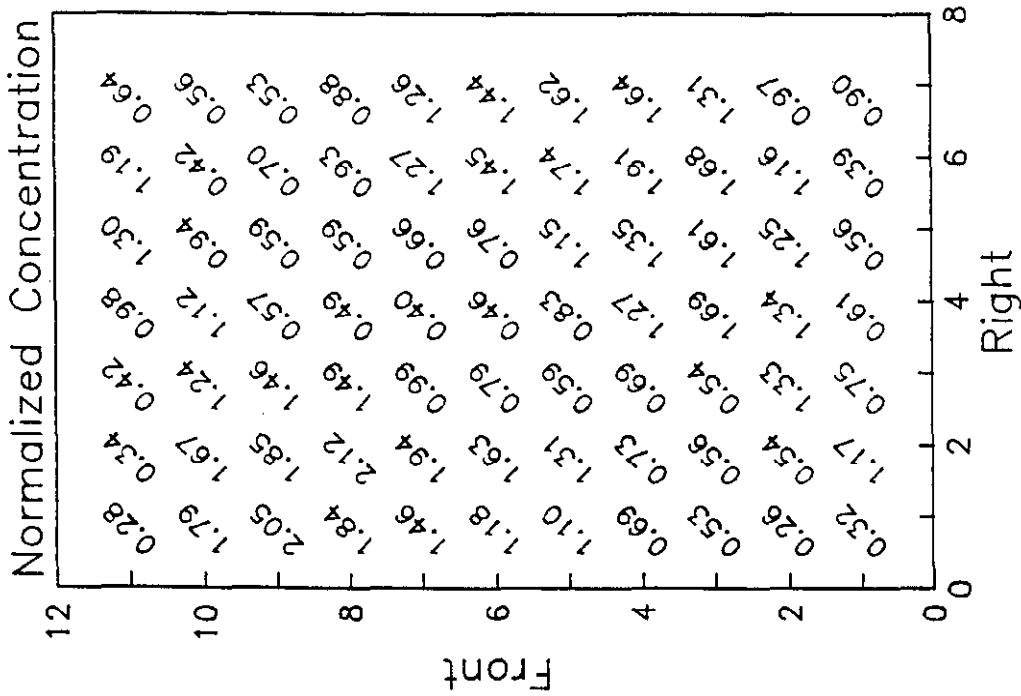


Figure 6-32

**SOUTHERN COMPANY SERVICES
 LANSING SMITH #2 FLOW MODEL**

NORMALIZED METHANE CONCENTRATION

Test Plane: 2

Test Date: 2/14/91

Firing System: LNCFS-II

Test ID: Configuration #5

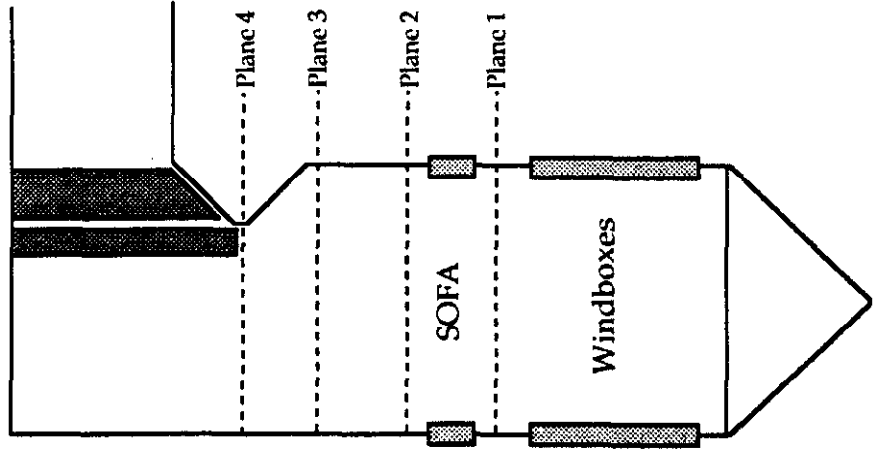
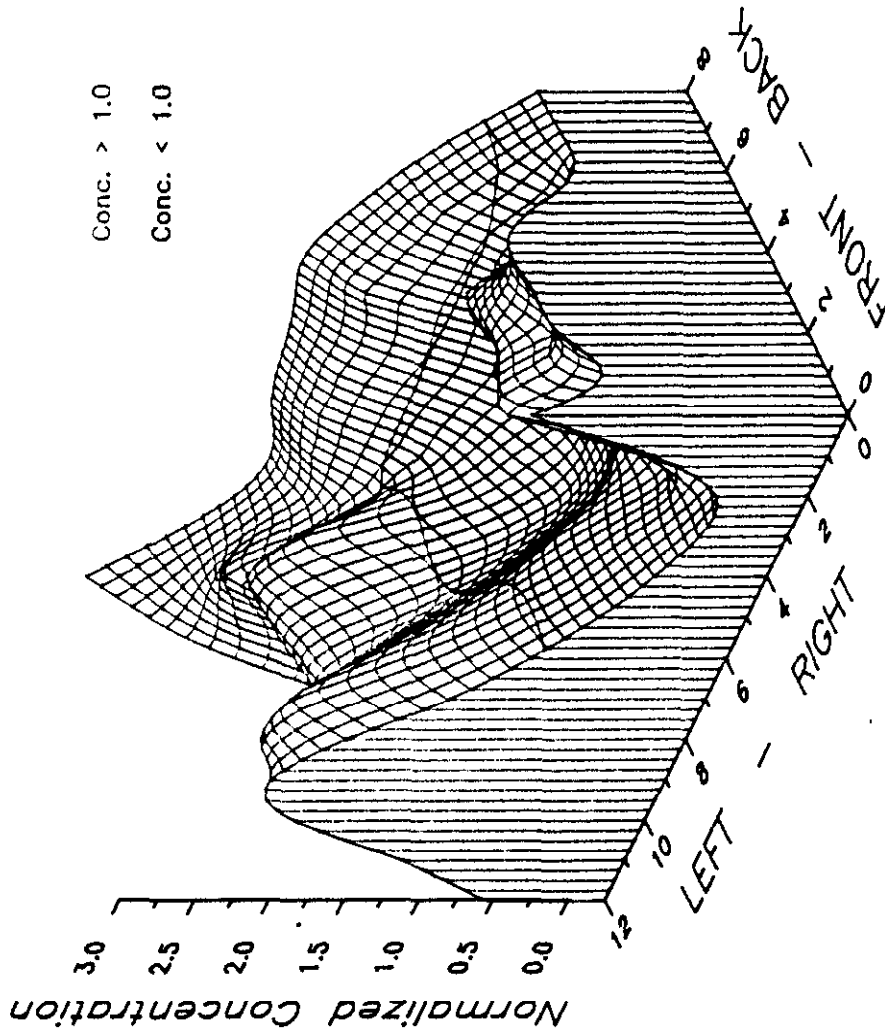


Figure 6-33

**SOUTHERN COMPANY SERVICES
LANSING SMITH #2 FLOW MODEL**

NORMALIZED METHANE CONCENTRATION

Test Plane: 2
 Test Date: 2/14/91
 Firing System: LNCFS-II
 Test ID: Configuration #5

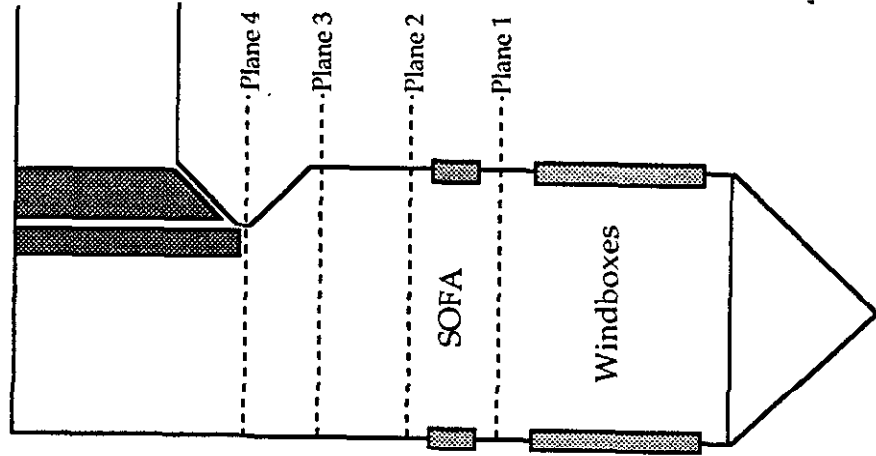
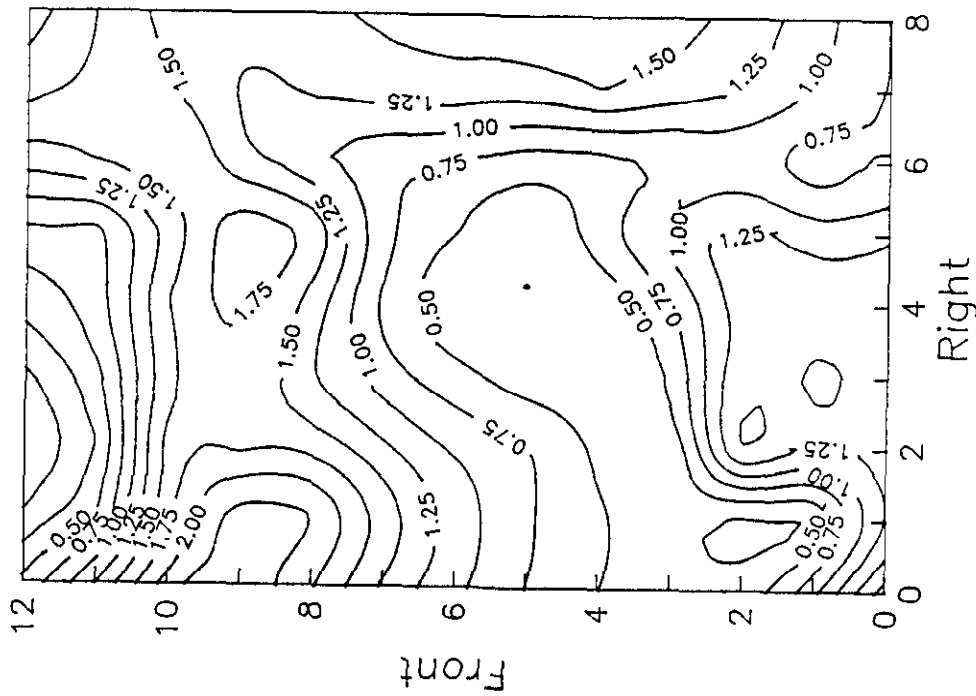


Figure 6-34
**SOUTHERN COMPANY SERVICES
 LANSING SMITH #2 FLOW MODEL**

NORMALIZED METHANE CONCENTRATION

Test Plane: 2
 Test Date: 2/14/91
 Firing System: LNCFS-II
 Test ID: Configuration #5

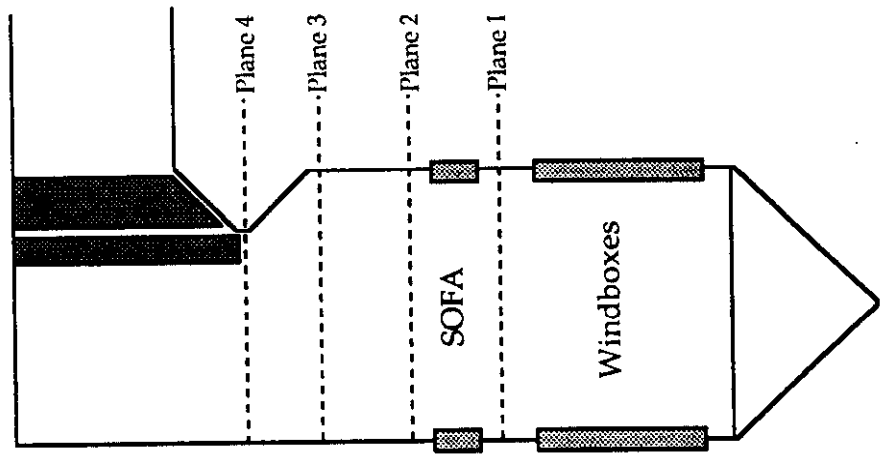
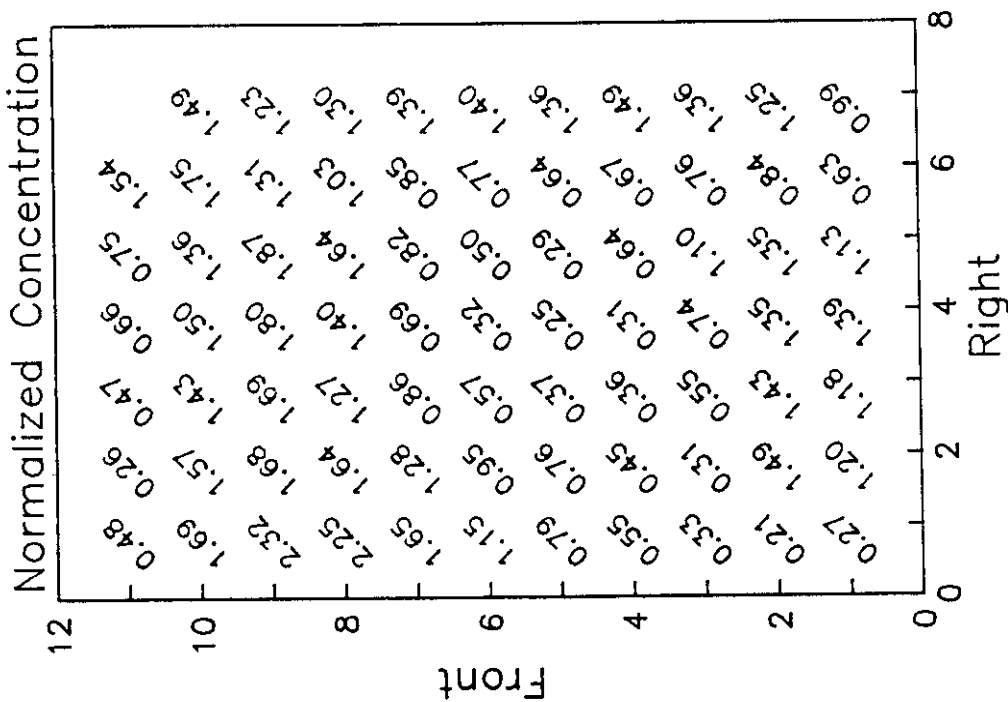
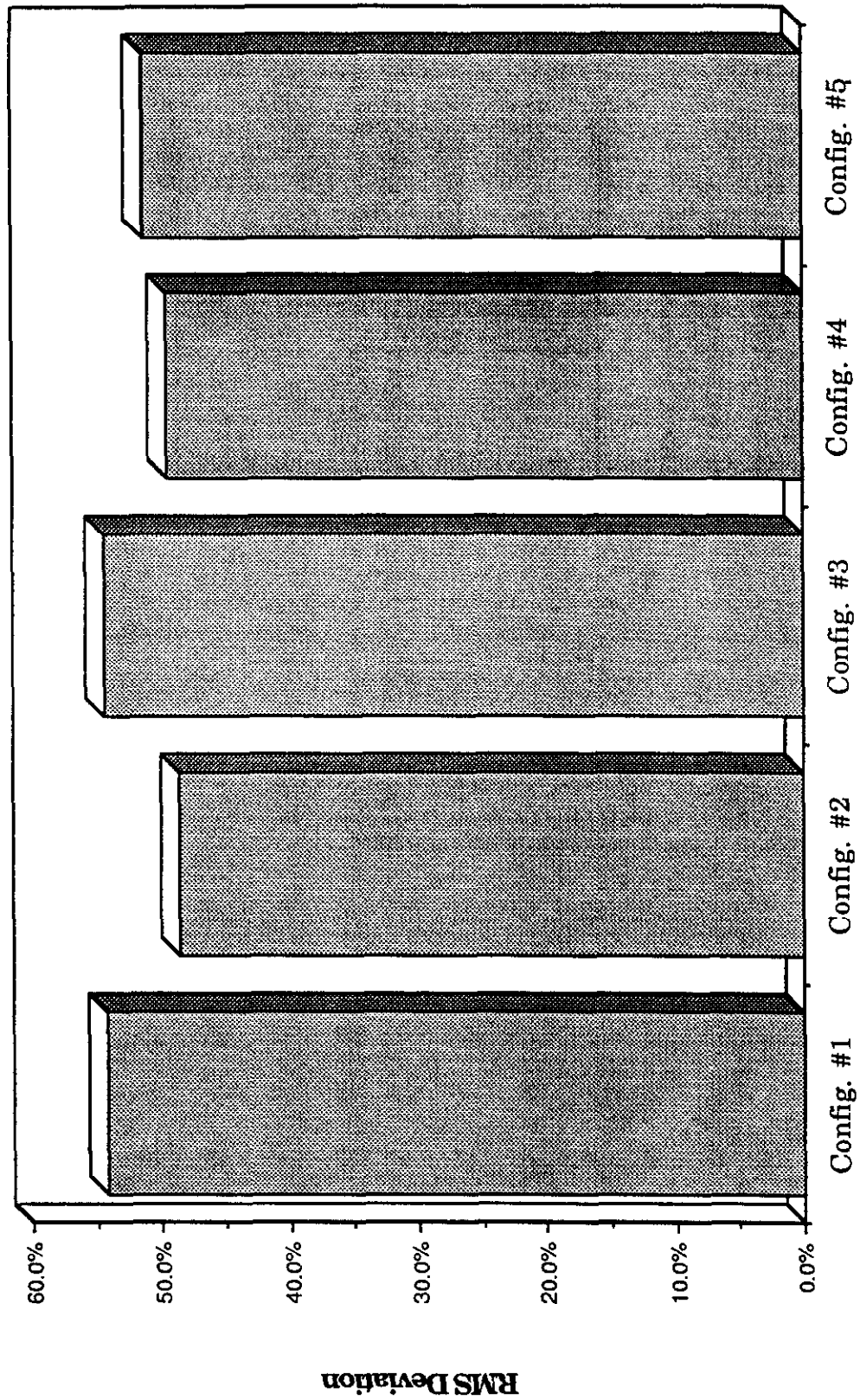


Figure 6-35

**SOUTHERN COMPANY SERVICES
 LANSING SMITH #2 FLOW MODEL**

ABB Combustion Engineering, Inc.
 Kreisinger Development Laboratory
 Mechanical Systems Engineering

**Lansing Smith Flow Model
Methane RMS Deviation - Plane 2**



Test Identification

Figure 6-36

NORMALIZED METHANE CONCENTRATION

Test Plane: 3

Test Date: 2/12/91

Firing System: LNCFS-II

Test ID: Configuration #1

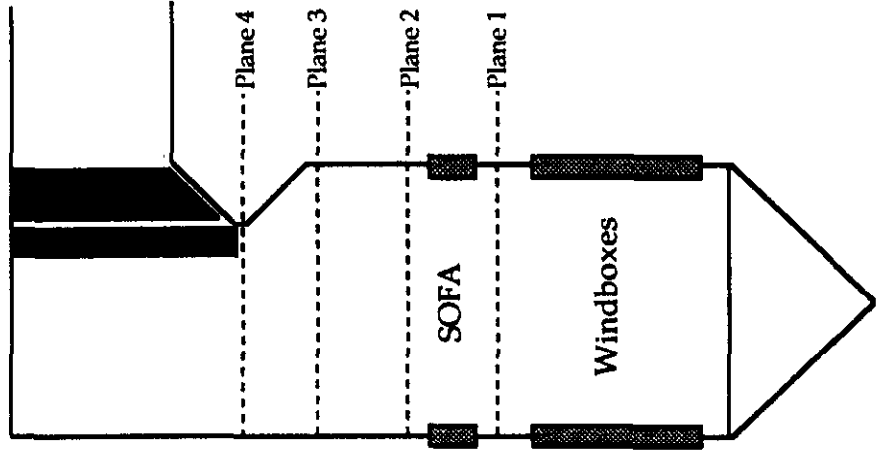
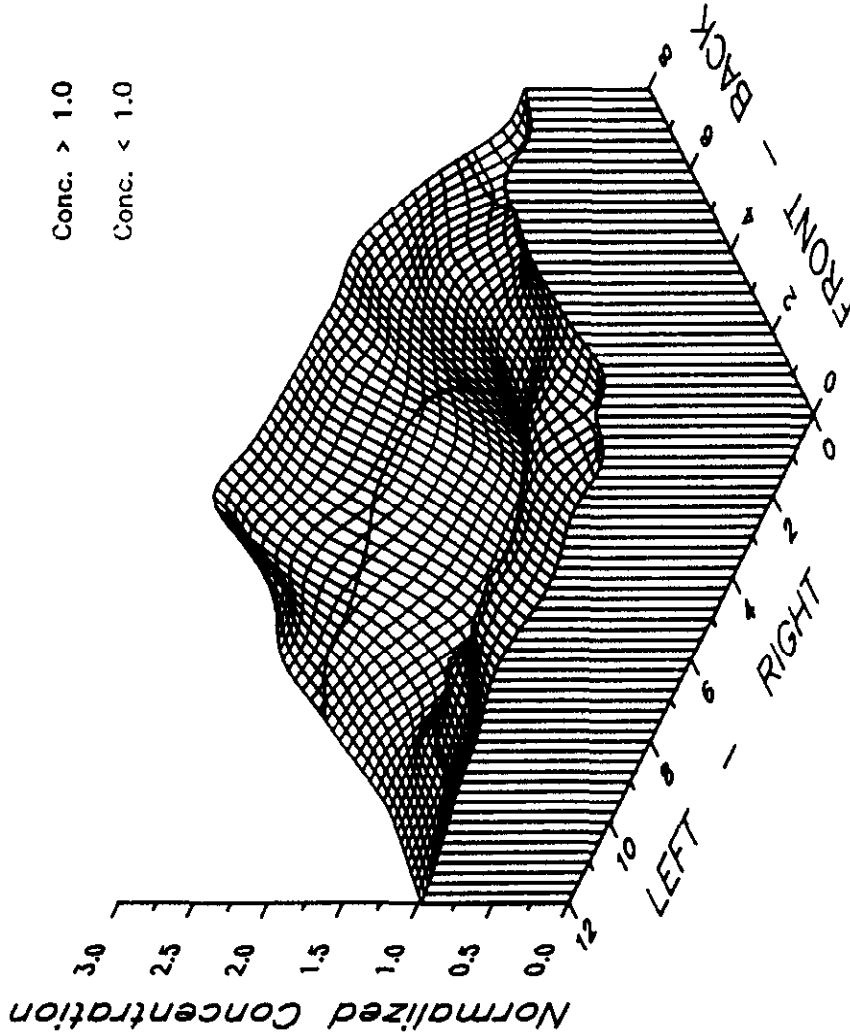


Figure 6--37

SOUTHERN COMPANY SERVICES LANSING SMITH #2 FLOW MODEL

NORMALIZED METHANE CONCENTRATION

Test Plane: 3
 Test Date: 2/12/91
 Firing System: LNCFS-II
 Test ID: Configuration #1

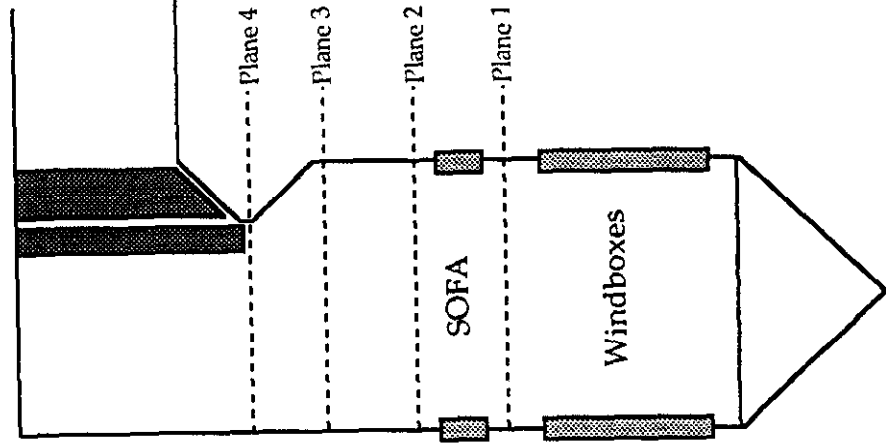
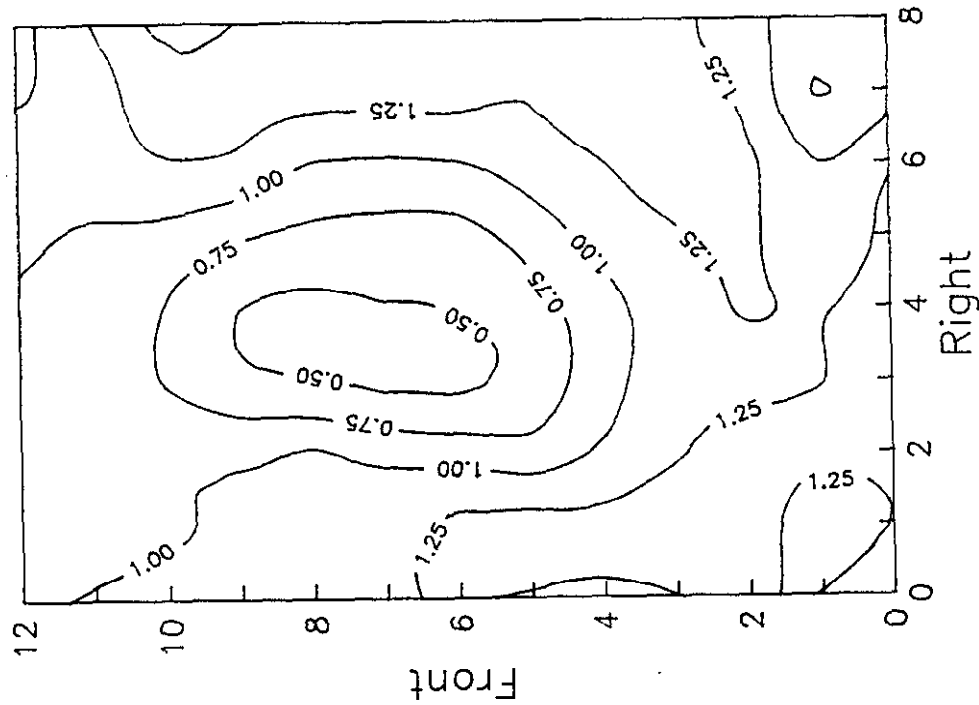


Figure 6-38

**SOUTHERN COMPANY SERVICES
 LANSING SMITH #2 FLOW MODEL**

ABB Combustion Engineering, Inc.
 Kreisinger Development Laboratory
 Mechanical Systems Engineering

NORMALIZED METHANE CONCENTRATION

Test Plane: 3
 Test Date: 2/12/91
 Firing System: LNCFS-II
 Test ID: Configuration #1

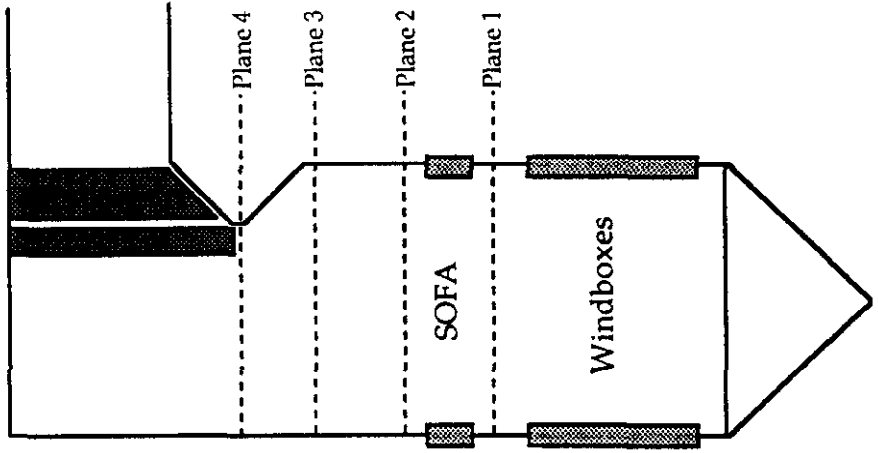
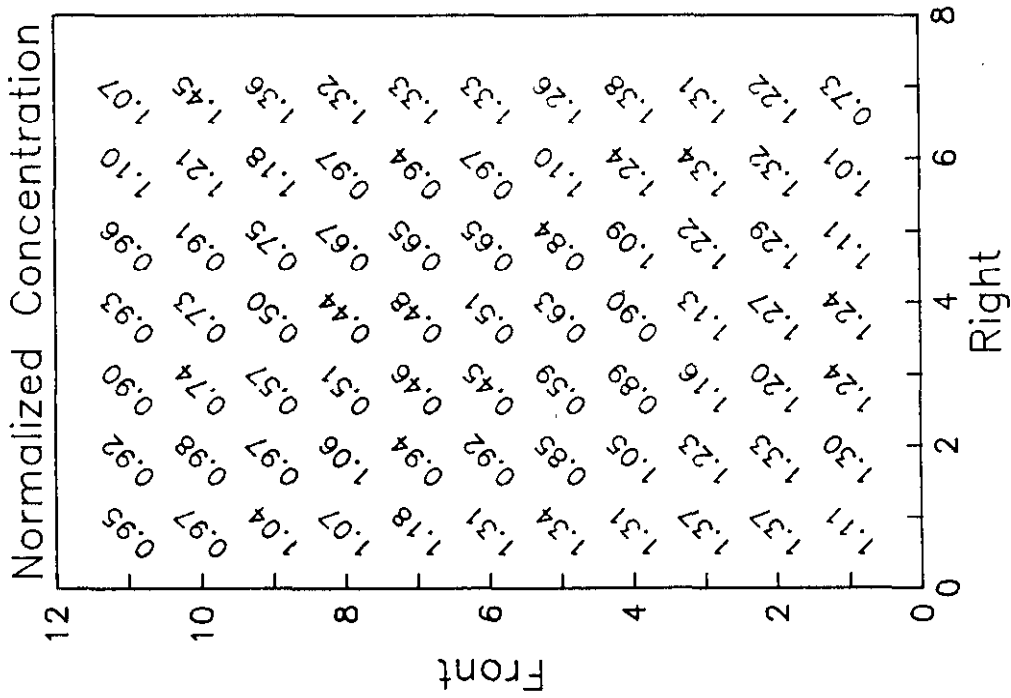


Figure 6-39

**SOUTHERN COMPANY SERVICES
 LANSING SMITH #2 FLOW MODEL**

NORMALIZED METHANE CONCENTRATION

Test Plane: 3

Test Date: 2/12/91

Firing System: LNCFS-II

Test ID: Configuration #2

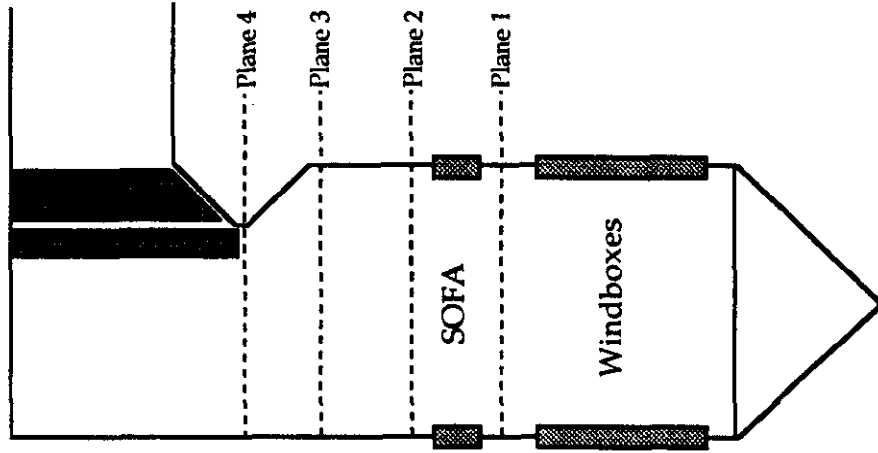
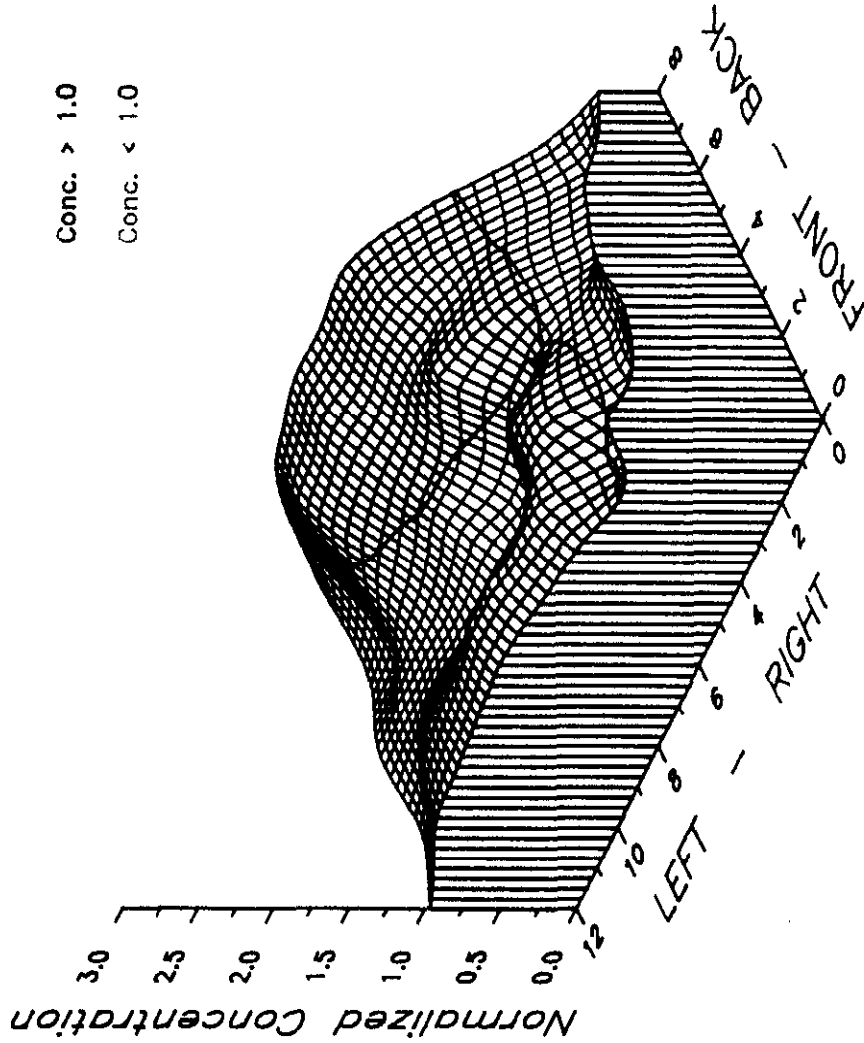


Figure 6-40

**SOUTHERN COMPANY SERVICES
LANSING SMITH #2 FLOW MODEL**

NORMALIZED METHANE CONCENTRATION

Test Plane: 3
 Test Date: 2/12/91
 Firing System: LNCFS-II
 Test ID: Configuration #2

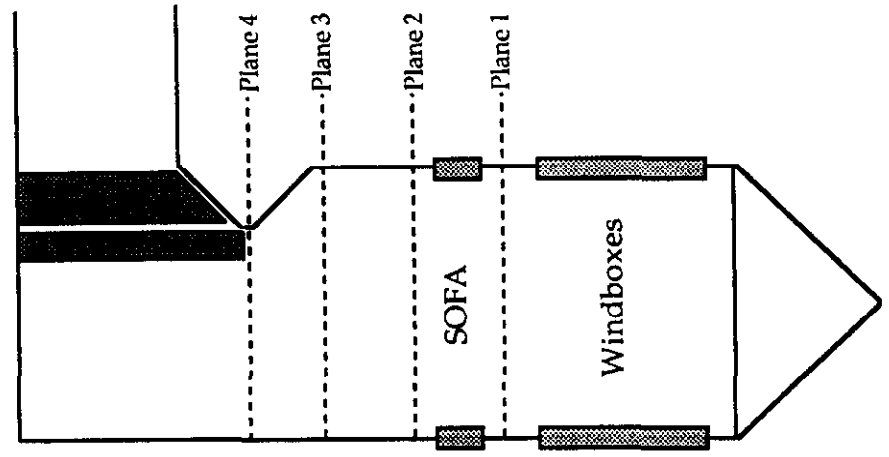
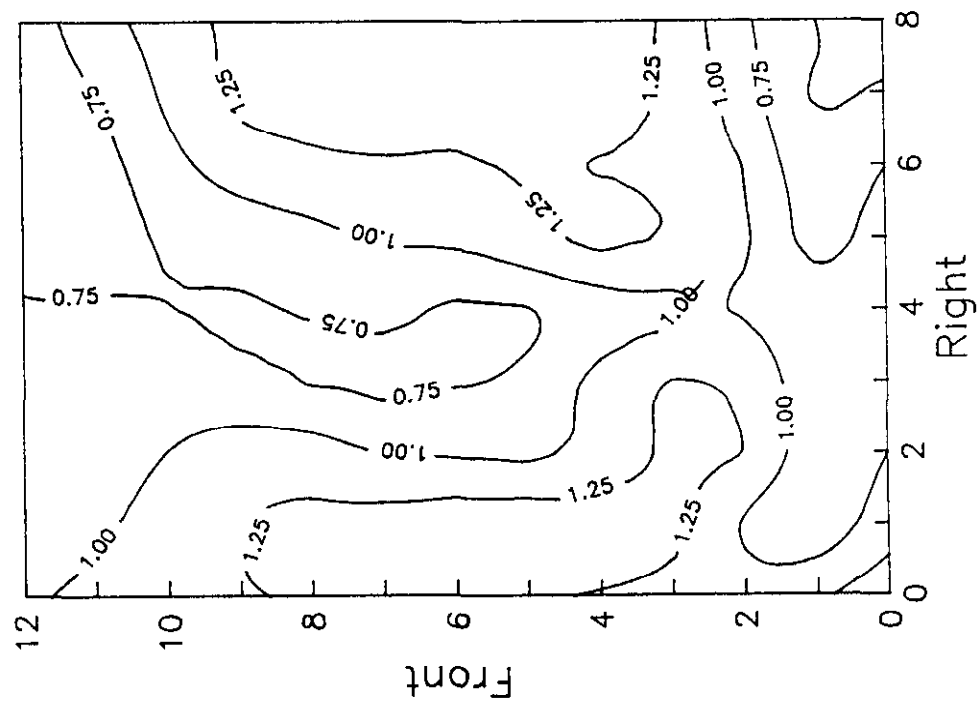


Figure 6-41

**SOUTHERN COMPANY SERVICES
 LANSING SMITH #2 FLOW MODEL**

ABB Combustion Engineering, Inc.
 Kreisinger Development Laboratory
 Mechanical Systems Engineering

NORMALIZED METHANE CONCENTRATION

Test Plane: 3
 Test Date: 2/12/91
 Firing System: LNCFS-II
 Test ID: Configuration #2

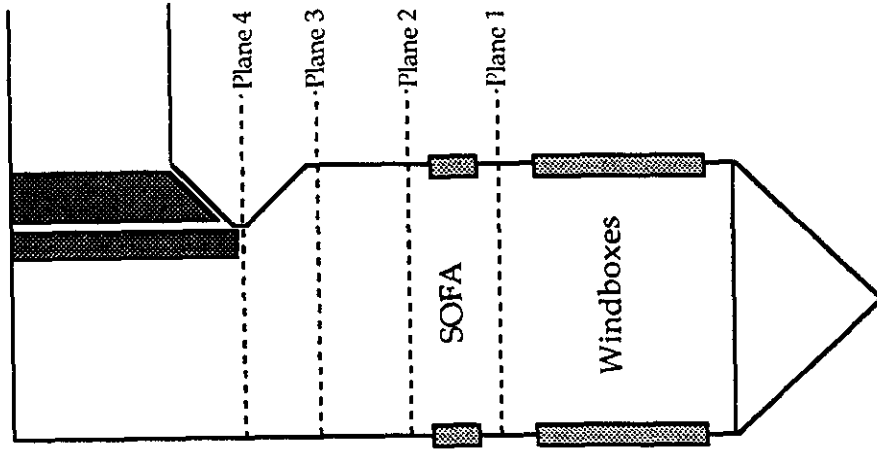
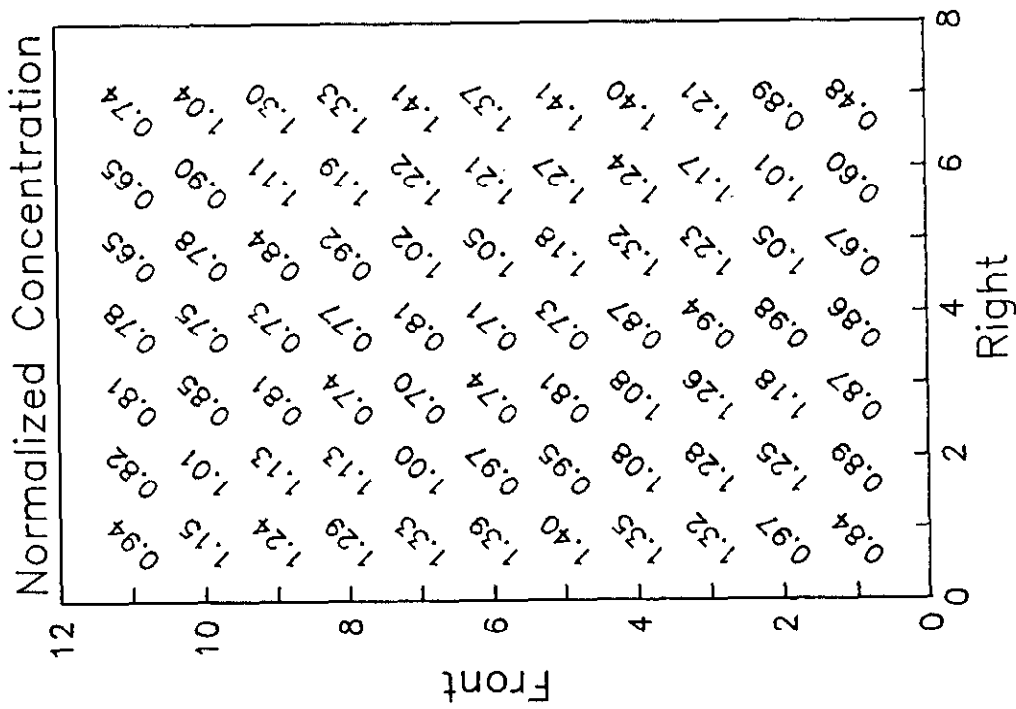


Figure 6-42

**SOUTHERN COMPANY SERVICES
 LANSING SMITH #2 FLOW MODEL**

NORMALIZED METHANE CONCENTRATION

Test Plane: 3

Test Date: 2/13/91

Firing System: LNCFS-II

Test ID: Configuration #3

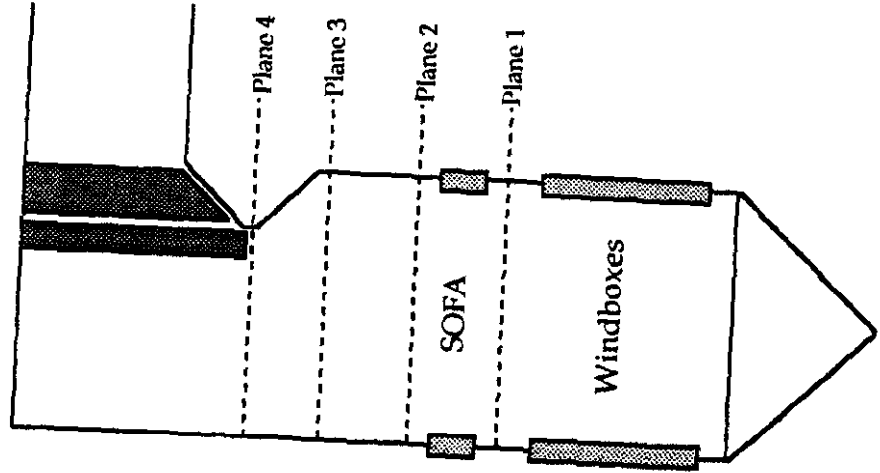
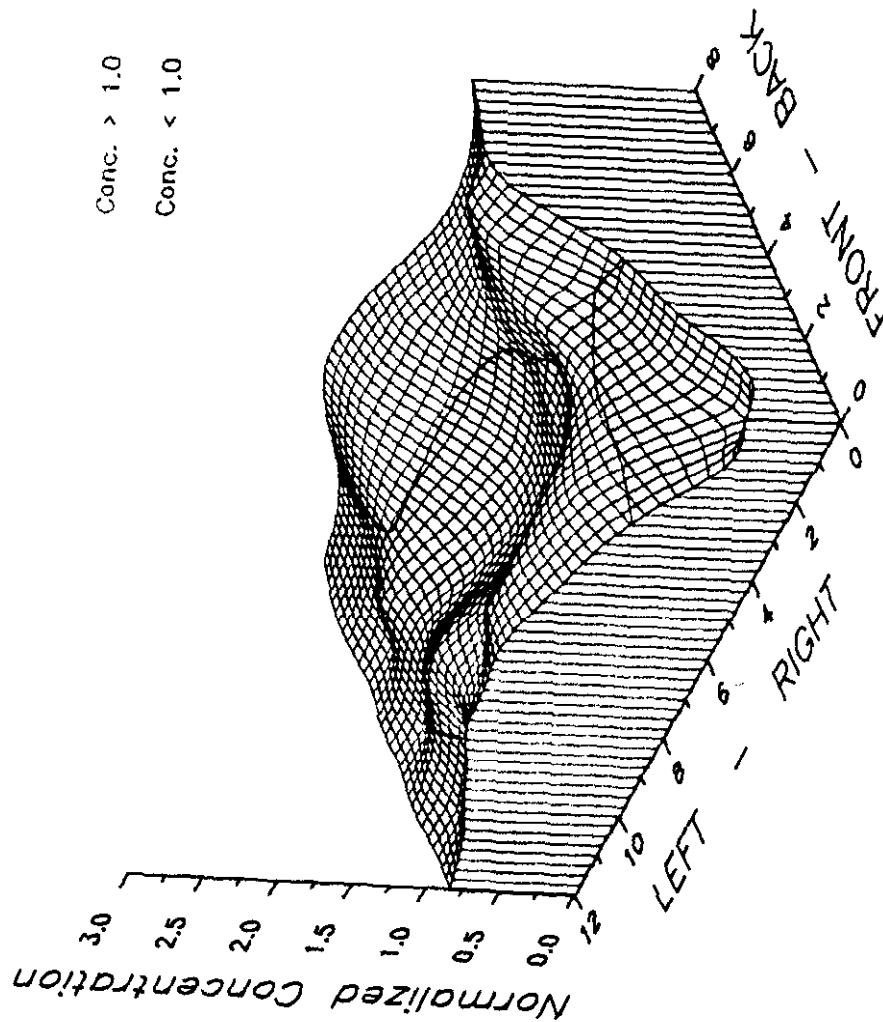


Figure 6-43

**SOUTHERN COMPANY SERVICES
LANSING SMITH #2 FLOW MODEL**

NORMALIZED METHANE CONCENTRATION

Test Plane: 3

Test Date: 2/13/91

Firing System: LNCFS-II

Test ID: Configuration #3

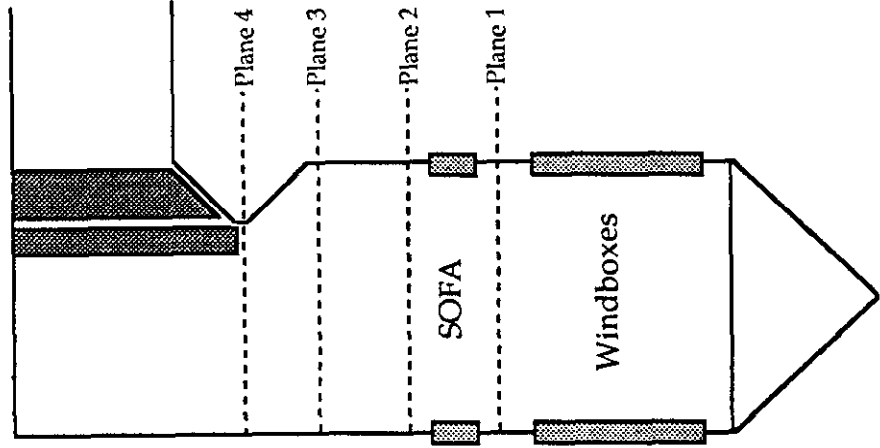
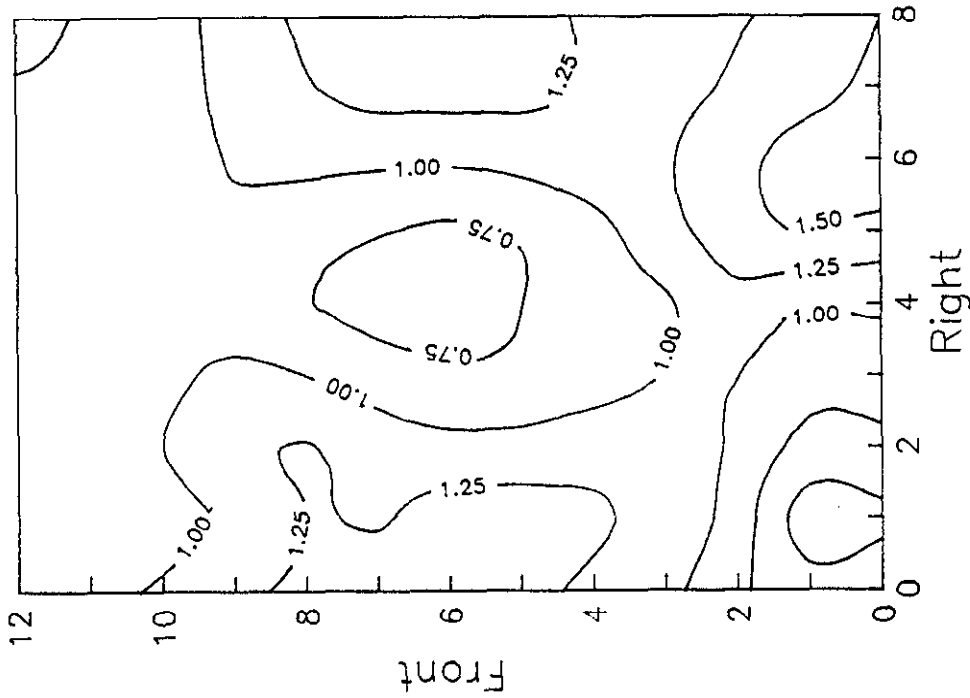


Figure 6-44

**SOUTHERN COMPANY SERVICES
LANSING SMITH #2 FLOW MODEL**

NORMALIZED METHANE CONCENTRATION

Test Plane: 3
 Test Date: 2/13/91
 Firing System: LNCFS-II
 Test ID: Configuration #3

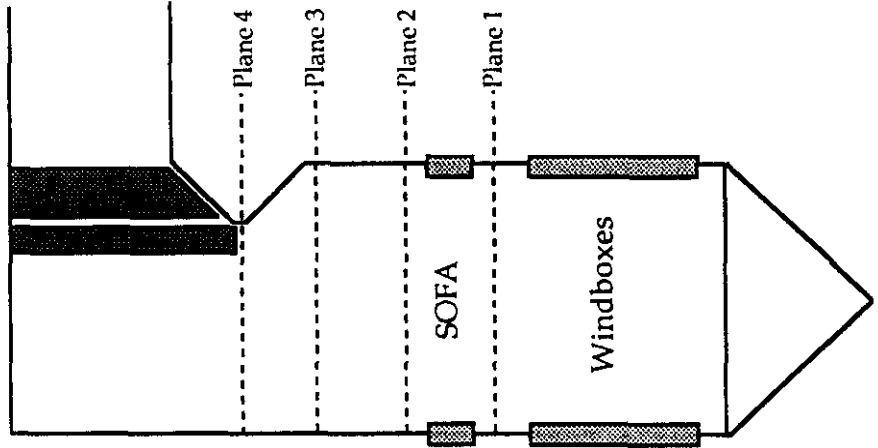
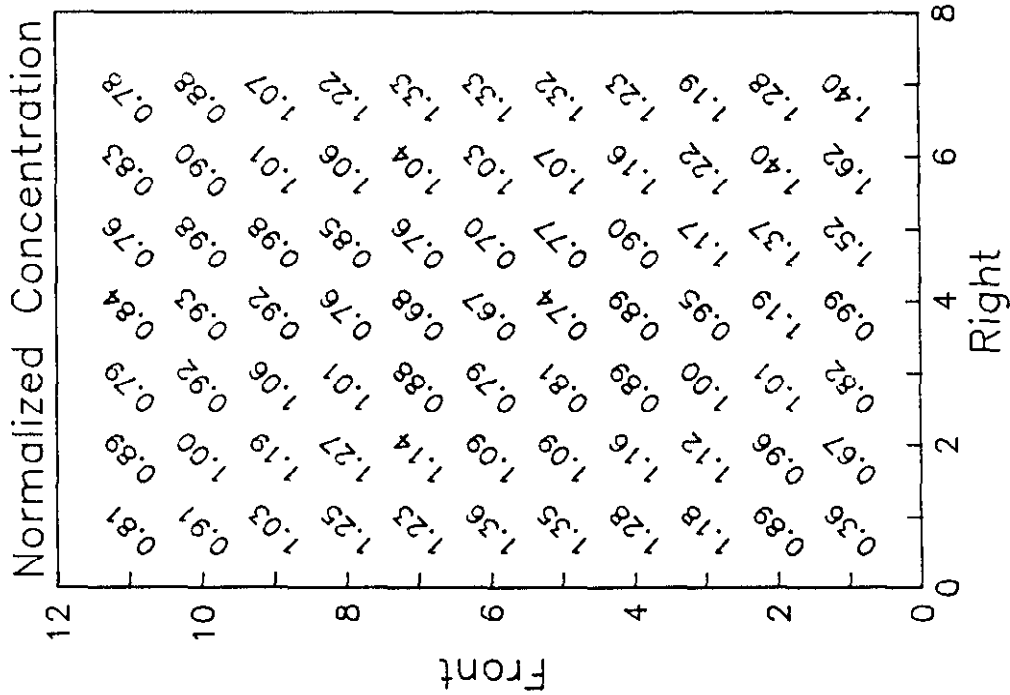


Figure 6-45

**SOUTHERN COMPANY SERVICES
 LANSING SMITH #2 FLOW MODEL**

NORMALIZED METHANE CONCENTRATION

Test Plane: 3

Test Date: 2/11/91

Firing System: LNCFS-II

Test ID: Configuration #4

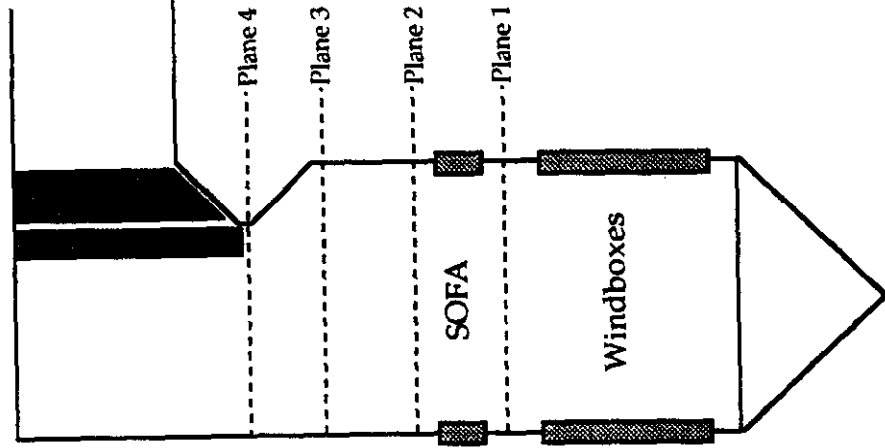
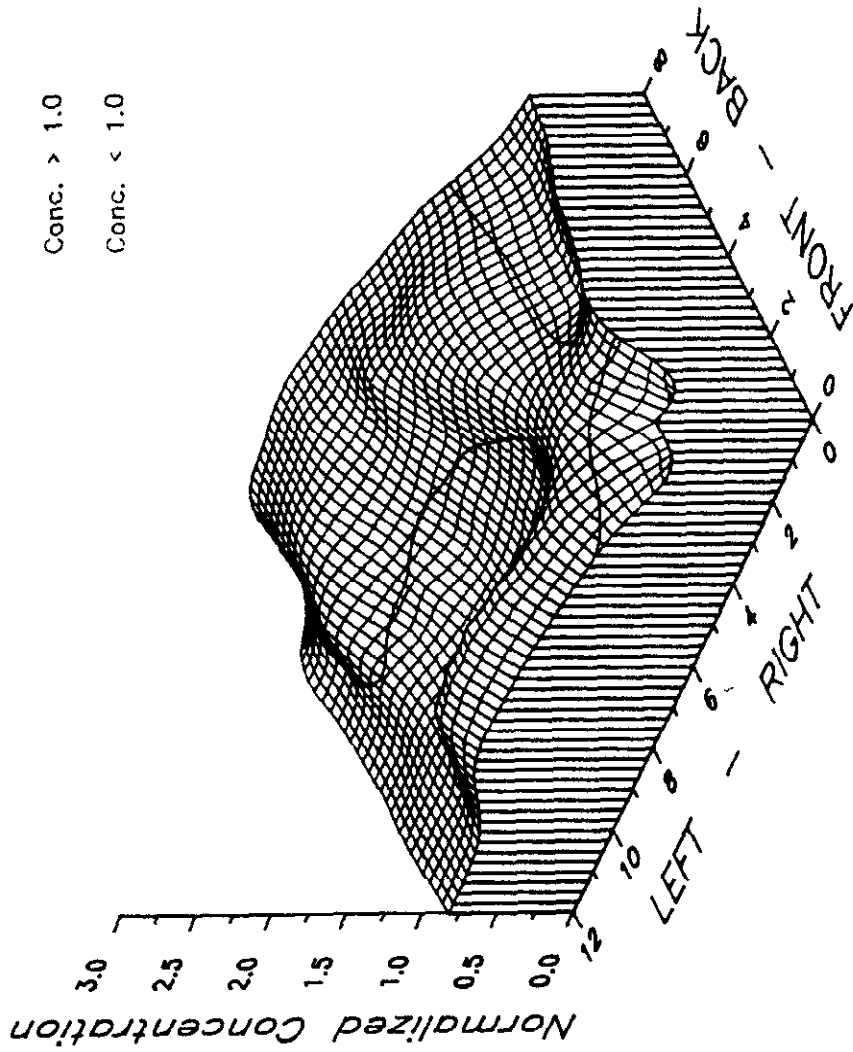


Figure 6-46

**SOUTHERN COMPANY SERVICES
LANSING SMITH #2 FLOW MODEL**

NORMALIZED METHANE CONCENTRATION

Test Plane: 3
 Test Date: 2/11/91
 Firing System: LNCFS-II
 Test ID: Configuration #4

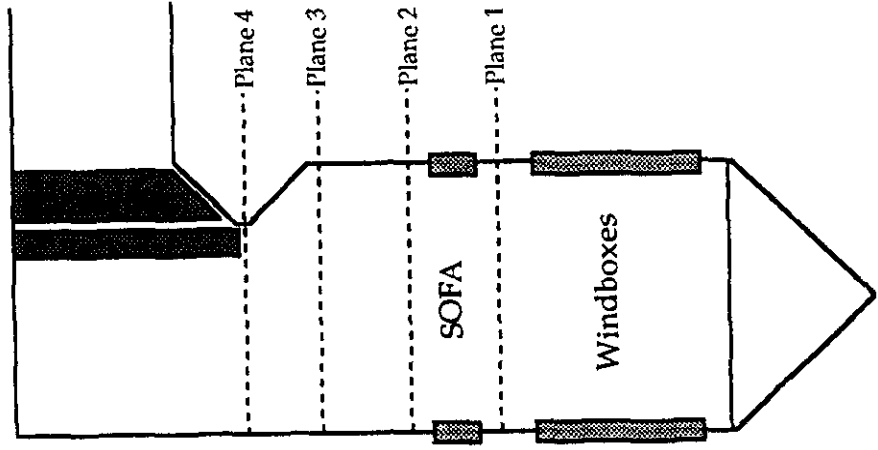
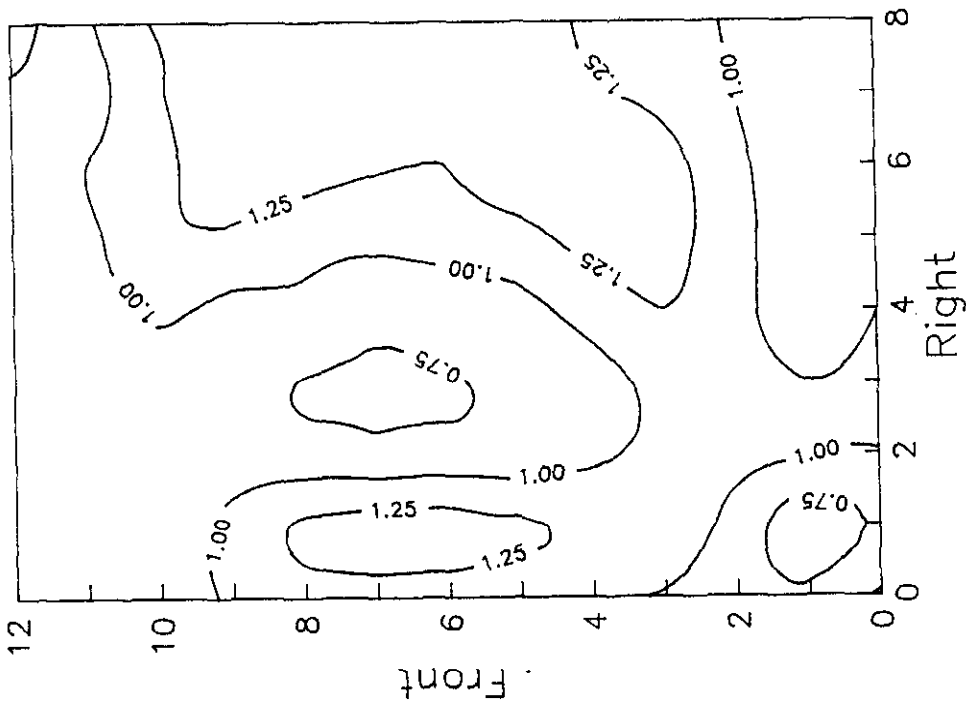


Figure 6-47

**SOUTHERN COMPANY SERVICES
 LANSING SMITH #2 FLOW MODEL**

ABB Combustion Engineering, Inc.
 Kreisinger Development Laboratory
 Mechanical Systems Engineering

NORMALIZED METHANE CONCENTRATION

Test Plane: 3
 Test Date: 2/11/91
 Firing System: LNCFS-II
 Test ID: Configuration #4

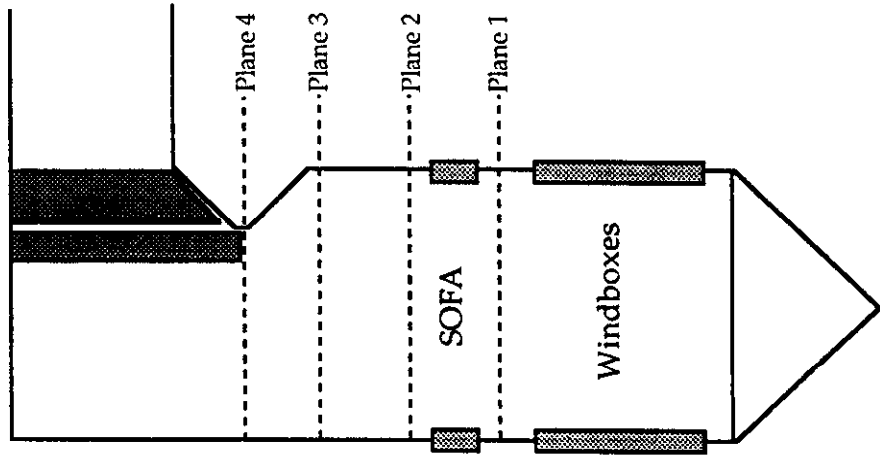
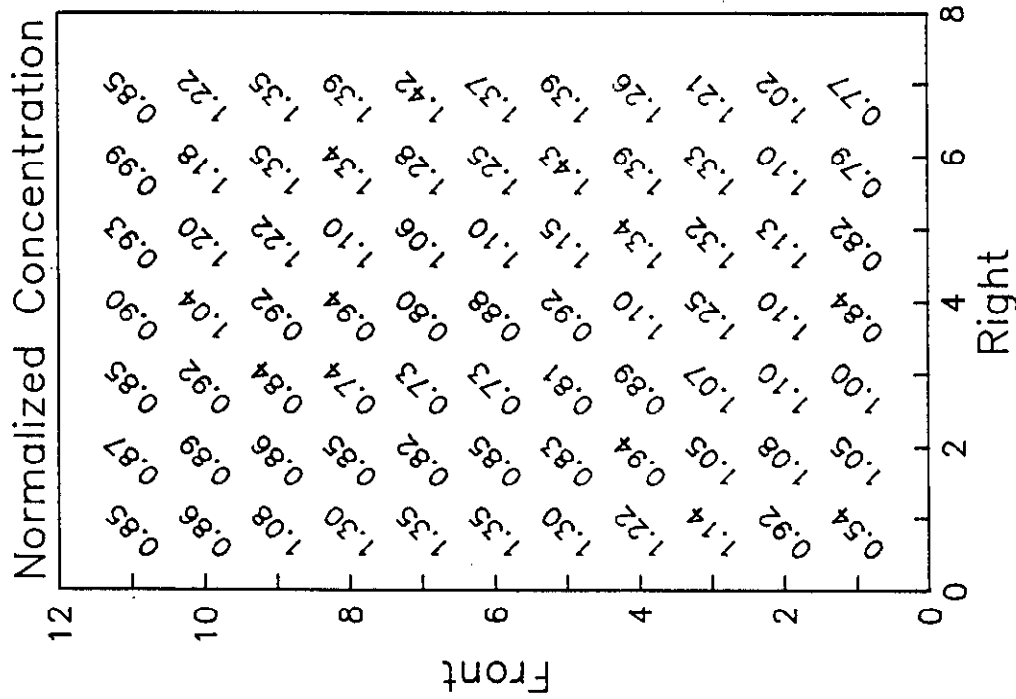


Figure 6-48

**SOUTHERN COMPANY SERVICES
 LANSING SMITH #2 FLOW MODEL**

ABB Combustion Engineering, Inc.
 Kreisinger Development Laboratory
 Mechanical Systems Engineering

NORMALIZED METHANE CONCENTRATION

Test Plane: 3

Test Date: 2/14/91

Firing System: LNCFS-II

Test ID: Configuration #5

Conc. > 1.0
 Conc. < 1.0

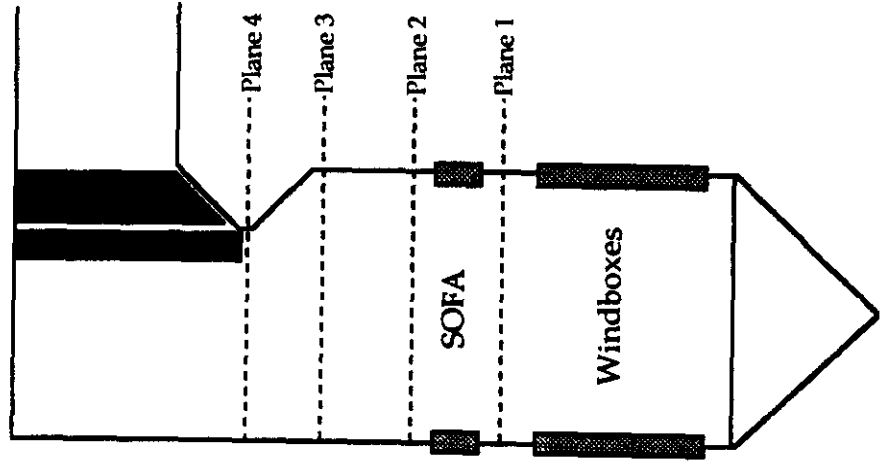
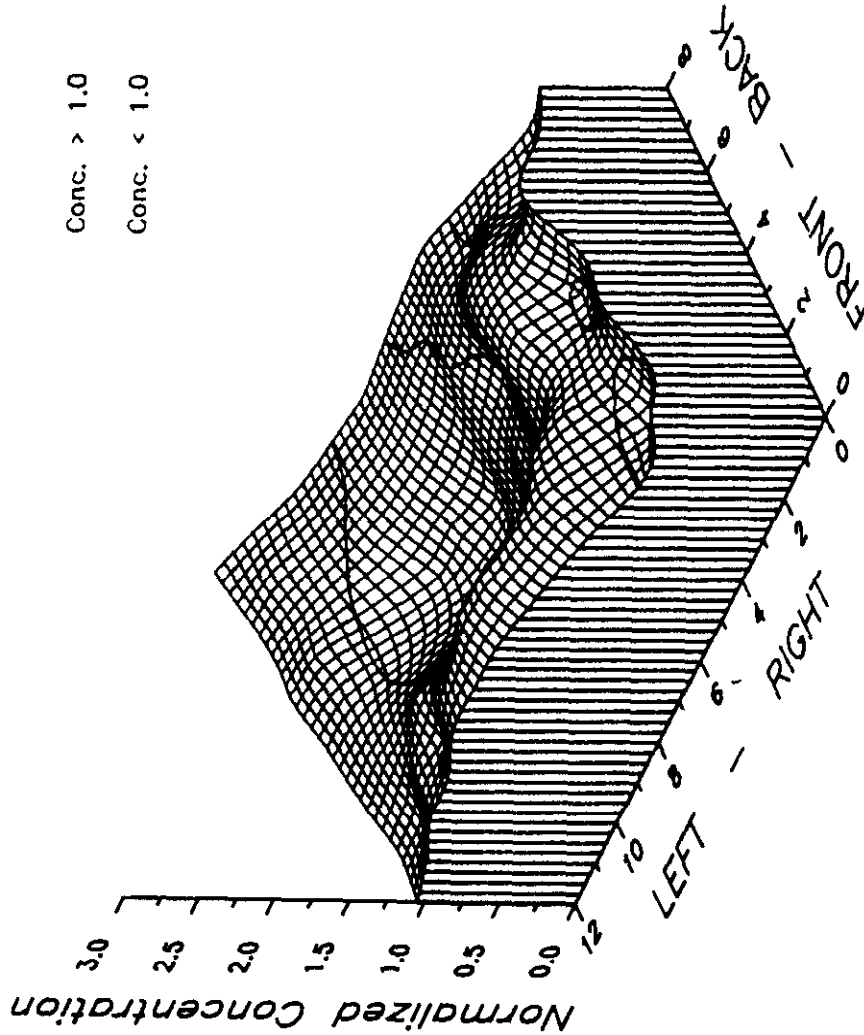


Figure 6-49

**SOUTHERN COMPANY SERVICES
 LANSING SMITH #2 FLOW MODEL**

NORMALIZED METHANE CONCENTRATION

Test Plane: 3

Test Date: 2/14/91

Firing System: LNCFS-II

Test ID: Configuration #5

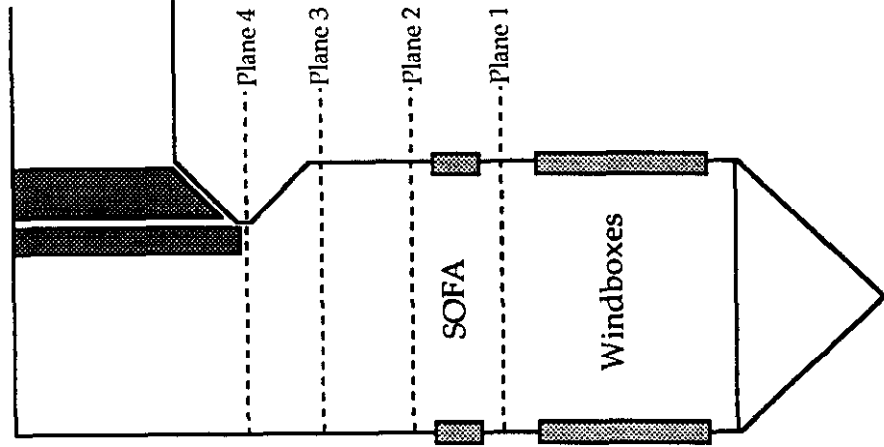
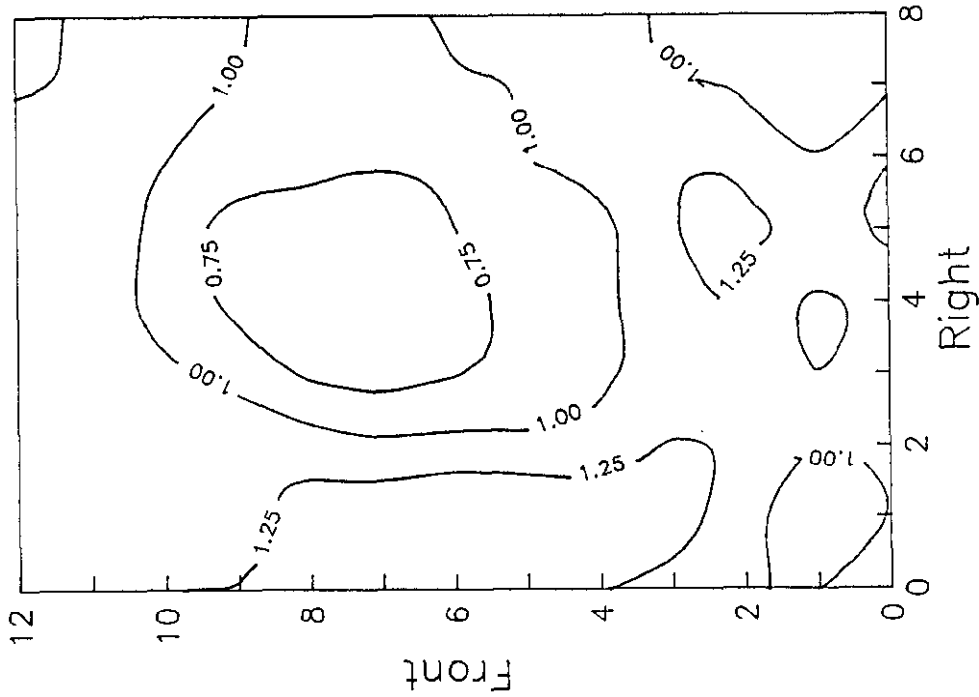


Figure 6-50

**SOUTHERN COMPANY SERVICES
LANSING SMITH #2 FLOW MODEL**

NORMALIZED METHANE CONCENTRATION

Test Plane: 3
 Test Date: 2/14/91
 Firing System: LNCFS-II
 Test ID: Configuration #5

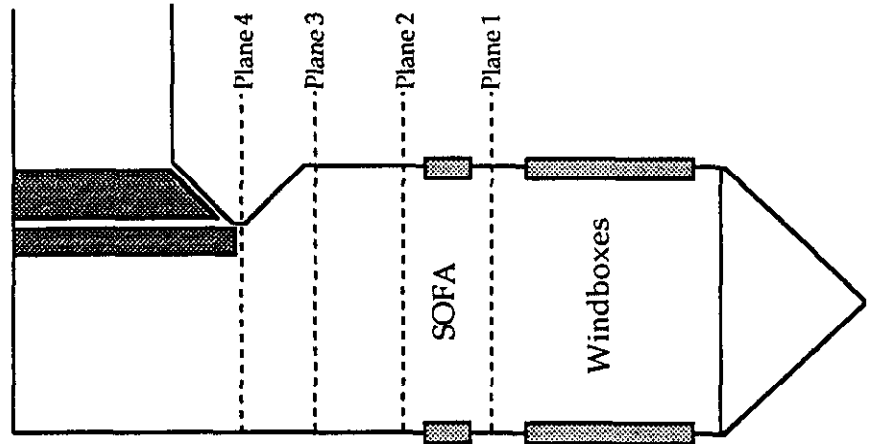
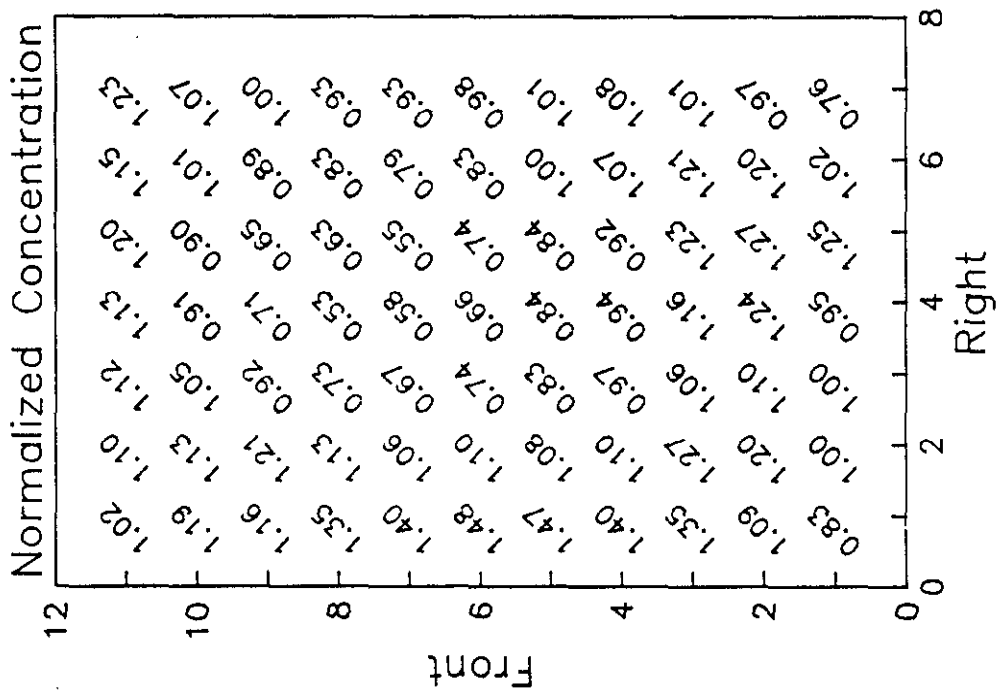
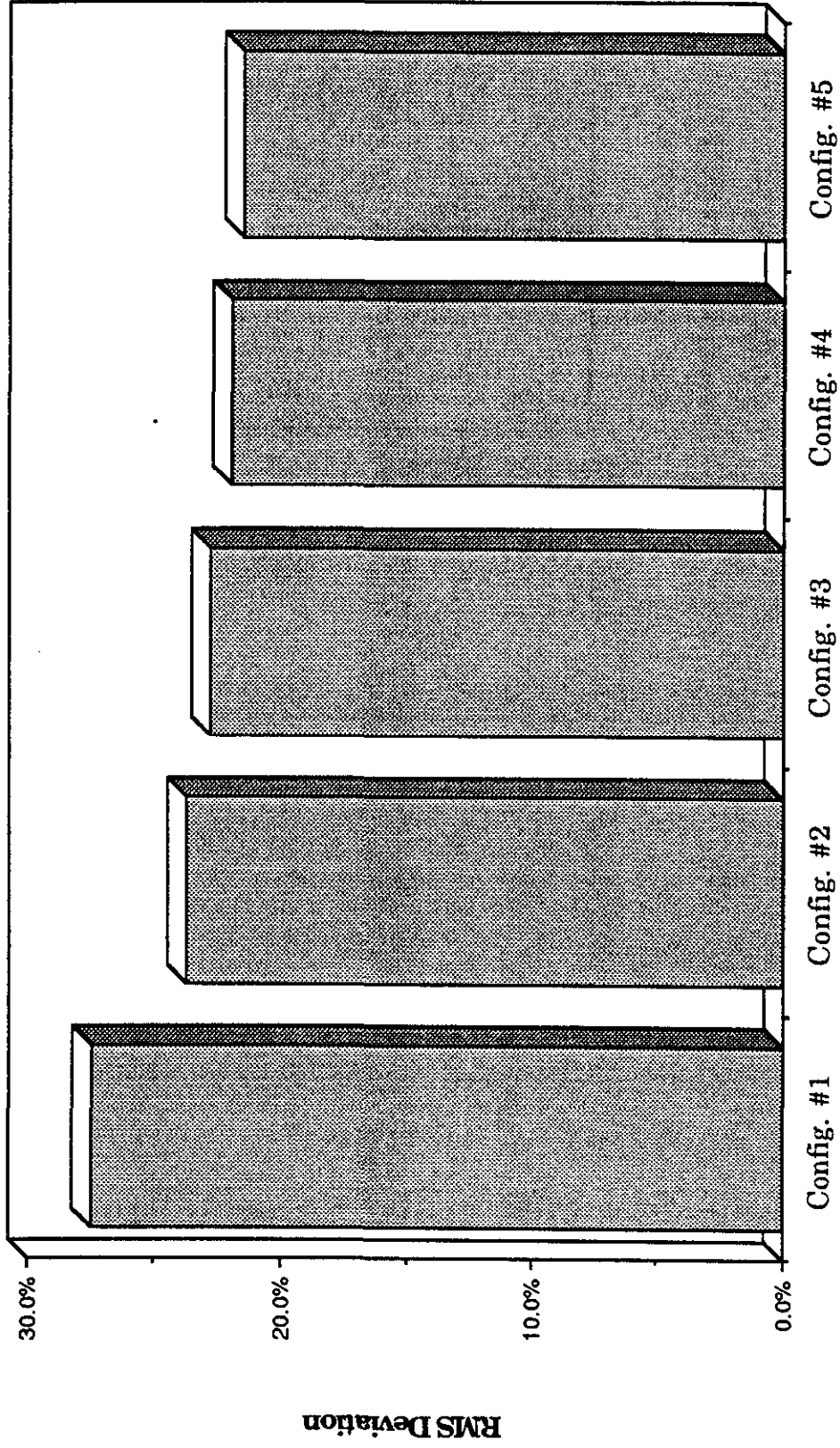


Figure 6-51

**SOUTHERN COMPANY SERVICES
 LANSING SMITH #2 FLOW MODEL**

**Lansing Smith Flow Model
Methane RMS Deviation - Plane 3**



Test Identification

Figure 6-52

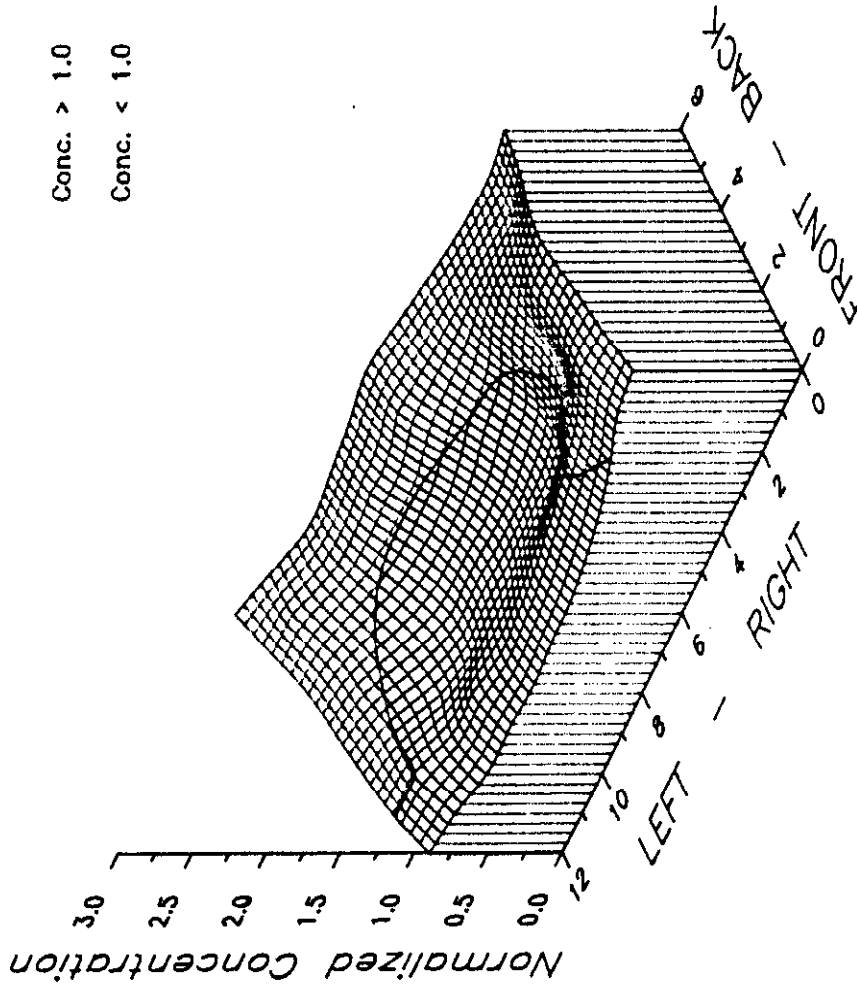
NORMALIZED METHANE CONCENTRATION

Test Plane: 4

Test Date: 2/12/91

Firing System: LNCFS-II

Test ID: Configuration #1



Conc. > 1.0

Conc. < 1.0

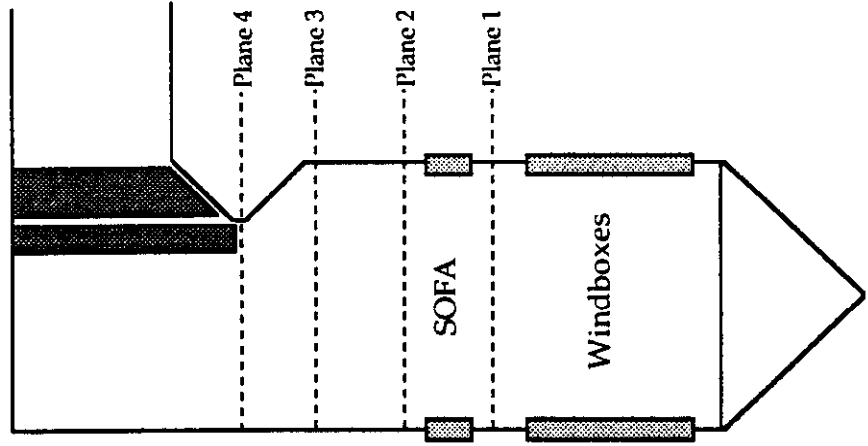


Figure 6-53

**SOUTHERN COMPANY SERVICES
LANSING SMITH #2 FLOW MODEL**

NORMALIZED METHANE CONCENTRATION

Test Plane: 4

Test Date: 2/12/91

Firing System: LNCFS-II

Test ID: Configuration #1

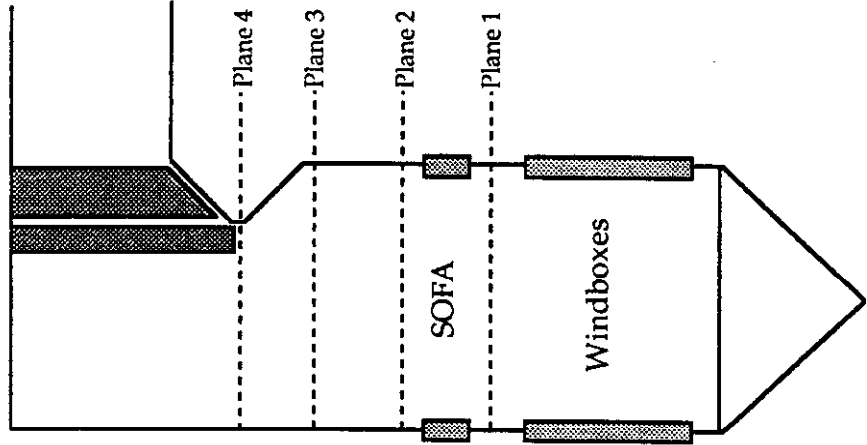
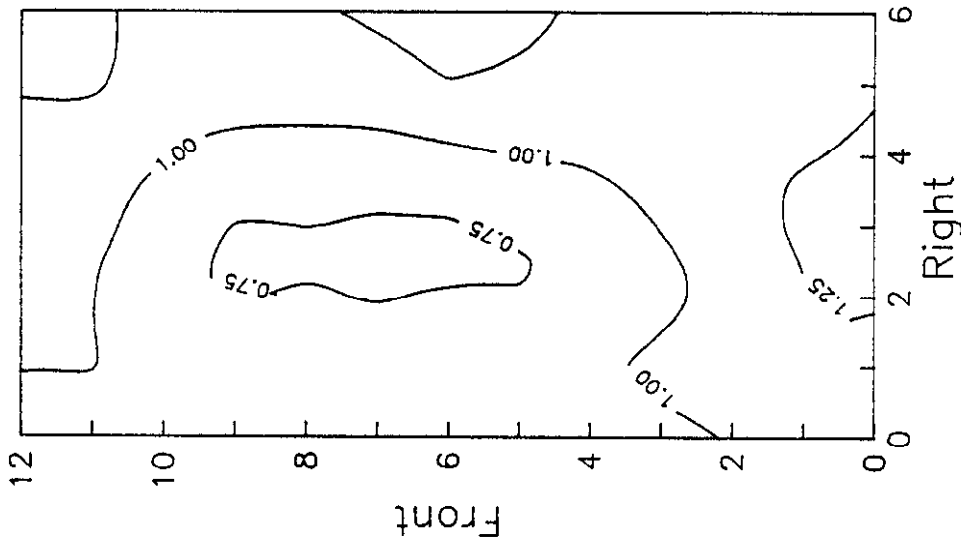
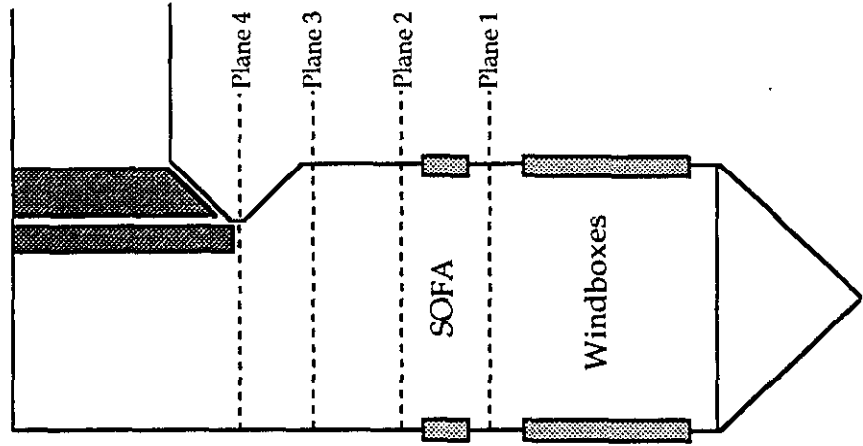
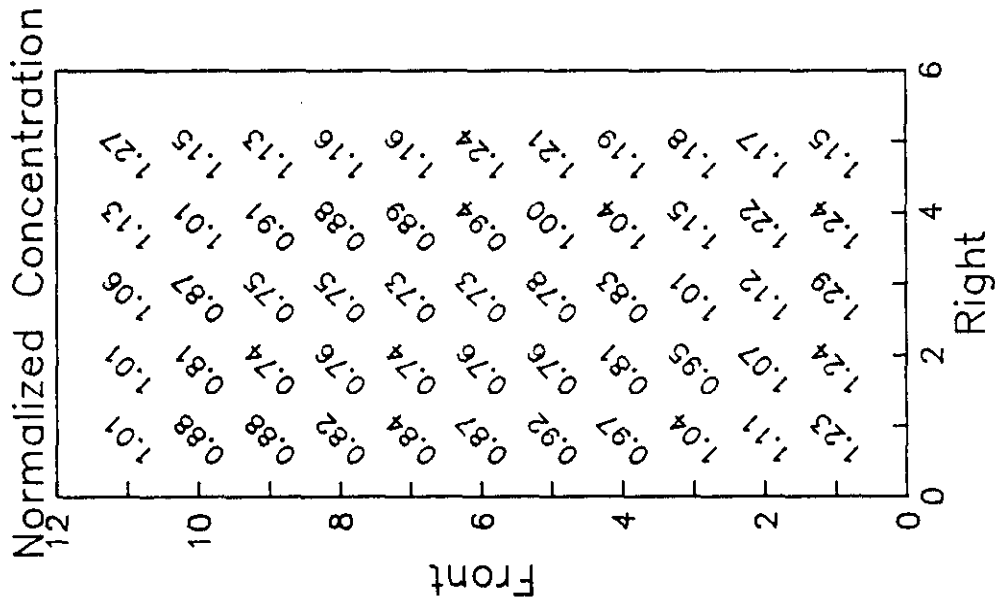


Figure 6-54

**SOUTHERN COMPANY SERVICES
LANSING SMITH #2 FLOW MODEL**

NORMALIZED METHANE CONCENTRATION

Test Plane: 4
 Test Date: 2/12/91
 Firing System: LNCFS-II
 Test ID: Configuration #1



SOUTHERN COMPANY SERVICES
LANSING SMITH #2 FLOW MODEL

Figure 6-55

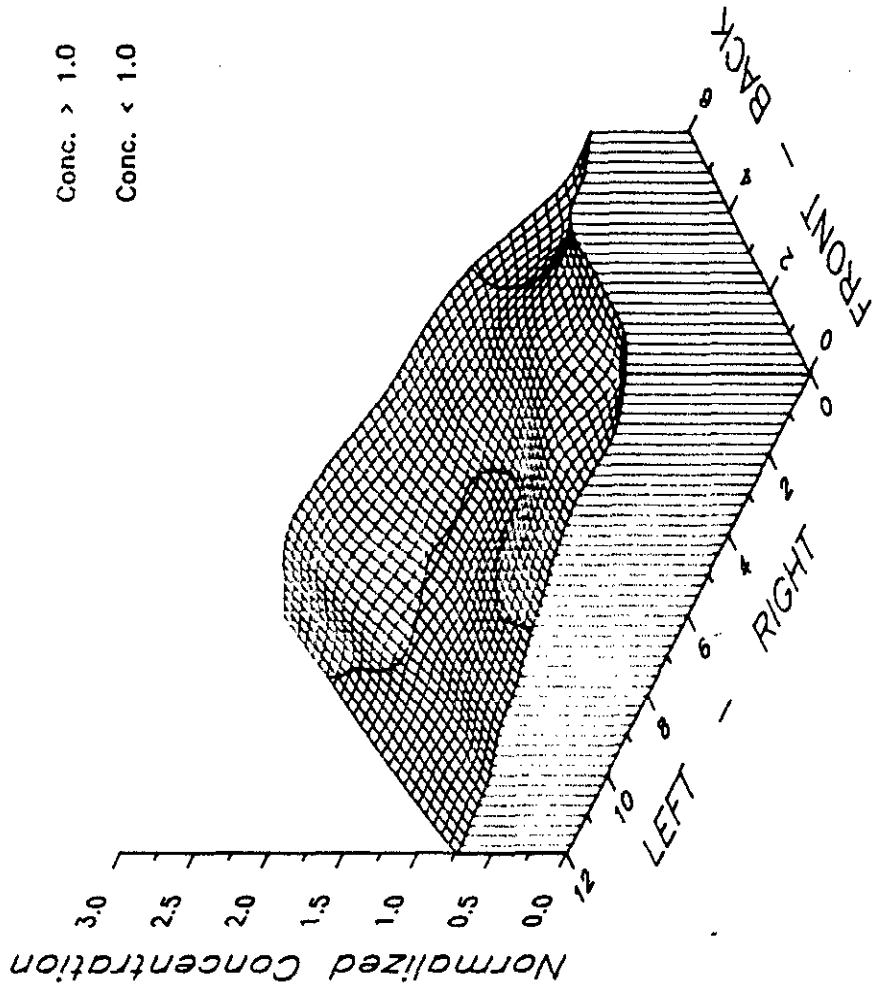
NORMALIZED METHANE CONCENTRATION

Test Plane: 4

Test Date: 2/12/91

Firing System: LNCFS-II

Test ID: Configuration #2



Conc. > 1.0

Conc. < 1.0

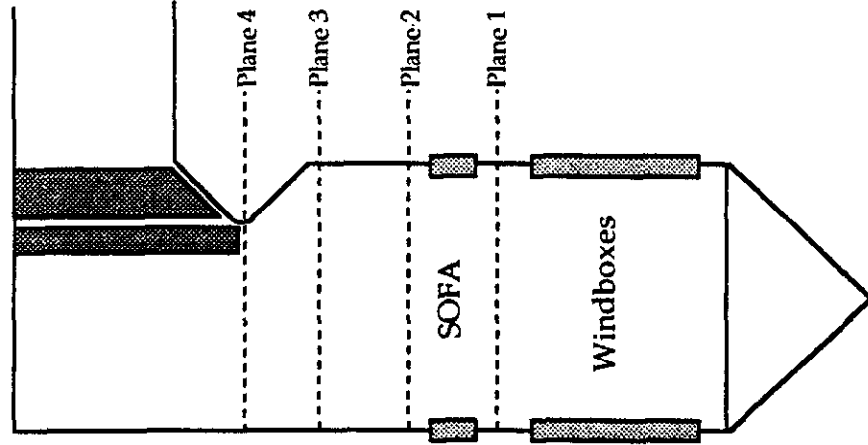


Figure 6-56

**SOUTHERN COMPANY SERVICES
LANSING SMITH #2 FLOW MODEL**

ABB Combustion Engineering, Inc.
Kreisinger Development Laboratory
Mechanical Systems Engineering

NORMALIZED METHANE CONCENTRATION

Test Plane: 4
 Test Date: 2/12/91
 Firing System: LNCFS-II
 Test ID: Configuration #2

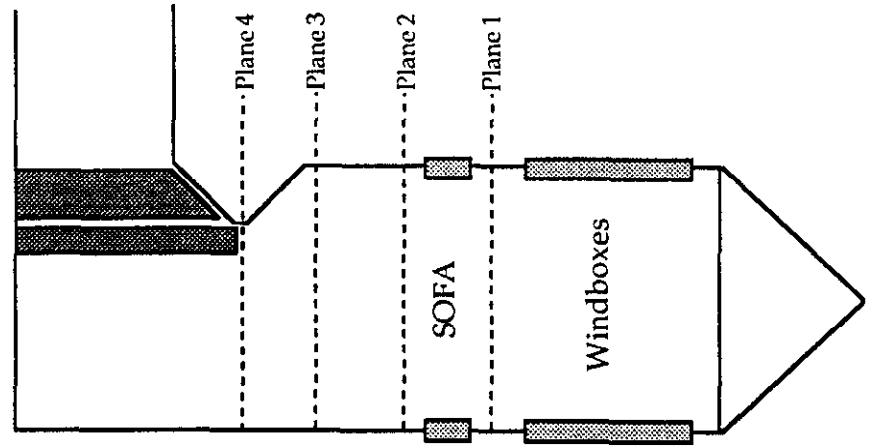
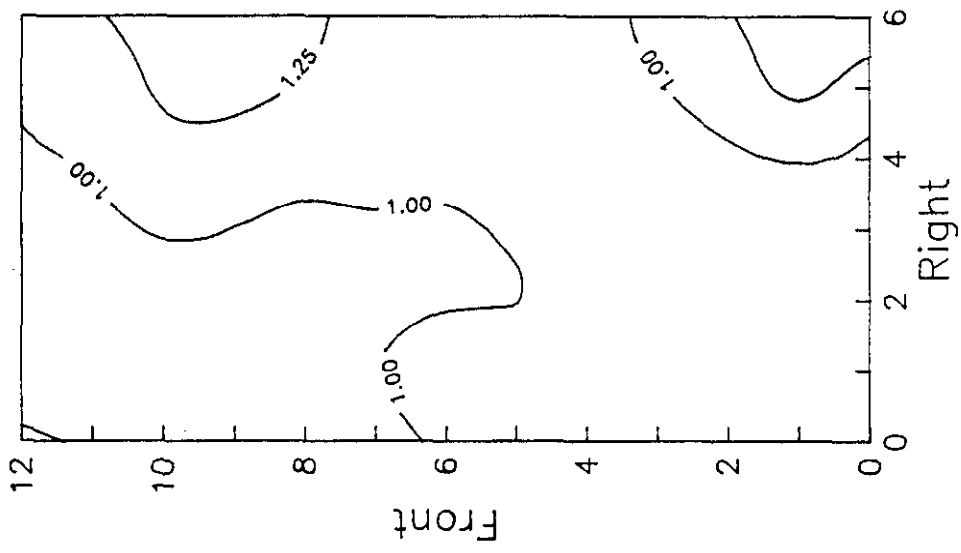
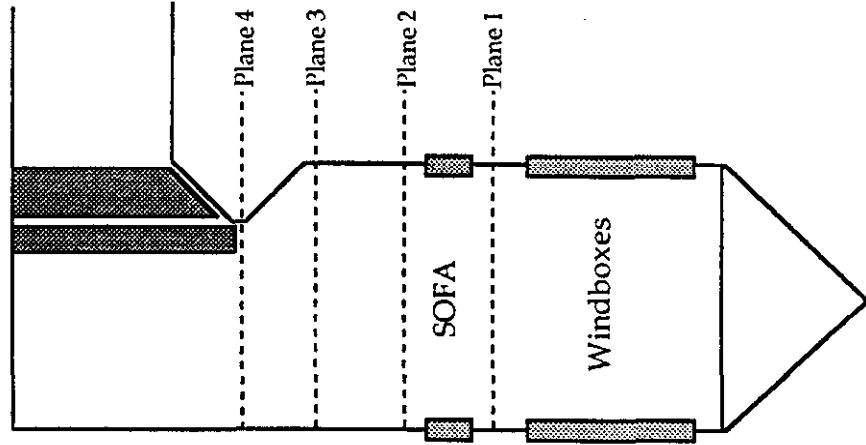
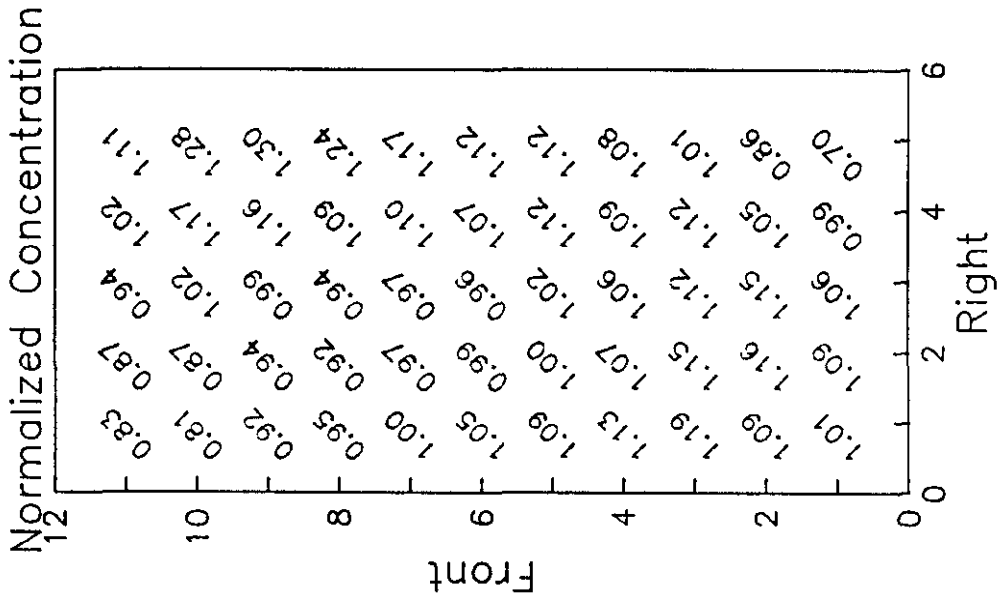


Figure 6-57

**SOUTHERN COMPANY SERVICES
 LANSING SMITH #2 FLOW MODEL**

NORMALIZED METHANE CONCENTRATION

Test Plane: 4
 Test Date: 2/12/91
 Firing System: LNCFS-II
 Test ID: Configuration #2



**SOUTHERN COMPANY SERVICES
 LANSING SMITH #2 FLOW MODEL**

Figure 6-58

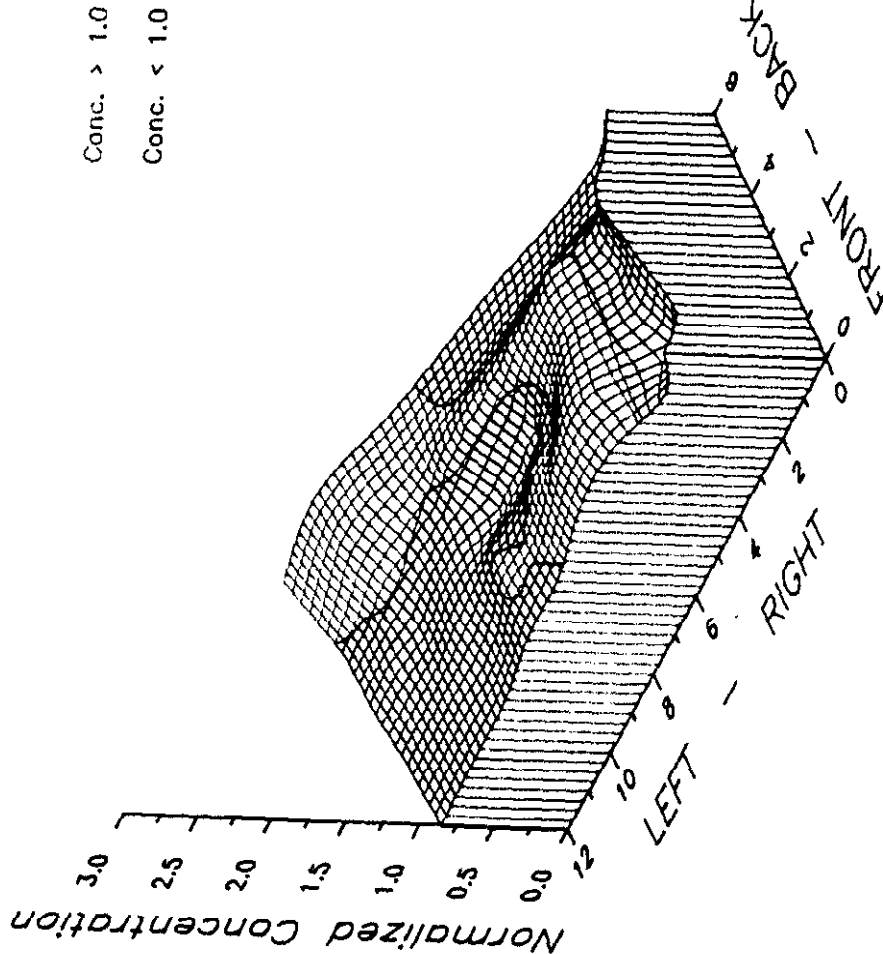
NORMALIZED METHANE CONCENTRATION

Test Plane: 4

Test Date: 2/13/91

Firing System: LNCFS-II

Test ID: Configuration #3



Conc. > 1.0

Conc. < 1.0

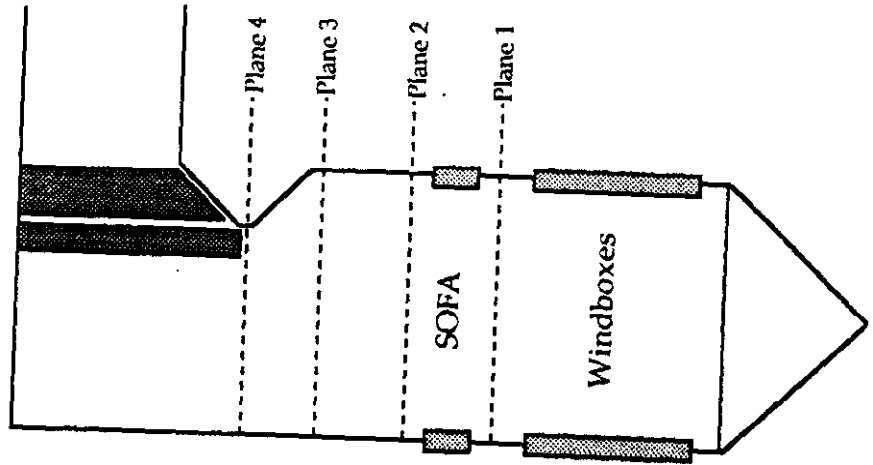


Figure 6-59

**SOUTHERN COMPANY SERVICES
LANSING SMITH #2 FLOW MODEL**

NORMALIZED METHANE CONCENTRATION

Test Plane: 4

Test Date: 2/13/91

Firing System: LNCFS-II

Test ID: Configuration #3

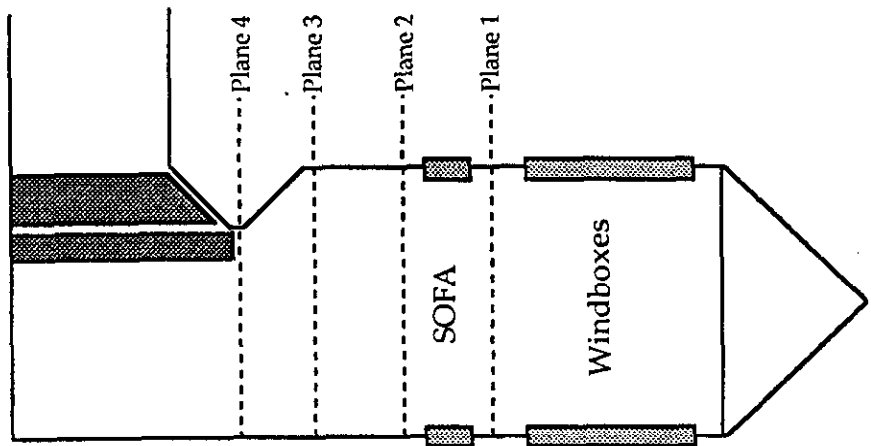
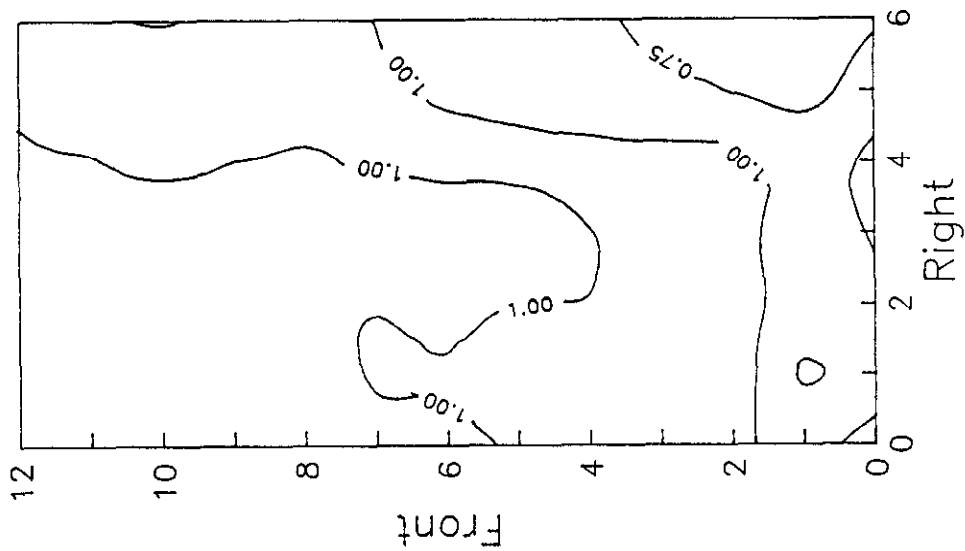


Figure 6-60

**SOUTHERN COMPANY SERVICES
LANSING SMITH #2 FLOW MODEL**

ABB Combustion Engineering, Inc.
Kreisinger Development Laboratory
Mechanical Systems Engineering

NORMALIZED METHANE CONCENTRATION

Test Plane: 4
 Test Date: 2/13/91
 Firing System: LNCFS-II
 Test ID: Configuration #3

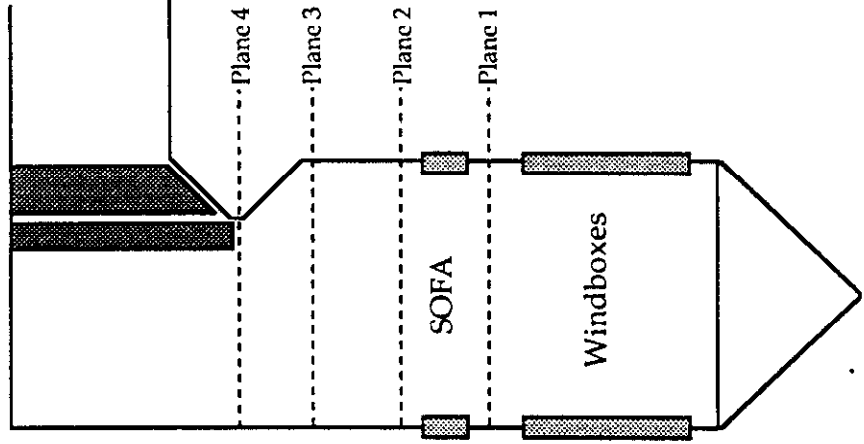
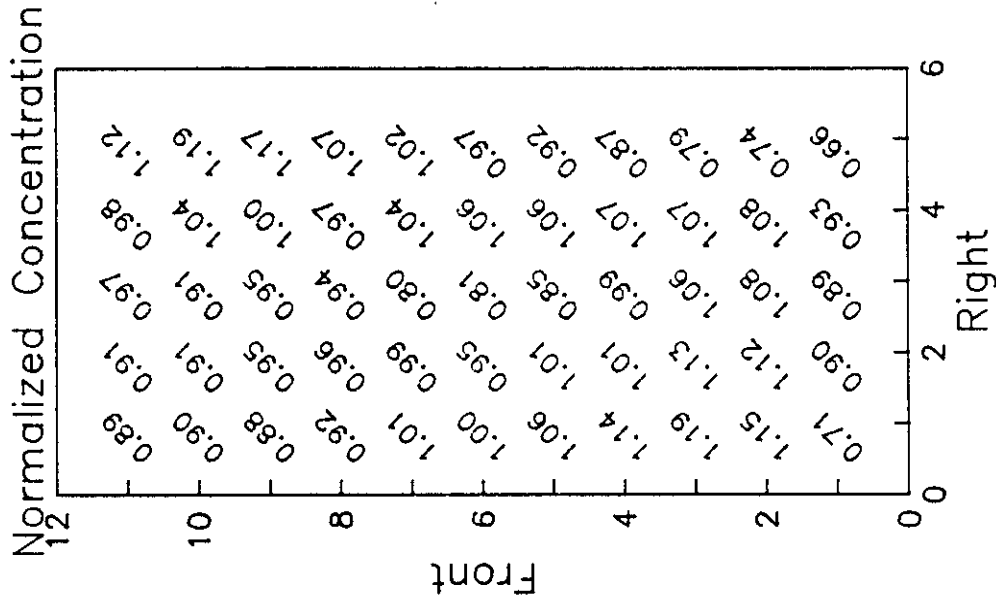


Figure 6-61

**SOUTHERN COMPANY SERVICES
 LANSING SMITH #2 FLOW MODEL**

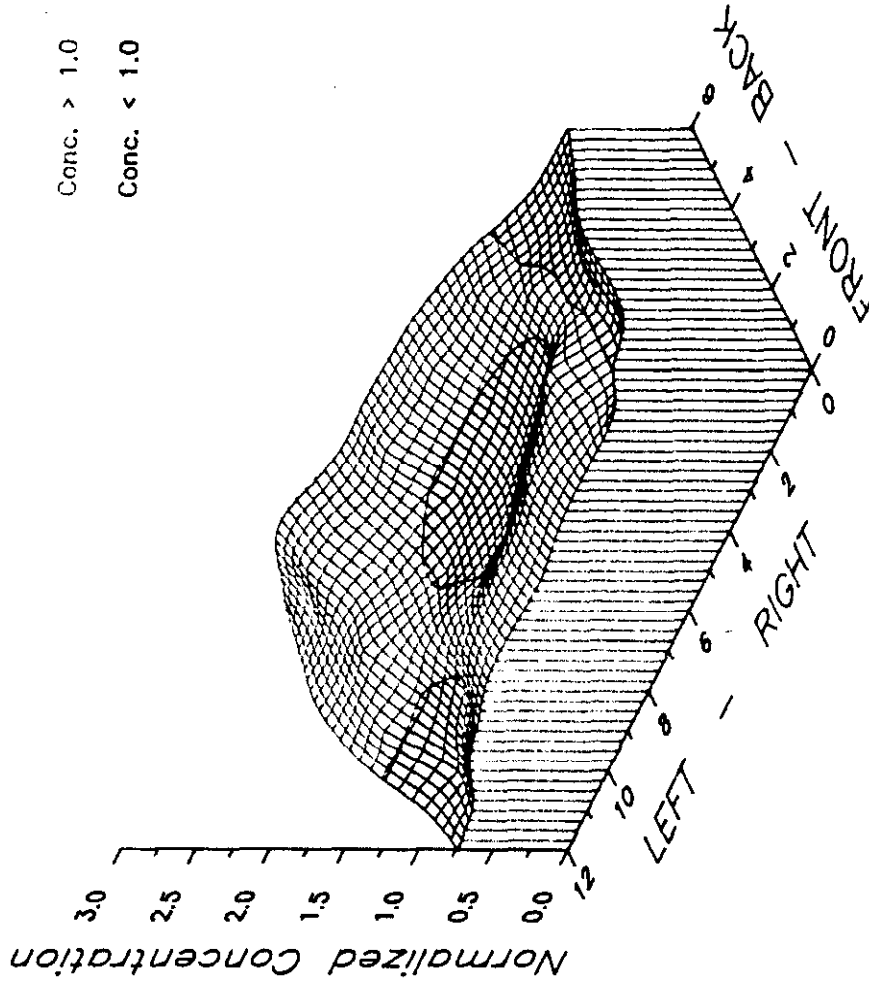
NORMALIZED METHANE CONCENTRATION

Test Plane: 4

Test Date: 2/11/91

Firing System: LNCFS-II

Test ID: Configuration #4



Conc. > 1.0

Conc. < 1.0

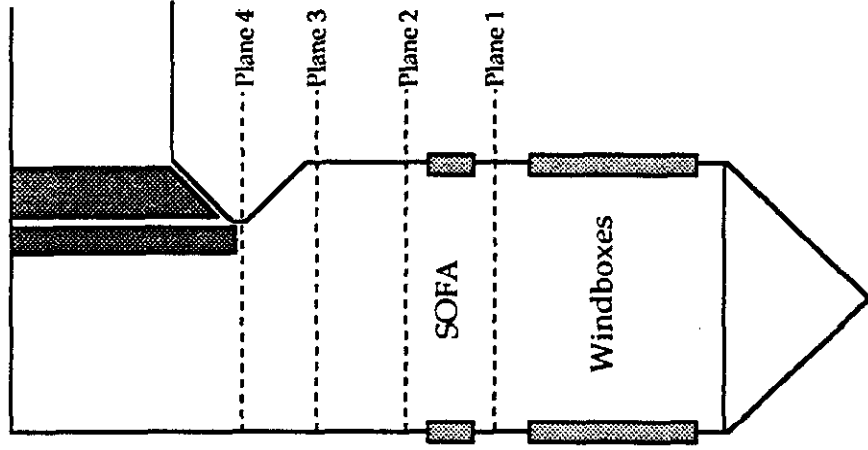


Figure 6-62

**SOUTHERN COMPANY SERVICES
LANSING SMITH #2 FLOW MODEL**

NORMALIZED METHANE CONCENTRATION

Test Plane: 4

Test Date: 2/11/91

Firing System: LNCFS-II

Test ID: Configuration #4

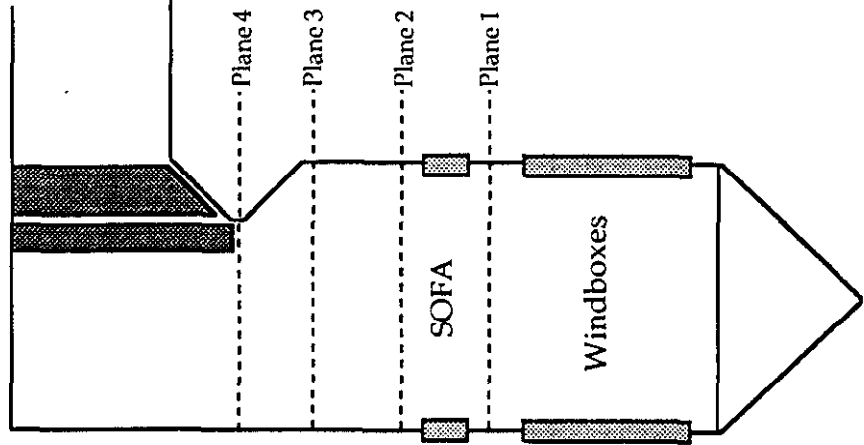
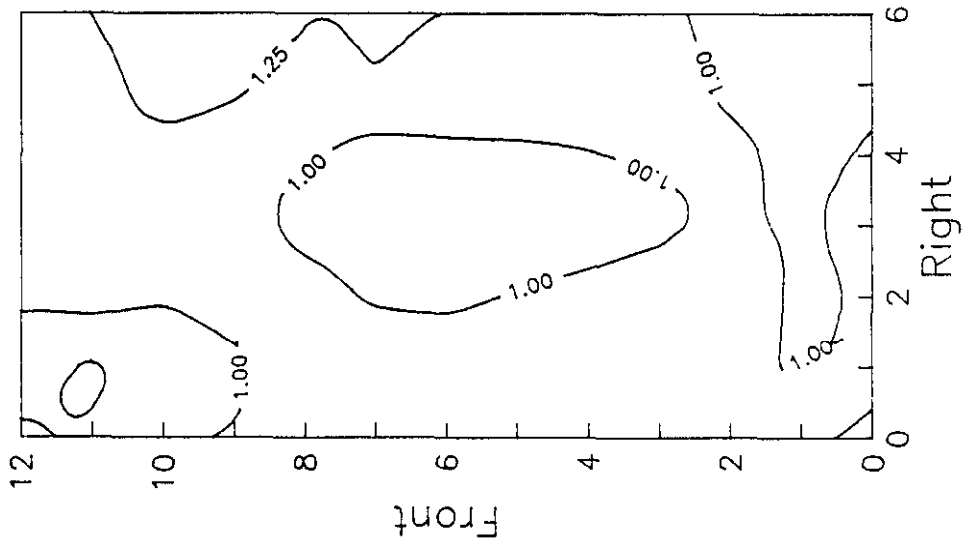


Figure 6-63

**SOUTHERN COMPANY SERVICES
LANSING SMITH #2 FLOW MODEL**

NORMALIZED METHANE CONCENTRATION

Test Plane: 4
 Test Date: 2/11/91
 Firing System: LNCFS-II
 Test ID: Configuration #4

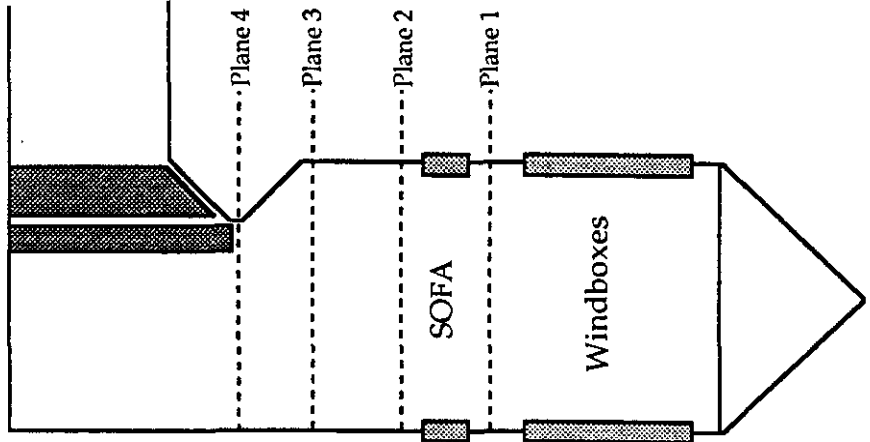
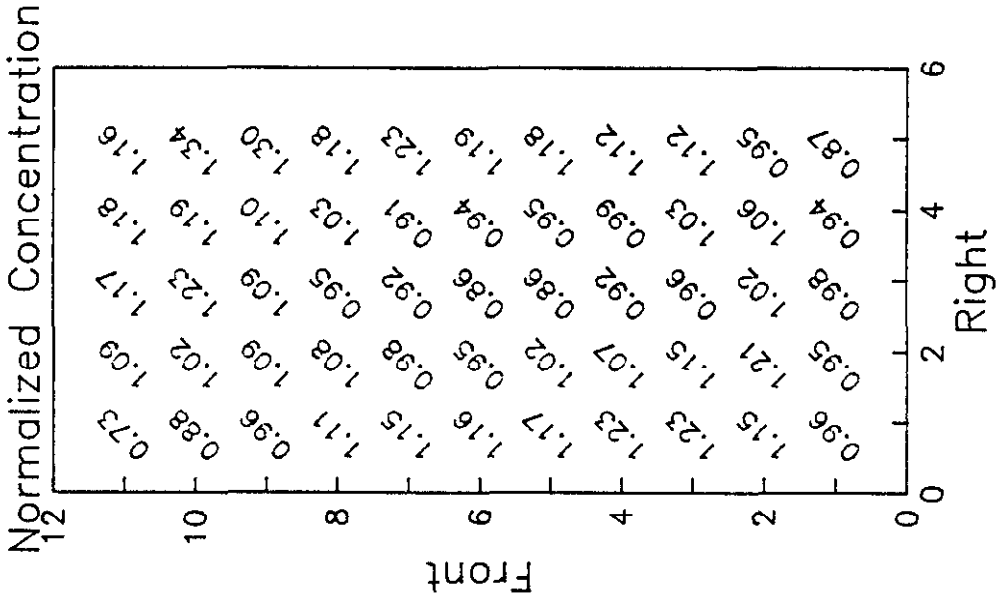


Figure 6-64

**SOUTHERN COMPANY SERVICES
 LANSING SMITH #2 FLOW MODEL**

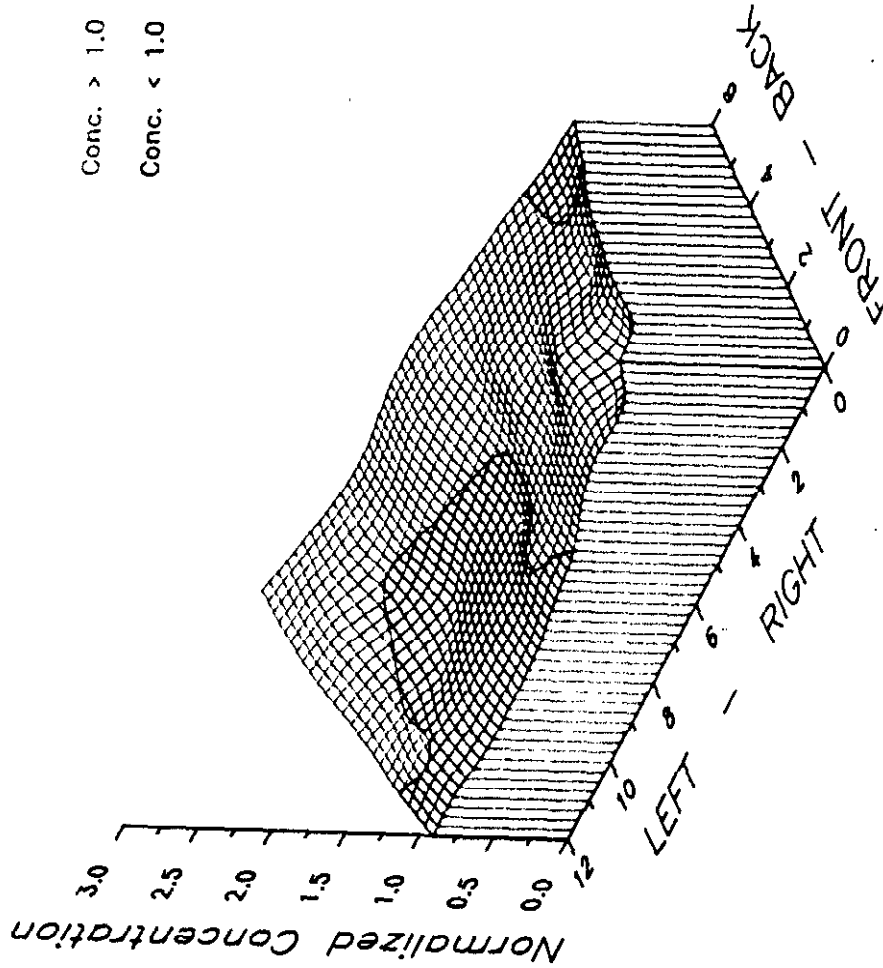
NORMALIZED METHANE CONCENTRATION

Test Plane: 4

Test Date: 2/13/91

Firing System: LNCFS-II

Test ID: Configuration #5



Conc. > 1.0

Conc. < 1.0

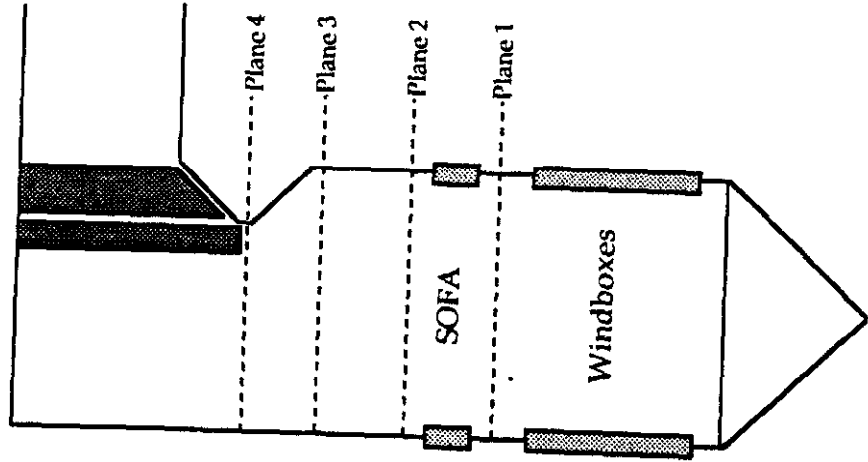


Figure 6-65

SOUTHERN COMPANY SERVICES LANSING SMITH #2 FLOW MODEL

NORMALIZED METHANE CONCENTRATION

Test Plane: 4

Test Date: 2/13/91

Firing System: LNCFS-II

Test ID: Configuration #5

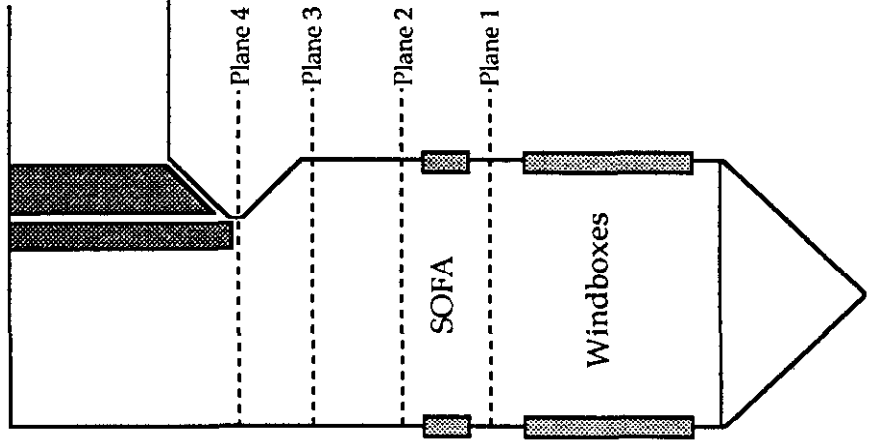
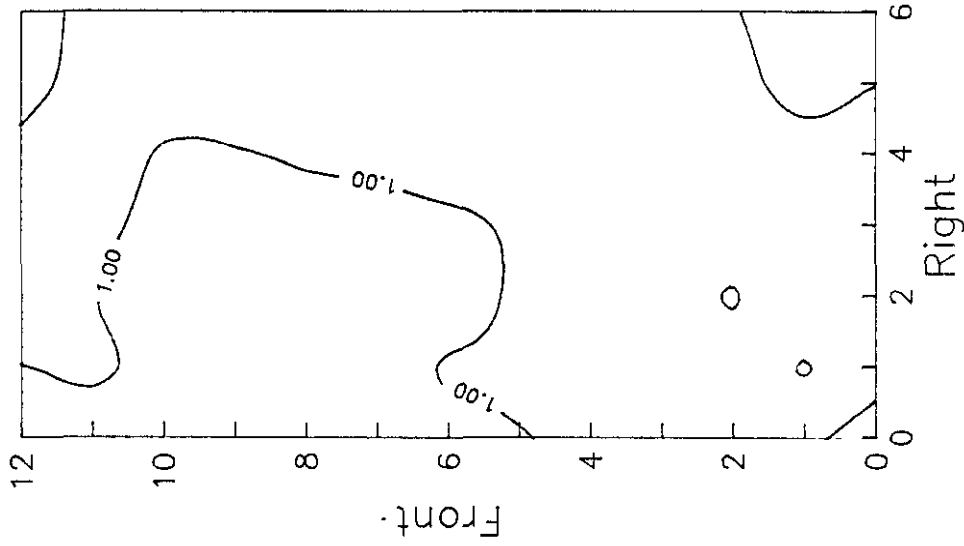


Figure 6-66

**SOUTHERN COMPANY SERVICES
LANSING SMITH #2 FLOW MODEL**

NORMALIZED METHANE CONCENTRATION

Test Plane: 4
 Test Date: 2/13/91
 Firing System: LNCFS-II
 Test ID: Configuration #5

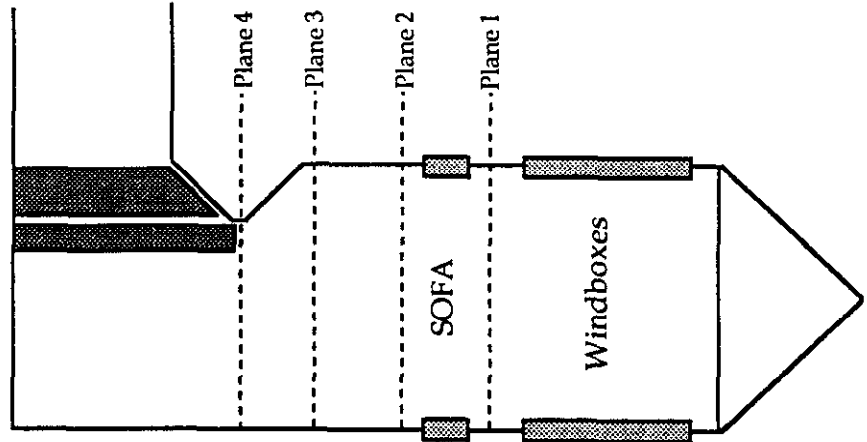
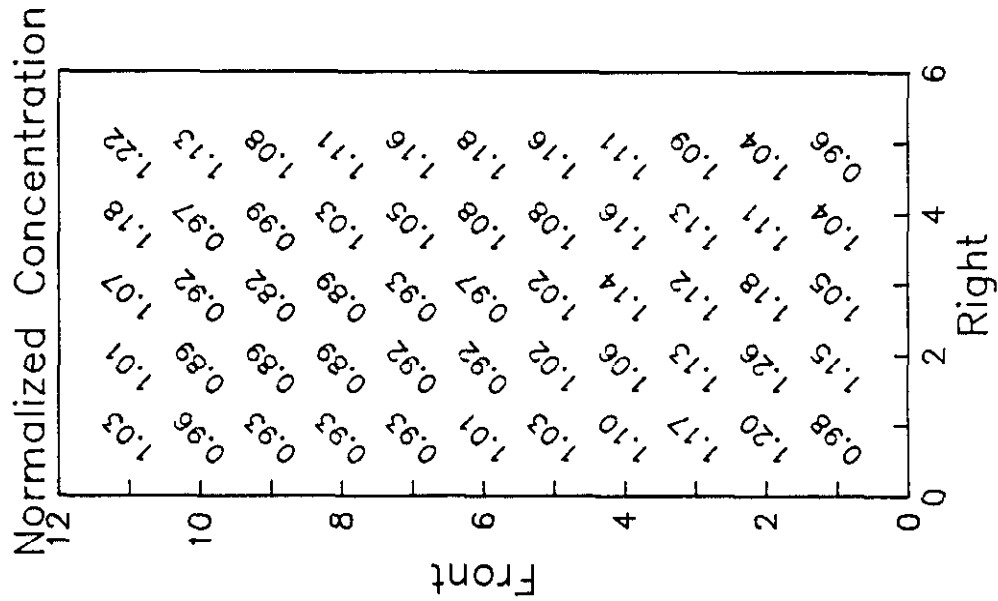
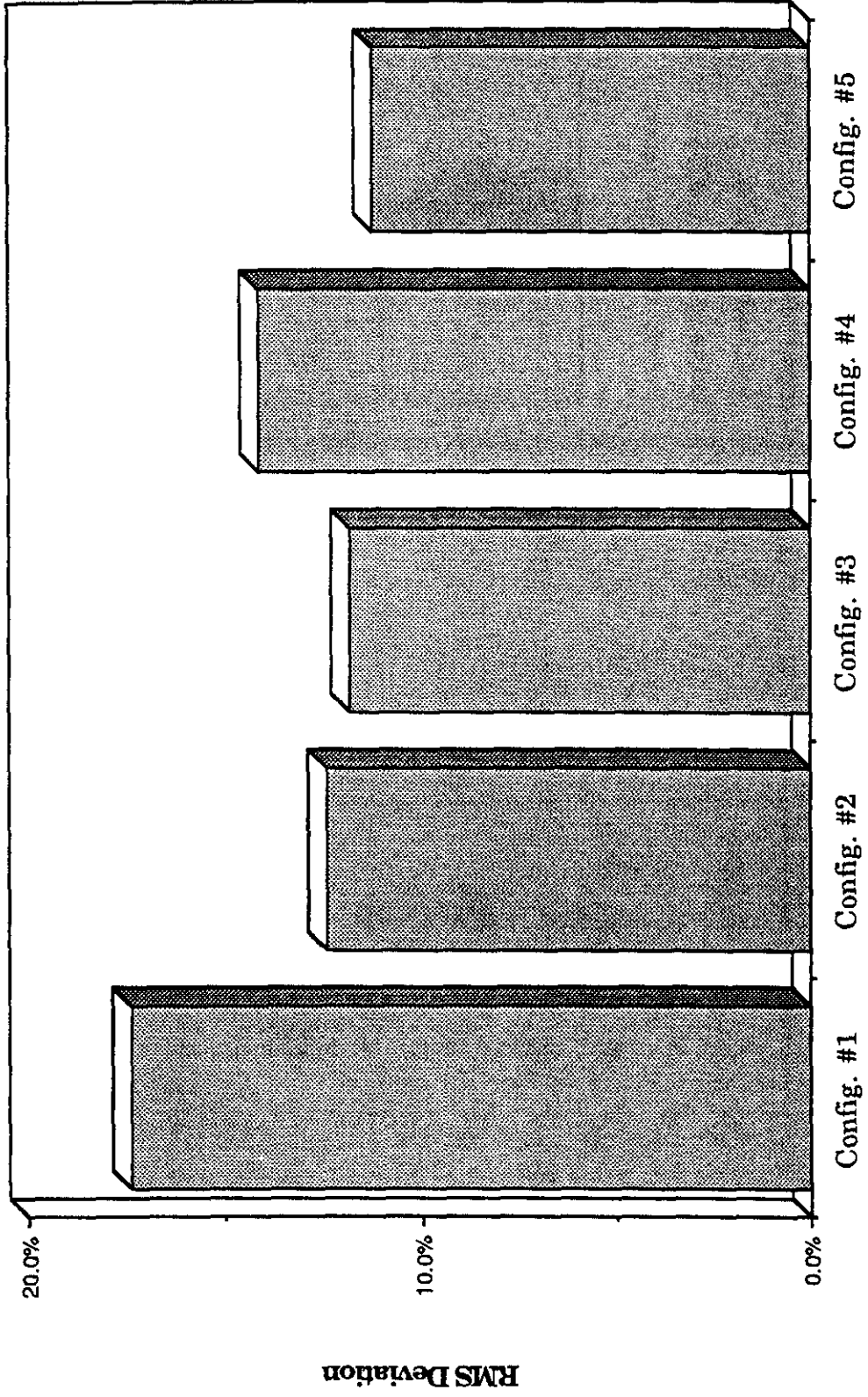


Figure 6-67

**SOUTHERN COMPANY SERVICES
 LANSING SMITH #2 FLOW MODEL**

Lansing Smith Flow Model
Methane RMS Deviation - Plane 4



Test Identification

Figure 6-68

Lansing Smith #2 Flow Model Overall Mixing Performance

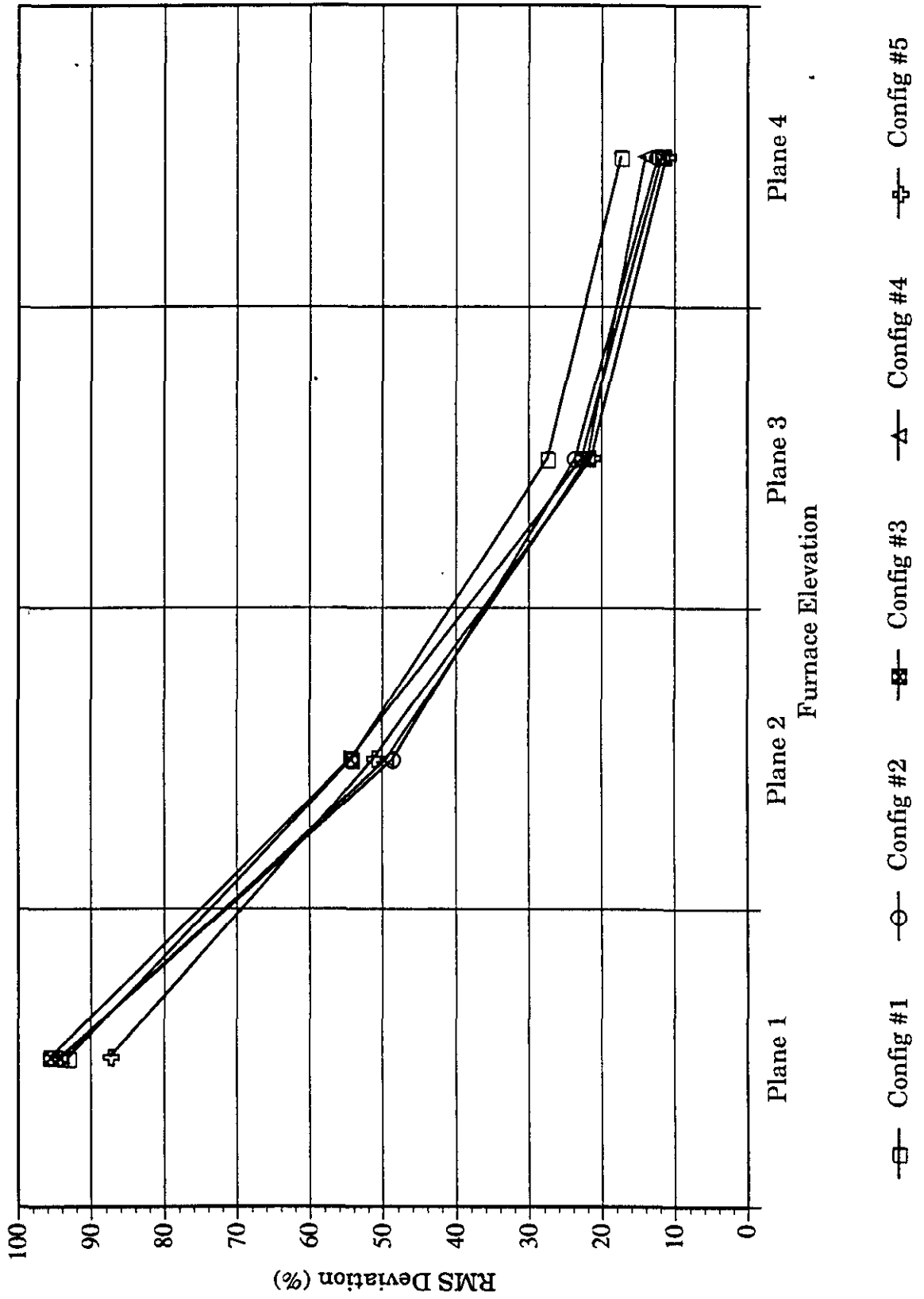


Figure 6-69

6.3 Velocity Testing

In addition to the methane gas mixing tests, three dimensional velocity test data was obtained for each of the five (5) OFA configurations and the baseline configuration. This velocity mapping was performed at the furnace outlet plane for each configuration to characterize the gas flow distribution leaving the furnace.

The velocity data was taken using the five hole pitot probe and the APTD, previously discussed. Pressure measurements were collected and stored in the data acquisition system and central computer, coupled to the APTD. The computer calculates the x, y, and z components of the flow, where the x direction is positive as the flow moves along the rear to the front of the furnace, the y direction is positive as the flow moves from left to right in the furnace, and the z direction is positive when the flow is upward in the furnace. The measured velocities were then reported in both tabular form, typical of Table 6-4, and graphical form.

From the three dimensional velocity data, the normalized upward velocity data was plotted as surface and contour plots, and is shown in Figures 6-70 through 6-81. Additionally, the normalized value of the axial (upward) velocity is presented in Figures 6-82 through 6-87. Results from these tests show that the upward flow leaving the furnace is concentrated along the left rear corner, typical of tangentially fired units. This is primarily due to the effects of the swirl on the leaving gasses. Furthermore, the higher flows occur along the walls of the model with reduced upward flow through the center. In general, the flow distribution at the furnace outlet plane was fairly well distributed, with RMS deviations between 20% and 25%, as shown in Figure 6-88. The RMS deviation for configuration #3 was 21.3%, which was the lowest of the configurations tested. In addition to the overall plane distribution, the side to side velocity distribution was also determined. This was done by taking the average velocity across the depth of the furnace and plotting it across the width. Figure 6-89 shows these values for each configuration. From this data, it can be seen that configuration #2 has a strong left to right imbalance. This imbalance may cause a temperature maldistribution at the furnace outlet

plane, resulting in high tube metal temperatures. Although the reason for this imbalance is not known, it should be noted that this is the only configuration tested which had all four (4) of the OFA nozzles at firing angle which were counter-rotational to the furnace swirl. Also, from this data, it can be seen that the side to side distribution for configuration #3 is fairly uniform, which may result in a more uniform temperature distribution at the superheater.

Additionally, the tangential velocities for each of these configurations are presented in the form of a vector plots. Each vector plot was generated using the same scaling factors, so that they could be compared, and are presented in Figures 6-90 through 6-96. From these plots, the counter clockwise swirl, imposed by the tangential firing system, can be easily seen. The center of this swirl is located near the center of the test plane, as expected. Generally, higher tangential velocities are found along the front and rear walls of the furnace, as these walls are longer than the side walls. This flow corresponds to that seen in the flow visualization tests.

AUTOMATIC PROBE TRAVERSING DEVICE

PROBE NUMBER : E18B4-2
 PROBE CAL DATE : 10/23/90
 FLANE NUMBER : 4
 NUMBER OF ROWS : 5
 NUMBER OF COLUMNS : 11

TEST ID : LNCFS VEL 5
 TEST NUMBER : 0005
 TEST DATE : 2/14/91

AVERAGE NORMAL VELOCITY = 22.64 FT/SEC

* X-VELOCITY (FT/SEC) *

	1	2	3	4	5	6	7	8	9	10	11
1	-1.16	-6.21	-7.03	-4.15	-4.39	1.09	0.08	0.46	2.87	3.07	9.84
2	-9.43	-10.22	-8.88	-9.86	-6.78	0.64	3.10	5.50	6.56	11.20	20.41
3	-13.75	-15.10	-12.20	2.53	-0.59	2.65	10.56	13.67	11.07	9.17	11.12
4	-20.54	-10.16	-1.04	0.60	7.01	8.02	5.32	13.42	12.16	13.71	19.77
5	-5.09	1.61	2.41	5.45	7.23	4.91	8.38	8.67	9.94	15.26	12.26

* Y-VELOCITY (FT/SEC) *

	1	2	3	4	5	6	7	8	9	10	11
1	-7.13	3.00	17.78	18.78	20.95	18.08	21.56	19.30	22.52	19.22	-1.09
2	0.91	7.25	17.14	14.05	9.49	11.68	15.01	8.57	3.86	0.92	0.03
3	-2.83	-1.44	-5.40	-5.73	0.18	-5.69	-6.14	-12.52	5.07	-0.23	2.50
4	-5.21	-3.83	-12.90	-14.25	-17.83	-15.05	-16.92	-22.31	-15.35	-14.39	-2.40
5	-10.32	-14.95	-16.14	-22.87	-24.14	-15.52	-22.68	-22.46	-24.68	-14.43	-5.59

* NORMAL VELOCITY (FT/SEC) *

	1	2	3	4	5	6	7	8	9	10	11
1	26.53	23.36	16.49	18.57	20.64	20.18	22.49	20.35	22.39	21.58	26.33
2	28.20	18.67	17.50	18.78	24.97	26.20	25.59	25.03	28.40	24.69	26.98
3	21.25	20.33	15.51	12.09	16.17	17.97	17.04	18.15	29.13	28.75	31.92
4	21.20	19.19	19.91	18.96	18.35	16.31	17.29	20.28	22.02	24.33	32.26
5	23.35	24.24	26.51	24.79	24.90	24.14	22.55	23.43	24.61	29.32	35.21

* TOTAL PRESSURE (IN-H2O) *

	1	2	3	4	5	6	7	8	9	10	11
1	-0.62	-0.65	-0.70	-0.71	-0.68	-0.74	-0.70	-0.73	-0.68	-0.63	-0.57
2	-0.63	-0.70	-0.73	-0.74	-0.70	-0.72	-0.75	-0.71	-0.71	-0.67	-0.61
3	-0.64	-0.66	-0.73	-0.78	-0.80	-0.75	-0.79	-0.69	-0.71	-0.67	-0.67
4	-0.58	-0.69	-0.66	-0.77	-0.76	-0.79	-0.75	-0.73	-0.74	-0.65	-0.59
5	-0.60	-0.62	-0.61	-0.63	-0.65	-0.69	-0.70	-0.69	-0.66	-0.64	-0.59

Table 6-4 Velocity Mapping Data - General Output

AUTOMATIC PROBE TRAVERSING DEVICE

PROBE NUMBER : R1884-2
 PROBE CAL DATE : 10/23/90
 PLANE NUMBER : 4
 NUMBER OF ROWS : 5
 NUMBER OF COLUMNS : 11

TEST ID : LNCFS VEL 5
 TEST NUMBER : 0005
 TEST DATE : 2/14/91
 AVERAGE NORMAL VELOCITY = 22.64 FT/SEC
 NORMAL VELOCITY RMS = 20.53 %

* NORMALIZED *
 * X-VELOCITY *

	1	2	3	4	5	6	7	8	9	10	11
1	-0.05	-0.27	-0.31	-0.18	-0.19	0.05	0.00	0.02	0.13	0.14	0.43
2	-0.42	-0.45	-0.39	-0.44	-0.30	0.03	0.14	0.24	0.29	0.49	0.90
3	-0.61	-0.67	-0.54	0.11	-0.03	0.12	0.47	0.60	0.49	0.41	0.49
4	-0.91	-0.45	-0.05	0.03	0.31	0.35	0.23	0.59	0.54	0.61	0.87
5	-0.22	0.07	0.11	0.24	0.32	0.22	0.37	0.38	0.44	0.67	0.54

* NORMALIZED *
 * Y-VELOCITY *

	1	2	3	4	5	6	7	8	9	10	11
1	-0.31	0.13	0.79	0.83	0.93	0.80	0.95	0.85	0.99	0.85	-0.05
2	0.04	0.32	0.76	0.62	0.42	0.52	0.66	0.38	0.13	0.04	0.00
3	-0.13	-0.06	-0.24	-0.25	0.01	-0.25	-0.27	-0.55	0.22	-0.01	0.11
4	-0.23	-0.17	-0.57	-0.63	-0.79	-0.66	-0.75	-0.99	-0.68	-0.64	-0.11
5	-0.46	-0.66	-0.71	-1.01	-1.07	-0.69	-1.00	-0.99	-1.09	-0.64	-0.25

* NORMALIZED *
 * NORMAL VELOCITY *

	1	2	3	4	5	6	7	8	9	10	11
1	1.17	1.03	0.73	0.82	0.91	0.89	0.99	0.90	0.99	0.95	1.16
2	1.25	0.62	0.77	0.83	1.10	1.16	1.13	1.11	1.25	1.09	1.19
3	0.94	0.90	0.68	0.53	0.71	0.79	0.75	0.80	1.29	1.27	1.41
4	0.94	0.85	0.88	0.84	0.81	0.72	0.76	0.90	0.97	1.07	1.42
5	1.03	1.07	1.17	1.09	1.10	1.07	1.00	1.03	1.09	1.30	1.56

Table 6-4 Velocity Mapping Data - General Output (cont)

AUTOMATIC PROBE TRAVERSING DEVICE

PROBE NUMBER : B1884-2
 PROBE CAL DATE : 10/23/90

TEST ID : LNCFS VEL 5
 TEST NUMBER : 0005
 TEST DATE : 2/14/91

PLANE NUMBER : 4
 NUMBER OF ROWS : 5
 NUMBER OF COLUMNS : 11

AVERAGE NORMAL VELOCITY = 22.64 FT/SEC

* RESULTANT VELOCITY VECTOR/ANGLE IN THE X-Y PLANE *

	1	2	3	4	5	6	7
1	7.22/189.	6.90/296.	19.12/338.	19.24/348.	21.40/348.	18.11/ 3.	21.56/ 0.
2	9.48/276.	12.53/305.	19.30/333.	17.16/325.	11.66/325.	11.70/ 3.	15.33/ 12.
3	14.04/258.	15.17/264.	13.34/246.	6.26/156.	0.62/287.	6.28/155.	12.22/120.
4	21.19/256.	10.86/249.	12.94/185.	14.26/178.	19.15/159.	17.06/152.	17.74/163.
5	11.51/206.	15.03/174.	16.32/172.	23.51/167.	25.20/163.	16.28/162.	24.18/160.
B		9	10	11			

1	19.30/ 1.	22.71/ 7.	19.46/ 9.	9.90/ 97.
2	10.19/ 33.	7.15/ 66.	11.24/ 85.	20.41/ 90.
3	18.54/133.	12.17/ 65.	9.18/ 92.	11.40/ 77.
4	26.04/149.	19.58/142.	19.88/137.	19.91/ 97.
5	24.07/159.	26.60/158.	21.01/134.	13.48/115.

Table 6-4 Velocity Mapping Data - General Output (cont)

NORMALIZED VELOCITY

Test Plane: 4

Test Date: 1/31/91

Firing System: LNCFS-II

Test ID: Baseline

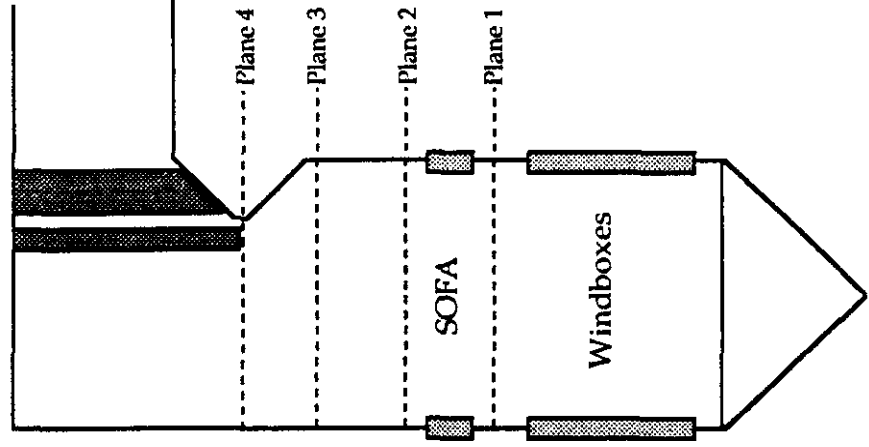
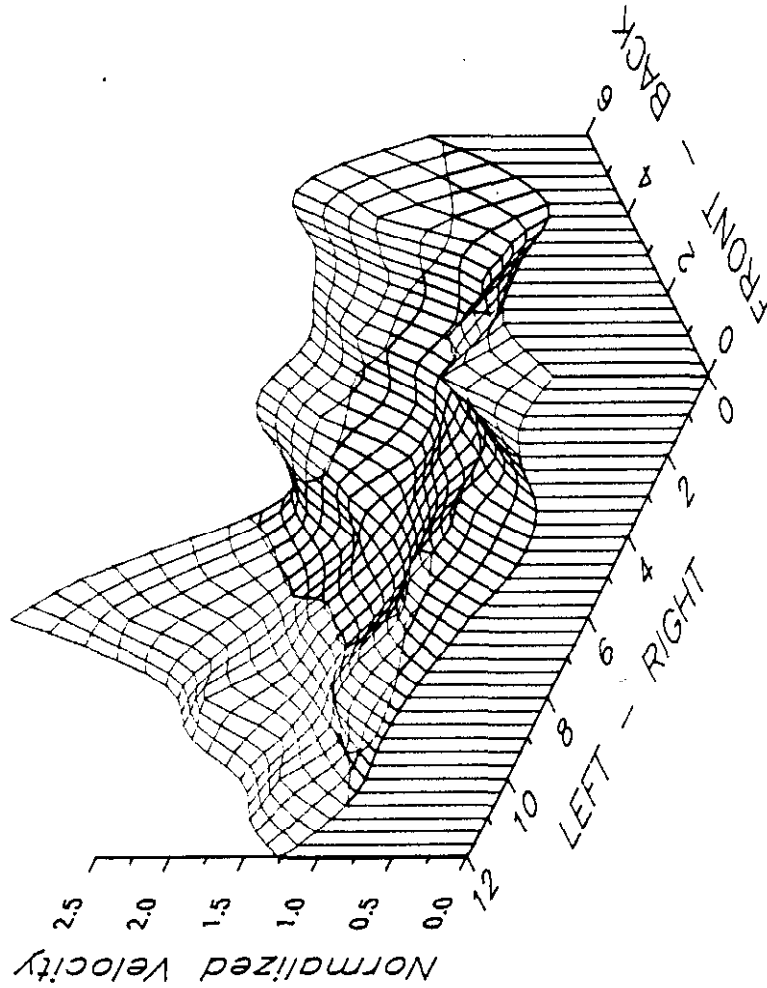


Figure 6-70

**SOUTHERN COMPANY SERVICES
LANSING SMITH #2 FLOW MODEL**

ABB Combustion Engineering, Inc.
Kreisinger Development Laboratory
Mechanical Systems Engineering

NORMALIZED VELOCITY

Test Plane: 4

Test Date: 1/31/91

Firing System: LNCFS-II

Test ID: Baseline

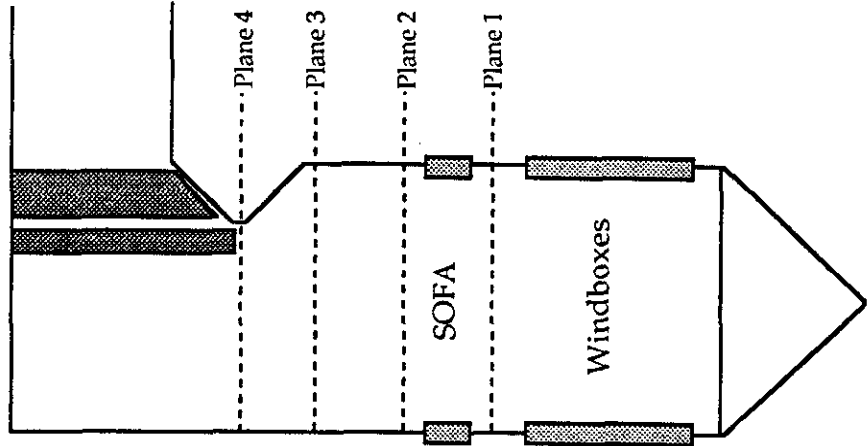
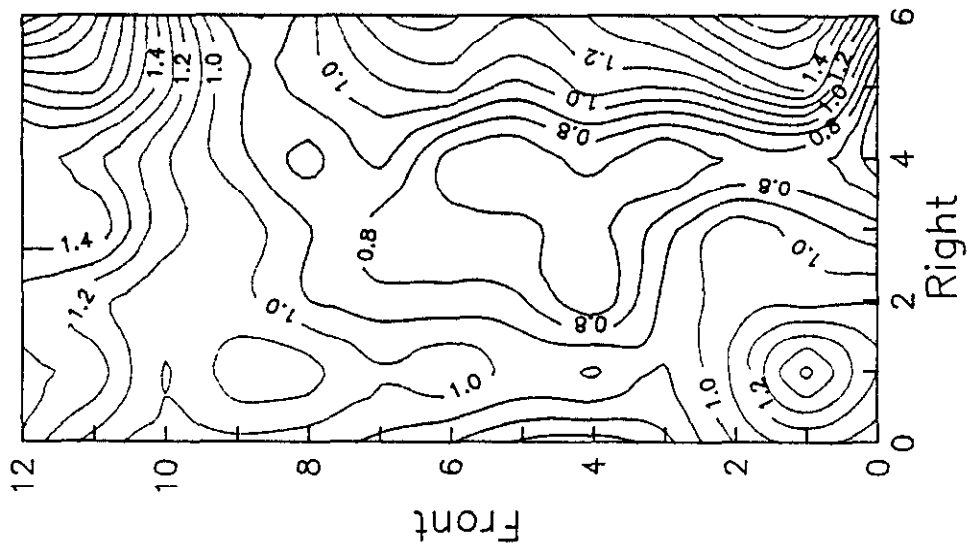


Figure 6-71

**SOUTHERN COMPANY SERVICES
LANSING SMITH #2 FLOW MODEL**

NORMALIZED VELOCITY

Test Plane: 4

Test Date: 2/4/91

Firing System: LNCFS-II

Test ID: Configuration #1

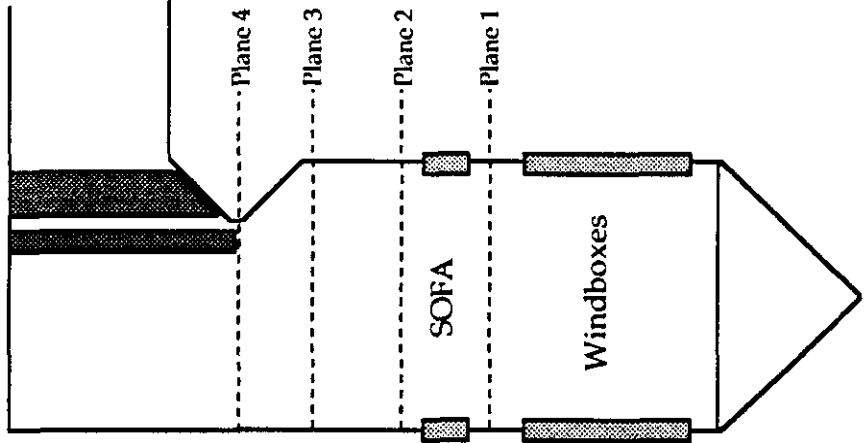
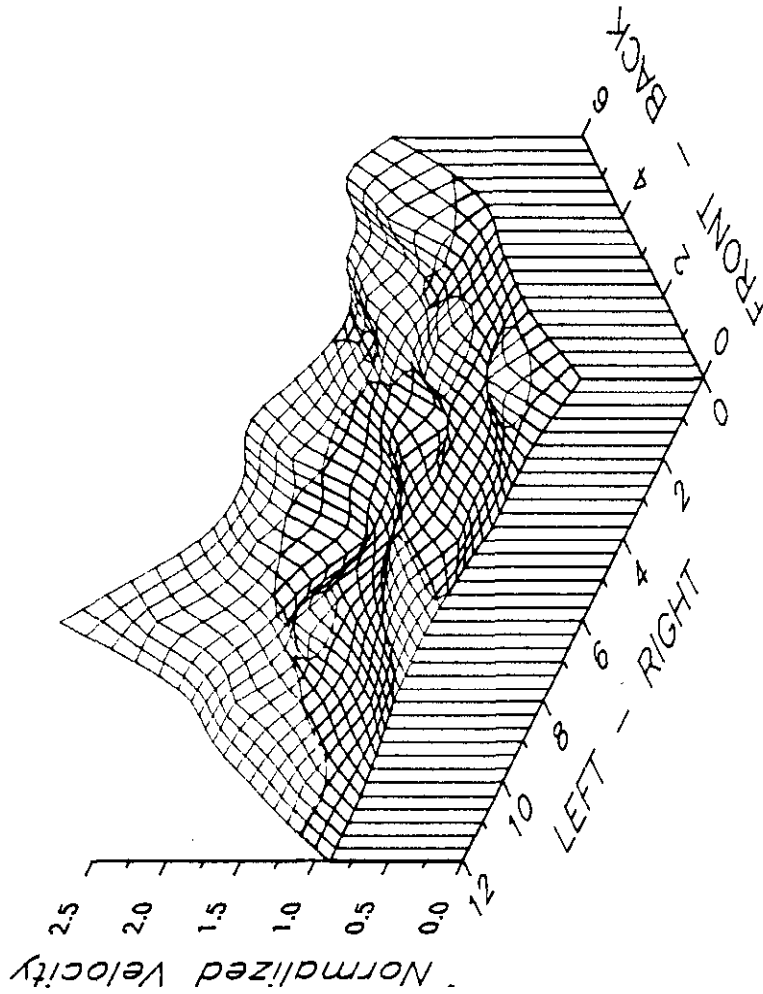


Figure 6-72

**SOUTHERN COMPANY SERVICES
LANSING SMITH #2 FLOW MODEL**

ABB Combustion Engineering, Inc.
Kreisinger Development Laboratory
Mechanical Systems Engineering

NORMALIZED VELOCITY

Test Plane: 4

Test Date: 2/4/91

Firing System: LNCFS-II

Test ID: Configuration #1

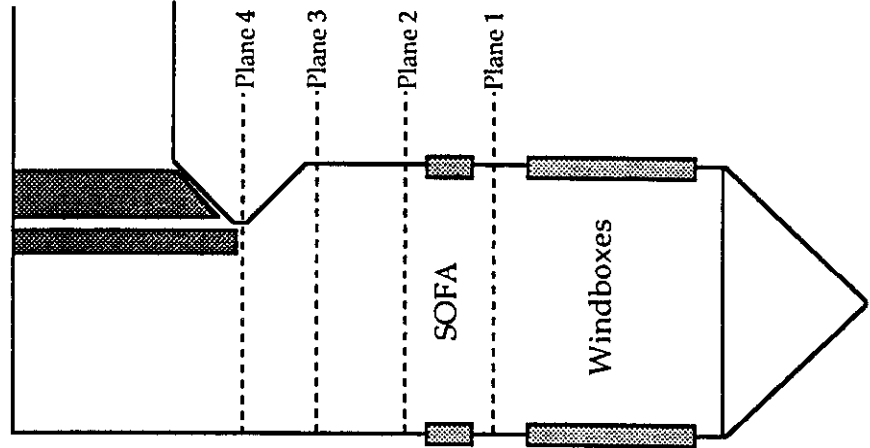
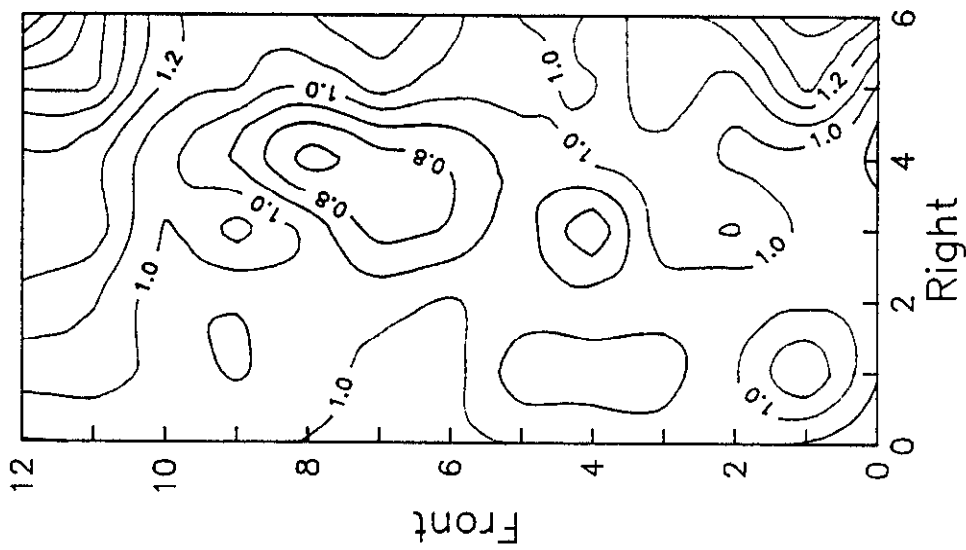


Figure 6-73
SOUTHERN COMPANY SERVICES
LANSING SMITH #2 FLOW MODEL

NORMALIZED VELOCITY

Test Plane: 4

Test Date: 2/5/91

Firing System: LNCFS-II

Test ID: Configuration #2

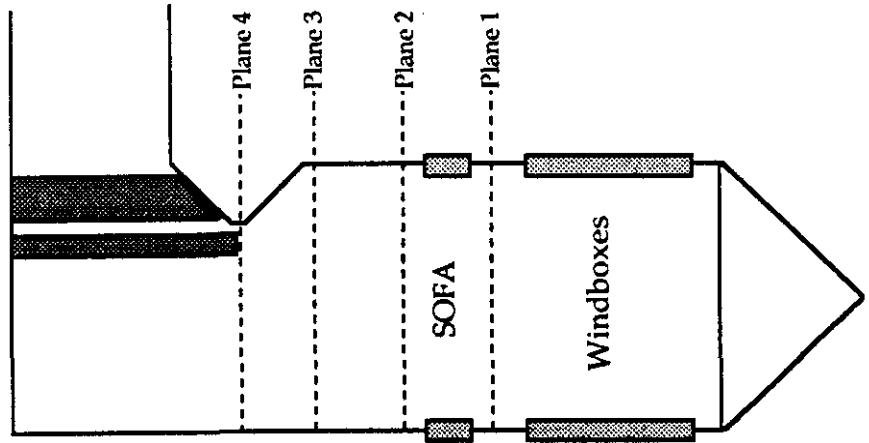
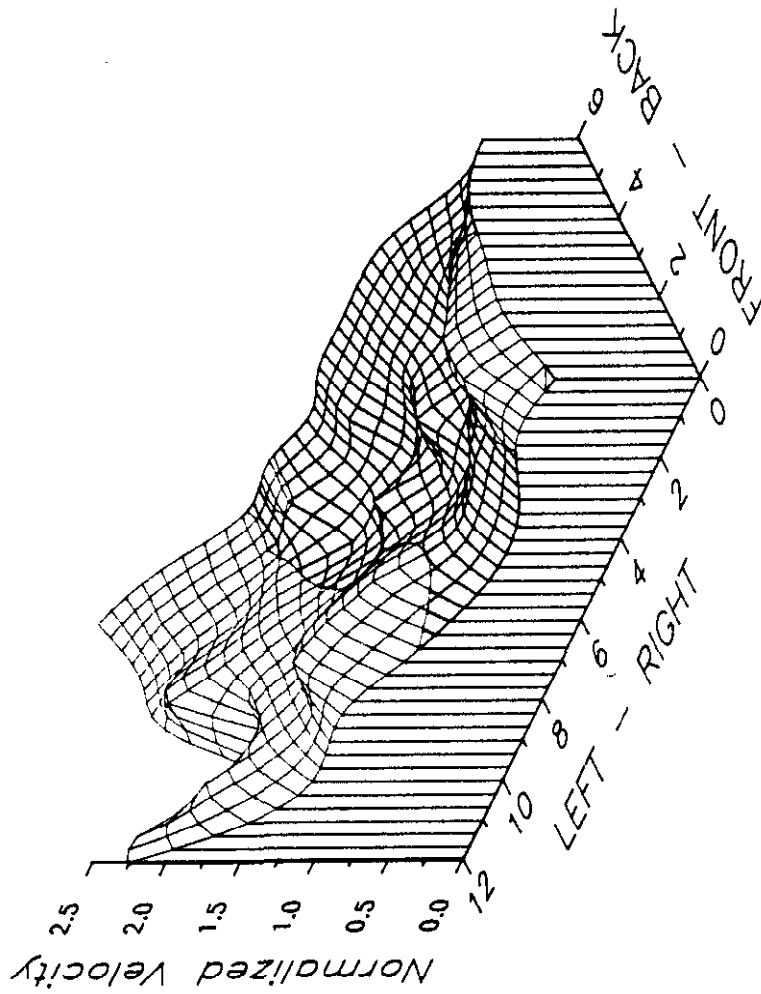


Figure 6-74

**SOUTHERN COMPANY SERVICES
LANSING SMITH #2 FLOW MODEL**

NORMALIZED VELOCITY

Test Plane: 4

Test Date: 2/5/91

Firing System: LNCFS-II

Test ID: Configuration #2

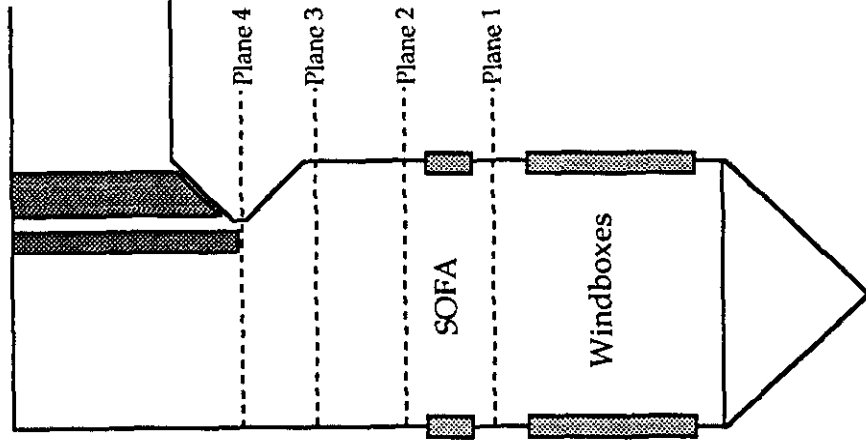
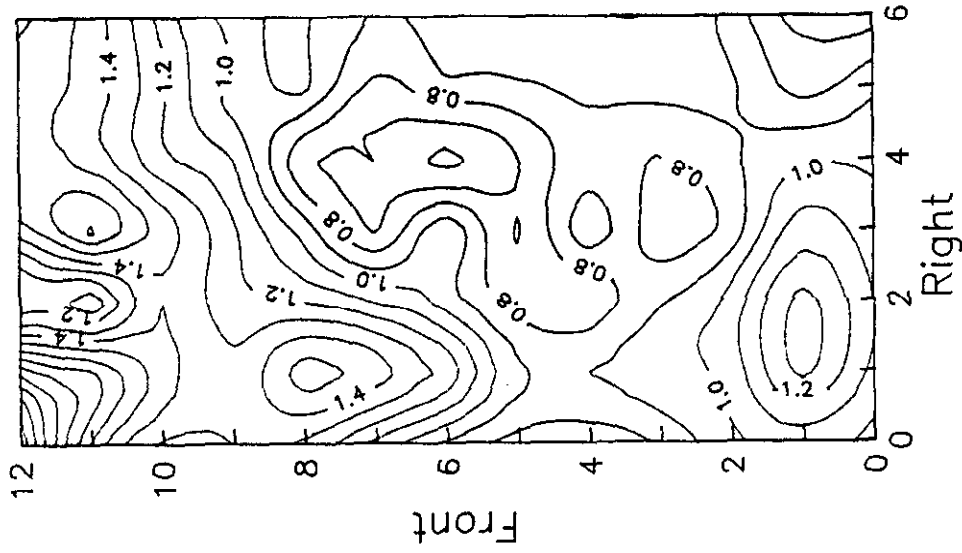


Figure 6-75

**SOUTHERN COMPANY SERVICES
LANSING SMITH #2 FLOW MODEL**

ABB Combustion Engineering, Inc.
Kreisinger Development Laboratory
Mechanical Systems Engineering

NORMALIZED VELOCITY

Test Plane: 4

Test Date: 2/5/91

Firing System: LNCFS-II

Test ID: Configuration #3

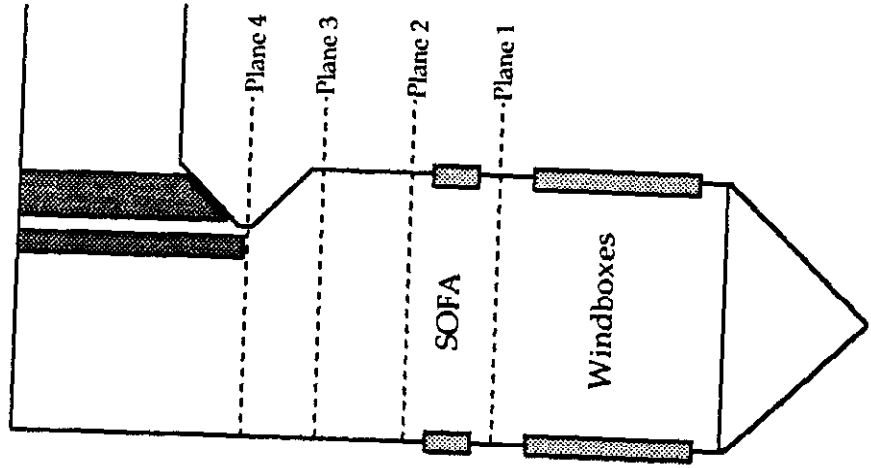
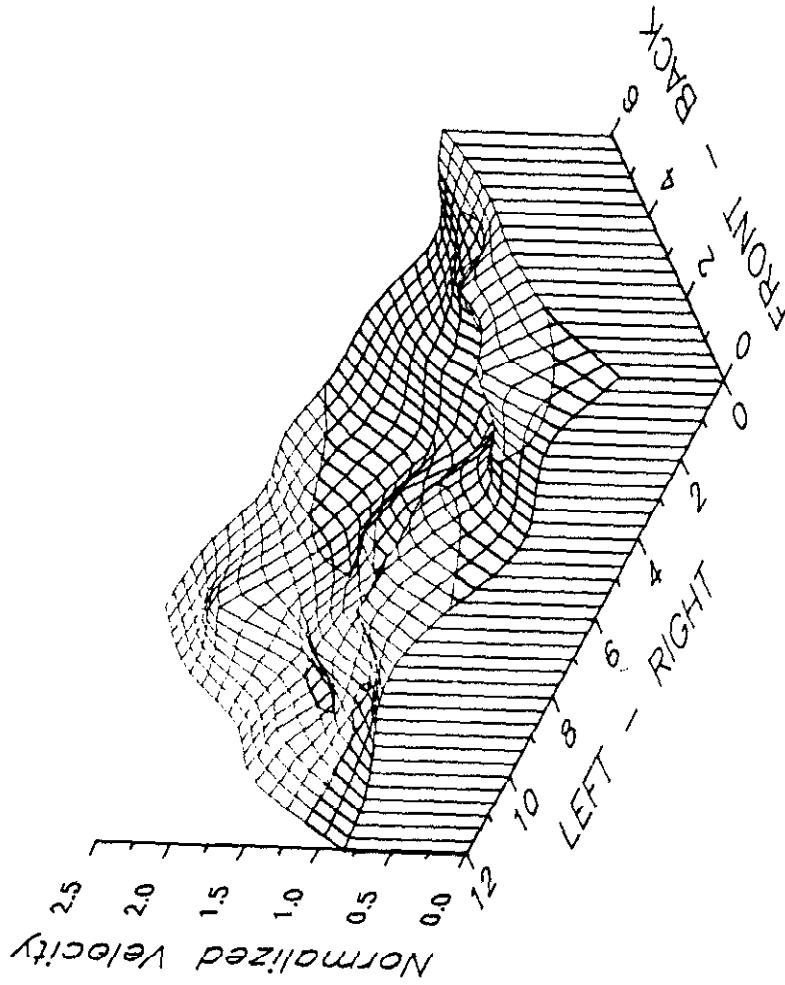


Figure 6-76

**SOUTHERN COMPANY SERVICES
LANSING SMITH #2 FLOW MODEL**

NORMALIZED VELOCITY

Test Plane: 4

Test Date: 2/5/91

Firing System: LNCFS-II

Test ID: Configuration #3

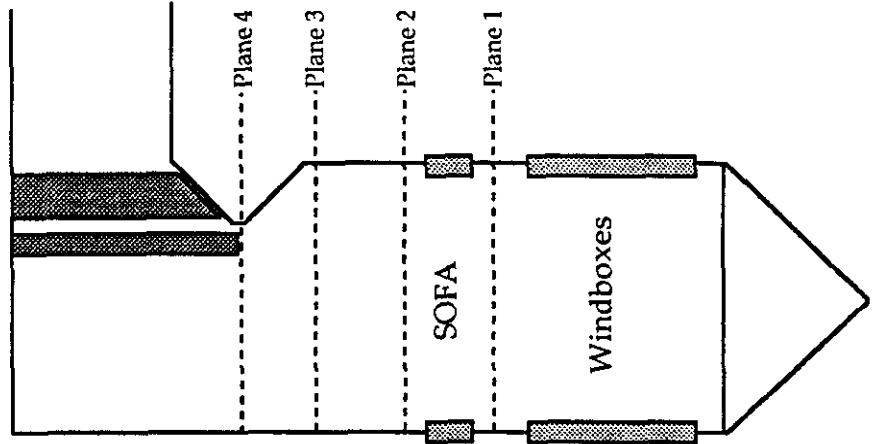


Figure 6-77

**SOUTHERN COMPANY SERVICES
LANSING SMITH #2 FLOW MODEL**

ABB Combustion Engineering, Inc.
Kreisinger Development Laboratory
Mechanical Systems Engineering

NORMALIZED VELOCITY

Test Plane: 4

Test Date: 2/7/91

Firing System: LNCFS-II

Test ID: Configuration #4

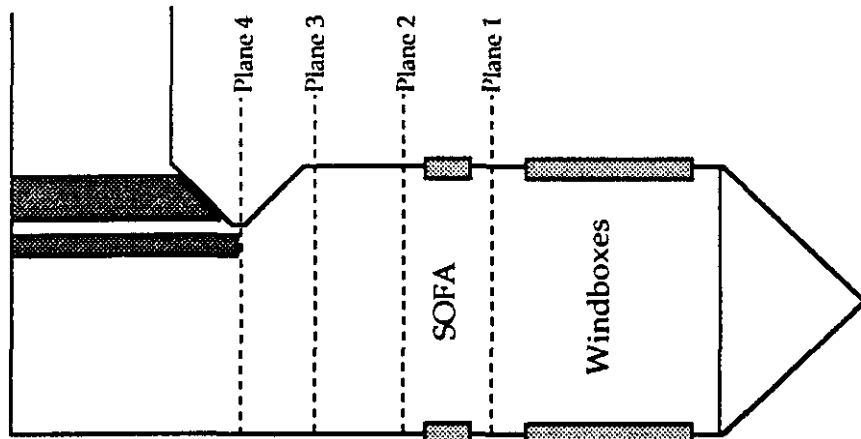
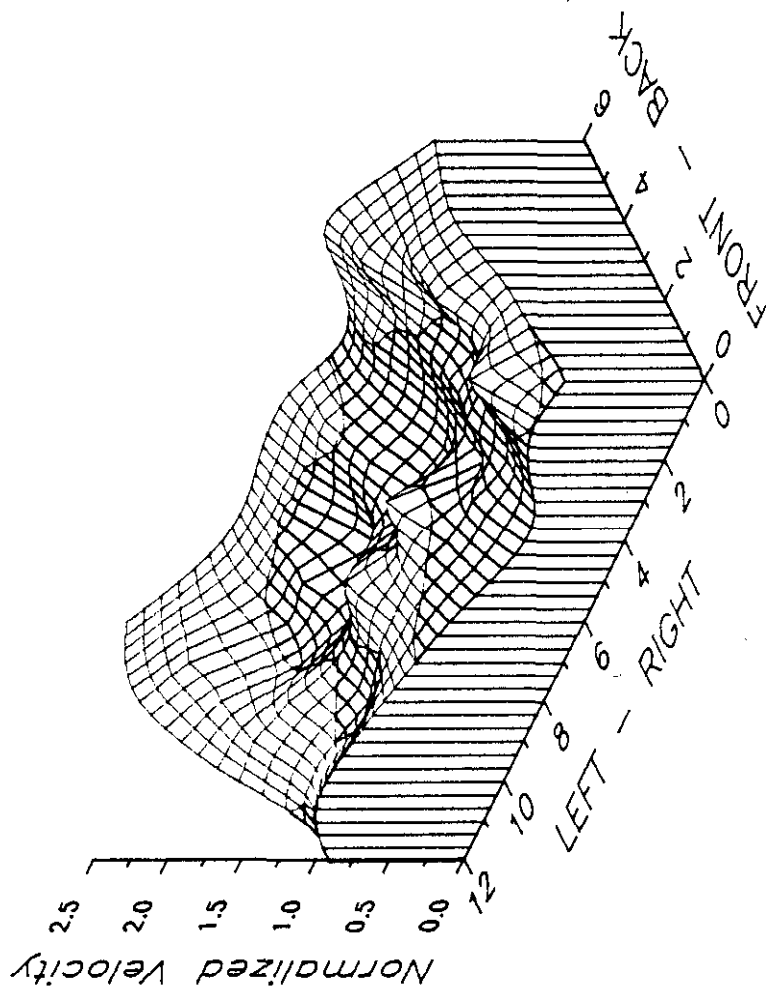


Figure 6-78

**SOUTHERN COMPANY SERVICES
LANSING SMITH #2 FLOW MODEL**

NORMALIZED VELOCITY

Test Plane: 4

Test Date: 2/7/91

Firing System: LNCFS-II

Test ID: Configuration #4

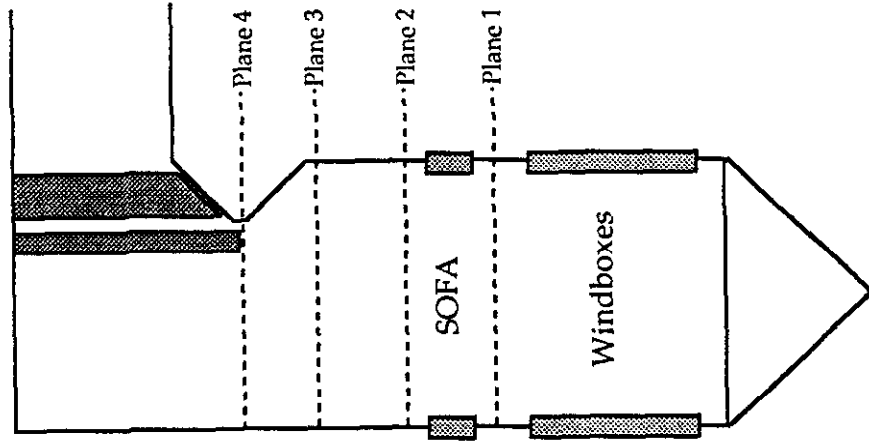
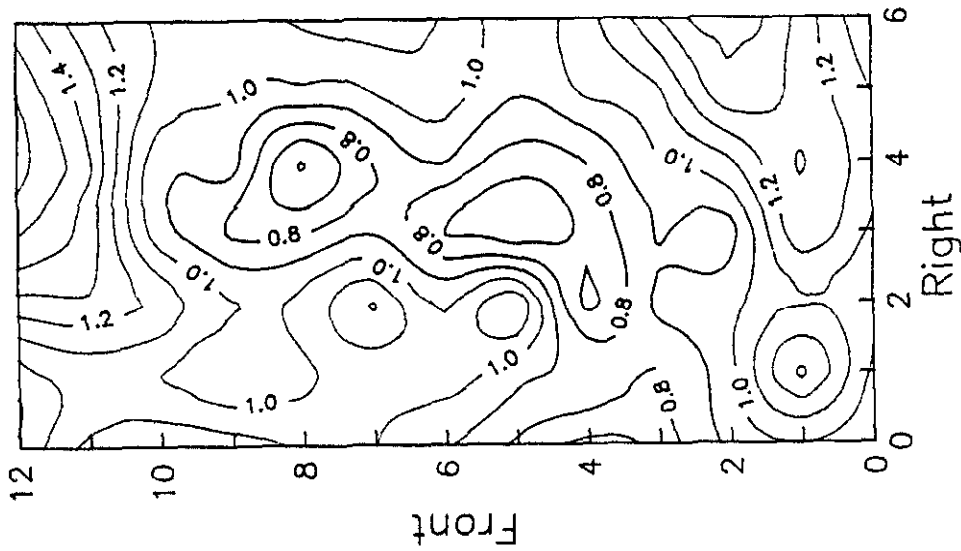


Figure 6-79
**SOUTHERN COMPANY SERVICES
LANSING SMITH #2 FLOW MODEL**

NORMALIZED VELOCITY

Test Plane: 4

Test Date: 2/14/91

Firing System: LNCFS-II

Test ID: Configuration #5

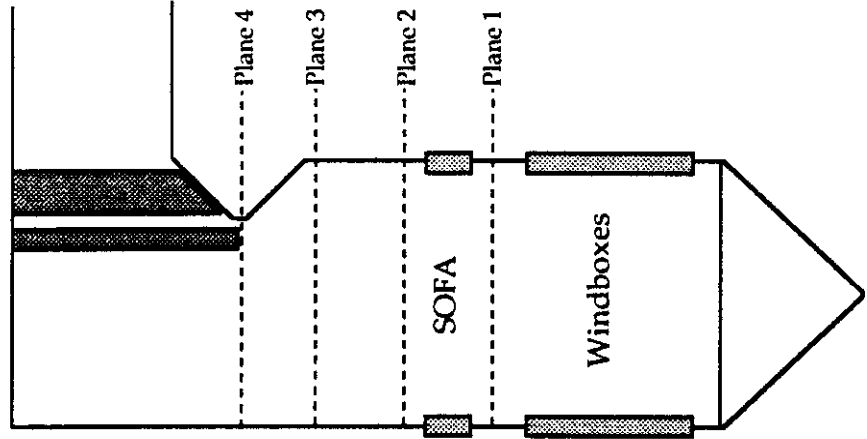
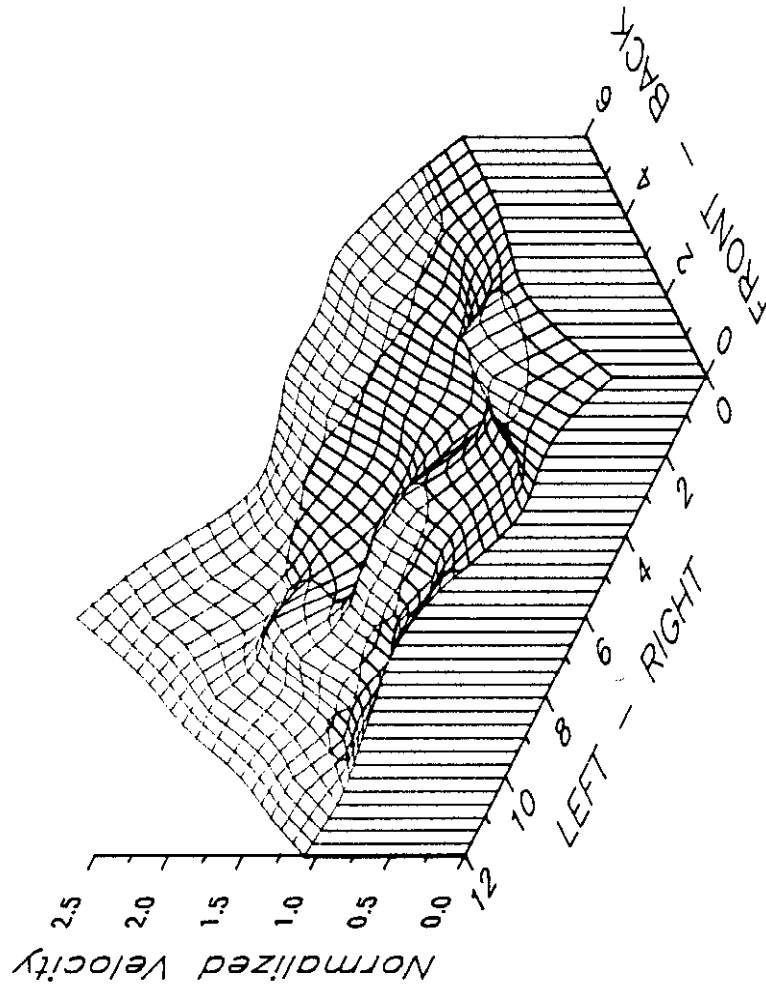


Figure 6-80

**SOUTHERN COMPANY SERVICES
LANSING SMITH #2 FLOW MODEL**

NORMALIZED VELOCITY

Test Plane: 4

Test Date: 2/14/91

Firing System: LNCFS-II

Test ID: Configuration #5

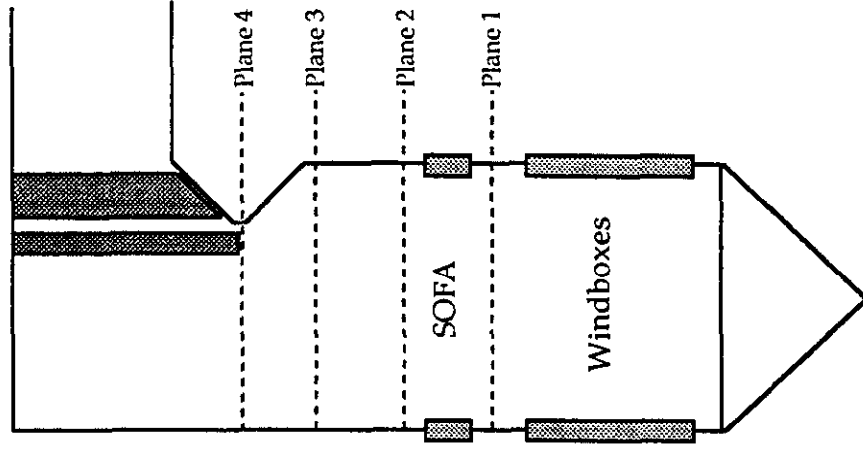
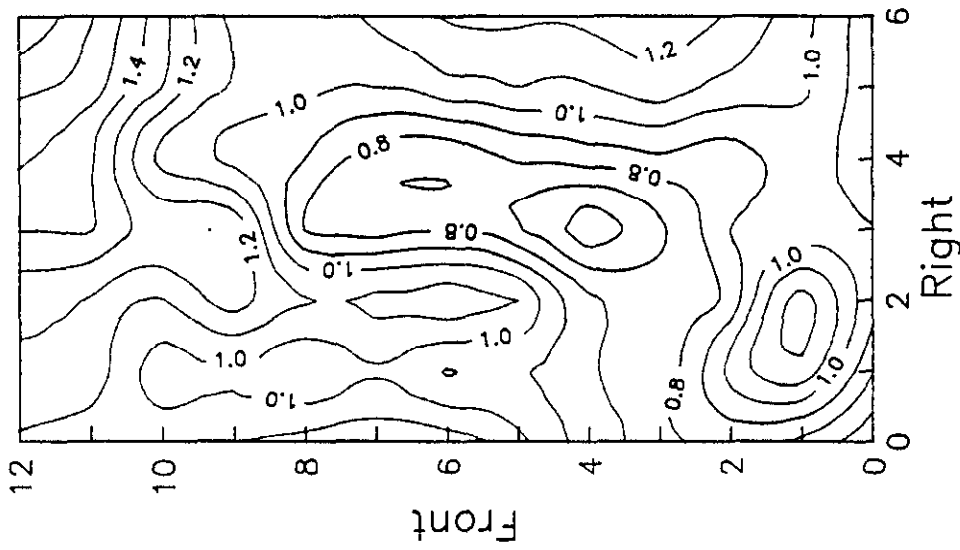


Figure 6-81

**SOUTHERN COMPANY SERVICES
LANSING SMITH #2 FLOW MODEL**

NORMALIZED VELOCITY

Test Plane: 4
 Test Date: 1/31/91
 Firing System: LNCFS-II
 Test ID: Baseline

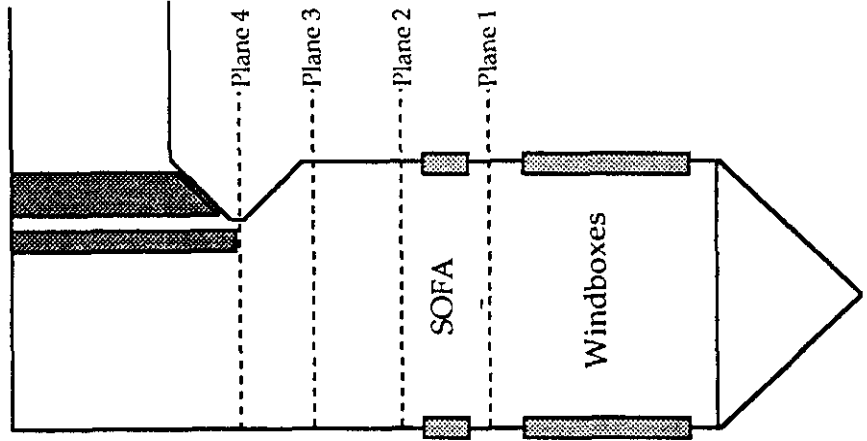
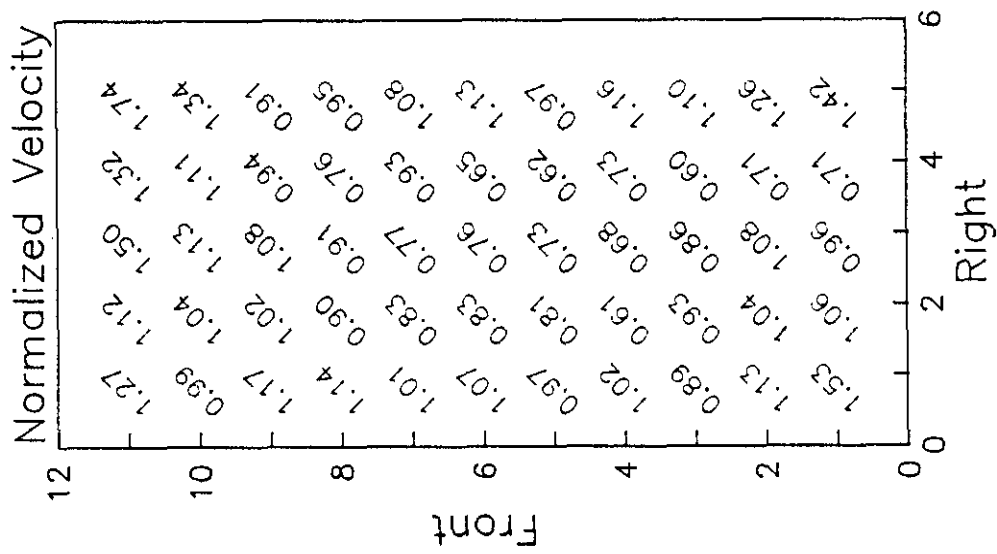


Figure 6-82

**SOUTHERN COMPANY SERVICES
 LANSING SMITH #2 FLOW MODEL**

NORMALIZED VELOCITY

Test Plane: 4

Test Date: 2/4/91

Firing System: LNCFS-II

Test ID: Configuration #1

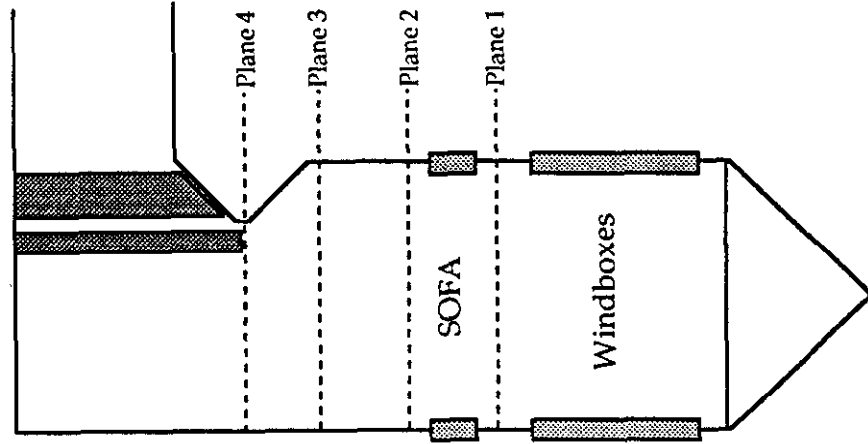
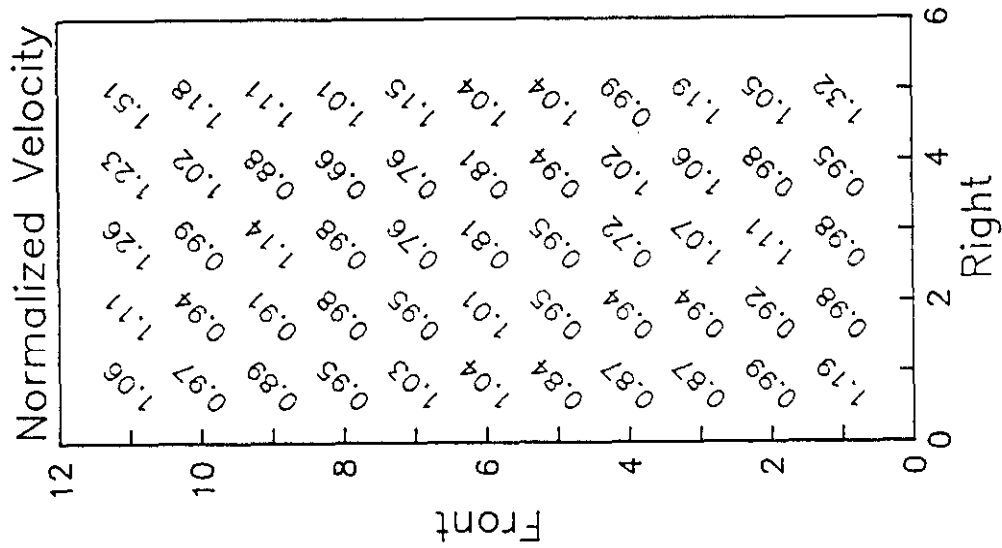


Figure 6-83

**SOUTHERN COMPANY SERVICES
LANSING SMITH #2 FLOW MODEL**

NORMALIZED VELOCITY

Test Plane: 4

Test Date: 2/5/91

Firing System: LNCFS-II

Test ID: Configuration #2

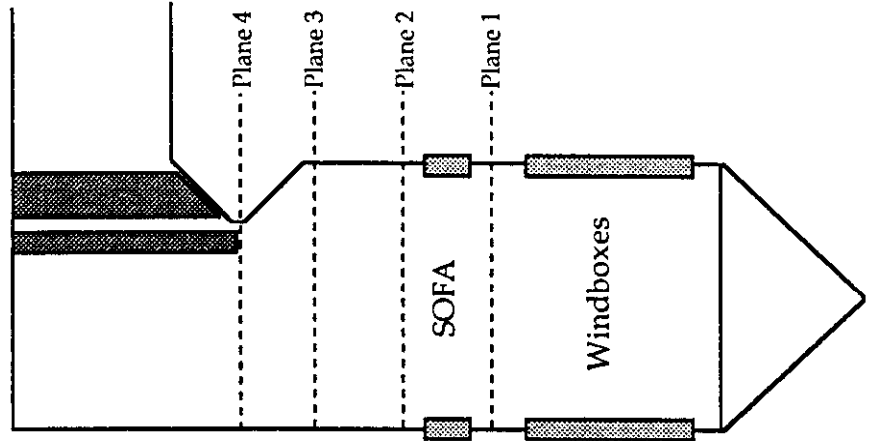
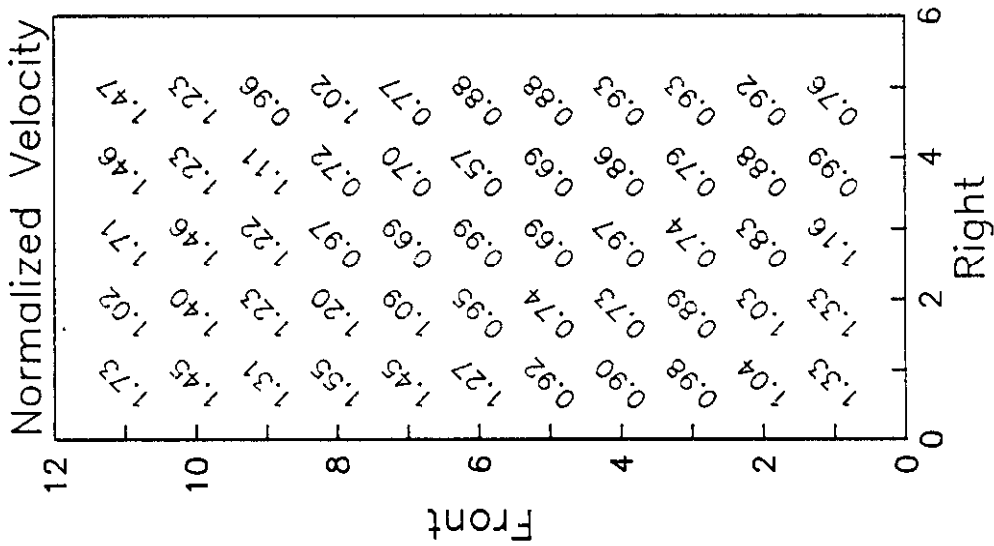


Figure 6-84

**SOUTHERN COMPANY SERVICES
LANSING SMITH #2 FLOW MODEL**

NORMALIZED VELOCITY

Test Plane: 4

Test Date: 2/5/91

Firing System: LNCFS-II

Test ID: Configuration #3

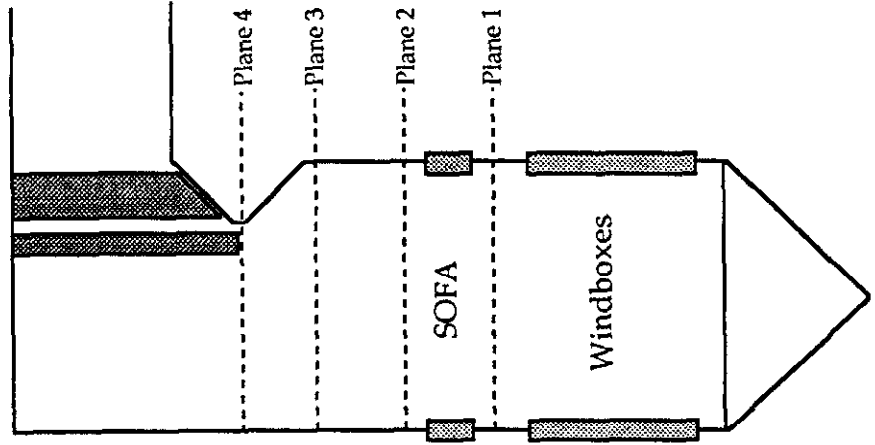
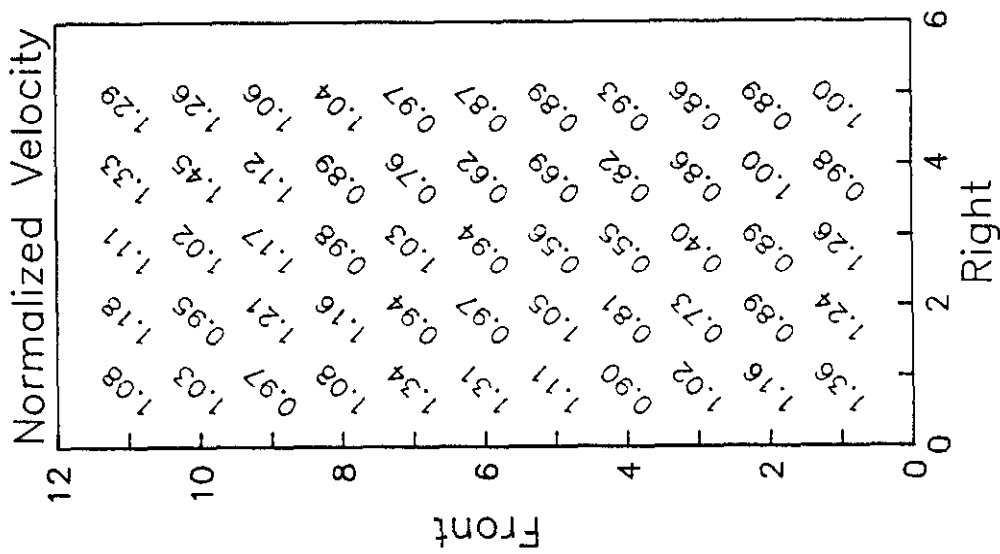
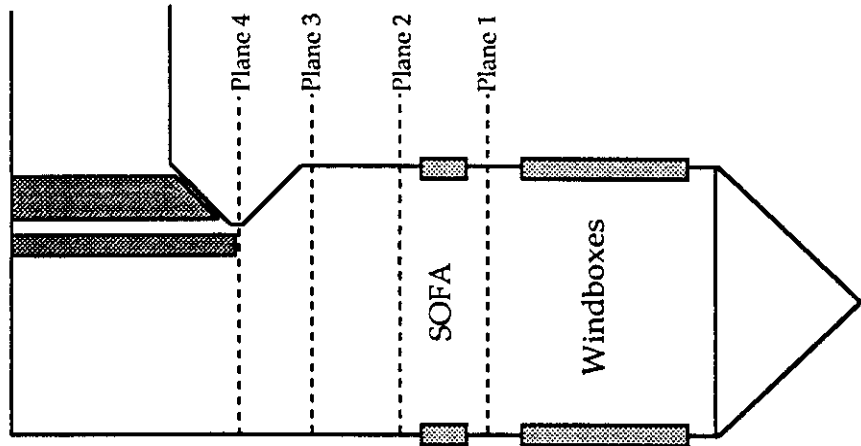
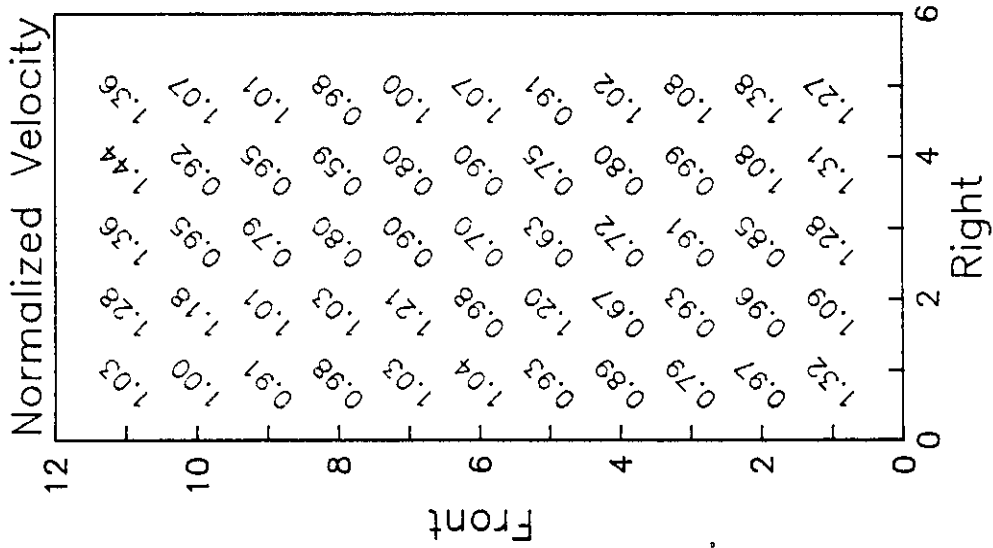


Figure 6-85

**SOUTHERN COMPANY SERVICES
LANSING SMITH #2 FLOW MODEL**

NORMALIZED VELOCITY

Test Plane: 4
 Test Date: 2/7/91
 Firing System: LNCFS-II
 Test ID: Configuration #4



SOUTHERN COMPANY SERVICES
LANSING SMITH #2 FLOW MODEL

Figure 6-86

NORMALIZED VELOCITY

Test Plane: 4
 Test Date: 2/14/91
 Firing System: LNCFS-II
 Test ID: Configuration #5

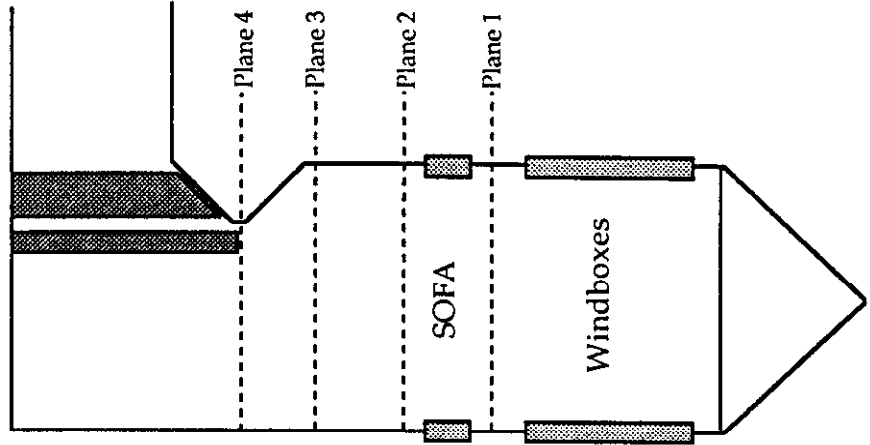
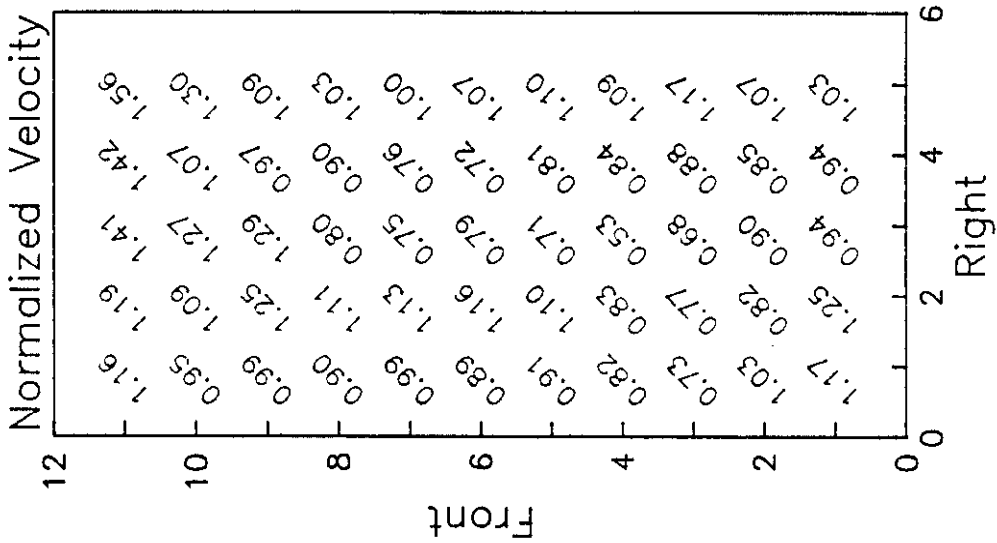
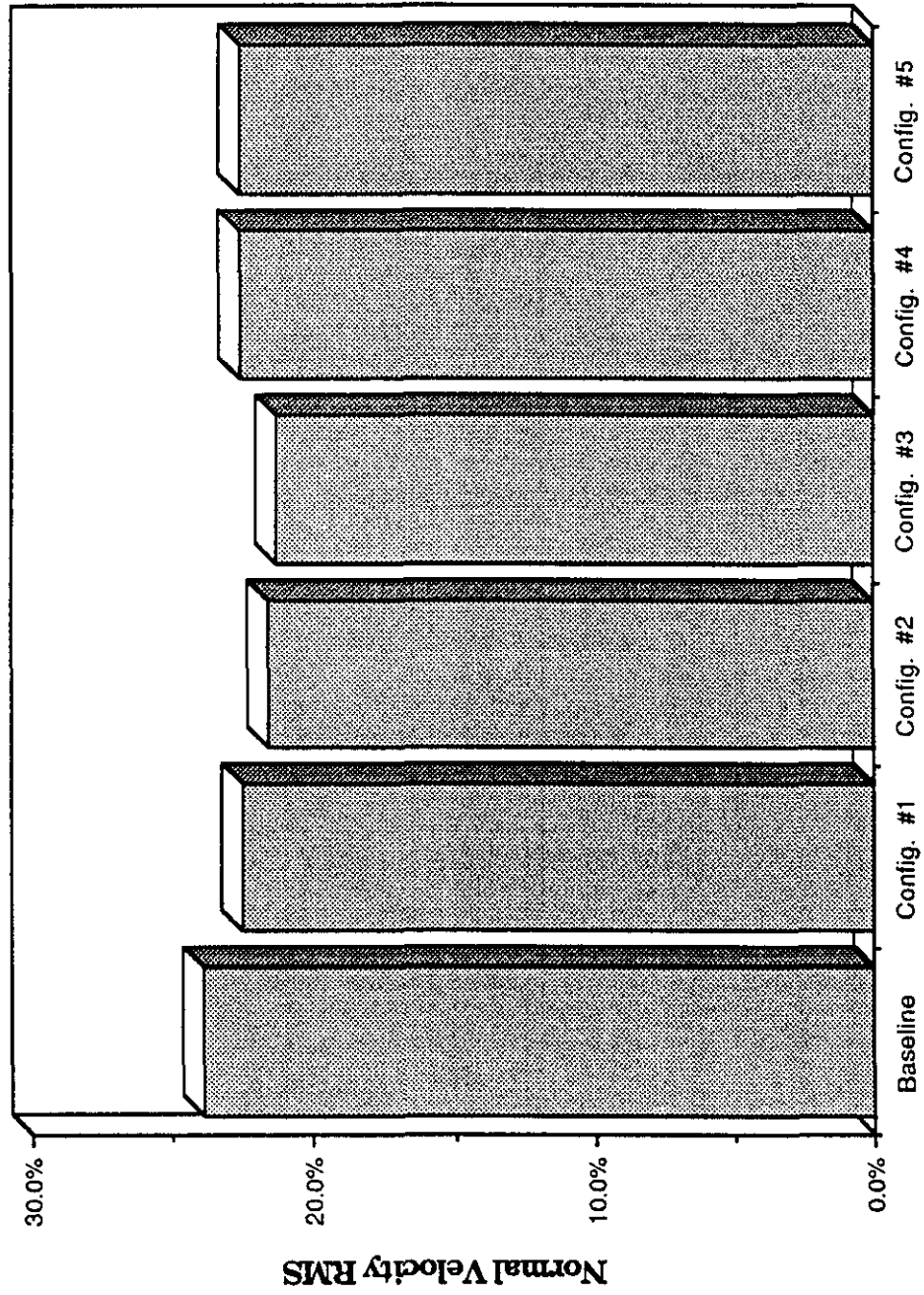


Figure 6-87

**SOUTHERN COMPANY SERVICES
 LANSING SMITH #2 FLOW MODEL**

**Lansing Smith #2 Flow Model
Velocity RMS at Furnace Outlet Plane**



Test Identification

Figure 6-88

Lansing Smith #2 Flow Model

Side to Side Velocity Distribution at Furnace Outlet Plane

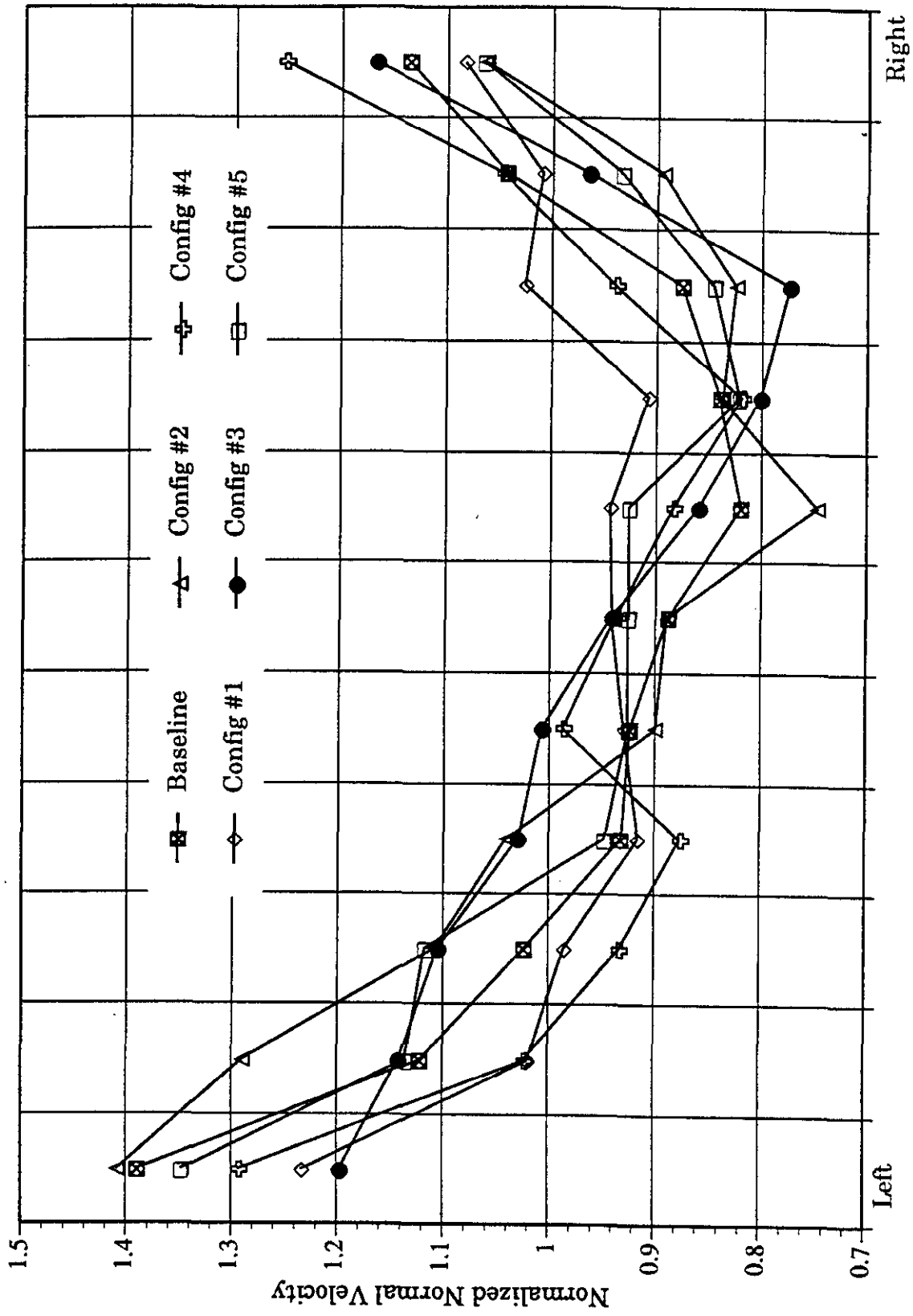
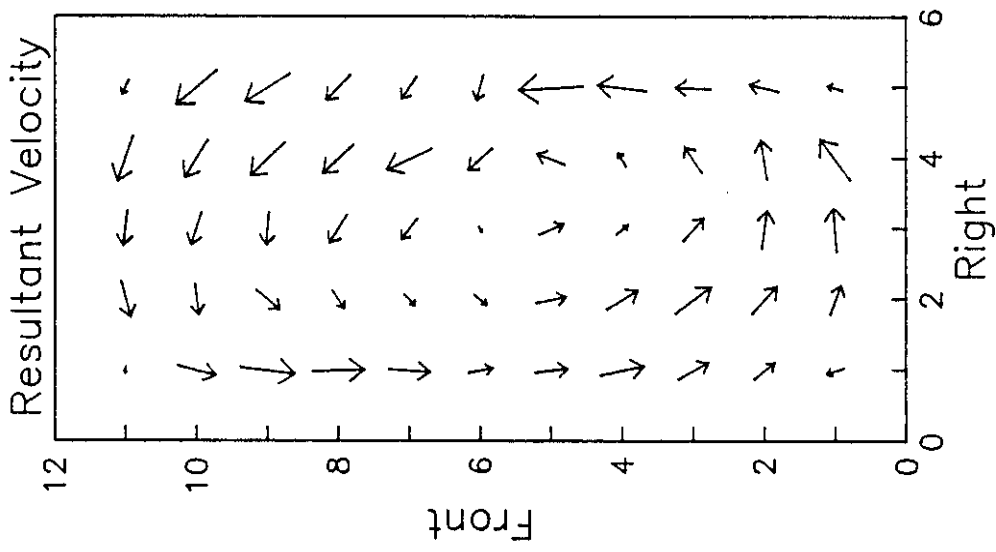


Figure 6-89



VELOCITY VECTORS

Test Plane: 4

Test Date: 1/31/91

Firing System: LNCFS-II

Test ID: Baseline

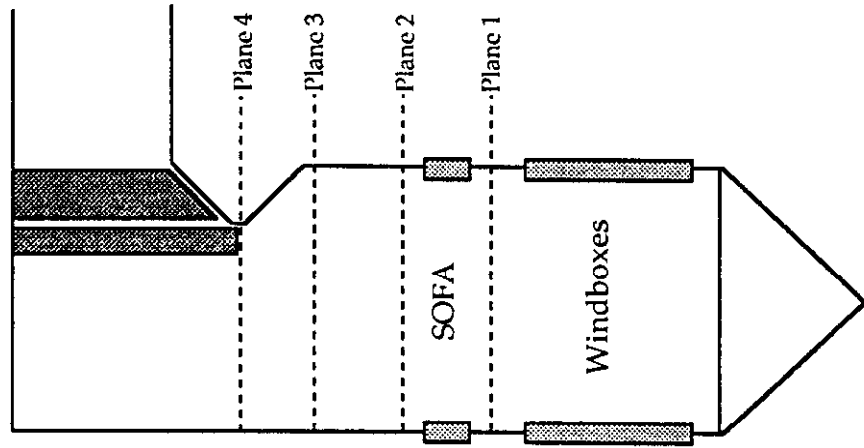


Figure 6-90

**SOUTHERN COMPANY SERVICES
LANSING SMITH #2 FLOW MODEL**

VELOCITY VECTORS

Test Plane: 4

Test Date: 2/4/91

Firing System: LNCFS-II

Test ID: Configuration #1

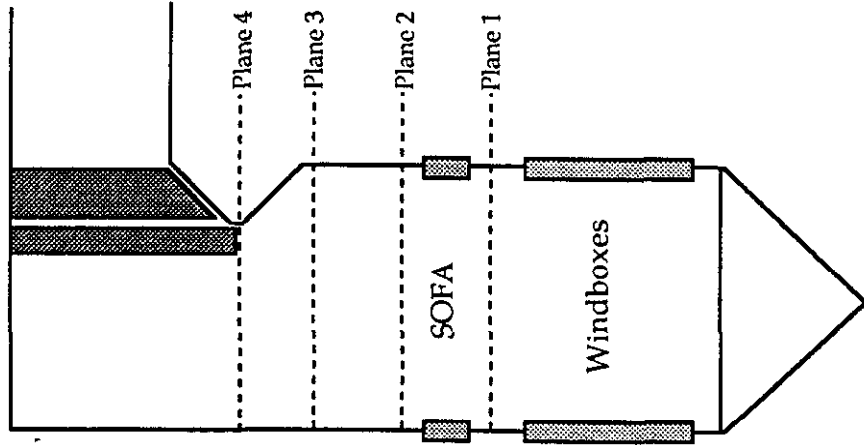
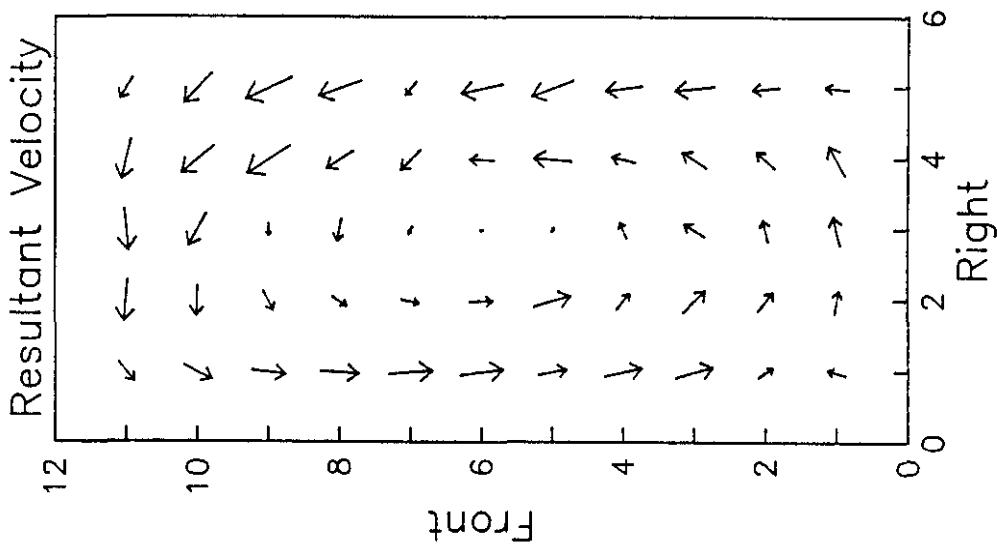
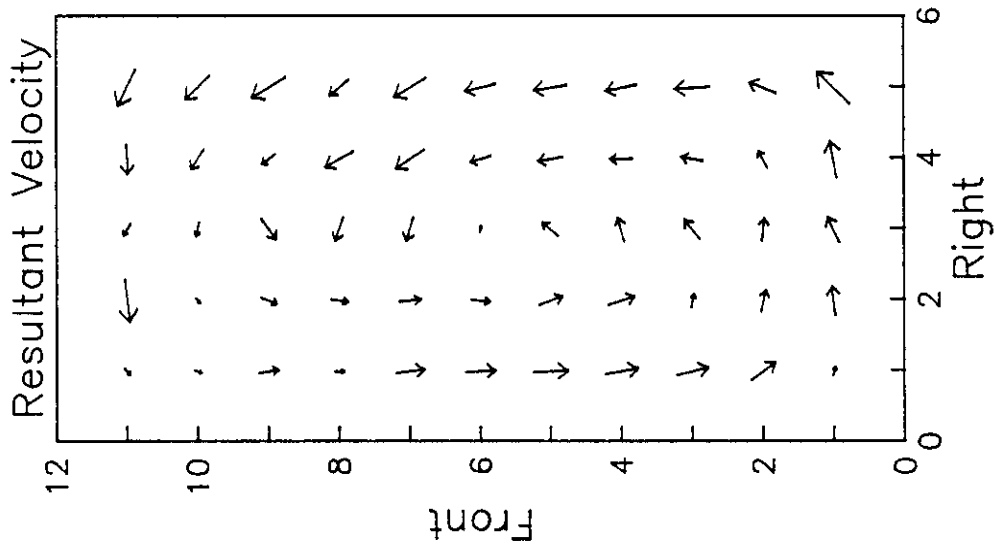


Figure 6-91

**SOUTHERN COMPANY SERVICES
LANSING SMITH #2 FLOW MODEL**



VELOCITY VECTORS
 Test Plane: 4
 Test Date: 2/4/91
 Firing System: LNCFS-II
 Test ID: Configuration #2

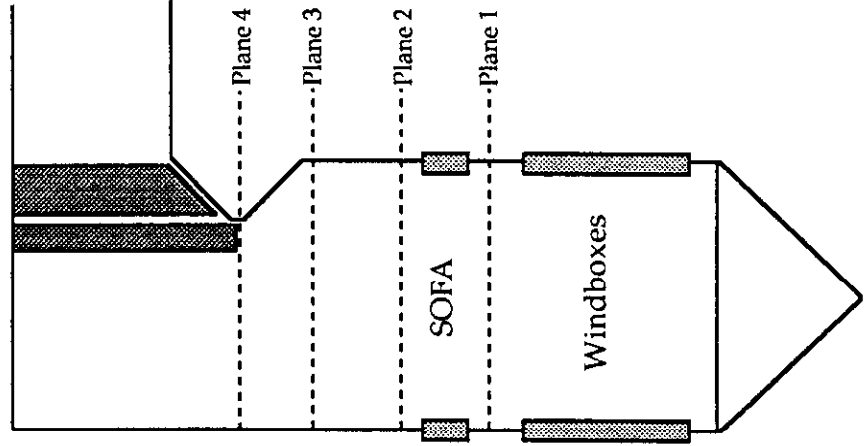


Figure 6-92

**SOUTHERN COMPANY SERVICES
 LANSING SMITH #2 FLOW MODEL**

VELOCITY VECTORS

Test Plane: 4

Test Date: 2/5/91

Firing System: LNCFS-II

Test ID: Configuration #3

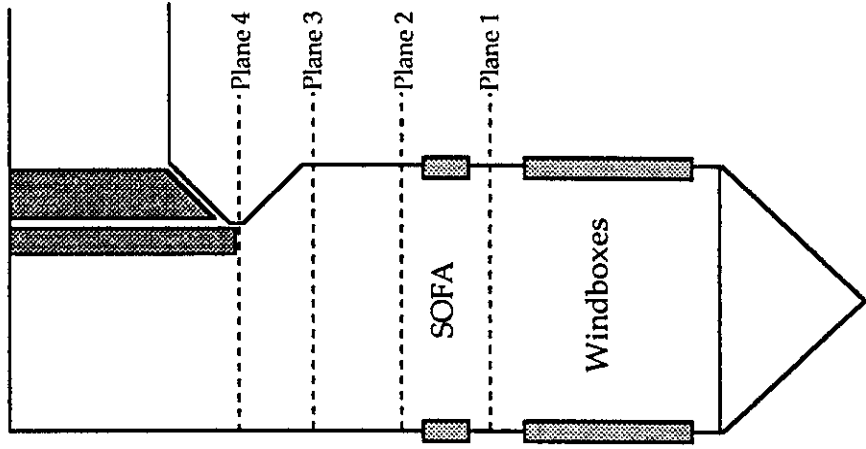
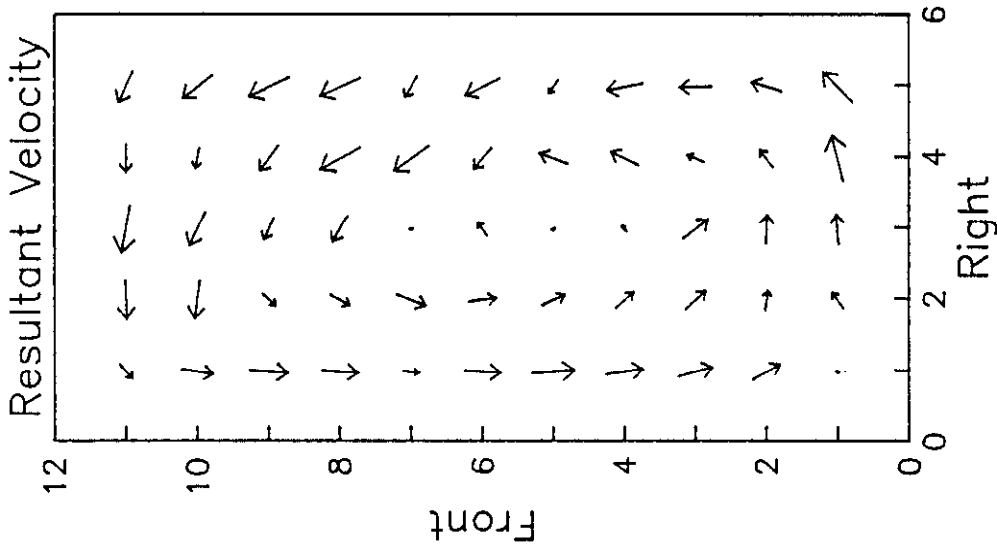


Figure 6-93

**SOUTHERN COMPANY SERVICES
LANSING SMITH #2 FLOW MODEL**

VELOCITY VECTORS

Test Plane: 4

Test Date: 2/7/91

Firing System: LNCFS-II

Test ID: Configuration #4

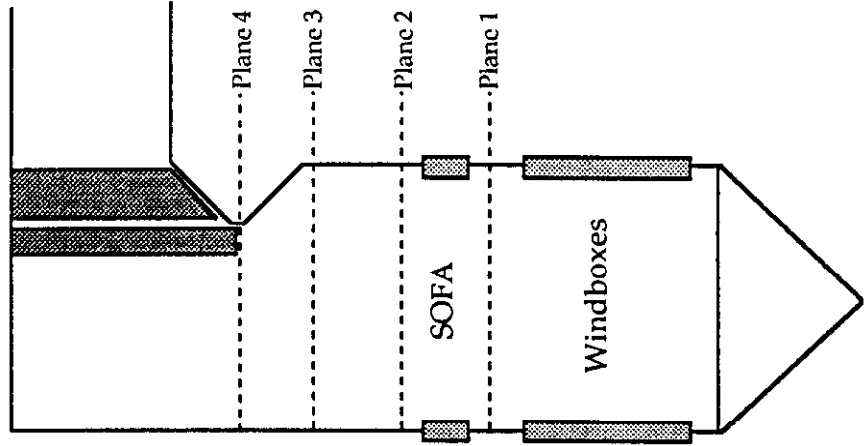
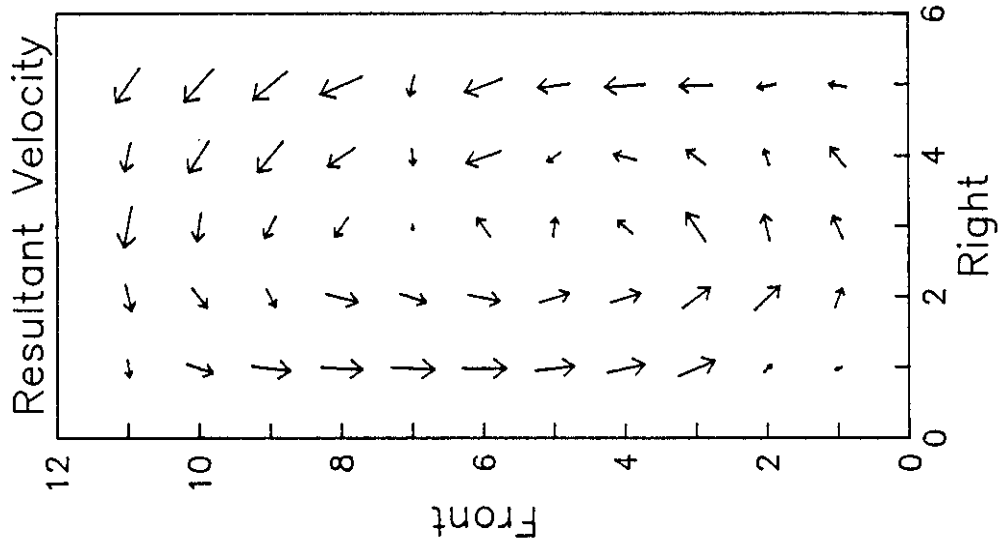


Figure 6-94

**SOUTHERN COMPANY SERVICES
LANSING SMITH #2 FLOW MODEL**

VELOCITY VECTORS

Test Plane: 4

Test Date: 2/14/91

Firing System: LNCFS-II

Test ID: Configuration #5

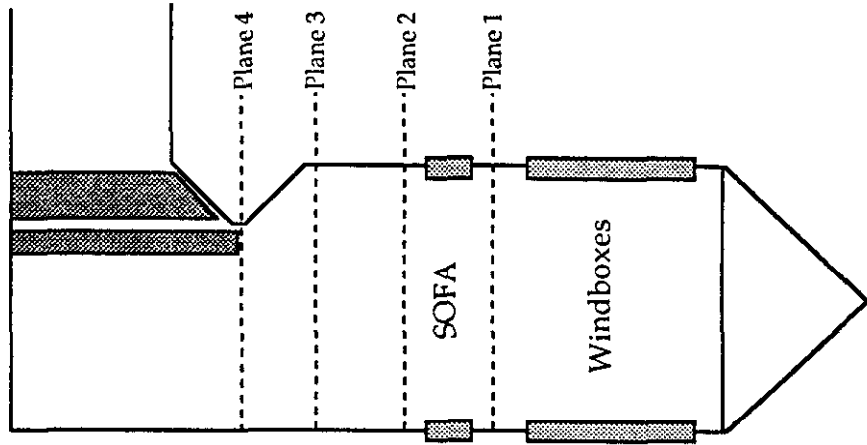
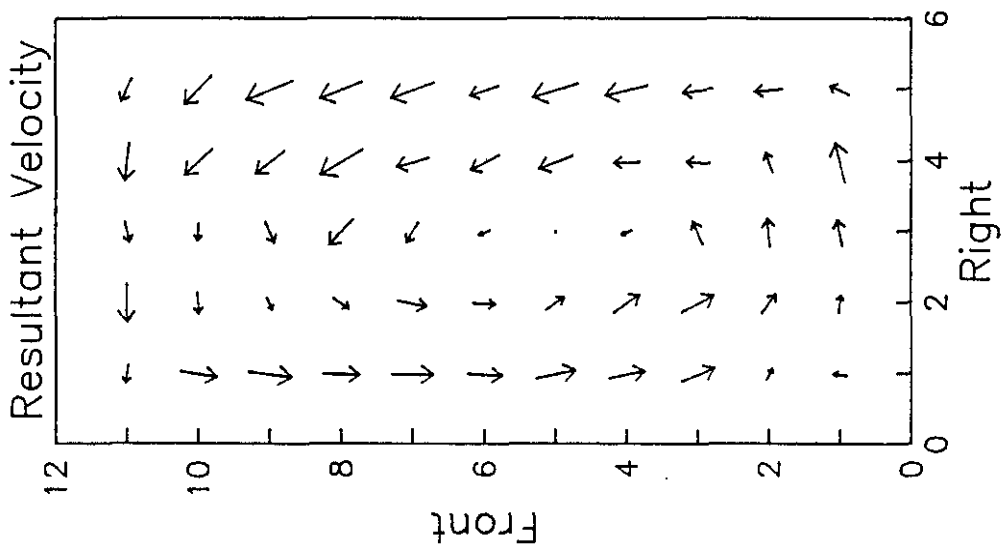


Figure 6-95

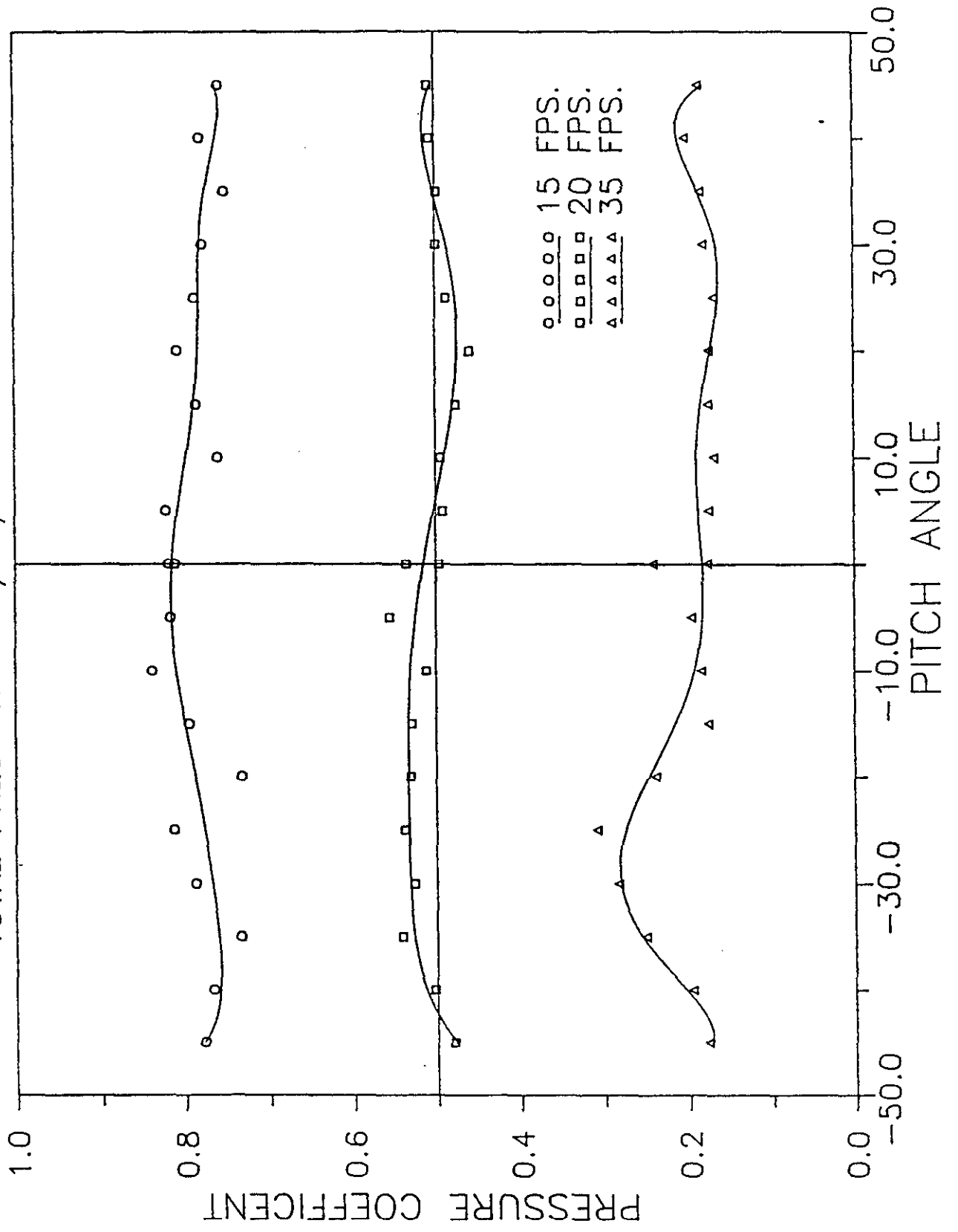
**SOUTHERN COMPANY SERVICES
LANSING SMITH #2 FLOW MODEL**

7.0 References

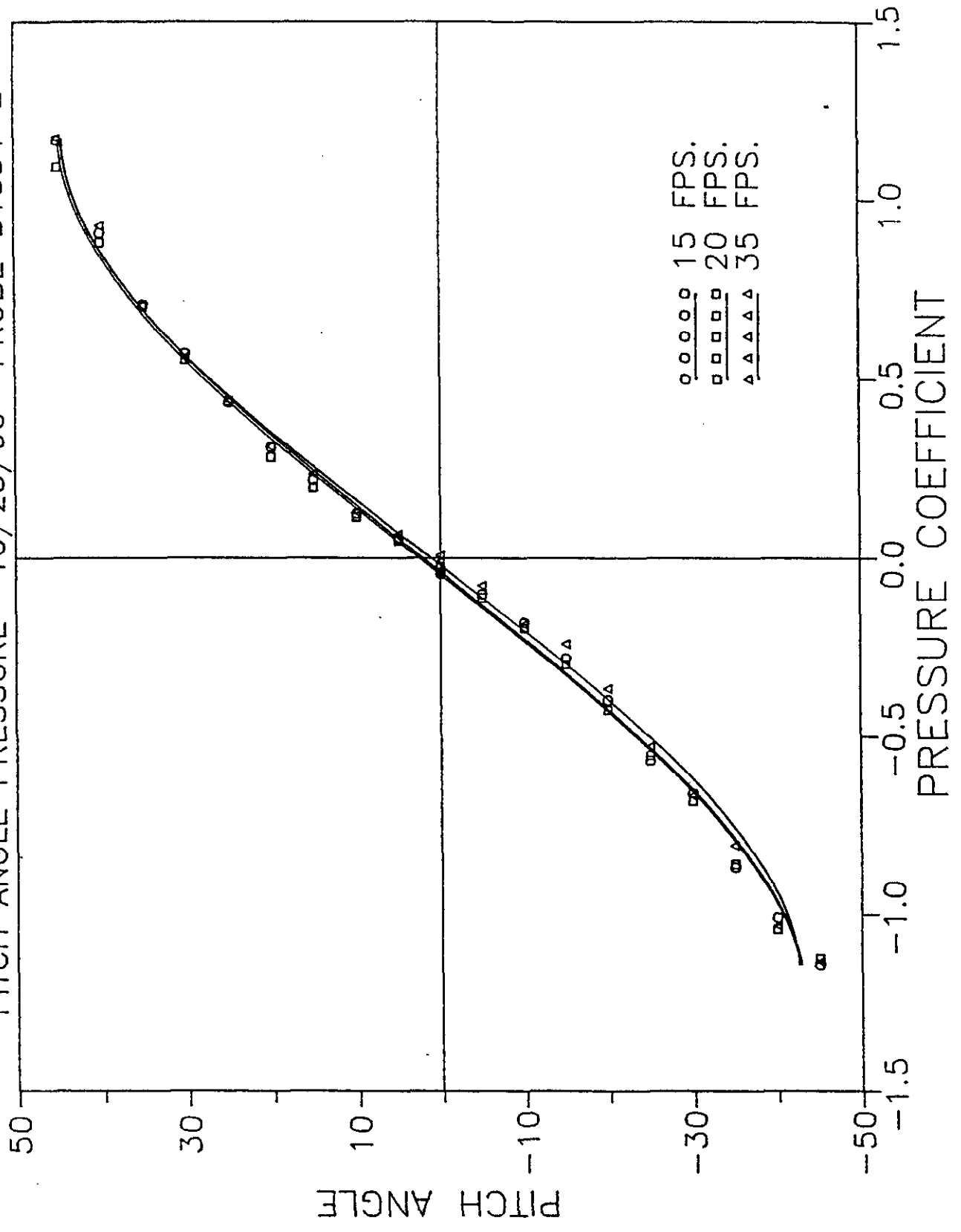
1. Anderson, D.K., Bianca, J.D., and McGowan, J.G., "Recent Developments in Physical Flow Modeling of Utility Scale Furnaces," Proc. 1986 Symposium on Industrial Combustion Technologies, Chicago, Illinois, 1986
2. Beer, J.M., "Significance of Modeling," J. Inst. Fuel, November, 1966
3. Beer, J.M., "Recent Advances in the Technology of Furnace Flames," J. Inst. Fuel, July 1972
4. Beer, J.M. and Chigier, N.A., Combustion Aerodynamics, Wiley, New York, 1972
5. Bianca, J.D., Bauver, W.P., and McGowan, J.G., "An Aerodynamic Study of an Operating Tangentially Fired Furnace," Fluid Mechanics of Combustion Systems, ASME, 1981
6. Chigier, N.A., "Application of Model Results to Design Industrial Flames", J. Inst. Fuel, September 1973
7. Johnstone, R.E., and Thirng, M.B., Pilot Plants, Models and Scale up Factors in Chemical Engineering, McGraw Hill, New York, 1947
8. Spaulding, D.B., "The Art of Partial Modeling," 9th International Symp. on Combustion, September, 1973
9. Thring, M.B., and Newby, M.P., "Combustion Length of Enclosed Turbulent Jet Flames," 9th Symp. on Combustion, September 1953

Appendix A
Five Hole Pitot Probe Calibration Curves

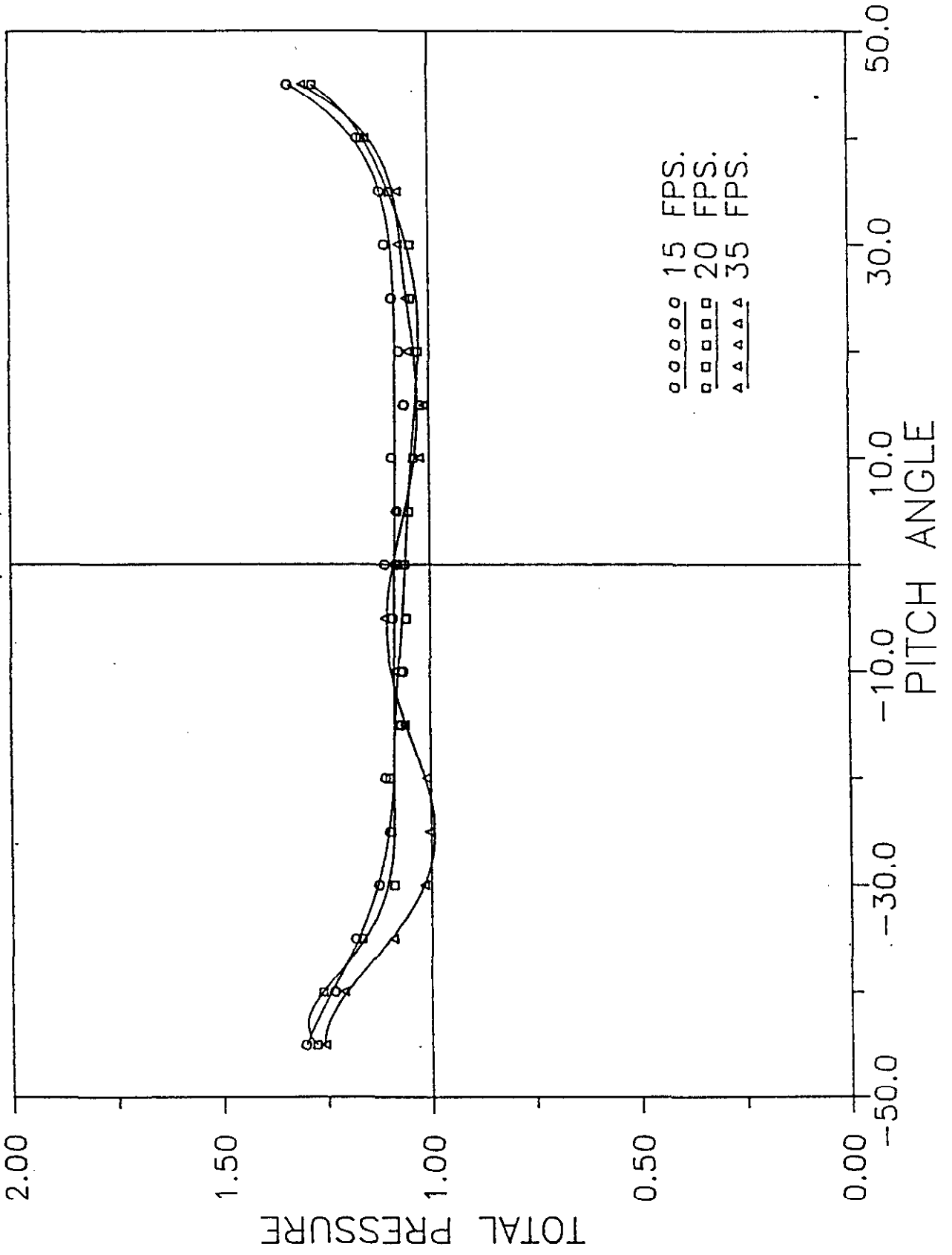
TOTAL PRESSURE 10/23/90 PROBE B1884-2



PITCH ANGLE PRESSURE 10/23/90 PROBE B1884--2



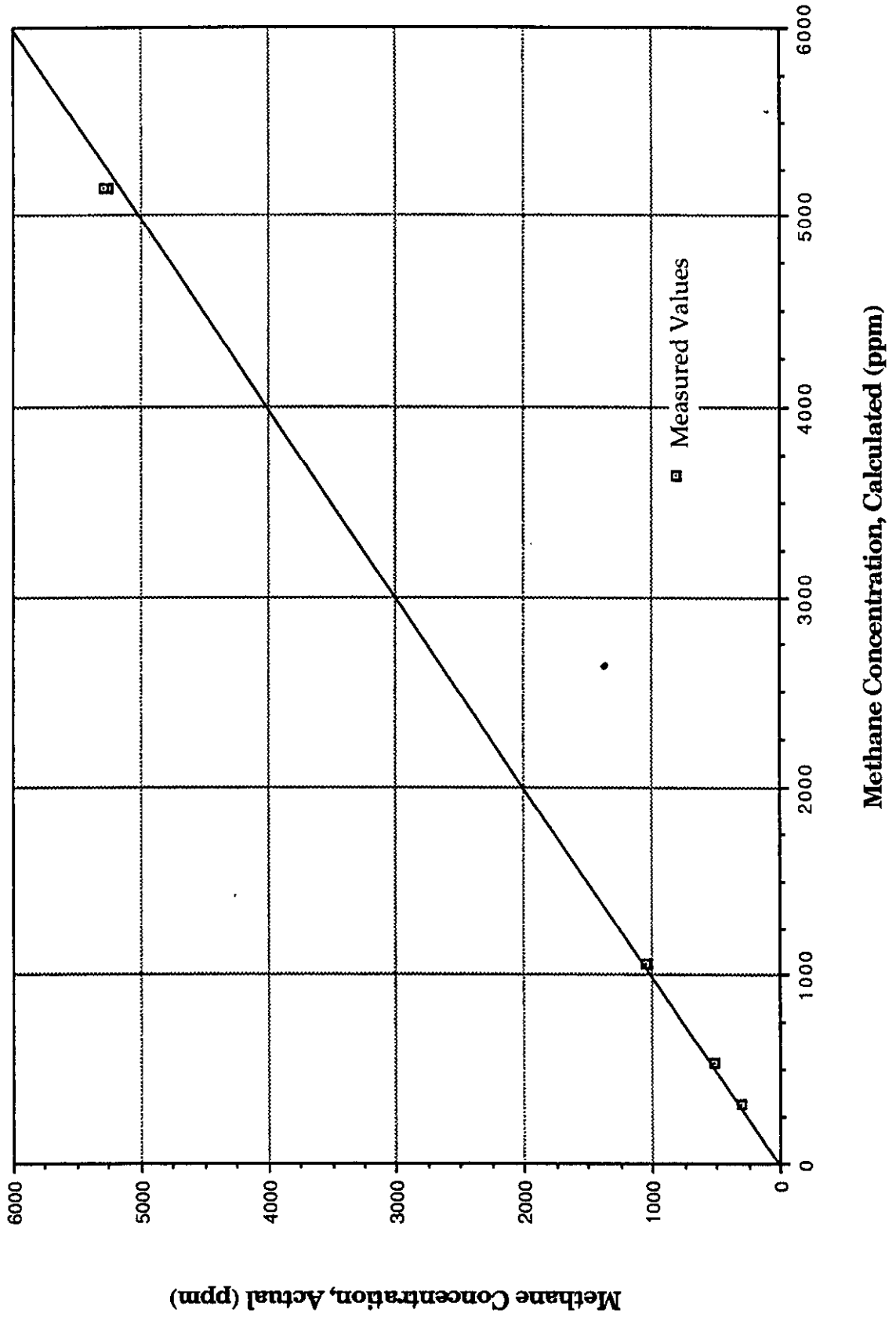
VELOCITY PRESSURE 10/23/90 PROBE B1884-2



○ ○ ○ ○ ○ 15 FPS.
□ □ □ □ □ 20 FPS.
△ △ △ △ △ 35 FPS.

Appendix B
Laser Absorption Spectrophotometer Calibration Curve

Laser Absorption Spectrophotometer Calibration Curve



SOUTHERN COMPANY SERVICES
LOW NO_x TANGENTIAL FIRING SYSTEM DEVELOPMENT
C-E CONTRACT #14664

TEST REPORT
PHYSICAL FLOW MODELING - TASK V
LNCFS-III OPERATING CONDITIONS

Project 901237

Mechanical Systems Engineering
Kreisinger Development Laboratory
KDL-91-17

Robert J. von Hein

May, 1991

DISCLAIMER

This report was prepared as an account of work sponsored by Southern Company Services. Neither Southern Company Services, ABB Combustion Engineering, nor any person acting on behalf of them:

- A. Makes any warranty, expressed or implied, with respect to the use of any information, apparatus, method, or process disclosed in this report or that such use *may not infringe privately owned rights: or*
- B. Assumes any liability with respect to the use of, or damages resulting from the use of any apparatus, method, or process disclosed in this report.

Table of Contents

<u>Section</u>	<u>Title</u>	<u>Page No.</u>
<i>i</i>	List of Figures	<i>i</i>
<i>ii</i>	List of Tables	<i>iv</i>
1.0	Introduction	1
2.0	Conclusions	3
3.0	Modeling Theory	5
4.0	Facility Description	9
4.1	Lansing Smith Flow Model	9
4.2	Automatic Probe traversing Device	13
4.3	Three Dimensional Pitot Tube Probe	16
4.4	Laser Absorption Spectrophotometer	19
4.5	Smoke Generator	21
5.0	Modeling and Testing Techniques	22
5.1	Modeling Theory	22
5.2	Testing Procedures	24
6.0	Results	27
6.1	Flow Visualization	27
6.2	Gas Mixing	38
6.3	Velocity	107
7.0	References	138
Appendix A Five Hole Pitot Probe Calibration Curves		
Appendix B Laser Methane Calibration Curves		

List of Figures

<u>Figure No.</u>	<u>Description</u>
3-1	Single Jet in a Crossflow
4-1	Lansing Smith #2 Flow Model
4-2	Side Elevation of Flow Model
4-3	KDL Model Test Facility
4-4	Flow Model Firing Circle
4-5	OFA Nozzles
4-6	Automatic Probe Traversing Device
4-7	5-Hole Pitot Tube
4-8	Laser Absorption Spectrophotometer
5-1	Flow Model Test Matrix
5-2	Model Test Plane Locations
6-1	Typical Flow Visualization Results - CCOFA Nozzles
6-2	Typical Flow Visualization Results - SOFA Nozzles
6-3	Typical Flow Visualization Results - SOFA Nozzles
6-4	Flow Visualization - Close Up of SOFA Nozzle
6-5	OFA Firing Circle
6-6	Schematic of Methane Injection System
6-7	Mixing Isoconcentration Plot - Config. #1, Plane 1
6-8	Mixing Contour Plot - Config. #1, Plane 1
6-9	Mixing Isoconcentration Plot - Config. #2, Plane 1
6-10	Mixing Contour Plot - Config. #2, Plane 1
6-11	Mixing Isoconcentration Plot - Config. #3, Plane 1
6-12	Mixing Contour Plot - Config. #3, Plane 1
6-13	Mixing Isoconcentration Plot - Config. #4, Plane 1
6-14	Mixing Contour Plot - Config. #4, Plane 1
6-15	Mixing Isoconcentration Plot - Config. #5, Plane 1
6-16	Mixing Contour Plot - Config. #5, Plane 1
6-17	Normalized Concentration - Config. #1, Plane 1
6-18	Normalized Concentration - Config. #2, Plane 1
6-19	Normalized Concentration - Config. #3, Plane 1
6-20	Normalized Concentration - Config. #4, Plane 1
6-21	Normalized Concentration - Config. #5, Plane 1
6-22	Mixing Isoconcentration Plot - Config. #1, Plane 2
6-23	Mixing Contour Plot - Config. #1, Plane 2
6-24	Normalized Concentration - Config. #1, Plane 2
6-25	Mixing Isoconcentration Plot - Config. #2, Plane 2

6-26	Mixing Contour Plot - Config. #2, Plane 2
6-27	Normalized Concentration - Config. #2, Plane 2
6-28	Mixing Isoconcentration Plot - Config. #3, Plane 2
6-29	Mixing Contour Plot - Config. #3, Plane 2
6-30	Normalized Concentration - Config. #3, Plane 2
6-31	Mixing Isoconcentration Plot - Config. #4, Plane 2
6-32	Mixing Contour Plot - Config. #4, Plane 2
6-33	Normalized Concentration - Config. #4, Plane 2
6-34	Mixing Isoconcentration Plot - Config. #5, Plane 2
6-35	Mixing Contour Plot - Config. #5, Plane 2
6-36	Normalized Concentration - Config. #5, Plane 2
6-37	Mixing RMS Deviation - Plane 2
6-38	Mixing Isoconcentration Plot - Config. #1, Plane 3
6-39	Mixing Contour Plot - Config. #1, Plane 3
6-40	Normalized Concentration - Config. #1, Plane 3
6-41	Mixing Isoconcentration Plot - Config. #2, Plane 3
6-42	Mixing Contour Plot - Config. #2, Plane 3
6-43	Normalized Concentration - Config. #2, Plane 3
6-44	Mixing Isoconcentration Plot - Config. #3, Plane 3
6-45	Mixing Contour Plot - Config. #3, Plane 3
6-46	Normalized Concentration - Config. #3, Plane 3
6-47	Mixing Isoconcentration Plot - Config. #4, Plane 3
6-48	Mixing Contour Plot - Config. #4, Plane 3
6-49	Normalized Concentration - Config. #4, Plane 3
6-50	Mixing Isoconcentration Plot - Config. #5, Plane 3
6-51	Mixing Contour Plot - Config. #5, Plane 3
6-52	Normalized Concentration - Config. #5, Plane 3
6-53	Mixing RMS Deviation - Plane 3
6-54	Mixing Isoconcentration Plot - Config. #1, Plane 4
6-55	Mixing Contour Plot - Config. #1, Plane 4
6-56	Normalized Concentration - Config. #1, Plane 4
6-57	Mixing Isoconcentration Plot - Config. #2, Plane 4
6-58	Mixing Contour Plot - Config. #2, Plane 4
6-59	Normalized Concentration - Config. #2, Plane 4
6-60	Mixing Isoconcentration Plot - Config. #3, Plane 4
6-61	Mixing Contour Plot - Config. #3, Plane 4
6-62	Normalized Concentration - Config. #3, Plane 4
6-63	Mixing Isoconcentration Plot - Config. #4, Plane 4
6-64	Mixing Contour Plot - Config. #4, Plane 4
6-65	Normalized Concentration - Config. #4, Plane 4
6-66	Mixing Isoconcentration Plot - Config. #5, Plane 4
6-67	Mixing Contour Plot - Config. #5, Plane 4
6-68	Normalized Concentration - Config. #5, Plane 4
6-69	Mixing RMS Deviation - Plane 4
6-70	Overall Mixing RMS
6-71	Velocity Isoconcentration Plot - Baseline, Plane 4

6-72	Velocity Contour Plot - Baseline, Plane 4
6-73	Velocity Isoconcentration Plot - Config. #1, Plane 4
6-74	Velocity Contour Plot - Config. #1, Plane 4
6-75	Velocity Isoconcentration Plot - Config. #2, Plane 4
6-76	Velocity Contour Plot - Config. #2, Plane 4
6-77	Velocity Isoconcentration Plot - Config. #3, Plane 4
6-78	Velocity Contour Plot - Config. #3, Plane 4
6-79	Velocity Isoconcentration Plot - Config. #4, Plane 4
6-80	Velocity Contour Plot - Config. #4, Plane 4
6-81	Velocity Isoconcentration Plot - Config. #5, Plane 4
6-82	Velocity Contour Plot - Config. #5, Plane 4
6-83	Normalized Axial Velocity - Baseline, Plane 4
6-84	Normalized Axial Velocity - Config. #1, Plane 4
6-85	Normalized Axial Velocity - Config. #2, Plane 4
6-86	Normalized Axial Velocity - Config. #3, Plane 4
6-87	Normalized Axial Velocity - Config. #4, Plane 4
6-88	Normalized Axial Velocity - Config. #5, Plane 4
6-89	Axial Velocity RMS Deviation - Plane 4
6-90	Side to Side Velocity Profiles
6-91	Velocity Vectors - Baseline, Plane 4
6-92	Velocity Vectors - Config. #1, Plane 4
6-93	Velocity Vectors - Config. #2, Plane 4
6-94	Velocity Vectors - Config. #3, Plane 4
6-95	Velocity Vectors - Config. #4, Plane 4
6-96	Velocity Vectors - Config. #5, Plane 4

List of Tables

<u>Table No.</u>	<u>Description</u>
6-1	Flow Visualization Test Matrix
6-2	Methane and Velocity Mapping Test Matrix
6-3	Methane Mixing Tests - General Output
6-4	Velocity Mapping Tests - General Output

1.0 Introduction

Southern Company Services (SCS), the Department of Energy (DOE), and ABB Combustion Engineering (CE) are involved in a program to develop advanced tangentially fired combustion modifications for reducing NO_x emissions. The intent of this program is to demonstrate, at "full scale," low NO_x technologies of a commercial prototype design. This demonstration includes the addition of Low NO_x Concentric Firing Systems (LNCFS) to Gulf Power Company's Lansing Smith #2 Unit. To investigate the fluid mechanic performance of the proposed low NO_x configurations, CE performed a physical isothermal flow model study at its Kreisinger Development Laboratory (KDL) in Windsor, CT.

The objective of the isothermal flow model study was to assure optimum performance of the Low NO_x tangential firing systems. The effort centers on understanding in-furnace flow and mixing phenomena for the various low NO_x firing systems as applied to the demonstration unit. This is being done through an evaluation of each proposed firing system, along with the evaluation of the burner only configuration, in the isothermal flow model.

Baseline testing was performed on the burner only configuration which exists in the Lansing Smith #2 Unit. This testing was followed by testing the LNCFS-II configuration, which included the addition of Separated Over Fire Air (SOFA), in the physical flow model. Finally, the LNCFS-III configuration was tested in the flow model. This configuration included the addition of Close Coupled Over Fire Air (CCOFA) and clustered burners, along with the SOFA. Each LNCFS configuration was evaluated from an Over Fire Air penetration, mixing, and dispersion standpoint. The results from the flow modeling was to provide specific flow field information to help access the merits of each of these configurations in the Lansing Smith #2 Unit.

This report presents the results of the physical cold flow modeling conducted under Task V of the SCS Low NO_x Development Program. The purpose of this task was to evaluate the flow fields within the LNCFS-III

configuration of the flow model. The furnace model, which was constructed under Task I of this project, is a 1/12 scale model of the Lansing Smith No. 2 Unit, from the hopper through the furnace backpass. In addition to LNCFS-II, modifications were made to the model in order to evaluate the addition of SOFA and CCOFA. The evaluation was divided into two (2) screening levels. In the first, flow visualization was used to evaluate a moderate number of operating conditions. These results were then used to select "the best" configurations for additional quantitative tests, three dimensional velocity mapping and gas mixing. The results from this cold flow model will provide a basis to assess performance of the proposed modifications to this unit.

2.0 Conclusions

An evaluation of the proposed LNCFS-III configuration for the Lansing Smith #2 Unit was performed through the use of flow visualization (screening level one), methane gas mixing, and three dimensional velocity mapping tests (screening level two.) From these tests, the following conclusions have been made:

1. In general, the OFA was found to be fairly well mixed at the furnace outlet plane for each of the configurations tested in the second screening level. That is, the RMS deviation of the mixing was typically less than 20%. It was also determined that the mixing could be improved with the adjustment of the OFA firing angles.
2. The recommended configuration for OFA operation, based on this flow model testing, is Configuration #5 (see Table 6-2.) For this configuration, the firing angles of each of the SOFA nozzles were determined in a manner such that the OFA jet penetration, mixing, and dispersion was maximized. It was not necessary to impose a horizontal tilt to the nozzles.
3. For the design operating conditions (15% CCOFA and 20% SOFA), the jets do not penetrate into the center of the furnace, but are redirected by the crossflow and dispersed along the outer perimeter of the furnace.
4. The overall penetration of the SOFA jets increases with higher velocities and decreases with lower velocities.
5. A downward tilt helps to improve the overall mixing level of the OFA jets. However, this occurs at the expense of the separation between the OFA and windbox firing zones. For the recommended configuration, no tilt in the OFA nozzles was necessary to obtain a good level of mixing.
6. An upward tilt to the OFA nozzles will obviously increase the separation between furnace zones. However, the overall mixing is reduced, mainly due to the decrease in OFA residence time.

7. For the higher SOFA operating rates (24% SOFA), the jet penetration, mixing, and dispersion is increased. However, the horizontal tilt becomes limited. With a down tilt of greater than 5°, the SOFA jets will begin to penetrate into the lower furnace firing zone. On the other hand, when an upward tilt is imparted, the mixing time of the jets is reduced.
8. At lower SOFA operating flow rates (12% SOFA), the jet penetration, mixing, and dispersion is reduced. To improve the overall mixing, it became necessary to impose a downtilt of 10° to the SOFA nozzles.
9. The side to side velocity distribution generally shows higher flow rates along the side walls of the furnace at the furnace outlet plane. There is also a side to side flow imbalance in which there is more flow along the side walls, with reduced flow at the center of the furnace.

3.0 Modeling Theory

Isothermal flow models have long been recognized as a cost effective way of evaluating the fluid mechanics within a furnace. Qualitative and quantitative information gathered from these models are especially useful in understanding and explaining unit performance and/or operation. Qualitative information is usually restricted to visual flow observations, whereas, quantitative information includes, but is not limited to, velocity profiles, pressure distributions, and gas mixing data.

For an accurate simulation of the flow within a furnace, a physical model must duplicate the fundamental controlling fluid mechanic phenomena. These include: mixing of fuel and air streams, mixing of crossflow jets with the main swirling flow, and the interaction of these jets in the combustion zone.

As detailed by Beer and Chigier (1972), it is possible to model combustion systems through the use of geometric, mechanical, and thermal similarities. However, Beer (1966) and Spaulding (1963) indicate that it is not possible to simultaneously reproduce all of the prototype's processes in any one model. It becomes an important engineering consideration, then, to critically select the most important parameters. This technique, known as the "art of partial modeling", is based on modeling only the dominant processes and relating the conditions occurring in the furnace to physical observations in the model.

The "art of partial modeling" has been successfully applied and verified in numerous studies at KDL, the most recent by Anderson and Bianca (1989). Here, the results of flow modeling studies were correlated to field observations and measurements in coal fired furnaces. Based on these results, and on those from the previously discussed references, the following criteria was used as guidelines for the isothermal flow modeling of the Gulf Power Company, Lansing Smith Station for Southern Company Services:

1. Geometric Scaling:

To the extent possible, the isothermal flow model must be constructed geometrically similar to the prototype. Scaling is achieved by applying a scale factor between all the dimensions in the model and prototype. As in any physical model, the linear scale factor, S , is defined as;

$$S = \frac{\text{dimension in prototype}}{\text{dimension in model}}$$

For the Southern Company Services Program, the value of S was 12. This value represents the scale of the physical model, constructed at KDL, to the Lansing Smith No. 2 Station of Gulf Power Company. Geometric scaling of the inlet air/fuel ports was not applicable, as discussed in section 3 below.

2. Reynolds Number

Based on experience in modeling internal flows, if the Reynolds number exceeds 10,000 (based on overall furnace conditions), the transfer process of mass, momentum and heat transfer are controlled by the turbulent flows in the model. In this case, the molecular transport processes can be neglected. Since the Reynolds number for the Lansing Smith No. 2 flow model is approximately 270,000, it is not necessary to equate the Reynolds number between the furnace and the model.

3. Mass and Momentum

As detailed by Beer, et.al. (1984), it is standard practice to oversize the burners in isothermal furnace models to account for the rapid expansion of gasses exiting the burners due to the combustion of the fuel and air. The Thring-Newby criteria (1953) has been utilized to size such burners at KDL for a number of years. In general, the area of the fuel/air admission assemblies is increased such that the total

burner area is equal to the ratio of the prototype's burner inlet to combustion zone gas densities. For the Southern Company Services Program, the windboxes (simulated fuel/air admission assemblies) were scaled according to this criteria.

4. Jet Penetration

In order to simulate jet penetration/dispersion of a "hot" prototype in an isothermal flow environment, it is necessary to scale the jets in the model based on equivalent mass flow ratios. Simplifying assumptions, based on modeling criteria developed by examining single jet trajectories in a crossflow, have been used in designing the jet components of three-dimensional airflow models. This approach insures the modeled jets behave in a similar fashion to furnace jets in the case of a hot uniform flow field. The cold flow model jet velocity and size are optimized to provide a conservative approximation of the jet penetration to the furnace centerline. Figure 3-1 describes the position of the jet centerline in a uniform crossflow. Jet penetration characteristics, as described by Patrick (1965) and Beer and Chigier (1972), have been studied in KDL to determine the appropriate criteria which will provide the desired model to prototype jet similitude.

In general, the mass flow rate ratio of the model is equivalent to the mass flow rate ratio of the prototype, where the mass flow rate ratio is expressed as the ratio of the mass flow rate of the jets to the mass flow rate of the crossflow. For the Southern Company Services flow model, the nozzle sizes were increased to compensate for the gas density differences between the hot furnace gasses and the much cooler over fire air.

Jet Parameters for Replicating Jet in Ideal Uniform Crossflow:

$$\text{Mass: } \frac{\rho_j A_j V_j}{\rho_{cf} A_{cf} V_{cf}}$$

$$\text{Momentum: } \frac{\rho_j A_j V_j^2}{\rho_{cf} A_{cf} V_{cf}^2}$$

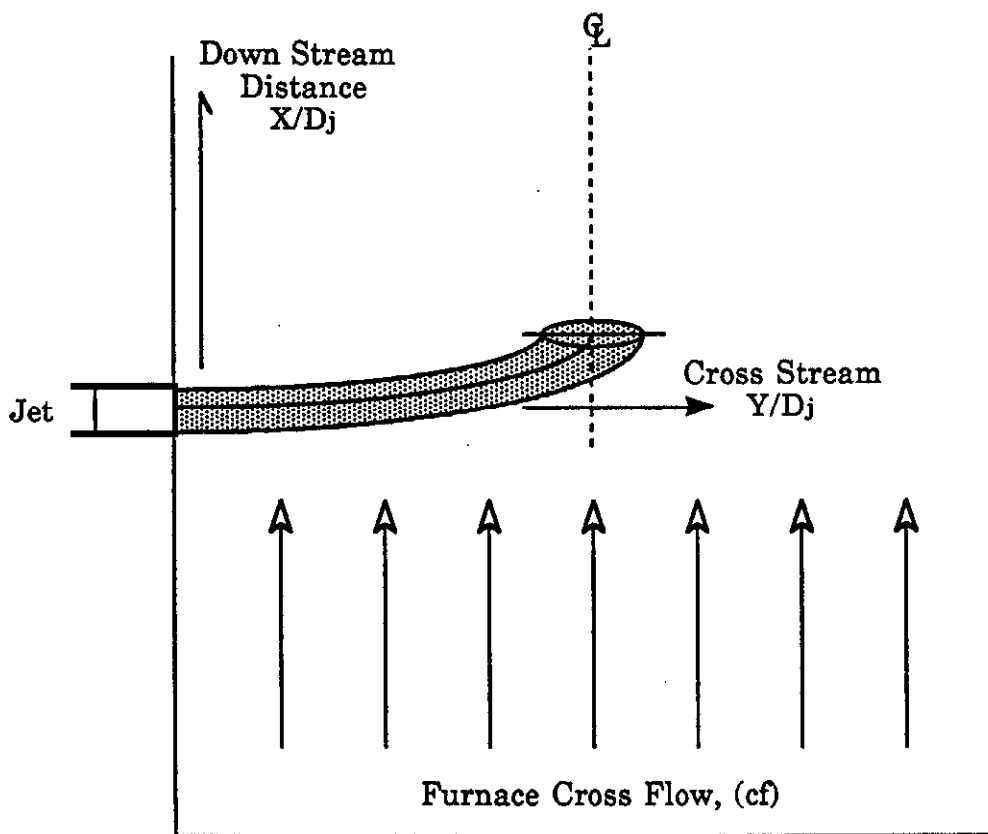


Figure 3-1 Single Jet in a Crossflow

4.0 Facility Descriptions

This section of the report describes the flow model, test facilities, and instrumentation systems used to perform the LNCFS-III evaluations.

4.1 Lansing Smith No. 2 Flow Model Description

Flow modeling was done on a 1/12 scale, geometrically similar model of the Lansing Smith No. 2 Unit, shown in Figure 4-1. The flow model encompasses the entire furnace from the hopper through the economizer outlet. Included in the flow model were the fuel admission assemblies, all radiant and convective heat transfer surfaces within the first sections of the upper furnace, along with the addition of the separated OFA nozzles. Figure 4-2 is a side elevation of the model, showing the nominal model dimensions and the test plane locations.

The furnace model was built primarily of 1/2" acrylic glass, permitting the recording of the flow visualization tests. All dimensions were maintained to a tolerance of $\pm 1/16$ ", which corresponds to $\pm 3/4$ " full scale. The flow model was erected in the KDL Flow Model Test Facility, Figure 4-3. This facility consists of a high volume fan and duct system capable of testing both suction and pressurized models at flow rates up to 20,000 SCFM. Where additional air sources are needed, (i.e. the OFA) supplemental air is supplied via a Lamson high pressure blower (4,000 SCFM @ 4.0 psi) or through the labs compressed air system (1,200 SCFM @ a header pressure of 90 psi.)

The flow model was operated under suction (induced draft) using ambient air as the working fluid. Bell mouths, added to the inlets of the windboxes, reduce the entrance losses and provide uniform velocity profiles at the inlet to the furnace model. Over fire air was supplied via a header which was attached to the high pressure Lamson blower. Each of these flows was independently controlled and monitored, so that the proper air flow splits could be obtained.

The heat transfer surfaces were constructed of perforated metal plate and

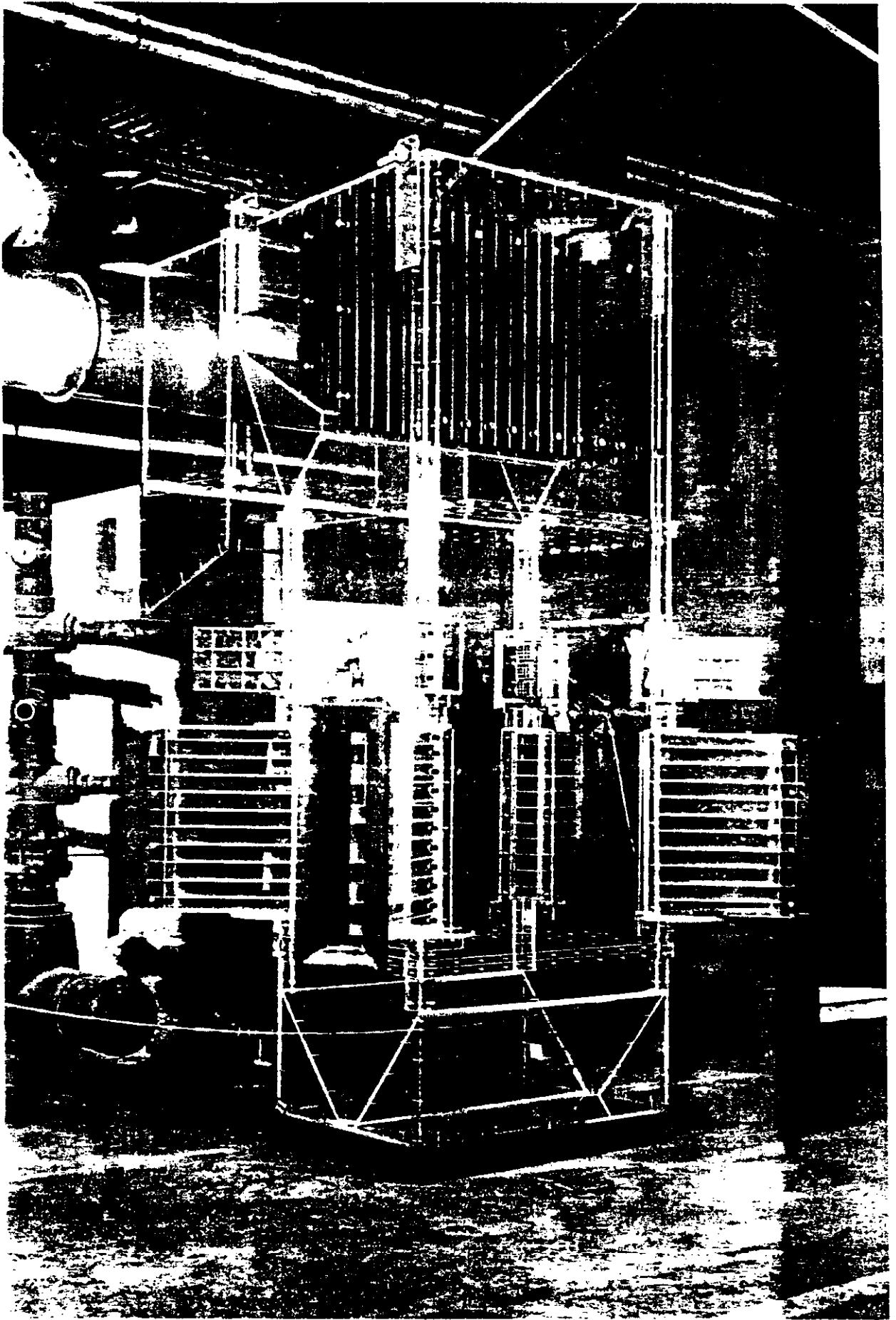


Figure 4-1 Lansing Smith #2 Flow Model

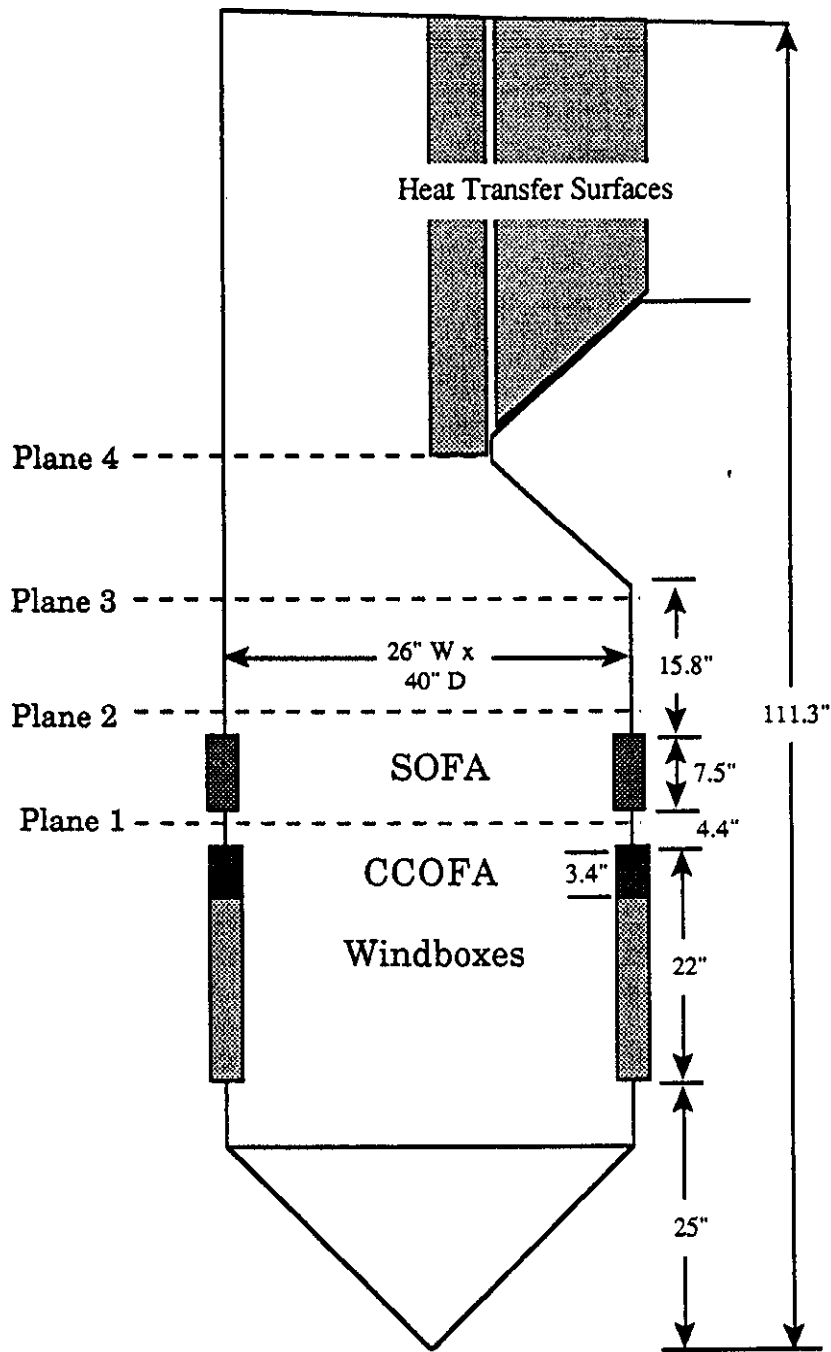


Figure 4-2 Lansing Smith Flow Model (Side View)

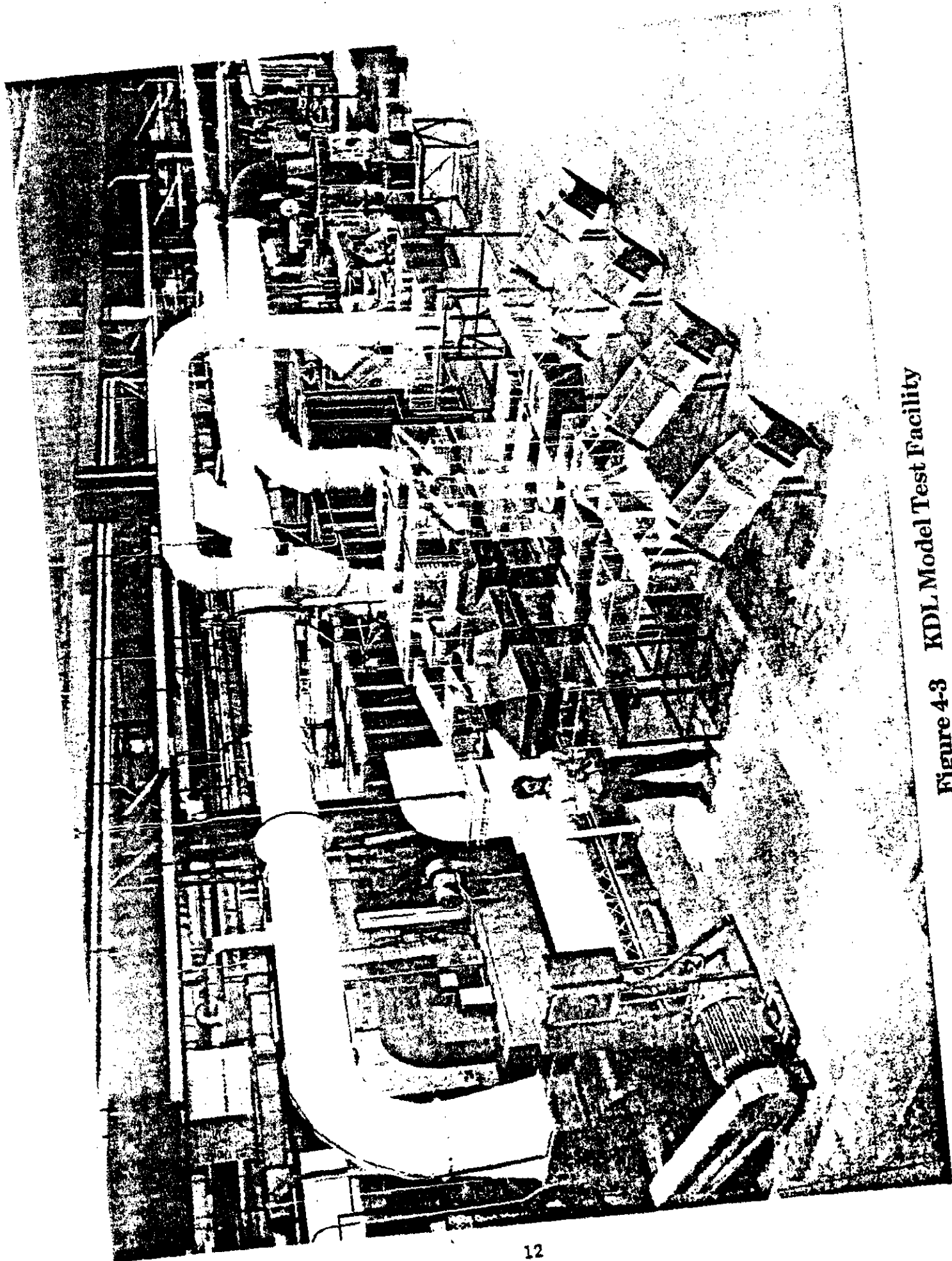


Figure 4-3 KDL Model Test Facility

paper tubing. These sections were shaped to simulate heat transfer surface geometry. The free areas of the plates and their spacing within the model were determined such that the axial and transverse pressure drop coefficients were accurately simulated.

The fuel admission assemblies and the Close Coupled Over Fire Air (CCOFA) were modeled as part of the windboxes. The free areas of the compartments were adjusted according to the Thring-Newby criteria, accounting for the change of density which occurs as a result of combustion within the furnace. Perforated plate was added to achieve the proper velocity splits between the primary air /coal nozzles and secondary air nozzles. The firing circle in the model was set to model that of the prototype through geometric scaling. A schematic of the modeled firing circle /angles is shown in Figure 4-4.

The Separated Over Fire Air (SOFA) injection nozzles were designed to simulate the corresponding jet trajectories in the prototype. Each nozzle was sized as a single jet, such that the mass and penetration ratios of the prototype jet and the model jet were equivalent. These nozzles were also constructed to allow for variable yaw and tilt settings within the model. Figure 4-5 shows a closer view of these nozzles.

Methane, used as a tracer gas for the mixing studies, was introduced into the over fire air at a point far upstream from the nozzle exits. This insured that the tracer gas was fully mixed with the OFA before entering the furnace.

4.2 Automatic Probe Traversing Device

All quantitative three dimensional velocity and pressure mapping within the flow model was performed with a calibrated five-hole pitot tube coupled to a computer controlled traversing device and data acquisition system. This system, developed and built at KDL, is called the Automatic Probe Traversing Device or APTD.

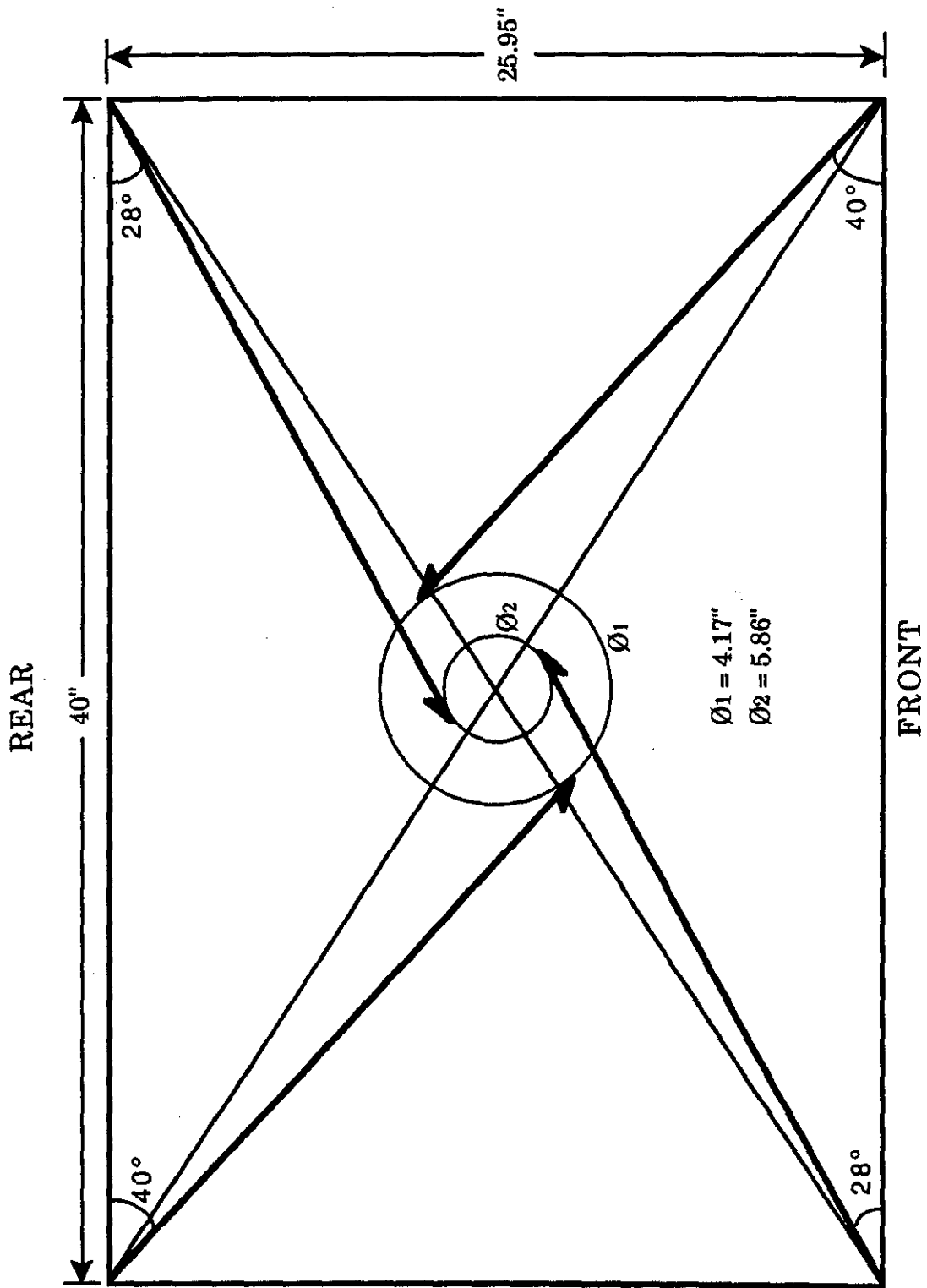
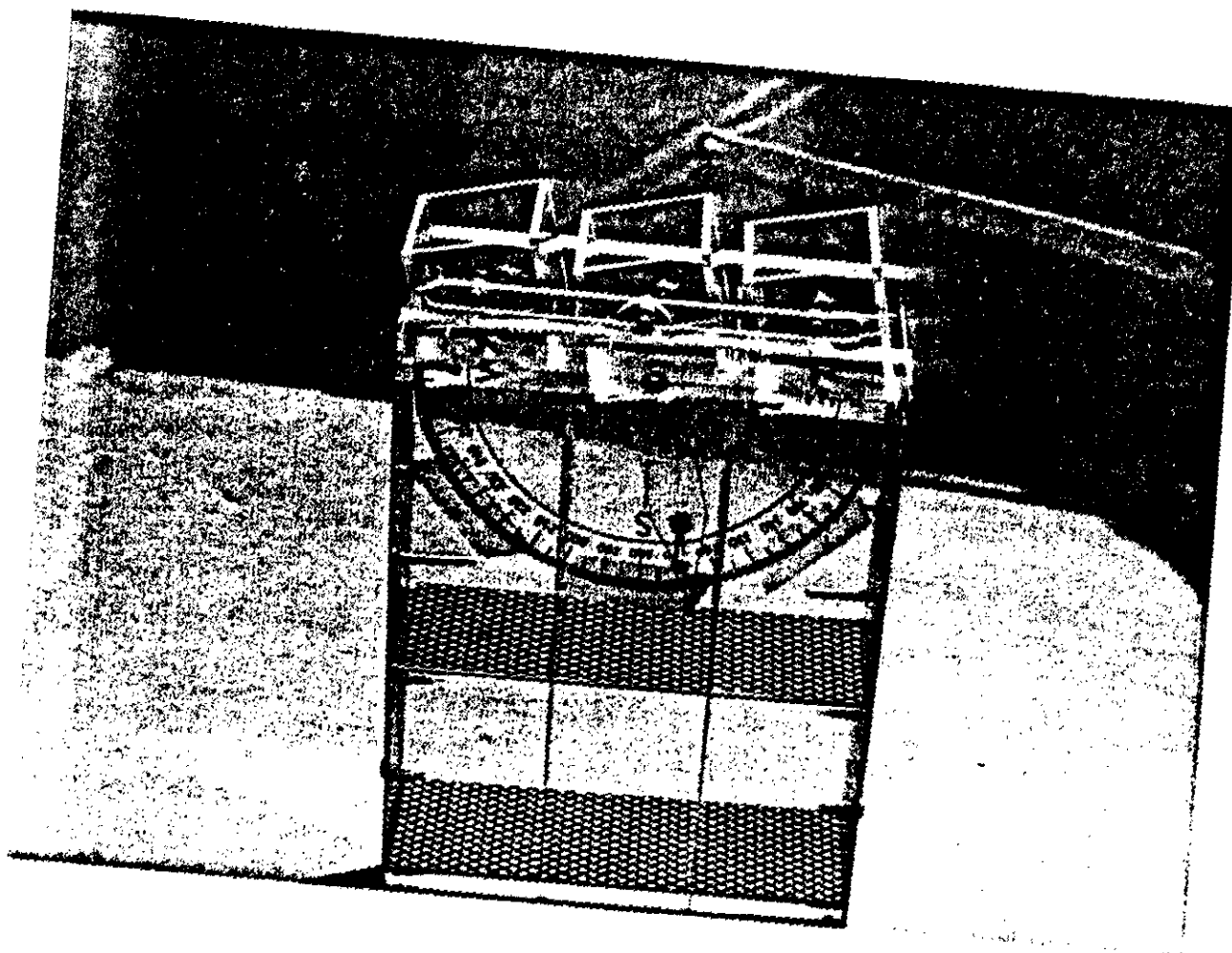


Figure 4-4 Firing Circle and Windbox Settings for Lansing Smith No. 2 Flow Model

Southern Company Services
Lansing Smith Unit #2
LNCFS-III Flow Model



OFA Nozzle with Variable Tilt

Figure 4-5 OFA Nozzle for Lansing Smith #2 Flow Model

The APTD is a programmable data acquisition system which automatically positions and nulls the five-hole pitot tube, and records all pressure readings on the laboratory's central computer system. Figure 4-6 shows the five-hole pitot tube, the APTD, and the local programmable controller/electronic manometer cabinet. The motion of the probe is controlled by a local processor. This processor is programmed by the facility operator at the start of each traverse by entering the appropriate operational parameters for the particular test. These parameters include: instrument type and serial number (for accessing the most recent calibrations), test number, test plane, the number of data points, the distance between each point, and the maximum distance of probe travel (a safety feature.) Once these operational parameters have been entered, the traverse is started by indicating the desired operational mode.

The processor controls stepping motors which move the probe to the pre-programmed test point location and rotates it until the direction of flow is obtained. The outputs of the four pressure transmitters attached to the probe are then recorded along with probe position, angle, test number, test plane, etc. by the central data acquisition computer.

4.3 Three Dimensional Pitot Tube Probe

A commercially available five-hole, directional sensing, pitot tube, shown in Figure 4-7, was used to obtain the velocity data. The probe has five pressure sensing holes located at its tip. The centrally located pressure hole, P1, measures the total or impact pressure of the fluid, while two lateral holes, P2 and P3, measure the static pressure. If the probe is rotated around its long axis until $P2=P3$, the plane of flow can be identified and measured. However, since the condition $P2=P3$ can be given at two locations 180° apart, the correct vector plane is identified when $P2=P3$ and P1 has its highest positive value with respect to P2 and P3. An angular encoder is attached to the probe at its base so that the angle of this vector plane, commonly called the yaw angle, can be measured. The yaw angle indicates the plane of flow but does not give the flow angle within this plane.

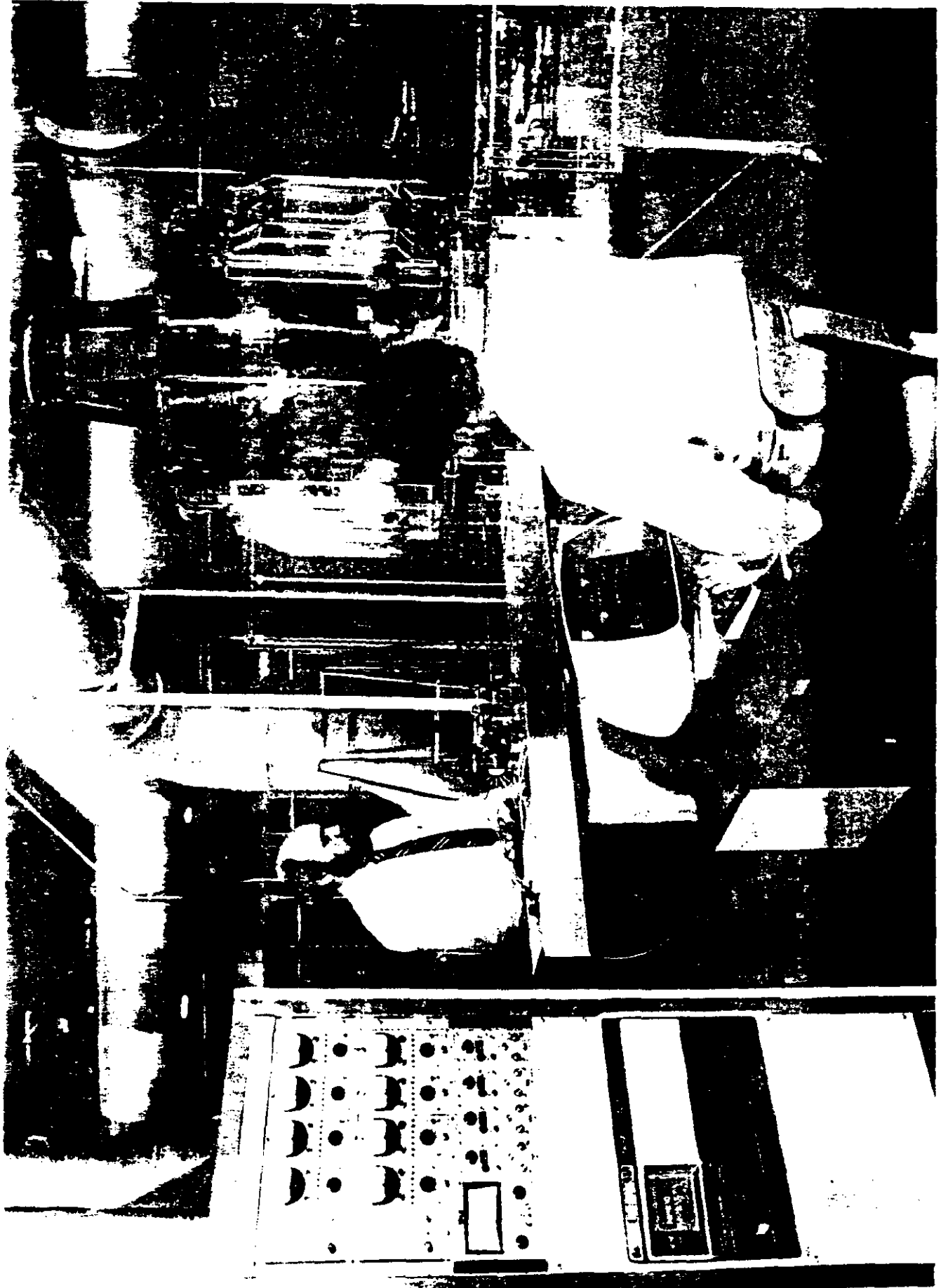


Figure 4-6 Automatic Probe Traversing Device

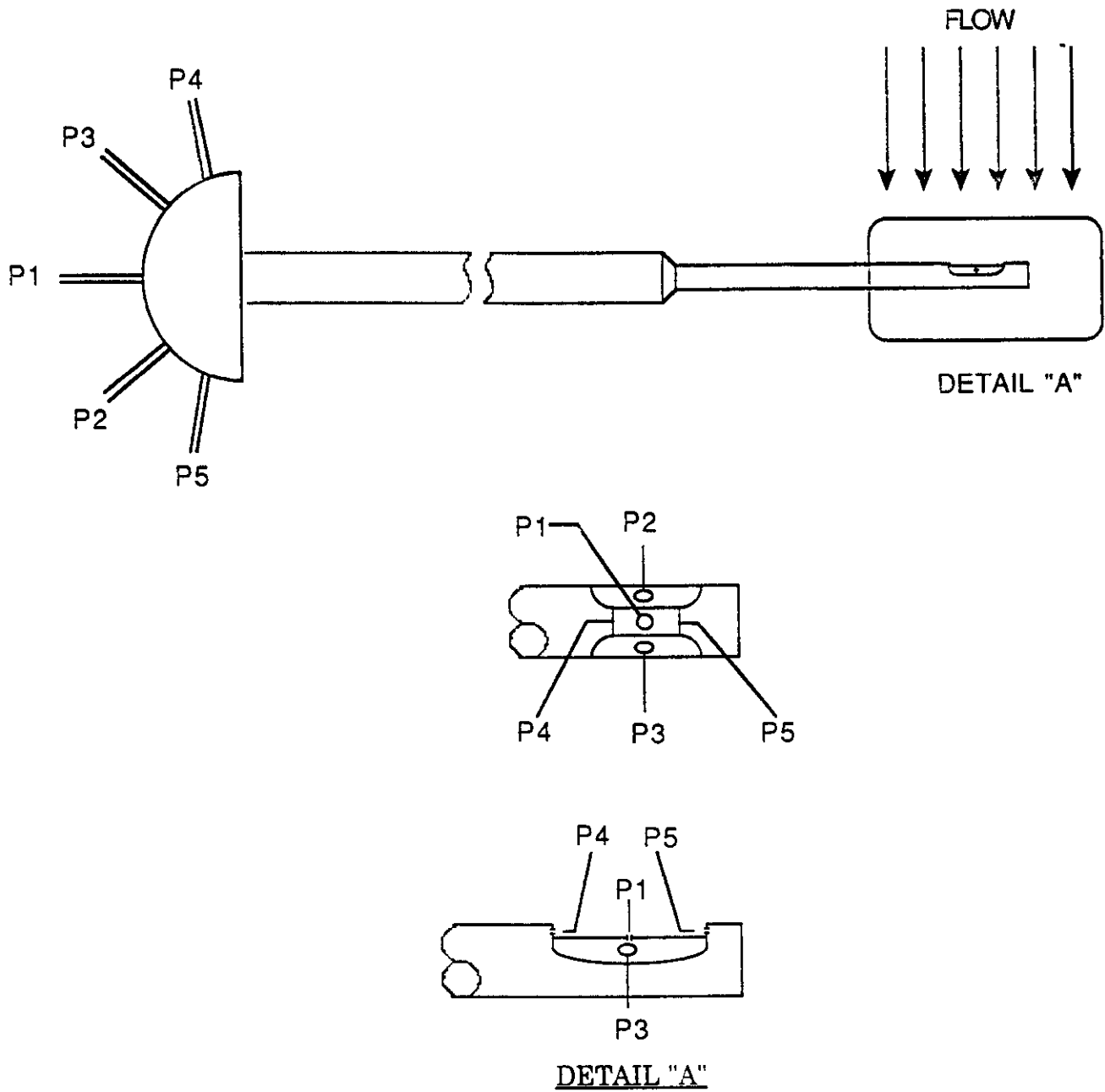


Figure 4-7 Five Hole Pitot Tube

This flow angle, known as the pitch angle, is determined by the differential pressure P4-P5.

In actual practice, four (4) differential pressure readings are required to fully define the flow at a particular point in the flow field. These pressure differentials are:

- P1-Patm = Indicated total pressure with respect to atmosphere
- P1-P2 = Indicated velocity pressure
- P2-P3 = Yaw angle pressure
- P4-P5 = Pitch angle pressure

Calibration curves are used to relate these pressure differentials to the actual pressures and pitch angles. These curves are generated through detailed probe calibrations, which were performed at the beginning of the test series. These curves, given in Appendix A, enable the determination of the actual velocity head and pitch angle at each measuring point. Knowing this data and the yaw angle, the x, y, z, or the normal, radial, and tangential velocity vectors are determined using simple geometric relationships.

4.4 Laser Absorption Spectrophotometer

An automatic laser based system, the Laser Absorption Spectrophotometer, has been developed in KDL to make tracer gas concentration measurements using the available APTD hardware. A schematic of this Laser Absorption Spectrophotometer is shown in Figure 4-8. The APTD positions the five-hole pitot probe at each of a matrix of points in a plane, as specified in the test set-up. A sample of the tracer gas is then extracted from the flow model by a suction pump attached to the probe and analyzed by the spectrophotometer.

The sample, in going from the probe to the pump exhaust, passes through a chamber through which one of two equally intense laser beams is passed. The wavelength of the laser light is tuned to the absorption frequency of the tracer gas, methane. The level of attenuation, when compared to the reference beam, is proportional to the concentration of the tracer gas at the sampling point in the flow model. Before and after each traverse into the

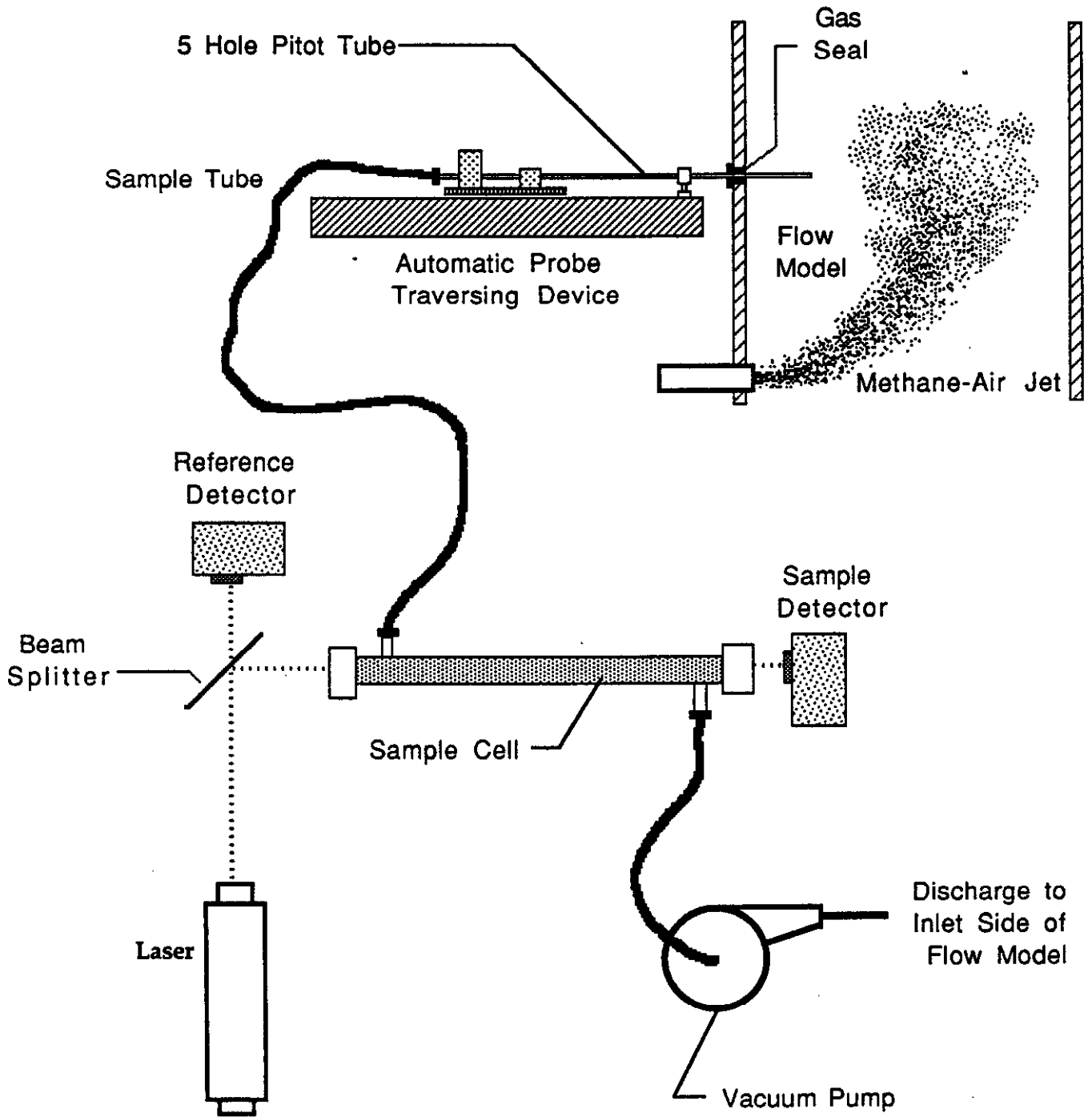


Figure 4-8 Laser Methane System

model, the system is zeroed. Two samples per test point are drawn and the results sent to the laboratory central data acquisition computer. A full calibration is performed on this system prior to the model testing. This calibration is given in Appendix B.

4.5 Smoke Generator

A commercially available smoke generator was utilized during the flow visualization tests. The smoke generation system consisted of a gas heater, a light oil smoke fluid reservoir, and tube coil. The fluid was pumped through the tube coil, which was heated, causing it to flash into a dense white stream of smoke. This stream was then injected into the various ports of interest within the model.

5.0 Lansing Smith Flow Model Testing

5.1 Flow Model Set Up

The Lansing Smith flow model and the criteria used to design it have been discussed in the previous sections. In general terms, the flow model is representative of the actual prototype. The final step in achieving model similitude is to configure the model inlet conditions such that they match, as closely as possible, the inlet conditions which exist in the prototype. Since the LNCFS-III configuration has not been installed in the prototype unit, actual field data is not available. Therefore, the model flow splits were modified such that they produced profiles similar to that of the design operating conditions.

The overall distribution of the flow quantities between the sources of air was handled in the following manner. The Lansing Smith flow model was nominally operated under induced draft. The total air flow through the model was measured using a venturi, which was installed in the main duct downstream of the Model Area Fan. The OFA flow was supplied through the Lamson blower and was measured independantly via an orifice, which was located at the blower inlet. The OFA flow was than subtracted from the total model air flow to obtain the flow through the windboxes. Dampers in the air source lines allowed for adjustment of the flow streams until the desired total flow ratios had been achieved.

Correctly modeling the initial flow distributions is necessary where the evaluation of multiple gas streams is considered. For the Lansing Smith model, it was necessary to model the windbox flows, including the CCOFA, as closely as possible in order to obtain meaningful measures of the gas mixing of the SOFA at higher levels in the furnace. Velocity ratios between the primary and secondary air nozzles were determined based on MCR operating conditions for the Lansing Smith Unit. In addition to this, the CCOFA flow rates were determined from the design operating conditions. The flow splits between the primary, secondary, and the Close Coupled Over Fire Air nozzles were controlled through the use of perforated plate in

the windboxes. The velocities through each of these nozzles were measured with a pitot tube and the flow through each was determined. Perforated plate was chosen such that the flow splits in the model matched those of the prototype.

5.2 Test Matrix

The isothermal flow model test program for the LNCFS-III configuration was divided into two (2) separate screening levels (Figure 5-1) designed to lead, in an interactive manner, to recommended OFA operation. In the first level, flow visualization tests were performed on twenty (20) different OFA configurations to evaluate those conditions which "look the best" from an OFA penetration, mixing, and dispersion standpoint. In the second level, quantitative tests were performed on those configurations which were chosen from the first level. These tests included methane gas mixing and 3-D velocity mapping. For each of these configurations, gas mixing data was taken at planes 1, 2, 3, and 4 while 3-D velocity data was taken only at plane 4. Each of these test planes were horizontal planes located above the windboxes, above the SOFA nozzles, below the arch, and at the furnace outlet plane, respectively. Figure 5-2 shows the location of these planes in the flow model.

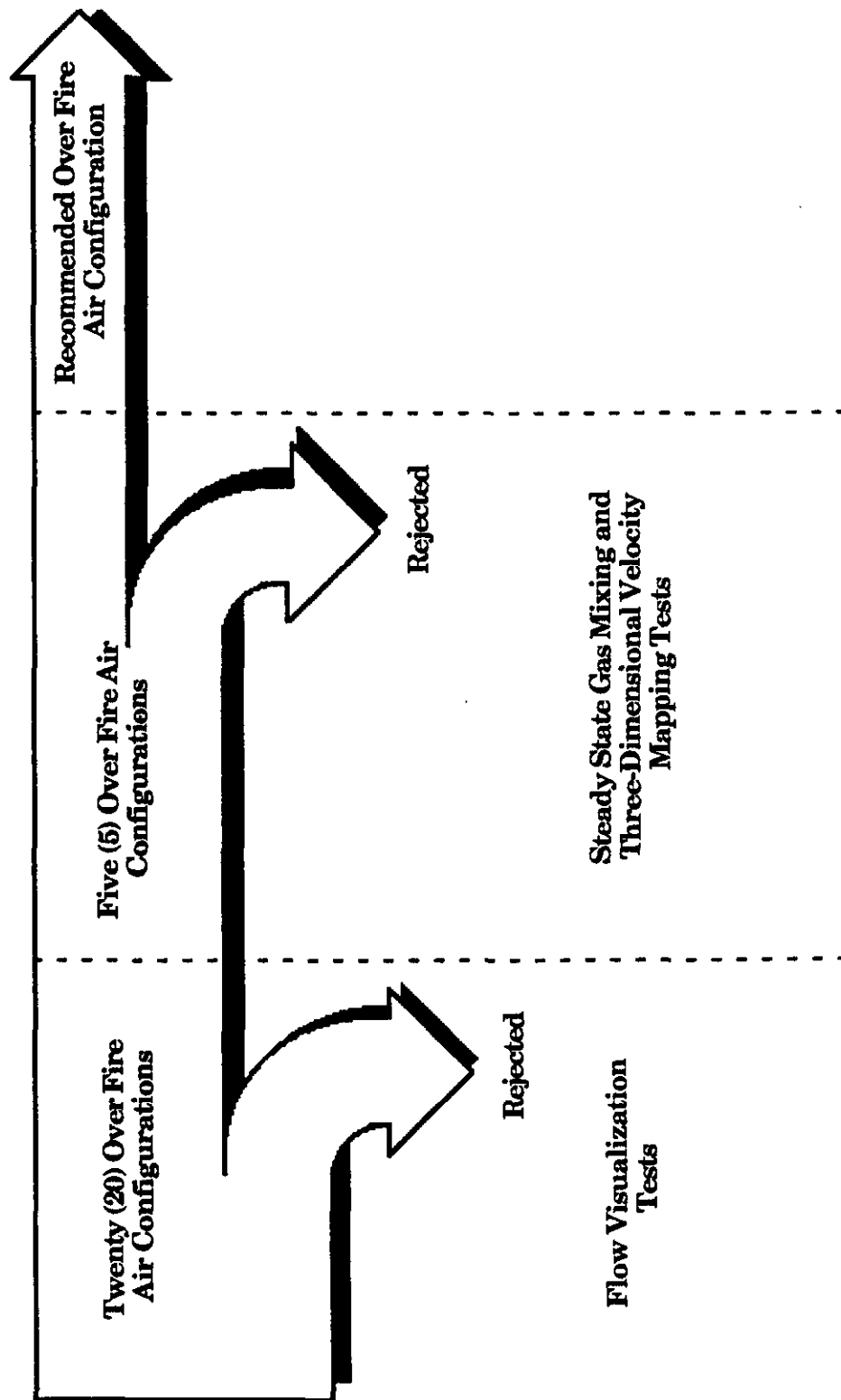


Figure 5-1 Lansing Smith Unit #2 Flow Model
LNCFS-III Test Matrix

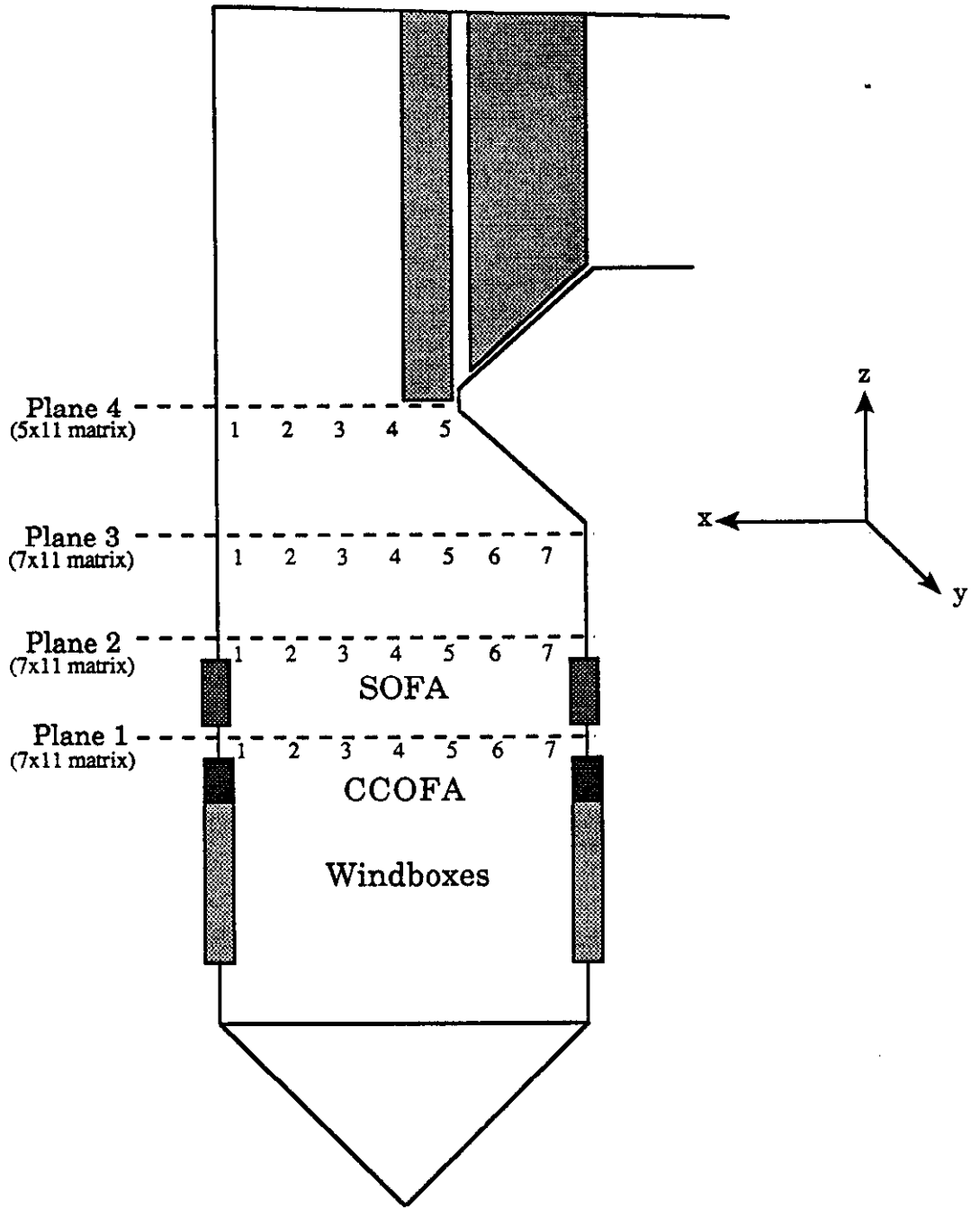


Figure 5-2 Test Plane Locations

6.0 Results

The objective of this flow modeling effort was to evaluate the in-furnace flow and mixing phenomena of the LNCFS-III configuration, which is to be installed in the Lansing Smith No. 2 Unit following the LNCFS-II testing. First, flow visualization tests were used as a preliminary screening tool to evaluate a moderate number of operating conditions. Results from this testing were then used to select those configurations which "looked the best," from an OFA penetration, dispersion, and mixing standpoint, for additional quantitative tests. The quantitative tests, methane gas mixing and three dimensional velocity mapping, were then used to select the OFA configurations providing the desired level of mixing in the furnace.

6.1 Flow Visualization

Flow visualization tests were used as a qualitative method of observing and evaluating the flow fields within the model. These tests were performed on the baseline configuration (no OFA), as well as twenty (20) different operating conditions of the LNCFS-III model configuration, consisting of both CCOFA and SOFA. Each of these tests represented a combination of furnace load and OFA firing angle. In addition to this, the effect of SOFA tilt was evaluated for each test configuration.

Model flow patterns were visualized by the injection of smoke through each of the windboxes, the CCOFA nozzles, and the SOFA nozzles. The smoke was used to evaluate the furnace swirl, along with the OFA jet penetration, mixing, and dispersion. This testing was performed at reduced model flow rates, while maintaining the proper scaling parameters and flow splits. These reduced flow rates were used to improve the visibility of the smoke within the flow model. A video camera was used to record the flow patterns, a copy of this tape is included as an Appendix. The information gained from these tests was used to develop the matrix for quantitative gas mixing and 3-D velocity tests.

Flow visualization tests were performed on the baseline model configuration to evaluate the flow fields within the furnace. The smoke was

injected through each of the four (4) windboxes to qualitatively evaluate the flow swirl and fireball characteristics. The patterns of the smoke as it entered through the different windbox compartments were also observed. Results from this testing showed that the flow entering the furnace through the lower windbox compartments experienced recirculation into the lower hopper, as was expected. For the higher windbox compartments, the windbox flow penetrated towards the center of the furnace and began to form the "fireball", located in the main firing zone. It could also be seen that this swirl was more of an oval shape than it was circular, due to the rectangular geometry of the furnace. Furthermore, it could be seen that the overall penetration of the windbox jets was not very strong. Typically, the flow would instead be redirected along the wall of the furnace before it reached the center.

After the baseline test was performed, smoke visualization tests were performed on twenty (20) OFA configurations. In addition to the different configurations tested to simulate design operation, tests were performed for 0% CCOFA, 0% SOFA, a reduced SOFA flow of 12%, and an increased SOFA flow of 24%. Each of these tests were intended to look at the performance of the CCOFA and the SOFA as a function of the SOFA firing angle and flow rate. A summary of these test configurations is given in Table 6-1. Instead of describing the results of each of these tests individually, the discussion will focus on the OFA performance for each of the OFA flows tested. For each of these, the performance will be evaluated as a function of the OFA nozzle firing angle and the tilt.

The first configuration tested was with 15% CCOFA and 0% SOFA. For this configuration, smoke was injected through each of the CCOFA nozzles and the flow patterns observed. From these tests, it could be seen that the jets penetrated towards the center of the furnace, similar to the windbox flow. As with the windbox, the overall penetration of the jets was not very strong, with the flow being redirected along the wall of the furnace. This flow behavior was typical for the CCOFA jets with the SOFA, also. Figure 6-1 shows typical flow visualization results for the CCOFA nozzles.

Next, the flow characteristics of the SOFA was observed, with and without CCOFA, for a 0° firing angle. In general, the performance for the 20% SOFA condition was as follows. The jets began to penetrate towards the center of the furnace, but became quickly entrained in the cross flow, as was expected. As this happened, the jets were redirected towards the walls and were dispersed along the outer perimeter of the furnace flow. Typical results of flow visualization tests are shown in Figures 6-2 through 6-4. When a downward tilt was imparted to these nozzles, the penetration increased, while the overall dispersion also improved. However, when this down tilt reached approximately 7°, the jets begin to mix with the windbox firing zone. In so doing, the separation zone required for staged burning is eliminated. Furthermore, as an upward tilt was imparted to these nozzles, no improvements were noticed in the jet penetration and mixing.

In general, the penetration and mixing of the OFA jets was improved with the adjustment of the nozzle firing angles, Figure 6-5. In the model, each corner was adjusted to optimize the furnace coverage. That is, a series of tests were performed in which the nozzle firing angles were adjusted to improve the penetration and mixing of individual corners. It was through this technique that those configurations tested in the next screening level were chosen, see Table 6-2.

For the reduced operation of 12% SOFA, the overall performance was much lower than 20% SOFA as far as jet penetration, mixing, and dispersion. This is expected because of the reduced jet velocities and penetration. In order to improve the overall mixing for this configuration, it was not only necessary to adjust the firing angles of each nozzle, but it was also necessary to impose a downtilt in the SOFA nozzles of 10°. In so doing, the SOFA remained in the furnace for a longer period of time. However, the downtilt in these nozzles reduced the separation zone between the windboxes and the SOFA.

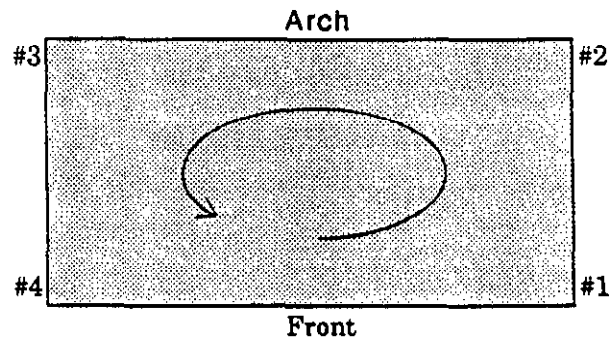
Finally, for the increased operation of 24% SOFA, the overall performance tends to improve from a penetration and mixing standpoint, as would be expected. The jets are able to penetrate deeper into the furnace cross flow

due to the higher velocities. An increase in mixing can also be seen at this setting. However, as more combustion air is injected at higher furnace elevations, the combustion process within the furnace will be effected. In addition to this, the higher jet velocities restricted the allowable tilt in these nozzles. Downtilt was limited to about 5° before the jets became entrained in the windbox firing zone. Also, when a positive tilt was imparted to the nozzles, the jets were carried to the back pass much more rapidly.

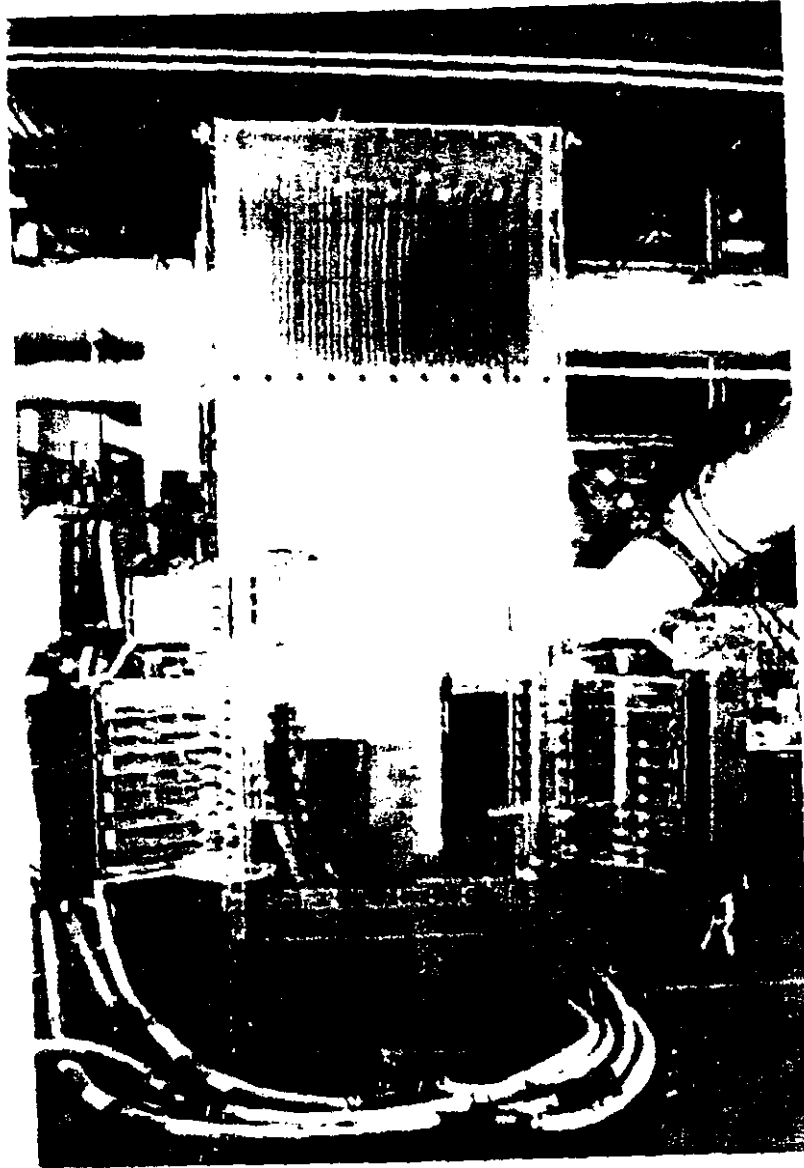
Table 6-1 Flow Visualization Test Matrix

Test No.	Load	% CCOFA	% SOFA	Corner 1	Corner 2	Corner 3	Corner 4
1	MCR	0%	0%	N/A	N/A	N/A	N/A
2	MCR	15%	0%	N/A	N/A	N/A	N/A
3	MCR	0%	20%	0°	0°	0°	0°
4	MCR	15%	20%	0°	0°	0°	0°
5	MCR	15%	20%	0°	-5°	0°	0°
6	MCR	15%	20%	0°	0°	-8°	-8°
7	MCR	15%	20%	0°	-8°	-5°	-5°
8	MCR	15%	20%	-8°	-8°	-8°	-8°
9	MCR	15%	20%	+5°	-8°	-8°	-8°
10	MCR	15%	20%	+7°	-8°	-5°	-10°
11	MCR	15%	20%	0°	-8°	-8°	-2°
12	MCR	15%	20%	0°	-8°	-3°	-8°
13	MCR	15%	20%	-3°	-8°	-5°	-3°
14	MCR	15%	20%	+2°	-5°	-7°	-2°
15	MCR	15%	20%	0°	0°	0°	0°
16	MCR	15%	12%	0°	0°	0°	0°
17	MCR	15%	12%	-3°	-8°	-5°	-3°
18	MCR	15%	12%	+2°	-5°	-7°	-2°
19	MCR	15%	24%	0°	0°	0°	0°
20	MCR	15%	24%	-3°	-8°	-5°	-3°
21	MCR	15%	24%	0°	-8°	-8°	-2°

Lansing Smith Flow Model Corner Reference



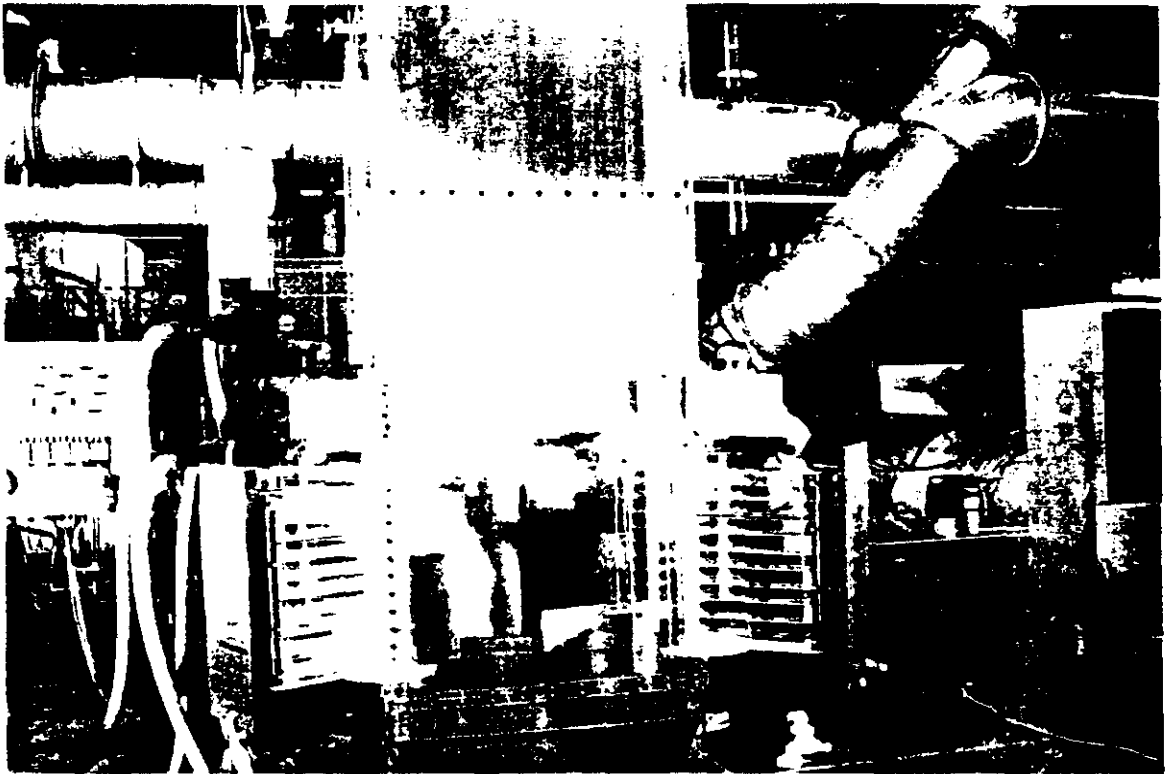
Southern Company Services
Lansing Smith Unit #2
LNCFS-III Model Configuration



Smoke Induced Through the CCOFA Nozzles

Figure 6-1 Typical Flow Visualization Results

Southern Company Services
Lansing Smith Unit #2
LNCFS-III Model Configuration



Smoke Induced Through SOFA Nozzles

Figure 6-2 Typical Flow Visualization Results

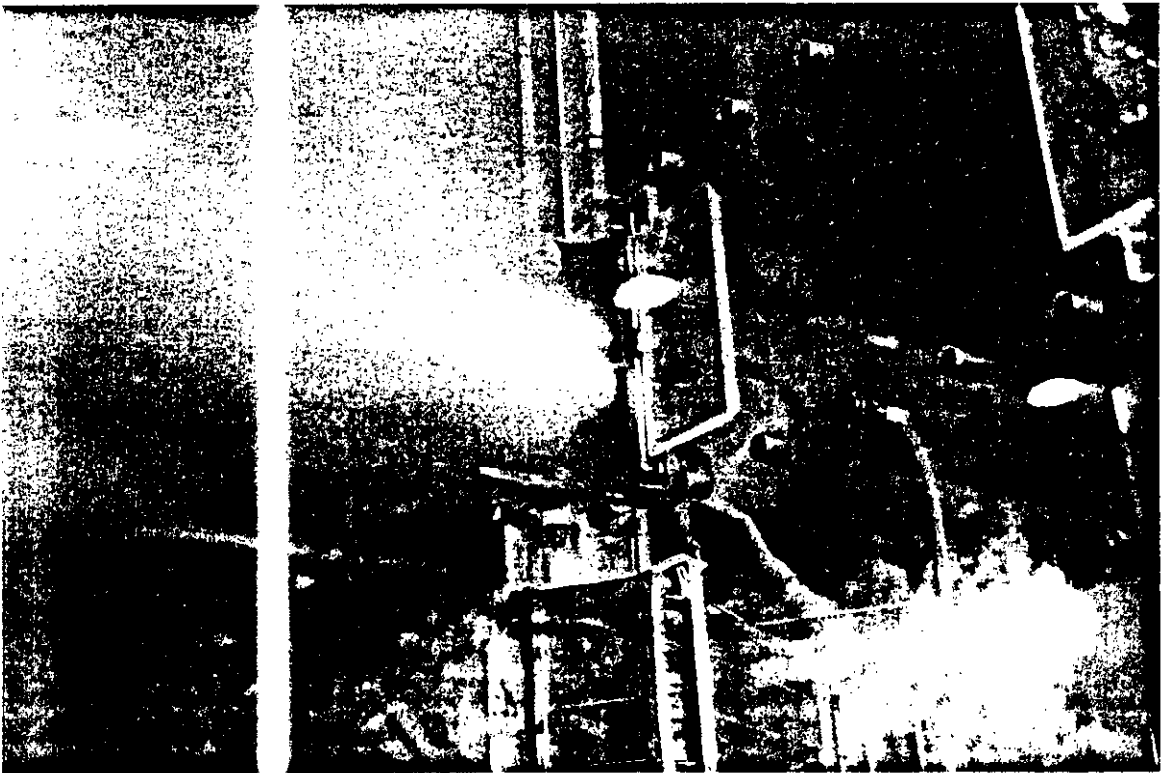
Southern Company Services
Lansing Smith Unit #2
LNCFS-III Model Configuration



Smoke Induced Through SOFA Nozzles

Figure 6-3 Typical Flow Visualization Results

Southern Company Services
Lansing Smith Unit #2
LNCFS-III Model Configuration



Close Up of Smoke Induced Through SOFA Nozzles

Figure 6-4 Typical Flow Visualization Results

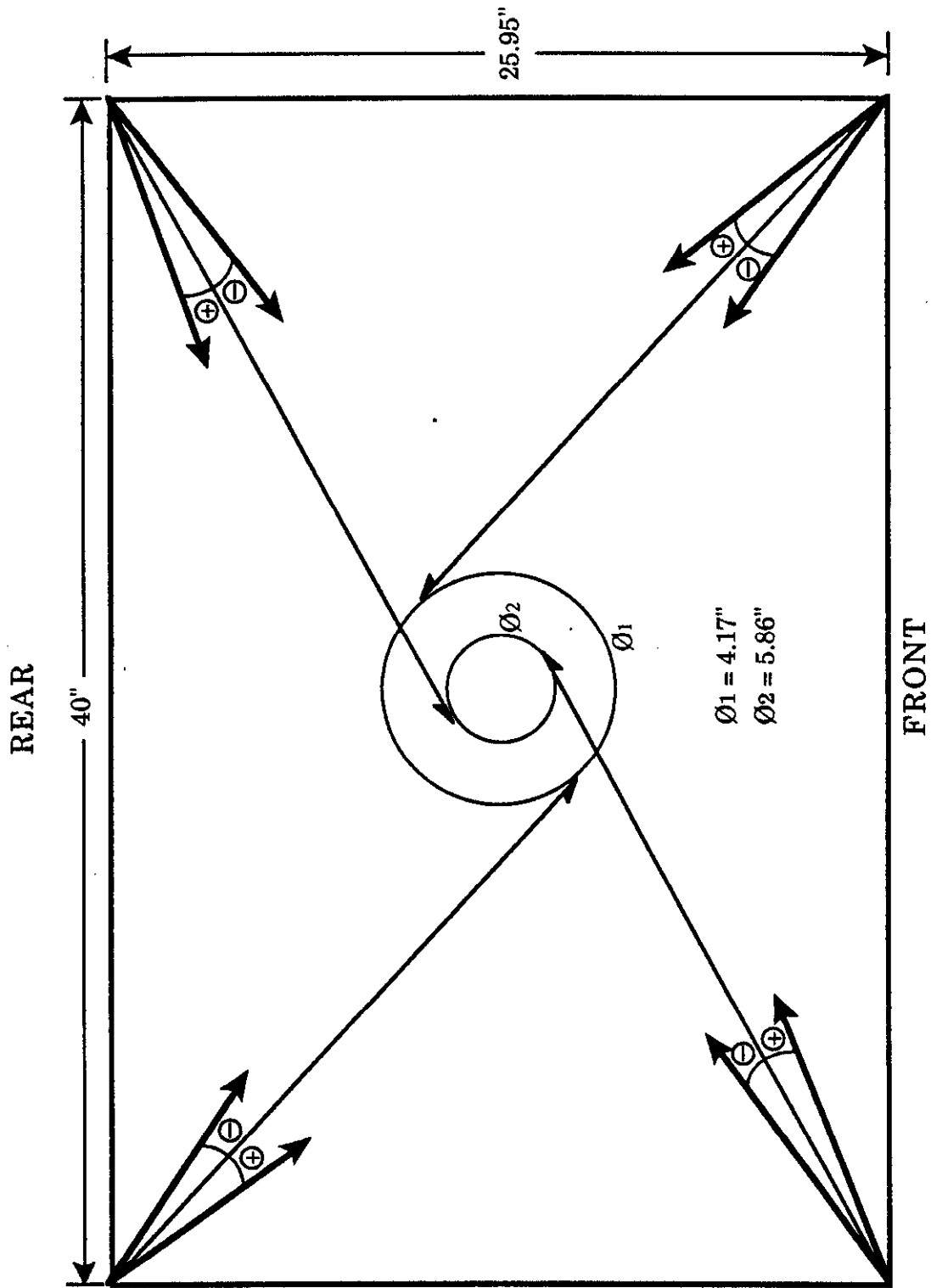


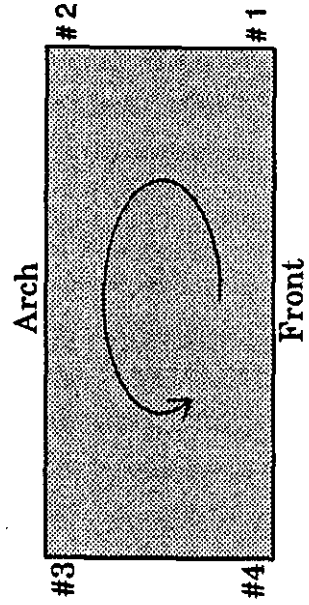
Figure 6-5 SOFA Nozzle Firing Circle Lansing Smith No. 2 Flow Model

Table 6-2 Methane Gas Mixing and Velocity Mapping Test Matrix

Configuration #	Load	% CCOFA	% SOFA	Corner 1	Corner 2	Corner 3	Corner 4	OFA Tilt
Baseline*	MCR	15%	0%	N/A	N/A	N/A	N/A	N/A
1	MCR	15%	20%	0°	0°	0°	0°	0°
2	MCR	15%	20%	+5°	-8°	-8°	-8°	0°
3	MCR	15%	20%	0°	-8°	-8°	-2°	0°
4	MCR	15%	20%	-3°	-8°	-5°	-3°	0°
5	MCR	15%	20%	+2°	-5°	-7°	-2°	0°

* Velocity mapping only

Lansing Smith #2 Flow Model Corner Reference



6.2 Methane Gas Mixing

Based on the results from the flow visualization, a test matrix for the second screening level was developed, as given in Table 6-2. This second screening level involved quantitative mixing tests of five (5) OFA configurations utilizing methane as a tracer gas. The purpose of these tests was to quantitatively measure the penetration, dispersion, and mixing of the OFA with the furnace gases in order to select optimum OFA configurations.

Methane samples were extracted from the flow model through the five hole probe, attached to the APTD. Samples were analyzed by the laser spectrophotometer, previously discussed, and stored in the lab's data acquisition system. This data was later transformed to gas concentrations (ppm) within the model. The measured gas concentrations were normalized to a reference value, taken as the "well mixed" value at the model's outlet. This data was reported in both tabular form, typical of Table 6-3, and graphical form.

For each of these tests, the flow model was operated at a simulated 100% MCR with 15% CCOFA and 20% SOFA. The flow model was operated under induced draft, with the SOFA under forced draft, the flow being provided by the high pressure Lamson blower. In order to assure a "well-mixed" tracer gas concentration at each of the SOFA nozzle outlets, the methane was injected into the discharge of this blower at a point far enough upstream to permit adequate mixing. The flow of methane was set using precision rotometers such that a "well-mixed" value of approximately 1200 ppm at the model outlet was achieved. A schematic of the methane injection system is shown in Figure 6-6. The concentration of the methane gas was then mapped over the four (4) test planes detailed previously in Figure 5-2. The concentration data obtained at each plane was normalized to the "well-mixed" concentration obtained at the model outlet, with each plot generated using the same scaling factors so that they could be compared. For the purpose of clarity, all the plots are presented at the end of this section. The degree of uniformity in concentration across the plane was statistically quantified as the RMS deviation of the mass weighted distribution of methane measured at the test plane. The lower the coefficient, the better the mixing is across the test plane.

Comparing the data at plane 1, contour and isoconcentration plots are presented in Figures 6-7 through 6-16. In addition to these plots, the normalized methane concentrations are shown in Figures 6-17 through 6-21. Plane 1 is located just under the SOFA nozzles and is used to show the separation zone between the windbox firing zone and the SOFA injection. Generally, it can be seen that there is little SOFA recirculation in this zone, with a clear separation between the windboxes and the SOFA nozzles. However, there are some areas of recirculation which should be noted. The first exists for configurations 2 through 5 and is located at the right, rear corner of the furnace. Although the cause of this is not known, it should be noted that for each of these configurations, the SOFA nozzle at this corner is set against the swirl of the furnace. Also, there is some recirculation along the front wall for configuration #1, which was set at the same firing angles as the windboxes.

Data at plane 2, contour and isoconcentration plots, along with the normalized methane concentrations, are presented in Figures 6-22 through 6-36. From this data, the penetration of the SOFA jets can be seen as peaks in the isoconcentration plots. Generally, these jets penetrate into the cross flow and, as they mix with the furnace gases, disperse along the furnace walls. Furthermore, the peaks in these jets are a function of the firing angles of the SOFA nozzles. This corresponds with the results from the flow visualization tests. Also, it can be seen that those jets which run along the front and rear walls of the furnace tend to have longer penetration lengths than those which run along the sides. Finally, the degree of "mixedness" is limited for this test plane because of the close proximity to the SOFA nozzles. Therefore, the RMS deviation, shown in Figure 6-37, for each of these configurations is high.

Contour and isoconcentration plots, along with the normalized methane concentration values, for plane 3 are presented in Figures 6-38 through 6-52. This plane, located just under the arch, shows the progression of the methane mixing within the furnace model. Generally, the overall mixing at this plane is greatly improved, with most of the concentrations falling between $\pm 25\%$ of the well mixed value, as can be seen from each of the

contour plots. As expected, the RMS deviation for this plane, Figure 6-53, is much lower than plane 2, due to the increased mixing time of the SOFA jets. From these plots, it can also be seen that there is higher methane concentrations located along the front and rear walls of the furnace model. This is more than likely a result of the aspect ratio and the furnace aerodynamics. With the front and rear walls of the furnace 1.54 times longer than the side walls, the SOFA jets which penetrate along the side walls will become entrained along the front and rear walls before those jets which come in along the front and rear walls move along the side walls. That is, there is more SOFA mass through the areas along the front and rear walls than there is along the side walls.

Finally, the plane 4 contour and isoconcentration plots, along with the normalized methane concentration values are presented in Figures 6-54 through 6-68. This plane, located at the nose of the arch, shows the progression of the SOFA mixing as the flow is exiting the furnace. Typically, an RMS deviation less than 20% at the furnace outlet plane is considered well mixed for industrial systems. For each of the configurations tested, the RMS deviation was less than 21%, with these values shown in Figure 6-69.

Overall, the best configuration tested from a gas mixing standpoint was Configuration #5. It provided the best overall mixing of any horizontal SOFA configuration tested, with an RMS deviation of 15.6% at the furnace outlet plane. The overall mixing characteristics for each of the configurations tested, from the SOFA nozzles through to the furnace outlet plane, is shown in Figure 6-70.

STEADY STATE LASER METHANE TRACER

TEST ID : LNCFS-111-4
 TEST NUMBER : 0014
 TEST DATE : 2/27/91

PLANE NUMBER :
 NUMBER OF ROWS :
 NUMBER OF COLUMNS

* EXTINCTION COEFFICIENT *

	1	2	3	4	5	6	7	8	9	10	11
1	0.657	0.569	0.520	0.515	0.527	0.552	0.589	0.632	0.673	0.682	0.734
2	0.612	0.587	0.597	0.601	0.611	0.635	0.630	0.632	0.663	0.684	0.727
3	0.616	0.623	0.623	0.655	0.712	0.739	0.773	0.747	0.725	0.725	0.716
4	0.647	0.637	0.633	0.657	0.720	0.743	0.788	0.792	0.773	0.742	0.718
5	0.697	0.592	0.583	0.624	0.661	0.720	0.738	0.733	0.733	0.708	0.736
6	0.708	0.559	0.549	0.572	0.612	0.630	0.634	0.619	0.632	0.642	0.709
7	0.711	0.631	0.561	0.531	0.532	0.517	0.559	0.548	0.561	0.582	0.702

* CONCENTRATION (PPM) *

	1	2	3	4	5	6	7	8	9	10	11
1	1175.08	1581.39	1826.61	1855.15	1790.05	1662.28	1481.44	1282.51	1109.54	1071.97	865.45
2	1371.08	1487.52	1443.00	1422.19	1376.52	1269.45	1291.89	1281.50	1150.50	1060.89	890.22
3	1353.68	1322.23	1321.97	1181.36	949.58	844.57	720.78	816.88	900.90	900.45	936.27
4	1219.52	1262.92	1280.42	1173.35	921.33	829.60	666.52	653.01	719.49	835.02	926.49
5	1008.81	1466.50	1507.51	1318.55	1158.38	919.92	848.60	868.06	868.51	966.50	858.55
6	964.03	1627.86	1675.24	1560.26	1372.22	1292.26	1273.73	1341.92	1284.03	1238.87	962.56
7	952.45	1286.17	1616.93	1770.44	1765.21	1842.24	1625.50	1679.62	1614.73	1515.25	991.93

NORMALIZED BY WELL MIXED CONCENTRATION*
 VALUE : 1191.58 PPM RMS DEV : 26.8 %

	1	2	3	4	5	6	7	8	9	10	11
1	0.9862	1.3271	1.5329	1.5569	1.5022	1.3950	1.2433	1.0763	0.9312	0.8996	0.7263
2	1.1506	1.2484	1.2110	1.1935	1.1552	1.0654	1.0842	1.0755	0.9655	0.8903	0.7471
3	1.1360	1.1096	1.1094	0.9914	0.7969	0.7088	0.6049	0.6855	0.7561	0.7557	0.7857
4	1.0234	1.0599	1.0746	0.9847	0.7732	0.6962	0.5594	0.5480	0.6038	0.7008	0.7775
5	0.8466	1.2307	1.2651	1.1066	0.9721	0.7720	0.7122	0.7285	0.7289	0.8111	0.7205
6	0.8090	1.3661	1.4059	1.3094	1.1516	1.0845	1.0689	1.1262	1.0776	1.0397	0.8078
7	0.7993	1.0794	1.3570	1.4858	1.4814	1.5460	1.3642	1.4096	1.3551	1.2716	0.8324

Table 6-3 Methane Mixing Data - General Output

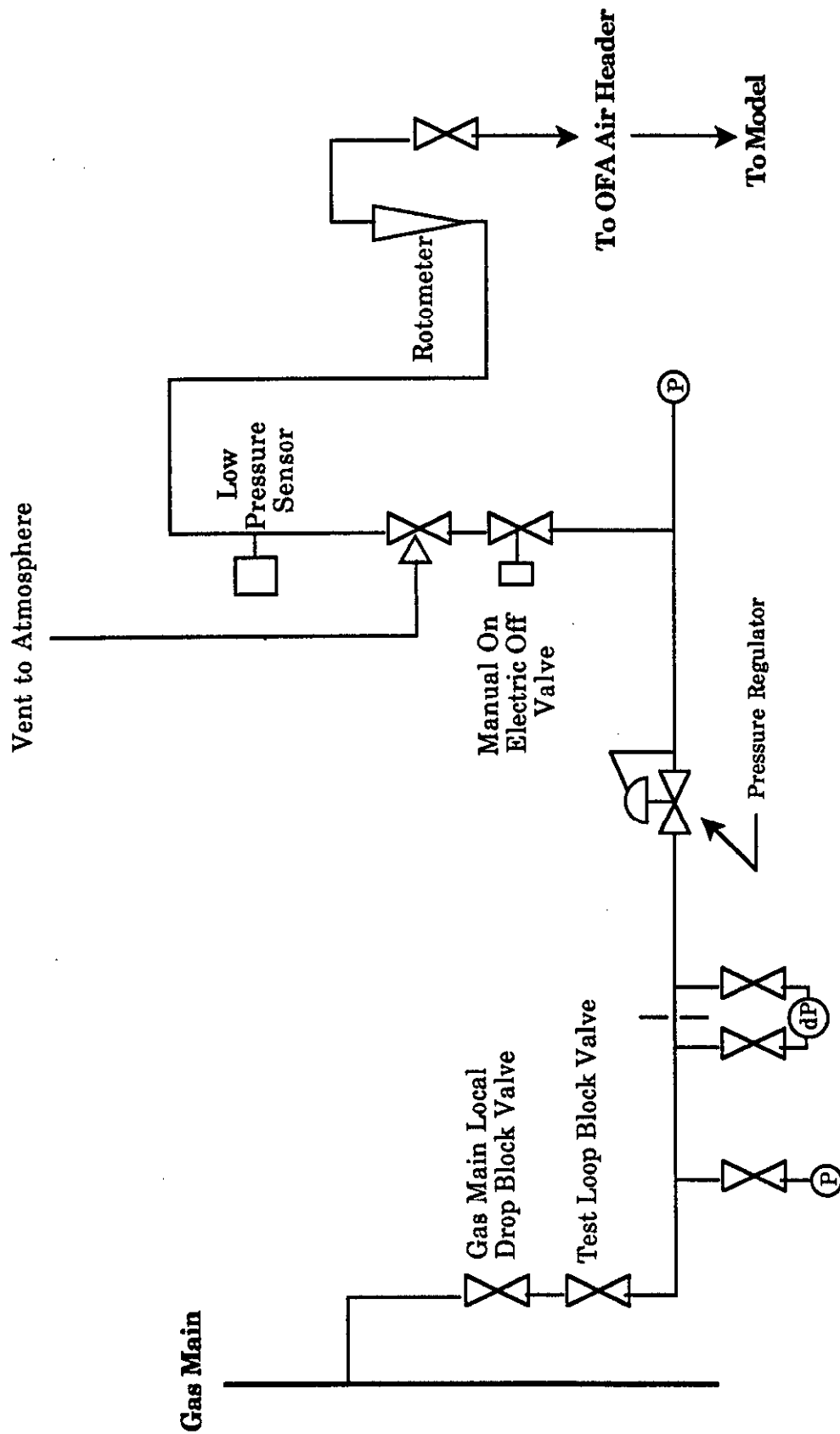


Figure 6-6 Schematic of Methane Injection System

NORMALIZED METHANE CONCENTRATION

Test Plane: 1

Test Date: 2/25/91

Firing System: LNCFS-III

Test ID: Configuration #1

Conc. > 1.0

Conc. < 1.0

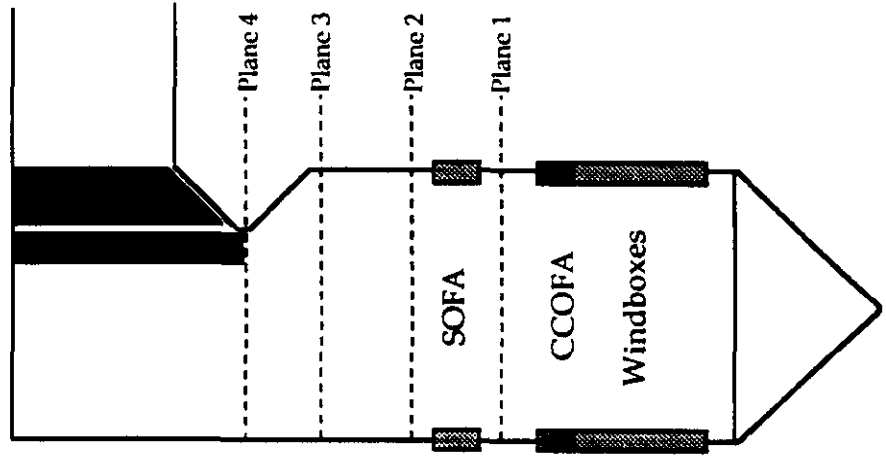
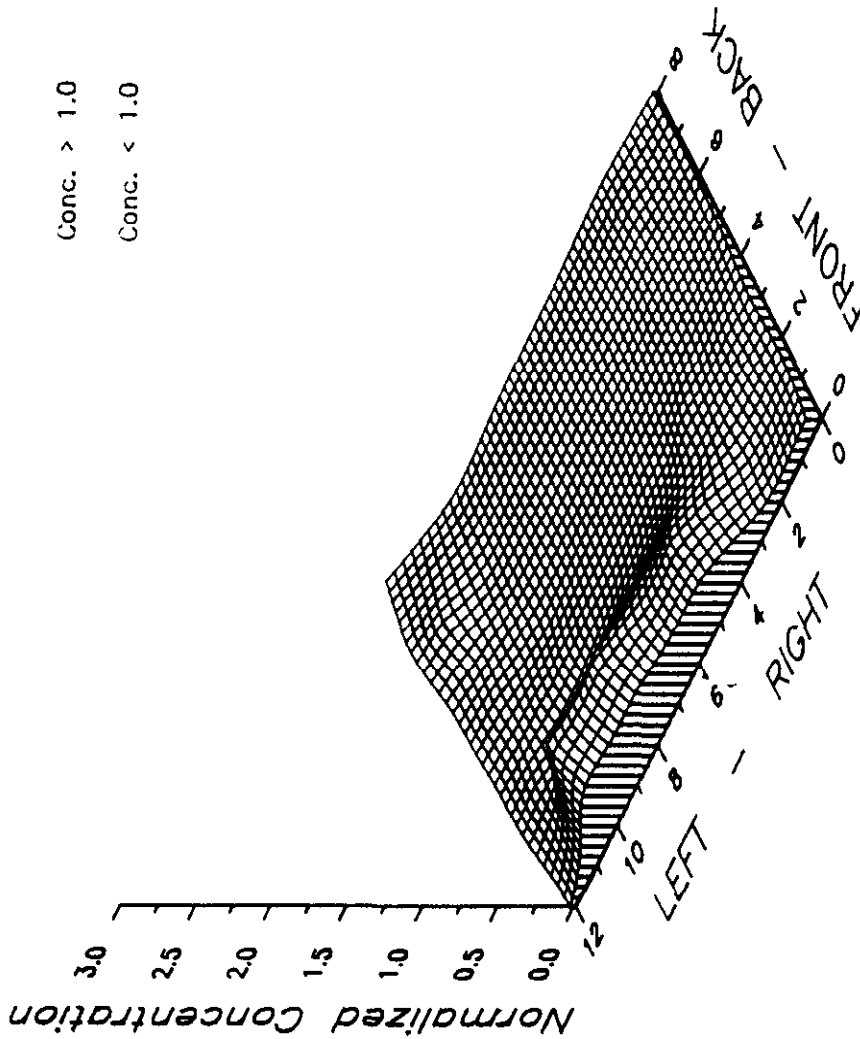


Figure 6-7

SOUTHERN COMPANY SERVICES LANSING SMITH #2 FLOW MODEL

NORMALIZED METHANE CONCENTRATION

Test Plane: 1
 Test Date: 2/25/91
 Firing System: LNCFS-III
 Test ID: Configuration #1

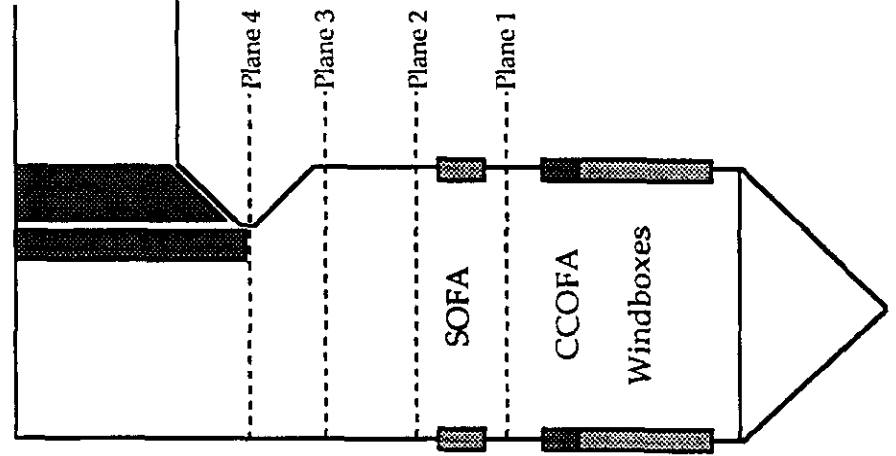
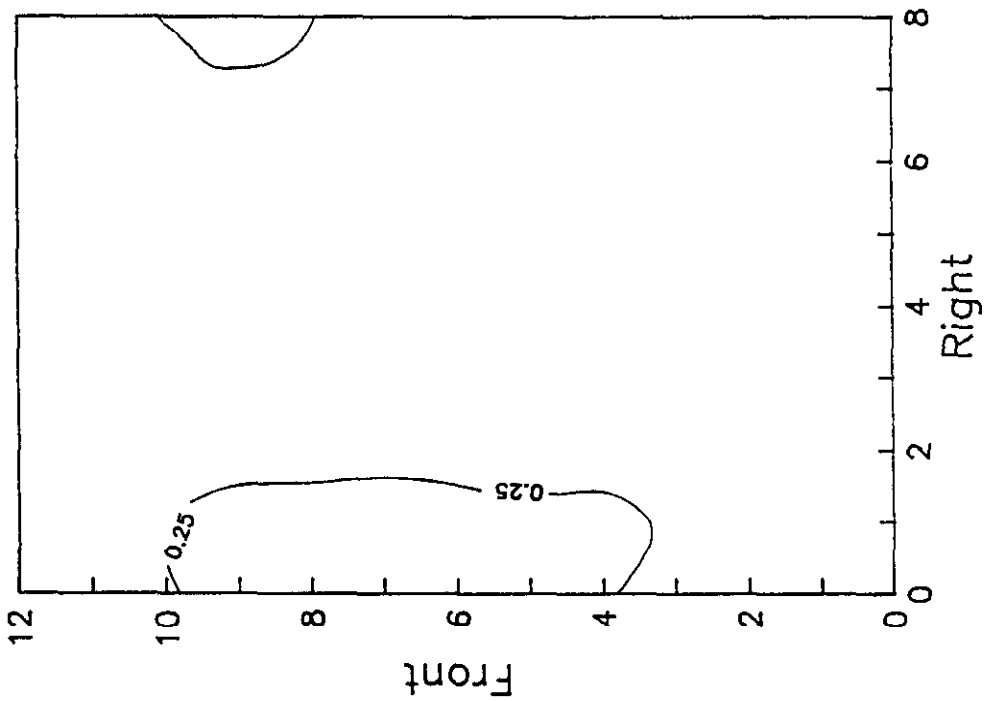


Figure 6-8

**SOUTHERN COMPANY SERVICES
 LANSING SMITH #2 FLOW MODEL**

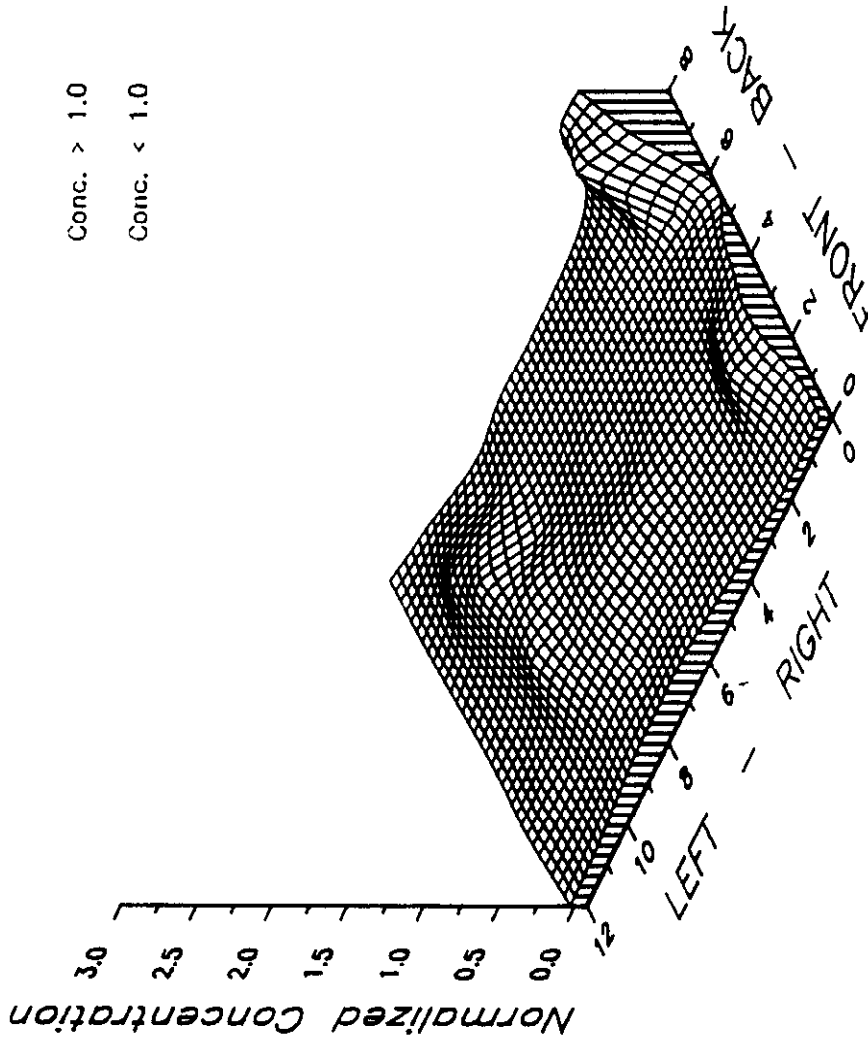
NORMALIZED METHANE CONCENTRATION

Test Plane: 1

Test Date: 2/26/91

Firing System: LNCFS-III

Test ID: Configuration #2



Conc. > 1.0

Conc. < 1.0

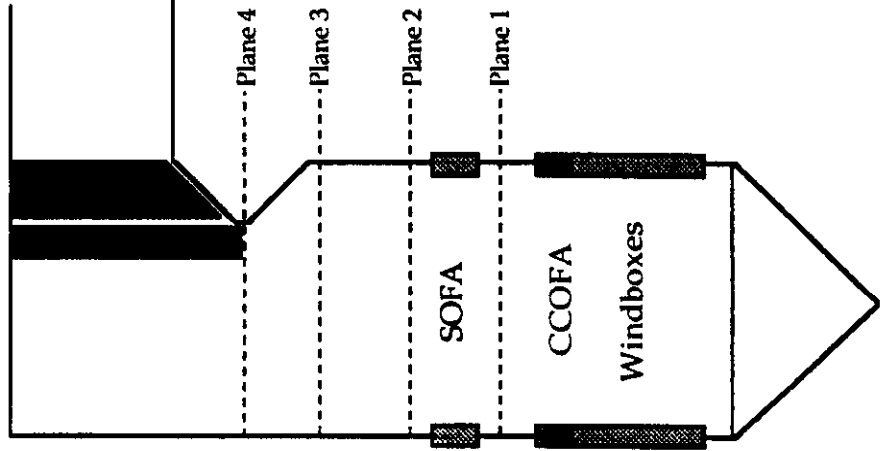


Figure 6-9

**SOUTHERN COMPANY SERVICES
LANSING SMITH #2 FLOW MODEL**

NORMALIZED METHANE CONCENTRATION

Test Plane: 1

Test Date: 2/26/91

Firing System: LNCFS-III

Test ID: Configuration #2

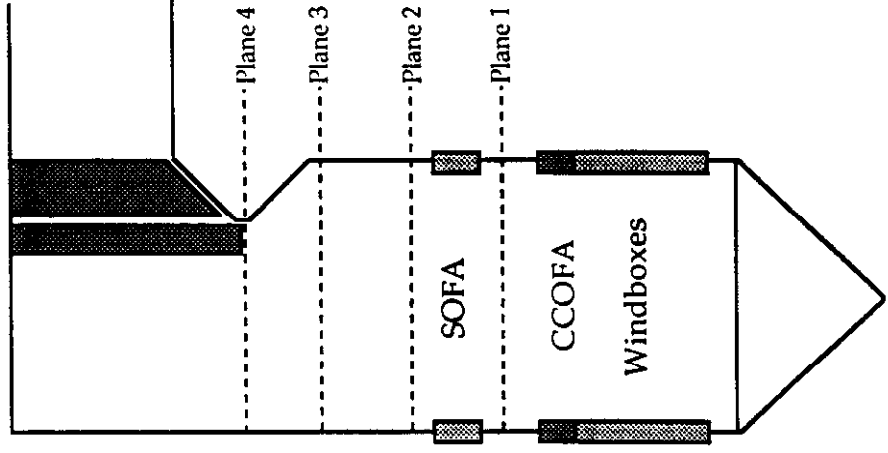
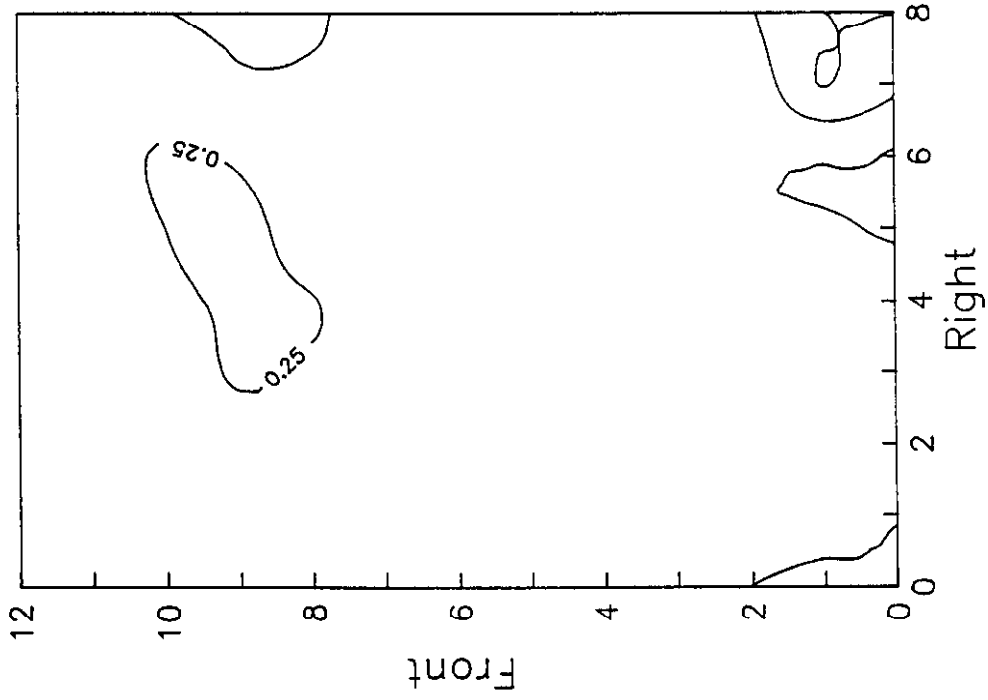


Figure 6-10

**SOUTHERN COMPANY SERVICES
LANSING SMITH #2 FLOW MODEL**

NORMALIZED METHANE CONCENTRATION

Test Plane: 1

Test Date: 2/27/91

Firing System: LNCFS-III

Test ID: Configuration #3

Conc. > 1.0

Conc. < 1.0

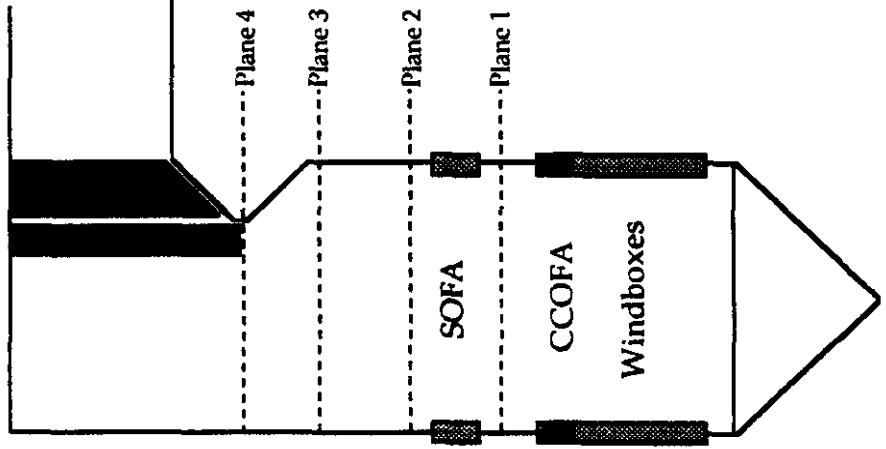
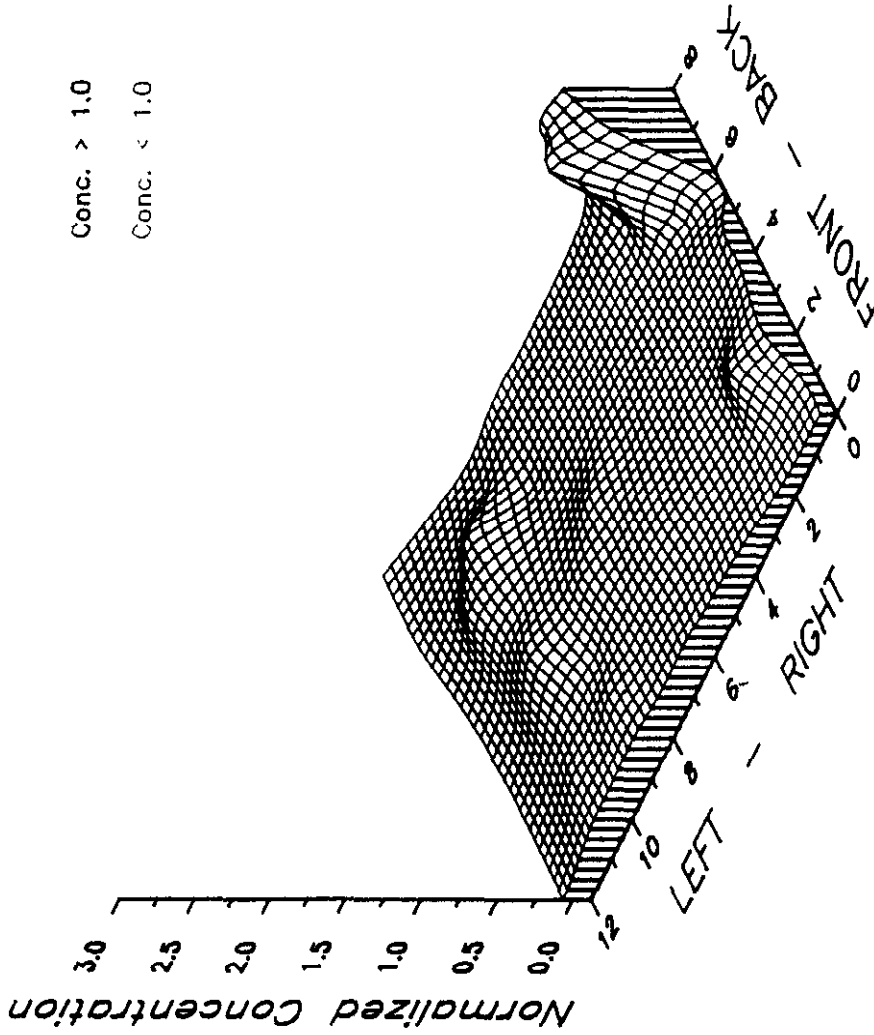


Figure 6-11

**SOUTHERN COMPANY SERVICES
LANSING SMITH #2 FLOW MODEL**

NORMALIZED METHANE CONCENTRATION

Test Plane: 1
Test Date: 2/27/91
Firing System: LNCFS-III
Test ID: Configuration #3

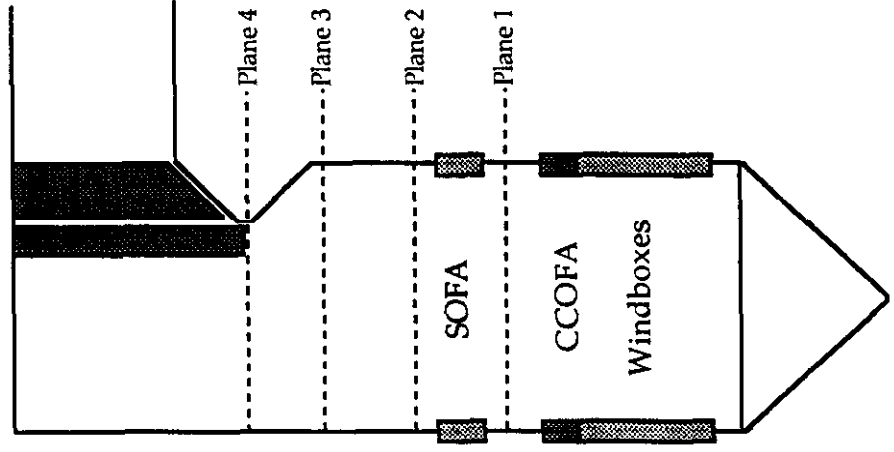
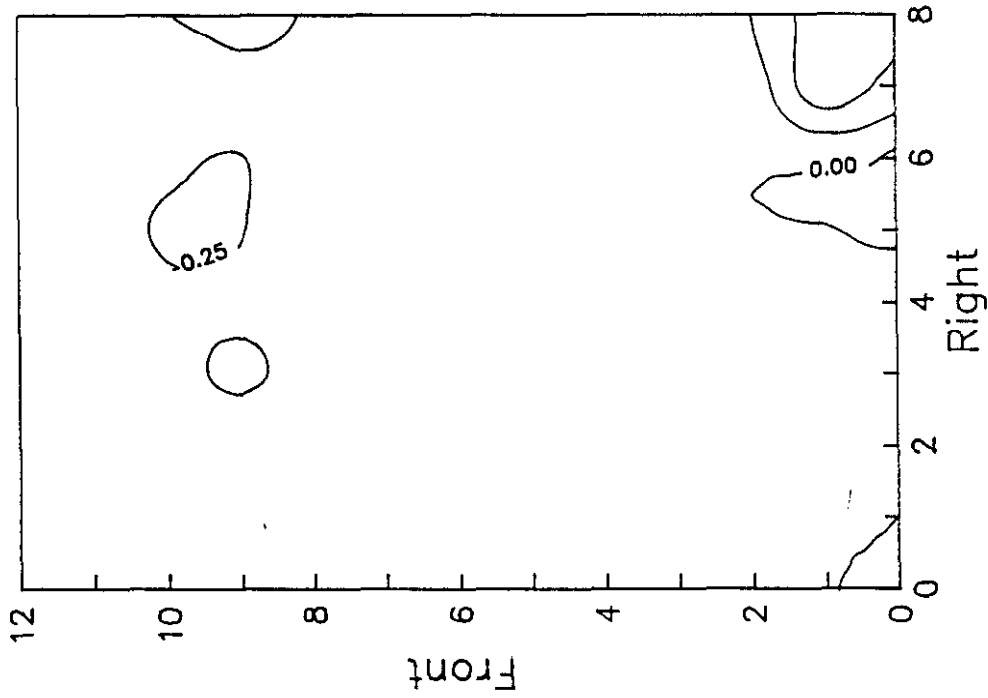


Figure 6-12

**SOUTHERN COMPANY SERVICES
LANSING SMITH #2 FLOW MODEL**

NORMALIZED METHANE CONCENTRATION

Test Plane: 1

Test Date: 2/27/91

Firing System: LNCFS-III

Test ID: Configuration #4

Conc. > 1.0

Conc. < 1.0

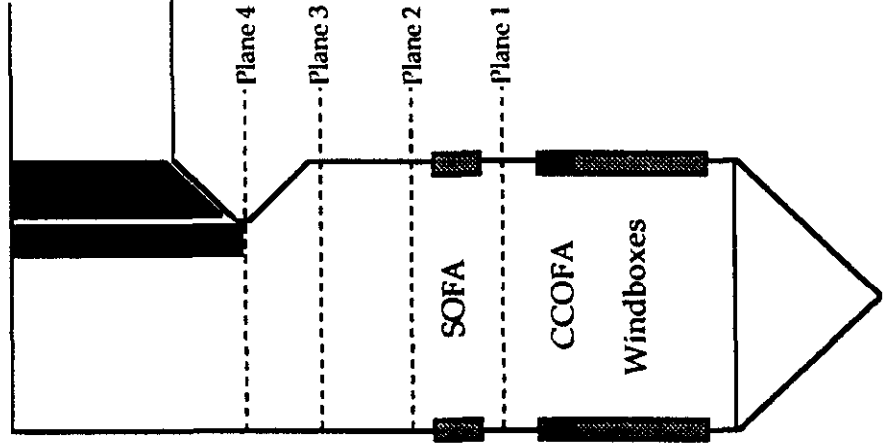
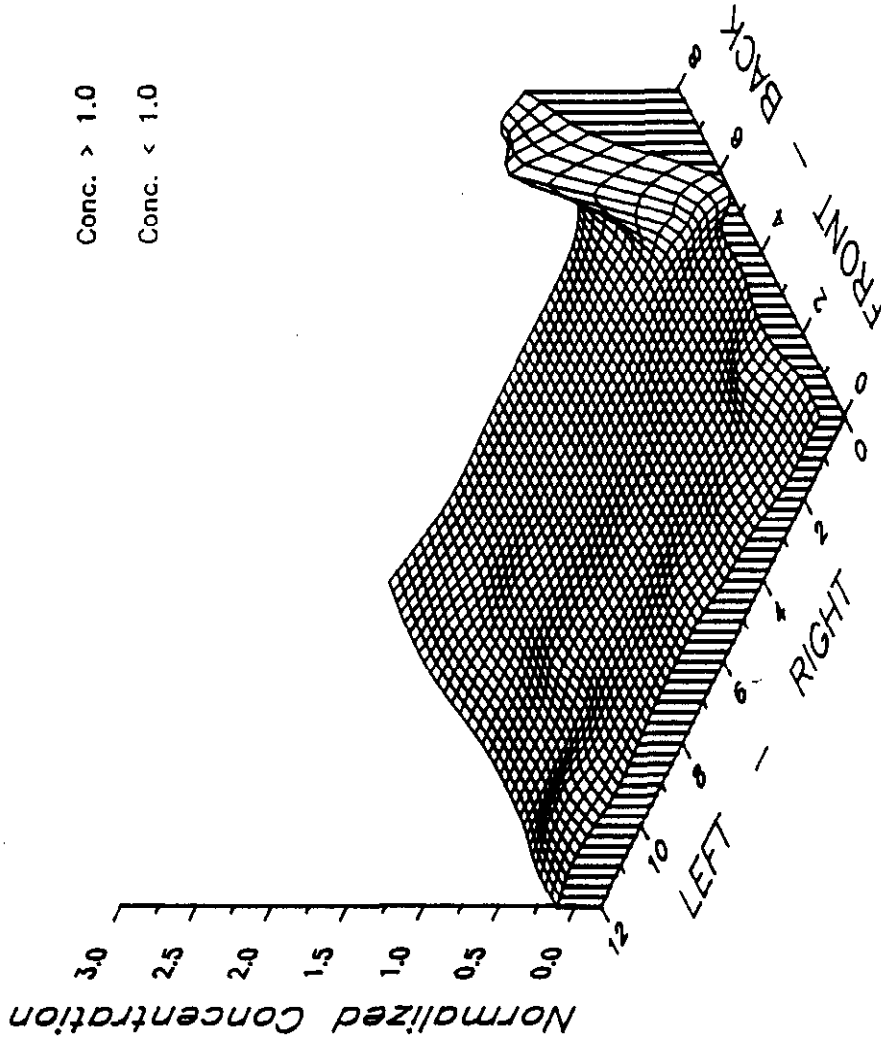


Figure 6-13

SOUTHERN COMPANY SERVICES LANSING SMITH #2 FLOW MODEL

NORMALIZED METHANE CONCENTRATION

Test Plane: 1

Test Date: 2/27/91

Firing System: LNCFS-III

Test ID: Configuration #4

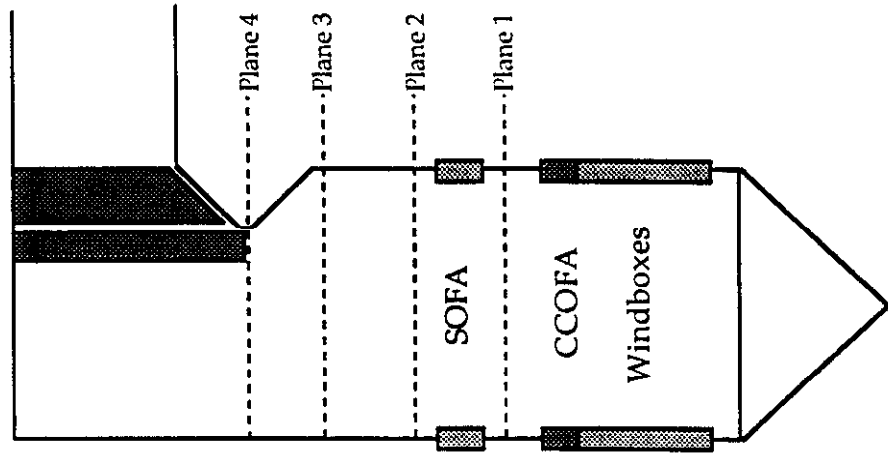
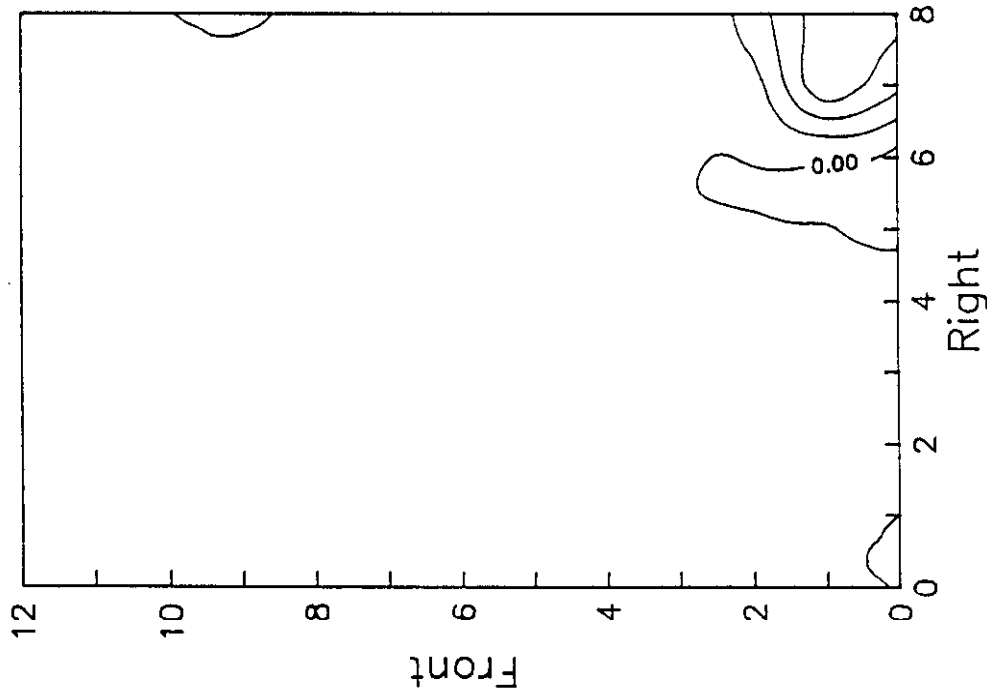


Figure 6-14

**SOUTHERN COMPANY SERVICES
LANSING SMITH #2 FLOW MODEL**

NORMALIZED METHANE CONCENTRATION

Test Plane: 1

Test Date: 2/27/91

Firing System: LNCFS-III

Test ID: Configuration #5

Conc. > 1.0

Conc. < 1.0

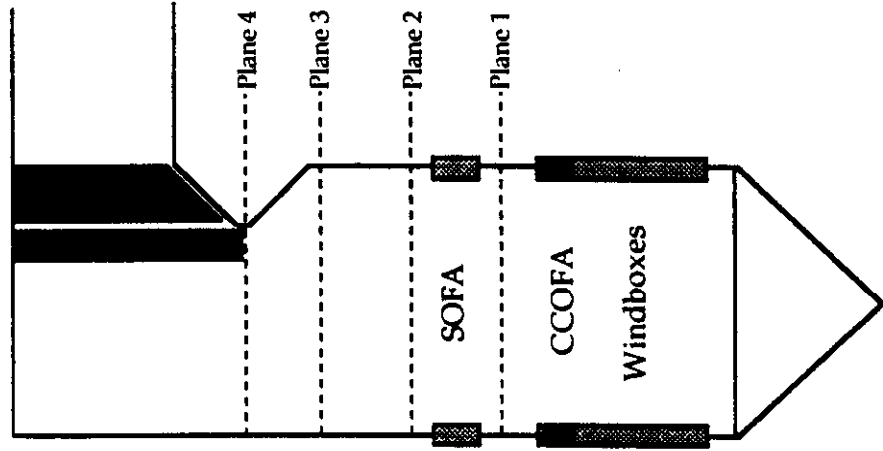
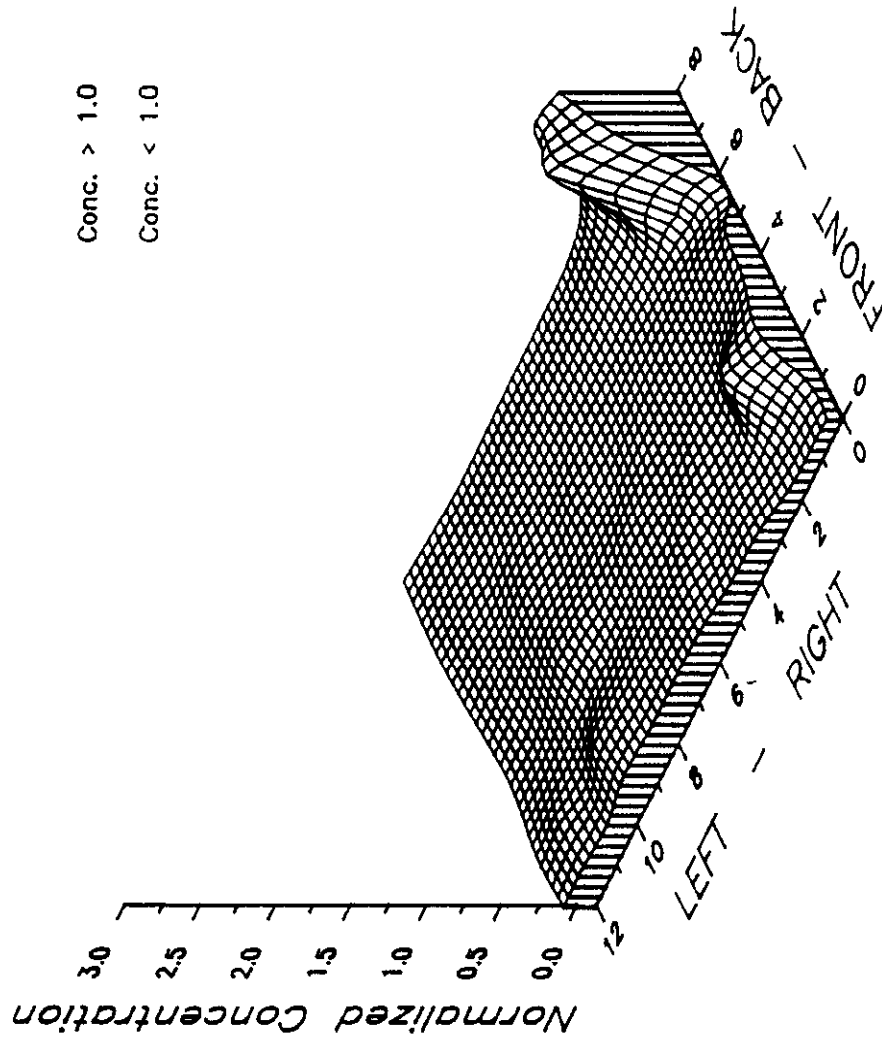


Figure 6-15

**SOUTHERN COMPANY SERVICES
LANSING SMITH #2 FLOW MODEL**

NORMALIZED METHANE CONCENTRATION

Test Plane: 1

Test Date: 2/27/91

Firing System: LNCFS-III

Test ID: Configuration #5

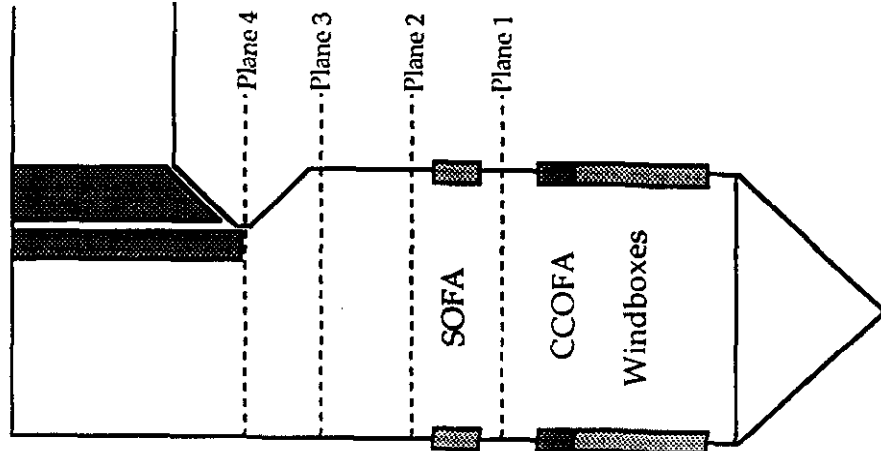
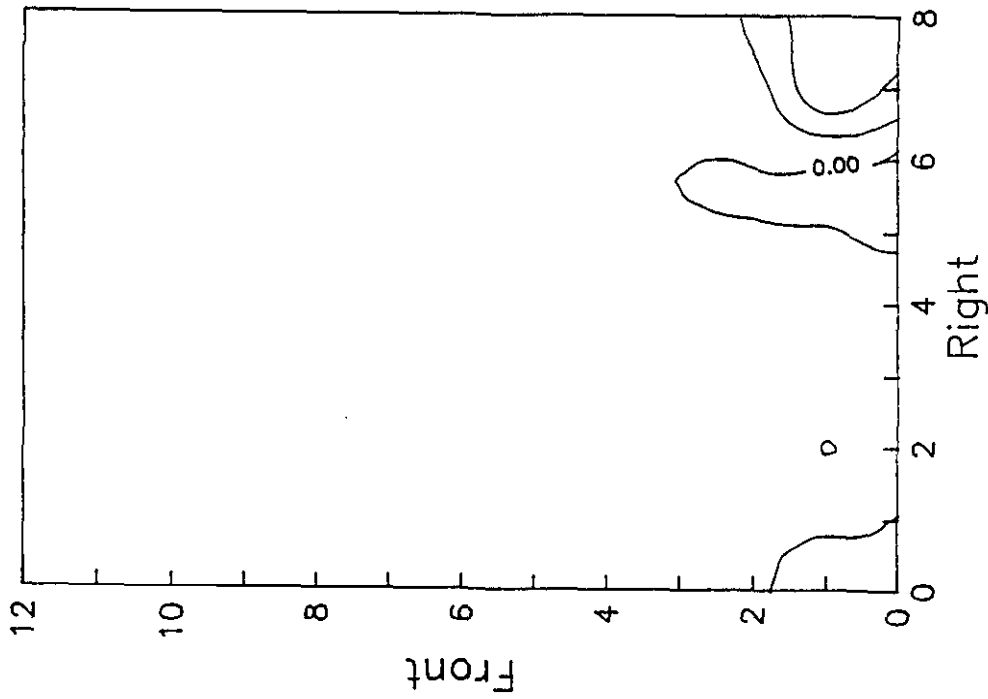


Figure 6-16

SOUTHERN COMPANY SERVICES LANSING SMITH #2 FLOW MODEL

NORMALIZED METHANE CONCENTRATION

Test Plane: 1
 Test Date: 2/25/91
 Firing System: LNCFS-III
 Test ID: Configuration #1

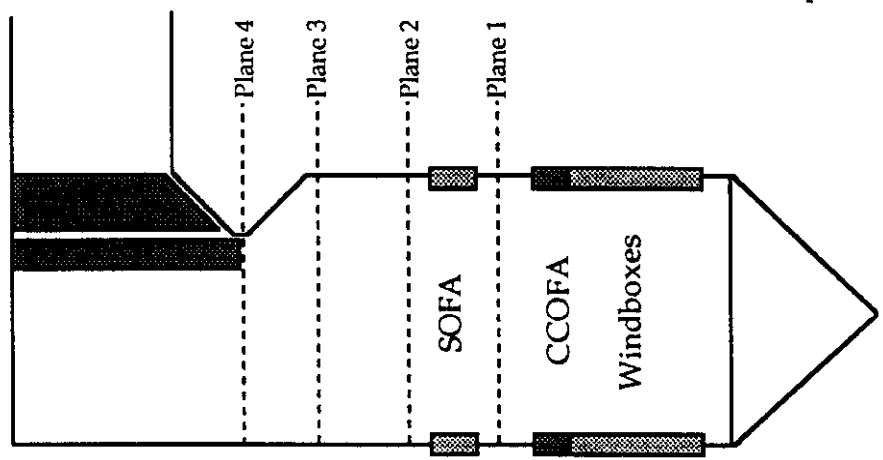
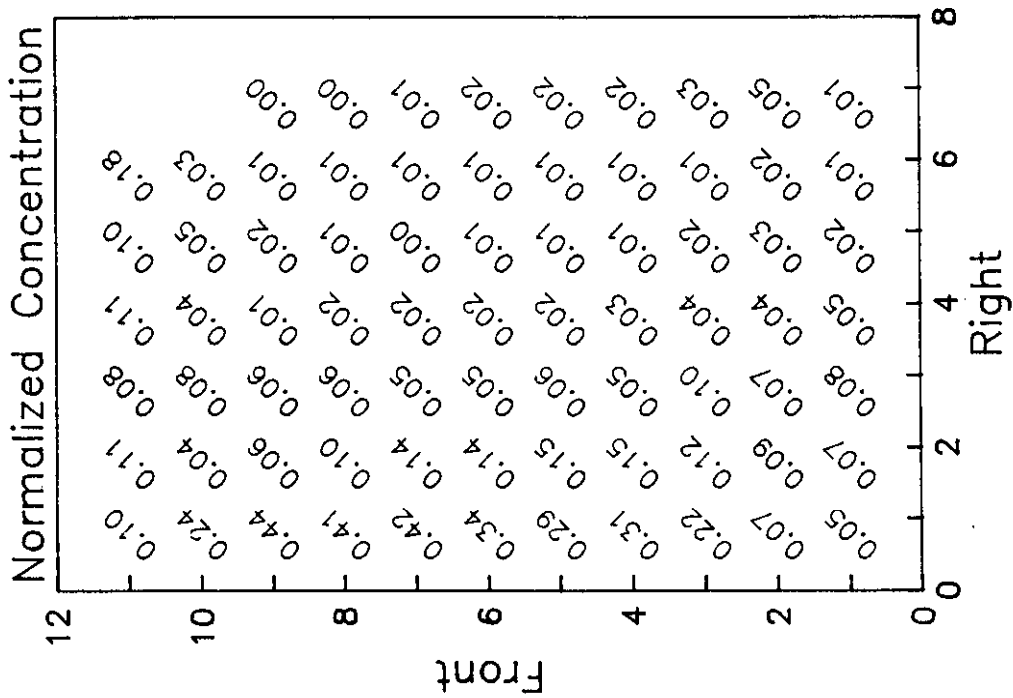


Figure 6-17

**SOUTHERN COMPANY SERVICES
 LANSING SMITH #2 FLOW MODEL**

NORMALIZED METHANE CONCENTRATION

Test Plane: 1
 Test Date: 2/26/91
 Firing System: LNCFS-III
 Test ID: Configuration #2

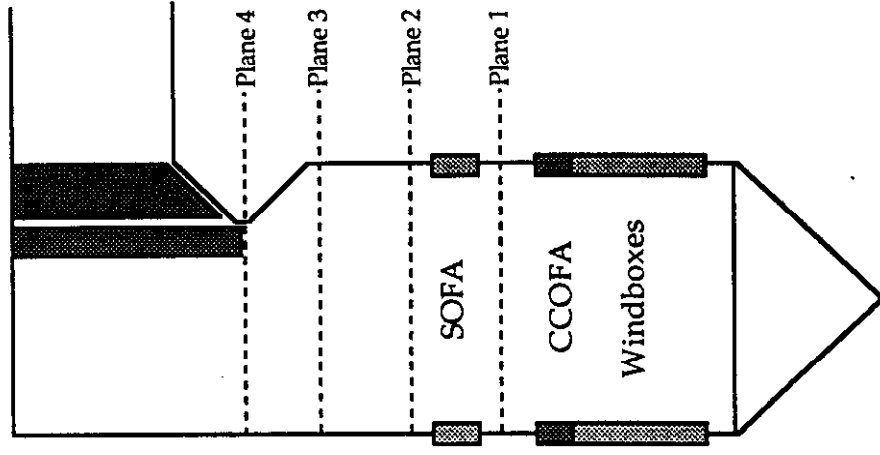
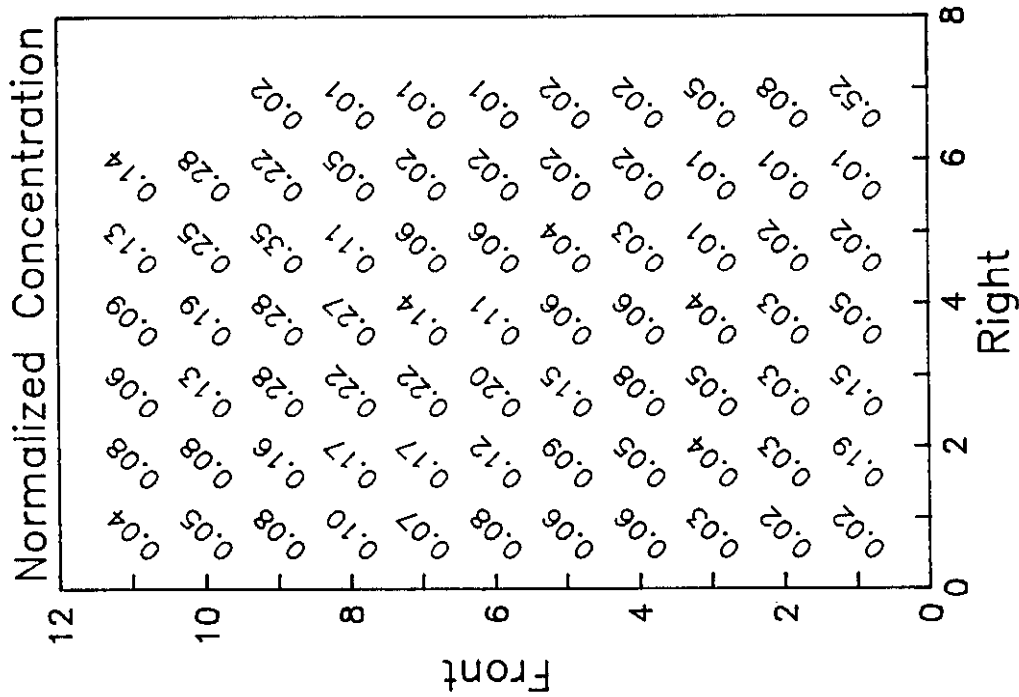


Figure 6-18

**SOUTHERN COMPANY SERVICES
 LANSING SMITH #2 FLOW MODEL**

NORMALIZED METHANE CONCENTRATION

Test Plane: 1

Test Date: 2/27/91

Firing System: LNCFS-III

Test ID: Configuration #3

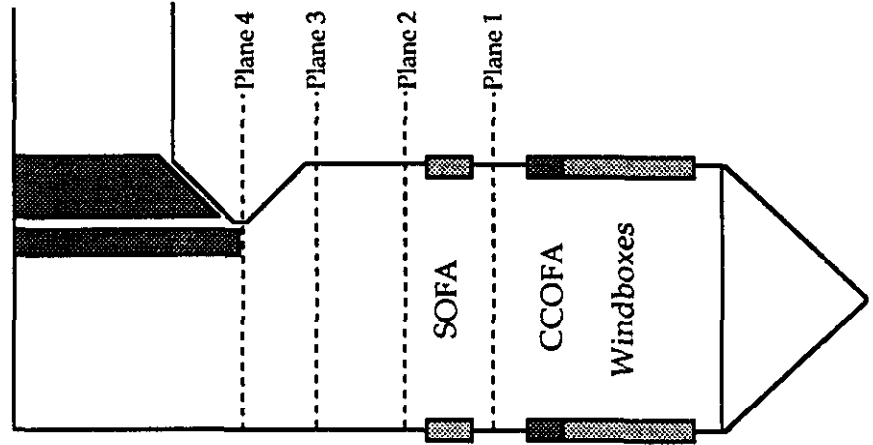
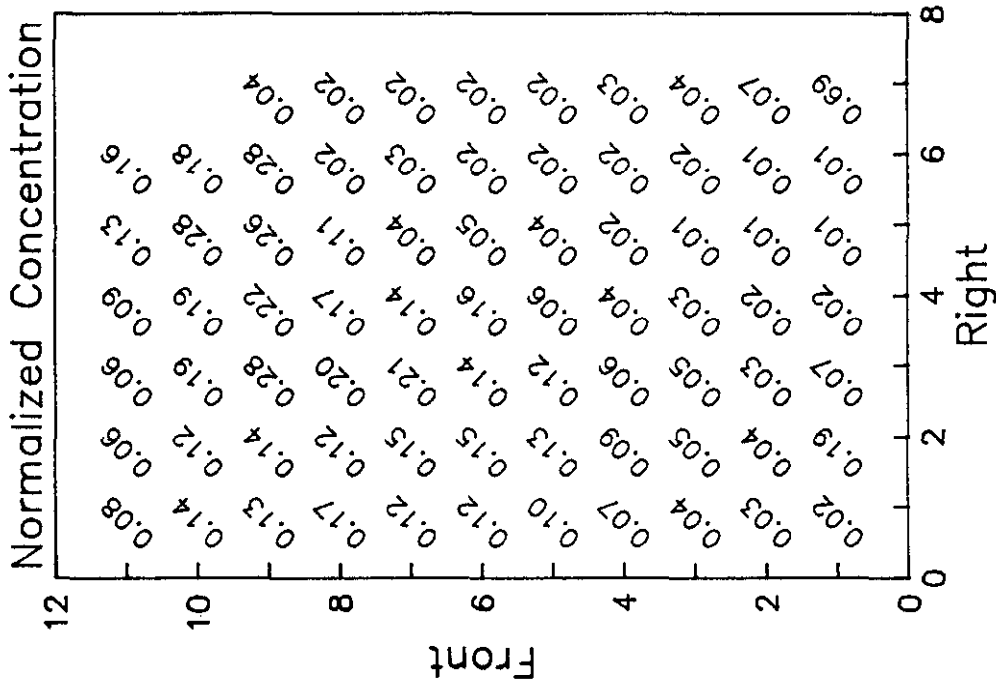


Figure 6-19

**SOUTHERN COMPANY SERVICES
LANSING SMITH #2 FLOW MODEL**

NORMALIZED METHANE CONCENTRATION

Test Plane: 1

Test Date: 2/27/91

Firing System: LNCFS-III

Test ID: Configuration #4

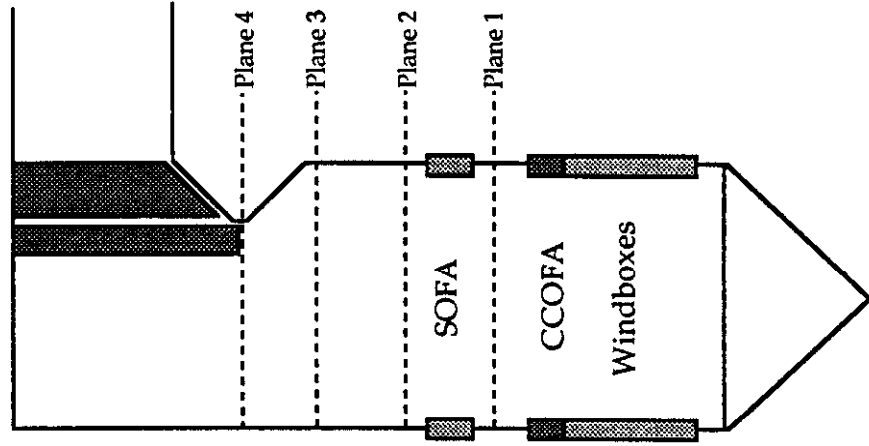
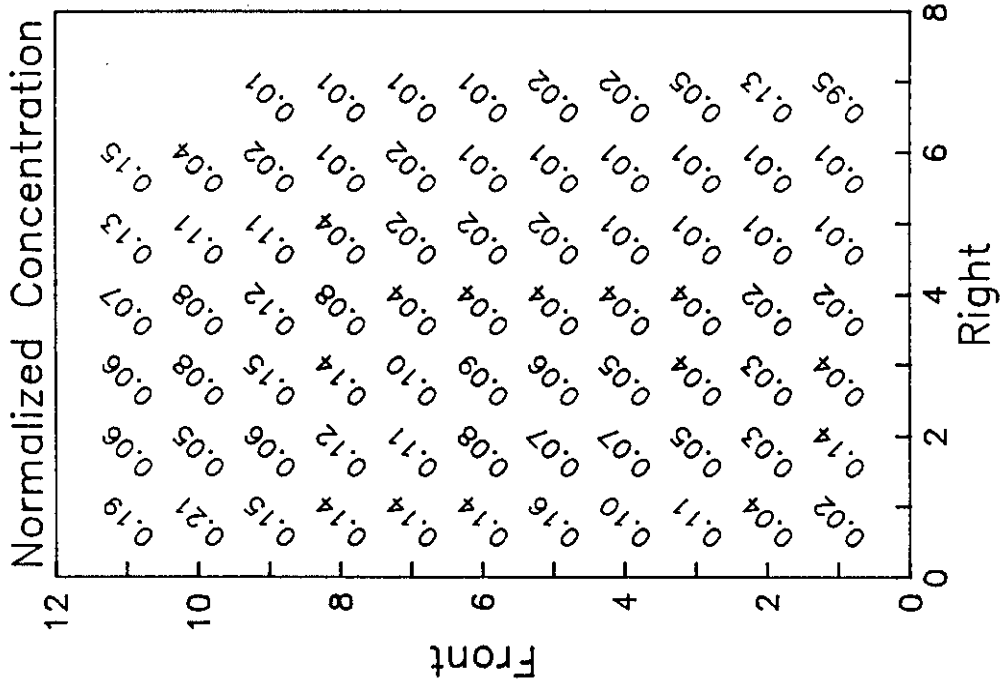


Figure 6-20

**SOUTHERN COMPANY SERVICES
LANSING SMITH #2 FLOW MODEL**

NORMALIZED METHANE CONCENTRATION

Test Plane: 1
 Test Date: 2/27/91
 Firing System: LNCFS-III
 Test ID: Configuration #5

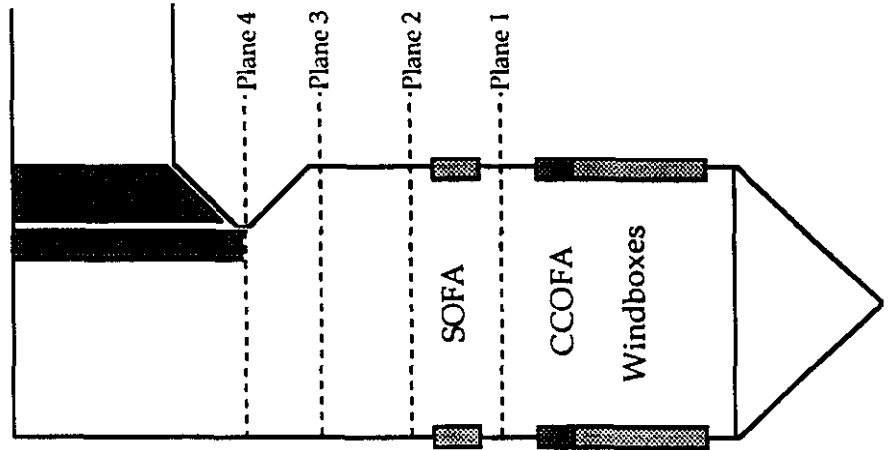
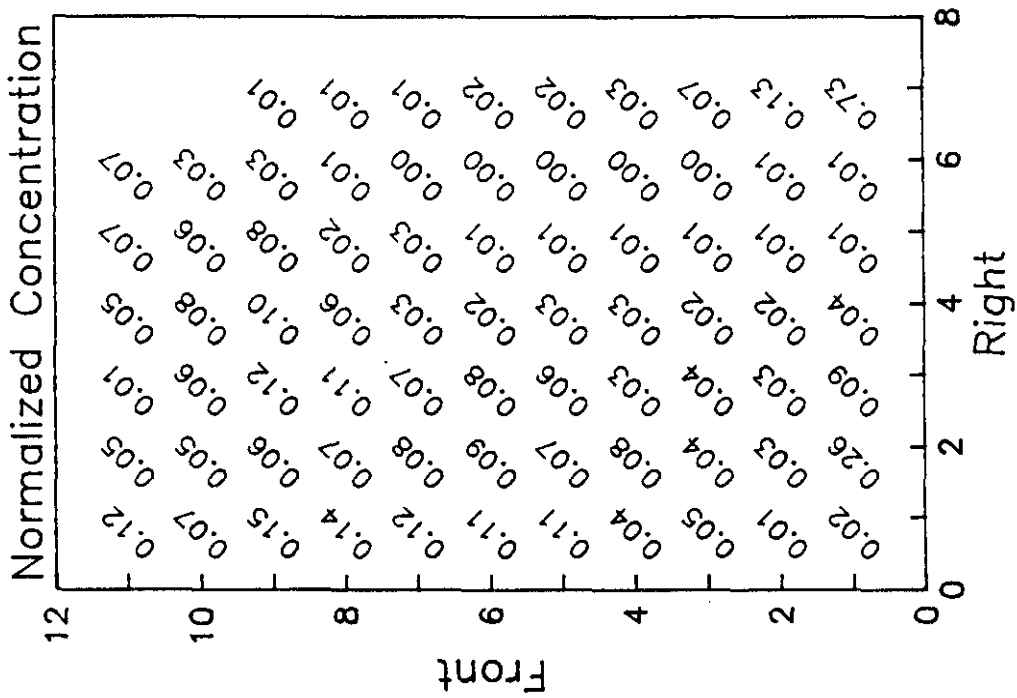


Figure 6-21

**SOUTHERN COMPANY SERVICES
 LANSING SMITH #2 FLOW MODEL**

NORMALIZED METHANE CONCENTRATION

Test Plane: 2

Test Date: 2/25/91

Firing System: LNCFS-III

Test ID: Configuration #1

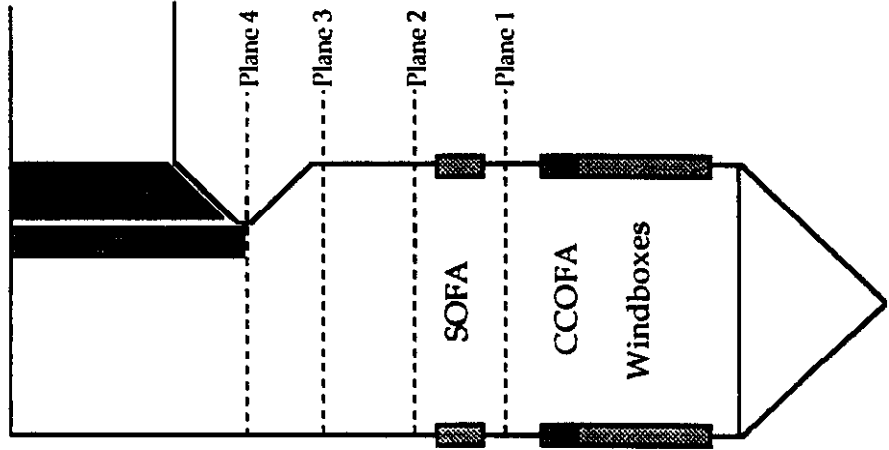
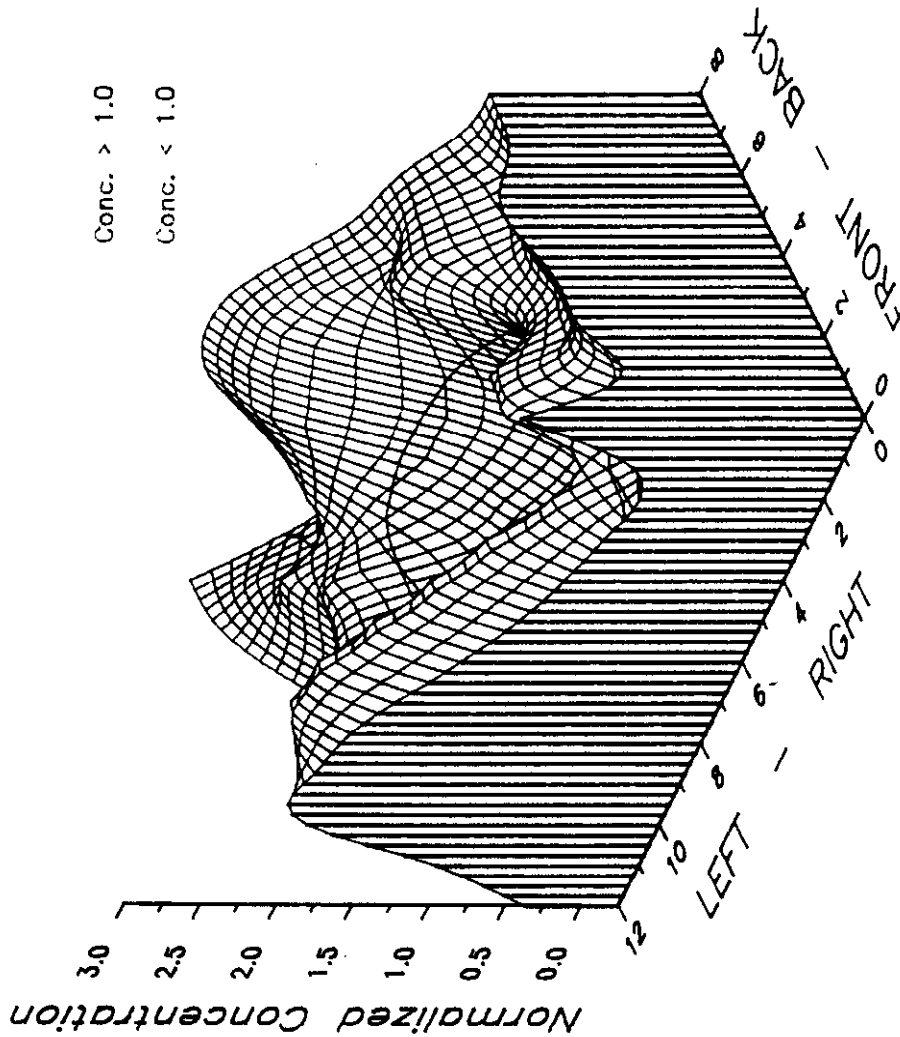


Figure 6-22

**SOUTHERN COMPANY SERVICES
LANSING SMITH #2 FLOW MODEL**

NORMALIZED METHANE CONCENTRATION

Test Plane: 2

Test Date: 2/25/91

Firing System: LNCFS-III

Test ID: Configuration #1

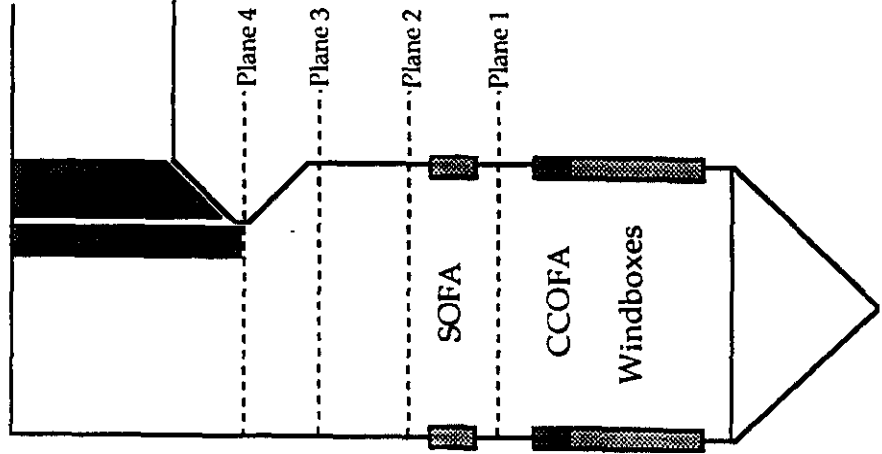
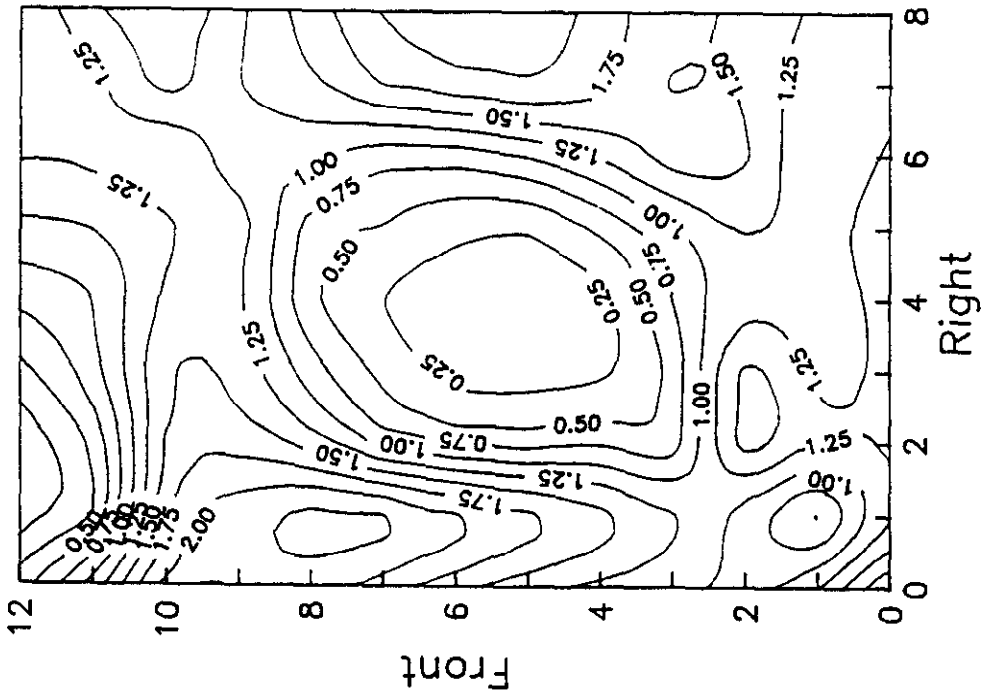


Figure 6-23

**SOUTHERN COMPANY SERVICES
LANSING SMITH #2 FLOW MODEL**

NORMALIZED METHANE CONCENTRATION

Test Plane: 2
 Test Date: 2/25/91
 Firing System: LNCFS-III
 Test ID: Configuration #1

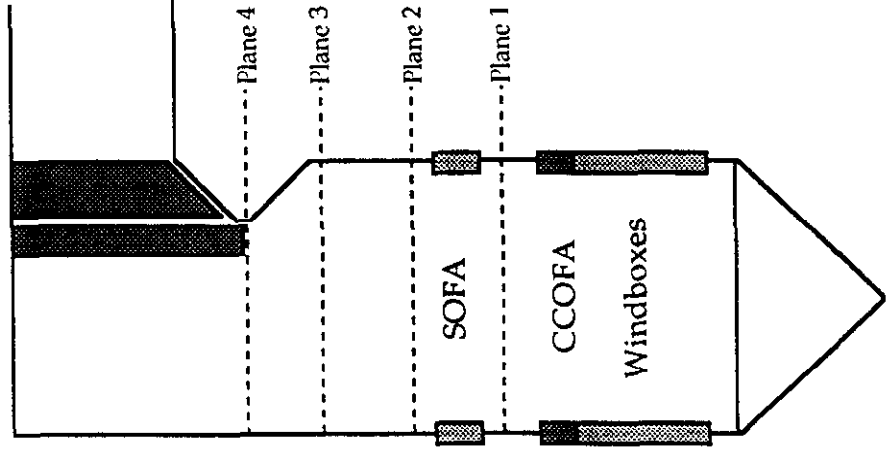
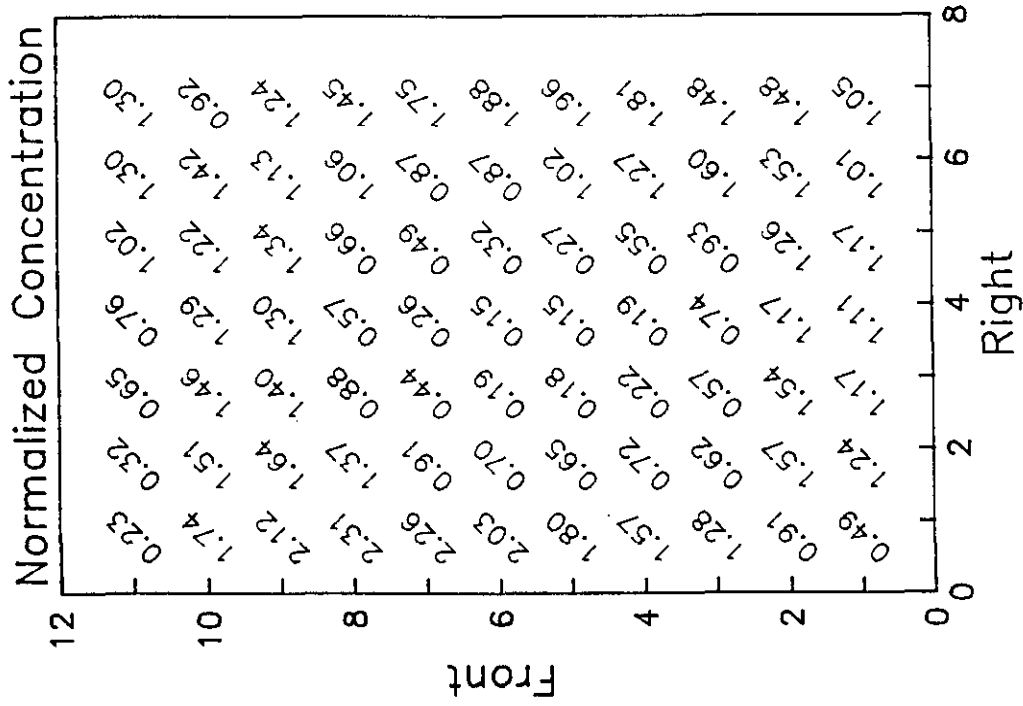


Figure 6-24

**SOUTHERN COMPANY SERVICES
 LANSING SMITH #2 FLOW MODEL**

NORMALIZED METHANE CONCENTRATION

Test Plane: 2

Test Date: 2/26/91

Firing System: LNCFS-III

Test ID: Configuration #2

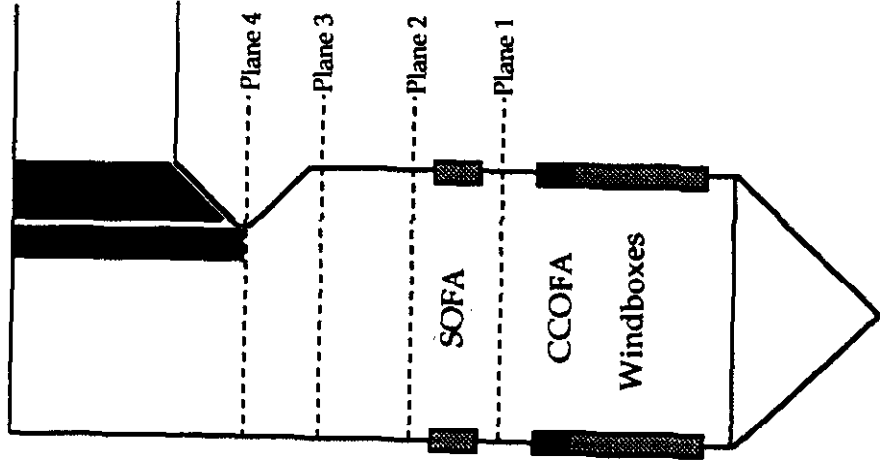
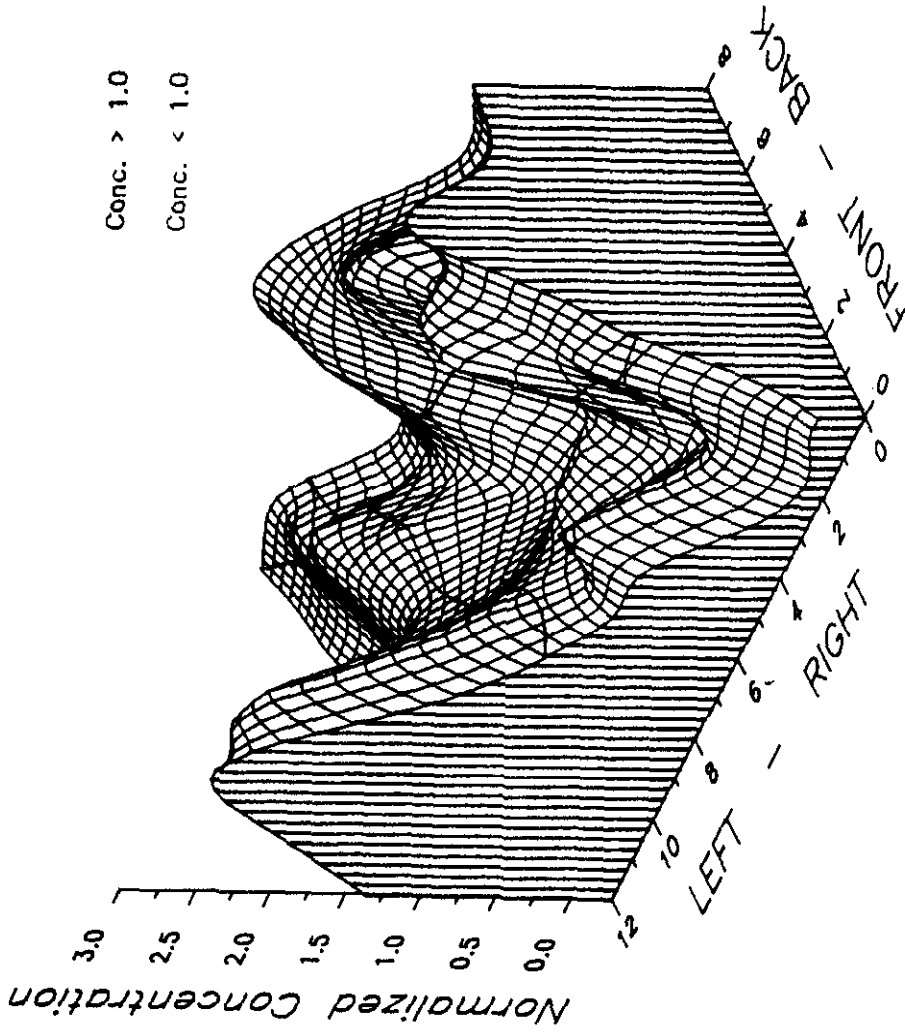


Figure 6-25
**SOUTHERN COMPANY SERVICES
LANSING SMITH #2 FLOW MODEL**

NORMALIZED METHANE CONCENTRATION

Test Plane: 2
 Test Date: 2/26/91
 Firing System: LNCFS-III
 Test ID: Configuration #2

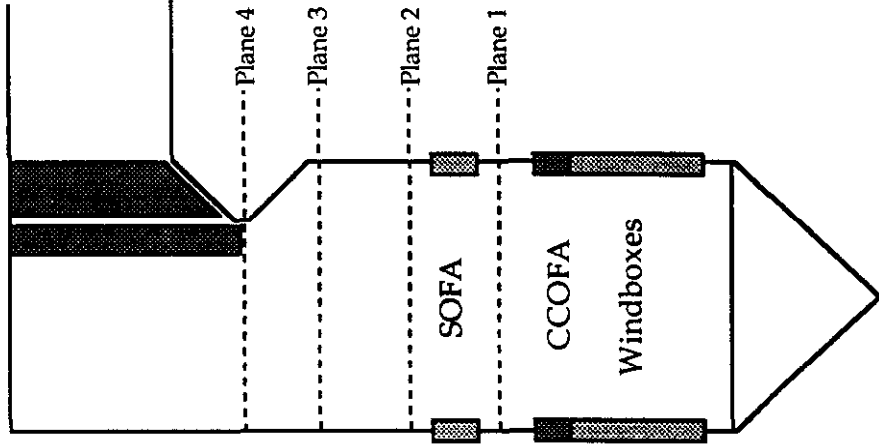
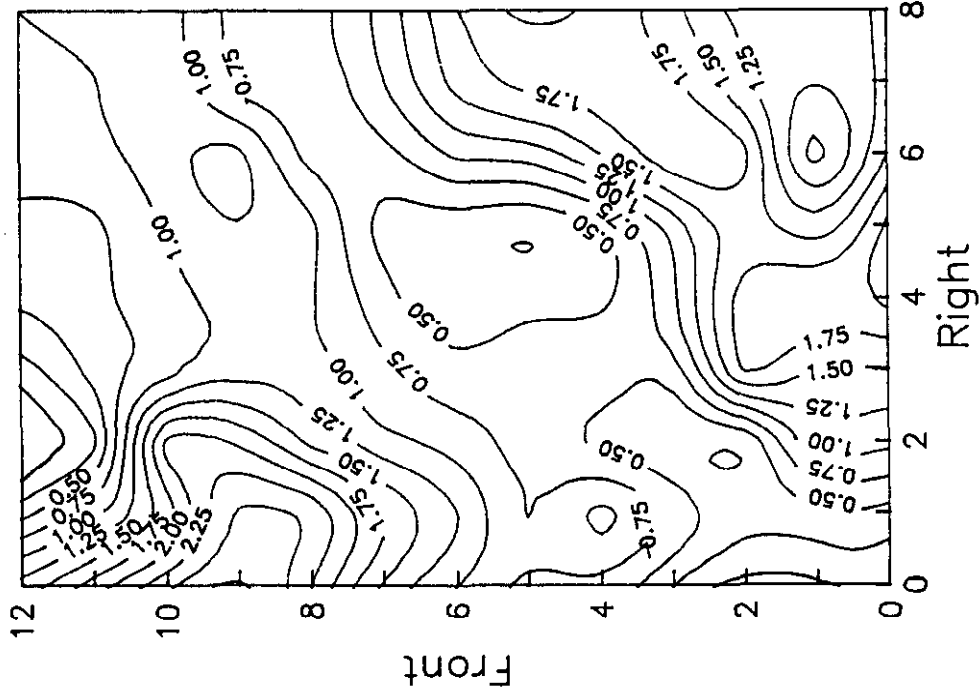


Figure 6-26

**SOUTHERN COMPANY SERVICES
 LANSING SMITH #2 FLOW MODEL**

NORMALIZED METHANE CONCENTRATION

Test Plane: 2
 Test Date: 2/26/91
 Firing System: LNCFS-III
 Test ID: Configuration #2

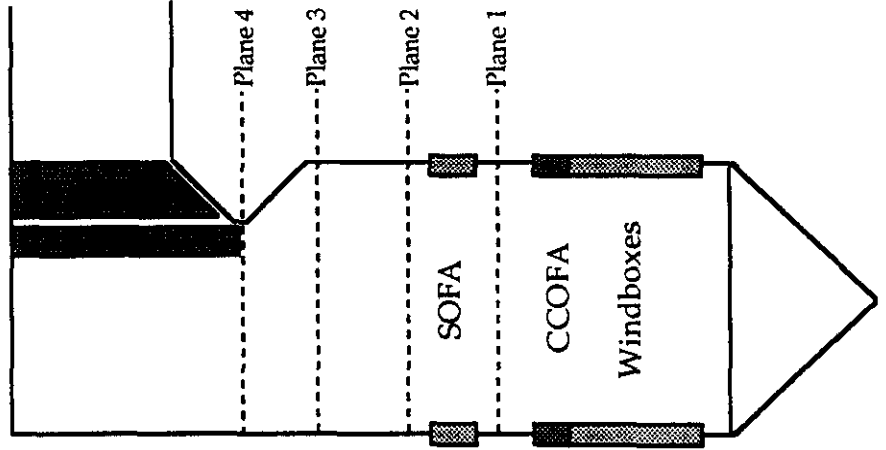
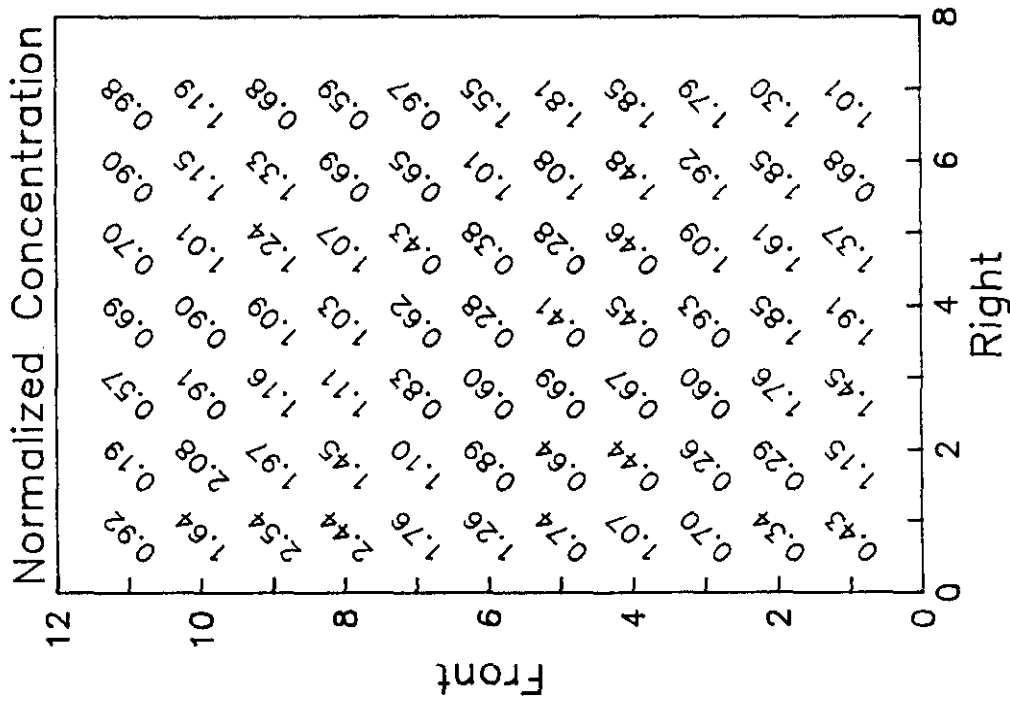


Figure 6-27

**SOUTHERN COMPANY SERVICES
 LANSING SMITH #2 FLOW MODEL**

NORMALIZED METHANE CONCENTRATION

Test Plane: 2

Test Date: 2/27/91

Firing System: LNCFS-III

Test ID: Configuration #3

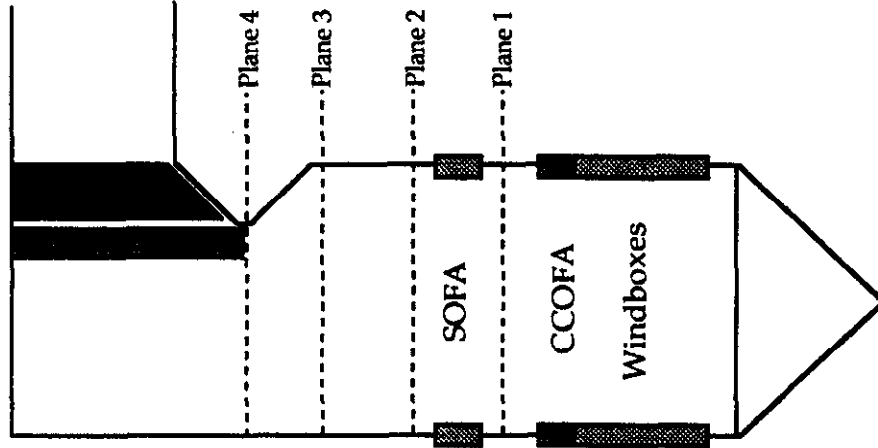
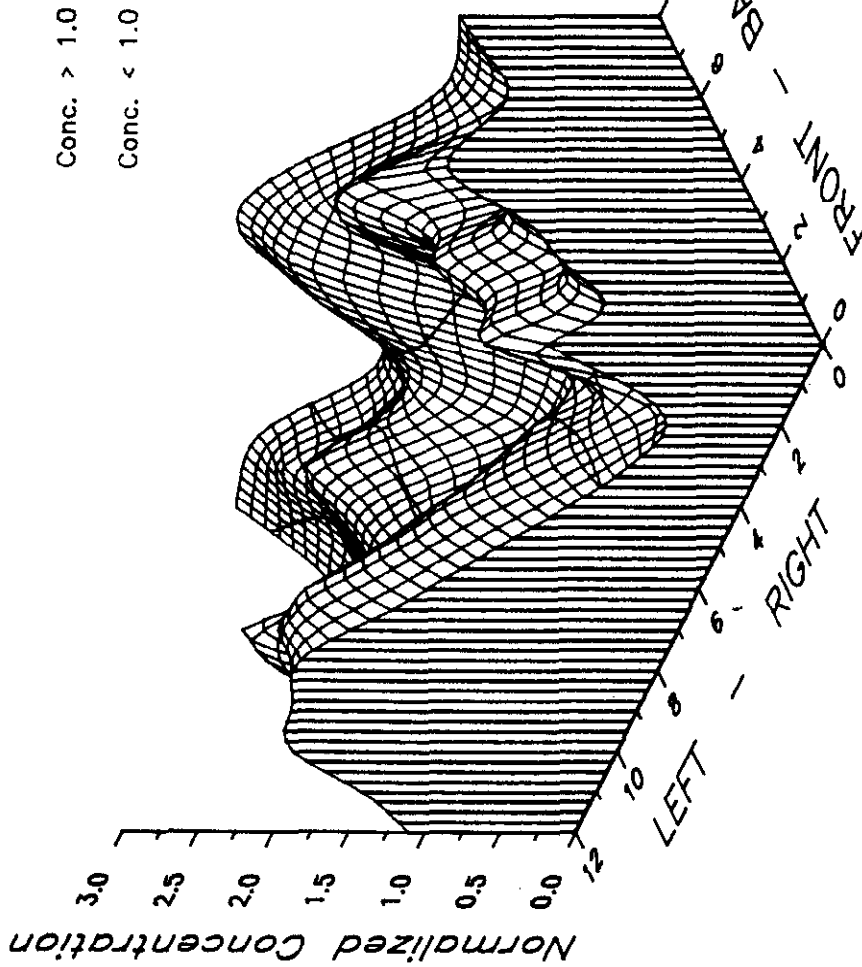


Figure 6-28

**SOUTHERN COMPANY SERVICES
LANSING SMITH #2 FLOW MODEL**

NORMALIZED METHANE CONCENTRATION

Test Plane: 2

Test Date: 2/27/91

Firing System: LNCFS-III

Test ID: Configuration #3

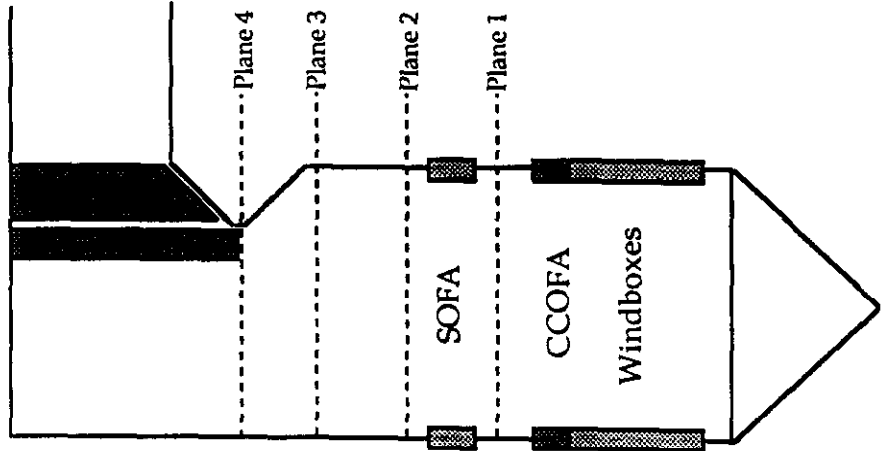
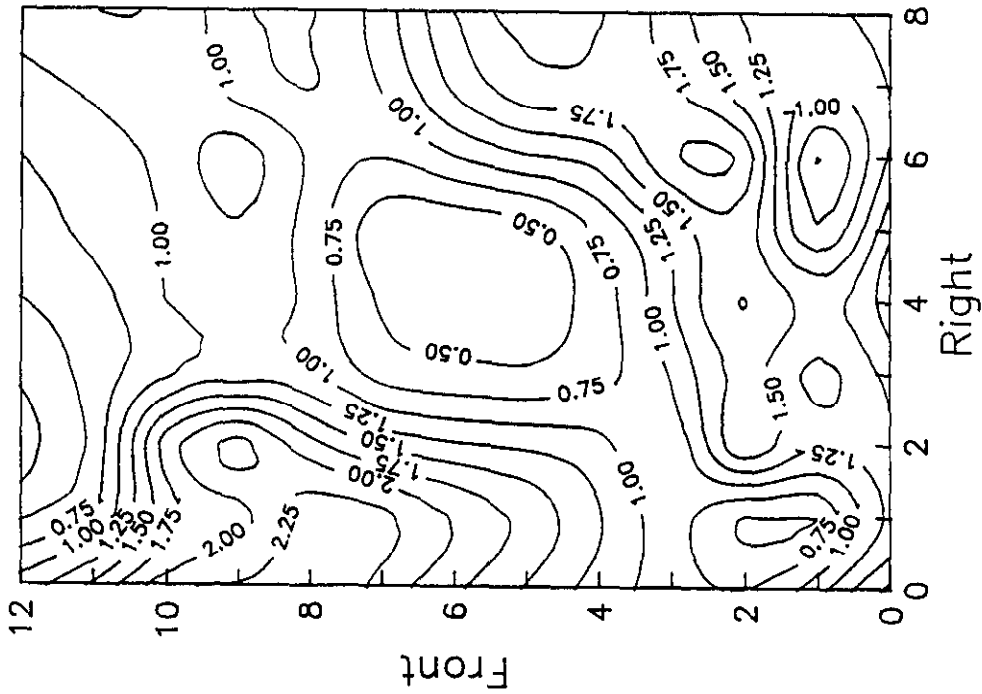
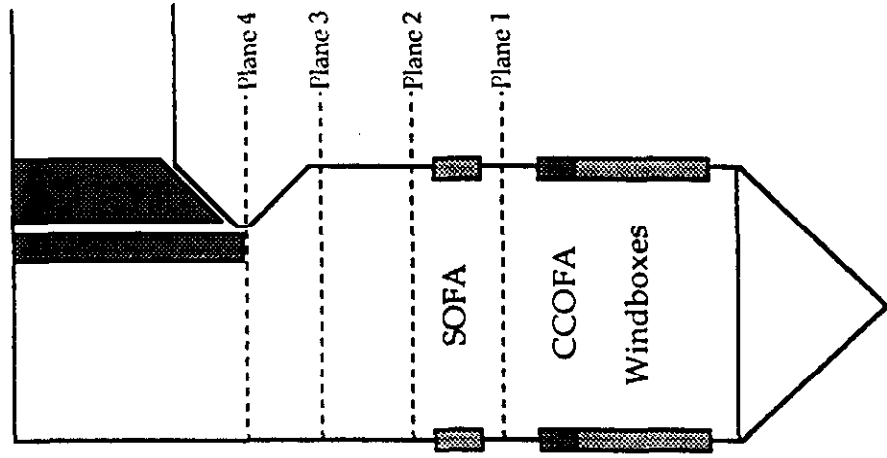
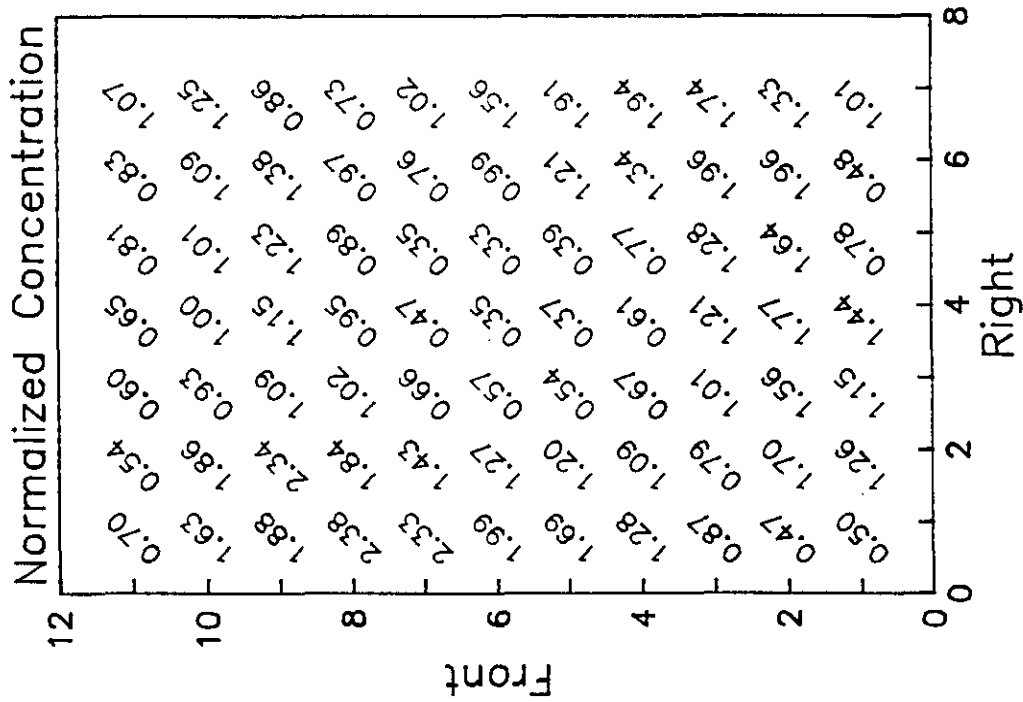


Figure 6-29

**SOUTHERN COMPANY SERVICES
LANSING SMITH #2 FLOW MODEL**

NORMALIZED METHANE CONCENTRATION

Test Plane: 2
 Test Date: 2/27/91
 Firing System: LNCFS-III
 Test ID: Configuration #3



SOUTHERN COMPANY SERVICES
LANSING SMITH #2 FLOW MODEL

Figure 6-30

NORMALIZED METHANE CONCENTRATION

Test Plane: 2

Test Date: 2/27/91

Firing System: LNCFS-III

Test ID: Configuration #4

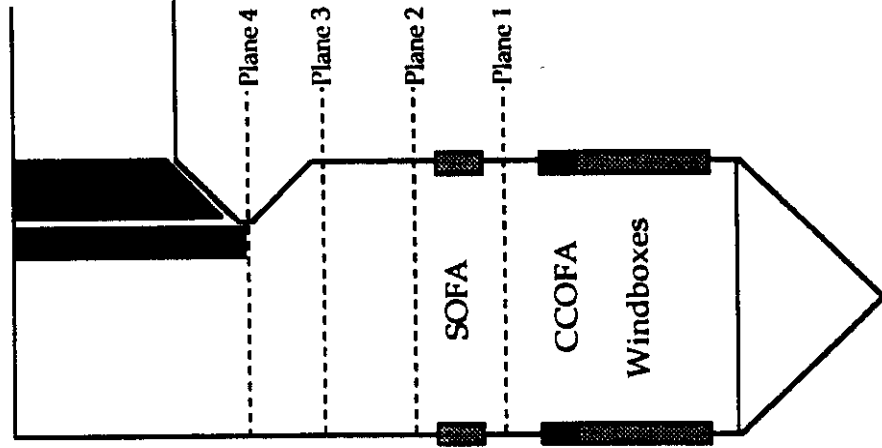
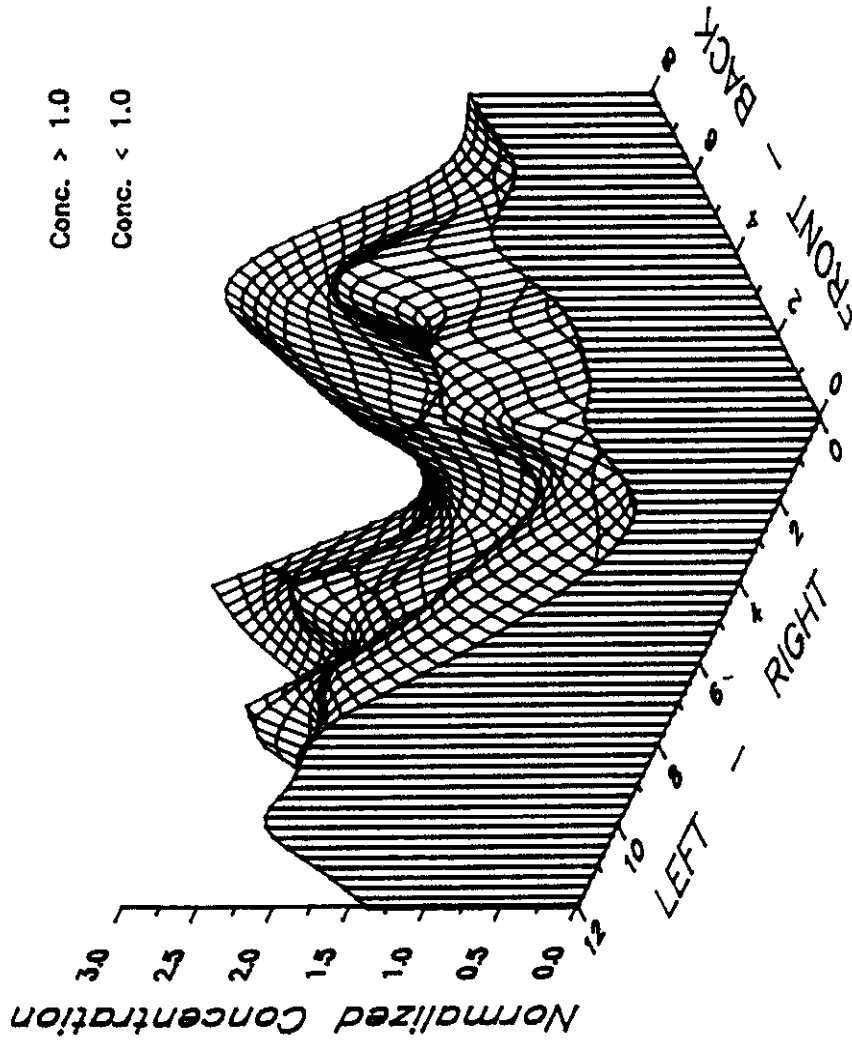


Figure 6-31

**SOUTHERN COMPANY SERVICES
LANSING SMITH #2 FLOW MODEL**

NORMALIZED METHANE CONCENTRATION

Test Plane: 2
Test Date: 2/27/91
Firing System: LNCFS-III
Test ID: Configuration #4

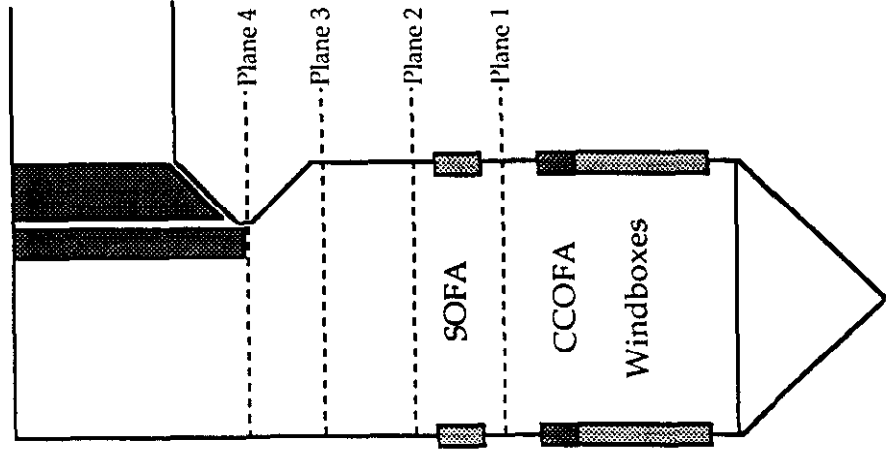
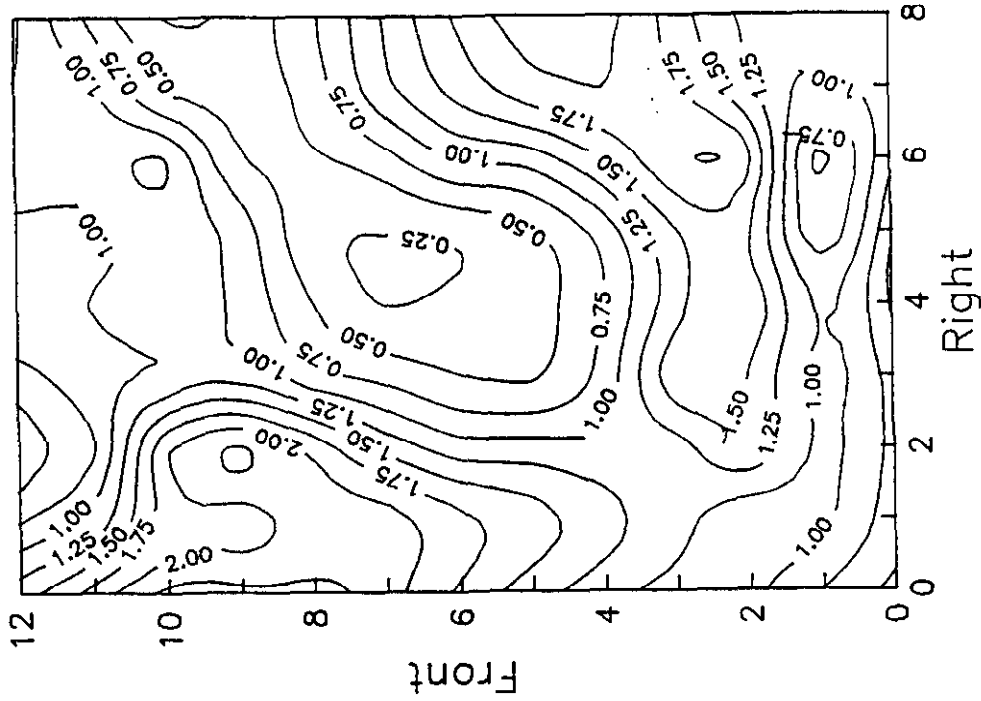


Figure 6--32
**SOUTHERN COMPANY SERVICES
LANSING SMITH #2 FLOW MODEL**

NORMALIZED METHANE CONCENTRATION

Test Plane: 2
 Test Date: 2/27/91
 Firing System: LNCFS-III
 Test ID: Configuration #4

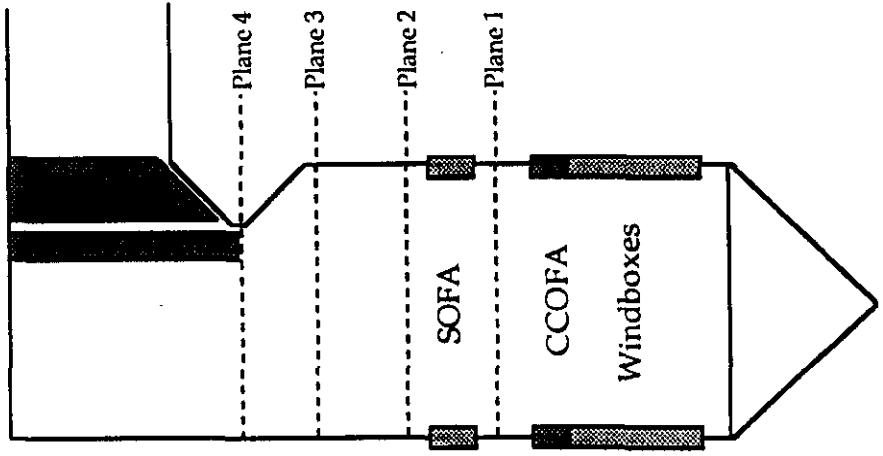
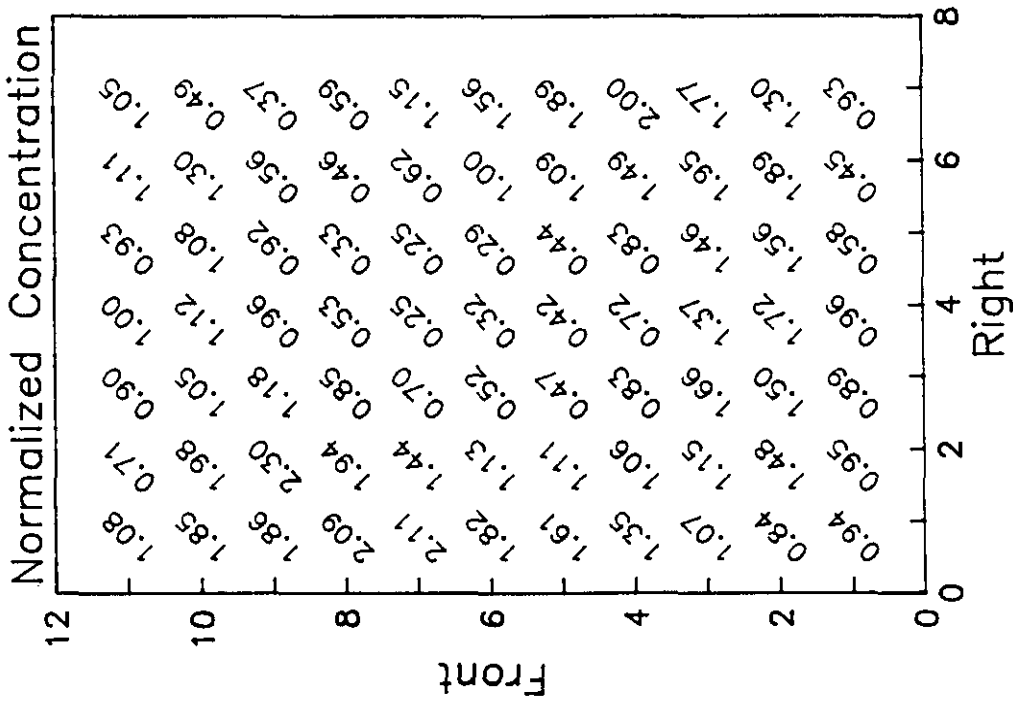


Figure 6-33

**SOUTHERN COMPANY SERVICES
 LANSING SMITH #2 FLOW MODEL**

NORMALIZED METHANE CONCENTRATION

Test Plane: 2

Test Date: 2/28/91

Firing System: LNCFS-III

Test ID: Configuration #5

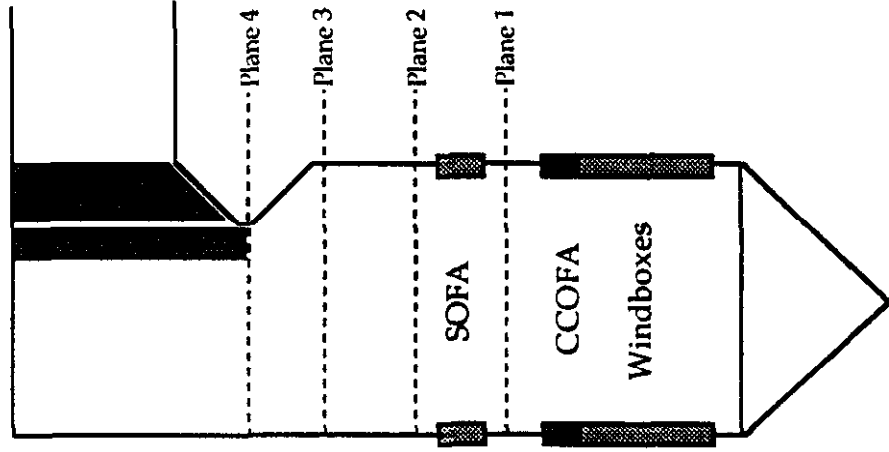
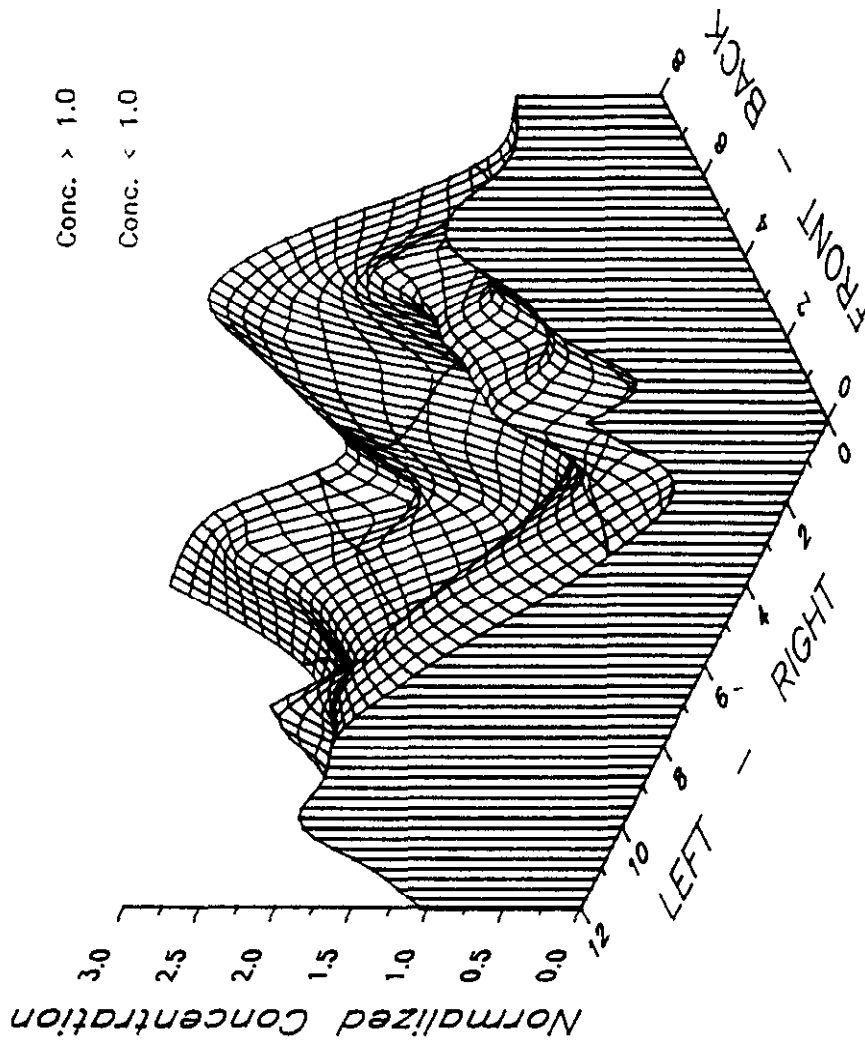


Figure 6-34

**SOUTHERN COMPANY SERVICES
LANSING SMITH #2 FLOW MODEL**

NORMALIZED METHANE CONCENTRATION

Test Plane: 2

Test Date: 2/28/91

Firing System: LNCFS-III

Test ID: Configuration #5

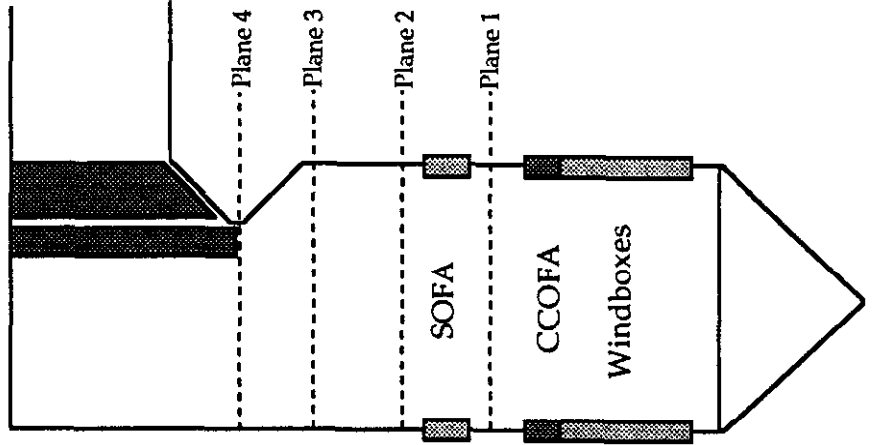
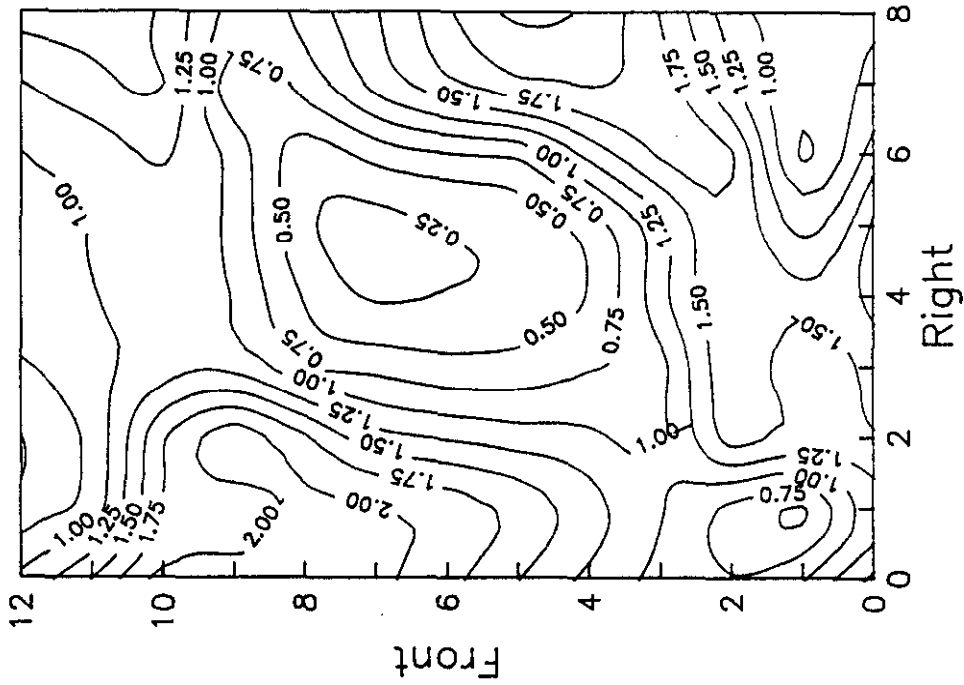


Figure 6-35

**SOUTHERN COMPANY SERVICES
LANSING SMITH #2 FLOW MODEL**

NORMALIZED METHANE CONCENTRATION

Test Plane: 2

Test Date: 2/28/91

Firing System: LNCFS-III

Test ID: Configuration #5

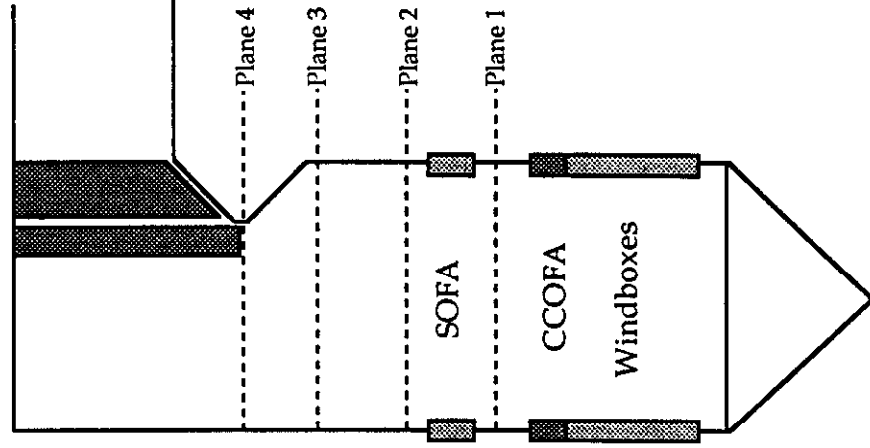
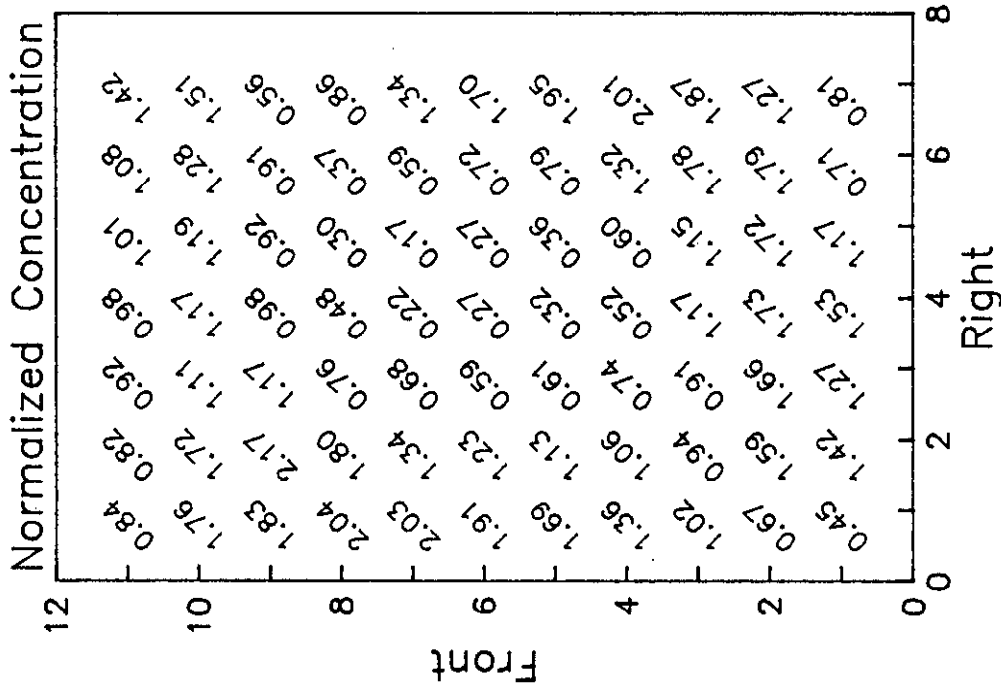
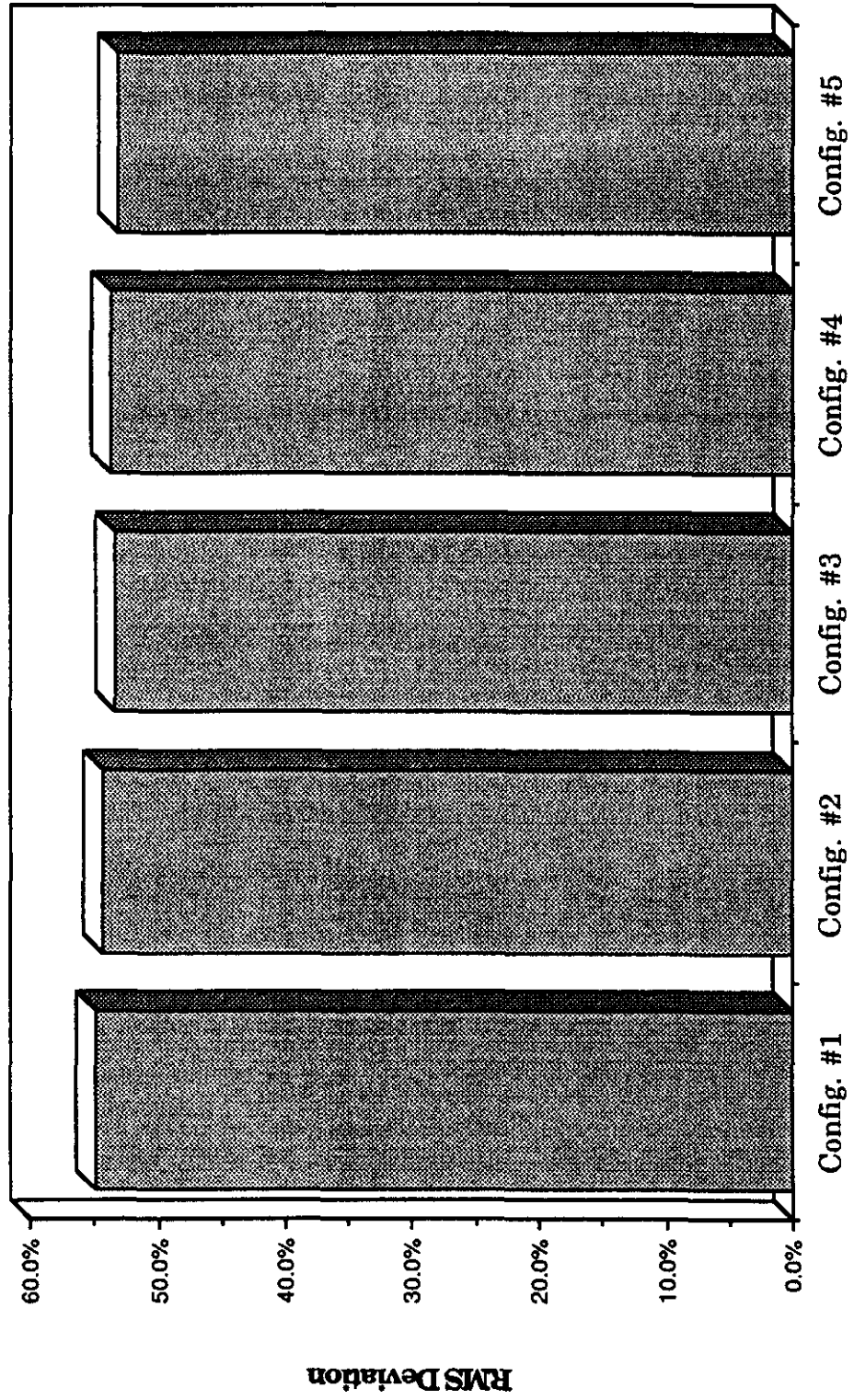


Figure 6-36

**SOUTHERN COMPANY SERVICES
LANSING SMITH #2 FLOW MODEL**

**Lansing Smith #2 Flow Model
Methane RMS Deviation - Plane 2**



Test Identification

Figure 6-37

NORMALIZED METHANE CONCENTRATION

Test Plane: 3

Test Date: 2/25/91

Firing System: LNCFS-III

Test ID: Configuration #1

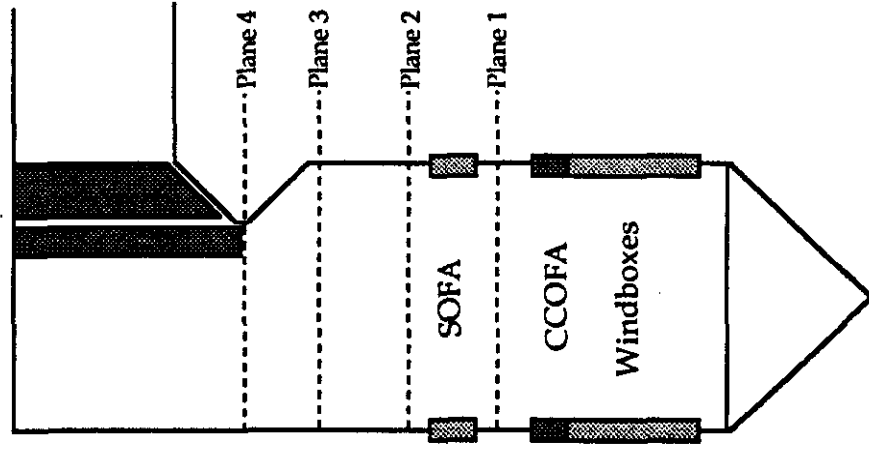
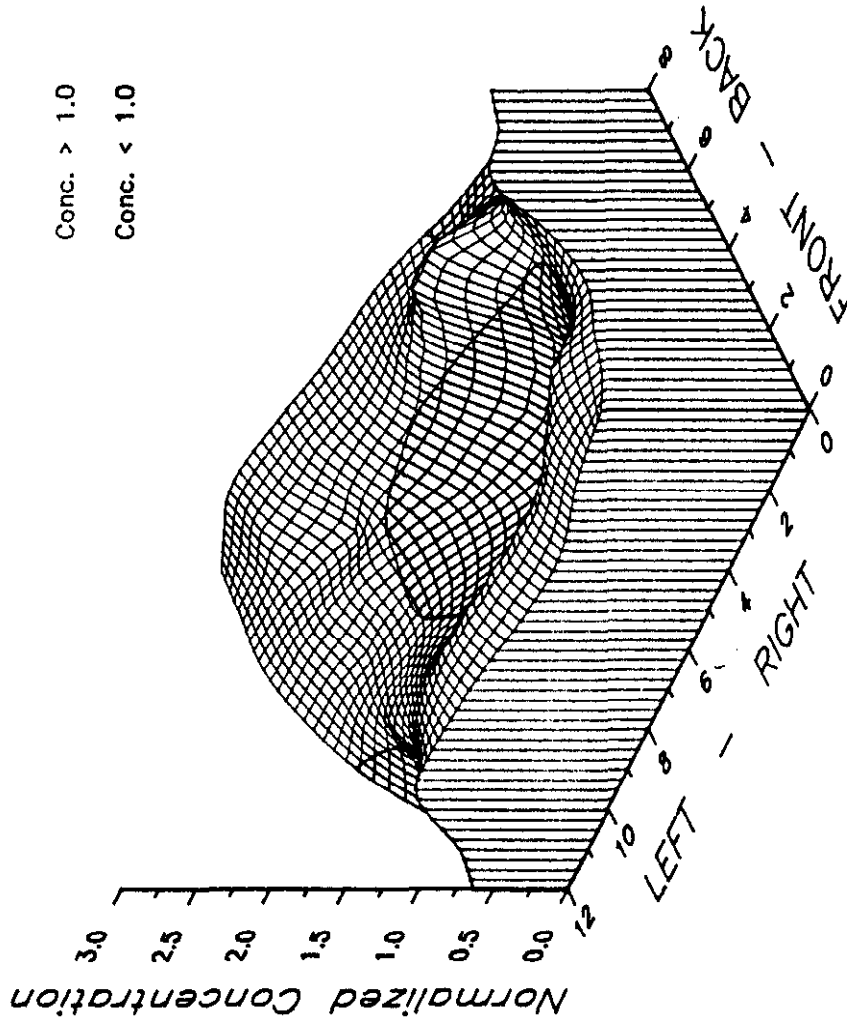


Figure 6-38
**SOUTHERN COMPANY SERVICES
LANSING SMITH #2 FLOW MODEL**

NORMALIZED METHANE CONCENTRATION

Test Plane: 3

Test Date: 2/25/91

Firing System: LNCFS-III

Test ID: Configuration #1

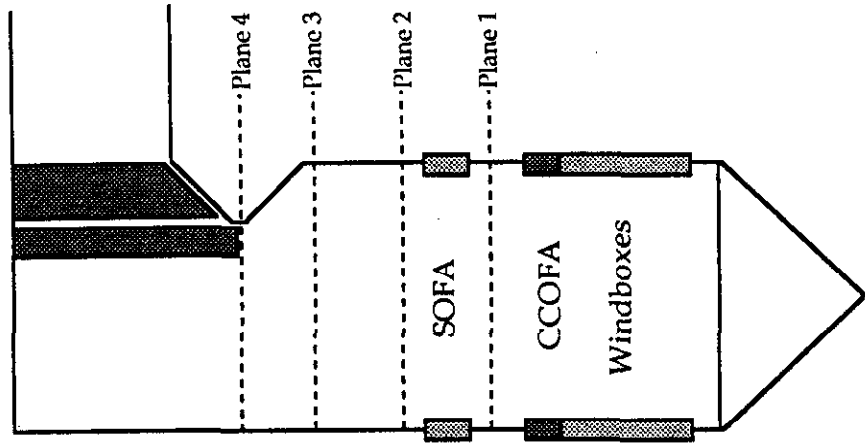
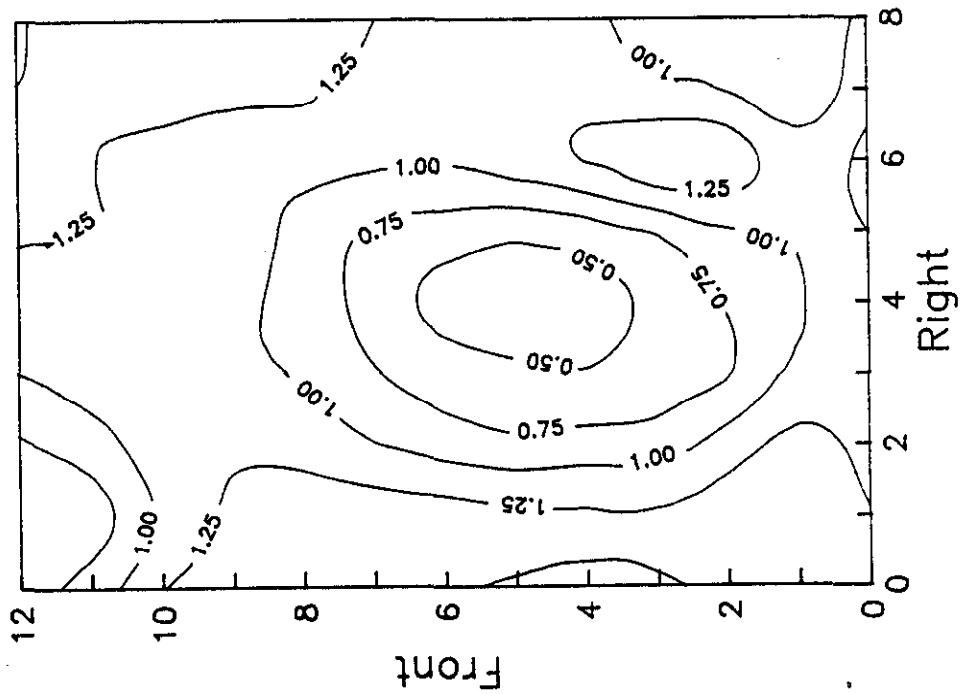


Figure 6-39

**SOUTHERN COMPANY SERVICES
LANSING SMITH #2 FLOW MODEL**

ABB Combustion Engineering, Inc.
Kreisinger Development Laboratory
Mechanical Systems Engineering

NORMALIZED METHANE CONCENTRATION

Test Plane: 3
 Test Date: 2/25/91
 Firing System: LNCFS-III
 Test ID: Configuration #1

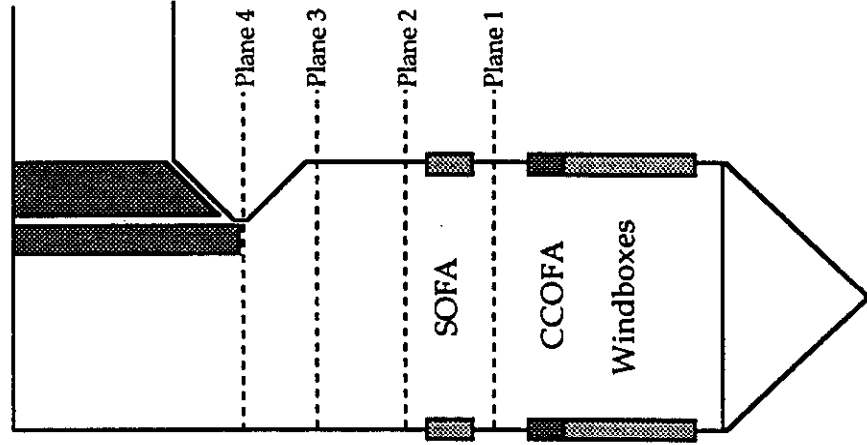
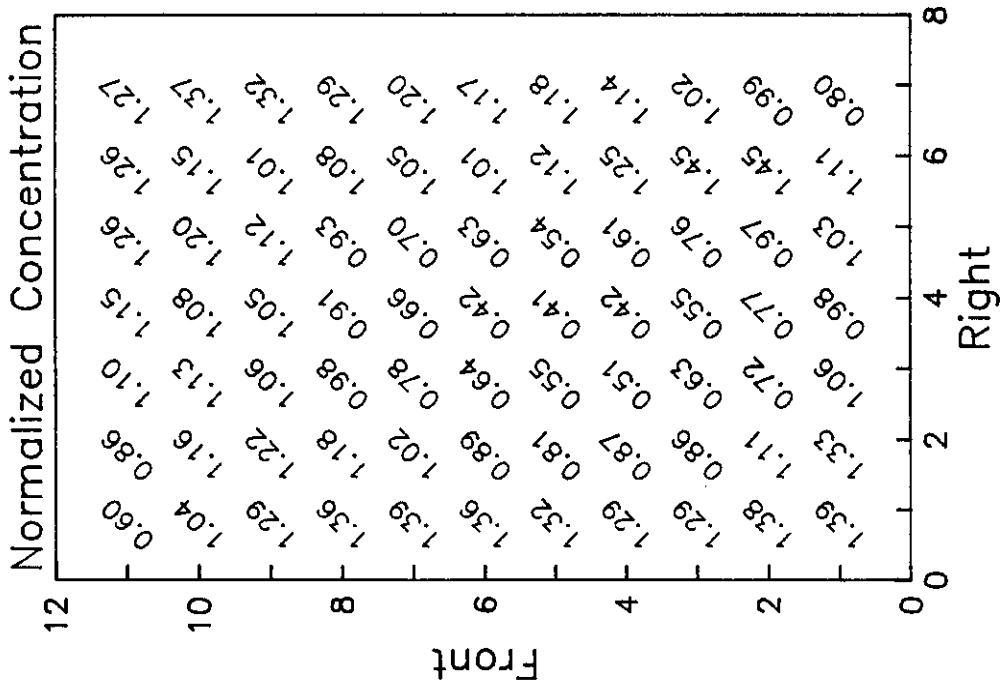


Figure 6-40

**SOUTHERN COMPANY SERVICES
 LANSING SMITH #2 FLOW MODEL**

NORMALIZED METHANE CONCENTRATION

Test Plane: 3

Test Date: 2/26/91

Firing System: LNCFS-III

Test ID: Configuration #2

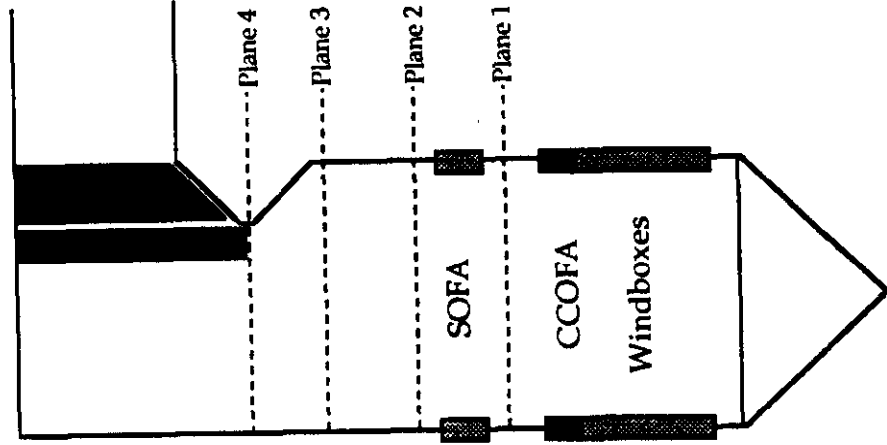
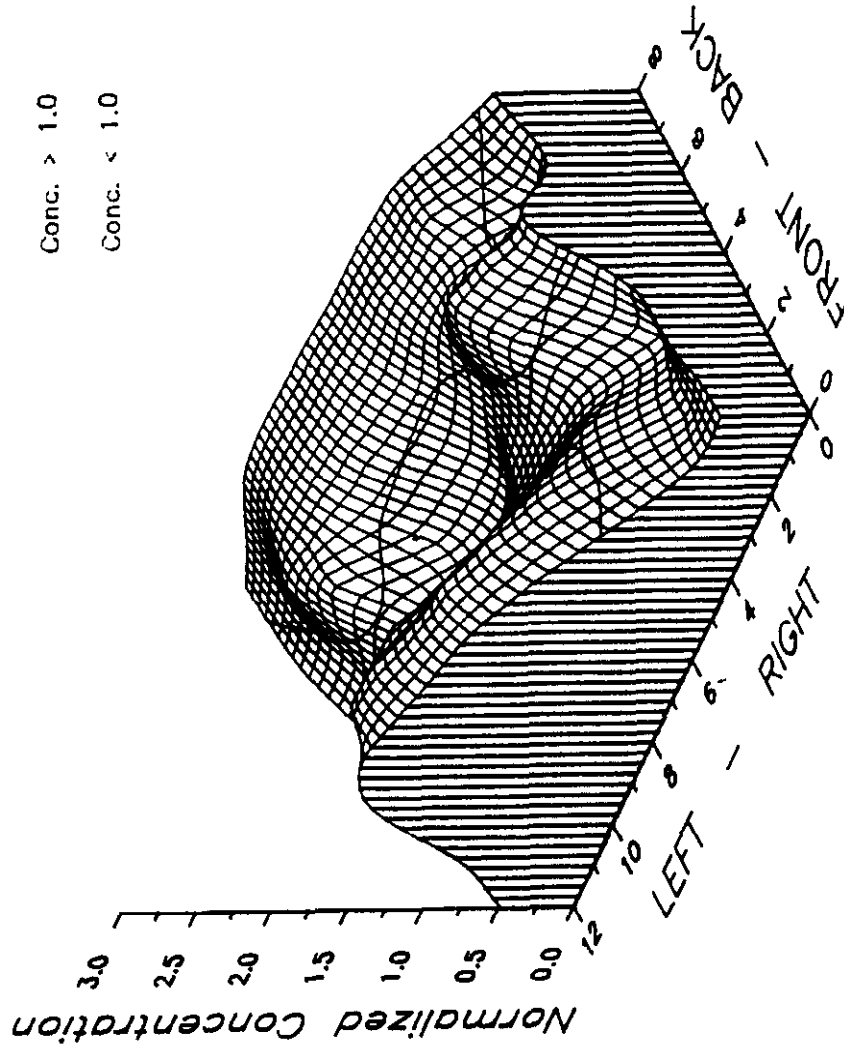


Figure 6-41

**SOUTHERN COMPANY SERVICES
LANSING SMITH #2 FLOW MODEL**

NORMALIZED METHANE CONCENTRATION

Test Plane: 3
Test Date: 2/26/91
Firing System: LNCFS-III
Test ID: Configuration #2

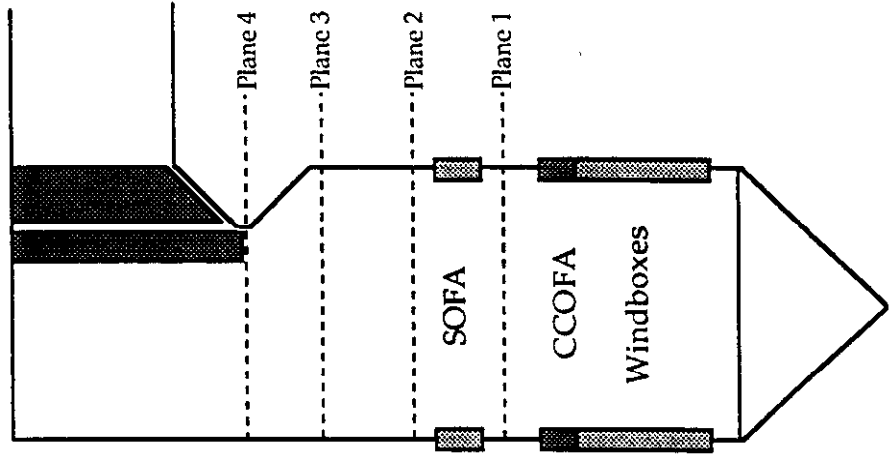
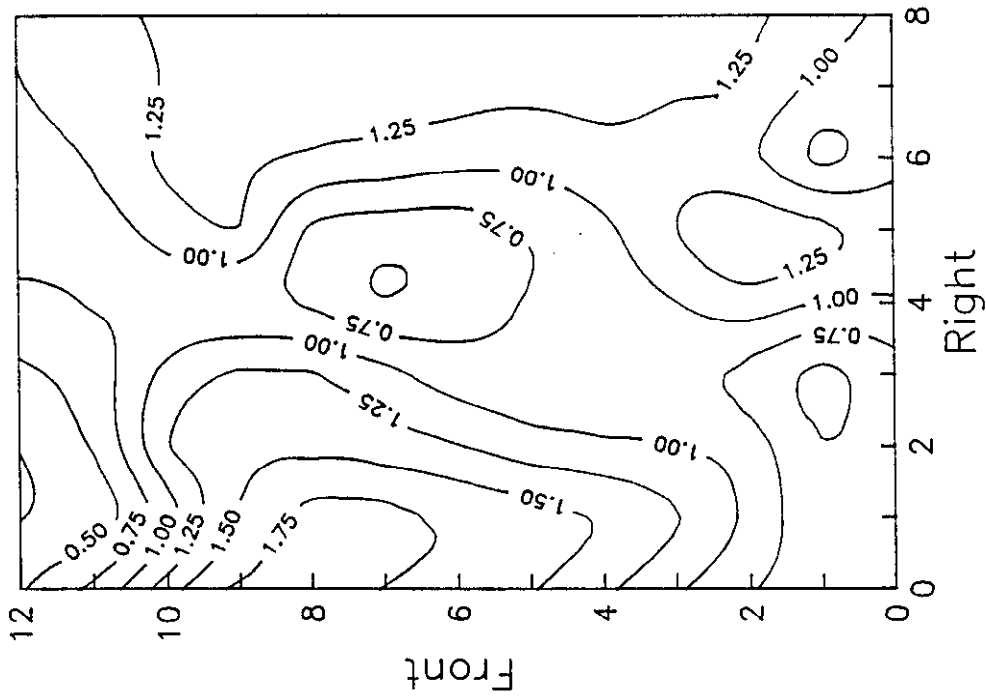


Figure 6-42
SOUTHERN COMPANY SERVICES
LANSING SMITH #2 FLOW MODEL

NORMALIZED METHANE CONCENTRATION

Test Plane: 3

Test Date: 2/26/91

Firing System: LNCFS-III

Test ID: Configuration #2

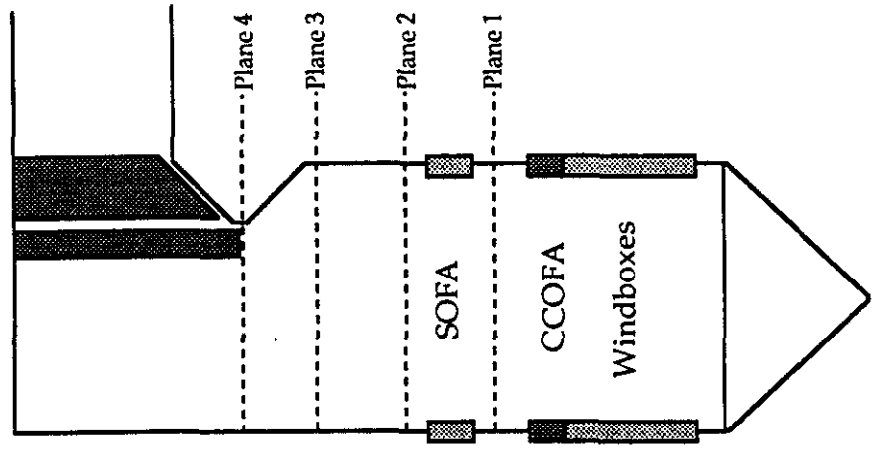
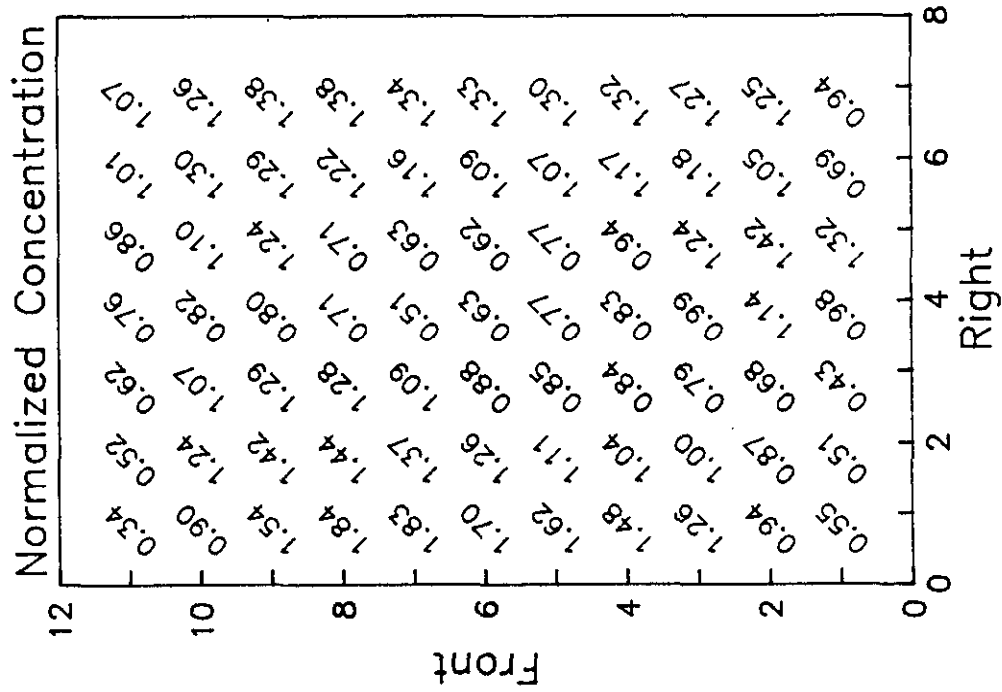


Figure 6-43

**SOUTHERN COMPANY SERVICES
LANSING SMITH #2 FLOW MODEL**

NORMALIZED METHANE CONCENTRATION

Test Plane: 3

Test Date: 2/26/91

Firing System: LNCFS-III

Test ID: Configuration #3

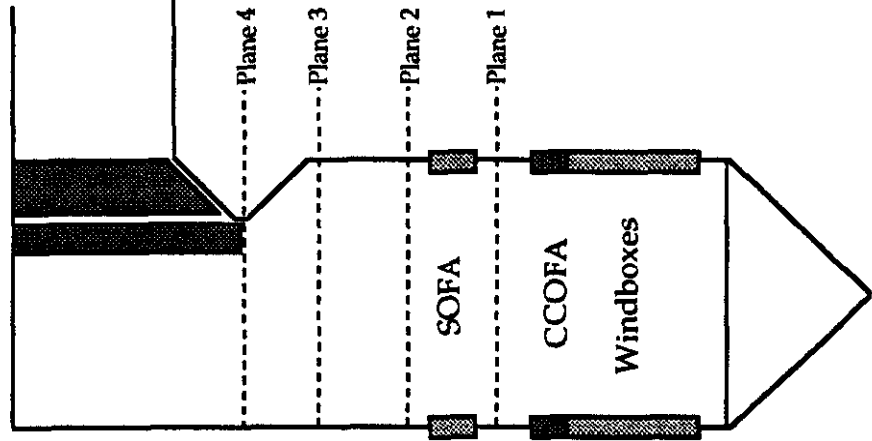
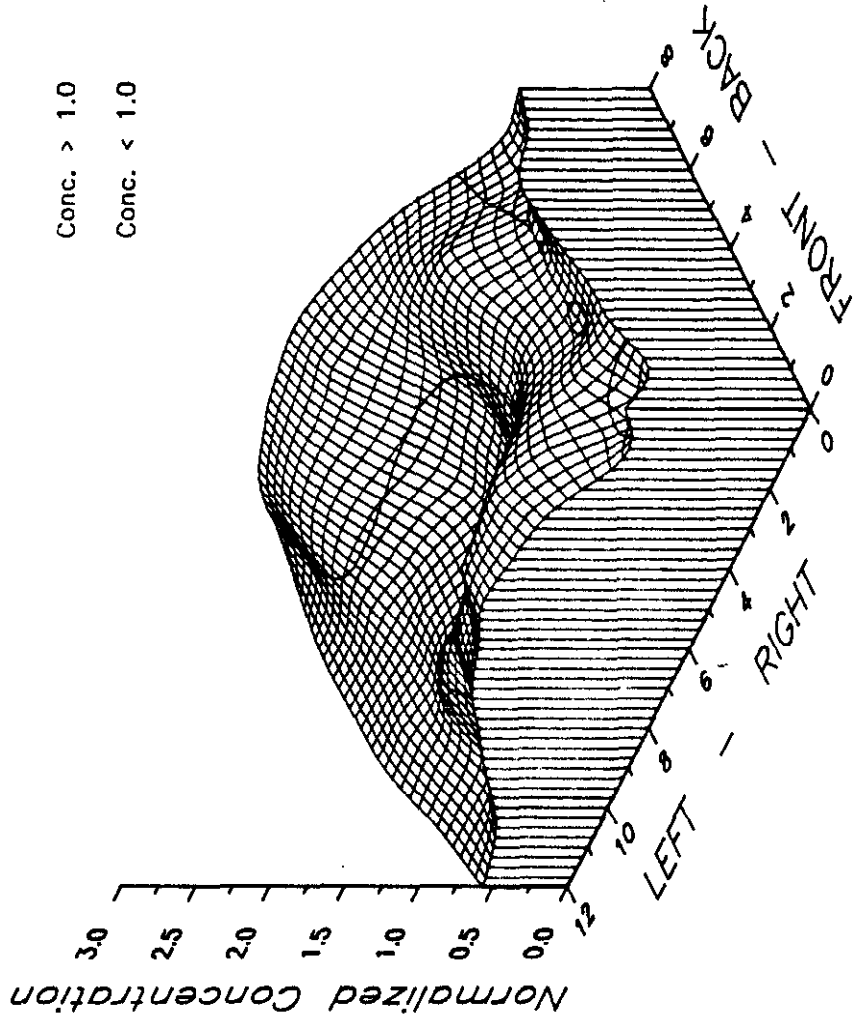


Figure 6-44

**SOUTHERN COMPANY SERVICES
LANSING SMITH #2 FLOW MODEL**

ABB Combustion Engineering, Inc.
Kreisinger Development Laboratory
Mechanical Systems Engineering

NORMALIZED METHANE CONCENTRATION

Test Plane: 3

Test Date: 2/26/91

Firing System: LNCFS-III

Test ID: Configuration #3

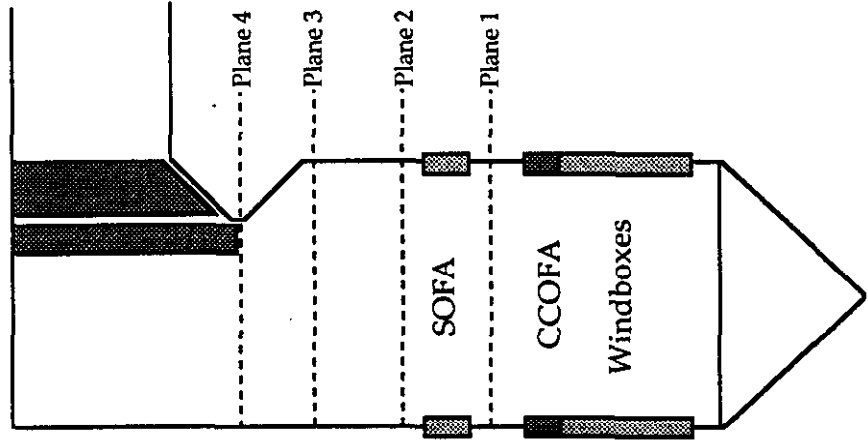
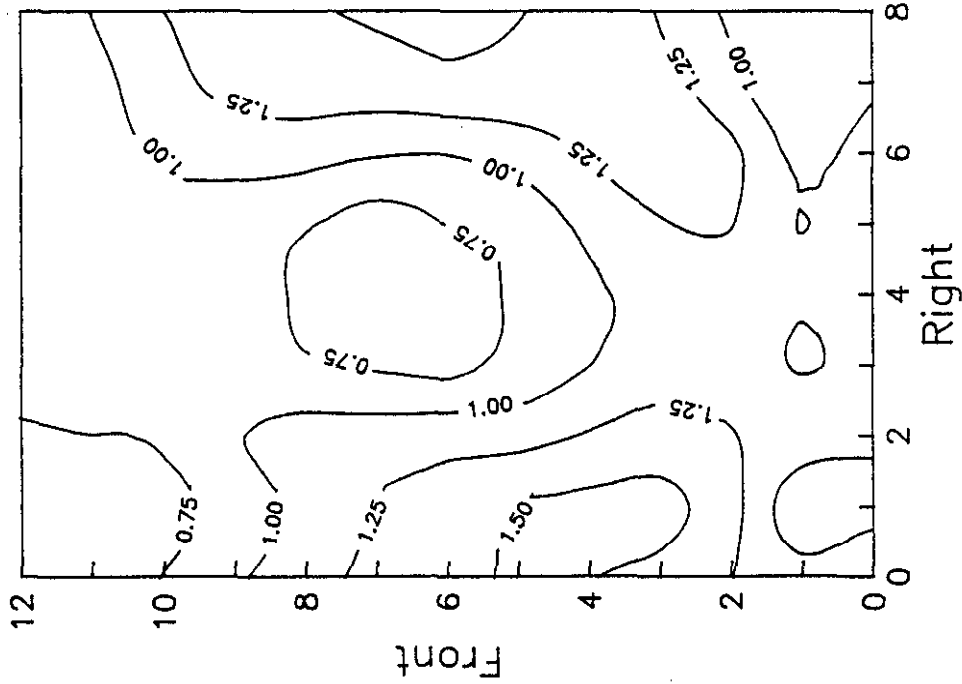


Figure 6-45
SOUTHERN COMPANY SERVICES
LANSING SMITH #2 FLOW MODEL

NORMALIZED METHANE CONCENTRATION

Test Plane: 3

Test Date: 2/26/91

Firing System: LNCFS-III

Test ID: Configuration #3

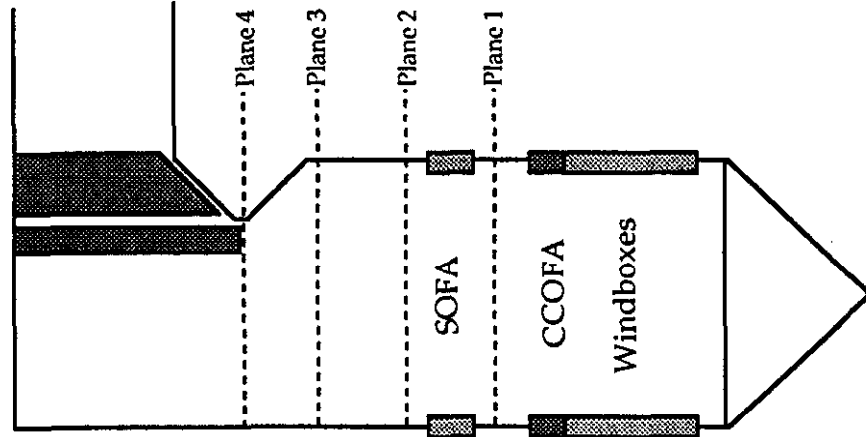
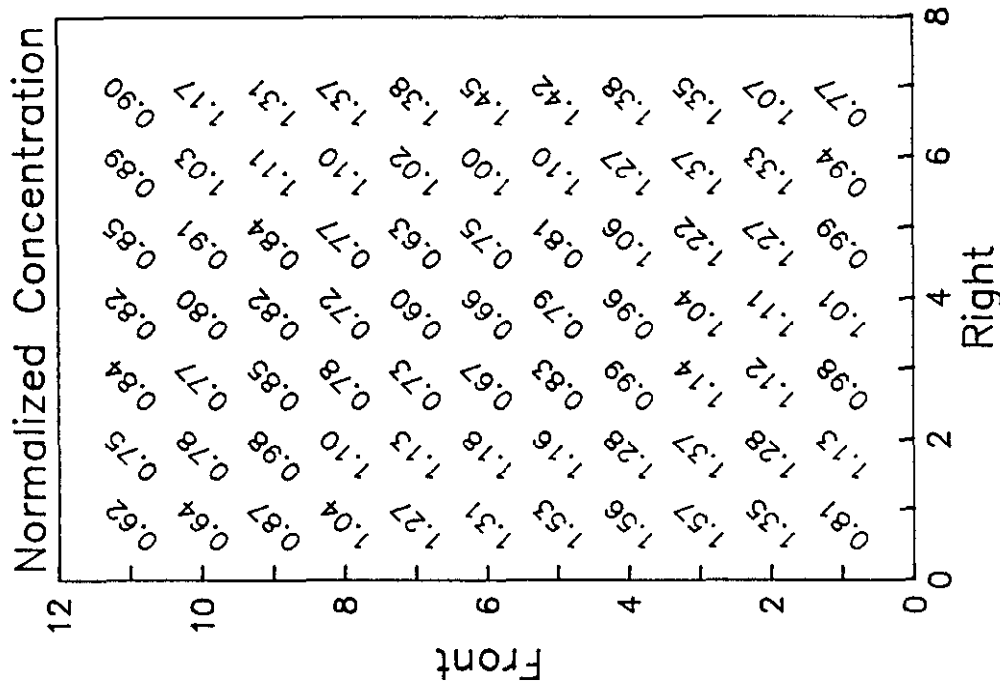


Figure 6-46

**SOUTHERN COMPANY SERVICES
LANSING SMITH #2 FLOW MODEL**

NORMALIZED METHANE CONCENTRATION

Test Plane: 3

Test Date: 2/27/91

Firing System: LNCFS-III

Test ID: Configuration #4

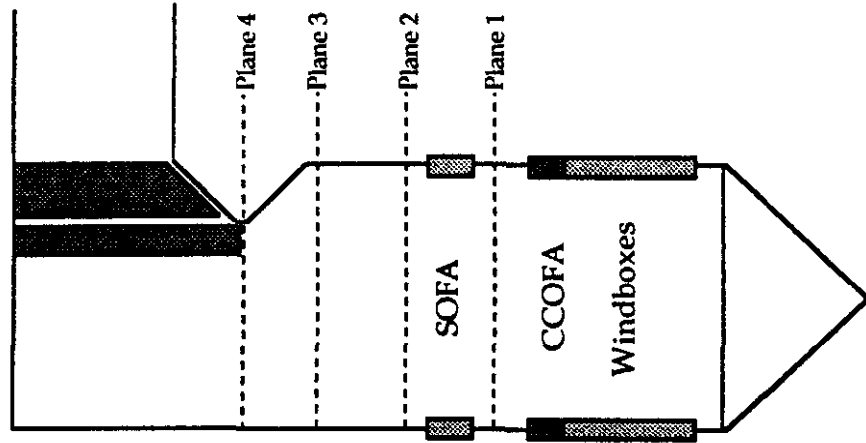
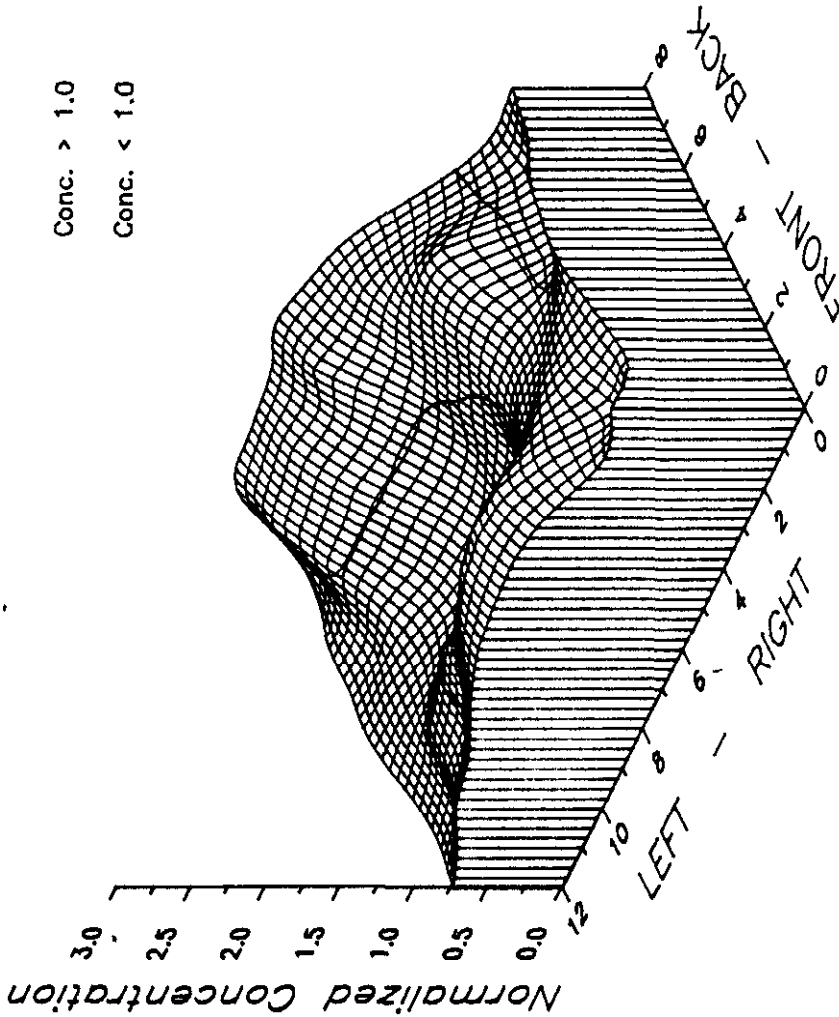


Figure 6-47

**SOUTHERN COMPANY SERVICES
LANSING SMITH #2 FLOW MODEL**

NORMALIZED METHANE CONCENTRATION

Test Plane: 3

Test Date: 2/27/91

Firing System: LNCFS-III

Test ID: Configuration #4

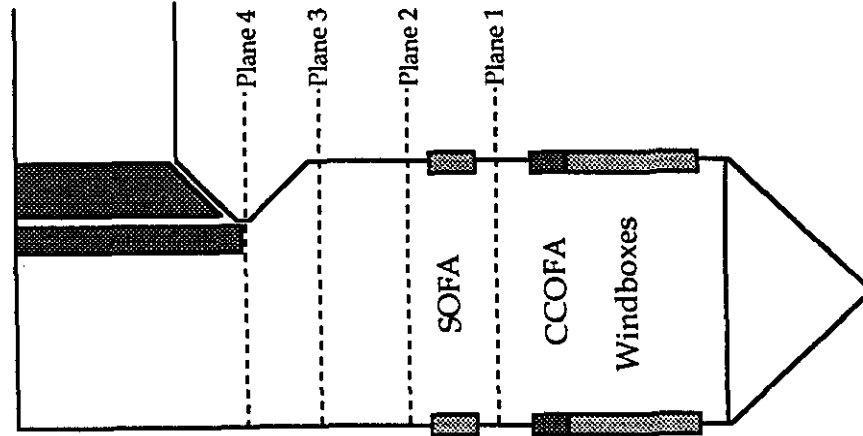
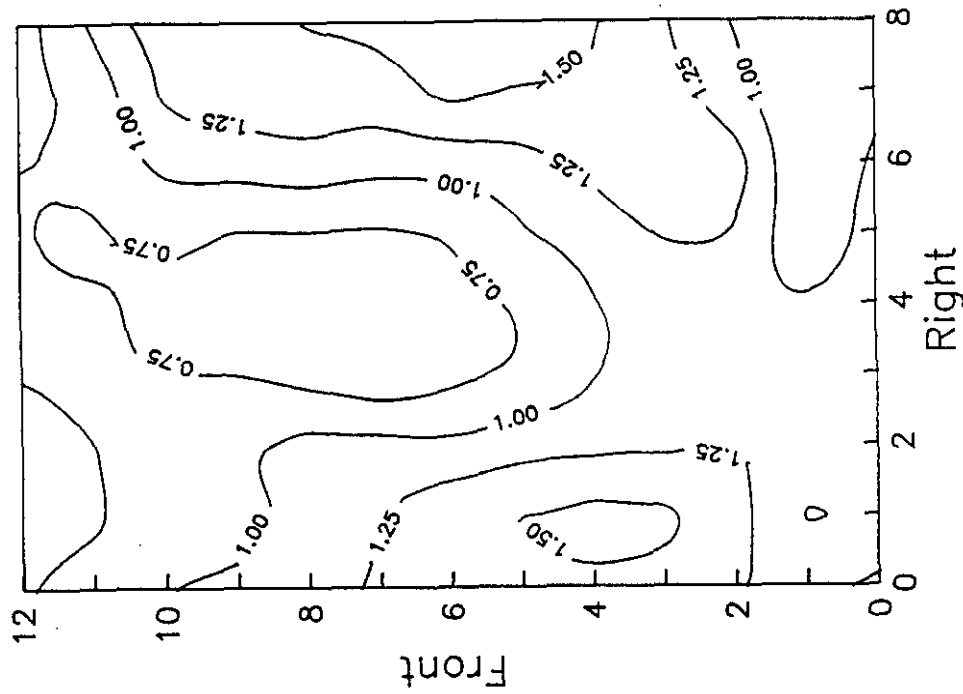


Figure 6-48

**SOUTHERN COMPANY SERVICES
LANSING SMITH #2 FLOW MODEL**

ABB Combustion Engineering, Inc.
Kreisinger Development Laboratory
Mechanical Systems Engineering

NORMALIZED METHANE CONCENTRATION

Test Plane: 3
 Test Date: 2/27/91
 Firing System: LNCFS-III
 Test ID: Configuration #4

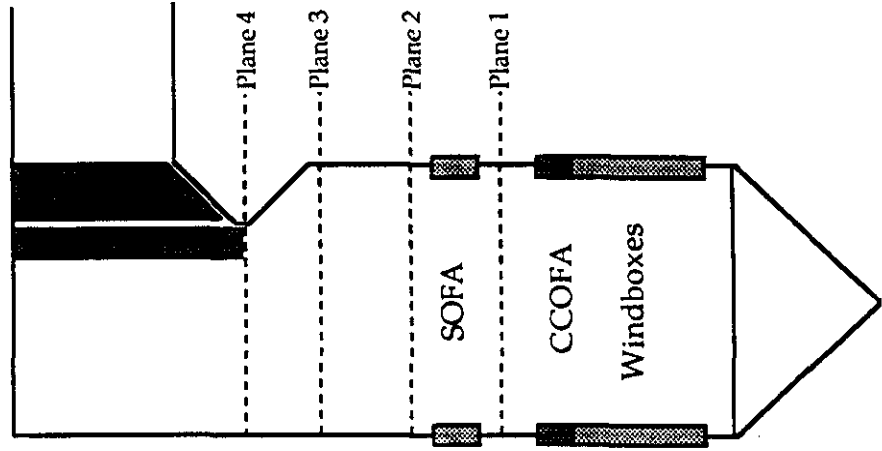
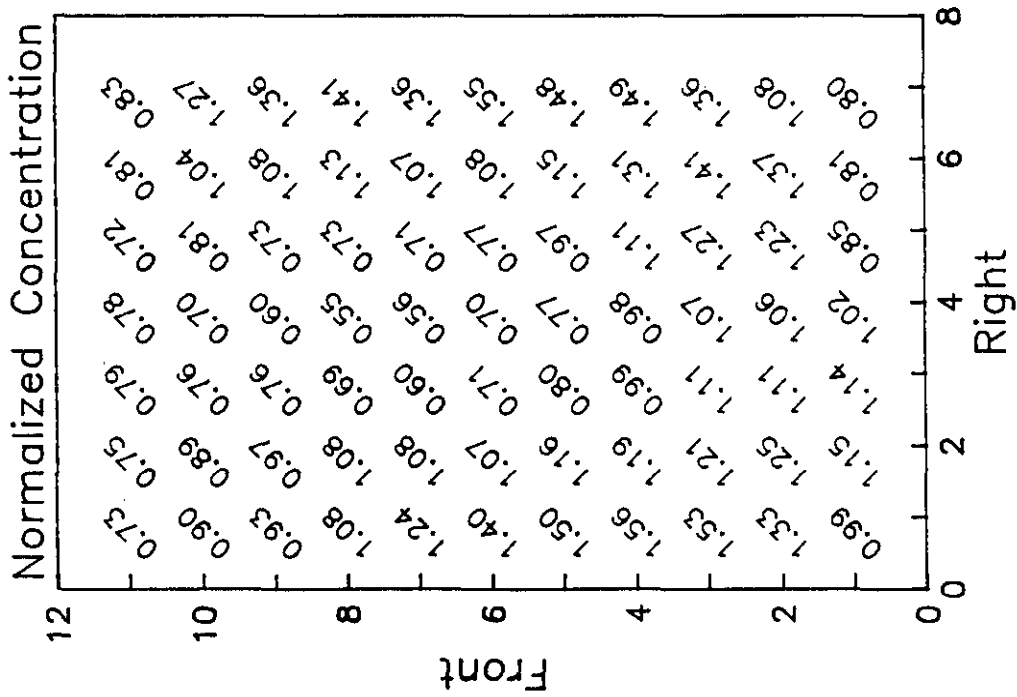


Figure 6-49
SOUTHERN COMPANY SERVICES
LANSING SMITH #2 FLOW MODEL

NORMALIZED METHANE CONCENTRATION

Test Plane: 3

Test Date: 2/28/91

Firing System: LNCFS-III

Test ID: Configuration #5

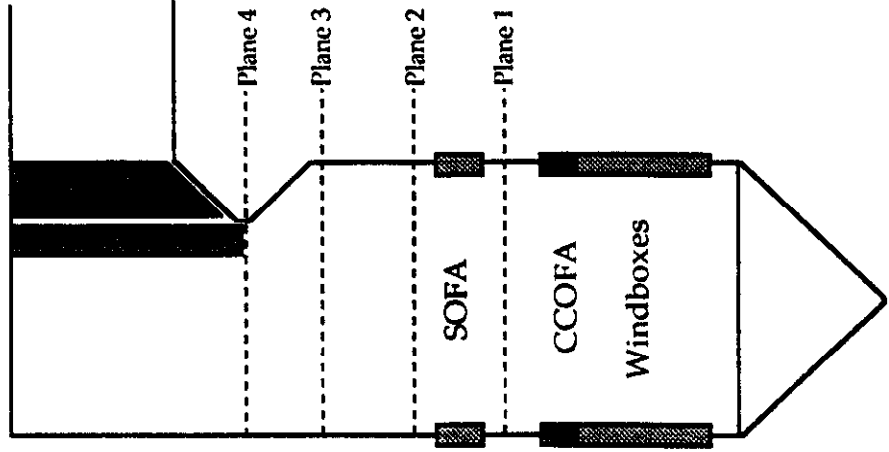
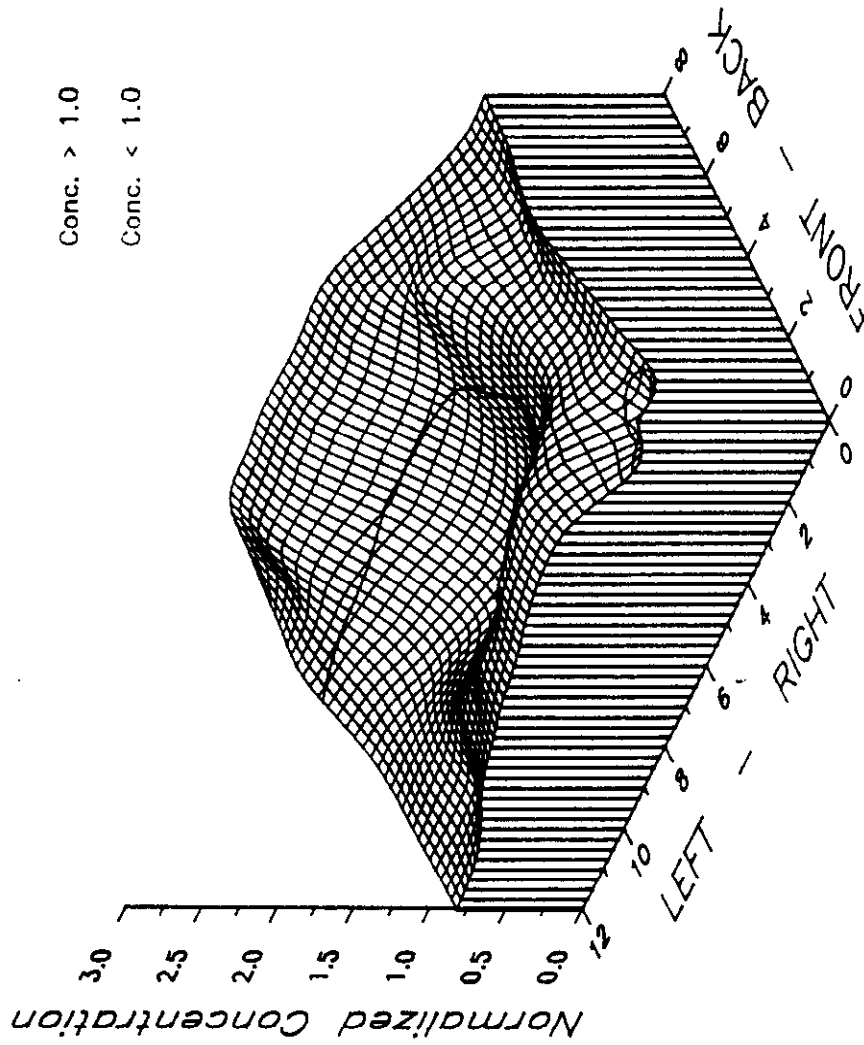


Figure 6-50

**SOUTHERN COMPANY SERVICES
LANSING SMITH #2 FLOW MODEL**

NORMALIZED METHANE CONCENTRATION

Test Plane: 3

Test Date: 2/28/91

Firing System: LNCFS-III

Test ID: Configuration #5

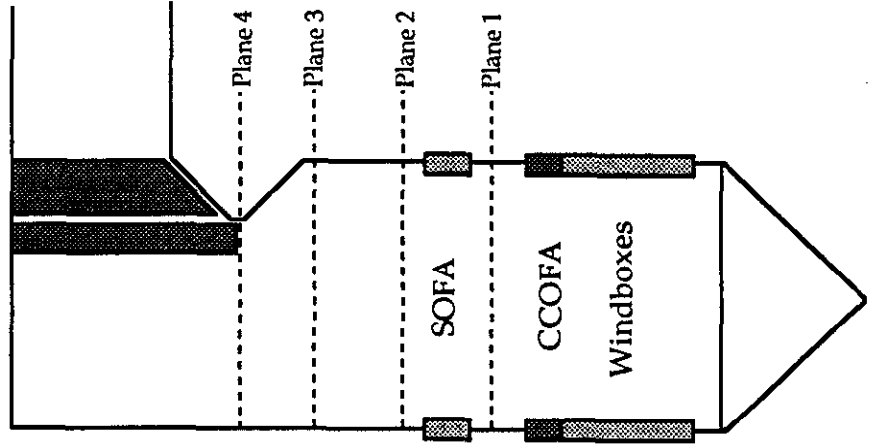
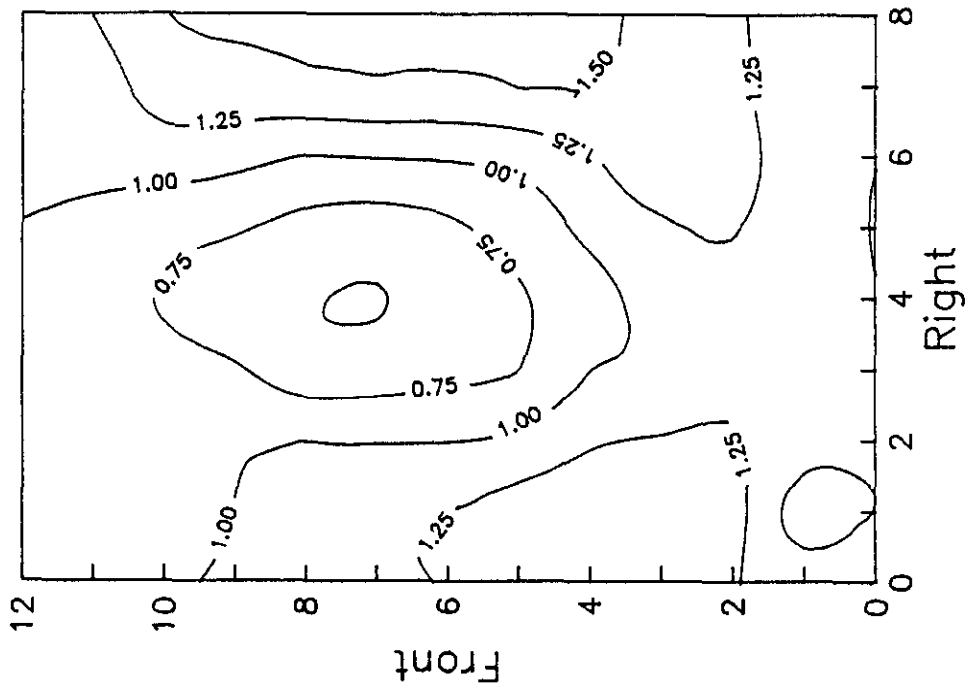


Figure 6-51

**SOUTHERN COMPANY SERVICES
LANSING SMITH #2 FLOW MODEL**

NORMALIZED METHANE CONCENTRATION

Test Plane: 3
 Test Date: 2/28/91
 Firing System: LNCFS-III
 Test ID: Configuration #5

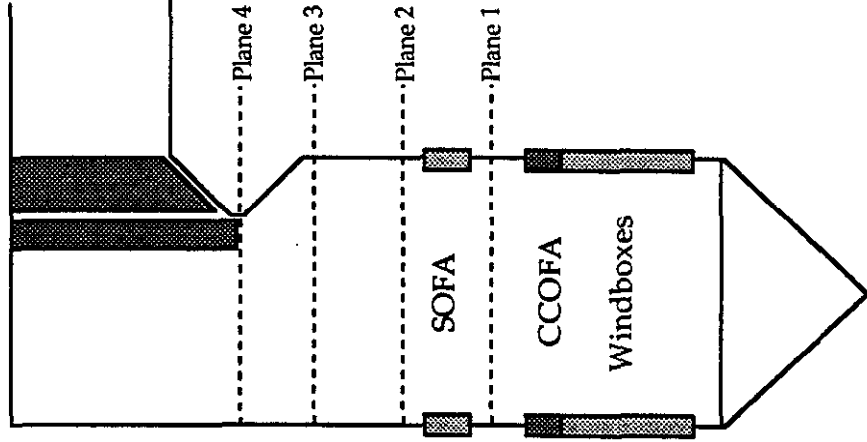
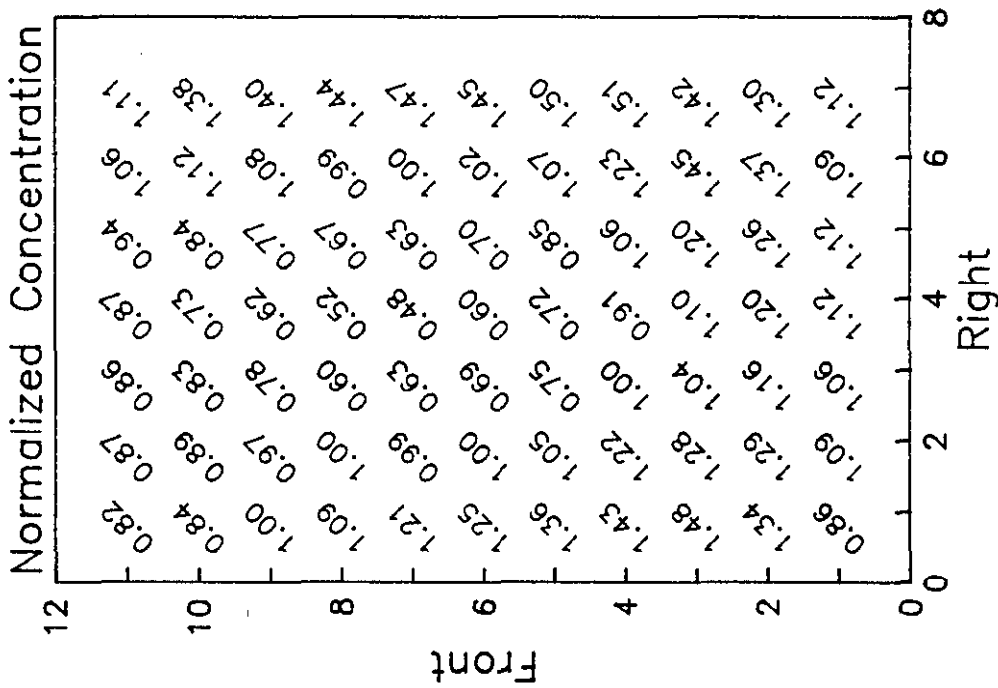


Figure 6-52

**SOUTHERN COMPANY SERVICES
 LANSING SMITH #2 FLOW MODEL**

**Lansing Smith #2 Flow Model
Methane RMS Deviation - Plane 3**

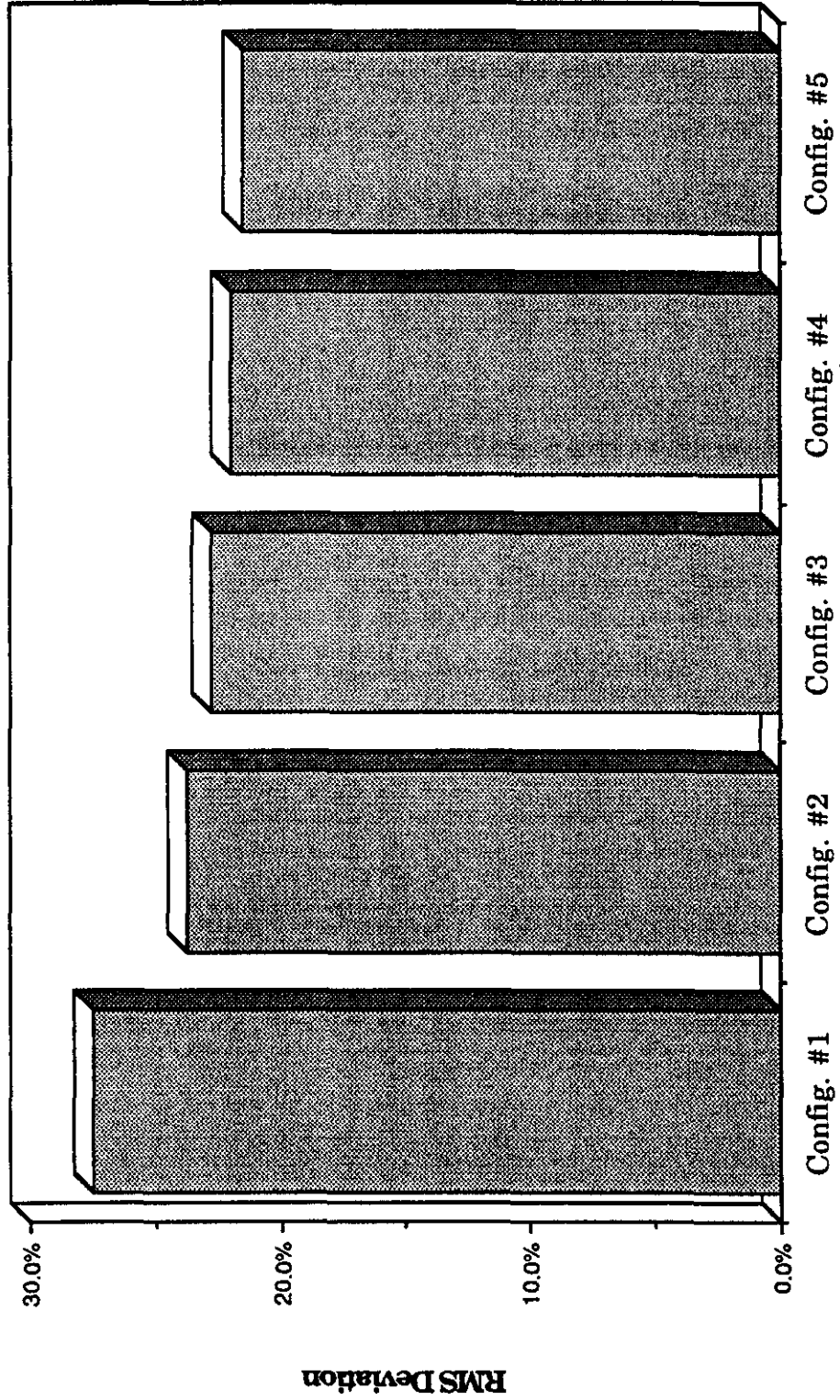


Figure 6-53

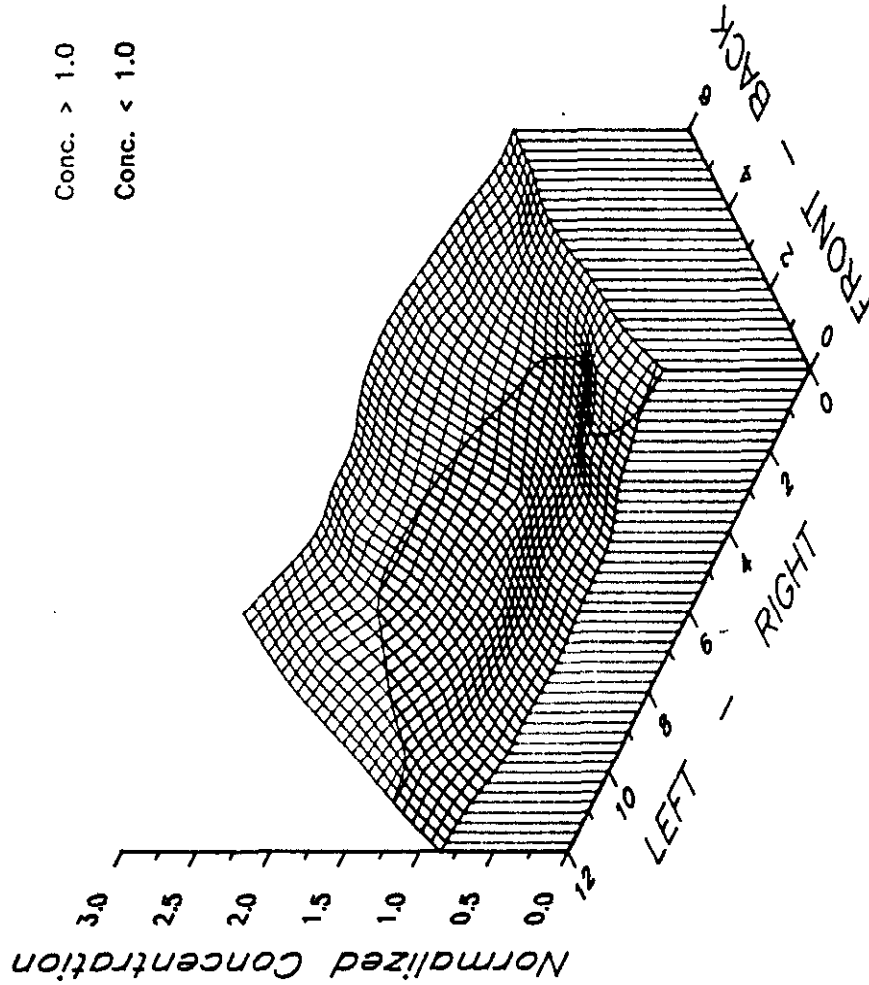
NORMALIZED METHANE CONCENTRATION

Test Plane: 4

Test Date: 2/25/91

Firing System: LNCFS-III

Test ID: Configuration #1



Conc. > 1.0

Conc. < 1.0

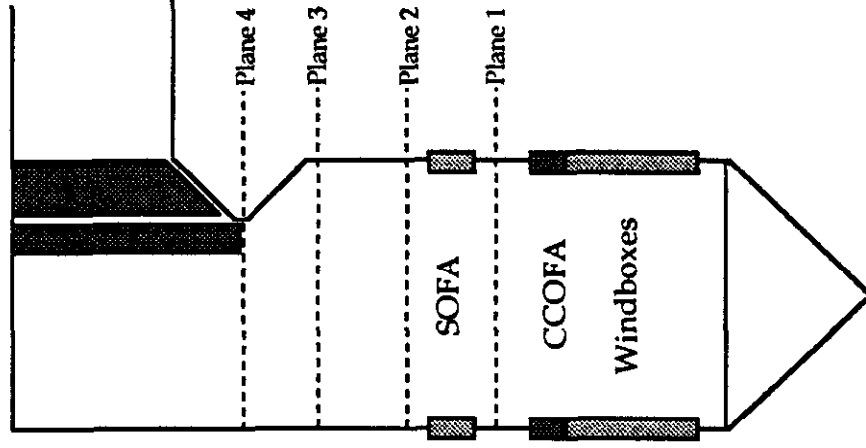


Figure 6-54

**SOUTHERN COMPANY SERVICES
LANSING SMITH #2 FLOW MODEL**

NORMALIZED METHANE CONCENTRATION

Test Plane: 4

Test Date: 2/25/91

Firing System: LNCFS-III

Test ID: Configuration #1

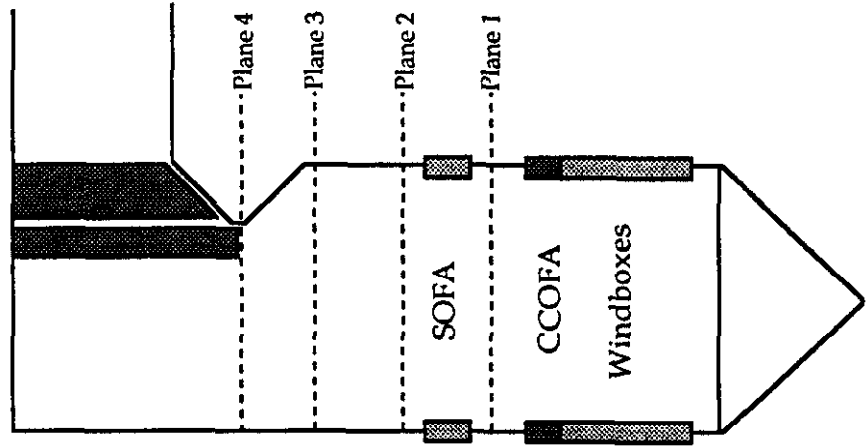
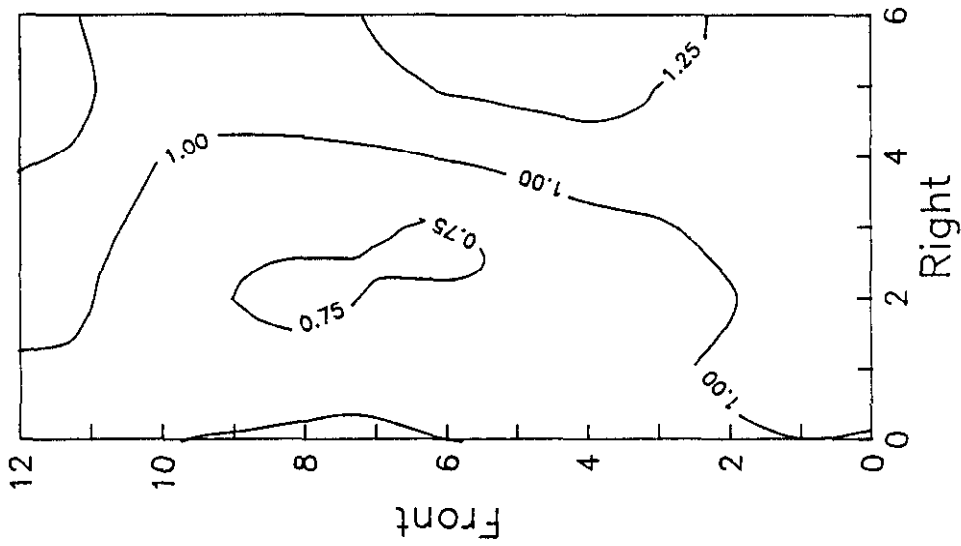


Figure 6-55

**SOUTHERN COMPANY SERVICES
LANSING SMITH #2 FLOW MODEL**

NORMALIZED METHANE CONCENTRATION

Test Plane: 4
 Test Date: 2/25/91
 Firing System: LNCFS-III
 Test ID: Configuration #1

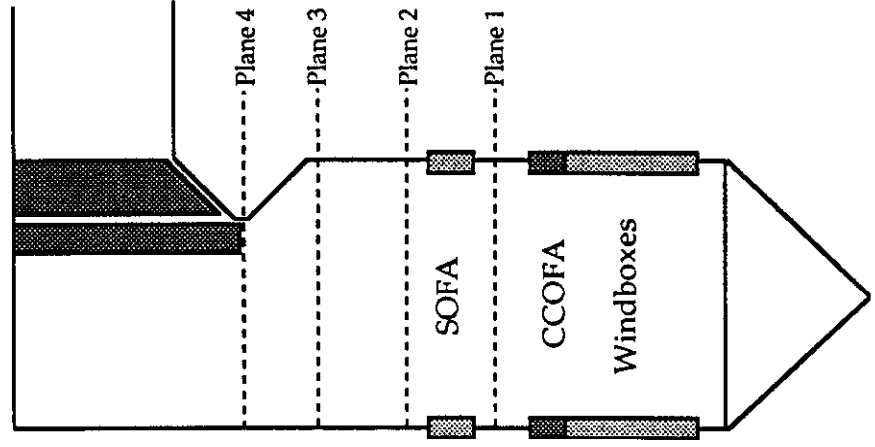
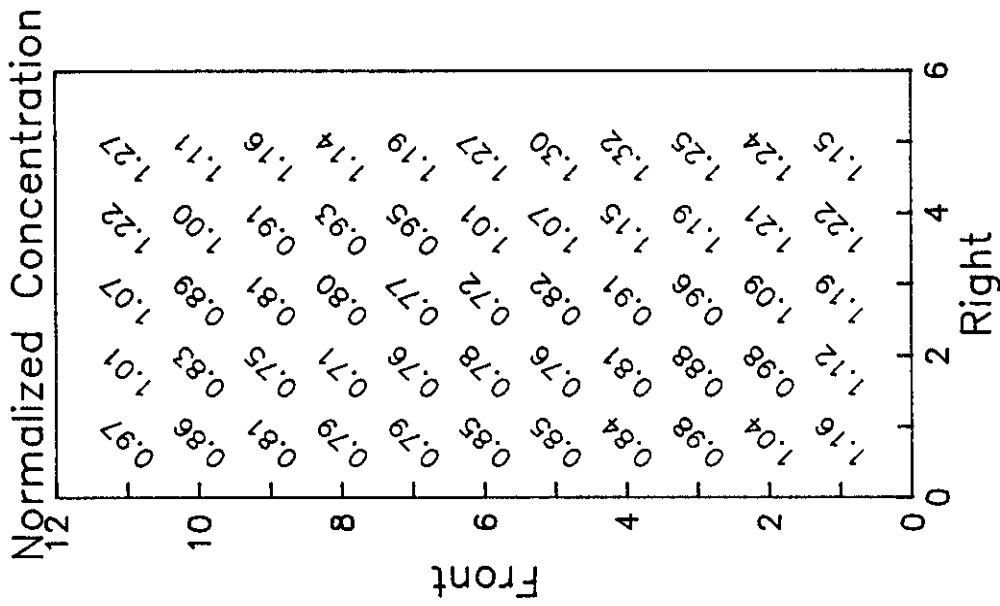


Figure 6-56

**SOUTHERN COMPANY SERVICES
 LANSING SMITH #2 FLOW MODEL**

ABB Combustion Engineering, Inc.
 Kreisinger Development Laboratory
 Mechanical Systems Engineering

NORMALIZED METHANE CONCENTRATION

Test Plane: 4

Test Date: 2/26/91

Firing System: LNCFS-III

Test ID: Configuration #2

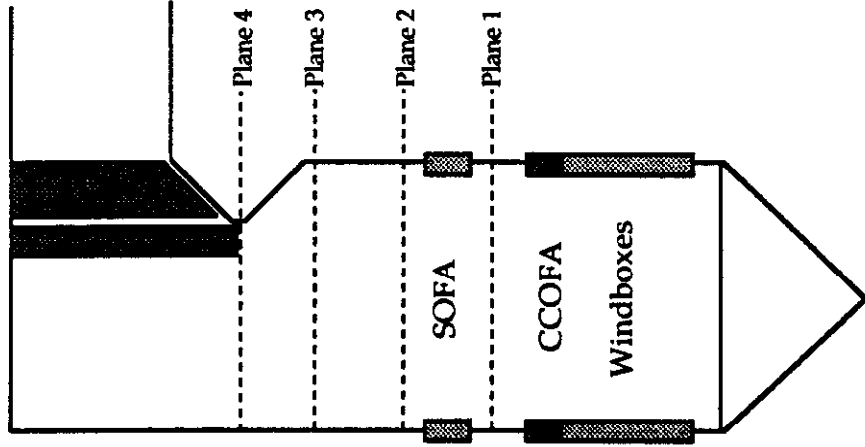
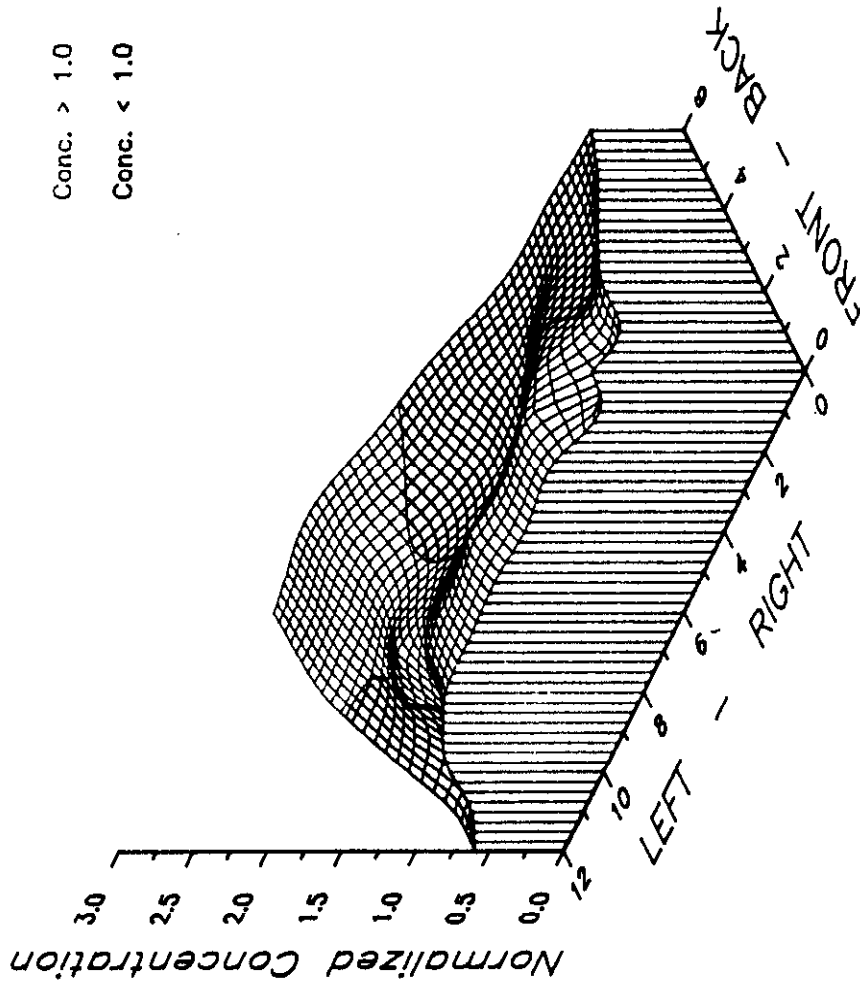


Figure 6-57

**SOUTHERN COMPANY SERVICES
LANSING SMITH #2 FLOW MODEL**

NORMALIZED METHANE CONCENTRATION

Test Plane: 4

Test Date: 2/26/91

Firing System: LNCFS-III

Test ID: Configuration #2

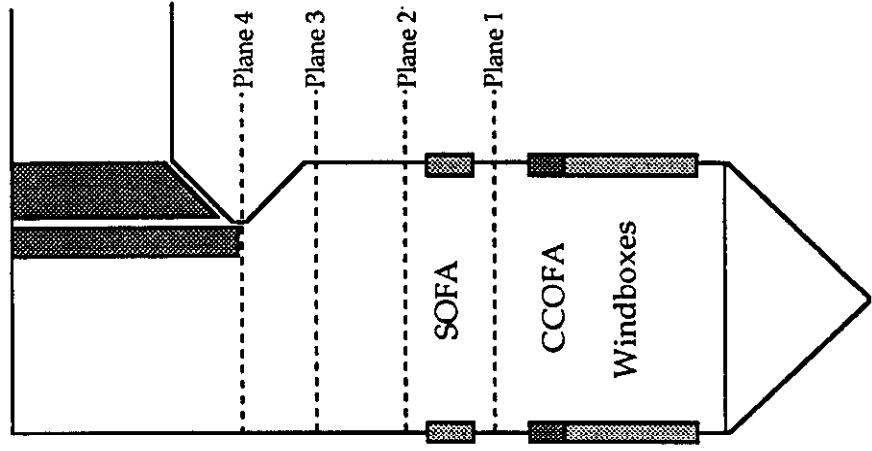
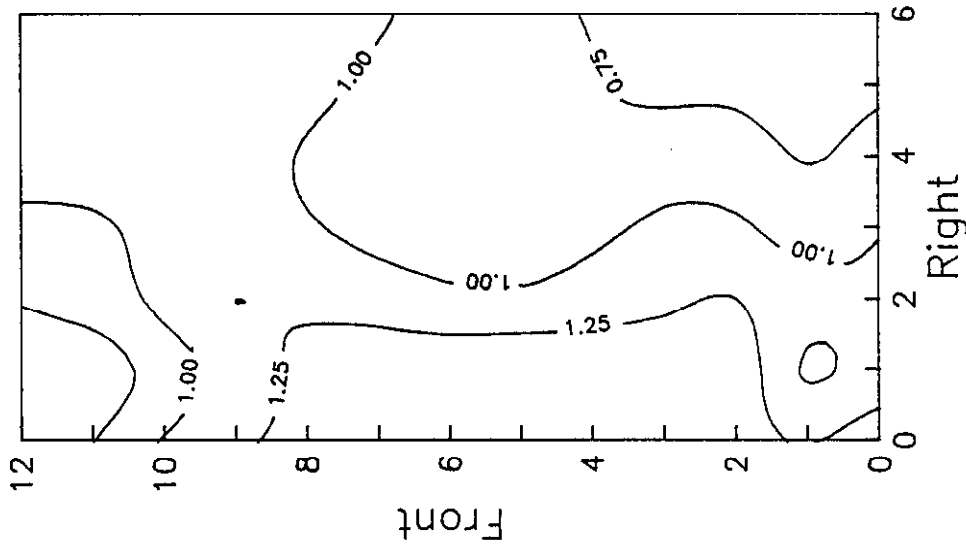


Figure 6-58

**SOUTHERN COMPANY SERVICES
LANSING SMITH #2 FLOW MODEL**

NORMALIZED METHANE CONCENTRATION

Test Plane: 4
 Test Date: 2/26/91
 Firing System: LNCFS-III
 Test ID: Configuration #2

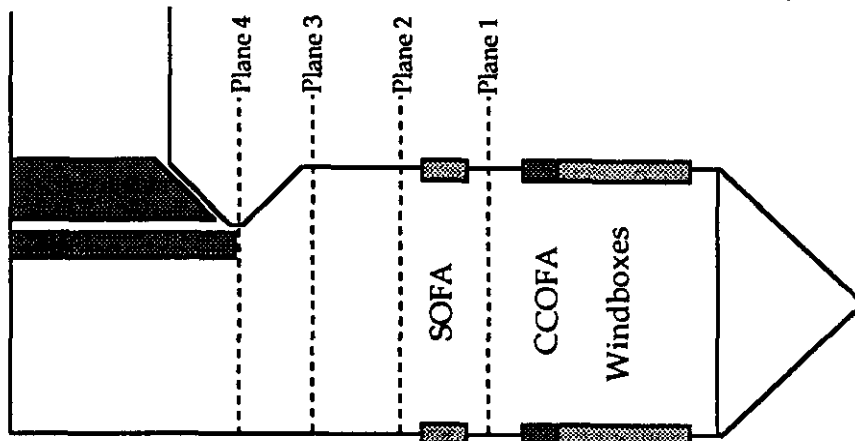
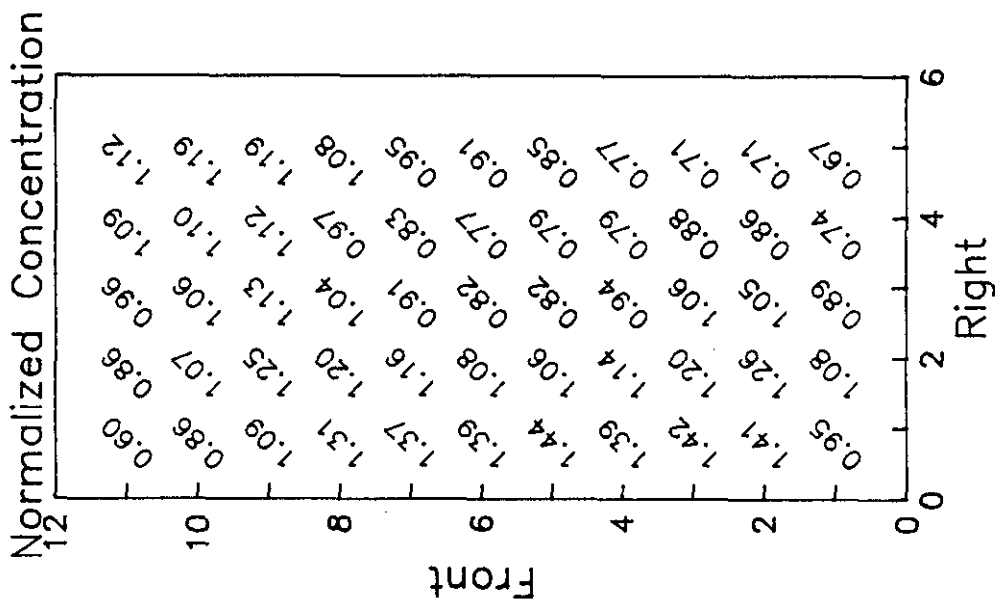


Figure 6-59

**SOUTHERN COMPANY SERVICES
 LANSING SMITH #2 FLOW MODEL**

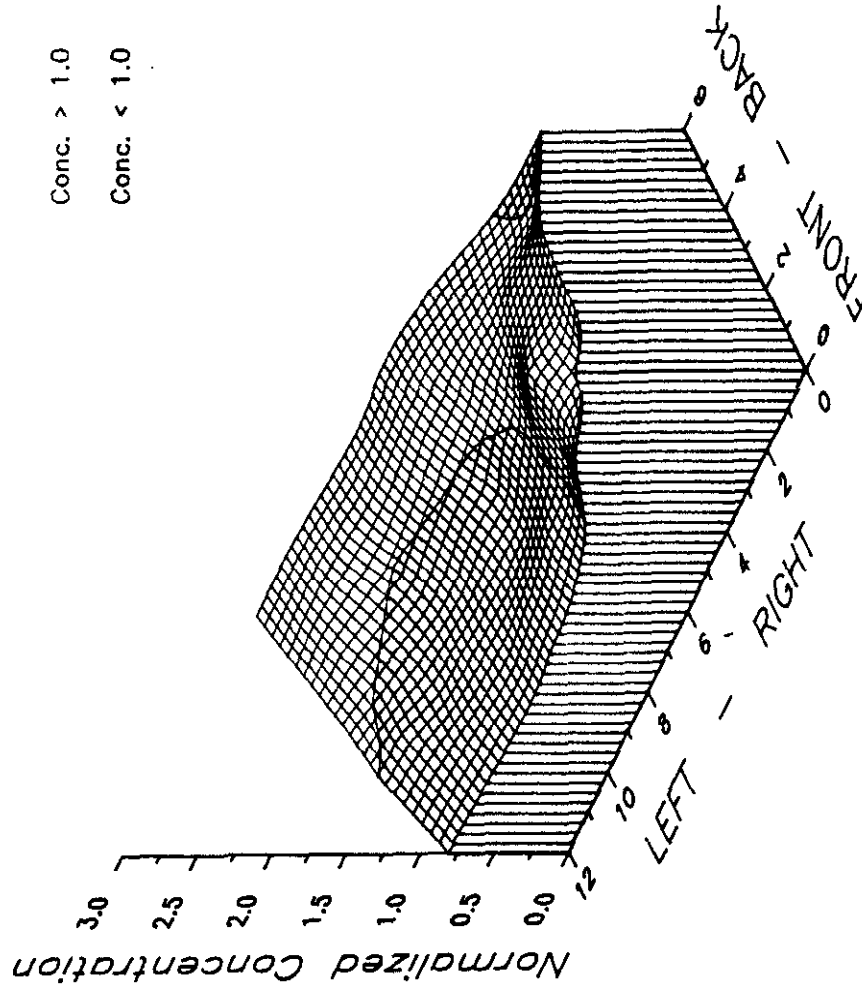
NORMALIZED METHANE CONCENTRATION

Test Plane: 4

Test Date: 2/26/91

Firing System: LNCFS-III

Test ID: Configuration #3



Conc. > 1.0

Conc. < 1.0

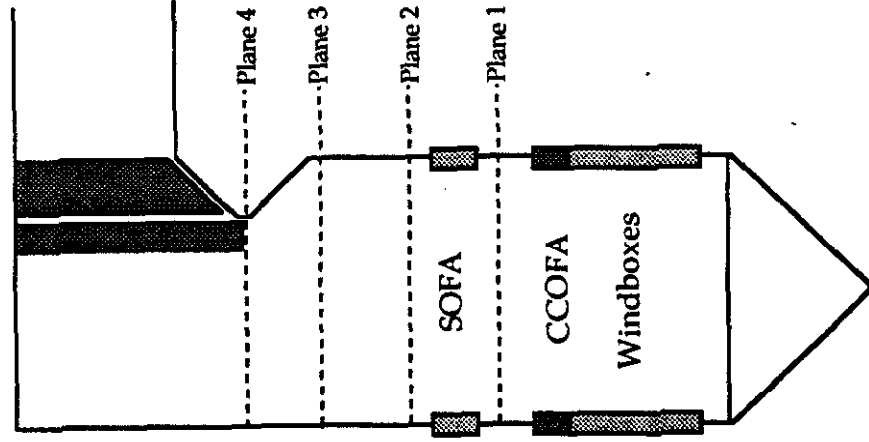


Figure 6-60

**SOUTHERN COMPANY SERVICES
LANSING SMITH #2 FLOW MODEL**

ABB Combustion Engineering, Inc.
Kreisinger Development Laboratory
Mechanical Systems Engineering

NORMALIZED METHANE CONCENTRATION

Test Plane: 4

Test Date: 2/26/91

Firing System: LNCFS-III

Test ID: Configuration #3

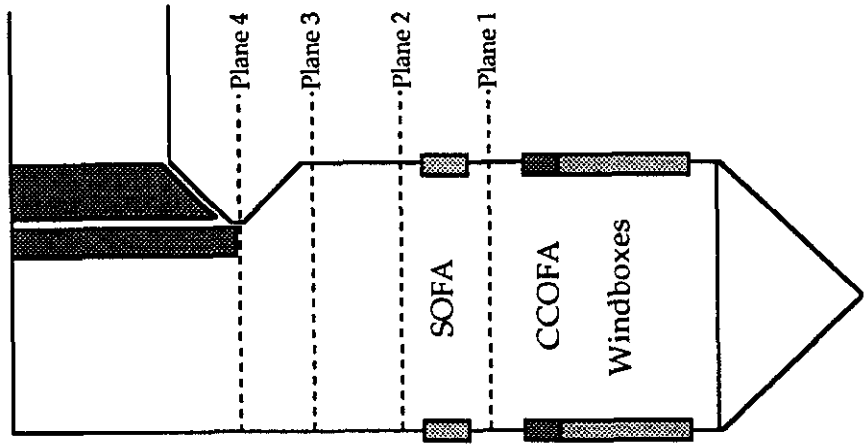
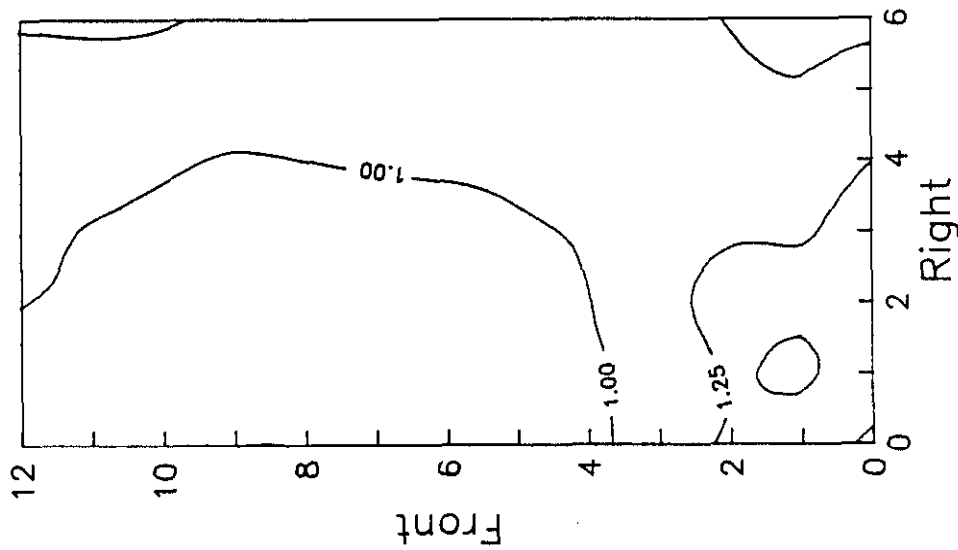


Figure 6-61

**SOUTHERN COMPANY SERVICES
LANSING SMITH #2 FLOW MODEL**

ABB Combustion Engineering, Inc.
Kreisinger Development Laboratory
Mechanical Systems Engineering

NORMALIZED METHANE CONCENTRATION

Test Plane: 4
 Test Date: 2/26/91
 Firing System: LNCFS-III
 Test ID: Configuration #3

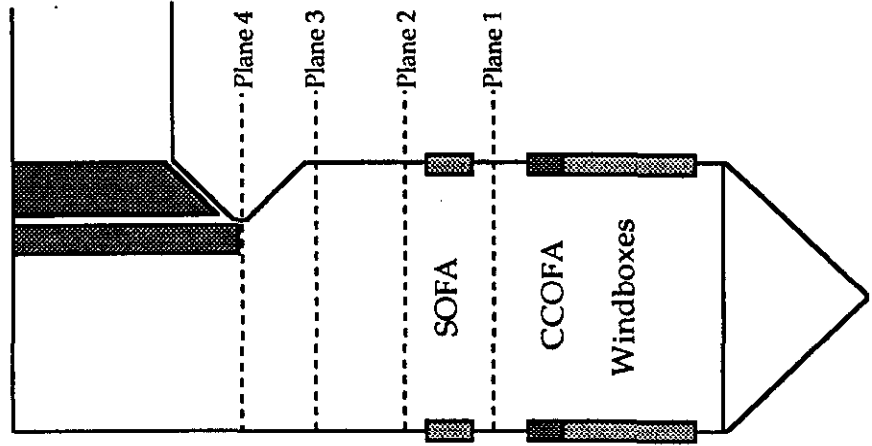
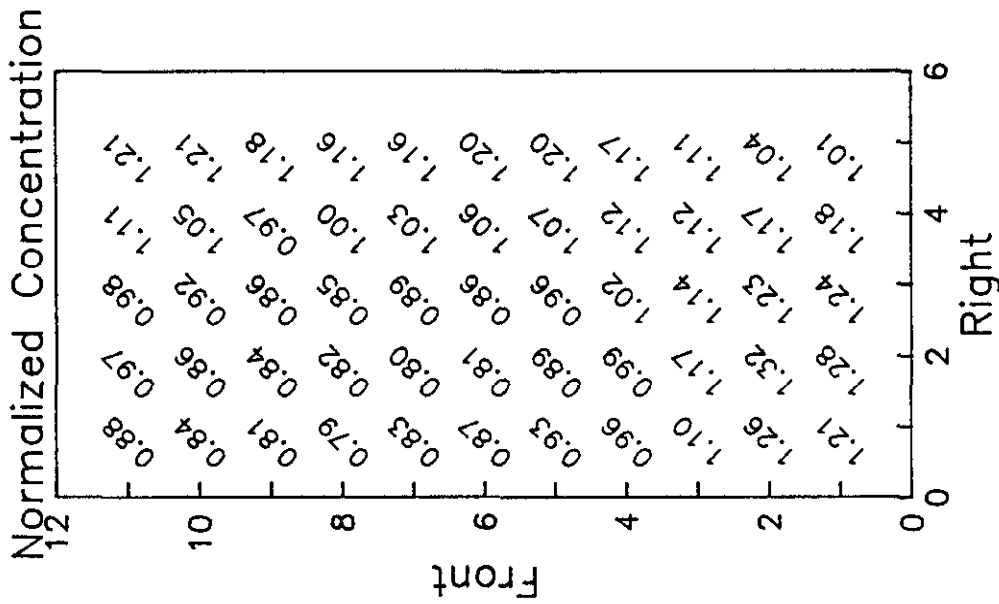


Figure 6-62

**SOUTHERN COMPANY SERVICES
 LANSING SMITH #2 FLOW MODEL**

ABB Combustion Engineering, Inc.
 Kreisinger Development Laboratory
 Mechanical Systems Engineering

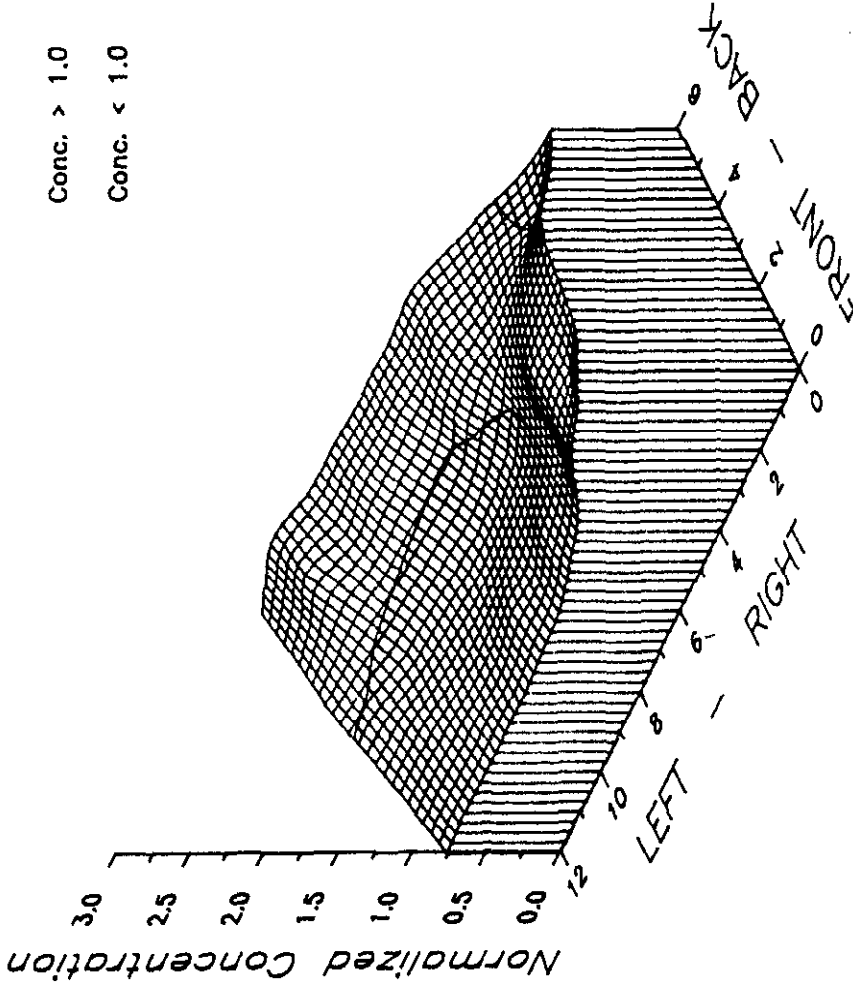
NORMALIZED METHANE CONCENTRATION

Test Plane: 4

Test Date: 2/27/91

Firing System: LNCFS-III

Test ID: Configuration #4



Conc. > 1.0

Conc. < 1.0

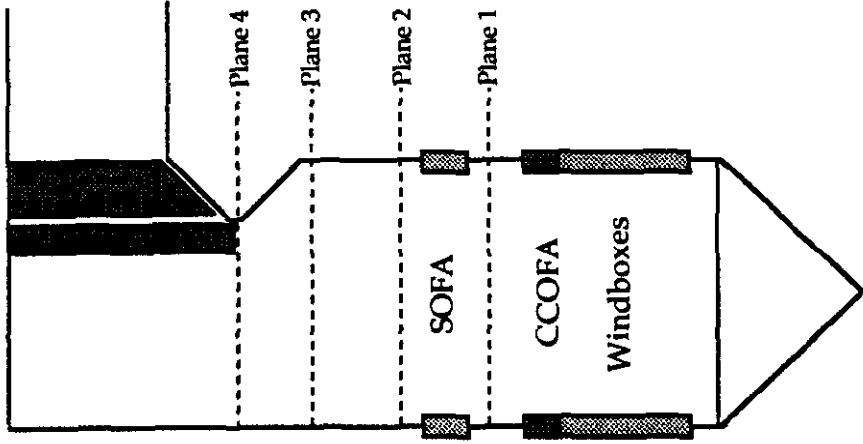


Figure 6-63

**SOUTHERN COMPANY SERVICES
LANSING SMITH #2 FLOW MODEL**

ABB Combustion Engineering, Inc.
Kreisinger Development Laboratory
Mechanical Systems Engineering

NORMALIZED METHANE CONCENTRATION

Test Plane: 4

Test Date: 2/27/91

Firing System: LNCFS-III

Test ID: Configuration #4

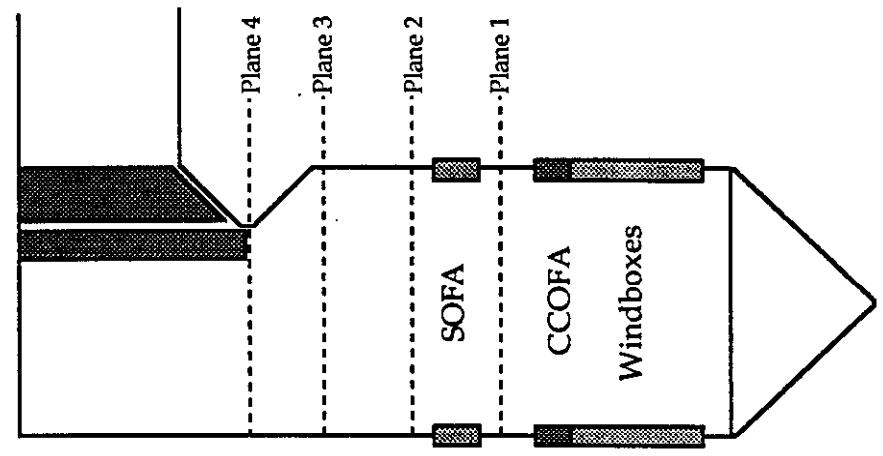
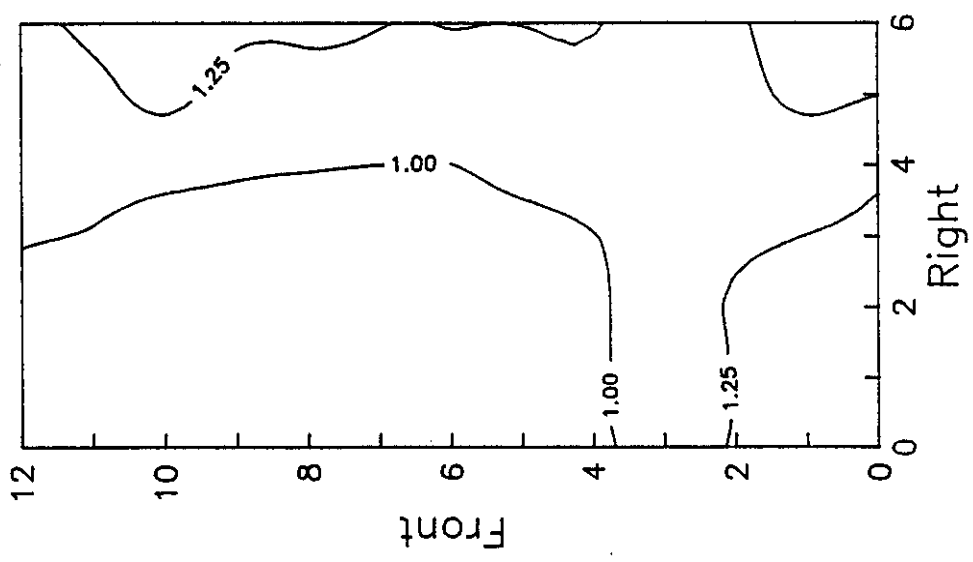


Figure 6-64

**SOUTHERN COMPANY SERVICES
LANSING SMITH #2 FLOW MODEL**

ABB Combustion Engineering, Inc.
Kreisinger Development Laboratory
Mechanical Systems Engineering

NORMALIZED METHANE CONCENTRATION

Test Plane: 4

Test Date: 2/27/91

Firing System: LNCFS-III

Test ID: Configuration #4

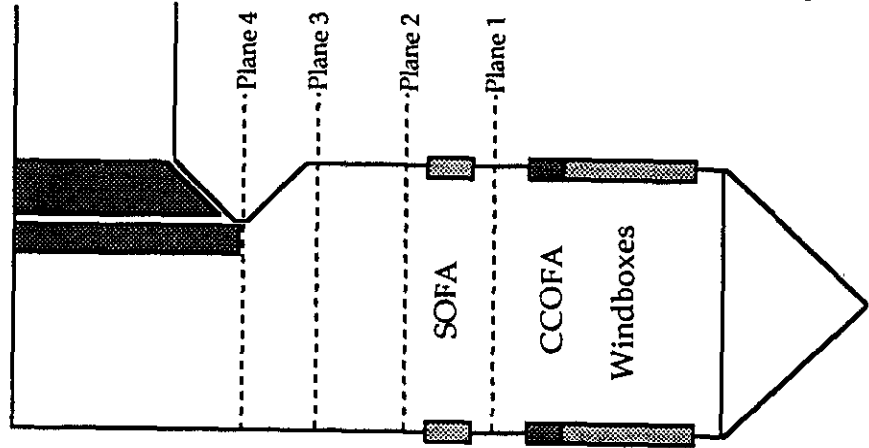
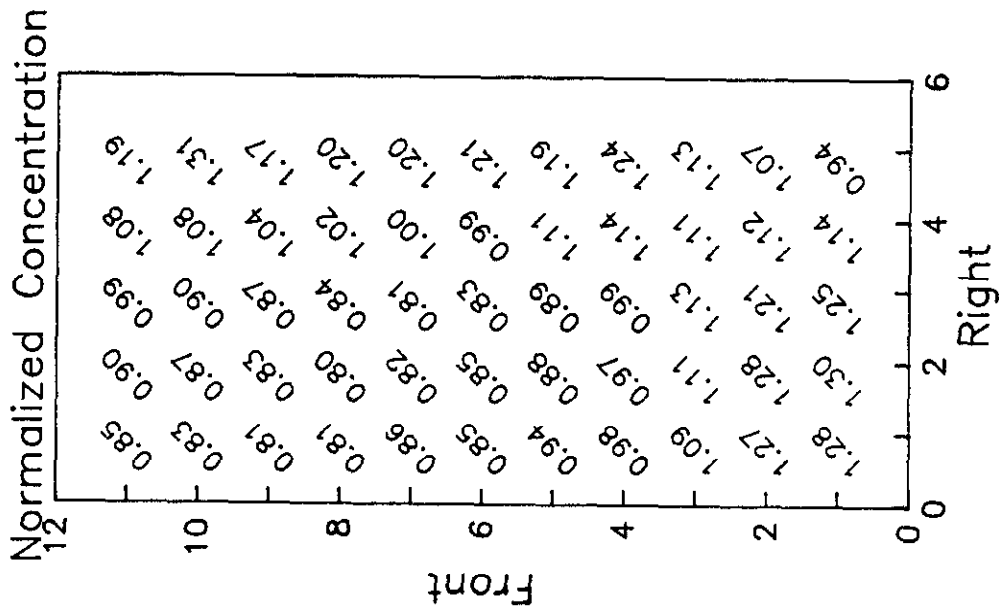


Figure 6-65

**SOUTHERN COMPANY SERVICES
LANSING SMITH #2 FLOW MODEL**

NORMALIZED METHANE CONCENTRATION

Test Plane: 4

Test Date: 2/28/91

Firing System: LNCFS-III

Test ID: Configuration #5

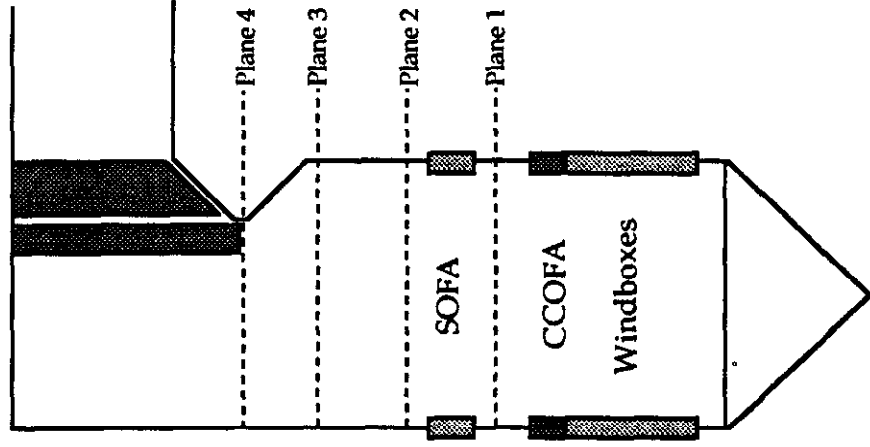
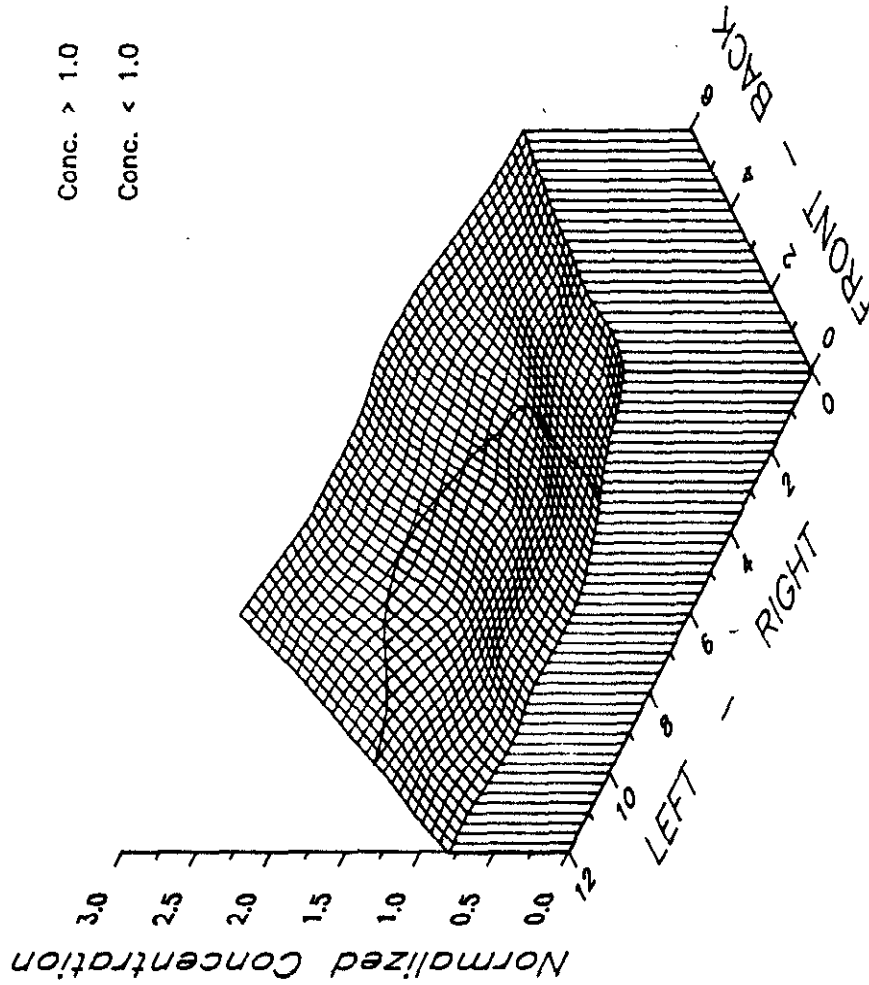


Figure 6-66

**SOUTHERN COMPANY SERVICES
LANSING SMITH #2 FLOW MODEL**

NORMALIZED METHANE CONCENTRATION

Test Plane: 4
 Test Date: 2/28/91
 Firing System: LNCFS-III
 Test ID: Configuration #5

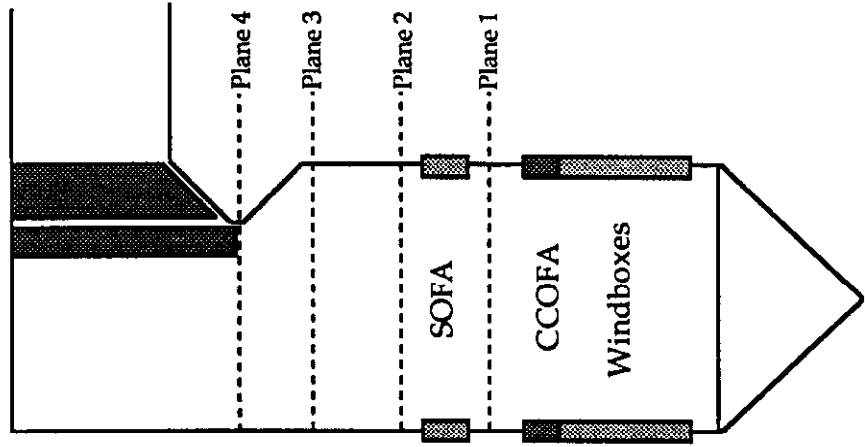
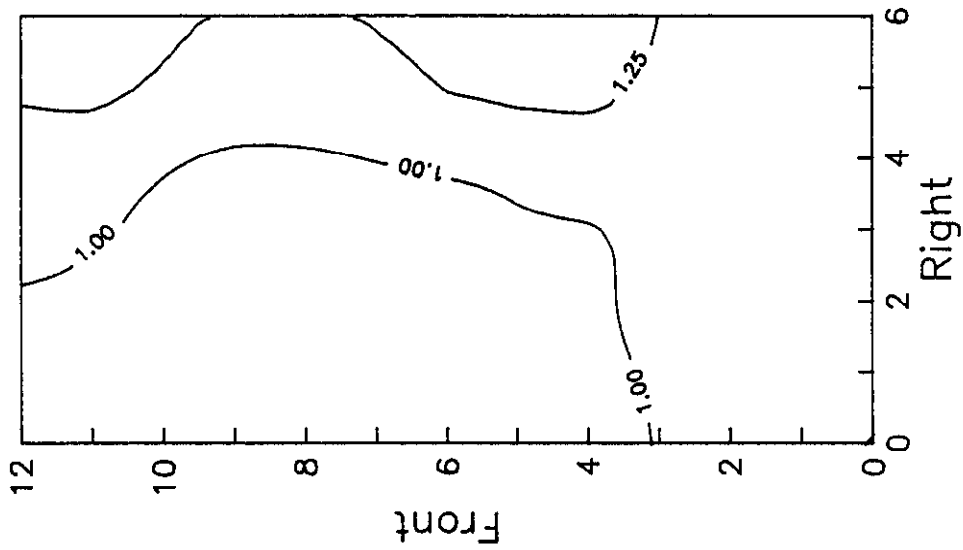
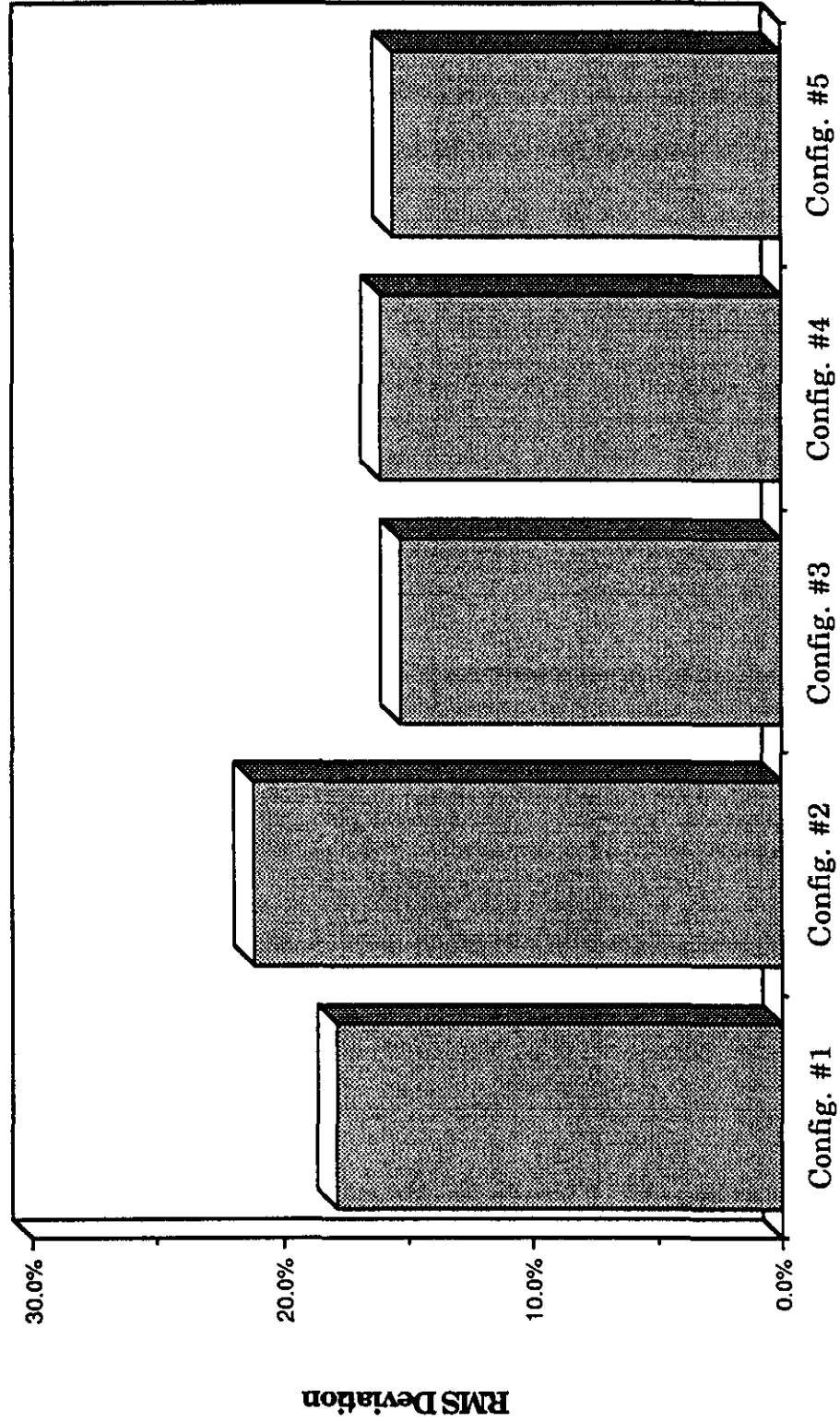


Figure 6-67

**SOUTHERN COMPANY SERVICES
 LANSING SMITH #2 FLOW MODEL**

**Lansing Smith #2 Flow Model
Methane RMS Deviation - Plane 4**



Test Identification

Figure 6-69

Lansing Smith #2 Flow Model Overall Mixing Performance (LNCFS-III)

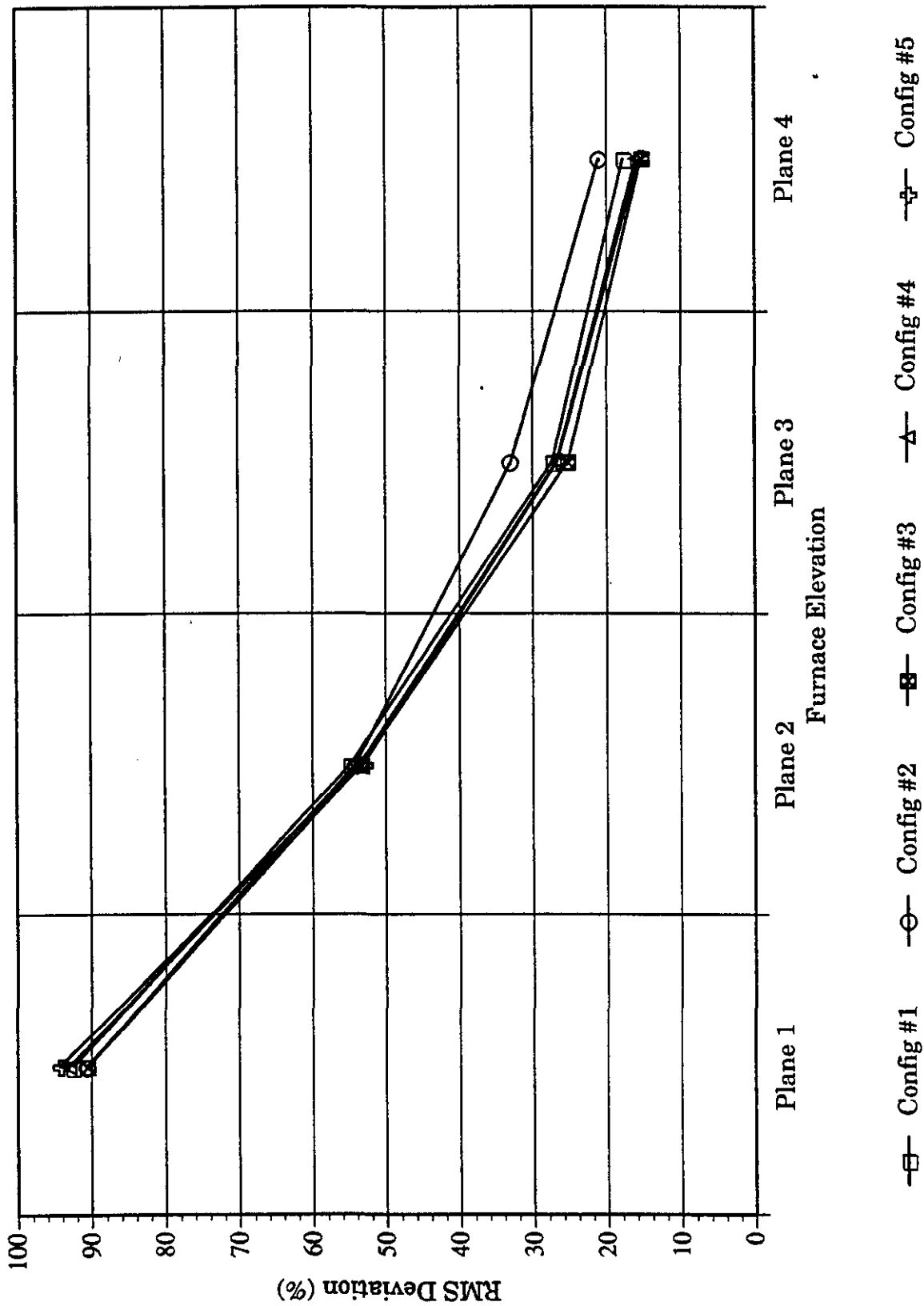


Figure 5-70

6.3 Velocity Testing

In addition to the methane gas mixing tests, three dimensional velocity test data was obtained for each of the five (5) OFA configurations, along with the baseline configuration. This velocity mapping was performed at the furnace outlet plane for each configuration to characterize the gas flow distribution leaving the furnace.

The velocity data was taken using the five hole pitot probe and the APTD, previously discussed. Pressure measurements were collected and stored in the data acquisition system and central computer, coupled to the APTD. The computer calculates the x, y, and z components of the flow, where the x direction is positive as the flow moves along the rear to the front of the furnace, the y direction is positive as the flow moves from left to right in the furnace, and the z direction is positive when the flow is upward in the furnace. The measured velocities were than reported in both tabular form, typical of Table 6-4, and graphical form.

From the three-dimensional velocity data, the normalized upward velocity data was plotted as surface and contour plots, and is shown in Figures 6-71 through 6-82. Additionally, the normalized value of the axial (upward) velocity is presented in Figures 6-83 through 6-88. Results from these tests show that the upward flow leaving the furnace is higher along the left rear corner, typical of tangentially fired units. This is primarily due to the effects of the swirl and the arch on the gasses leaving the furnace. Furthermore, the higher flows occur along the walls of the model with reduced upward flow through the center. In general, the flow distribution at the furnace outlet plane was fairly well distributed, with RMS deviations between 17% and 22%, as shown in Figure 6-89. The RMS deviation for Configuration #5 was 19.6%.

The side to side velocity and mass distribution at the furnace outlet plane is shown in Figure 6-90. From this figure, it can be seen that the side to side distributions for each of the configurations were consistent. In each case, the flow in the center was fairly uniform, with higher flows along the side walls. This is expected due the tangential nature of the furnace flow field. Because

high flow imbalances at the furnace outlet plane may result in an uneven temperature distribution at the superheater, the side to side velocity distribution for OFA operation should not be significantly different than baseline operation. For Configuration #5, the velocity profile leaving the furnace is better than the baseline configuration.

The tangential velocities for each of these configurations are presented in the form of vector plots. Each vector plot was generated using the same scaling factors, so that they could be compared, and are presented in Figures 6-91 through 6-96. From these plots, the counter-clockwise swirl of the furnace gasses can be easily seen. The tangential component of the flow is directed towards the rear of the unit along the right side, while being directed towards the front of the unit along the left side. The center of the flow swirl is located near the center of the test plane for each of the configurations, with higher tangential and axial velocity components located along the walls of the unit. Note that the swirling flow is more oval than circular, due to the rectangular geometry of the furnace. The results from this data corresponds to the results of the flow visualization tests.

PROBE NUMBER : B1884-2
 PROBE CAL DATE : 10/23/90

TEST ID : LNCFS-111-V3
 TEST NUMBER : 0023
 TEST DATE : 3/ 1/91

PLANE NUMBER : 4
 NUMBER OF ROWS : 5
 NUMBER OF COLUMNS : 11

AVERAGE NORMAL VELOCITY = 22.74 FT/SEC
 NORMAL VELOCITY RMS = 21.91 %

 * NORMALIZED *

* X-VELOCITY *

	1	2	3	4	5	6	7	8	9	10	11
1	-0.09	-0.26	-0.24	-0.15	-0.05	-0.06	-0.14	-0.01	0.01	0.16	0.38
2	-0.45	-0.51	-0.42	-0.24	-0.23	0.02	0.07	0.13	0.20	0.46	1.04
3	-0.66	-0.44	-0.36	-0.42	-0.27	0.16	-0.16	0.32	0.60	0.55	0.95
4	-0.61	-0.20	-0.09	0.07	0.43	0.24	0.38	0.54	0.47	0.74	0.87
5	-0.35	0.08	0.23	0.28	0.38	0.21	0.32	0.39	0.52	0.69	0.56

 * NORMALIZED *

* Y-VELOCITY *

	1	2	3	4	5	6	7	8	9	10	11
1	-0.08	0.51	0.68	0.86	0.67	0.94	0.92	0.88	0.89	0.57	0.42
2	-0.31	0.21	0.31	0.37	0.61	0.71	0.66	0.14	0.47	0.01	-0.10
3	-0.05	-0.22	-0.49	-0.52	-0.62	-0.28	-0.35	-0.11	-0.63	-0.44	-0.14
4	-0.29	-0.59	-0.32	-0.79	-0.67	-0.56	-0.08	-0.91	-0.74	-0.53	-0.25
5	-0.33	-0.86	-0.97	-1.01	-0.96	-0.93	-0.98	-0.98	-1.11	-0.49	-0.57

 * NORMALIZED *

* NORMAL VELOCITY *

	1	2	3	4	5	6	7	8	9	10	11
1	1.31	0.63	0.80	0.86	0.90	0.94	1.02	1.08	0.90	0.99	1.00
2	0.99	0.84	0.79	0.87	0.71	0.92	1.10	1.20	1.14	1.27	1.27
3	1.08	0.80	0.78	0.73	0.72	0.71	0.93	0.79	0.91	1.04	1.28
4	1.03	0.92	0.85	0.94	0.79	0.65	0.70	0.84	0.93	1.16	1.53
5	1.18	1.00	1.22	1.18	1.09	1.16	1.06	1.14	1.27	1.43	1.64

Table 6-4 Velocity Mapping Data - General Output

AUTOMATIC PROBE TRAVERSING DEVICE

PROBE NUMBER : B1884-2
 PROBE CAL DATE : 10/23/90

TEST ID : LNCFS-111-V3
 TEST NUMBER : 0023
 TEST DATE : 3/ 1/91

PLANE NUMBER : 4
 NUMBER OF ROWS : 5
 NUMBER OF COLUMNS : 11

AVERAGE NORMAL VELOCITY = 22.74 FT/SEC

* X-VELOCITY (FT/SEC) *

	1	2	3	4	5	6	7	8	9	10	11
1	-2.14	-5.96	-5.51	-3.49	-1.18	-1.38	-3.19	-0.30	0.25	3.71	8.53
2	-10.18	-11.59	-9.56	-5.35	-5.21	0.40	1.61	3.02	4.46	10.56	23.68
3	-14.98	-10.06	-8.20	-9.46	-6.23	3.60	-3.68	7.26	13.65	12.46	21.61
4	-13.91	-4.64	-2.14	1.68	9.71	5.41	8.58	12.33	10.59	16.87	19.81
5	-7.86	1.82	5.28	6.29	8.62	4.69	7.36	8.77	11.82	15.62	12.82

* Y-VELOCITY (FT/SEC) *

	1	2	3	4	5	6	7	8	9	10	11
1	-1.81	11.49	15.46	19.45	15.18	21.32	20.93	19.95	20.33	12.96	9.55
2	-7.00	4.66	7.13	8.49	13.85	16.08	14.93	3.12	10.67	0.22	-2.25
3	-1.24	-4.91	-11.19	-11.77	-14.18	-6.31	-8.00	-2.53	-14.34	-10.05	-3.16
4	-6.58	-13.44	-7.23	-18.06	-15.17	-12.62	-1.79	-20.76	-16.88	-12.15	-5.69
5	-7.53	-19.46	-22.17	-23.05	-21.88	-21.22	-22.18	-22.21	-25.34	-11.06	-12.85

* NORMAL VELOCITY (FT/SEC) *

	1	2	3	4	5	6	7	8	9	10	11
1	29.82	14.25	18.24	19.58	20.40	21.32	23.30	24.53	20.51	22.44	22.71
2	22.55	18.99	17.98	19.83	16.04	20.81	24.93	27.37	25.82	28.85	28.93
3	24.53	18.14	17.74	16.66	16.32	16.23	21.10	18.07	20.78	23.63	29.20
4	23.42	20.92	19.39	21.41	18.03	14.86	16.00	18.99	21.05	26.48	34.74
5	26.89	22.68	27.70	26.80	24.76	26.31	24.08	25.90	28.81	32.46	37.24

* TOTAL PRESSURE (IN-H2O) *

	1	2	3	4	5	6	7	8	9	10	11
1	-0.54	-0.64	-0.62	-0.64	-0.67	-0.61	-0.62	-0.61	-0.65	-0.58	-0.59
2	-0.05	-0.63	-0.68	-0.69	-0.69	-0.69	-0.66	-0.64	-0.68	-0.61	-0.53
3	-0.03	-0.62	-0.61	-0.65	-0.67	-0.73	-0.67	-0.75	-0.67	-0.60	-0.53
4	-0.03	-0.61	-0.66	-0.65	-0.70	-0.74	-0.71	-0.66	-0.62	-0.57	-0.50
5	-0.06	-0.57	-0.53	-0.57	-0.62	-0.58	-0.62	-0.62	-0.59	-0.58	-0.47

Table 6-4 Velocity Mapping Data - General Output (con't)

AUTOMATIC PROBE TRAVERSING DEVICE

PROBE NUMBER : B1884-2
 PROBE CAL DATE : 10/23/90

TEST ID : LNCFS-111-U3
 TEST NUMBER : 0023
 TEST DATE : 3/ 1/91

PLANE NUMBER : 4
 NUMBER OF ROWS : 5
 NUMBER OF COLUMNS : 11

AVERAGE NORMAL VELOCITY = 22.74 FT/SEC

* RESULTANT VELOCITY VECTOR/ANGLE IN THE X-Y PLANE *

	1	2	3	4	5	6	7
1	2.80/230.	12.94/333.	16.41/340.	19.76/350.	15.23/356.	21.37/356.	21.17/351.
2	12.36/235.	12.49/292.	11.92/307.	10.03/328.	14.80/339.	16.09/ 1.	15.02/ 6.
3	15.03/265.	11.19/244.	13.87/216.	15.11/219.	15.49/204.	7.27/150.	8.80/205.
4	15.38/245.	14.22/199.	7.54/196.	18.14/175.	18.01/147.	13.73/157.	8.76/102.
5	10.89/226.	19.54/175.	22.79/167.	23.89/165.	23.51/159.	21.73/168.	23.37/162.
	8	9	10	11			
1	19.95/359.	20.33/ 1.	13.48/ 16.	12.81/ 42.			
2	4.34/ 44.	11.57/ 23.	10.56/ 89.	23.79/ 96.			
3	7.69/109.	19.80/137.	16.01/129.	21.84/ 99.			
4	24.15/149.	19.93/148.	20.79/126.	20.62/106.			
5	23.87/159.	27.96/155.	19.14/125.	18.16/135.			

Table 6-4 Velocity Mapping Data - General Output (con't)

NORMALIZED VELOCITY

Test Plane: 4

Test Date: 3/4/91

Firing System: LNCFS-III

Test ID: Baseline

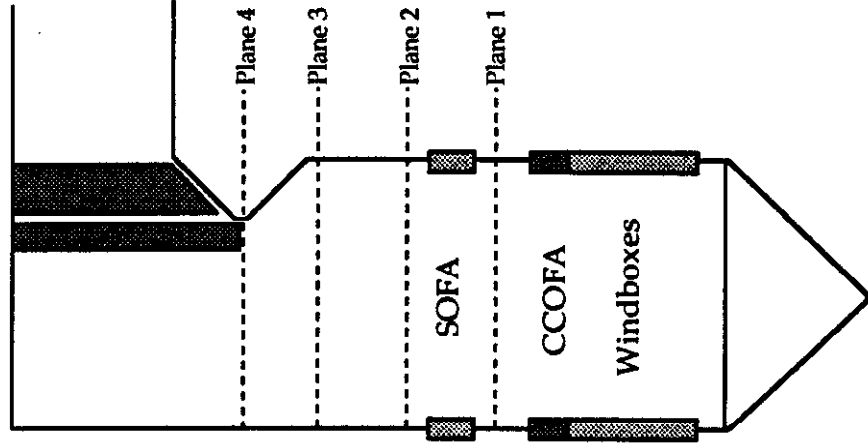
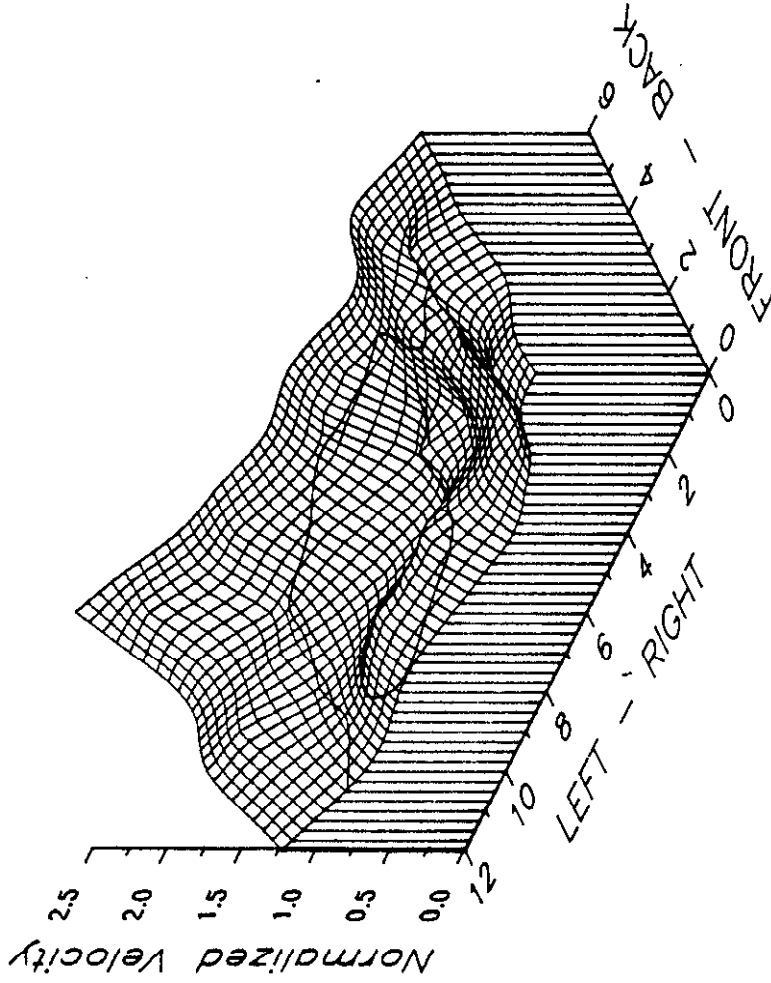
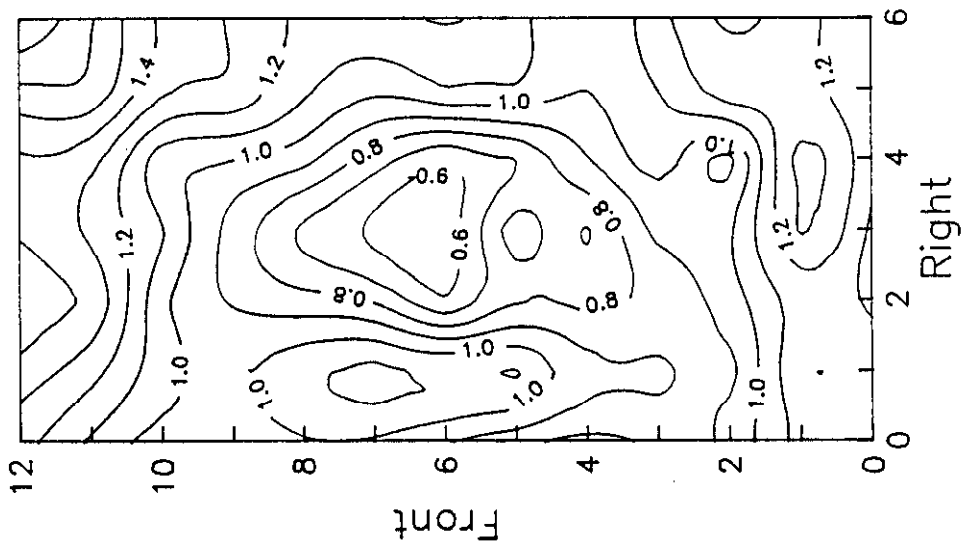


Figure 6-71

**SOUTHERN COMPANY SERVICES
LANSING SMITH #2 FLOW MODEL**



NORMALIZED VELOCITY

Test Plane: 4

Test Date: 3/4/91

Firing System: LNCFS-III

Test ID: Baseline

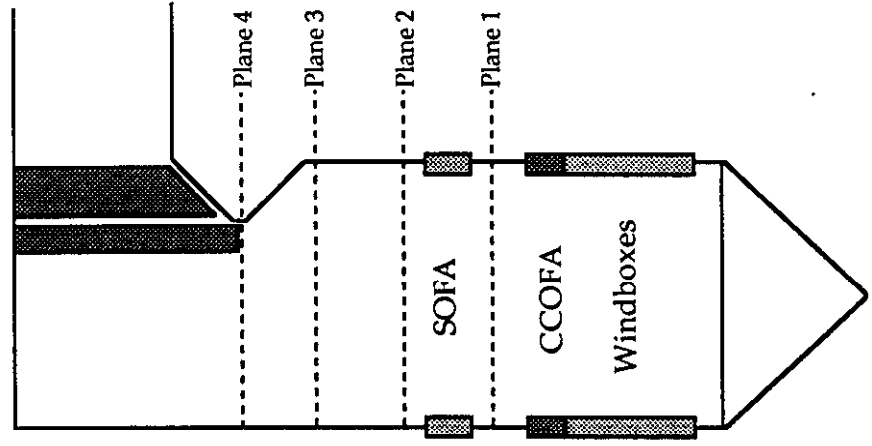


Figure 6-72

**SOUTHERN COMPANY SERVICES
LANSING SMITH #2 FLOW MODEL**

NORMALIZED VELOCITY

Test Plane: 4

Test Date: 3/1/91

Firing System: LNCFS-III

Test ID: Configuration #1

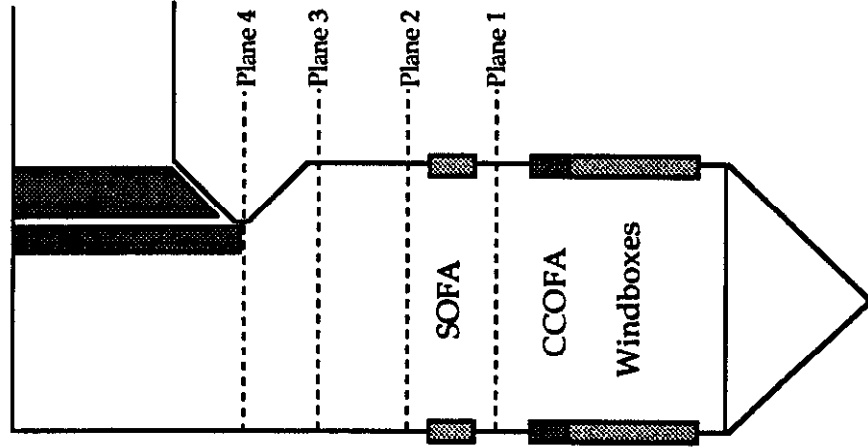
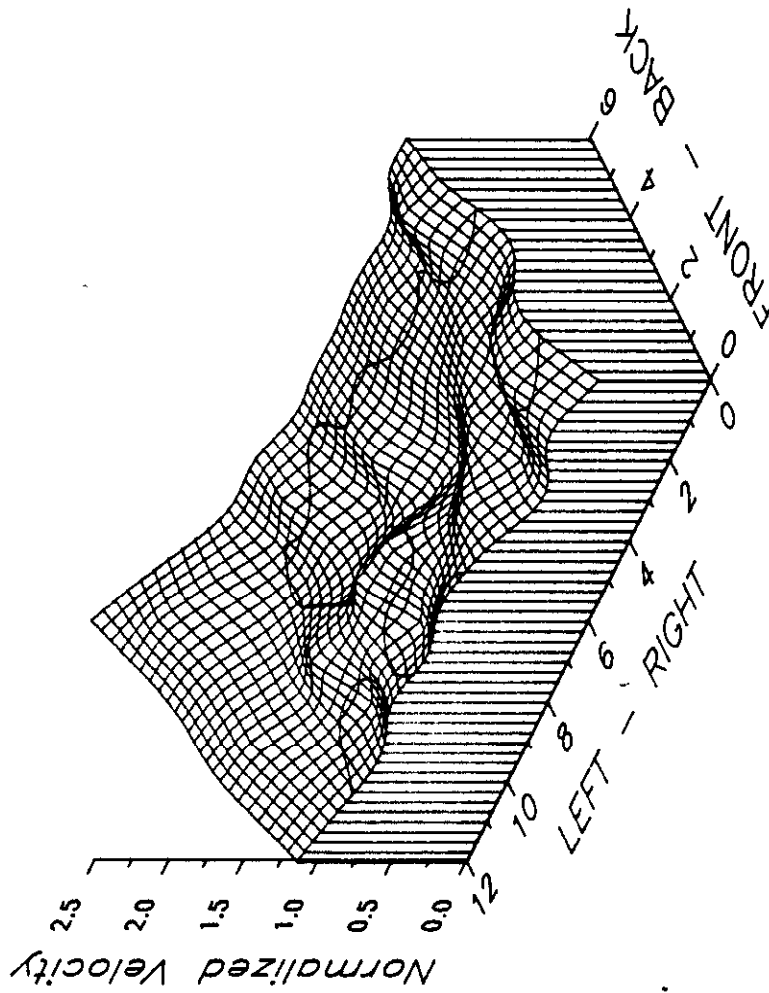
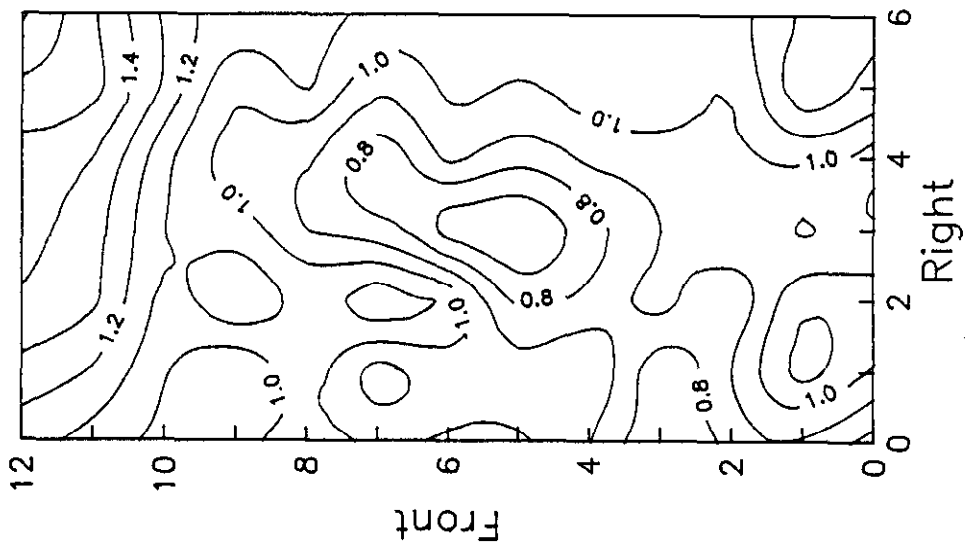


Figure 6-73

**SOUTHERN COMPANY SERVICES
LANSING SMITH #2 FLOW MODEL**



NORMALIZED VELOCITY

Test Plane: 4

Test Date: 3/1/91

Firing System: LNCFS-III

Test ID: Configuration #1

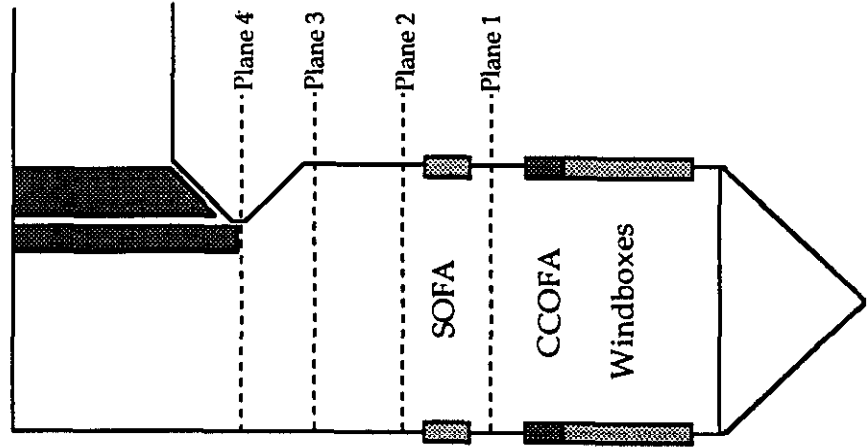


Figure 6-74

**SOUTHERN COMPANY SERVICES
LANSING SMITH #2 FLOW MODEL**

NORMALIZED VELOCITY

Test Plane: 4

Test Date: 3/1/91

Firing System: LNCFS-III

Test ID: Configuration #2

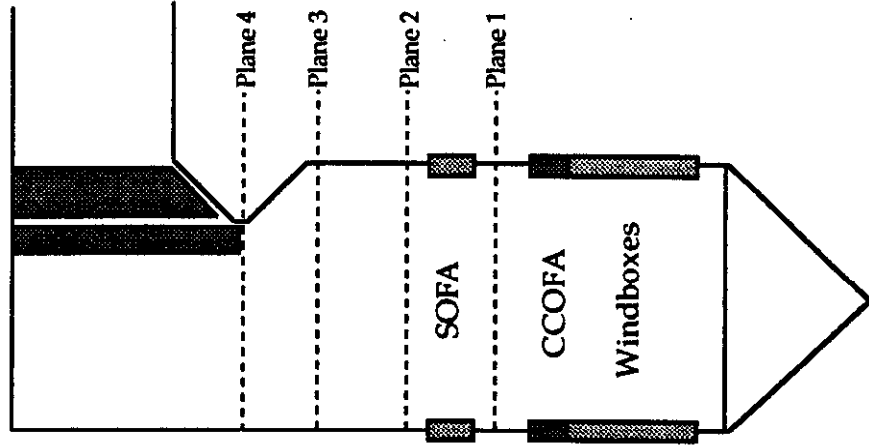
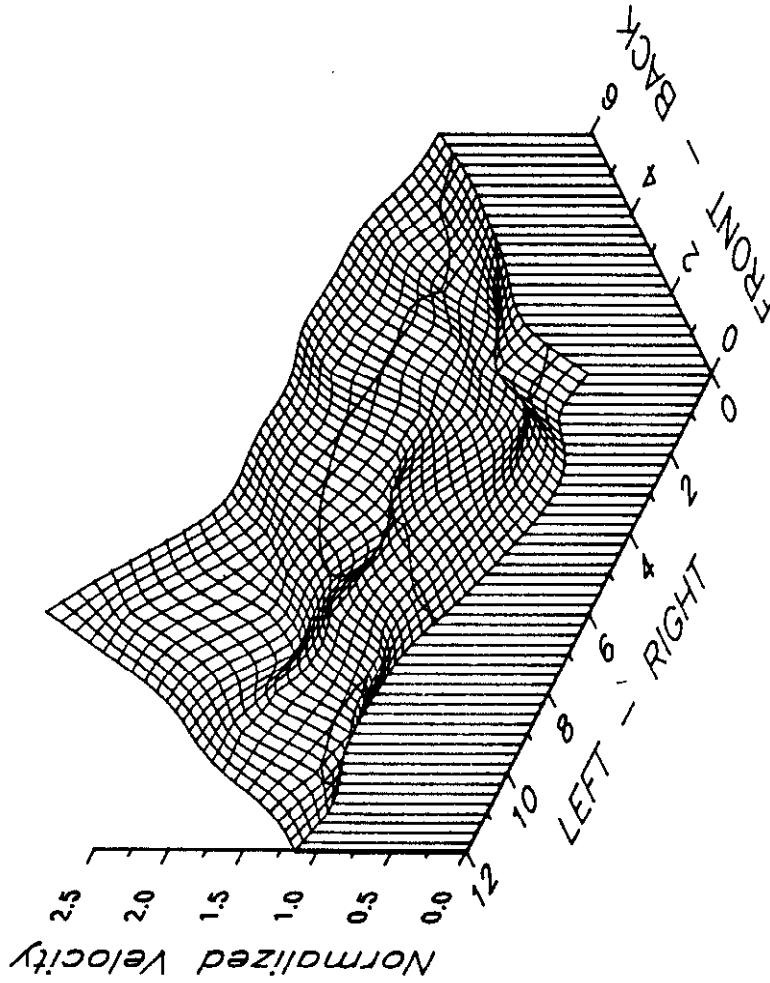
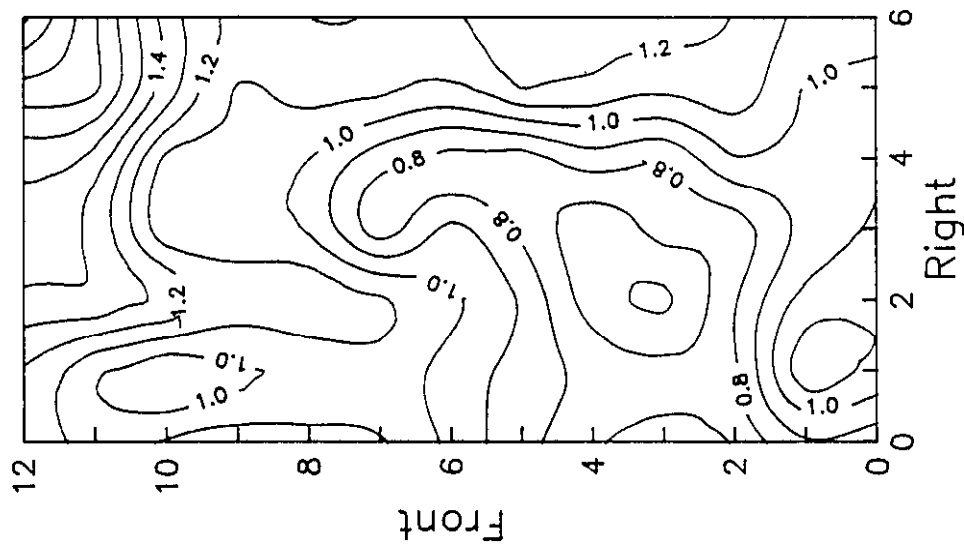


Figure 6-75

**SOUTHERN COMPANY SERVICES
LANSING SMITH #2 FLOW MODEL**



NORMALIZED VELOCITY
 Test Plane: 4
 Test Date: 3/1/91
 Firing System: LNCFS-III
 Test ID: Configuration #2

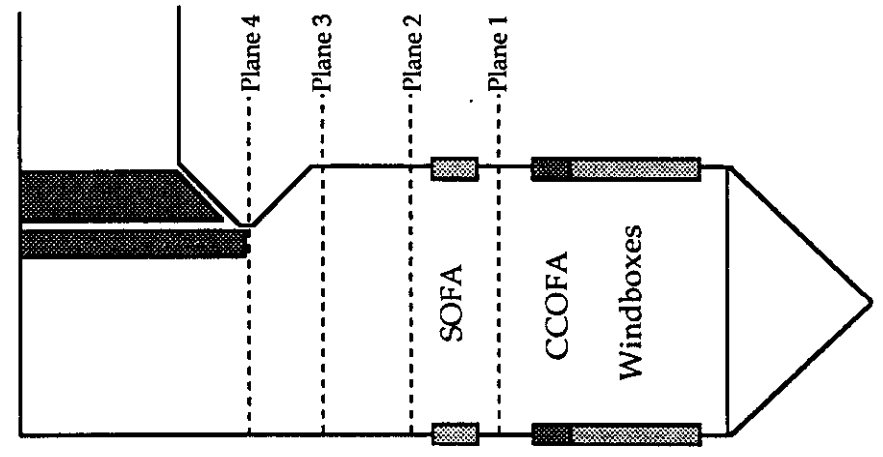


Figure 6-76

**SOUTHERN COMPANY SERVICES
 LANSING SMITH #2 FLOW MODEL**

NORMALIZED VELOCITY

Test Plane: 4

Test Date: 3/1/91

Firing System: LNCFS-III

Test ID: Configuration #3

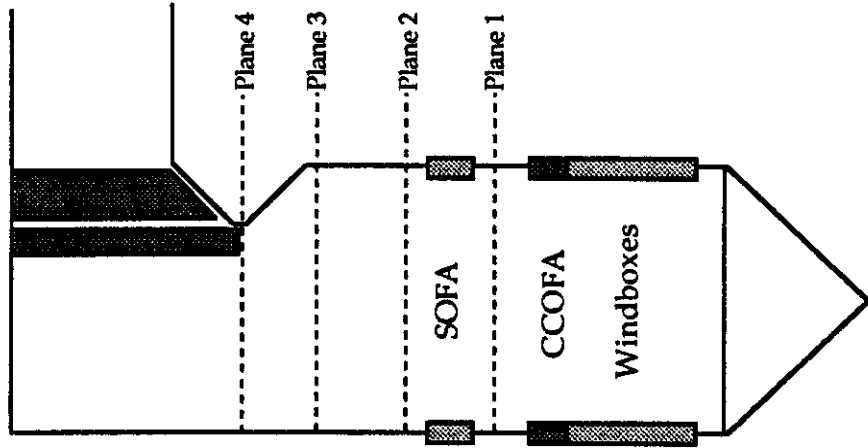
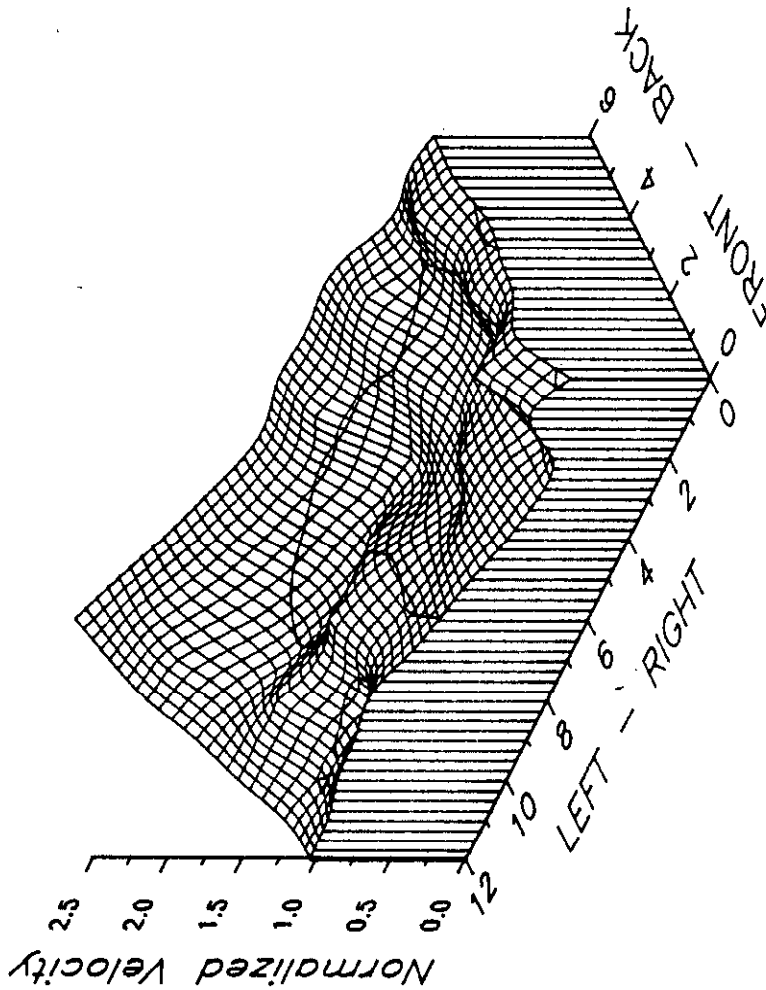
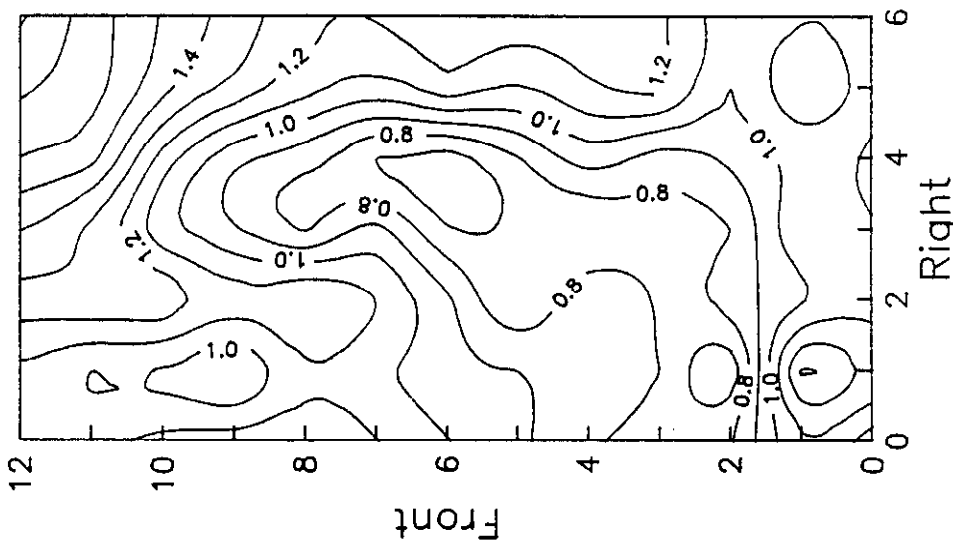


Figure 6-77

**SOUTHERN COMPANY SERVICES
LANSING SMITH #2 FLOW MODEL**



NORMALIZED VELOCITY

Test Plane: 4

Test Date: 3/1/91

Firing System: LNCFS-III

Test ID: Configuration #3

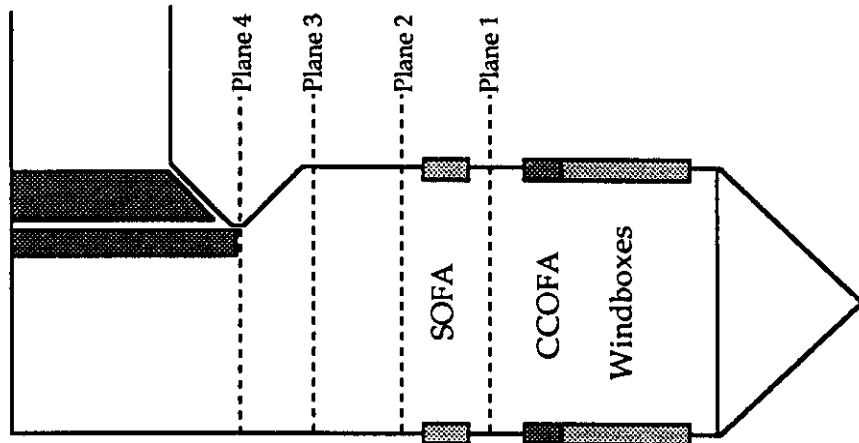


Figure 6-78

**SOUTHERN COMPANY SERVICES
LANSING SMITH #2 FLOW MODEL**

NORMALIZED VELOCITY

Test Plane: 4

Test Date: 3/1/91

Firing System: LNCFS-III

Test ID: Configuration #4

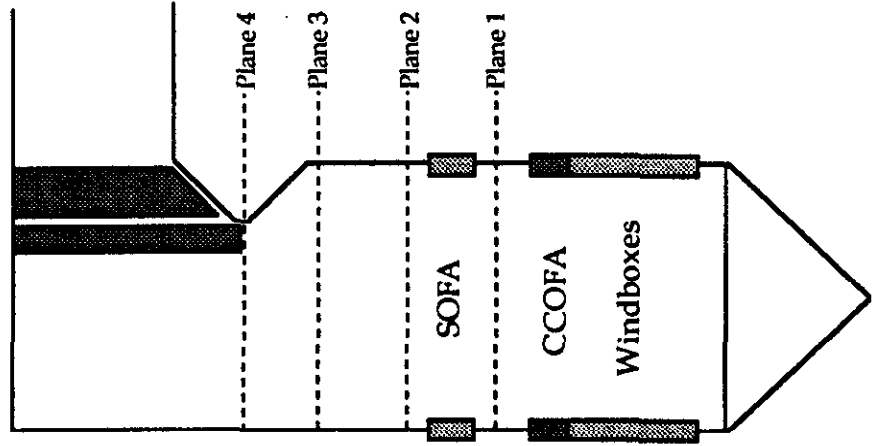
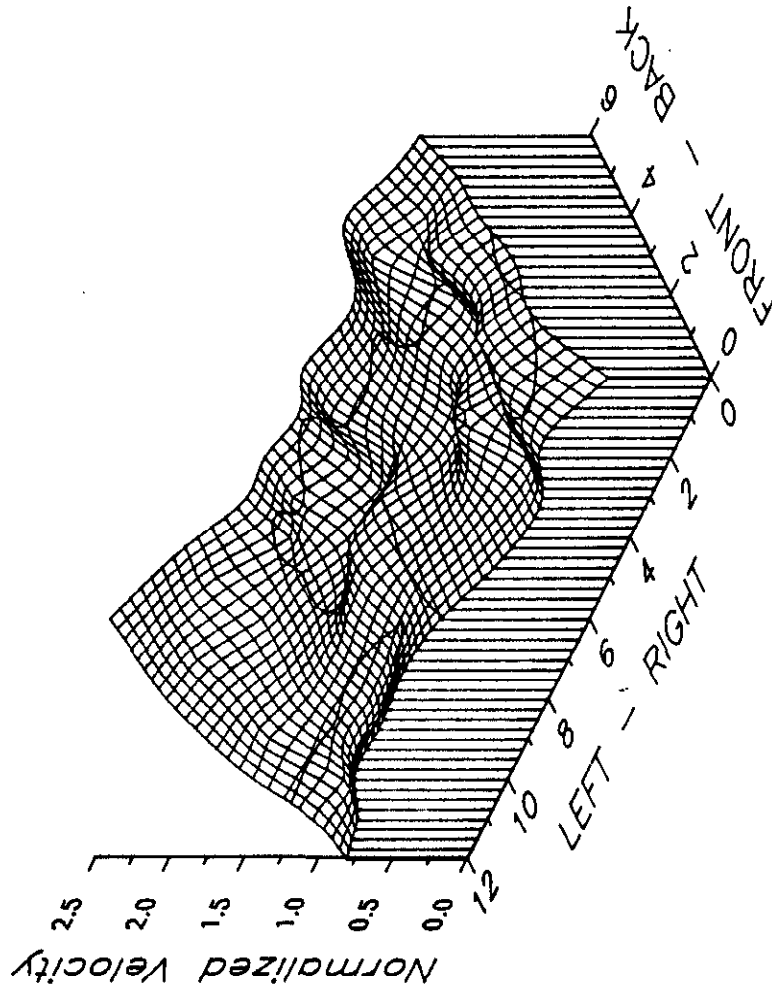


Figure 6-79

**SOUTHERN COMPANY SERVICES
LANSING SMITH #2 FLOW MODEL**

NORMALIZED VELOCITY

Test Plane: 4

Test Date: 3/1/91

Firing System: LNCFS-III

Test ID: Configuration #4

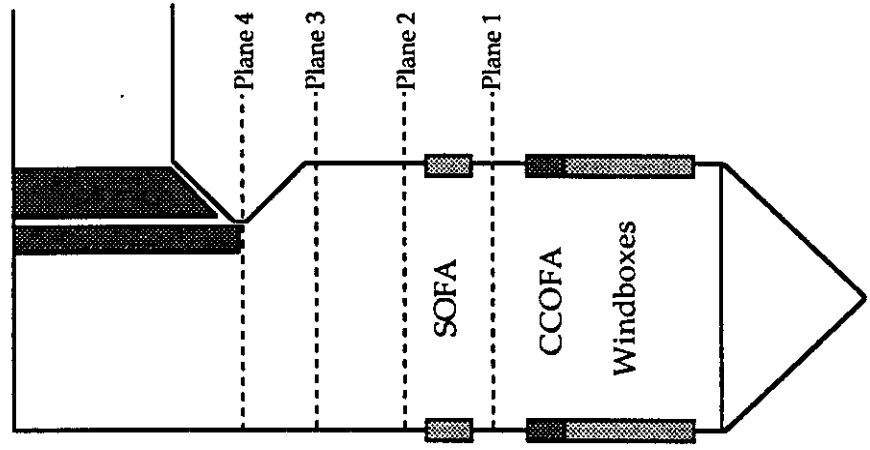
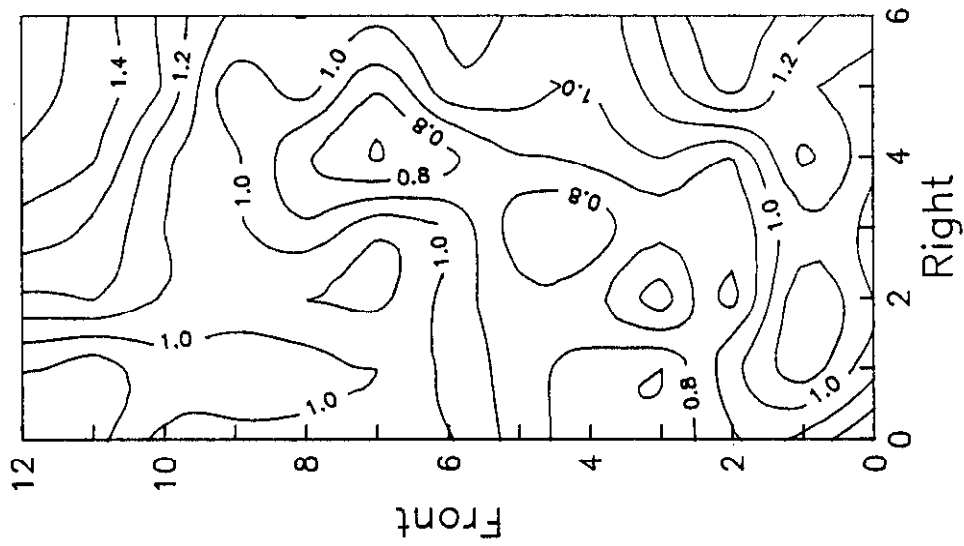


Figure 6-80

**SOUTHERN COMPANY SERVICES
LANSING SMITH #2 FLOW MODEL**

NORMALIZED VELOCITY

Test Plane: 4

Test Date: 2/28/91

Firing System: LNCFS-III

Test ID: Configuration #5

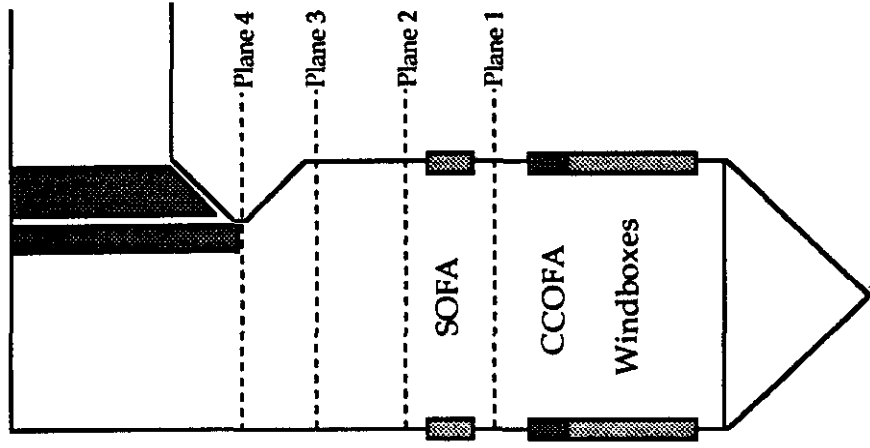
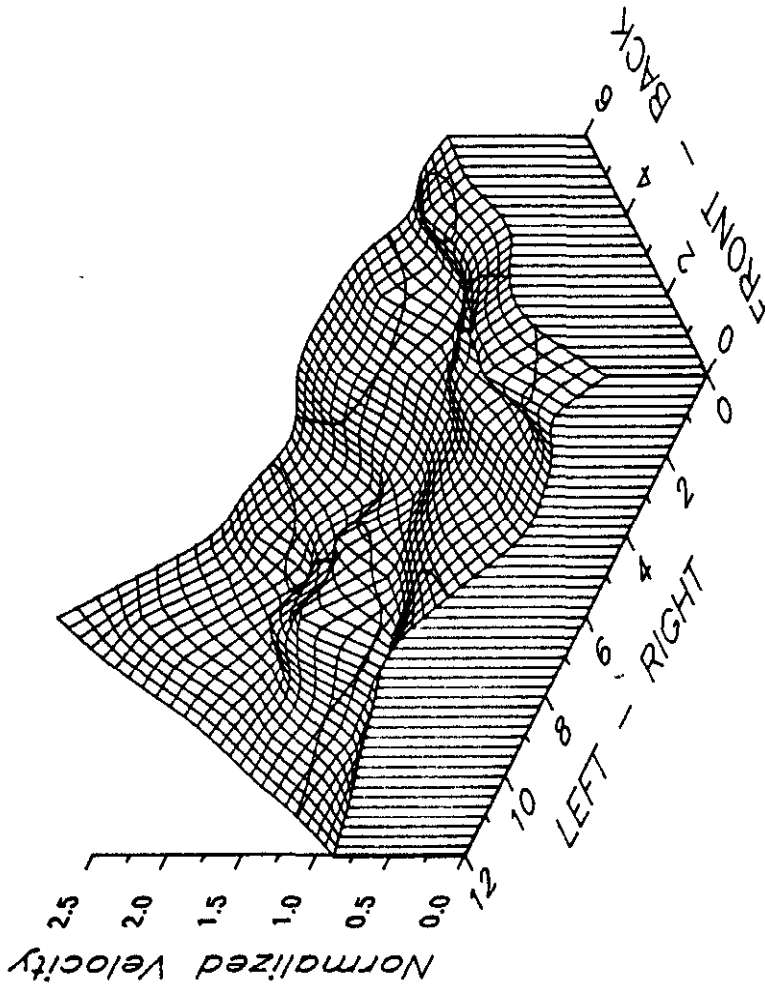


Figure 6-81

**SOUTHERN COMPANY SERVICES
LANSING SMITH #2 FLOW MODEL**

ABB Combustion Engineering, Inc.
Kreisinger Development Laboratory
Mechanical Systems Engineering

NORMALIZED VELOCITY

Test Plane: 4

Test Date: 2/28/91

Firing System: LNCFS-III

Test ID: Configuration #5

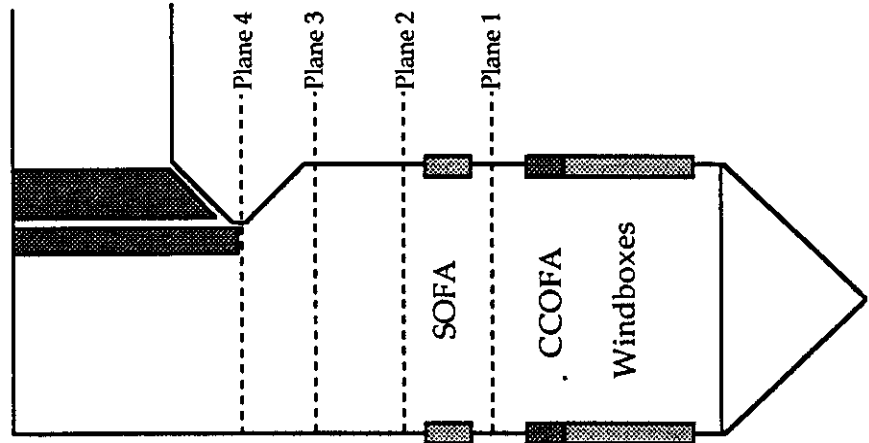
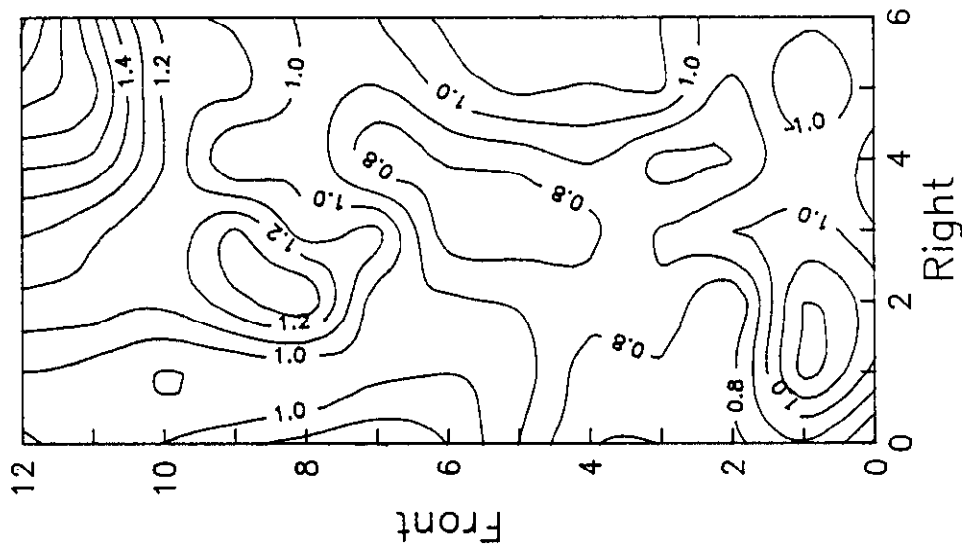


Figure 6-82

**SOUTHERN COMPANY SERVICES
LANSING SMITH #2 FLOW MODEL**

NORMALIZED VELOCITY

Test Plane: 4
 Test Date: 3/4/91
 Firing System: LNCFS-III
 Test ID: Baseline

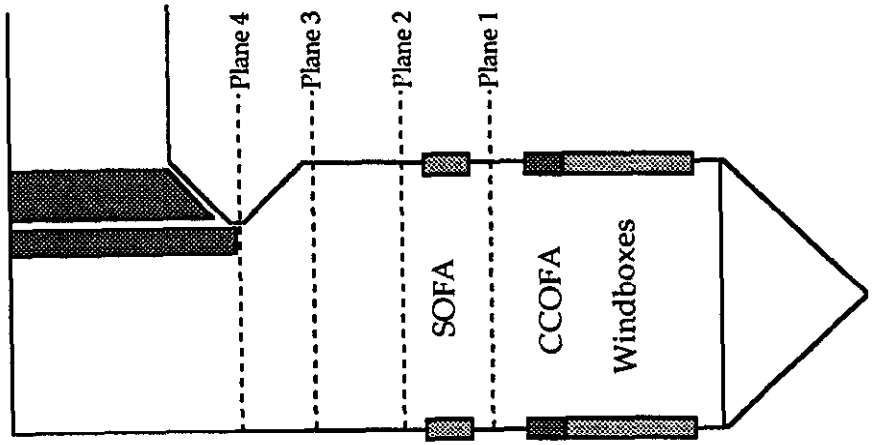
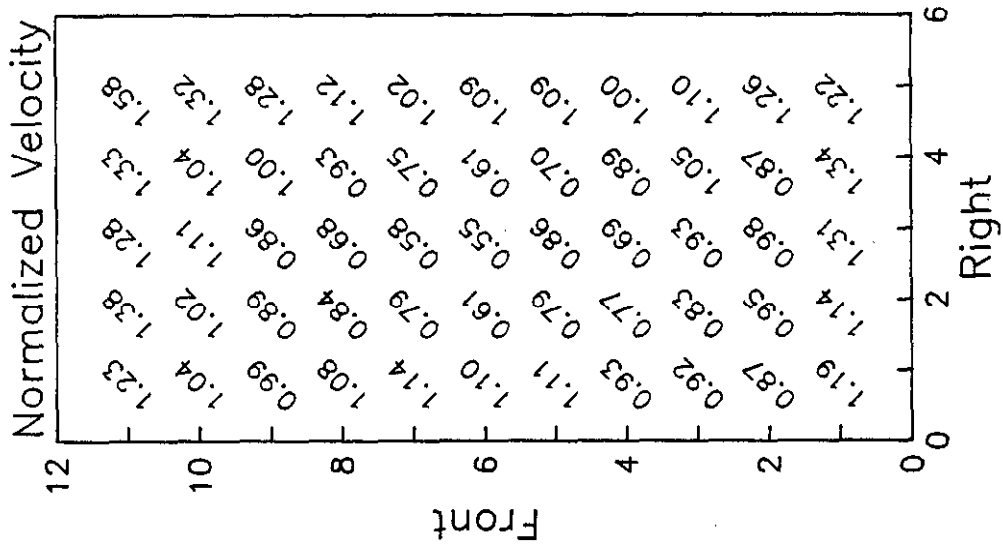


Figure 6-83

**SOUTHERN COMPANY SERVICES
 LANSING SMITH #2 FLOW MODEL**

ABB Combustion Engineering, Inc.
 Kreisinger Development Laboratory
 Mechanical Systems Engineering

NORMALIZED VELOCITY

Test Plane: 4
 Test Date: 3/1/91
 Firing System: LNCFS-III
 Test ID: Configuration #1

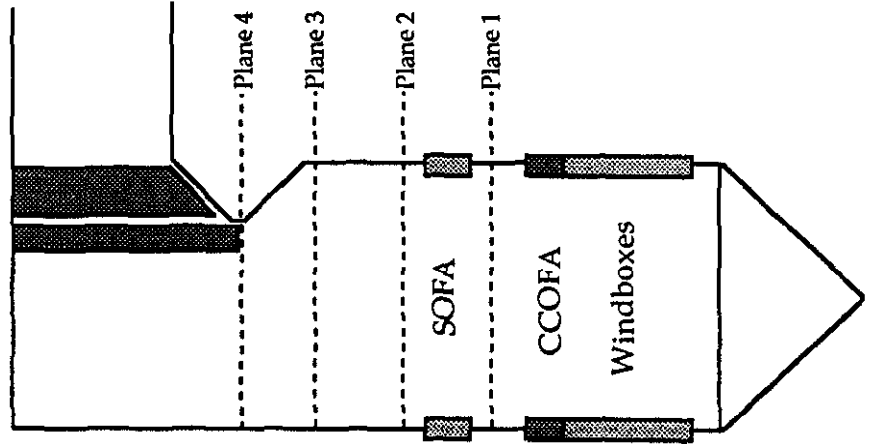
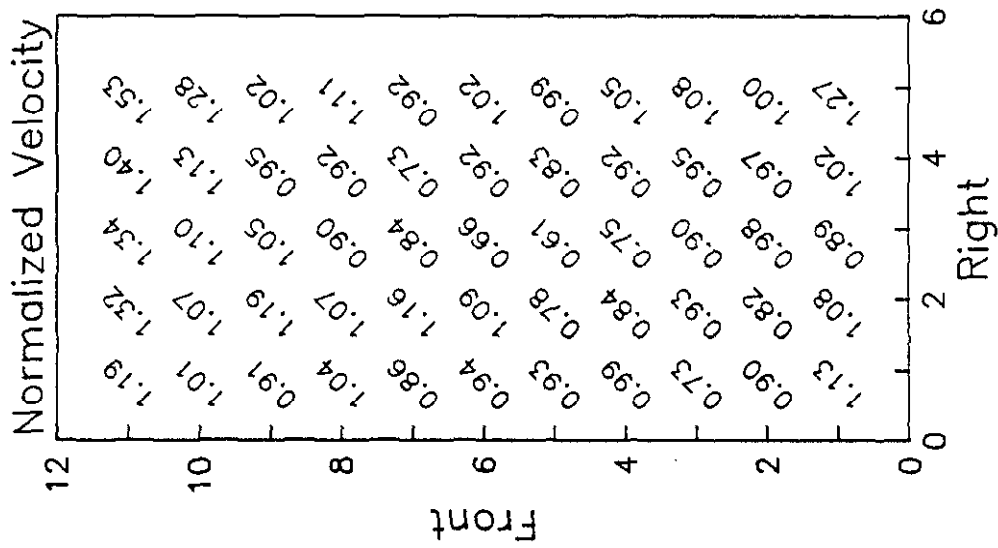


Figure 6-84

**SOUTHERN COMPANY SERVICES
 LANSING SMITH #2 FLOW MODEL**

NORMALIZED VELOCITY

Test Plane: 4
 Test Date: 3/1/91
 Firing System: LNCFS-III
 Test ID: Configuration #2

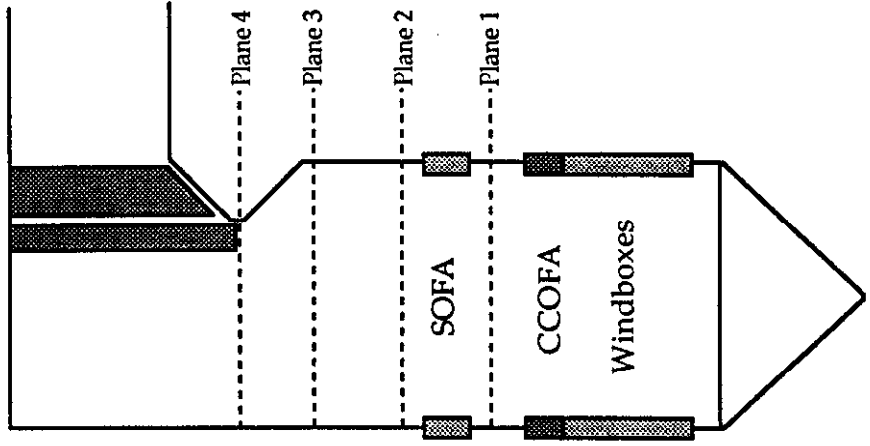
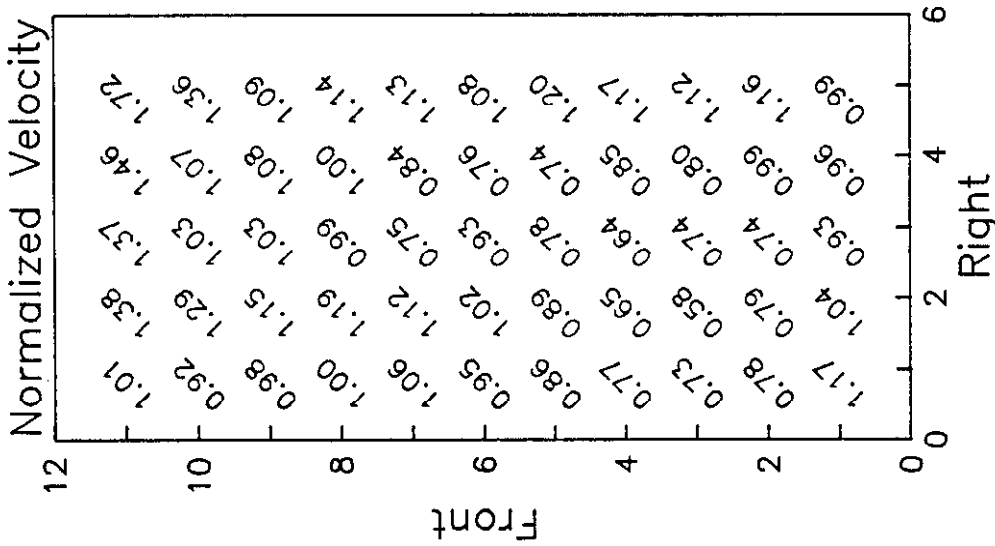
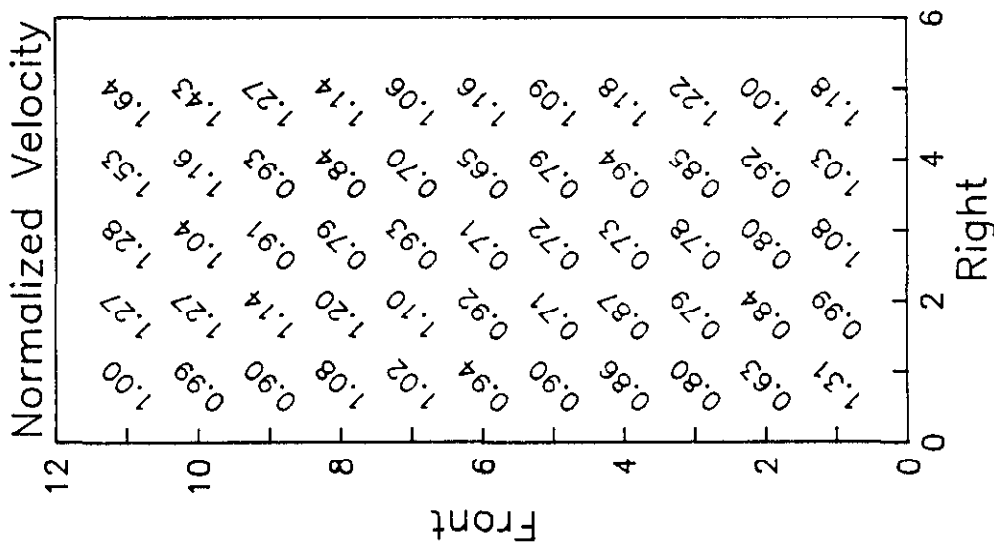


Figure 6-85

**SOUTHERN COMPANY SERVICES
 LANSING SMITH #2 FLOW MODEL**



NORMALIZED VELOCITY

Test Plane: 4

Test Date: 3/1/91

Firing System: LNCFS-III

Test ID: Configuration #3

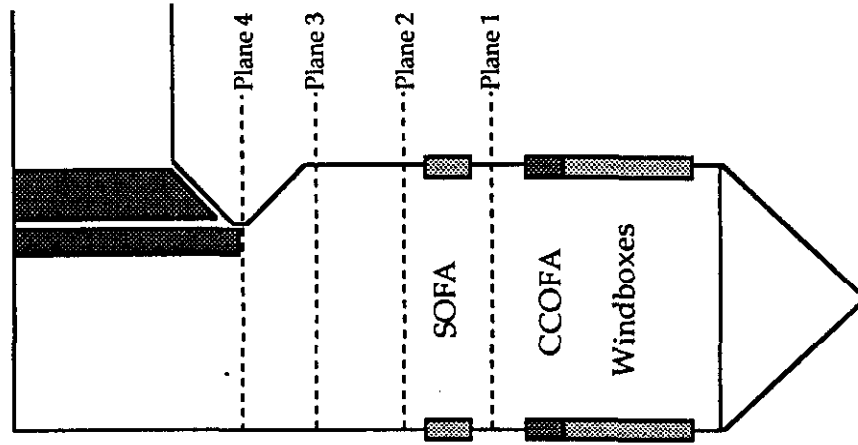


Figure 6-86

**SOUTHERN COMPANY SERVICES
LANSING SMITH #2 FLOW MODEL**

NORMALIZED VELOCITY
 Test Plane: 4
 Test Date: 3/1/91
 Firing System: LNCFS-III
 Test ID: Configuration #4

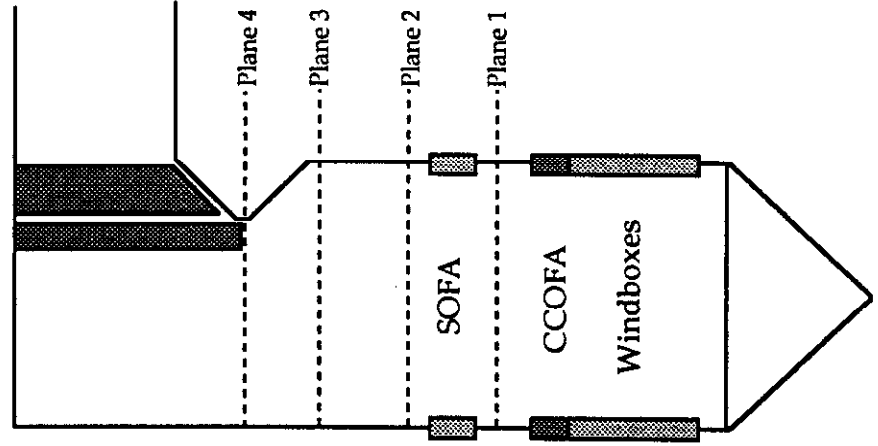
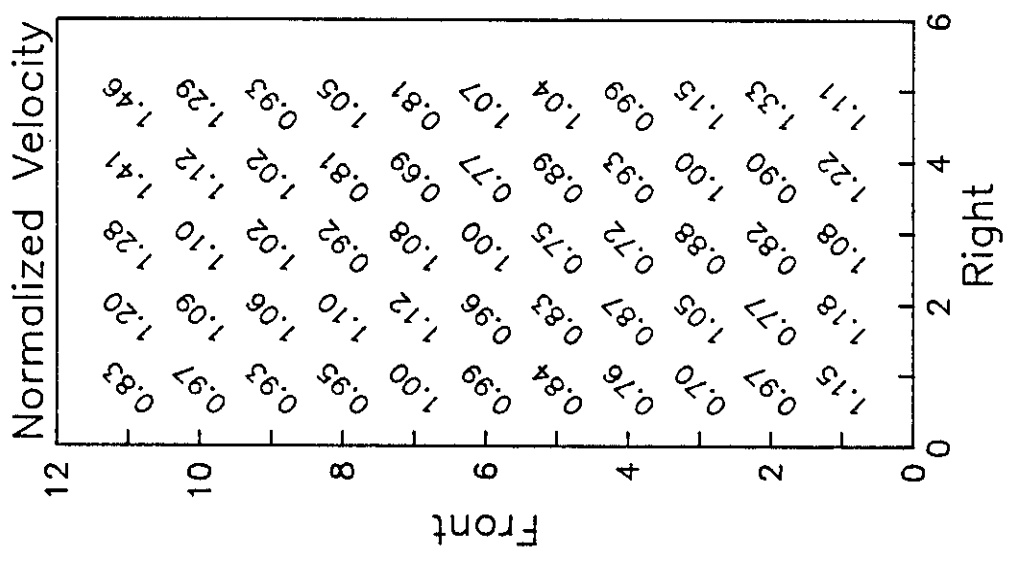


Figure 6-87

**SOUTHERN COMPANY SERVICES
 LANSING SMITH #2 FLOW MODEL**

NORMALIZED VELOCITY

Test Plane: 4
 Test Date: 2/28/91
 Firing System: LNCFS-III
 Test ID: Configuration #5

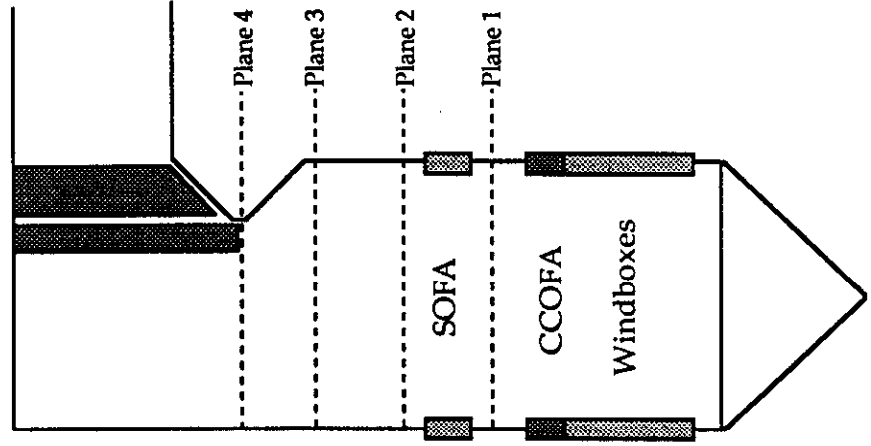
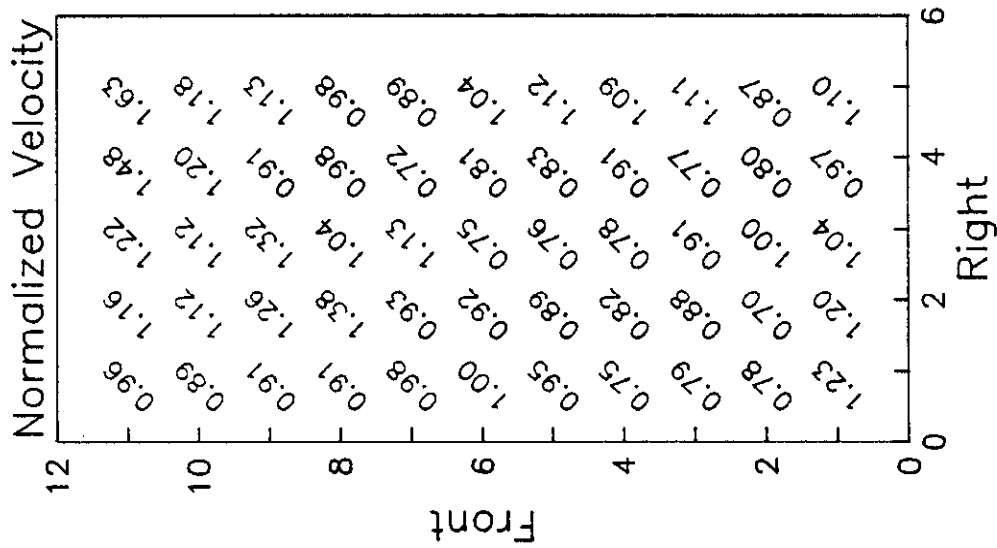


Figure 6-88

**SOUTHERN COMPANY SERVICES
 LANSING SMITH #2 FLOW MODEL**

**Lansing Smith #2 Flow Model
Velocity RMS at Furnace Outlet Plane**

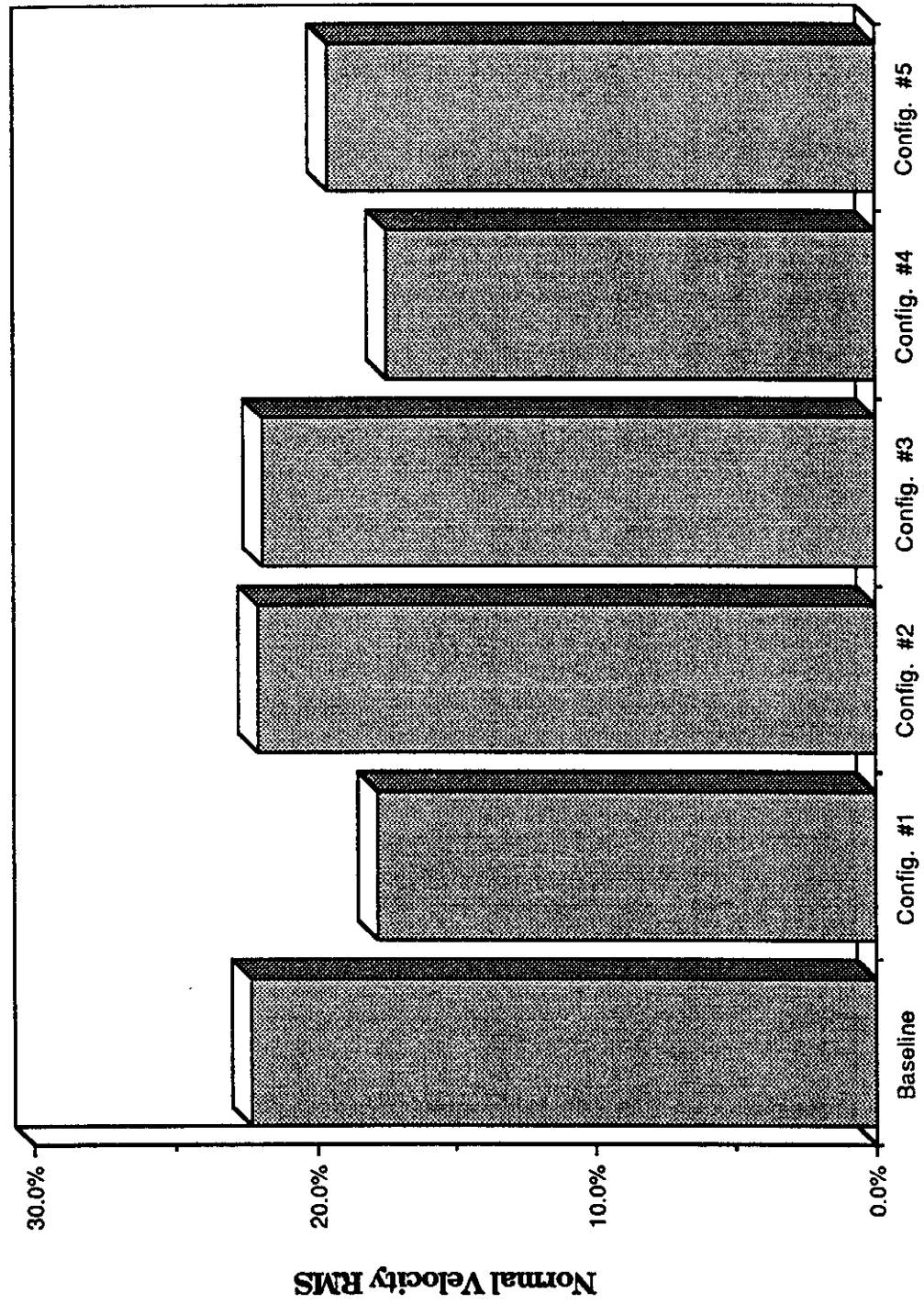


Figure 6-89

Lansing Smith #2 Flow Model

Side to Side Velocity Distribution at Furnace Outlet Plane

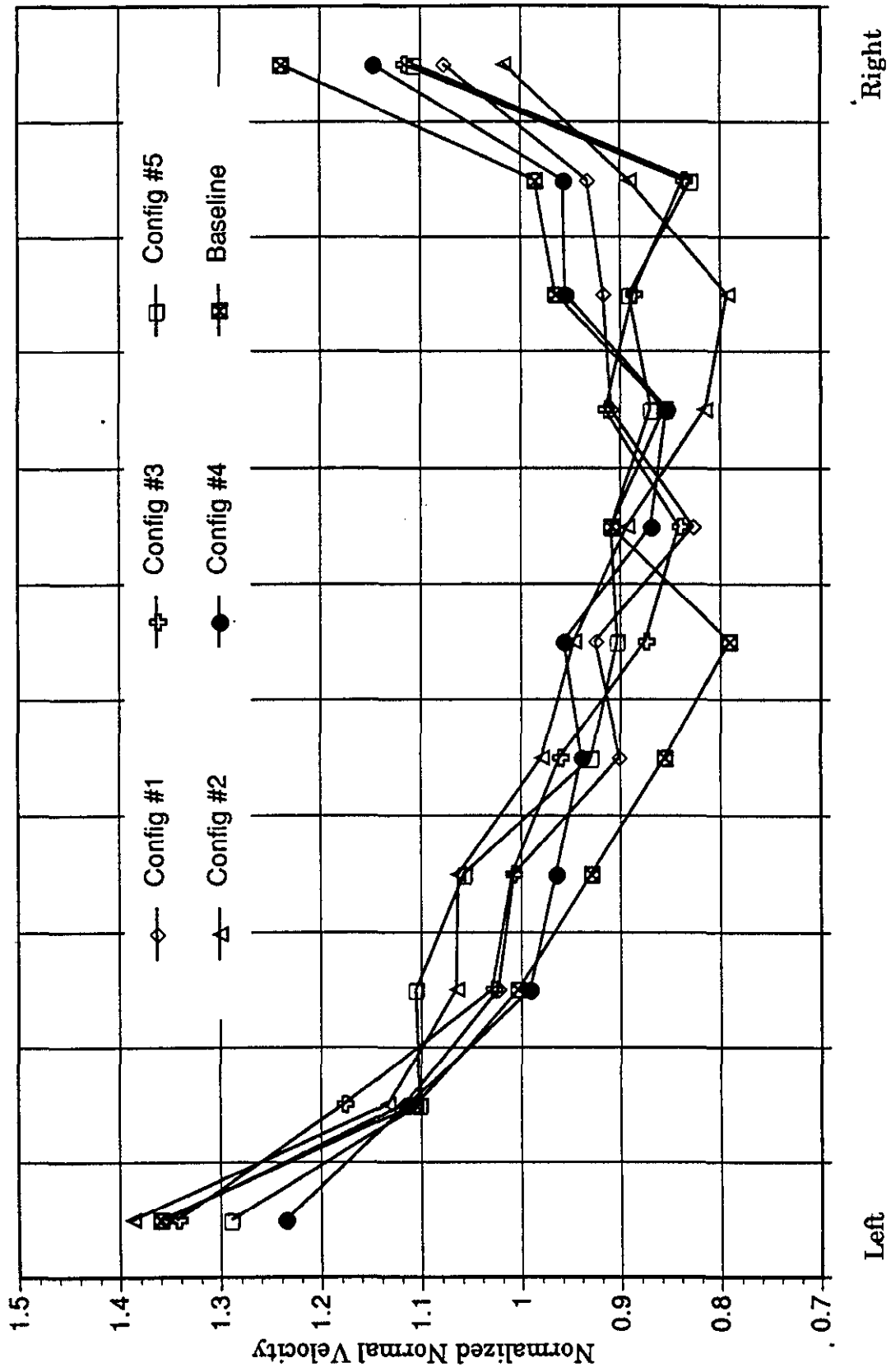


Figure 6-90

VELOCITY VECTORS

Test Plane: 4

Test Date: 3/4/91

Firing System: LNCFS-III

Test ID: Baseline

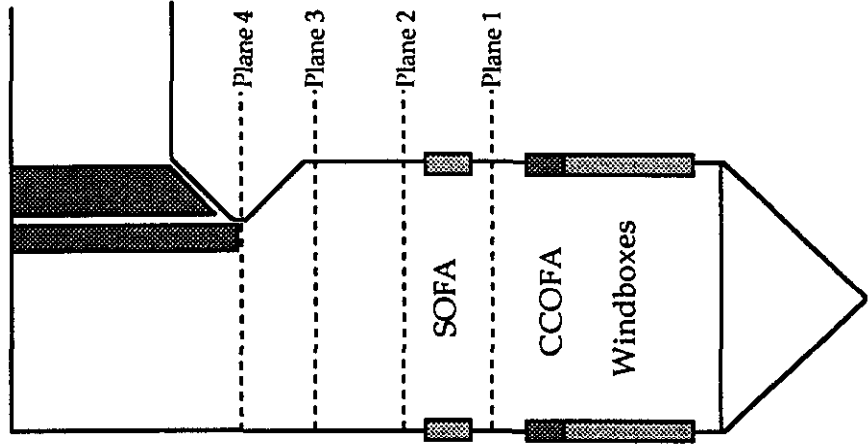
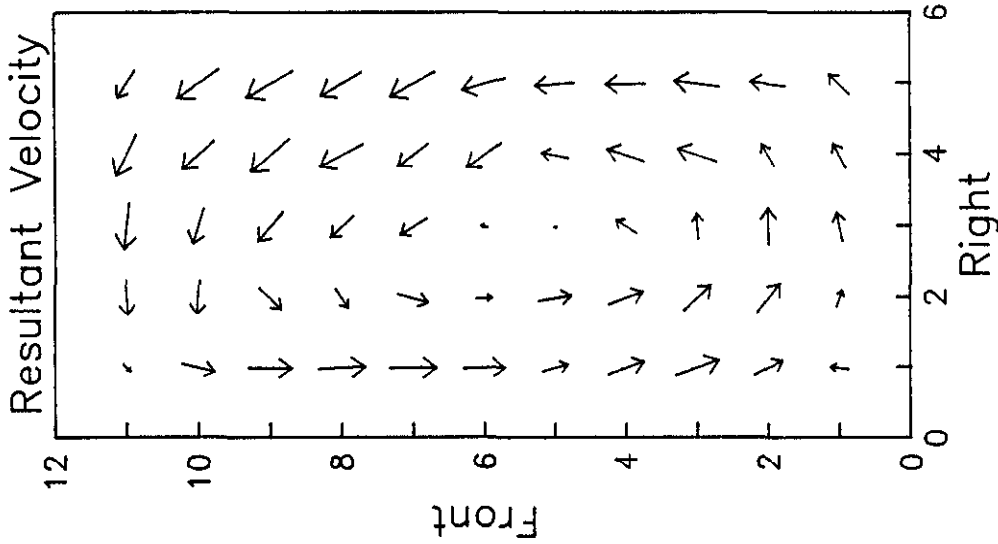


Figure 6-91

**SOUTHERN COMPANY SERVICES
LANSING SMITH #2 FLOW MODEL**

VELOCITY VECTORS

Test Plane: 4

Test Date: 3/1/91

Firing System: LNCFS-III

Test ID: Configuration #1

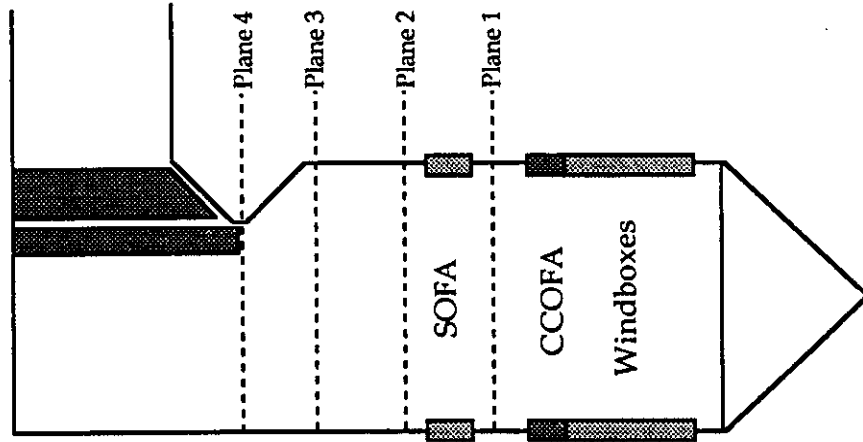
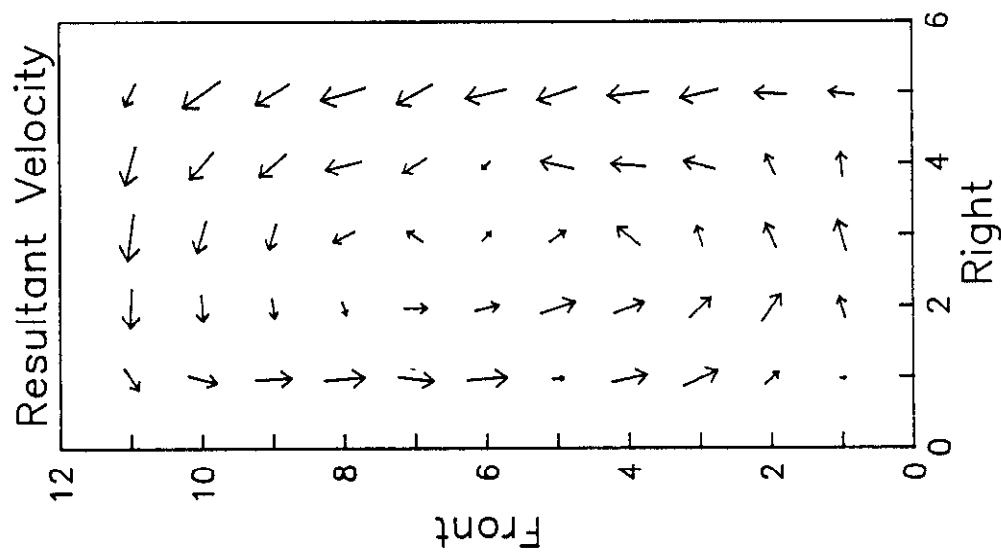


Figure 6-92

**SOUTHERN COMPANY SERVICES
LANSING SMITH #2 FLOW MODEL**

VELOCITY VECTORS

Test Plane: 4
 Test Date: 3/1/91
 Firing System: LNCFS-III
 Test ID: Configuration #2

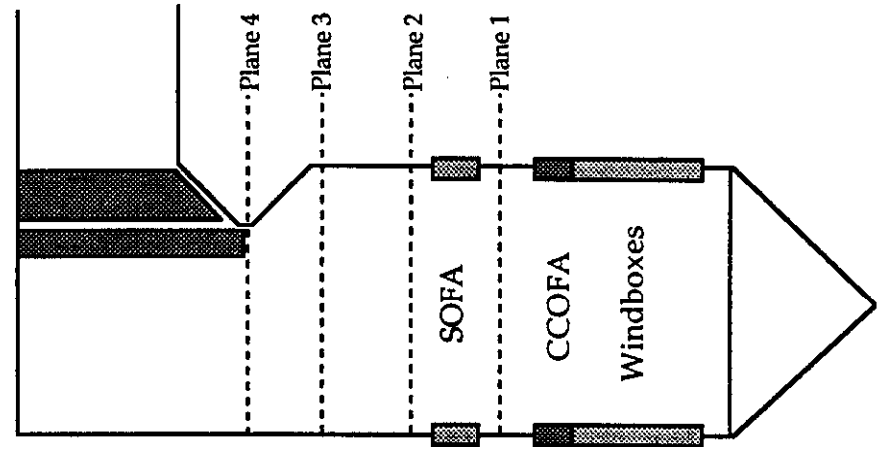
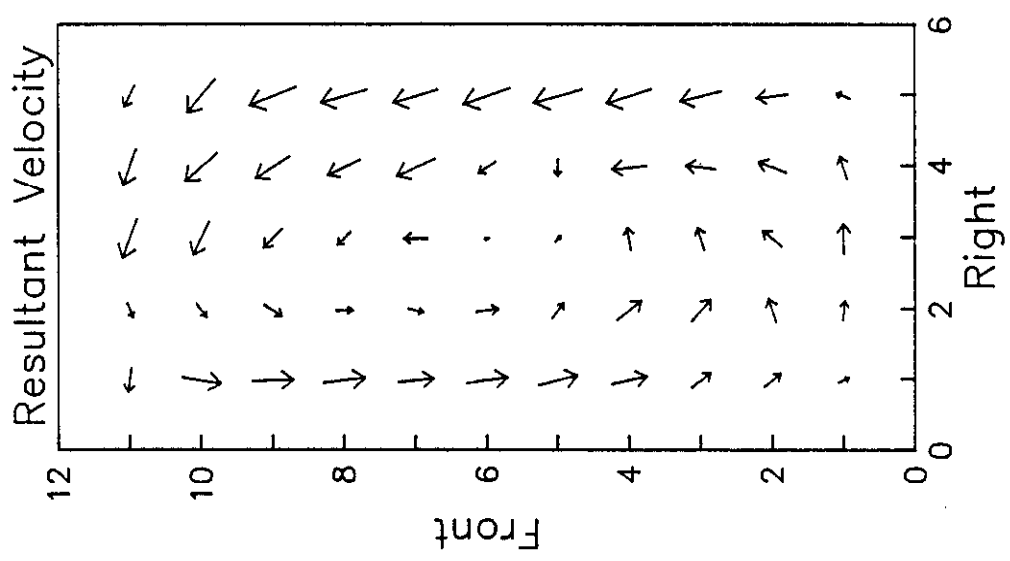


Figure 6-93

**SOUTHERN COMPANY SERVICES
 LANSING SMITH #2 FLOW MODEL**

ABB Combustion Engineering, Inc.
 Kreisinger Development Laboratory
 Mechanical Systems Engineering

VELOCITY VECTORS

Test Plane: 4

Test Date: 3/1/91

Firing System: LNCFS-III

Test ID: Configuration #3

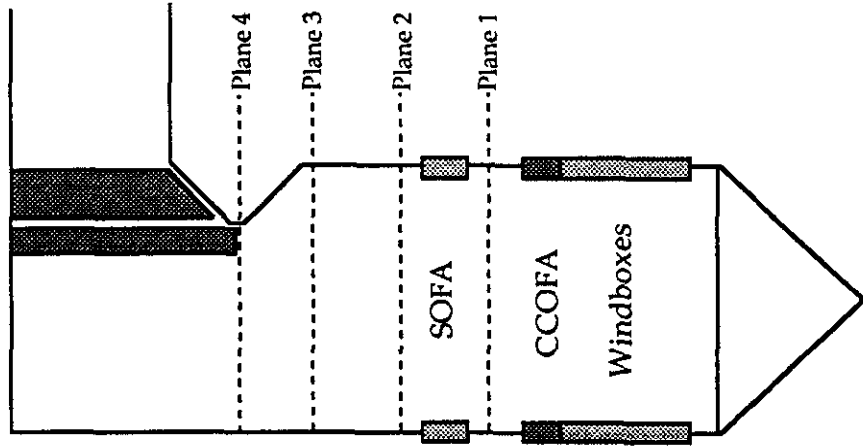
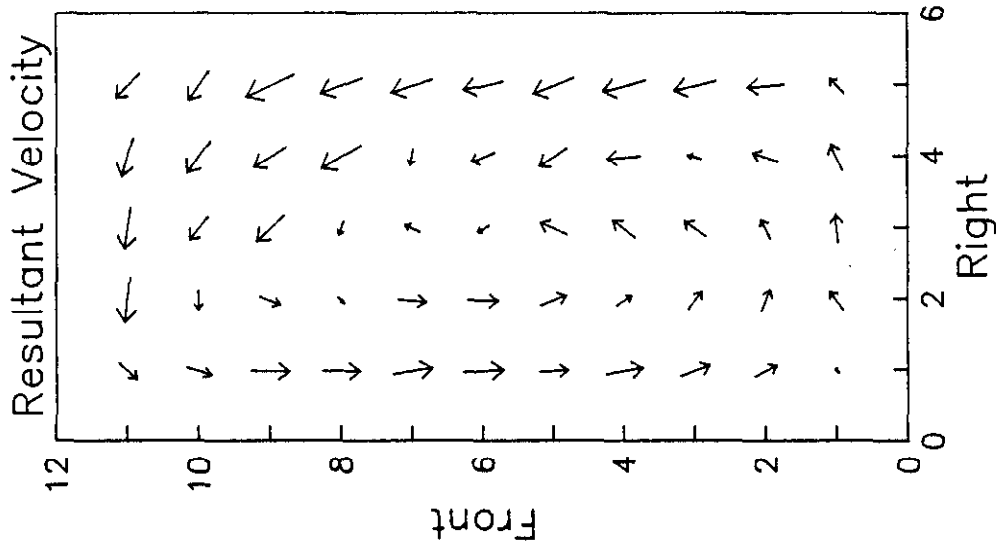


Figure 6-94

**SOUTHERN COMPANY SERVICES
LANSING SMITH #2 FLOW MODEL**

VELOCITY VECTORS

Test Plane: 4

Test Date: 3/1/91

Firing System: LNCFS-III

Test ID: Configuration #4

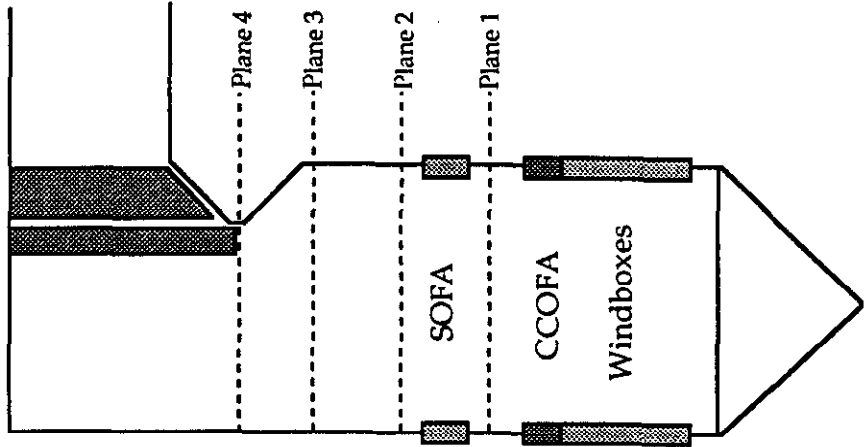
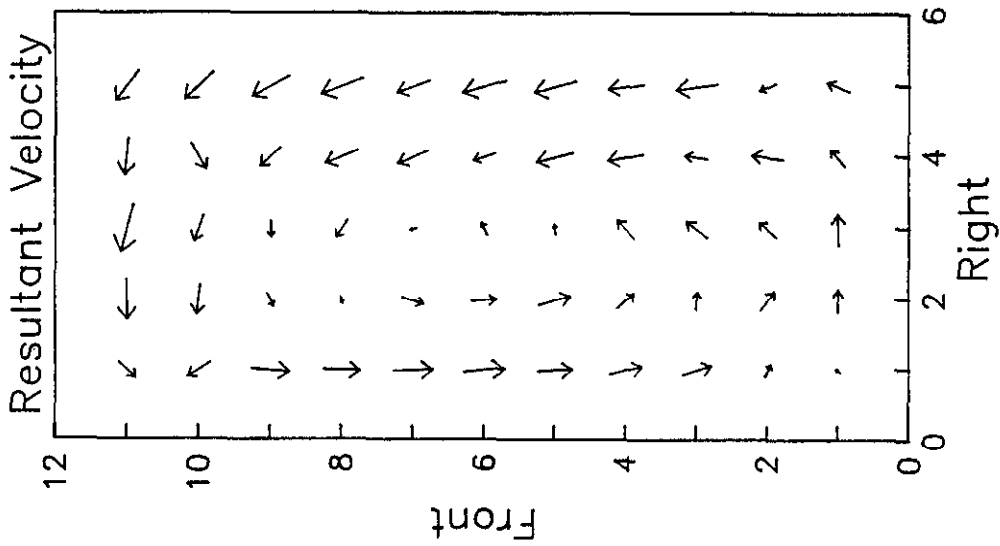
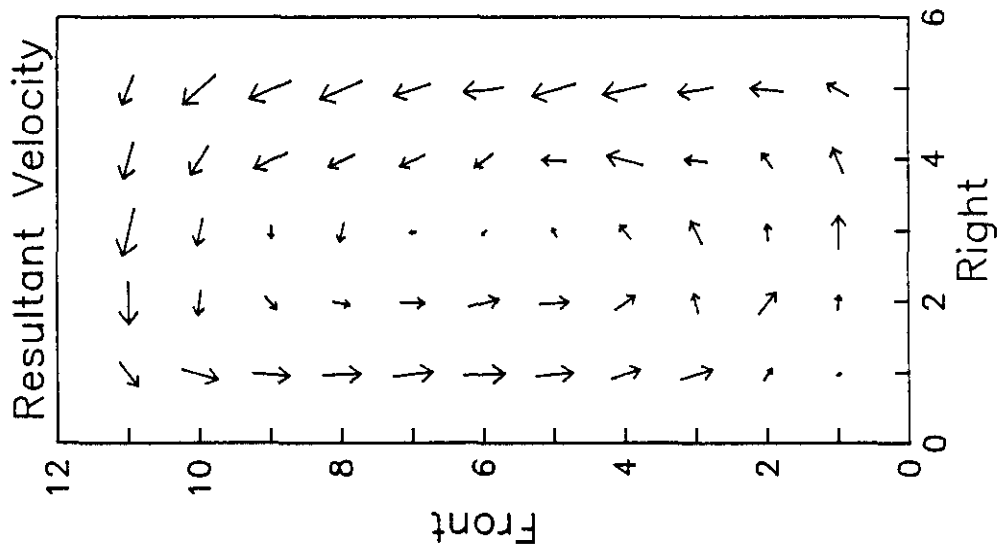


Figure 6-95

**SOUTHERN COMPANY SERVICES
LANSING SMITH #2 FLOW MODEL**

ABB Combustion Engineering, Inc.
Kreisinger Development Laboratory
Mechanical Systems Engineering



VELOCITY VECTORS

Test Plane: 4

Test Date: 2/28/91

Firing System: LNCFS-III

Test ID: Configuration #5

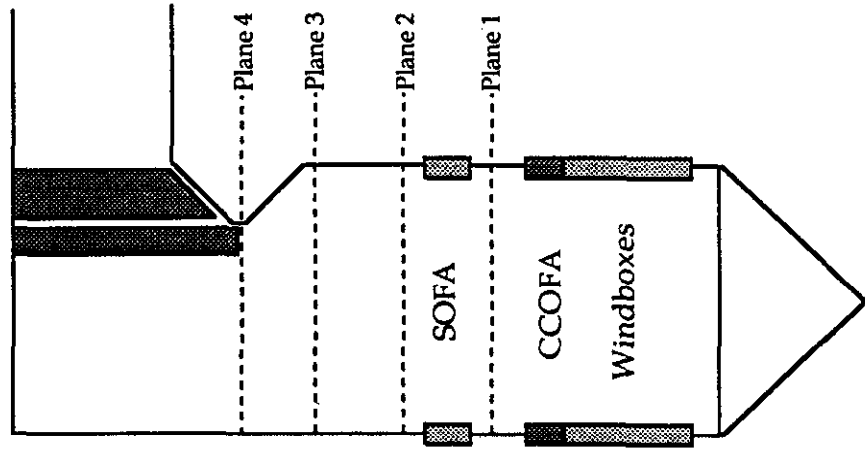


Figure 6-96

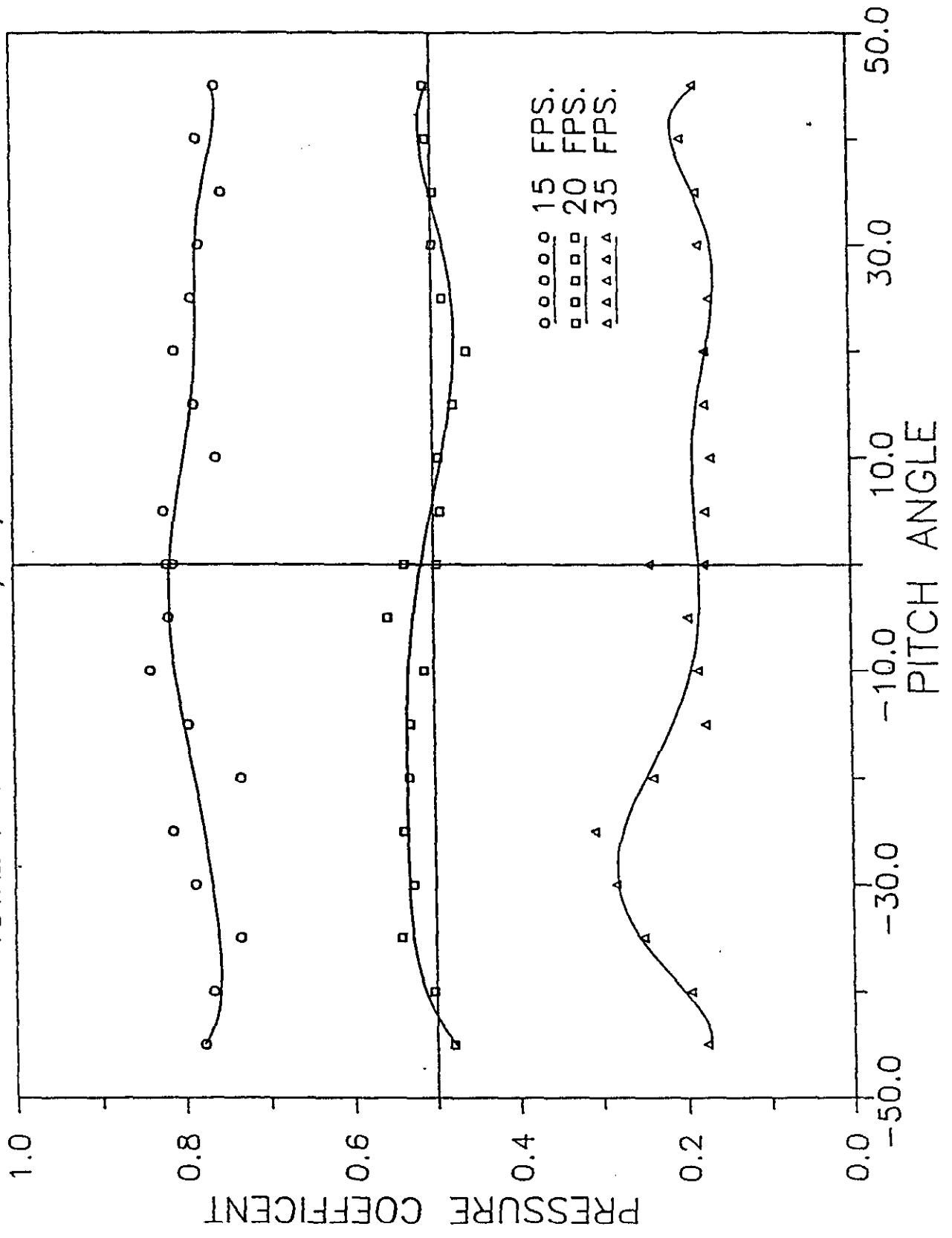
**SOUTHERN COMPANY SERVICES
LANSING SMITH #2 FLOW MODEL**

7.0 References

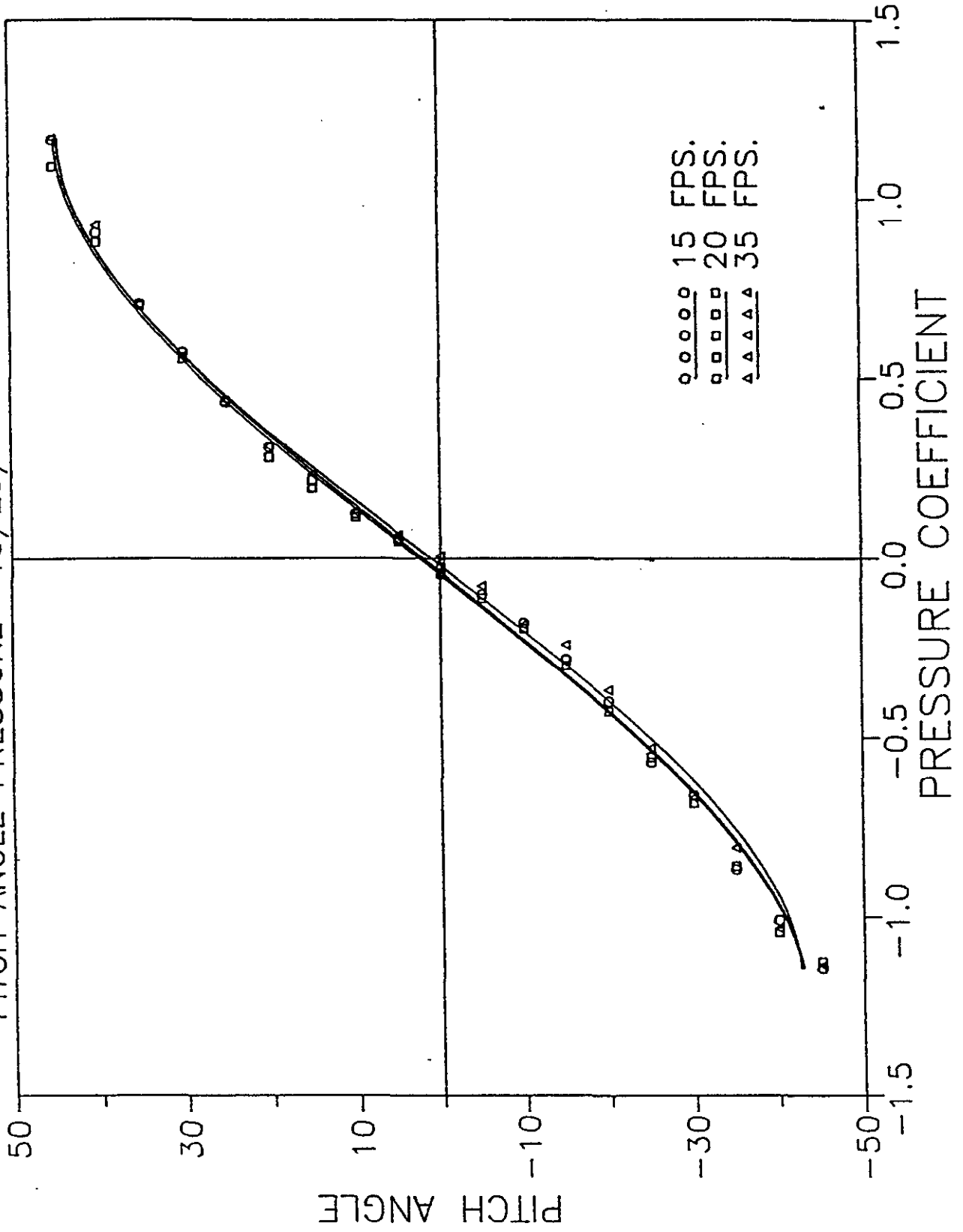
1. Anderson, D.K., Bianca, J.D., and McGowan, J.G., "Recent Developments in Physical Flow Modeling of Utility Scale Furnaces," Proc. 1986 Symposium on Industrial Combustion Technologies, Chicago, Illinois, 1986
2. Beer, J.M., "Significance of Modeling," J. Inst. Fuel, November, 1966
3. Beer, J.M., "Recent Advances in the Technology of Furnace Flames," J. Inst. Fuel, July 1972
4. Beer, J.M. and Chigier, N.A., Combustion Aerodynamics, Wiley, New York, 1972
5. Bianca, J.D., Bauver, W.P., and McGowan, J.G., "An Aerodynamic Study of an Operating Tangentially Fired Furnace," Fluid Mechanics of Combustion Systems, ASME, 1981
6. Chigier, N.A., "Application of Model Results to Design Industrial Flames", J. Inst. Fuel, September 1973
7. Johnstone, R.E., and Thirng, M.B., Pilot Plants, Models and Scale up Factors in Chemical Engineering, McGraw Hill, New York, 1947
8. Spaulding, D.B., "The Art of Partial Modeling," 9th International Symp. on Combustion, September, 1973
9. Thring, M.B., and Newby, M.P., "Combustion Length of Enclosed Turbulent Jet Flames," 9th Symp. on Combustion, September 1953

Appendix A
Five Hole Pitot Probe Calibration Curves

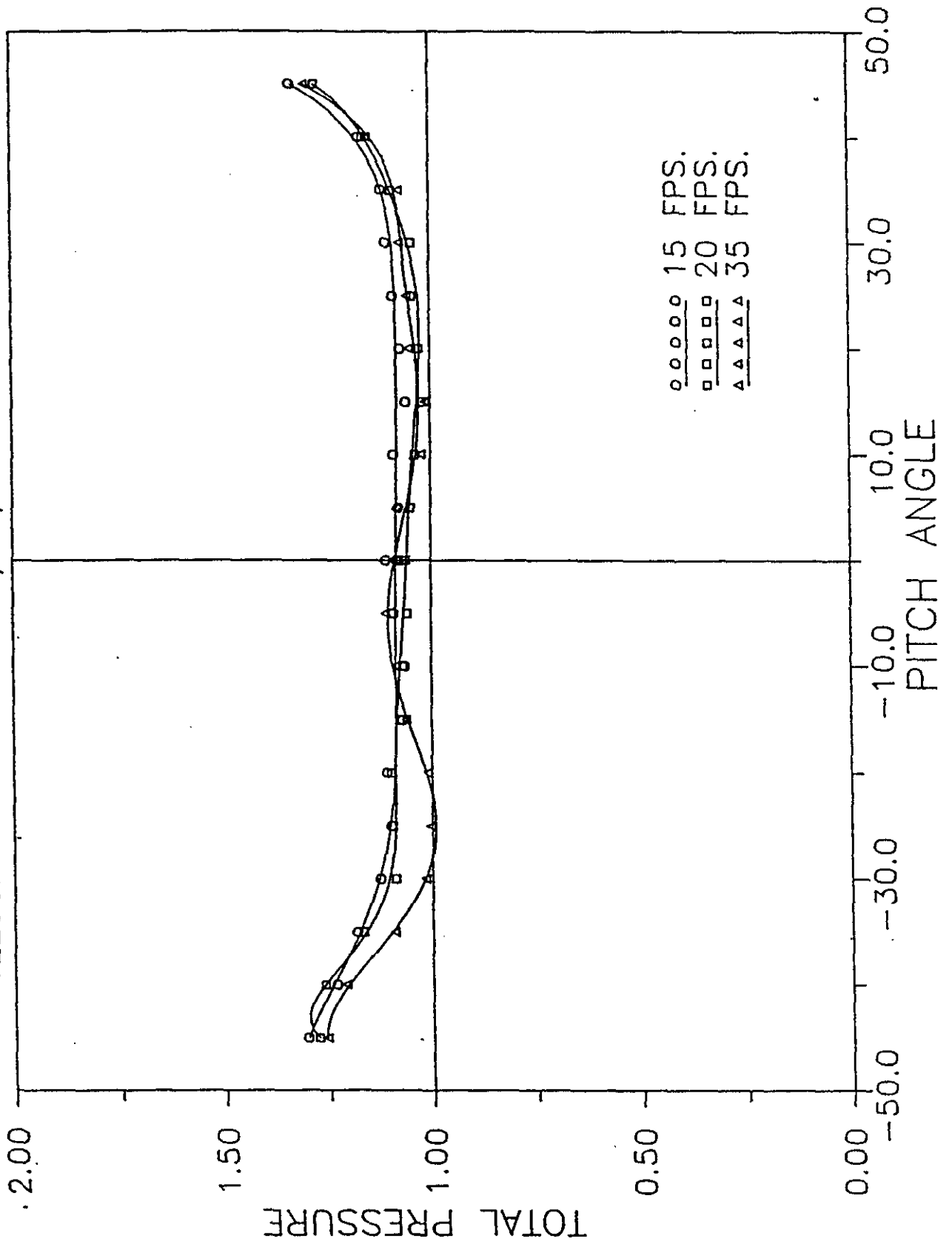
TOTAL PRESSURE 10/23/90 PROBE B1884-2



PITCH ANGLE PRESSURE 10/23/90 PROBE B1884-2



VELOCITY PRESSURE 10/23/90 PROBE B1884-2



Appendix B

Laser Absorption Spectrophotometer Calibration Curve

Laser Absorption Spectrophotometer Calibration Curve

